

**NASA TECHNICAL  
TRANSLATION**

**NASA TT F-339**



**NASA TT F-339**

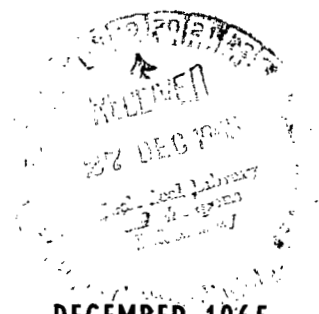
*2.1*



**ELECTRIC CONTACTS**

*by B. S. Sotskov, et al*

*Izdatel'stvo Energiya,  
Moscow-Leningrad, 1964*



**NATIONAL AERONAUTICS AND SPACE ADMINISTRATION - WASHINGTON, D. C. - DECEMBER 1965**



## ELECTRIC CONTACTS

By B. S. Sotskov, I. Ye. Dekabrun, B. N. Zolotych,  
R. S. Kuznetsov, and Z. S. Kirillova

Translation of "Elektricheskiye kontakty."  
Izdatel'stvo Energiya,  
Moscow - Leningrad, 1964

NATIONAL AERONAUTICS AND SPACE ADMINISTRATION

---

For sale by the Clearinghouse for Federal Scientific and Technical Information  
Springfield, Virginia 22151 - Price \$7.45



## ANNOTATION

/2

This work contains the proceedings of the Third All-Union Conference on Electric Contacts and Contact Materials which took place in Moscow from 11th to the 14th of December 1962.

As before, the proceedings cover problems associated with physical processes which take place during the operation of contacts, with the construction of contacts and contact elements, with the characteristics of contact materials and with their production. A series of reports contained in the present volume is devoted to the problems of contact reliability as well as the reliability of devices using contacts.

The work is intended for scientists, engineers, and technicians who develop, investigate, design and operate equipment containing contact elements.





## CONTENTS

	Page
Preface	v
PART I. THE PHYSICS OF THE PROCESSES	
The Nature of Energy Transfer to Electrodes in a Pulse Discharge with Small Gaps B. N. Zolotykh	1
Theoretical Determination of the Contact Gap Restorable Strength I. S. Tayev	16
Selectivity in the Emission of Material from Solid Binary Alloys during Pulse Discharges in Air O. I. Avseyevich and I. G. Nekrashevich	32
Effect of Components Percentage on the Electric Erosion of Binary Alloys N. V. Afanas'yev and A. G. Goloveyko	36
Erosion of Precious Metal Electrodes in an Arc Discharge A. D. Gut'ko	45
Investigation of Nonequilibrium Processes at Electrodes in an Arc A. A. Kuranov	64
Nature of Forces which Eject Metal during Electric Erosion A. S. Zingerman	66
Computing the Contact Areas of Stationary and Sliding Contacts I. V. Kragel'skiy, N. B. Demkin and N. N. Mikhin	77
Energy Losses in Closing Contacts Measured by Means of an Oscillograph V. S. Pellinets	92
Transient Currents and Voltages which Occur in Breaking Contacts in a Low Voltage dc Inductive Circuit B. Ye. Kravchuk	99

	Page
Welding of Electric Contacts at High Currents O. B. Bron and N. G. Myasnikova	113
Application of the Additivity Principle to the Erosion of Electrodes in Pulse Discharges with Low Interelectrode Gaps A. I. Kruglov	126
Investigation of the Fine Transfer of Material on Silver Contacts A. Khench	137
PART II. CONSTRUCTION AND APPLICATION	
Arc Quenching at Critical dc Current Values R. S. Kuznetsov, P. M. Zemskov and V. A. D'yachkova	144
Quenching of an Electric Arc when Switching Off Currents of 5-150 A at 660 V V. A. Kleymenov and N. I. Korbal'	148
Silver Contacts at Elevated Temperatures with Prolonged Loading O. B. Bron and M. Ye. Yevseyev	158
The deterioration of Contacts during the Switching of Low Voltage (up to 220 V) dc and ac Currents V. T. Nezhdanov and B. A. Vasil'yev	169
Resistance of Contact Materials to Electric Wear O. F. Gayday	178
A Phenomenon at the Contacts of a Sealed Relay A. V. Gordon, V. N. Gimmel'brodskiy and O. N. Mikheyeva	185
Effect of Moisture on the Formation of Current-Carrying Bridges across Electric Contacts Made of Different Materials G. N. Volosevich	193
Investigation of Cam Contacts of Punched Card Machines V. Dauknis, I. Mayauskas, G. Prantskyavichyus and V. Ryauka	205
Investigation of New Contact Systems for Miniature High- Frequency Switches I. G. Mordukhovich and N. P. Barshteyn	212

	Page
Investigation of Plug-Type Connectors Operating with Microcurrents at Microvolts A. I. Fedorov and G. Z. Zakirov	222
PART III. CONTACT MATERIALS	
Heavy Duty Cermet Switching Contacts I. P. Melashenko and K. V. Gubar'	234
Development and Investigation of Heavy Duty Finely Dispersed Contacts N. N. Smaga, B. A. Yudin and Ye. V. Markov	245
Cu-Cd and Ag-Cd Cermet Contacts A. B. Al'tman and E. S. Bystrova	252
Investigation of Electric Contact Erosion of Tungsten- Rhenium Electrodes M. I. Tishkevich	258
Investigation of Breaking Contacts for Ignition Assemblies Z. S. Kirillova and A. G. Morozova	261
The Possibility of Using Cermets to Replace Tungsten G. A. Bugayev	270
Special Features of Switching Low Level Currents and Voltages by Means of Contacts T. K. Shtremberg and D. V. Gayevskaya	276
Contacts of Relay-Type Elements and Microswitches which Commutate Low Level Signals S. F. Solov'yeva, I. I. Sigachev, N. A. Surkova, and Ye. V. Kogteva	301
Electroplating of Switching Contacts S. Ya. Grilikhes and D. S. Isakova	332
Alloys of Palladium with Tungsten, Rhenium, Osmium and Iridium Ye. M. Savitskiy, M. A. Tylkina, V. P. Polyakova, I. A. Tsyganova and Ch. V. Kopetskiy	348
Stability of Elastic Elements of Communications Equipment at Elevated Temperatures R. I. Mishkevich	358

## IV. RELIABILITY OF CONTACTS

The Reliability of the Electric Contact B. S. Sotskov and I. Ye. Dekabrun	376
The Reliability of Electromagnetic Relay Contacts According to Operational Data G. Ya. Rybin	385
The Useful Life of Platini-Iridium Relay Contacts as a Function of Load Current T. K. Shtremberg and N. A. Belozerova	388
Determining Norms from the Basic Electric Parameters of Connector Contacts V. S. Savchenko	407
A System for Recording Failures A. Yu. Gorodetskiy	426

## PREFACE

13

One of the basic problems encountered today is concerned with the improvement of equipment reliability. This problem cannot be solved without a deep understanding of the physical processes which form the basis for the operation of all components which make up a piece of equipment.

In spite of the wide development of contactless equipment, electric contacts still form an integral part of any circuit, device or installation. This is explained both by their natural properties (high control coefficient, low resistance in operating state, ability to control ac and dc currents, ability to control high powers per unit volume, etc.) and by the successes in understanding their physical behavior, which makes their design fabrication and operation more intelligent.

The present volume is devoted to the proceedings of the Third All-Union Conference on Electric Contacts and Contact Materials which took place from the 11th to the 14th of December 1962 in Moscow at the Institute of Automation and Remote Control. Like the preceding volumes, the present one contains reports on the physics of the processes, on design methods and on the methods of applying and developing new materials. In addition to this, a special part of the volume is devoted to the problem of contact reliability.

The conference has shown that there has been a substantial increase in the number of organizations concerned with the problems of contacts and contact devices and most of the works are now oriented in the direction of problems associated with the investigation of physical processes which take place when the contacts operate and with the reliability of contact operation. During preceding conferences, the presentations were concerned primarily with the physical investigation of related disciplines: electro-erosion machining of metals, electric welding, etc. /4

We should also point out that because the questions of electric erosion are not clearly defined from the standpoint of physical principles of operation, the present volume contains papers which present several different points of view.

The committee which organized the conference and the editorial board of the present volume hope that the published papers will be useful to persons who are concerned with the design and utilization of contact equipment.

## PART I. THE PHYSICS OF THE PROCESSES

### THE NATURE OF ENERGY TRANSFER TO ELECTRODES IN A PULSE DISCHARGE WITH SMALL GAPS

B. N. Zolotykh

A pulse discharge (with a current duration of  $10^{-6}$  to  $10^{-3}$  sec) takes 5\* place when the contacts make and break and is widely used for electric spark machining. In this article we shall consider a discharge when the current reaches tens, hundreds and even thousands of A, while the voltage at the electrodes (when they are open) does not exceed 100-200 V. In air these voltages correspond to gaps of the order of several microns, while in a dielectric liquid (oil, kerosene) they are of the order of tens of microns.

References 1 and 2 presented the results of investigations on the distribution of the potential in the channel of a pulse discharge over small gaps. The results of these investigations have shown that the energy liberated in the spark interval may be divided into two basic parts

$$W_i = W_e + W_c$$

where  $W_i$  is the total energy liberated in the gap during one pulse;

$W_e$  is the energy liberated at the electrodes for the case of dc current;

$W_c$  is the energy in the discharge column.

It is the quantity  $W_e$  which is responsible for the phenomenon of electrode erosion.

Therefore, both from the point of view of electric contact wear and from the point of view of electric spark machining, it is interesting to consider the mechanism of energy liberation at the electrodes and to consider those 6 physical factors which affect the quantity  $W_e$ .

---

\*Numbers given in the margin indicate the pagination in the original foreign text.

Apparently, in the case of electric contacts, the conditions for which  $W_e$  would be a minimum are of interest. For the case of electric spark machining, it is desirable to generate conditions when  $W_e$  reaches a maximum.

As we have shown experimentally in our works (refs. 1 and 2), the potential drop in the discharge channel may be represented in the following form

$$U_{\text{gap}} = U_a + U_k + U_c$$

where  $U_{\text{gap}}$  is the total voltage drop across the gap;

$U_a$  is the anode drop;

$U_k$  is the cathode drop;

$U_c$  is the drop in the discharge column.

Experience has shown that the quantity  $U_a + U_k$  is practically independent of time.

The quantity  $U_c$  depends substantially on time and may be represented in the form  $U_c = \ln E_n(t)$ .

It has been shown experimentally that the quantity  $U_c$  varies by a factor of 3 to 8 during the period of the pulse, while the quantity  $U_a + U_k$  varies only by 10 - 20 percent during the same period of time.

If we use the methods of the theory of quasistationary plasma, we can obtain the following expression for the potential gradient which agrees well with the experiments

$$E_n(t) = \text{const } g_2 \frac{\frac{1}{4} + \frac{V_i}{4V_a}}{R(t)^{\frac{3}{2}}}, \quad (1a)$$

or in explicit form

$$E_n(t) = \text{const } g \frac{\frac{1}{4} + \frac{V_i}{4V_a}}{t^{\frac{3}{4}}}. \quad (1b)$$



If we note that  $W_e = l_p \int_0^t E_n(t) I(t) dt$ , it becomes clear that when  $W_i = \text{const}$ , the portion  $W_e$  relative to  $W_c$  decreases when  $W_c$  increases; i.e., from the point of view of decreasing the erosion it is advantageous to operate with high values of  $l_p$  with short pulses and consequently with relatively small discharge channel cross sections. However, before we can draw final conclusions, it is desirable to consider a whole series of questions. /7

We maintain the point of view that the basic role in the erosion process is played by two-dimensional heat sources. This concept has been extensively verified by experiment. For this reason we shall discuss some of the processes of energy transfer to the electrodes which according to our viewpoint are most probable, specifically:

- (1) the bombardment of the anode by electrons and of the cathode by ions under the action of the field in the regions adjoining the electrodes;
- (2) radiation of the discharge column;
- (3) the thermal (gaskinetic) bombardment with particles contained in the discharge channel;
- (4) energy exchanged between electrons due to vapor flares which occur at the anode and at the cathode (for small gaps).

The nature of energy transfer processes at the anode and at the cathode is substantially different. To emphasize this it is sufficient to remember that at the anode all of the current is transported by electrons, while at the cathodes, in addition to the ion current, there is an electron current component and the topography of the anode and cathode spots is radically different, etc. We shall, therefore, consider the processes at the anode and the cathode separately.

For our case we may assume that the electrons have a Maxwellian distribution of velocities. We can neglect the kinetic energy accumulated by the electrons during their motion in the discharge column, because the mean free path in the plasma of the discharge in our case is small and represents a quantity whose order of magnitude is not greater than  $10^{-5} - 10^{-6}$  cm. Therefore, in spite of the relatively high potential gradient the voltage drop along the mean free path is a fraction of a volt, i.e., it is less than the anode drop by one or two orders. With this in mind we may write the following equation for the energy transported by the electrons at the anode

$$W_a^e = (U_a + \varphi) en_e, \quad (2)$$

where  $W_a^e$  is the energy transmitted by the electrons to the anode;

$U_a$  is the anode drop;

$\varphi$  is the work function of the electron;  
 $e$  is the electron charge;  
 $n_e$  is the number of electrons.

/8

During the pulse time  $t_i$  the energy transmitted by the electrons to the anode will obviously be equal to

$$W_a^e = (U_a + \varphi) \int_0^{t_i} I(t) dt. \quad (3)$$

The energy transmitted to the anode by radiation is given by the Stefan-Boltzmann expression

$$W_a^i = \delta \epsilon \sigma S_{\text{eff}}^4 t_i, \quad (4)$$

(subscript ef = effective)

where  $W_a^i$  is the energy transmitted to the anode by radiation;

$\delta$  is the coefficient of light absorption by the surface of the metal;  
 $\epsilon$  is the blackbody coefficient of the plasma;  
 $\sigma$  is the Stefan-Boltzmann constant equal to  $5.673 \cdot 10^{-5}$  erg/cm<sup>2</sup>·sec<sup>-10</sup>·deg<sup>4</sup>;  
 $S$  is the area of the radiator;  
 $t_i$  is the pulse duration.

Because a region of gas heated to a high temperature is retained for a certain period of time after the pulse ends, we may expect that in the last stage of current development, and for some time thereafter, there is a thermal bombardment of the electrode surface.

Evaluating this quantity from gaskinetic considerations, we obtain a value

$$W_a^r = b^{1/2} (p_{\text{ef}} - p_0), \quad (5)$$

where  $b$  is the coefficient of energy transfer whose magnitude depends on the type of particles which collide with the electrodes; obviously the following relation is always true:  $0 < b \leq 1$ .

Now let us estimate the quantity of energy obtained by the anode, when the flare formed at the cathode is retarded at its surface. A large number of experimental data as well as data obtained by us with the aid of high speed photography show that when a current pulse exists, metal vapor flares are given off from the electrodes. The liberation of metal vapors from the anode and from the cathodes are substantially different, both in the speed of the flares and in their structures.

/9

It follows from the theory of heat transfer that the heat flux transmitted to a unit surface by the gas, which is retarded at a rigid wall, is equal to

$$q_g = \alpha(T^* - T_n) \quad (6)$$

where  $q_g$  is the heat flux conducted from the boundary layer to the wall;

$\alpha$  is the coefficient of heat transfer;

$T$  is the retardation temperature;

$T_n$  is the temperature of the surface which retards the gas.

From hydrodynamic considerations, the retardation temperature is expressed in the following manner

$$T^* = T_g \left( 1 + \frac{k-1}{2} M^2 \right). \quad (7)$$

Here  $T_g$  is the gas temperature;

$$k = c_p / c_v;$$

$M$  is the ratio of the flare velocity (the group velocity of the particles) to the velocity of sound.

We can write the expression for the heat transfer coefficient in a turbulent flow  $\alpha$  in the following manner

$$\alpha = \frac{1}{2} c_p \rho_g v_g k_f, \quad (8)$$

where  $\rho_g$  is the gas density;

$v_g$  is the gas velocity;

$k_f$  is the coefficient of friction;

$c_p$  is the specific heat at constant pressure.

The quantity  $k_f$  is usually determined experimentally. If we assume that the gas temperature is constant and equal to some effective value, we can obtain from equations (6)-(8) the following expression for the total quantity of energy transmitted to the anode surface

$$W_a^F = \frac{A}{2} c_p \rho_{CF} v_{CF} k_f \left[ T_F \left( 1 + \frac{k-1}{2} M^2 \right) \right] S_{iF}. \quad (9)$$

Here  $W_a^F$  is the energy transmitted by the flare to the anode;

/10

$A$  is the mechanical heat equivalent;

$\rho_{CF}$  is the density of the cathode flare;

$v_{CF}$  is the velocity of the cathode flare;

$T_F$  is the temperature of the flare;

$S$  is the area of the surface on which the flare is retarded;

$t_F$  is the action time of the flare.

On the basis of what we have presented, we find the total quantity of energy received by the anode during the period of one pulse

$$W_a = W_a^e + W_a^i + W_a^T + W_a^F.$$

The results obtained in evaluating the components which constitute the energy are shown in table 1.

The quantity  $W_a^F$  entering the anode is most difficult to evaluate because part of the quantities contained in the equation for  $W_a^F$ , which in itself is approximate, is unknown.

TABLE 1

Component	Magnitude, Joules	Cathode material
Electron $W_a^e$	$(3-10) \cdot 10^{-2}$	-
Radiant $W_a^i$	$3 \cdot 10^{-3}$	-
Gasketic $W_a^T$	$1 \cdot 10^{-3}$	-
Flare $W_a^F$	$2 \cdot 10^{-2}$	Tungsten
	$1 \cdot 10^{-2}$	Molybdenum
	$7 \cdot 10^{-3}$	Iron
	$(5-6.3) \cdot 10^{-3}$	Nickel
	$4 \cdot 10^{-3}$	Copper
	$1 \cdot 10^{-3}$	Aluminum

Ion component at the cathode is  $W_k^i \sim (1-3) \cdot 10^{-2}$  J.

Thus, for example, we do not know the magnitude of  $C_p$  for metallic vapors at temperatures of 3,000-5,000°C, the density of vapors, the velocity of sound in metal vapors, etc.

The sound velocity in the discharge channel may be evaluated /11 roughly by using the equation for an ideal gas. As we know from thermodynamics, the sound velocity in an ideal gas is given by the following equation

$$c = \sqrt{\frac{c_p}{c_v} \cdot \frac{RT}{\mu}},$$

where  $R$  is the gas constant;  
 $\mu$  is the molecular weight of the gas.

This equation gives us approximate values, because even when an insignificant amount of liquid droplets is present in the vapor the velocity of sound decreases substantially.

The velocity of sound computed by means of this equation for different metal vapors at their boiling point yields the following results:

Metal	W	Mo	Fe	Ni	Cu	Al
Velocity of Sound cm/sec	520	640	645	680	570	880

In accordance with experimental data, the initial velocity at which the flare flies out of the cathode is practically independent of the cathode material, and under our conditions may be evaluated as  $10^3$  m/sec.

The metal vapor density under pressures of 10-20 atm may be approximated by the quantity  $\rho \cdot 10^{-3}$ , where  $\rho$  is the density in the solid state. If we assume that the flare is completely retarded at the surface of the opposite electrode, we may assume roughly that  $k_f = 1$ . The specific heat for vapors at the boiling point may be approximated roughly by quantities which correspond to the critical temperature.

It follows from (9) that when all other conditions are equal, the quantity of energy transmitted to the anode by the flare, which originated at the cathode, depends on the temperature difference between the flare and the anode spot. Consequently, when the cathode boils at a higher temperature and other conditions are equal, a greater quantity of heat will be transmitted to the anode. The quantity of heat increases proportionately to the density of vapors and to the velocity of the flare. Thus, this mechanism of energy transfer will be significant when the flare velocity is higher and the vapor is denser.

The maximum value of anode erosion for the same material will be observed in the case when the cathode material is tungsten, and the minimum value /12 will be observed when the cathode material is aluminum.

In the case when the anode is made out of copper and the cathodes are made of various materials, experiments conducted with discharges in the liquid medium give the following results (table 2).

TABLE 2. ANODE-COPPER, MEDIUM-KEROSENE

Cathode material	Extent of erosion per 10,000 pulses when $W_1$ has the following value in J			
	0.5	1	2	3
W	0.33	0.34	1.74	2.42
Mo	0.30	0.71	1.28	1.64
Fe	0.22	0.54	0.88	1.33
Ni	0.21	0.49	0.84	1.22
Cu	0.19	0.46	0.80	1.20
Al	0.18	0.45	0.63	1.10

Thus the flare component of the energy transmitted to the anode may be substantial, if the cathode is made from a material with a higher boiling temperature. However, the magnitude of the flare component depends not only on the material but on a series of other factors--duration of pulses, the magnitude of the zone occupied by the discharge at the cathode, and others. For this reason, the approximation of the flare component may be looked upon as qualitative.

To verify these propositions and to refine the role of the flare component, we performed special experiments. The cathode flare was isolated from the discharge (by using the Mandel'shtamm method) and then, after thermal dispersion, the magnitude of the erosion produced by the flare on a metal plate not connected to the circuit was investigated. In this case we used a unipolar pulse, since the discharge was produced by means of a thyatron. Experiments showed that the amount of erosion decreases with a decrease in the flare velocity, as predicted by the theoretical equation. It is interesting to note that the track of the flare on the plate has a discrete structure, although there was no current on this plate, and consequently we cannot consider channel migration.

Figure 1 shows this flare track. The magnitudes of erosion in this case are comparable to the magnitude of erosion in the liquid medium.<sup>1</sup> /13

Similar results are obtained by using current pulses with a steep front, when the magnitudes of active surface of the cathode are limited.

<sup>1</sup>K. Kh. Gioyev participated in this work.

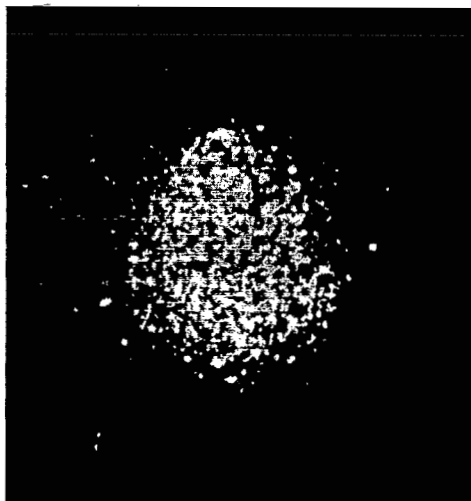


Figure 1. Flare track produced by pulse discharge on steel plate when discharge was in air. X 10.

Limiting the cathode zone subjected to the discharge showed that a decrease in the cathode region produces a sharp increase in anode erosion.

Figures 2a and 2b show the results of flare action on a steel plate. The limitation in the size of the cathode zone was accomplished by putting the cathode in a ceramic tube of corresponding dimensions or by placing masks of insulating materials with openings of required size.

With an active cathode region diameter of 0.5 mm, the erosion /15  
was  $2.5 \cdot 10^{-3}$  g with  $W_i = 10$  J, i.e., not less than the amount of erosion in a liquid.

When the area of the cathode was not limited artificially, the magnitude of cathode erosion under the same conditions was smaller by two orders of magnitude (fig. 2b).

In accordance with equation (9) which determines the flare component, the magnitude of erosion increases with the flare velocity. A limitation of the cathode area occupied by the discharge leads to a sharp increase in energy density at the cathode; this in turn produces a sharp increase in the quantity of vapors released from the cathode and produces an increase in their average temperature and consequently increases the group velocity of the flare.

Consequently, from the standpoint of decreasing the erosion effect it is desirable to use relatively dense current pulses. In this case it is also desirable to have a cathode material which contains components of relatively

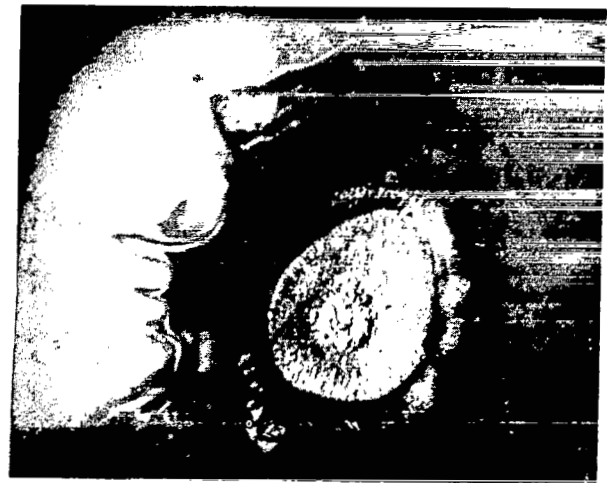
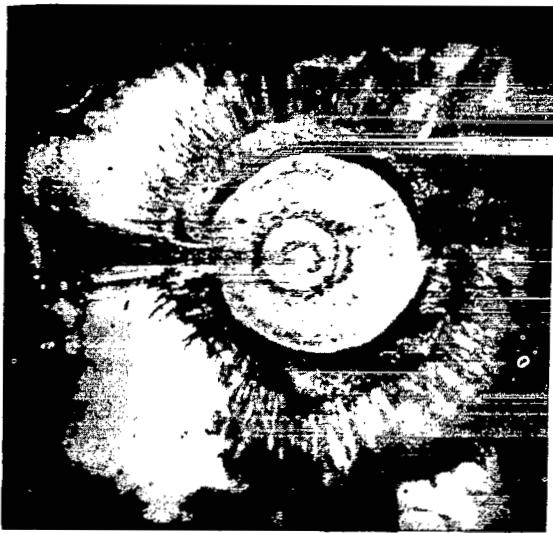


Figure 2. Track produced by flare. a, limitation in size of active surface ( $\times 10$ ); b, same without limitation ( $\times 10$ ).

light materials or oxides with low boiling temperatures. However, at the same time it is desirable to select these components in such a way that their heat of vaporization is sufficiently high, so that these vapors carry away a substantial portion of the energy, even when their velocity is relatively small. In addition, it is rational to produce conditions for a substantial expansion of the discharge channel, which can be done, for example, by producing a current pulse of special shape.

For the electro-erosion machining this requirement will be opposite, because we must now use part of the energy arriving from the cathode to increase the erosion of the anode.

Now, if we consider the problem of energy transfer to the cathode, we can make the following conclusions.

Because the anode and the cathode are equivalent from the standpoint of radiant and gas kinetic components, there is no point in repeating these discussions. We can merely state that the magnitude of these components is small and they can be neglected.

The flare component does not depend on the polarity of the electrode and is determined only by the nature of energy liberation. All of the discussions which we carried out for the anode process remain valid for this component. The only difference is that the ion bombardment is more significant in this case, and not all of the current at the cathode is transported by the ions: part of the energy is transported by the electron current. /16



If we take into account the kinetic energy of the ion and also the energy for its neutralization and assume that the ion current is from 0.2 to 0.5 I

total, we can estimate the quantity  $W_k^i$ , shown in table 1, for the case  $W_i =$

0.16 J,  $t_i = 20 \mu \text{ sec}$ , which has the same order of magnitude as the electron

component of energy transmitted to the electrode. The flare component may be rather substantial, particularly if the anode is made of a material with a high boiling temperature. This is well known, for example, in electro-erosion machining. In the machining of hard alloys or of tungsten by means of a brass cathode, there is a sharp increase in the wear of the cathode (up to 300-400 percent, compared with the anode), whereas when tungsten or a hard alloy is machined with an electrode made from a copper-tungsten composition, the magnitude of cathode wear drops sharply and is only 20-30 percent of the anode erosion.

It is desirable to clarify one other problem, although it is not directly connected with the mechanism of energy transfer to the electrodes, but is related to the electro-erosion destruction.

At the present time there is convincing proof that in the final analysis erosion has a thermal nature. It is also obvious that the magnitude of erosion depends on the nature of the heat source and on the depth to which the surface layer is melted. We shall not concern ourselves with the question of heat propagation in the electrode: this question has been considered in sufficient detail in our published works, the works of I. G. Nekrashevich and his co-workers and the works of other investigators. We shall consider only some results of this process of heat propagation not adequately covered in the literature.

The nonstationary temperature field and also the occurrence of a melted layer on the surface of the contacts produces fields of elastic and residual stresses.

As it applies to the conditions of electrosark machining, this question has been thoroughly studied experimentally by A. P. Aleksandrov for a series of steels and alloys (ref. 3). The nature of the stresses which are /17 produced by the erosion process is such that in the upper layer there are significant tensile stresses, whose magnitude decreases as the observation point is moved deeper into the body of the electrode. The magnitude of these tensile stresses is such that in a series of cases it exceeds the strength of the contact material or of the electrode and produces a network of microscopic cracks. This fact is well known for heat-resistant and solid alloys and for several other cermet compositions. Similar phenomena are observed for some contact materials. The redistribution of stresses in the surface layer frequently leads to warping of the contacts.

The periodic discharges produce periodic loads on the contact or electrode material which leads to thermal fatigue of the electrode surface material. In the end this leads to a sharp local decrease in the strength of the material and

consequently to the formation of cracks or to the scaling of surface regions. The destruction of the contacts or of the electrode takes place much more rapidly than is to be expected for a purely erosion effect.

These phenomena are observed most frequently for materials with a sharply heterogeneous structure from the standpoint of thermal expansion (cermet alloys). From this standpoint it is desirable to note several factors controlling the distribution and magnitude of elastic and residual stresses.

First of all, it is obvious that the integral magnitude of residual stresses and mass forces due to them, depends on the thickness of the molten layer, which in turn depends on the discharge parameters  $W_\mu$  and  $t_i$ .

$$h_{\text{molten}} \approx k \sqrt{t_i}$$

where

$$k = f(a, W_\mu, T_m)$$

(subscript m = melting).

Consequently the shorter the pulse duration, the smaller is the zone /18 occupied by substantial residual stresses. From the solution of the thermal problem we can also estimate the total depth of the zone which contains residual and elastic stresses. For periodic pulses

$$L = 2 \sqrt{\pi a t_i},$$

where  $a = \frac{\lambda}{c \rho}$ ;

$t_i$  is the pulse duration;

$L$  is the depth at which the initial temperature does not vary from the temperature after the action of the pulse.

Thus, to reduce the zone which is subjected to elastic and residual thermal stresses, when other conditions are equal it is advantageous to select materials with a small coefficient of heat transfer.

In the practical utilization of electric contacts and in electrospark machining, a case is sometimes encountered when foreign films form on the surface of the electrode. Let us consider the role of such films from a purely thermal aspect and the possibility of their effect on the magnitude of erosion.

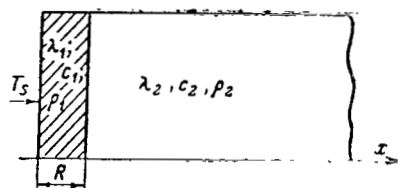


Figure 3. Diagram for solution of thermal problem of the effect on the magnitude of film erosion forming on the foreign surface of the electrode.

If we consider the problem of heat propagation in this system consisting of two bodies, e.g., two rods, one limited and the other unlimited, with different thermal properties, we can get some idea of the effect of thin films and the erosion of the electrode. Figure 3 shows the diagram where the region of magnitude  $R$  corresponds to the film and has thermal constants different from those in the region where  $x > R$ . The designations with subscript 1 refer to  $x < R$ , while designations with subscript 2 refer to the region  $x > R$ , i.e., to the basic electrode material.

The problem is solved by assuming that the natural temperature /19  
of the film and of the electrode is the same, and that the external boundary of the film has some temperature  $T_c = \text{const.}$  The solution of the problem is

achieved by combining the solutions for the first and second regions in a manner similar to that in the problem of Stefan (refs. 1 and 2). The solution of this problem for the temperature in the second region (for the electrode) has the form

$$T_2(x,t) = \frac{T_c}{1+\delta} \sum_{n=1}^{\infty} (-h)^{n-1} \operatorname{erfc} \left[ \frac{(x-n) + (2n-1)R \sqrt{\frac{a_2}{a_1}}}{2\sqrt{a_2 t}} \right]$$

Here

$$\delta = \sqrt{\frac{\lambda_2 c_2 \rho_2}{\lambda_1 c_1 \rho_1}}; \quad h = \frac{1-\delta}{1+\delta}; \quad \operatorname{erfc} = 1 - \operatorname{erf} = \text{the Cramp function,}$$

where  $\lambda_{1,2}$  is the heat conductivity;

$c_{1,2}$  is the specific heat;

$\rho_{1,2}$  is the density.

If we note that when the argument of the Cramp function is greater than 2.9, it becomes equal to 0, for the case  $x = R$  we can obtain an expression which determines the thickness of the film, for which  $T_2 = 0$ , i.e., the basic elec-

trode metal will not be heated and consequently will not be subject to erosion. This takes place when

$$R = 5.8 \sqrt{a_1 t_1}.$$

Consequently, the smaller the temperature conductivity of the film, the more it will protect the electrode, i.e., it will have the effect of a unique heat shield. Thus, a graphite film on the surface of the copper, whose thickness is several tens of microns, should completely protect the copper from destruction by erosion. We should point out that a practical use of this effect requires that certain auxiliary conditions be observed.

First of all, the film itself will be destroyed and consequently, if it is to protect an electrode, we must provide for its own regeneration. This regeneration of the film takes place in some cases of electro-erosive machining (refs. 4 and 5). In addition, several other properties are important /20 for cases of electric contacts--transitional resistance, mechanical strength, etc.

Summarizing our presentation we can draw the following conclusions:

1. The most significant factor which controls the transfer of energy by the electrode during pulse discharge is electron and ion bombardment.
2. Under definite conditions the energy exchange between electrodes produced by flares may be significant.
3. In selecting contact materials or materials for the electrode used in electrosark machining, we should take into account the nature of energy liberation and the thermal properties of the material in accordance with the considerations presented in this report.
4. The formation of films on the surface of the electrode or of the contact with low temperature conductivity may provide a substantial reduction of their wear.

#### REFERENCES

1. Zolotikh, B. N. Energy Balance in the Spark Gap During a Low Voltage Pulse Discharge in a Liquid Dielectric Medium (O balanse energii v iskrovom promezhutke pri nizkovol'tnom impul'snom razryade v zhidkoy dielektricheskoy srede). Vestnik Elektropromyshlennosti, No. 11, 1959.
2. --- The Principal Questions of the Qualitative Theory of Electrosark Machining in a Liquid Dielectric Medium (Osnovnyye voprosy kachestvennoy teorii elektroiskrovoy obrabotki v zhidkoy dielektricheskoy srede), in Collected Works "Problems of Electric Machining of Materials" (Problemy elektricheskoy obrabotki materialov), Izd-vo AN SSSR, 1962.
3. Aleksandrov, V. P. Residual Stresses, Prolonged and Fatigue Strength After Electro-Erosion Machining of Heat Resistant Alloys (Ostatochnyye napryazheniya, dlitel'naya i ustalostnaya prochnost' posle elektro-erozionnoy obrabotki zharoprochnykh splavov). Trudy Vsesoyuznoy Mezhvuzovskoy Konferentsii, Izd-vo Kuybyshevskogo Aviatsionnogo Instituta, 1962.
4. Nekrashevich, I. G., Bakuto, I. A. and Mitskevich, M. K. Special Properties of the Electric Erosion of Porous Electrodes (Ob osobennosti elektricheskoy erozii poristyykh elektrodov). Trudy FTI AN BSSR, Izd-vo AN BSSR, 1956.

5. Aronov, A. I. Formation of Carbonaceous Substances during Electric Pulse Machining, Using Tools Made of Graphitized Materials (O protsessakh obrazovaniya uglerodistykh veshchestv pri elektroimpul'snoy obrabotki instrumentami iz grafitirovannykh materialov), in Collected Works "Electric Pulse and Electric Contact Method of Machining Metals" ("Elektroimpul'snyy i elektrokontaktnyy sposoby obrabotki metallov"), No. 3, Izd-vo TsBTI Goskomiteta po Avtomatizatsii i mashinostroyeniyu, 1962.

## THEORETICAL DETERMINATION OF THE CONTACT GAP RESTORABLE STRENGTH

I. S. Tayev

When an electric circuit is turned off, the contact gap is transformed <sup>/21</sup> from a conductor to a dielectric. When the contacts are closed, the electric resistance of the gap is equal to the transitional resistance of the contacts and the electric strength is equal to 0. When the contacts are open and the arc column is dispersed, the resistance of the gap is practically equal to 0, while the strength is equal to the breakdown voltage of the gas layer formed between the contacts. When the device opens the circuit, there is an increase in the strength of the gap, known as the restorable strength. The law governing the restorable strength is a basic characteristic of the arc quenching system. This strength resists the increasing voltage at the contacts. The nature of this increase is determined by the properties of the circuit, which is switched off, and by the resistance of the contact gap.

When the circuit is open, the gas discharge column is destroyed and different stages of the discharge may take place: arc discharge, glow discharge, Townsend discharge, until a dielectric is achieved. In the arc discharge state, the restorable strength, which is determined by the balance between the delivered and removed power, is equal to

$$U_{\text{res}} = \sqrt{R_{\text{arc}} P_0 l_{\text{arc}}}, \quad V, \quad (1)$$

where  $R_{\text{arc}}$  is the resistance of the arc;  
 $P_0$  is the power removed from a unit arc length into the surrounding medium;  
 $l_{\text{arc}}$  is the length of the arc.

In the glow discharge stage, the drop  $U_{\text{nc}}$  near the cathode may be obtained theoretically by using the method of Engel and Steinbeck. The breakdown voltage during the Townsend discharge is obtained from the Townsend equation. However, neither relationship takes into account the effect of the following on  $U_{\text{nc}}$ : the breakdown voltage of the electrons in the residual thermal ionization contained in the gas and of the thermal emission electrons released in the heated <sup>/22</sup> contact--from the cathode into the gas discharge column. It is obvious that during any discharge state these electrons affect the electrical strength of the contact gap.

The streamer discharge stage, as it applies to low voltage devices, is not considered, because apparently it will not take place here; when the heated column is diffused, the field required to produce a streamer will not exist in the head of the avalanche.

According to Townsend, the condition for the breakdown of the gaseous gap of length  $l$  in a uniform field is

$$\gamma(e^{\alpha l} - 1) = 1. \quad (2)$$

Here  $\gamma$  is the second Townsend coefficient, which determines the number of electrons knocked out of the cathode when the latter is hit by one positive ion.

The first Townsend coefficient,  $\alpha$ , i.e., the number of acts of shock ionization performed by 1 electron over a path of 1 cm during its motion in the field with intensity  $E$ , is a probability function, because it is determined as a product of the number of electron collisions per unit path and the probability of ionization

$$\frac{\alpha}{p} = A_0 U_{i \text{ ac}} e^{-\frac{B_0 U_{i \text{ ac}}}{(E/p)}} \quad (3)$$

(Subscript ac = acting.)

Here  $p$  is the gas density.

The air density is equal to

$$p = 3.54 \cdot 10^{-4} \frac{P}{T}, \text{ g/cm}^3,$$

where  $P$  is the pressure in  $\text{g/cm}^2$ ;  
 $T$  is the temperature in  $^{\circ}\text{K}$ ;  
 $U_{i \text{ ac}}$  is the acting ionization potential in volts;  
 $A_0$  and  $B_0$  are constants.

Condition (2) has a definite physical meaning. If 1 electron forms at random at the cathode, then, as it moves along the path  $l$ , it will produce

$(e^{\alpha l} - 1)$  positive ions due to shock ionization; if we multiply this number by  $\gamma$ , we obtain the number of electrons knocked out of the cathode. If this number is equal to 1, it means that the electron which has appeared at random at the cathode has replaced itself and that the discharge has become self-supporting. Let us assume that, due to thermionic emission, the cathode continues to liberate  $N_e$  electrons per unit time from a unit surface. Then these

$N_e$  electrons will produce  $N_{ey}(e^{\alpha l} - 1)$  positive ions, and if these ions knock out

only 1 electron from the cathode, the discharge will continue to develop and the number of electrons in the gap will be continuously increased. Instead of  $N_e$  electrons at the cathode, there will be  $(N_e + 1)$  electrons in the next instant of time, because  $N_e$  electrons will be liberated by the cathode as before. Thus, when  $N_e$  electrons are constantly emitted by the cathode, the critical condition for the breakdown will have the form

$$(1 + N_e) \gamma (e^{\alpha l} - 1) = 1. \quad (4)$$

Here unity in the term  $(1 + N_e)$  represents the random electron which may appear at the cathode. It is necessary to take it into account, so that condition (4) is transformed into condition (2) when  $N_e = 0$ .

The physical formulation of the breakdown is more justified than the purely formal approach, when the denominator in the well-known Townsend expression for the current is set equal to 0. This formal approach was criticized by Loeb, since from the mathematical point of view such a criterion has no meaning. At least one electron is necessary for the discharge, and this electron cannot be identified with a rational explanation of the discharge current  $i_0$ . The current equation is derived for a stationary state and cannot be referred to a transient state such as a breakdown. If we proceed with the purely formal approach for establishing the breakdown criterion, the breakdown voltage becomes independent of the initial electron current from the cathode, which is in agreement with experimental data.

The physical formulation of the breakdown conditions makes it possible to dispense with the shortcomings associated with the formal approach and reflects more accurately the physical nature of the processes within the limits of existing conditions. In their time Engel and Steinbeck took into account the effect of thermionic emission from the cathode on the magnitude of the cathode <sup>/24</sup> drop, when glow discharge was transformed into arc discharge. They reduced the effect of thermionic emission to an increase in coefficient  $\gamma$ . Some effective coefficient  $\gamma'$  became equal to

$$\gamma' = \gamma + \frac{1 + \gamma}{i/i_e - 1},$$

where  $i = i_+(1 + \gamma) + i_e$  is the total current;

$i_+$  is the positive ion current;

$i_e$  is the thermionic emission current from the cathode.



We can carry out the following transformations

$$\begin{aligned}\gamma' &= \gamma \left[ 1 + \frac{1+\gamma}{\gamma(i_e/i_e - 1)} \right]; \\ \gamma' &= \gamma \left[ 1 + \frac{1+\gamma}{\gamma \left\{ \frac{i_+ (1+\gamma) + i_e}{i_e} - \frac{i_e}{i_e} \right\}} \right]; \\ \gamma' &= \gamma \left[ 1 + \frac{(1+\gamma)i_e}{\gamma i_+ (1+\gamma)} \right] = \gamma \left[ 1 + \frac{i_e}{\gamma i_+} \right].\end{aligned}$$

However,  $i_e = eN_e$  and  $i_+ = eN_+$  (the charge of the ion is equal to the charge of the electron). Then

$$\gamma' = \gamma \left[ 1 + \frac{eN_e}{\gamma eN_+} \right] = \gamma \left[ 1 + \frac{N_e}{\gamma N_+} \right].$$

If we assume that  $\gamma N_+ = 1$  for the critical condition (the positive ions knock out 1 electron), we obtain

$$\gamma' = \gamma(1 + N_e).$$

This is the same expression which was used by us to take into account the effect of thermionic emission in expression (4).

Let us determine the cathode drop for the glow discharge  $U_{nc}$  and the breakdown voltage during the Townsend discharge  $U_{bd}$ , taking into account the effect of thermionic emission and cathode heating as well as of the residual gas ionization temperature on these. These values will determine the restorable strength of the contact gap for the respective discharge stages in the gap. The basis of this calculation will be the breakdown condition (4).

Townsend Discharge Stage. When we have a uniform field intensity  $E$ , /25  
we obtain from (4) and (3) an expression for the value of the breakdown voltage

$$U_{bd} = \frac{B_0 U_{i \text{ ac}}(\rho l)}{\ln \left\{ \frac{A_0 U_{i \text{ ac}}(\rho l)}{\ln \left[ 1 + \frac{1}{\gamma(1+N_e')} \right]} \right\}}. \quad (5)$$

This expression is valid for  $N_e$  electrons, which exist simultaneously at the cathode. Actually, due to the field, the electrons liberated by the heated cathode are distributed over an interval. The distribution density of thermionic electrons over the interval may be determined in the following manner. Let us assume that  $N_e^0$  electrons are released per unit time from a unit cathode surface of area  $S_{hs}$ . We assume that  $S_{hs}$  is the area of the hot spot which emits thermionic electrons. The value  $N_e^0$  is determined from Richardson equation

$$N_e^0 = (37.4 - 62.5) \cdot 10^{18} T_c^2 e^{-\frac{11600 \varphi_{WF}}{T_c}} \quad (6)$$

The electron distribution density in the arc column depends on the velocity of the electrons  $v_e$  which is equal to the product of electron mobility  $K_e$  and the field intensity  $E$ . Actually,  $v_e$  is the path traveled by the electron in 1 sec. The ratio of  $N_e^0$  to  $v_e$  will represent the quantity of emitted electrons in a unit volume

$$N_{e0} = \frac{N_e^0}{v_e} = \frac{N_e^0}{K_e E}$$

If we assume that the cross section of the column occupied by these electrons does not change in length, we obtain the following formula for the number of electrons per unit length:

$$N_{e0} = \frac{N_e^0 S_{hs}}{K_e E}, \text{ 1/cm.}$$

For air

$$K_e \approx 93 \cdot 10^3 \sqrt{\frac{T_g}{EP}}, \frac{\text{cm/sec}}{\text{V/cm}}$$

If we take into account the expression for the gas density, the mobility will be equal to

26

$$K_e \approx \frac{1.750}{V^{1/2} E}, \frac{\text{cm/sec}}{\text{V/cm}}$$

Finally for a uniform field in air we have

$$N_{e0} = \frac{N_e^0 S_{hs}}{1750} \sqrt{\frac{\rho l}{U_{bd}}}, 1/cm \quad (7)$$

$$(N_e^0 - 1/cm^2 \cdot sec; S_{hs} - cm^2; \rho = gram/cm^3; U_{bd} - volt; l - cm).$$

When determining  $N_e^0$  by means of (6), the cathode temperature  $T_c$  is taken in degrees K, the work function of the electron  $\phi_{WF}$  is taken in eV.

The total number of electrons per unit length of the gap, taking into account their content in the gas volume, due to temperature ionization is equal to

$$N_z = N_{e0} + n_0 S_D, 1/cm. \quad (8)$$

Here  $n_0$  is determined by taking into account the Saha equation

$$n_0 = 191 \cdot 10^{15} T_D^{0.25} P^{1/2} e^{-\frac{5800 U_i}{T_D} \frac{ac}{D}}, \quad (9)$$

where  $S_D$  is the cross section of the heated gas column (the temperature along the radius is assumed to be constant and equal to  $T_D$ ).

If we know the total number of electrons per unit length of the gas discharge gap  $N_\Sigma$ , we can determine the number of positive ions produced by shock ionization. Let us isolate an element of gap with length  $dx$  at the distance  $x$  from the cathode. The number of electrons along this length is equal to  $N_\Sigma dx$ .

The number of ions which appear as a result of shock ionization along the length  $x$  is equal to

$$N_\Sigma (e^{\alpha x} - 1) dx.$$

Along the entire length of gap  $l$  there will be  $n_m$  positive ions

$$n_m = \int_0^l N_\Sigma (e^{\alpha x} - 1) dx = \frac{N_\Sigma}{\alpha} (e^{\alpha l} - 1) - N_\Sigma l.$$

If to this quantity we add the number of ions  $n_0 S_D l$ , which are in /27  
the gap (due to thermal ionization), we obtain the total quantity of positive ions.

$$n_i = \frac{N_e}{\alpha} (e^{\alpha l} - 1) - N_{oe} l.$$

If we take into account the single random electron which appears at the cathode, the total number of positive ions in the gap will be equal to

$$1(e^{\alpha l} - 1) + \frac{n_0 S_D}{\alpha} (e^{\alpha l} - 1) + \frac{N_{oe}}{\alpha} (e^{\alpha l} - 1) - N_{oe} l.$$

In this case the condition of similarity analogous to condition (4) will be

$$\gamma \left[ \left( 1 + \frac{n_0 S_D}{\alpha} + \frac{N_{oe}}{\alpha} \right) (e^{\alpha l} - 1) - N_{oe} l \right] = 1. \quad (10)$$

This gives us an expression for the breakdown voltage of the gap which takes into account all of these factors

$$U_{bd} = \frac{B_0 U_{i \text{ ac}} (\rho l)}{\ln \left\{ \ln \left[ 1 + \frac{1 + N_{oe} l \gamma}{\gamma \left( 1 + \frac{N_{oe} + n_0 S_D}{\alpha} \right)} \right] \right\}}. \quad (11)$$

Figure 1 shows the design relationships of the breakdown voltage of the gap as a function of gas temperature  $T_D$  for air, without taking into account thermionic emission from the cathode ( $N_e^0 = 0$ ) under the following conditions:  $\gamma = 0.025$ ; channel cross section  $S_D$ ,  $0.5 \text{ cm}^2$ ; channel length  $l = 1/\text{cm}$ ; pressure  $P = 1,035 \text{ g/cm}^2$ ;  $\alpha = 0.012$ . The assumption that  $\alpha$  is constant is not too much out of the way because this quantity is contained twice under the logarithmic sign in eq. (11). The basic effect of  $\alpha$  on the results of the calculation is taken into account in deriving equation (11). The constants for the air are assumed to be equal to  $A_0 = 24.9 \cdot 10^4$  and  $B_0 = 12.2 \cdot 10^6$ .

Calculations were carried out for two values of the acting ionization potential  $eU_{ac} = 8$  and  $15 \text{ eV}$ . The same graph shows the calculated values of  $U_{bd}$ ,

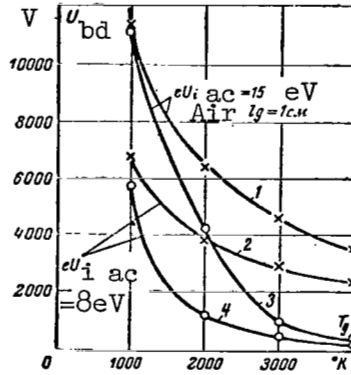


Figure 1. Computed variations in  $U_{bd}$  of air as function of temperature  $T_D$ : 1 and 2, without taking into account thermal ionization; 3 and 4, taking into account thermal ionization.

without taking into account the thermal ionization ( $n_0 = 0$ ); in this case, only the effect of temperature on the density of the gas and consequently on the breakdown voltage is taken into account. /28

The variation in  $U_{bd}$ , as a function of contact-cathode temperature is computed for argon. In this case it is possible to compare the design data with experimental data (ref. 1). If we take into account the corresponding constants  $A_0$  and  $B_0$ , equation (11) takes on the following form for argon

$$U_{bd} = \frac{2820U_{i\text{ ac}}(Pl)}{169U_{i\text{ ac}}(Pl)} T \ln \left\{ \ln \left[ 1 + \frac{1 + N_{e0}l\gamma}{\gamma \left( 1 + \frac{N_{e0}}{\alpha} \right)} \right] \right\} \quad (11a)$$

Instead of density  $\rho$ , this equation contains temperature  $T$  and pressure  $P$ . As an example, let us consider the following values:  $eU_i = 15$  eV; tungsten cathode,  $\phi_{WF} = 4.54$  eV;  $\gamma = 0.02$ ,  $Pl = 8$  mm of Hg;  $T = 273$  °K;  $S_{hs} = 0.01$  cm<sup>2</sup> (according to more accurate data  $U_{bd} = 450$  V for argon corresponds to  $Pl = 8$  mm of Hg and not 3.75 mm of Hg, as assumed in reference 1). The experimental curve for a in figure 2 is obtained under these conditions.

The same variation in the breakdown voltage as a function of cathode temperature is computed from equations (6), (10) and (11) for the same

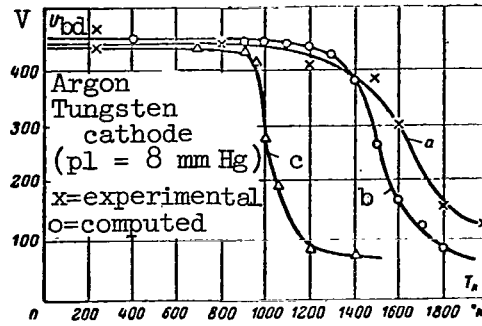


Figure 2. Breakdown voltage in argon as function of tungsten cathode temperature.

conditions--curve b in figure 2. Under these conditions temperature ionization does not take place ( $T_D = 273^\circ\text{K}$ ;  $n_0 = 0$ ). Curve b is computed taking into

account the electron field emission along the gap. The same curve shows the design variation computed directly by means of equations (5) and (6), without taking into account this effect (curve c, fig. 2).

Glow Discharge. Because the length of the cathode drop region is small, the effect of electrons produced by the thermal ionization of gas on  $U_{nc}$  will not be taken into account. In addition, the degree of thermal ionization near the cathode is quite low, because the temperature of the gas cannot be very high at this point: it is limited by the value of the boiling temperature of the cathode material.

In accordance with (4), when the field is nonuniform in the region of the cathode drop, the conditions for the stationary state of the discharge will be:

$$(1 + N_e) \gamma \left( e^{\int_0^{l_k} \alpha dx} - 1 \right) = 1; \quad (12)$$

$$\int_0^{l_k} \alpha dx = \ln \left[ 1 + \frac{1}{(1 + N_e) \gamma} \right]. \quad (12a)$$

In this equation  $l_k$  is the length of the cathode drop zone.

The variation in the electric field intensity in the cathode drop zone may be approximated by means of the following equation

$$E = \frac{2U_{nc}}{a_1 x + l_k}, \quad (13)$$

where  $U_{nc}$  is the cathode drop;

$x$  is the distance from the cathode to the considered point in the cathode drop zone;

$a_1$  is a constant.

If we substitute (13) into the expression for  $\alpha$  and if we substitute (3) into (12a) and integrate, we obtain an approximate expression for the value of the cathode drop in a glow discharge: /30

$$U_{nc} \approx - \frac{B_0 U_{i \text{ ac}} (\rho l_K)}{2 \left[ 1 - \frac{\ln \left[ 1 + \frac{1}{\gamma (1 + N_0)} \right]}{A_0 U_{i \text{ ac}} (\rho l_K)} \right]}. \quad (14)$$

In deriving this expression, we assumed that

$$e^{-r} \approx 1 - r, \quad \text{and} \quad r = \frac{B_0 U_{i \text{ ac}} (\rho l_K)}{2 U_{nc}},$$

which is valid in the limits  $r = 0-0.5$ .

The second Townsend coefficient  $\gamma$  for various metals may be determined in terms of the work function  $\phi_{WF}$  by means of an approximate empirical equation, obtained experimentally from data presented by different authors

$$\gamma \approx \frac{0.115}{\phi_{WF}}.$$

For the case of glow discharge it is characteristic to have a constant value for the product of gas pressure (or density) at a given temperature and the length of the cathode drop zone. For air at room temperature

$$(\rho l_K)_{gd} = 0.705 \cdot 10^{-6}, \text{ g} \cdot \text{cm/cm}^3.$$

In the region of the Paschen curve minimum, the constants  $A_0$  and  $B_0$  for air will be somewhat different from those assumed above, specifically

$$A_0 = 0.74 \cdot 10^6 \text{ and } B_0 = 24 \cdot 10^6.$$

After substituting all of these data into expression (14), we obtain an equation for determining the cathode drop for the case of glow discharge in air

$$U_{nc} = \frac{8.45U_{i\ ac}}{1 - \frac{1.92}{U_{i\ ac}} \ln \left( 1 + \frac{8.7\varphi_{WF}}{1 + N_e} \right)} \quad (15)$$

On the basis of what we have stated, this expression gives reliable values of  $U_{nc}$ , if the ratio of  $U_{i\ ac}$  to  $U_{nc}$  is within 0-0.06.

Table 1 shows the values of the glow discharge cathode drop computed /31 by means of equation (15), as well as their experimental values for different cathode materials, when thermionic emission is absent ( $N_e = 0$ ).

The variation in the glow discharge cathode drop as a function of cathode temperature may be computed by means of equation (15), if we substitute into this equation the number of emission electrons  $N_e$  obtained from (6). A calculation of this type has been carried out for a copper cathode (in air). The results are presented in table 2; the corresponding curve is shown in figure 3 (curve a). In the calculations the area of the hot spot on the cathode was assumed to be equal to  $S_{hs} = 0.01\text{ cm}^2$ .

However, this calculation again presents an inadequate picture of the processes, because it does not take into account the fact that the emission electrons are distributed along the cathode drop zone due to the forces of the electric field. If we take into account the average value of the electric field intensity, we have

$$E_{av} = \frac{U_{nc}}{l_k} = \frac{U_{nc}\rho}{0.705 \cdot 10^{-6}}.$$

We obtain the number of thermal emission electrons per unit length, using the method employed for the Townsend discharge stage, equation (7) /32

$$N_{eo} = \frac{0.48 \cdot 10^{-6} N_e^0 S_{hs}}{U_{nc}^{1/2}} \quad (16)$$

Here  $S_{hs}$  is the area of the hot spot on the cathode.

TABLE 1

Cathode material	Pt	Cu	Mg	Al	Fe	Ni
$\varphi_{WF}$ , eV	6.27	4.6	--	--	4.77	5.03
$\gamma$	0.017	0.025	0.033	0.035	0.02	0.036
Computed $U_{nc}$ , V	271	240	217	220	256	220
Experimental $U_{nc}$ , V	277	252	234	229	269	226



TABLE 2

$T, ^\circ\text{K}$	850	900	950	980	1015	1040	1070
$N_e^0, 1/\text{cm}^2$	0.33	8.9	240	1500	$16 \cdot 10^3$	$36 \cdot 10^3$	$15.5 \cdot 10^4$
$U_{nc}, \text{V}$	250	237	170	100	50	40	30

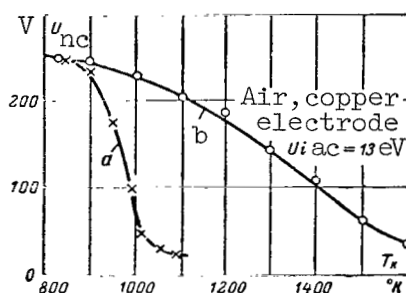


Figure 3. Computed variation in glow discharge near the cathode drop as function of cathode temperature.

If we perform the same mathematical operations as in the case of the Townsend discharge, we obtain an approximate expression for the drop near the cathode, which takes into account the distribution of thermal electrons along the gap

$$U_{nc} = \frac{8.45 U_{i \text{ ac}}}{1 - \frac{1.92}{U_{i \text{ ac}}} \ln \left[ 1 + \frac{8.7 \varphi_{WF}}{1 + \frac{N_{e0}}{\alpha}} \right]} \quad (17)$$

The computed curve  $U_{nc} = f(T_k)$  for the case considered above and obtained from (17) is shown in figure 3 (curve b).

If the gap has the Townsend stage of this discharge or a glow discharge, its restorable strength is equal, respectively, to  $U_{bd}$  or  $V_k$ , given by equation

(11) or (17). These equations take into account the thermionic emission from the heated contact-cathode, the effect of thermal gas ionization produced by its high temperature and the value of the restorable strength of the gap between the contacts.

Experimental investigations of the restorable strength in low voltage ac equipment, directly at the point where the sinusoidal current passes through zero, give values for the restorable strength which are tens or hundreds

of volts. In their order of magnitude these experimental values coincide with the computed values obtained for the true temperature of the arc support points on the contacts and with the temperature of the gas in the arc column.

The magnitude of the restorable strength for both gas discharge stages depends substantially on the acting ionization potential  $U_{ac}$ . For a mixture of two gases it is determined by the well-known equation

$$U_{i \text{ ac}} = -8.6 \cdot 10^{-5} T \ln \left\{ \frac{N_1}{N_\Sigma} e^{-\frac{11600 U_{i1}}{T}} + \frac{N_2}{N_\Sigma} e^{-\frac{11600 U_{i2}}{T}} \right\}, \quad (18)$$

where  $N_1$  and  $N_2$  are the concentrations of the mixture components;

$$N_\Sigma = N_1 + N_2;$$

$U_{i1}$  and  $U_{i2}$  are the ionization potentials of the mixture components.

When a gas discharge exists in the gap between the contacts of a switching device, there is usually an intense evaporation of the contact material in the gap. It is known that the ionization potential of metal vapors is substantially less than the ionization potential of gas, and the effective ionization potential in a mixture of gas and metal vapors is, therefore, sharply reduced for this reason. The restorable strength must also decrease for this reason, as follows from the expressions presented before. Therefore, it is important to evaluate the quantity  $U_{i \text{ ac}}$  correctly under actual conditions of arc quenching, which occurs between the contacts of the device when the circuit is switched off.

If we are to determine  $U_{i \text{ ac}}$ , taking into account the effect of metal particles evaporating from the contacts, it is necessary to know the number of metal particles per unit volume of the arc. An approximate evaluation is possible, if we consider the value of the plasma transport of the metal from the cathode to the anode when the arc burns. The quantity of contact metal <sup>/34</sup>  $G$  transported from the cathode by current  $I$  during a period of time  $t_1$ , is equal to

$$G = \gamma_k I t.$$

The value of  $\gamma_k$ ,  $\text{cm}^3/\text{k}$  is equal to: for Ag  $0.2-0.4 \cdot 10^{-6}$ , for Pt  $0.9 \cdot 10^{-6}$ , for W  $0.04 \cdot 10^{-6}$ , for Cu  $1.5 \cdot 10^{-6}$ , for CH  $40-0.6 \cdot 10^{-6}$ .

The number of metal molecules per unit volume is equal to

$$N_M = 0.603 \cdot 10^{24} \frac{\delta_M}{\mu_M},$$

where  $\delta_M$  is the specific weight of the metal;

$\mu_M$  is the molecular weight of metal particles.

The product  $GN_M$  represents the number of metal molecules transported from the cathode during a period of time  $t$ , when the current is  $I$ . The number of transported metal molecules per unit time is equal to

$$M = 0.603 \cdot 10^{24} \frac{\delta_M \gamma_K I}{\mu_M}.$$

The cross section of the arc column, as shown experimentally, may be expressed by the following approximation as a function of current

$$S_D \approx 0.05 I, \text{ cm}^2.$$

The current density at the anode  $j_a$  is also usually known; therefore, the cross section of the gas discharge column at the contacts may be estimated by means of the expression

$$S_a \approx \frac{I}{j_a}.$$

From experimental data  $j_a \approx 1000 \text{ a/cm}^2$  for copper contacts.

With these data we can determine the number of molecules transmitted per 1 sec through a unit area of the cross section:

at the anode

$$M_0 = 0.603 \cdot 10^{24} \frac{\delta_M \gamma_K j_a}{\mu_M}, \frac{\text{molecules}}{\text{cm}^2 \cdot \text{sec}};$$

in the arc column

$$M_0 = 11.3 \cdot 10^{24} \frac{\delta_M \gamma_K}{\mu_M}, \frac{\text{molecules}}{\text{cm}^2 \cdot \text{sec}}.$$

The number of metal vapor particles per unit volume depends on the velocity of their motion  $V_{\text{vapor}}$ . It can be obtained if we divide the expression

for  $M_0$  by  $V_{\text{vapor}}$ . We obtain:

at the anode

$$M_a = 0.603 \cdot 10^{24} \frac{\delta_M \gamma_k / j_a}{\mu_M v_{\text{vapor}}}, \frac{\text{molecules}}{\text{cm}^3}, \quad (19a)$$

in the arc column

$$M_D = 11.3 \cdot 10^{24} \frac{\delta_M \gamma_k}{\mu_M v_{\text{vapor}}}, \frac{\text{molecules}}{\text{cm}^3}. \quad (19b)$$

According to data presented in the literature, the velocity of copper vapors lies in the limits corresponding to temperatures 4100-27,200°K. If we transform from temperatures to velocities, we obtain the following value for copper contacts

$$V_{\text{vapor}} = (7.86-20.3) \cdot 10^4 \text{ cm/sec.}$$

Experimental data show that for a mercury contact

$$V_{\text{vapor}} = (1.0-1.9) \cdot 10^5 \text{ cm/sec;}$$

while for a carbon contact

$$V_{\text{vapor}} = (1.5-4.0) \cdot 10^3 \text{ cm/sec.}$$

As an example we have computed the number of metal vapor particles per unit volume of the column at the anode and in the arc channel proper, which have evaporated from copper contacts under the following conditions:  $\mu_M = 163.54$ ;

$$\delta_M = 8.9 \text{ g/cm}^3; \gamma_k = 1.5 \cdot 10^{-6} \text{ cm}^3/\text{k}; j_a = 10^3 \text{ A/cm}^2; V_{\text{vapor}} = 7.86 \cdot 10^4 \text{ cm/sec.}$$

The following values were obtained for the specific content of metal particles:

$$\text{at the anode } M_a = 2.42 \cdot 10^{13} \text{ mol/cm}^3; \text{ in the arc column } M_D = 0.455 \cdot 10^{13} \text{ mol/cm}^3.$$

If we assume that under the specified conditions the total number of gas parti-

cles per unit volume is equal to (when  $p = 2000 \text{ gm wt/cm}^2$  and  $T = 2000 \text{ }^\circ\text{K}$ )  $n_0 =$

$0.764 \cdot 10^{19}$ , we find from equation (18) the effective ionization potential of the mixture of copper vapor and air at the temperature of 2000°K with the stated ratios of  $M$  to  $n_0$ : at the anode  $U_{i \text{ ac}} = 9.8 \text{ V}$ ; in the arc column  $U_{i \text{ ac}} = 10.2 \text{ V}$ .

Thus, the material we presented makes it possible to evaluate the magnitude of the effective ionization potential under specific conditions.

The material which we have presented is a first attempt to determine /36 theoretically the value of the electric strength of the contact gap, by taking into account the basic factors which play a role in the formation of this strength, when the devices are used to turn off an electric circuit. These factors, which have not been considered previously, include the thermionic emission from the contact heated by the arc and the temperature ionization of the gas.

#### REFERENCE

1. Kaptsov, N. A. and Afanas'yev, N. V. The Transition of a Discharge With a Red Hot Cathode to a Glow Discharge (Perekhod razryada s raskalennym katodom k tleyushchemu). Zhurnal Tekhnicheskoy Fiziki, Vol. 3, No. 7, 1933.

## SELECTIVITY IN THE EMISSION OF MATERIAL FROM SOLID BINARY ALLOYS DURING PULSE DISCHARGES IN AIR

O. I. Avseyevich and I. G. Nekrashevich

The thermal nature of electric erosion in pulse discharges at atmospheric temperature is now universally accepted. However, the mechanism of heat release at the electrodes is controversial, because there are several concepts concerning this mechanism. /36

An investigation of the selectivity in the entry of material during pulse discharges in air is of interest, because it may contribute to some extent to the understanding of processes which take place at the electrodes.

As we know, in the energy balance equation at the electrodes

$$dQ = \rho j^2 dt + \operatorname{div} (\lambda \operatorname{grad} T) dt$$

the first term of the right side gives the direct heating of the microscopic volume of electrode material, which joins the plasma due to volumetric release of heat; the second term gives the heat flux transmitted from the heel of the channel into the depth of the electrode. This heat may be transmitted to the surface of the electrode either by the hot plasma or by some other process (for example, the bombardment of the surface with charged particles). /37

In most cases, the products of erosion contain both the solid spherical solidified droplets of the alloy and the oxidized vaporous products of ejection. Since the alloy components have different partial vapor pressures at high temperatures (above the melting temperature of the alloy), the solidified particles should have a concentration of one of the alloy components, while the vapors should have a concentration of the other component. The total composition of the products of erosion during their explosive ejection must be the same as in the electrode. If, however, the surface sources of heat play the principal role in the energy balance at the electrode, we can expect that the flow of electrode material into the discharge zone will take place in a more quiet form, by means of surface evaporation without explosive processes, and products of erosion will concentrate the alloy component whose partial vapor pressure is greater at the given surface temperature.

Thus, from the selectivity of electrode material emission we can establish the prevailing role of a particular mechanism for transmitting the material into the discharge zone.

To study this problem, we investigated the emission of an electrode fabricated from Cu-Zn alloys with a Cu content of 100, 93, 83, 73, 54, 22, 11.5 and 0 percent.

The opposite electrode consisted of a carbon rod ground to an angle of 30°. A special arrangement conducted each successive discharge onto a freshly polished surface of the alloy electrode. The products of erosion were deposited on the walls of the discharge chamber, lined with decalcified damp filter paper.

Rectangular pulses with a duration of 130  $\mu$ sec were used with amplitude values 455, 910, 1215, 1520 and 1900 A with corresponding voltages of 600, 1200, 1600, 2000 and 2500 V. The rectangular wave generator was a model of a long line. /38

After 240 discharges, the collected products of erosion were processed by separating the solidified droplets from the oxidized vapor phase. The vapor products and the droplets were subjected to polarographic analysis. Then the weight and composition of these products was established.

The results of the investigation are shown by curves giving the variation in the quantity of anode material and cathode material ejected into the discharge zone and variation in their relative composition of the erosion products during one pulse as a function of pulse current. As an example, figures 1a, b and c show the results for 3 Cu-Zn alloys of different concentration. /39

The general laws uncovered in these experiments are as follows:

1. The erosion of the anode has a maximum for alloys with Cu concentration greater than 44 percent with currents 1200-1500 A; for alloys with a smaller concentration of Cu the maximum occurs at 1520 A. Apparently the presence of a maximum can be explained by the fact that when the current increases in the pulse the initial breakdown voltage increases linearly and causes an increase of the gap and its volume in which the discharge is localized. This apparently leads to a decrease in the energy density of this volume.

2. The anode products of erosion contain a vapor phase and solidified small spherical droplets of the alloy.

The concentration of zinc is greater in the vapor phase of the anode erosion products than in the anode material. The relative concentration of copper decreases, when its concentration in the alloy decreases. The concentration of copper in the liquid phase of the anode erosion products is higher than in the anode material. In the range of investigated states there is no clearly defined correlation between the discharge state and the selectivity of electrode emission.

3. The total composition of the vapor phase and the liquid phase of the anode erosion products has a somewhat increased concentration of copper compared with the electrode material. This is explained by the fact that part of the vapor phase with a concentration of zinc is not captured during the

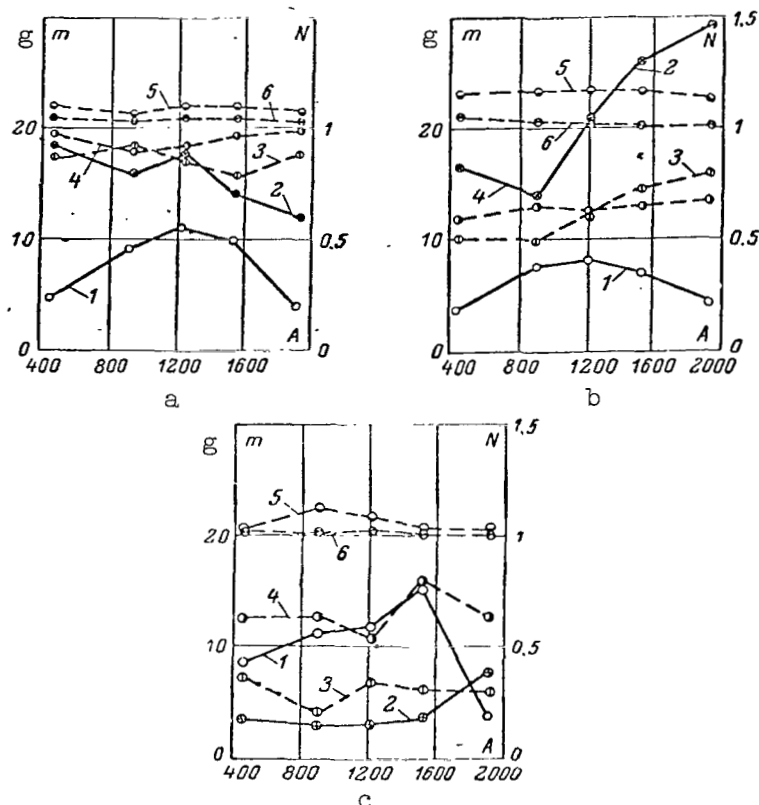


Figure 1. Erosion characteristics of Cu-Zn alloys (solid lines) and relative composition of products of erosion N (broken line) for various current amplitudes: a, Cu-Zn-83 alloy; b, Cu-Zn-54 alloy; c, Cu-Zn-22 alloy; 1, anode  $N \cdot 10^5$

g/discharge; 2, cathode  $N \cdot 10^7$  g/discharge (for Cu-Zn-22,

$N \cdot 10^6$  g/discharge); 3, cathode vapors; 4, anode vapors; 5, solidified droplets of anode erosion products; 6, total anode erosion products.

experiment. All this points to a volumetric heating effect and an explosive nature of material ejection from the anode.

4. The movement of the material from the cathode to the decomposition zone is of a more quiescent nature. Solidified particles were not observed in the cathode erosion products, and the relative concentration of Cu is less than in the alloy, i.e., there is a clearly defined selectivity. The relative copper concentration N decreases with a decrease of copper in the alloy (increased selectivity). The effect of discharge state on the selectivity of cathode material emission was not observed.

5. The magnitude of cathode erosion is 30-40 times smaller than the anode erosion under equal conditions, and there is a maximum which depends on the state and composition of the alloy.



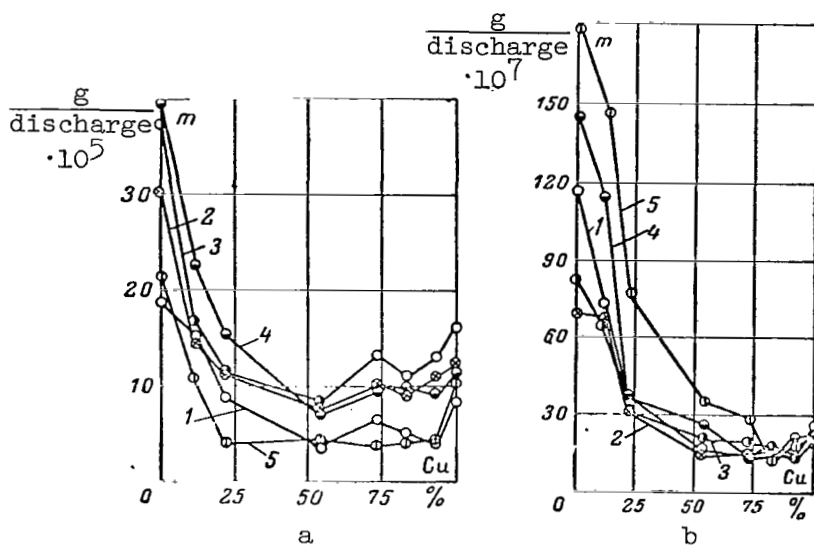


Figure 2. Erosion characteristics for Cu-Zn alloy systems at various pulse current amplitudes: a, anode; b, cathode; 1, 455 A; 2, 910 A; 3, 1,215 A; 4, 1,520 A; 5, 1,900 A.

6. The erosion diagrams which show the variation in the erosion as a function of alloy composition are shown in figures 2a and b and have the following characteristics:

(a) in all states the anode erosion has a maximum value for pure zinc, decreases with copper concentration and achieves a maximum value for an alloy which is close to Cu-Zn-50; then there is a small maximum for Cu-Zn-73 alloy and another increase for pure copper.

(b) The behavior of the erosion characteristics is similar at the cathode, with the only difference that the minimum erosion takes place in an alloy close to Cu-Zn-83.

The results obtained under conditions of our experiments may be summarized as follows:

(1) a surface erosion effect takes place on the cathode and the emission selectivity of the alloy electrode material is clearly shown; /41

(2) volumetric heat liberation effects take place at the anode, associated with the explosive mechanism of material emission, which is confirmed by the identical composition of the total erosion products and the anode material.

## EFFECT OF COMPONENTS PERCENTAGE ON THE ELECTRIC EROSION OF BINARY ALLOYS

N. V. Afanas'yev and A. G. Goloveyko

It is well known that electric contact wear during switching is produced by a combination of physical and chemical phenomena such as electric erosion, corrosion, mechanical grinding, etc. For this reason contact materials must satisfy various requirements which depend on the operating conditions of the contact pair. /41

In general these materials must resist corrosion and electrical erosion, must have a high electric conductivity and thermal conductivity, must possess sufficient hardness, must be easily machinable, must not fuse during breaking and making and must be relatively inexpensive.

None of the pure metals satisfies these wide requirements. For example, gold and silver have high resistance to corrosion, but their erosion properties are not as good as that of iron and molybdenum and they are also very expensive materials; iron and molybdenum have good resistance to erosion and are relatively inexpensive, but corrode extensively in air.

Thus we have a need for alloys with two, three or more components which would satisfy even approximately the various conditions encountered in switching networks.

Although electric contacts have been used for over 150 years, there is no rigorous theory which makes it possible to design contact materials with given properties providing for reliable operation of contact pairs under specific conditions. Unfortunately, the solution of these problems is still largely empirical. The reason for this is the rather large range of properties which the contact material must have, and the insufficient information on the mechanism of electric erosion producing the wear of electric contacts. /42

An analysis of physical properties, which could, to some degree, affect the value of electric erosion of pure metals, has been presented in the literature. It follows from this analysis that it is impossible to develop a relationship between the magnitude of erosion and such metal constants as hardness, density and specific electric resistance. It has also been shown that of the thermal constants of metals (specific heat, heat conductivity, melting temperature and vaporization temperature), only the heat of vaporization is related to the magnitude of erosion, apparently playing the most significant role in the electric wear of metals. When all other conditions are equal, the

erosion of a metal becomes greater when the specific heat of vaporization of this metal becomes smaller.

In contact engineering and in electro-erosion machining, most of the materials which are used are alloys, and therefore it is desirable to investigate alloys of various compositions.

Investigations were carried out using heterogeneous alloys of easily fusible metals: Zn-Sn, Pb-Bi, Cd-Bi, Al-Zn with different percentages of components and Cu-Ni alloys with a high melting temperature, which produce a continuous series of solid unlimited solutions. The cermet composition of Cu-Ni was also investigated, with different percentages of components.

Investigations were carried out by means of a RC erosion setup in air and in kerosene for two electric states: (1)  $C = 40 \text{ mf}$ ;  $U = 120 \text{ V}$  and (2)  $C = 40 \text{ mf}$ ;  $U = 360 \text{ V}$ .

#### Results of Investigation

/43

Figures 1, 2 and 3 show the results of the investigation carried out in kerosene and in air ( $C = 40 \text{ mf}$ ;  $U = 120 \text{ V}$ ), using 3 types of materials: heterogeneous alloys, continuous solid solution and cermet composition. The percentage of components is shown on the axis of the abscissas, while the magnitude of anode erosion  $\Delta m_a$ , cathode erosion  $\Delta m_k$  and total erosion  $\Delta m$ , computed for

each discharge, are shown along the axis of the ordinates.

The erosion diagram for the Zn-Sn alloys in kerosene (figure 1a) is typical for the alloys of heterogeneous systems.

As we can see from the diagram, there is no linear relation between the erosion of the alloys and the percentage of components. This shows that the erosion of an alloy does not follow an additive law with respect to the erosion of the components.

Figure 1b shows the erosion diagram of the same alloys when discharge takes place in the air. We note that  $\gamma = \Delta m_k / \Delta m_a$  varies as a function of component

percentage, and for some alloy compositions there is an inversion of electrode erosion; for example, when there is 0 and 40 percent of Sn in the alloy /44  $\gamma < 1$ , while for 20, 60, 80 and 100 percent Sn  $\gamma > 1$ . A small variation of this quantity is also observed when discharge takes place in kerosene, and in the latter case  $\gamma < 1$  when we have 100 percent Sn.

We should note that the magnitude of erosion for these alloys, when discharge takes place in the air, is substantially less than when the discharge takes place in kerosene.

Figure 2a shows the erosion diagram for the Cu-Ni system alloys during discharge in kerosene. The special feature of the erosion diagram of these

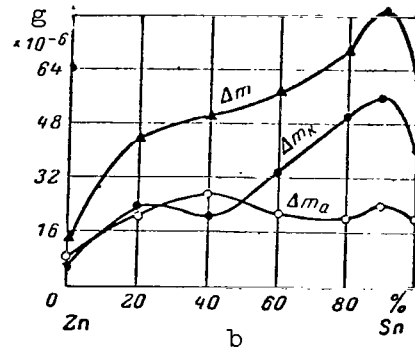
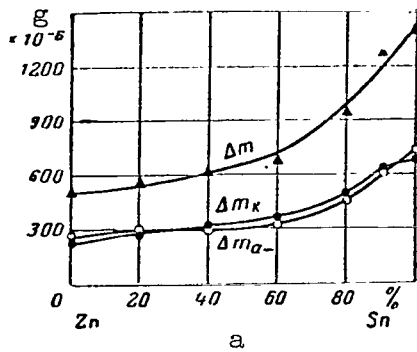


Figure 1. Erosion diagram of Zn-Sn alloy:  
a, discharges in kerosene; b, discharges in air.

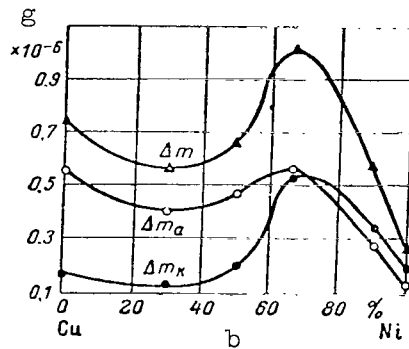
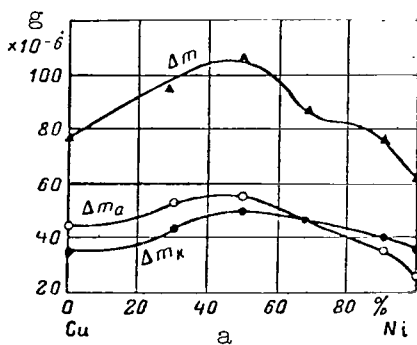


Figure 2. Erosion diagram of Cu-Ni alloy:  
a, for discharge in kerosene; b, for discharge in air.

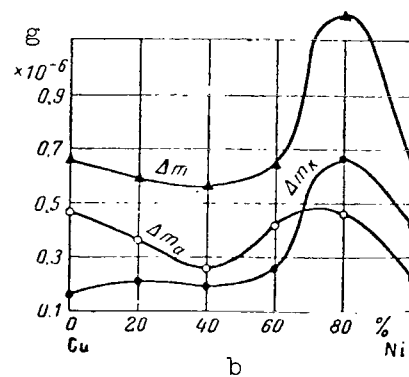
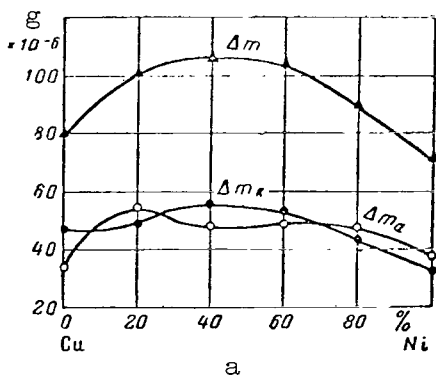


Figure 3. Erosion diagram of Cu-Ni cermet:  
a, for discharges in kerosene; b, for discharges in air.

alloys, which are continuous solid solutions, is the presence of a maximum in the region where the component composition is 50 percent, both for the total erosion as well as for the cathode and anode erosion. It is also interesting that up to 60 percent Ni  $\gamma < 1$ , and after 60 percent Ni  $\gamma > 1$ . Thus the inversion lies near 60 percent Ni in the alloy.

Figure 2b shows the erosion diagram of the same alloy for discharge in air. In this case maximum erosion also takes place in the region where we have a little more than 60 percent Ni; however, together with the maximum, there is a minimum of erosion in the region of 30 percent Ni. The inversion point lies in the region 70 percent Ni. As in the case of heterogeneous alloys, erosion in air is substantially less than in kerosene.

Figure 3a shows the erosion diagram of the Cu-Ni cermet during discharge in kerosene.

/45

The form of the total erosion curve and its magnitude are approximately the same as for the Cu-Ni alloy. The special feature of the cermet Cu-Ni system is the erosion of the cathode and of the anode for different percentages of components. Whereas for pure copper (fig. 2a)  $\gamma < 1$ , for a copper electrode, which is a cermet,  $\gamma > 1$ . The situation is the same for nickel electrode. For cast nickel,  $\gamma > 1$ ; for cermet nickel  $\gamma < 1$ . It is also interesting to note that for the Cu-Ni alloys there is one inversion point (~60 percent Ni); for the Cu-Ni cermet there are 3 points of inversion near 10 percent Ni, 28 percent Ni and 75 percent Ni.

Figure 3b shows the erosion diagram of the Cu-Ni system for discharge in air. This diagram also has a maximum for the total erosion, and for the anode and cathode erosion. Compared with figure 2b, this maximum is displaced towards the higher percentage of Ni and lies in the 80 percent region. There is also a small minimum in erosion for 40 percent Ni. The situation is different from erosion in kerosene and  $\gamma < 1$  for Cu, while  $\gamma > 1$  for Ni. There is also only one point of inversion (70 percent Ni) instead of three points, as shown in figure 3a.

/46

Figures 4a and 4b show the erosion diagrams of Cu-Ni cermet systems at constant voltage ( $U = 360$  V) for discharges in kerosene, with other parameters remaining unchanged.

/47

As we can see from figure 4a, the total erosion and the cathode and anode erosion increase, compared with the same values at a voltage of  $U = 120$  V (fig. 2a) and they achieve a maximum also for a 50 percent composition.

We should point out that at increased voltage the form of the curve for total erosion retains its basic characteristics exhibited at low voltage. However, it is displaced to the Cu side at higher voltages, and the inversion point is near 30 instead of 70 percent Ni (fig. 2a).

The erosion diagram of the Cu-Ni cermet system at increased voltage is shown in figure 4b. By comparing the diagrams in figures 4b and 3a, it follows that increased voltage erosion increases and the curves for total erosion have approximately the same form.

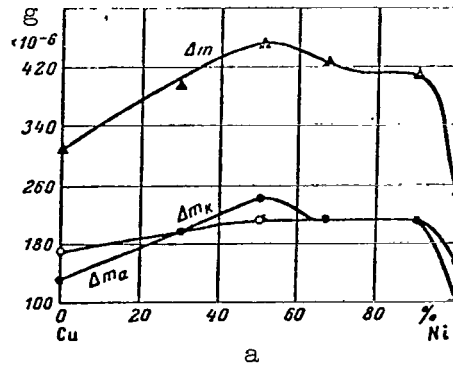


Figure 4a. Cu-Ni alloy erosion diagram for discharge in kerosene at increased electrode voltage ( $U = 360$  V).

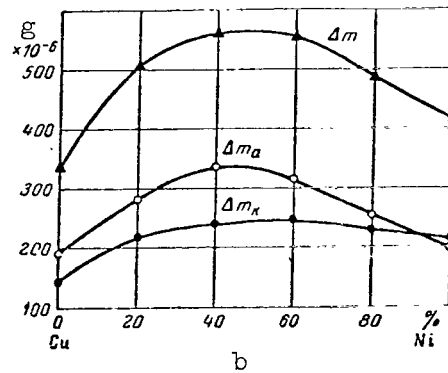


Figure 4b. Cermet Cu-Ni erosion diagram for discharge in kerosene at increased electrode voltage ( $U = 360$  V).

The erosion curves of the cathode and of the anode differ slightly.

#### Analysis of Results

The explanation of the laws which we have obtained should be sought in the specific properties of electric erosion of alloys.

In considering this problem, we proceeded from the proposition that the electrical erosion during electric discharge is caused by a thermal effect at the electrodes due to the bombardment of the cathode by positive ions and the bombardment of the anode by electrons.

We should also realize that the passage of high density current through the surface of the electrodes liberates heat, which increases the thermal effect due to the bombardment of electrodes by charged particles.

As a result of these processes, two-dimensional and volumetric sources of heat are produced in the regions where the spark touches the electrodes. These sources propagate into the depth of the electrode and increase the temperature of local electrode volumes to boiling. Due to the intense heat liberation, <sup>/48</sup> the boiling of the liquid metal in the lune is accompanied by a violent evaporation of the metal in the entire volume of the microbath.

As shown by Adamson, the spark discharge is accompanied by shock waves, whose photograph is shown in figure 5. It is reasonable to assume that when these waves reach the surface of the microbath with the liquid metal, they force the boiling metal out of this bath and into the gap in the form of spray; part of the fused metal remains in the microbath due to the forces of surface tension. The energy liberated in the microbath produces an additional melting and evaporation of the metal, and the subsequent shock waves cause an additional ejection of the metal from the lune. The evacuation of the metal from the lune takes place in a discrete manner with the vaporous and liquid phases entering the gap as discrete portions of the material. As a result the lune is not <sup>/49</sup> formed immediately, but becomes deeper gradually during a discharge.

Thus, the metal evacuated from the electrodes constitutes a two-phase system consisting of metal vapor and metal liquid which are ejected into the surrounding medium in the form of spherical elements of various dimensions.

These concepts of the mechanism of erosion agree with the results obtained by B. N. Zolotikh, who studied the dynamics of lune formation and the ejection of material into the spark gap by means of high speed photography and an X-ray pulse tube.

During the discharge in the gaseous medium, the resulting shock waves displaced part of the liquid material from the microbath. When the coefficient of surface tension is small and the shock wave pressure is large, a greater amount of metal is ejected.

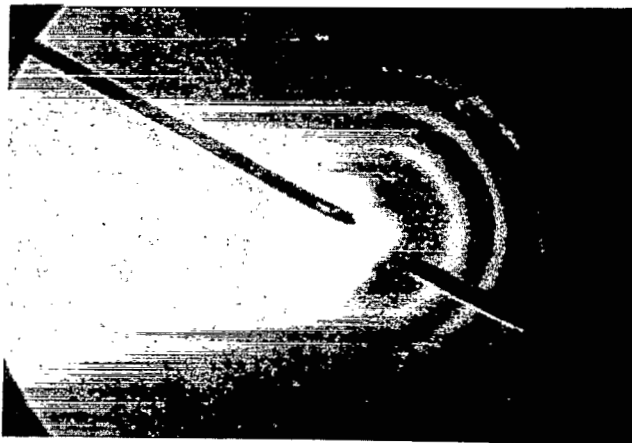


Figure 5. Photograph of shock waves accompanying spark discharge.

These concepts explain the behavior of the erosion process and, in particular, interpret the results of our experiments.

Figure 6 shows the curves  $\Delta m_{\text{ker}}/\Delta m_{\text{air}}$ , which give the ratio of alloy erosion in kerosene to erosion in air. As we can see from the graphs for alloys with components A and B and with small coefficients of surface tension, of the order 300-500 dyn/cm, the ratios  $\Delta m_{\text{ker}}/\Delta m_{\text{air}}$  are measured in units. Thus, for example, for the Cd-Bi and Pb-Bi alloys with the same percentage of components, the ratio  $\Delta m_{\text{ker}}/\Delta m_{\text{air}}$  is equal to 2.1 and 2.9, respectively.

For alloys whose components have the value  $\alpha$  of the order 500-800 dyn/cm, the ratio  $\Delta m_{\text{ker}}/\Delta m_{\text{air}}$  is measured in tens of units; thus, for Zn-Sn and Al-Zn alloys with a 50 percent content of components,  $\Delta m_{\text{ker}}/\Delta m_{\text{air}}$  is equal to 12 and 55, respectively.

For alloys whose components have  $\alpha$  of the order of 1000 dyn/cm, the ratio  $\Delta m_{\text{ker}}/\Delta m_{\text{air}}$  has values which are measured in hundreds of units. Examples of such alloys are the Cu-Ni alloy and the Cu-Ni cermet. For these, with a 50 percent content of components,  $\Delta m_{\text{ker}}/\Delta m_{\text{air}}$  is equal to 180 and 163 units, respectively.

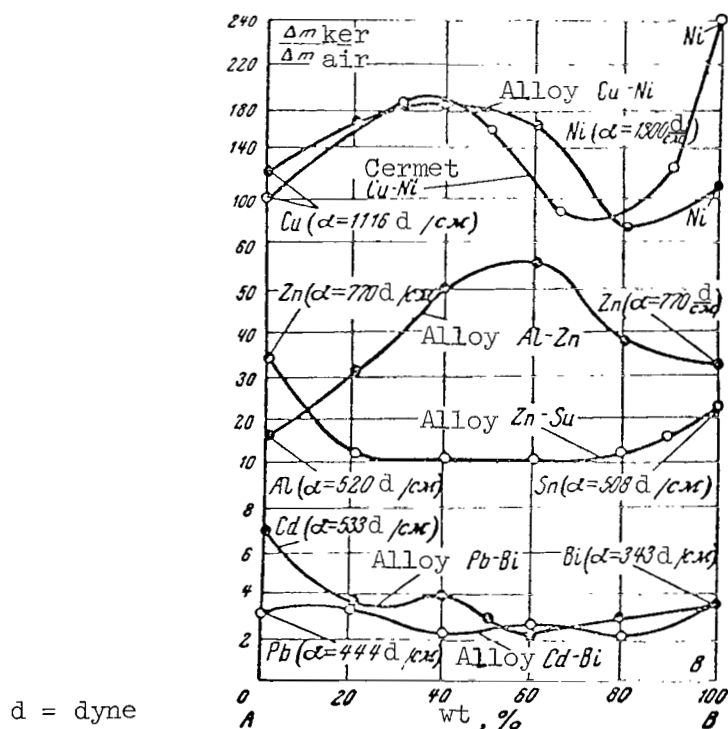


Figure 6. Graph showing variation in ratio of erosion in kerosene to erosion in air as function of component percentage.



When we consider the erosion of alloys, we note the special features of this process because the electrodes consist of two, three or more components. As in the case of pure metals, the energy liberated at the electrodes made of alloys causes the melting and evaporation of the latter, but the liquid phase in the microbaths in this case is not a single component phase, but rather represents a liquid solution. /50

It is known that if a liquid solution consists of components with different boiling temperatures, the component with a lower boiling temperature is evaporated more intensely, so that the liquid with the higher boiling temperature becomes more concentrated.

Of course, the metal with the higher melting temperature will also evaporate, but its relative amount depends on the ratio between the boiling temperatures of these metals. /51

For these reasons the surface of the contacts will change after many discharges and will have concentrations of the component with the higher melting temperature.

This concentration of high melting component was pointed out by I. P. Melashenko, who observed the concentration of tungsten on the surface contact layers made from a silver-tungsten composition and the concentration of nickel in contacts made from silver-nickel composition.

The metal vapor flares which enter the spark gap come in contact with the surfaces of the opposite electrodes and form a complex vapor above the liquid metal phase in the microbath: the electrode material vapor from which it is formed and the vapor of the opposite electrode material. The presence of a "foreign" vapor above the liquid metal in the microbath affects the value of the surface tension coefficient of this metal and consequently the magnitude of erosion for this electrode. This effect of the "foreign" vapor on the coefficient of surface tension for the metal in the microbath may be different. Depending on the material in the microbath, the type of "foreign" vapor and its pressure, the surface tension coefficient may be smaller or greater. In the first case, the erosion of the electrode will increase, while in the second case it will decrease.

The effect of flares on the erosion of the opposite electrode was noted in the work of S. L. Mandel'shtamm and S. M. Rayskogo.

These authors explain erosion as a result of mechanical destruction of electrode surface by the action of the flares. We assume that the action of the flare on the opposite electrode produces a variation in the surface tension of the metal in the microbath, which affects the magnitude of electrode erosion.

This mechanism of erosion shows that there is a complex relationship between the magnitude of erosion and the percentage of components in the alloys whose diagrams are shown in figures 1, 2, 3 and 4.

In low voltage discharges when there is a direct contact between the electrodes, the situation is further complicated by the fact that when the molten regions of the electrodes are in contact, the metal may be transported from one electrode to the other. /52

## Conclusions

The experimental investigation of the variation in the magnitude of alloy erosion as a percentage of components has made it possible to construct erosion diagrams, which show that the erosion of an alloy is not the sum of the erosions of the components; the latter, in turn, shows that the additive properties for all thermal constants of the component are not applicable when computing the magnitude of alloy erosion.

The analysis of curves in the erosion diagrams of alloys and the photographs of the deposited products of electric erosion give a new explanation for the mechanism of erosion in pure metals and in alloys; we can make several conclusions concerning the laws of the erosion process.

1. The electric erosion of electrodes is due to the thermal effect produced by the two-dimensional (bombardment of electrodes by electrons and positive ions) and volumetric (Joule) heat sources.
2. The evacuation of the material from the surface of the electrodes takes place in a discrete manner--in a vapor and liquid phase.
3. The vapor phase is caused by the rapid evaporation of the liquid metal in the microbath.
4. The ejection of the liquid phase from the microbath is caused by the pulse pressure of the shock wave. The most intense ejection of the liquid phase takes place at the end of the discharge, after the molten metal has obtained a high temperature and a resulting low surface tension coefficient.
5. The flare component, when it reaches the opposite electrode, does not produce its mechanical destruction, but changes the coefficient of surface tension  $\alpha$  of the liquid metal in the microbath. If in this case  $\alpha$  decreases, the ejection of the liquid phase and consequently the erosion of the electrode /53 increases.
6. When a discharge takes place between the electrodes made of alloys, there is a selective evaporation of alloy components: the component with the low melting temperature evaporates faster, leaving a concentration of the component with the higher melting temperature in the microbath.

## EROSION OF PRECIOUS METAL ELECTRODES IN AN ARC DISCHARGE

A. D. Gut'ko

The electric erosion of metals in pulse (spark) discharges has been studied in considerable detail (refs. 1-5). The problems concerned with the physical mechanism of electric erosion in an arc have received less attention, although this form of electric discharge is also of great practical interest. /53

### Erosion of the Cathode

It has been shown in references 6-12 that in a dc arc the destruction of the cathode exceeds the erosion of the anode by a factor of 2-20.

As determined by G. P. Skorniyakov (ref. 7), when the arc discharge acts on the cathode, we cannot consider any of the thermal constants as characteristic for the quantity of metal evaporated from the electrode. G. Ye. Zolotukhin and N. M. Zykova (ref. 8) came to the conclusion that the destruction of the cathode does not depend on the thermal conductivity of metals or alloys which are used as electrodes. V. P. Borzov (ref. 10) explains the decrease of the burning time at the cathode by the entry of unoxidized cathode particles into the discharge. L. I. Kiselevskiy and N. S. Svintitskiy (ref. 11) explain the increased erosion in the arc by the explosive nature of material entering the interelectrode space, associated with the rapid increase in current density at the initial stage of the discharge.

These authors assume that a significant role in the destruction of the cathode is played by the positive ion shocks in the glow discharge phase; they also point to the possibility that atoms may break off from the heated regions of electrodes in the arc phase of the discharge, due to a decrease in the work function of these atoms. /54

The study of the electric erosion of cathodes made of platinum metals, gold, silver and certain base metals were carried out in a unipolar arc with a current of 2.0-10.0 A and a distance of 1.0-4.5 mm between the electrodes. The source of the arc discharge was a generator with an electronic device (GEU-1), which made it possible to obtain the necessary operating conditions with sufficient stability. The discharge was carried out in air and in argon at normal pressures. The criterion of the electric erosion of the cathode was

the average decrease in the weight of the electrode per unit time, and also the value of the relative intensity of the spectral lines of the element, which was contained in the investigated metals in different quantities. The electrodes consisted of metallic rods, with a diameter of 5-6 mm and a length of 8-12 mm, inserted into holders cooled by flowing water (ref. 13); the second electrode was made of graphite.

Table 1 shows the values for the erosion of cathodes made of precious metals and their basic physical characteristics. We can see from this table that there is a closer relationship between the value of erosion in metals and the ionization energy of a given element than between the magnitude of erosion and other physical characteristics of the elements.

TABLE 1. COMPARISON OF THE MAGNITUDE OF CATHODE EROSION WITH THE PHYSICAL CONSTANTS OF METALS.

( $v_k$ --cathode erosion in  $\text{mg}/\text{sec} \cdot 10^{-3}$ ;  $T_f$  and  $T_b$  are the melting and

boiling temperatures,  $^{\circ}\text{C}$ ;  $\lambda$  is the heat conductivity,  $\text{cal}/\text{cm} \cdot \text{sec} \cdot \text{deg}$ ;  $C$  is the specific heat,  $\text{cal}/\text{g} \cdot \text{deg}$ ;  $L$  and  $r$  is the specific heat of fusion and evaporation,  $\text{cal}/\text{g}$ ;  $U_{ca}$  is the binding energy of atoms, in

$\text{eV}$ ;  $U_i$  is the energy of ionization of the atoms, in  $\text{eV}$ .)

Cathode material	$v_k$	$T_f$	$T_b$	$\lambda$	$C$	$L$	$r$	$U_{ca}$	$U_i$
Gold	-115.0	1,063	2,966	0.74	0.032	15.3	400	4.00	9.22
Platinum	-82.0	1,773	3,827	0.17	0.035	26.3	620	5.50	9.0
Palladium	-26.0	1,553	3,168	0.18	0.065	36.3	980	4.76	8.33
Iridium	-27.0	2,454	4,527	0.14	0.035	26.1	980	5.20	9.0
Copper	-8.0	1,083	2,595	0.92	0.100	50.6	1,200	3.52	7.72
Rhodium	-14.0	1,985	3,880	0.21	0.058	31.2	1,200	5.00	7.46
Ruthenium	-2.5	2,450	4,227	-	0.061	-	-	5.20	7.36
Silver	-1.9	960.5	2,212	1.05	0.062	26.0	600	2.95	7.57

The same relationship may be observed by using the results of <sup>155</sup> other investigators (refs. 14-17). A comparison of the magnitudes of contact erosion for different values of the ionization energy is shown in table 2 and is based on the results reported in references 16 and 17.

The energy of ionization was assumed to be equal to the resulting ionization potential computed by means of the following equation

$$U_i \text{ resultant} = \sum_{j=1}^n \frac{N_j}{N_0} U_{ij}, \quad (1)$$

where  $N_j$  is the number of atoms of a given element in a unit volume;

$N_0$  is the total number of atoms in the same volume;

$U_i$  is the ionization potential of atoms entering into the composition of the alloy.

It is not possible to compute the effective ionization potential (ref. 18) because the temperature of the arc near the cathode layer is unknown and because of the high degree of ionization of the contact alloy components. Therefore, we had to limit our calculations to a rough approximation, using the resultant ionization potential. The effective ionization potential reflects more accurately the true picture of the processes which take place in the arc. These depend to a larger degree on the magnitude of ionization potentials of the alloy components than on their relative concentrations. The magnitude of the effective ionization potential depends also on the arc temperature; a more accurate concept may therefore be obtained only by using this temperature.

It was assumed in the calculation that the composition of the vapor corresponds to the composition of the alloy and that the ions reach the cathode in their initial ratio.

We can see from tables 1 and 2 that a transition to metals with a smaller ionization potential and also the introduction of metals into the alloy with a small ionization potential (when other physical characteristics are identical or close) lead to a decrease in the erosion of the cathode, and vice versa.

A deviation from this law is observed in alloys which contain such elements as magnesium, beryllium, cadmium and others. We can see from the data presented in table 3 (refs. 19-21), that the addition of cadmium to 57 silver or to copper and also to copper-silver alloys does not lead to an increase, but rather leads to a decrease in the erosion of the contact cathode. The observed phenomenon is due to the fact that the atoms of the elements in the second group of the periodic table have favorable energy states for the step ionization (refs. 22 and 23). When the cadmium ions and ions of other elements in the second group of the periodic table are neutralized, the electrons may enter one of the triplet metastable states rather than the normal singlet state. The presence of metastable atoms with the metastable state energy greater than 1-2 eV may be looked upon as an admixture of vapor with low ionization energy. The numbers in the parentheses in table 3 show the magnitude of the resultant ionization potential, computed by taking into account the metastable state. Consequently, the "anomalous" erosion of alloys with metals of the second group may be explained by taking into account the energy states of the atom.

If we compare the data on the erosion of metals with the values 58 of the ionization potentials given in tables 1 and 2, we can see that there is a nonlinear relationship between the quantities of interest to us. For metals with close physical properties this relationship may be expressed by an exponential of the form

$$m \approx ae^{-b/U_i}, \quad (2)$$

TABLE 2. RELATION BETWEEN THE EROSION OF AN ALLOY AND THE VALUE OF THE IONIZATION POTENTIAL.

( $U_i, U'_i$  and  $U_{i \text{ resultant}}$  are ionization potentials of the base, admixture and of the resultant;  $\gamma$  and  $\gamma'$  are the cathode erosion (in the first case it is expressed in mg, in the second it is expressed in percent), according to data contained in references 16 and 17.)

Composition of contacts, %	$U_i$	$U'_i$	$U_{i \text{ res}}$	$\gamma$
Pd	8.33	—	8.33	—33.0
Pd+10Ag	8.33	7.57	8.25	—31.0
Pd+30Ag	8.33	7.57	8.11	—31.0
Pd+40Ag	8.33	7.57	8.04	—25.5
Pd+50Ag	8.33	7.57	7.94	—23.0
Pd+60Ag	8.33	7.57	7.87	—23.0
Pd+70Ag	8.33	7.57	7.80	—36.0
Pd+80Ag	8.33	7.57	7.72	—8.2
Pd+90Ag	8.33	7.57	7.61	—17.0
Ag	7.57	—	7.57	—7.6
Pd	8.33	—	8.33	—33.0
Pd+10Rh	8.33	7.46	8.12	—42.0
+20Rh	8.33	7.46	8.00	—23.0
Pd	8.33	—	8.33	—33.0
Pd+10Ir	8.33	9.2	8.38	—45.0
Pd+15Ir	8.33	9.2	8.42	—29.0
Pd+18Ir	8.33	9.2	8.42	—35.6
Au	9.22	—	9.22	+7.7
Pt	9.0	—	9.0	—14.4
Ir	9.2	—	9.2	—5.6
Rh	7.46	—	7.46	—4.66
Ru	7.36	—	7.36	—2.49
Ag	7.57	—	7.57	—2.45
Pt	9.0	—	9.0	—14.4
Pt+40Ir	9.0	9.2	9.1	—9.5—15.6
Pt+25Ir	9.0	9.2	9.0	—12.6—13.5
Pt+25Ru	9.0	7.36	8.37	—11.0
Pt+40Rh	9.0	7.46	8.13	—10.2
Pt+25Mo	9.0	7.10	8.04	—6.63
Ir	9.2	—	9.2	—5.6
Ir+34W+5Ni	9.2	8.0; 7.6	8.63	—6.5
Ir+20Rh+5Pt	9.2	7.46; 9.0	8.61	—4.0
Ir+33W+21Rh+5Ni	9.2	8.0; 7.5; 7.6	8.11	—2.55
Pd+20Ir	8.33	9.2	8.43	—32.0
Au+3Ni	9.22	7.63	9.09	—155.0
Au+20Ag	9.22	7.57	8.69	—67.0
Au+85Pg	9.22	8.33	8.42	—37.0
Rh	7.46	—	7.46	—4.66
Rh+20W+5Ni	7.46	8.0; 7.6	7.57	—1.78
Rh+40Ir	7.46	9.2	7.9	—7.9
Ru	7.36	—	7.36	—2.49
Ru+35W+5Ni	7.36	8.0; 7.6	7.53	—7.3
Ru+75Pt	7.36	9.0	8.37	—11.0

Note: All commas in tables represent decimal points.

TABLE 3. EROSION OF COPPER, SILVER AND COPPER-SILVER ALLOYS WITH CADMIUM OXIDE ( $U_i$  resultant --THE RESULTANT IONIZATION POTENTIAL, eV;  $\gamma$ --CATHODE EROSION)

Composition of alloy, %	$U_i$ res	$\gamma$ , $\text{mg} \cdot 10^6$	
Cu	7.72	6.5	
Cu+1.5CdO	7.72	2.9	
Cu+5.0CdO	7.77 (7.65)	2.5	
Cu+15.0CdO	7.81 (7.45)	3.0	
Cu	7.72	6.5	
Cu+5Ag+3.8Cd	7.70	0.8	
Cu+5Ag+4.3Cd	7.70	0.9	
		2 A	5 A
Ag	7.57	12.8	46.4
Ag+12CdO	7.72 (7.3)	11.6	27.0
Ag+15CdO	7.78 (7.1)	10.8	26.6

where  $m$  is the mass of the eroded metal per unit time, mg/sec;  
 $U_i$  is the ionization potential in electron volts;

$a$ ,  $b$ , are constants which depend on the physical properties of the cathode material, the electric parameters of the arc and the composition of the atmosphere in which the discharge takes place.

In addition to the ionization energy, the kinetic energy of positive ions and atoms is liberated at the cathode. However, only part of the kinetic energy is transmitted to the cathode. This energy is determined by the accommodation coefficient which is equal to 0.3-0.9.

A. Engel (ref. 24) makes the following rough qualitative approximation for the energy brought to the cathode when the arc burns between copper electrodes

$$E = a(E_{\text{pot}} + \alpha E_{\text{kin}} - \varphi) = a[7.7 + 4.5 - 4.5], \quad (3)$$

where  $a$  is the portion of the ion current;  
 $E_{\text{pot}}$  is the potential energy equal in value to the ionization potential;  
 $\alpha$  is the accommodation coefficient (in this case  $\alpha = 0.5$ );  
 $E_{\text{kin}}$  is the kinetic energy;  
 $\varphi$  is the work function of the electron.

From this rough calculation we can see that the energy transmitted to the cathode by the ions is determined primarily by the ionization energy of the atoms.

To compute the value of erosion, the equation for the erosion of metals by a spark discharge (refs. 25 and 26) was slightly changed

$$m = \frac{2 \cdot 10^{-3} I t e^{-b/U_i} - a \lambda (T_{ev} - T_0)}{c(T_{ev} - T_0) + L + r + 21 \frac{T_{ev}}{A}}, \quad (4)$$

where  $m$  is the mass of the diffuse substance, milligrams /59

$I$  is the arc current, A;

$t$  is the time, sec;

$U_i$  is the ionization energy, eV;

$a$  is the quantity proportional to the area of the cathode spot;

$\lambda$  is the heat conductivity, cal/cm·sec·deg;

$c$  is the specific heat, cal/g·deg;

$L$  is the specific heat of fusion, cal/g

$r$  is the specific heat of vaporization, cal/g;

$A$  is the atomic weight;

$T_{ev}$  is the evaporation temperature, °K;

$T_0$  is the temperature of the electrode at a point removed from the cathode spot, °K.

The physical constants shown in table 1 were used in the calculations. It was also assumed that the current density at the cathode was  $10^6$  A/cm<sup>2</sup> and that the ion current was 3-5 percent of the total current.

TABLE 4. RELATIVE EROSION OF INVESTIGATED METALS OBTAINED IN DIFFERENT WAYS

Cathode material	Calculations	Determined by decrease in weight of cathode	Spectroscopic method
Gold	5.0	4.4	3.6
Platinum	3.1	3.1	1.9
Palladium	1.0	1.0	1.0
Iridium	2.8	1.0	-
Copper	0.38	0.31	-
Rhodium	0.32	0.54	0.26
Silver	0.52	0.07	0.08
Iron	0.38	0.54	-
Nickel	0.28	0.27	-

Table 4 shows the values of the relative erosion of the investigated metals, obtained experimentally (from a decrease in cathode weight and from the intensity of spectral lines) and by means of calculations. We can see from the



table that the values of erosion obtained experimentally (from the decrease in cathode weight) and obtained by means of calculations are close for gold, platinum, copper and nickel. For rhodium and iron, there is a larger discrepancy while the discrepancy for iridium and silver cathodes reaches a factor of 3-7. The discrepancy between experimental and computed data for iridium is due to the instability of many physical characteristics, including the ionization energy of iridium atoms. As we have established earlier the erosion of silver, due to high thermal conductivity and a relatively low ionization energy of the atoms, takes place more intensely at the anode. /60

The use of the energy balance equation cannot serve as a convincing argument for supporting any proposition, because there is an absence of data which characterize the metal parameters at high temperatures and because the processes in the microvolume of the cathode spot have not been fully investigated. However, the equation may be used to evaluate the relative destruction of the cathode.

The third column in table 4 is obtained by evaluating the degree of cathode erosion using the spectroscopic method. Preceding investigations (ref. 27) have shown that under these conditions the anode material does not participate in the discharge to any appreciable degree. This is confirmed by figure 1; the second spectrum was obtained for a cathode made of platinum and the anode was made of copper. The third spectrum was obtained with the opposite polarity, i.e., the anode was made of platinum and the cathode was made of copper. The first spectrum was obtained with both electrodes made of platinum, and the fourth spectrum was obtained with both electrodes made of copper. We can see from figure 1 that the cathode material determines the structure of the spectrum. Consequently, the evaporation of the anode is insignificant, and it is possible that the cathode material transported to the anode evaporates at the anode. We can assume, therefore, that since the destruction takes place primarily at the cathode, we can use the intensity of spectral lines to evaluate the degree of cathode destruction. The same quantity of copper was introduced into the platinum, palladium, rhodium, gold and silver electrodes (in our case we prepared standards for each metal with a copper content of 0.5; 1.0; 2.0 and 5.0 percent, and the degree of cathode destruction was determined from the spectral lines belonging to the copper atoms and ions (table 5). /61

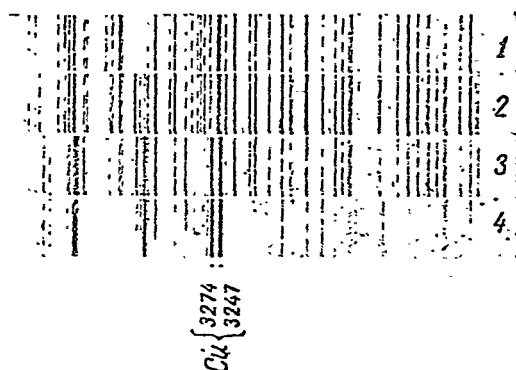


Figure 1. Spectra of platinum and copper obtained in unipolar ac arc with identical and combined electrodes.

TABLE 5. CHARACTERISTIC OF COPPER LINES USED IN THE SPECTROSCOPIC METHOD OF EVALUATING CATHODE EROSION ( $I_a$  AND  $I_s$  ARE THE INTENSITIES OF THE ARC AND SPARK COPPER LINES IN RELATIVE UNITS;  $E_i$  IS THE EXCITATION ENERGY OF THE LINES IN V).

Wavelength of copper line, Å	$I_a$	$I_s$	$E_i$	Superposition (element and wavelength)
I 2824.37	1000	300	5.78	Ag 2824.37 Pt 2824.41
I 2618.37	500	100	6.12	Rh 2618 (not shown in tables)
II 2369.89	20	300	5.76	Ag 2369.88
II 2247.00	30	500	5.51	Pd 2247.01

Calculations were made by means of the equation

$$\lg \frac{(N_{Cu})_i}{(N_{Cu})_{Pd}} = \lg \frac{(I_{Cu})_i}{(I_{Cu})_{Pd}} - \lg \frac{[1 - (x_{Cu})_i]}{[1 - (x_{Cu})_{Pd}]} - 0.43 \frac{E(T_i - T_{Pd})}{kT_{Pd}T_i}, \quad (5)$$

where  $N$  is the concentration of atoms in unit volume;

$I_{Cu}$  is the spectral intensity of the copper line;

$X_{Cu}$  is the degree of copper ionization;

$E$  is the excitation energy of the given line;

$k$  is the Boltzmann constant;

$T$  is the arc temperature °K;

$i$  is the coefficient which designates the metal from which the copper atoms evaporated (i.e., platinum, rhodium, gold or silver). /62

The temperature and the degree of ionization of copper atoms in the investigated metals were determined by means of arc and spark lines of copper and palladium, using techniques widely known in spectroscopy.

The lower value of erosion obtained in this way may be explained by the fact that a relatively large amount of copper was added to the investigated metals, and this copper lowered the degree of erosion of gold, platinum and palladium electrodes.

The spectroscopic evaluation of cathode erosion may be used only for metals with high melting points. For metals with low melting points (lead, zinc, cadmium, tin and others) the main mass of the substance is spattered by the arc discharge, and only 12-37 percent is converted into vapor. For gold, platinum, rhodium and silver the spattering of the metal under the test conditions did not exceed 8-13 percent, while for palladium it did not exceed 19 percent of the total cathode weight loss.

A large effect on the magnitude of erosion particularly in metals which resemble oxygen is produced by the atmosphere in which the discharge takes place. Thus, the replacement of air by argon decreases the erosion of lead, zinc, cadmium, tin and even tungsten by a factor of 0.5-3. These observations agree with the data presented in reference 28. The erosion of precious metals in an ac arc is practically independent of atmospheric composition.

From data contained in the literature and also from observations carried out in the laboratory we may assume that the anode erosion occurs as the result of a relatively quiescent evaporation of this material from the surface of the electrode, while the mechanism for the transformation of cathode material into vapor is of a more complex nature. This difference may be due to the difference in the nature of the particles which interact with the cathode surface and also to a different mechanism (compared with the anode) for the transmission of energy to the cathode atoms.

It is well known that the anode is bombarded by electrons which have a definite supply of kinetic energy obtained from the electric field, in addition to that performed to remove the electron from the metal. At the <sup>63</sup>anode the kinetic energy of electrons is first transmitted to the electrons of the anode, and from these is transmitted to the atoms or ions of the crystal lattice, where it is converted into thermal energy.

The cathode bombards more complex particles--excited and unexcited atoms and ions. In addition to kinetic energy, they have a definite supply of potential energy, which consists of the ionization energy and the excitation energy of atoms and ions. The energy transmitted to the cathode by the ions is transferred directly to the atoms or ions of the crystal lattice.

L. S. Palatnik and A. A. Levchenko (ref. 29) showed that the lune at the anode has the form of a circle and does not depend on the orientation of the crystallographic plane of the monocrystal, while the form of the lunes on the cathode depends on the crystallographic orientation of the monocrystal boundary or of the grain in a polycrystalline sample.

The difference in the nature of the particles, in their energy balance and in the mechanism of energy transfer produces a difference in the processes which take place at the surface of the cathode and the anode. The ions bring a relatively large portion of the energy to the cathode, which exceeds substantially the binding energy of atoms in the crystalline lattice. Therefore, the energy brought to the cathode is used up not only to evaporate the substance, but also to draw the atoms from the lattice of the metal and to form microexplosions on the surface of the cathode.

The presence of such a complex mechanism produces a substantial increase in cathode erosion, compared to erosion produced by thermal effects developing on the surface of the anode.

However, in spark discharges the erosion of the anode is comparable with the erosion of the cathode or exceeds it. Such a phenomenon, as a rule, is observed in electric discharges, which take place over a very short interval of time or when the distance between the electrodes is very small. Due

to the low mobility of ions during short-term action of the electric discharge, only a small portion of them reaches the cathode and transmits its energy. A decrease in the number of ions, which bombard the cathode surface, produces a decrease in cathode erosion. The dimensions of anode and cathode spots <sup>/64</sup> and the difference between them produces a large effect on the destruction of the anode. As pointed out by B. N. Zolotykh (ref. 2), the basic role in the determination of the erosion polarity is played by the intensity of thermal energy liberated at the surface of the electrodes. From our discussion it follows that:

1. The erosion of the cathode in an arc discharge depends on the elementary processes which take place in the region adjoining the arc and on the surface of the electrodes, i.e., on the ionization energy of atoms and their number, and also on the magnitude of the excitation energy of the metastable atomic states.

2. In designing the composition of alloys for contacts, in addition to the thermal and mechanical constants of the material it is necessary to take into account the ionization energy of the alloy components and the structure of their electron shells.

3. To obtain a negative contact (cathode) which is stable with respect to destruction, it is of interest to study binary and more complex alloys of platinum, palladium and iridium with rhodium and ruthenium, platinum metals (palladium, rhodium and ruthenium) with molybdenum, vanadium, chromium, manganese and others, and also with the elements of the second group and with the rare earth elements, whose atoms have an ionization energy equal to 5.6-6.2 eV.

#### Anode Erosion

The experiments for investigating the anode erosion were conducted under the same conditions as those for the investigation of cathode erosion (ref. 1). The only difference was that in these experiments the metallic rod served as the anode, while the graphite rod served as the cathode. The results of the observations are presented in table 6.

We can see from table 6 that the magnitude of anode erosion also depends on the ionization energy of the metallic atoms of which it consists. Unlike the cathode, the anode is destroyed with more power when the ionization energy of its atoms is lower. The observed law for anode erosion depends on the processes which take place in the arc near the anode, and first of all on the nature of electron interaction with anode atoms in the vapor state. The <sup>/65</sup> electrons which enter from the positive column of the arc and which are accelerated in the region of anode drop ionize the atoms which are evaporated from the anode. The electrons which are freed during ionization augment the basic current, and their number will be large when the ionization energy of anode atoms is low. The relation between the number of electrons and the ionization energy of atoms is expressed in the following form (refs. 2-4).

$$n = n_0 A e^{-\frac{eU_i}{kT_e}} \left(1 + \frac{eU_i}{kT_e}\right), \quad (6)$$

where  $n_0$  is the number of electrons which enter the region near the anode per unit time;  
 $A$  is a quantity which depends on pressure, electron temperature, etc.;  
 $e$  is the electron charge;  
 $U_i$  is the ionization potential;  
 $k$  is the Boltzmann constant;  
 $T_e$  is the electron temperature.

In addition to the increase in the number of "auxiliary" electrons, whose specific weight in the general energy balance is apparently small, the anode potential drop increases when the ionization energy of anode atoms decreases. This increase is caused by the decrease in the potential of the positive arc column, also by the more rapid decrease in the positive space charges and an increase in the negative space charges. This is caused by the diffusion processes, the electric field of the arc, and also the anode and cathode streams of material evaporating from the electrodes. These phenomena cause the electric erosion, and consequently the energy transported to the anode, to depend on the ionization potential of the anode atoms. /66

TABLE 6. COMPARISON OF ANODE EROSION VALUES WITH THE PHYSICAL CONSTANTS OF THE METALS ( $\gamma_a$ , anode erosion, mg/sec. $\cdot 10^{-3}$ ;  $T_f$  and

$T_b$  are the melting and boiling points,  $^{\circ}\text{C}$ ;  $\lambda$  is the heat conduc-

tivity, cal/cm. $\cdot$ sec. $\cdot$ deg;  $C$  is the specific heat cal/g. $\cdot$ deg;  $L$  and  $r$  are the specific heat of fusion and of evaporation, cal/g;  $U_{be}$  is

the binding energy of atoms, eV;  $U_i$  is the ionization energy of atoms).

Anode material	$\gamma_a$	$r_f$	$r_b$	$\lambda$	$C$	$L$	$r$	$U_{be}$	$U_i$
Ruthenium	-11.0	2 450	4 227	—	0.061	—	—	5.20	7.36
Rhodium	-6.0	1 985	3 880	0.21	0.058	31.2	1 200	5.00	7.46
Silver	-3.5	960.5	2 212	1.05	0.062	26.0	600	2.95	7.57
Palladium	-3.5	1 553	3 168	0.18	0.065	36.3	980	4.76	8.33
Iridium	-1.2	2 454	4 527	0.14	0.035	26.1	980	5.20	9.2
Copper	-1.0	1 083	2 595	0.92	0.100	50.6	1 200	3.52	7.72
Platinum	-0.8	1 773	3 827	0.17	0.035	26.3	620	5.50	9.0
Gold	-0.5	1 063	2 966	0.74	0.032	15.3	400	4.00	9.22

Table 7 shows the values of relative erosion (the erosion of palladium is assumed to be unit), determined experimentally from the decrease in the anode weight and by means of calculations. The calculations used the same equations that were used in computing the erosion of the cathode (refs. 5, 6 and 1), but the energy transported to the anode was determined by taking into account the number of electrons formed in the region of the arc close to the anode.

We can see from the table that the magnitudes of relative anode erosion obtained experimentally and by means of calculations are in satisfactory agreement.

The same variation in the magnitude of anode erosion as a function of the resultant ionization potential may be observed from experimental data presented in references 7-10. /67

We can see from table 8 that the introduction of additives into the alloy with a smaller ionization potential, as a rule, increases the anode erosion. Contact materials which have high electric conductivity and high thermal conductivity, high specific heat, high melting points and high boiling points, etc. are subject to less electric wear. In addition to the enumerated properties,

TABLE 7. RELATIVE EROSION OF INVESTIGATED METALS DURING EVAPORATION FROM THE ANODE (mg/sec. $\cdot 10^{-3}$ ).

Anode material	Erosion determined	
	Experimentally	Determined by calculations
Ruthenium	3.0	—*
Rhodium	1.7	2.2
Silver	1.0	1.3
Palladium	1.0	1.0
Iridium	0.3	0.0**
Copper	0.3	0.5
Platinum	0.2	0.0**
Gold	0.14	0.0**

\*The calculations for ruthenium were not carried out because certain tabulated data were not available.

\*\*The outflow of heat according to the calculations exceeds the influx of heat.

TABLE 8. RELATION BETWEEN ANODE EROSION AND THE RESULTANT IONIZATION POTENTIAL ACCORDING TO DATA PRESENTED IN REFERENCES 7-10.

Anode material	Anode erosion	Resultant
Pt+10Ir	-2.6 mg, 12·10 <sup>4</sup> cycles	8.98
Pd+18Ir	-1.2 " 12·10 <sup>4</sup> "	8.42
Pd+10Ir	-1.3 " 12·10 <sup>4</sup> "	8.38
Pd+35Ag+5Co	-1.8 " 12·10 <sup>4</sup> "	8.04
Pd+40Ag	-1.6 " 12·10 <sup>4</sup> "	8.03
Pd+80Ag	-5.3 " 12·10 <sup>4</sup> "	7.72
Ag	-6.3 " 12·10 <sup>4</sup> "	7.57
Pt+25Re	-6.5 %	8.35
Pt+25Mo	-19.0 %	8.04
Cu+1,2Cd	-6.3 μg	7.72*
Cu+2,0Cd	-6.6 μg	7.72
Cu+5Ag+2,1Cd	-6.1 μg	7.70
Cu+5Ag+3,8Cd	-8.2 μg	7.70
Cu+5Ag+4,3Cd	-10.1 μg	7.68
W	+2.5 mV·10 <sup>-6</sup>	7.98
W+30Ag	-40.0 mg·10 <sup>-6</sup>	7.80
W+50Ag	-47.7 mg·10 <sup>-6</sup>	7.73

\*The resultant ionization potential of alloys which contain cadmium is computed by taking into account step ionization.

the cathode and anode of electric contacts must consist of materials whose atoms have an ionization energy (ionization potential) providing for minimum electric wear. /68

From experimental data we can see that the requirements for cathode and anode materials are opposite from the standpoint of ionization energy of the atoms. Therefore, to obtain contacts with high resistance to electric wear, it is necessary to fabricate the cathode and anode from different materials: the cathode should be fabricated from a material whose atoms have the lowest possible ionization potential, while the anode should be fabricated from a material whose atoms have a large ionization potential. However, in designing contact pairs prime attention should be devoted to the selection of the cathode material because the magnitude of cathode erosion exceeds the anode erosion for most metals and alloys.

To study the erosion of electrodes when the cathode and anode were fabricated of different metals, the electrode pairs were selected in such a way that the anode had high ionization potential and the cathode had low ionization potential.

The magnitudes of erosion of electrodes made of dissimilar metals are shown in table 9, from which it follows that the replacement of the platinum, palladium or gold cathode with a metal having a lower ionization energy leads to a substantial decrease in the erosion of electrodes. The same effect is achieved, as we can see from table 4, if ruthenium, silver or aluminum anode is replaced with an anode from a metal with a high ionization potential. In addition, as we can see from the data presented in table 9, the anode material has an insignificant effect on the magnitude of cathode erosion. However, the replacement of the cathode with another metal decreases the quantity of substance which has precipitated on the anode due to a decrease in cathode erosion, while in some cases it produces conditions for the destruction of the anode.

The insignificant variation in the weight of the aluminum cathode is apparently due not only to the low ionization potential, but also to chemical processes which form a stable oxide film on the surface of the aluminum.

The severe destruction of the titanium cathode is due to the fact that at high temperatures it readily absorbs oxygen, hydrogen and carbon dioxide from the air (ref. 13), which naturally lowers its resistance to electric wear.

The advantage of contact pairs made of dissimilar metals has been shown experimentally by a series of investigators (references 9, 10, 11 and 12). Thus, T. K. Shtrenberg and M. P. Repner (ref. 11) investigated contact pairs, including pairs consisting of dissimilar metals: alloy of platinum with 10 percent iridium (cathode)--tungsten (anode) and alloys with a palladium base paired with tungsten. The alloy of palladium with 40 percent silver, or palladium with 40 percent copper, served as the anode, while the cathode <sup>70</sup> was made of tungsten. On the basis of experimental investigations they discovered that the pair most resistant to destruction consists of a palladium alloy with 40 percent copper used as anode and a tungsten cathode.

These observations correspond to our concepts on the effect of ionization energy on the degree of electrode destruction. Thus, the utilization of contact pairs consisting of tungsten (anode) and a palladium alloy with 10 percent iridium (cathode) cannot lead to a low erosion of the alloy because it contains metals with high ionization energies, which produce a noticeable erosion of the cathode. Of the contact pairs, tungsten-cathode and alloys of palladium with silver or copper-anode, the palladium alloy with 40 percent copper was the most stable with respect to erosion. This also contradicts the relation between the magnitude of erosion and the energy of ionization.

V. I. Fiks and M. A. Gurevich (ref. 12) point to a low erosion stability of contact pairs of tungsten (cathode) and silver (anode), basically due to the substantial erosion of the silver. This example also confirms the fact that the elements with low ionization energy have low resistance to electric wear when they serve as anodes.



TABLE 9. EROSION OF ELECTRODES WHEN THE CATHODE AND THE ANODE ARE MADE OF DISSIMILAR METALS,  $\gamma$ ,  $\text{mg/sec} \cdot 30^{-3}$  (the upper numbers refer to the change in weight of the anode, while the lower numbers show the change in weight of the cathode).

Cathode	Anode					$U_i$
	Plati- num	Palla- dium	Gold	Graph- ite (car- bon)	Both electrodes made of same material	
Aluminum	+0.5	-6.0	+0.4	-	-12.0	5.98
	+1.0	-1.0	+1.5	+2.0	+16.0	
Ruthenium	-6.0	-6.0	+0.4	-	-14.0	7.36
	-5.0	+1.0	-2.0	-2.0	+4.0	
Silver	+1.5	+2.0	+1.0	-	-6.0	7.57
	-5.0	-5.3	-2.8	-1.9	+3.0	
Nickel	-13.0	-5.0	+1.5	-	+0.5	7.63
	-10.0	-9.0	-11.0	-7.9	-7.0	
Copper	+3.5	-2.0	-0.2	-	-2.0	7.72
	-10.0	-12.0	-13.0	-8.0	-17.0	
Rhodium	+10.0	-5.0	+7.0	-	+6.0	7.46
	-24.0	-23.0	-19.0	-14.0	-16.0	
Titanium	-0.5	-50.0	-0.4	-	-15.0	6.82
	-112.0	-110.0	-90.0	-150.0	-100.0	
Both electrodes made of same metal	+47.0	+14.0	+70.0	-	-	-
	-110.0	-24.0	-142.0	-	-	

A. P. Adakhovskiy and Ye. A. Lyukevich (ref. 9) show that the application of various materials for the cathode and the anode sharply reduce the electric erosion of contacts.

The use of a cathode and anode fabricated from dissimilar metals opens up a wide possibility for developing contact pairs which are resistant to erosion. This possibility becomes even greater, if the magnitude of cathode erosion and anode erosion are varied when preparing alloys by taking into

account the ionization of atoms constituting these alloys. The material designed for the anode must contain an addition of atoms with high ionization energy and with a higher vapor elasticity than the base alloy. The cathode must consist of metals whose atoms have a low ionization energy or which have metastable states with excitation energy having a value of several electron volts.

It is of considerable interest to alloy the cathode with rare earth elements, whose atoms have an ionization energy equal to 5.6-6.2 eV.

From the information presented in the second half of the article /71 we can make the following conclusions.

1. It has been established that the erosion of the anode, like the erosion of the cathode, is associated with elementary processes which take place in the region of the arc close to the electrodes.
2. The destruction of the anode is more intense when the ionization of its atoms is lower; for the cathode it is more intense when the ionization energy is greater.
3. To obtain contacts which are stable to erosion, it is necessary in many cases to make the anode and the cathode from different metals or alloys.
4. A more intense destruction of the anode compared with the cathode is due to a definite combination of ionization energy of the atoms, of the thermal characteristics of the metal or alloy and also apparently of the corresponding structure of the metal crystal lattice. Examples of this are rhenium and ruthenium (ref. 14), whose anode erosion exceeds the cathode destruction.

#### REFERENCES

1. Lazarenko, B. R. and Lazarenko, N. I. The Physics of Electrosark Method of Machining Metals (Fizika elektroiskrovogo sposoba obrabotki metallov). TsBTI MEP, 1946.
2. Zolotyykh, B. N. Physical Principles of Electrosark Machining (Fizicheskiye osnovy elektroiskrovoy obrabotki). Gostekhizdat, 1953.
3. Mandel'shtam, S. L., Sukhadrev, N. K. and Shabanskiy, V. P. Proceedings of the Tenth All Union Conference on Spectroscopy, Publication of the L'vov University (Materialy X Vsesoyuznogo soveshchaniya po spektroskopii). Izd-vo L'vovskogo Universiteta, Vol. 2, 1958.
4. Nekrashevich, I. G., Olekhovich, N. M. and Labuda, A. A. Propagation of Current Along the Surface of Electrodes during Electric Pulse Discharge (O raspredelenii toka na poverkhnosti elektrodov pri elektricheskoy impul'snoy razryade), in Collected Works "Electric Contacts," Proceedings of the Conference (Sbornik "Elektricheskiye kontakty," Trudy soveshchaniya). Gosenergoizdat, 1960.

5. Zolotikh, B. N. Basic Problems of the Physical Theory of Electric Erosion in the Pulse State (Osnovnyye voprosy fizicheskoy teorii elektricheskoy erozii v impul'snom rezhime), in Collected Works "Electric Contacts," Proceedings of the Conference (Sbornik "Elektricheskiye Kontakty," Trudy soveshchaniya). Gosenergoizdat, 1960.
6. Prokof'yev, V. K. Mechanism of the Evaporation of Solid Electrode Material in the Spectro Analysis Light Sources (O mekhanizme ispareniiya veshchestva tverdykh elektrodov v spektroanaliticheskikh istochnikakh sveta). Izvestiya AN SSSR, seriya fizich., 11, No. 3, 1947.
7. Skorniyakov, G. P. Evaporation of Metallic Electrodes in a dc arc (Ob isparenii metallicheskih elektrodov v duge postoyannogo toka). Izvestiya AN SSSR, seriya fizich., 19, No. 1, 1955.
8. Zolotukhin, G. Ye., Zykova, N. M. The Influence of Length of Discharge on the Velocity of Particle Evaporation from the Surface of Metallic Arc Electrodes (Vliyaniye dlitel'nosti razryada na skorost' ispareniiya chastits s poverkhnosti metallicheskih elektrodov dugi) Izvestiya AN SSSR, seriya fizich. 23, No. 9, 1959.
9. Silin'sh, E. A. and Taure, L. F. Investigating the Role of Sample Polarity During the Excitation of the Spectrum in an ac Arc (Issledovaniye roli polyarnosti obraztsa pri vozbuzhdenii spektra v duge peremennogo toka). Izvestiya AN SSSR, seriya fizich., 23, No. 9, 1959.
10. Borzov, V. P., Inzhenerno-fizicheskiy zhurnal, Vol. 3, No. 6, 1960.
11. Kiselevskiy, L. I. and Svintitskiy, N. S. Role of Polarity in the Introduction of Electrode Material into Light Sources During Spectroanalysis (O roli polyarnosti postupleniya materiala elektrodov v istochnikakh sveta pri spektral'nom analize). Inzhenerno-fizicheskiy zhurnal, No. 9. 1959. /72
12. Gut'ko, A. D. and Shchurova, Ye. I. Some Questions of Emission and Molecular Spectroscopy (Nekotoryye voprosy emissionnoy i molekulyarnoy spektroskopii). TsBTI Krasnoyarskogo Sovnarkhoza, 1960.
13. Gut'ko, A. D. Method of Analyzing Platinum Metals, Gold and Silver (Metody analiza platinovykh metallov, zolota i serebra), in Collection of Scientific Works (Sbornik nauchnykh trudov). Metallurgizdat, 1960.
14. Lazarenko, B. R. and Lazarenko, N. I. Electrosark Machining of Current Conducting Metals in a Spark Discharge (Elektroiskrovaya obrabotka tokoprovodyashchikh metallov v iskrovom razryade). Izvestiya AN SSSR, seriya fizich., 18, No. 2, 1954.
15. Raykhbaut, Ya. D. and Krest'yaninov, A. G. The Question of Electric Erosion of Metals in a Spark Discharge (K voprosu ob elektricheskoy erozii metallov v iskrovom razryade). Izvestiya AN SSSR, seriya fizich. 18, No. 2, 1954.

16. Kirillova, Z. S. Alloys for Electric Contacts With Low Transitional Resistance, Collected Works "Electric Contacts" (Proceedings of the Conference) (Splavy dlya elektricheskikh kontaktov s malym perekhodnym soprotivleniyem), Sbornik "Elektricheskiye kontakty". Gosenergoizdat, 1958.
17. Adakhovskiy, A. P. and Lyukevich, Ye. A. Some Prospects for Breaking Contacts Using Precious Metals, Collected Works "Electric Contacts" (Proceedings of the Conference) (Nekotoryye perspektivnyye materialy dlya razryvnykh kontaktov na osnove dragotsennykh metallov, Sbornik, "Elektricheskiye kontakty"). Gosenergoizdat, 1960.
18. Semenova, O. P. The Effective Ionization Potential of a Gaseous Mixture During Thermal Ionization (Ob effektivnom ionizatsionnom potentsiale gazovoy smesi pri termicheskoy ionizatsii). (Izvestiya VUZov, Fizika, No. 1, 1958.
19. Dekabrun, I. Ye. The Characteristics of Some Cermet Contact Materials, Collected Works "Electric Contacts" (Proceedings of the Conference) Kharakteristiki nekotorykh metallo-keramicheskikh kontaktnykh materialov, Sbornik, "Elektricheskiye kontakty"). Gosenergoizdat, 1956.
20. Feyler, G. O. The Resistance to Wear of Contactor Contacts and Controller Contacts for dc Current, Collected Works "Electric Contacts" (Proceedings of the Conference) (Iznosoustoychivost' kontaktov kontaktorov i kontrollerov postoyannogo toka, Sbornik, "Elektricheskiye kontakty"). Gosenergoizdat, 1958.
21. Al'tman, A. B. and Bystrova, E. S. Cadmium Bronze as a Material for Breaking Electric Contacts, Collected Works "Electric Contacts" (Proceedings of the Conference) (Kadmiyevaya bronza kak material dlya razryvnykh elektricheskikh kontaktov, Sbornik, "Elektricheskiye kontakty"). Gosenergoizdat, 1960.
22. Kesayev, I. G. The Minimum Potentials of the Arc Discharge and the Question Concerning the Two Forms of an Arc With Gold Cathodes (Minimal'nyye potentsialy dugovogo razryada i vopros o dvukh formakh dugi s kholodnym katodom). Doklady AN SSSR, 140, No. 6, 1961.
23. Braun, S. Elementary Processes in the Plasma of a Gaseous Discharge (Elementarnyye protsessy v plazme gazovogo razryada). Gosatomizdat, 1961.
24. Engel', A. Ionized Gases (Ionizovannyye gazy). Fizmatgiz, 1959.
25. Jones, S. Brit. Journ. Appl. Phys. 1, 60, 1950; Nature, 157, 480, 1946.
26. Meek, J. and Craig, J. Electric Breakdown in Gases (Elektricheskiy proboy v gazakh). Izd-vo Inostrannoy Literatury (I. L.), 1960.

27. Gut'ko, A. D. The Role of Polarity During the Evaporation of Platinum Metals in an Arc Discharge (Rol' polyarnosti pri isparenii platinovykh metallov v dugovom razryade). Presented at the First Siberian Conference on Spectroscopy at the City of Kemerovo, February, 1962.
28. Ozawa, M., Morita, J. and Omura, K., Energy Balance at Electrode of Arcs, Bull. Electrotechn. 20, No. 10, 1956.
29. Palatnik, L. S. and Levchenko, A. A. The Nature of Erosion in Monocrystals, Collected Works "Electric Contacts" (Proceedings of the Conference (O kharaktere elektricheskoy erozii na monokristallakh, Sbornik, "Elektricheskiye kontakty"). Gosenergoizdat, 1960; "Kristallografiya", 3, No. 5, 1959.
30. Engel', A. and Shteynbek, M. The Physics and Engineering of Electric Discharge in Gases, (Fizika i tekhnika elektricheskogo razryada v gazakh). ONTI, Vol. 1, 1935; Vol.2, 1936. /73
31. Leb, L. Basic Processes of Electric Discharges in Gases (Osnovnyye protsessy elektricheskikh razryadov v gazakh). Gostekhzdat, 1950.
32. Shtremberg, T. K. and Repner, N. R. The Question of Increasing the Useful Life of Contacts Used in Polarized Telegraph Relays, Collected Works "Electric Contacts" (Proceedings of the Conference) (K voprosu ob uvelichenii sroka sluzhby kontaktov peredayushchikh telegrafnykh polyarizovannykh rele), Sbornik, "Elektricheskiye kontakty". Gosenergoizdat, 1960.
33. Fiks, V. I. and Gurevich, M. A. Contacts of Vibrator Voltage Regulators, Collected Works, "Electric Contacts" (Proceedings of the Conference) (O kontaktakh vibratsionnykh regulyatorov napryazheniya, Sbornik, "Elektricheskiye kontakty"). Gosenergoizdat, 1958.
34. Andreyeva, V. V. and Kazarin, V. I. New Structural Chemically Stable Metallic Materials (Novyye konstruktsionnyye khimicheski stoykiye metallicheskiye materialy). Goskhimizdat, 1961.
35. Savitskiy, Ye. M., Tylkina, M. A. and Dekabrun, I. Ye. Rhenium as a Material for Electric Contacts, Collected Works "Electric Contacts" (Proceedings of the Conference) (Reniye v kachestve materiala dlya elektricheskikh kontaktov, Sbornik, "Elektricheskiye kontakty"). Gosenergoizdat, 1960.

# INVESTIGATION OF NONEQUILIBRIUM PROCESSES AT ELECTRODES IN AN ARC

A. A. Kuranov

A study of the erosion mechanism is very important in the selection of /73 contact pairs. The diverse processes which take place at contact surfaces make the study of this mechanism very difficult. For this reason it is useful to use simulation to clarify certain mechanisms which take place.

In an arc discharge we can show the formation of a zone of molten metal which on one side is in contact with the solid metal phase and on the other with the region of the arc discharge. The metal enters the region of the arc discharge from the liquid phase. It is interesting to know the mechanism of this material migration.

It has been shown by L. M. Filimonov (ref. 1) that the liquid-vapor system in the arc discharge is close to a state of equilibrium and is described by the following expression:

$$\lg \frac{c'_1}{c'_2} = \lg \frac{c_1}{c_2} + \lg \frac{P_1^0}{P_2^0} + \lg \frac{\gamma_1}{\gamma_2}, \quad (1)$$

where  $c'_1$  and  $c'_2$  are the concentrations of elements 1 and 2 in the vapors;

$c_1$  and  $c_2$  are the concentrations of elements 1 and 2 in the /74 liquid;

$P_1^0$  and  $P_2^0$  are the vapor pressures of elements 1 and 2 for pure substances;

$\gamma_1$  and  $\gamma_2$  are activity coefficients which characterize the deviation of the system from the Raoult law.

If the vapor pressure of element 1 is higher than the vapor pressure of element 2 a depletion of the evaporation surface by element 1 takes place. This situation is confirmed by investigating the kinetic relations. Thus for these elements there is a drift which decreases the amount of component 1 in the liquid phase. We should point out that the diffusion coefficient for

molten metals has a value which is of the order of  $10^{-4}$ - $10^{-5}$  cm<sup>2</sup>/sec. If we simulate the shape of the molten metal in the form of a cylinder with impermeable

sides, we can solve the diffusion equation, taking into account the convection of the fused metal. From the expression obtained in this way and the theory of activities we obtain the following expression

$$\lg \frac{c_1}{c_1^0} = \lg \frac{c_1}{c_2} + \lg \frac{P_1^0}{P_2^0} - \frac{0.43\pi^2 D t}{h^2} - \frac{0.43 v^2 t}{4D} + \frac{0.43 v h}{2D} + \lg \frac{\gamma_1}{\gamma_2}, \quad (2)$$

where D is the diffusion coefficient of element 1;  
t is the duration of the process;  
h is the height of the fused metal;  
v is the convection velocity.

Spectroscopic investigations of fused metal show that expression (2) is satisfied qualitatively in the crater of a carbon electrode. In addition, for elements with the same vapor pressure removed from the metal with a lower vapor pressure, the variation of the kinetic curves may be different. For this reason we may assume that the basic rule in the neutralization process of the fused composition is played by the diffusion of element 1. /75

The mechanism for the solid-liquid transition was not considered by us. We can only point out that it will take place in accordance with the state diagram. A substantial role will also be played by the structure of the contact material because diffusion over the surfaces and intercrystalline members is greater by a factor of 5-6 than the volumetric diffusion. As a rule, however, the impurities are concentrated at the grain boundaries.

The concepts presented by us may be useful in selecting contact materials.

#### REFERENCES

1. Filimonov, L. M. The Relationship between the Composition of the Test Sample and the Emitting Cloud in Light Sources for Spectral Analysis (K voprosu o svyazi sostava proby i izluchayushchego oblaka v istochnikakh sveta dlya spektral'nogo analiza). Materialy X Vsesoyuznogo soveschaniya po spektroskopii, Vol. 2, Izd-vo L'vovskogo Universiteta, 1958.
2. Kuranov, A. A. The Mechanism of the Global Arc (K voprosu o mekhanizme global'noy dugi). Izvestiya AN SSSR, ser. fizich., Vol. 26, 1962.
3. Arkharov, V. I., Klotzman, S. M. and Timofeyev, A. N. The Effect of Small Admixtures on the Diffusion Coefficients in Polycrystalline Materials. III. The Effect of Thallium on the Self-Diffusion of Silver (O vliyanii malykh primesey na koeffitsienty diffuzii v polikristallicheskih materialakh. III. Vliyaniye talliya na samodiffuziyu serebra). Vol. 8, No. 5, 1959.

## NATURE OF FORCES WHICH EJECT METAL DURING ELECTRIC EROSION

A. S. Zingerman

### Mechanism of the Process of Metal Ejection during Electric Erosion

The phenomenon of electric erosion was discovered a long time ago. Of the many propositions on the mechanism of electric erosion, experimental investigations have confirmed a hypothesis which explains this phenomenon by the action of thermal processes. However, within the framework of the thermal hypothesis there are two basic theories. One theory states that the principal thermal role is played by volumetric sources, i.e., sources which liberate heat in the electrode due to the Joule-Lenz effect. The second theory assumes that the basic heating factor consists of a surface heat source, i.e., the heat is transferred to the electrode from the discharge channel.

The thermal processes in electrodes depend not only on the nature of the heat source, but also on the manner and time of metal removal from the electrode. Zingerman et al. consider the effect of various metal ejection mechanisms on the thermal processes and on electron erosion when a surface heat source is present. The following propositions can be made concerning the mechanism for metal ejection from the electrode. /76

Mechanism No. 1. The heat from the discharge channel is transferred into the electrode. The point of contact between the channel and the electrode surface is heated to the fusion point, and as the metal is fused, it is removed from the electrode in liquid state. The electrode remains solid in the aggregation state.

Mechanism No. 2. During the fusion of the surface layer, the forces which remove the metal are absent. The amount of fused metal in the hole increases. Heat is transmitted to the electrode through a liquid layer of metal. The surface layer of the liquid metal is overheated, but does not reach the evaporation temperature. It is only at the end of the discharge that the molten metal is removed by a single act. The zone of heated metal exists in two aggregate states--liquid and solid.



Mechanism No. 3. The surface layer of the liquid metal is overheated and reaches the evaporation temperature before the discharge has ended. The metal is gradually removed by quiescent evaporation.

Mechanism No. 4. The metal is removed by quiescent evaporation during the discharge. However, at the end of the discharge the accumulated liquid metal is removed in a single act.

Mechanism No. 5. When there is very intense transmission of heat (a sharp front of energy pulses), the propagation of heat inside the electrode due to heat conductivity does not play a substantial role. In this case there is extremely rapid local heating of a small region of the electrode to the evaporation temperature, and the evaporation itself takes on a very vigorous nature, occurring in the form of an explosion.

#### Results of Experimental Verification

Experiments were conducted to determine which of the enumerated mechanisms actually takes place. The results of these experiments are presented below.

Experiments were conducted with energy pulses from 300-4,000 W and a duration of 40-400  $\mu$ . In each series of experiments the power remained constant and the duration was varied. The discharge took place between two steel electrodes: a flat electrode (65 $\cdot$ 45 mm) and a rod electrode with a diameter of 2-4 mm with a hemispherical end. The surface of the electrodes was carefully polished. A gap of 25  $\mu$  was established between the electrodes a few drops of mineral oil were placed in the gap. After each pulse the flat electrode was displaced, while the rod electrode was replaced. The lunes on the flat electrode were measured by a double microscope or a profilograph with graduations of 1  $\mu$ . The measurements obtained from 10-50 lunes under identical conditions were averaged out. The variation in the depth of lunes as a function of pulse duration obtained experimentally with powers of 300-1,870 W are shown in figures 1 and 2, curves 5. /77

In order to compare the experimental data with theoretical conclusions, it was necessary to make the experimental conditions as close as possible to the basic premises in the conclusions. It was shown in reference 2 that when premises 1 and 2 are not strictly satisfied, an error is produced which /78 does not exceed several percent, if the following relationships exist between the depth of the lune  $h$ , its radius  $b$ , pulse duration  $t$  and electrode temperature conductivity  $a$

$$b:h \geq 3 \quad \text{and} \quad b:2\sqrt{at} \geq 1.5.$$

Figure 3 shows the profile of the lunes obtained experimentally, from which we can see that the required conditions are satisfied for steel rods and are not satisfied for brass rods.

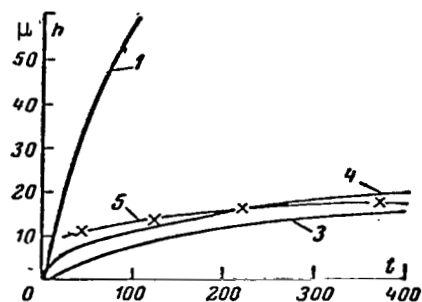


Figure 1. Variation in depth of lunes in steel as function of discharge duration with pulse power of 300 W. 1-4, theoretical curves corresponding to different transport mechanisms; 5, experimental curve.

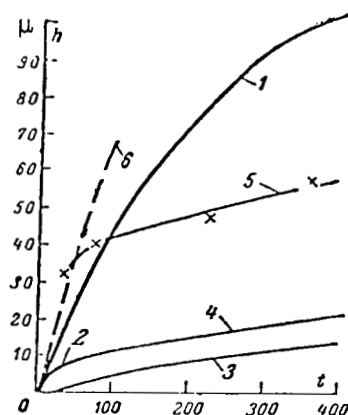


Figure 2. Variation in depth of lunes in steel as function of discharge duration when pulse power is 1,870 W. 1-4, theoretical curves; 5, experimental curve; 6, theoretical curve for mechanism No. 1 when energy ratio of anode to cathode is equal to 3:1.

From the current and voltage oscillograms shown in figure 4 we can see that during the pulse the average power of the source remains constant with an accuracy of  $\pm 4$  percent, which is within the limits of accuracy of the ex-

periment.<sup>1</sup> It is known that the cross section of the discharge channel increases in the course of the discharge. Consequently, the energy density is decreased. Figure 5 shows the variation in the area of the heat source as a function of discharge duration, when the powers are 300 and 1,870 W.

$$\vartheta = \frac{P}{S_0 + ft},$$

<sup>1</sup>A slight drop in the current on the oscillogram is produced by distortion when the oscillograms are taken.

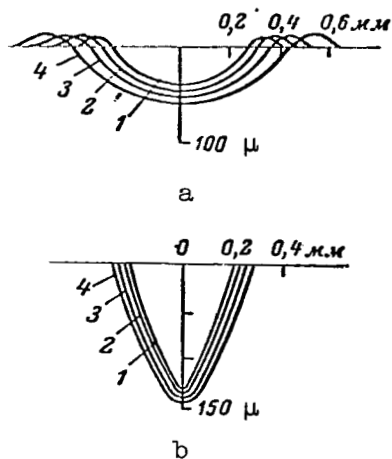


Figure 3. Average values of lune profiles. a, steel electrode, power of 1,870 W, pulse duration 1-40, 2-120, 3-220, 4-370 μsec; b, brass anode, power of 4,000 W, pulse duration 1-60, 2-88, 3-304, 4-357 μsec.

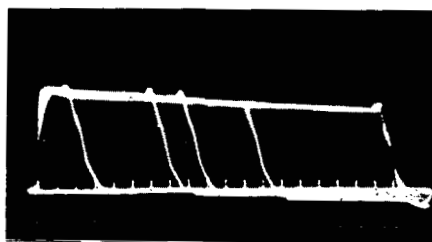


Figure 4. Oscillograms of current (upper curve) and voltage (lower curve) between time markers of 20 μsec.

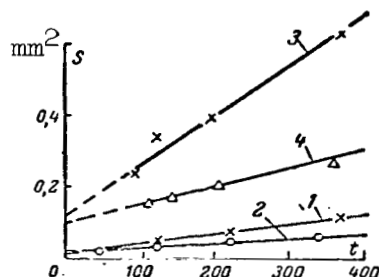


Figure 5. Variation in area of heat source as function of pulse duration. 1, steel, power of 300 W, positive polarity; 2, same with negative polarity; 3, same with power of 1,870 W, negative polarity; 4, brass, power of 400 W, positive polarity.

which does not satisfy four premises. Introducing the corresponding correction we obtain the following expression for the depth of the lune, when mechanism No. 1 is present

$$h_1 = \frac{1.15P}{fq_E\gamma} \lg \frac{S}{S_1},$$

where P is the pulse power;  
 $q_E$  is the enthalpy of 1 g of liquid metal;  
 $\gamma$  is the density of the solid metal; /79  
 S is the area of the source corresponding to time t;  
 $S_1$  is the area of the source when  $t = t_f$  where  $t_f$  is the time required for heating the electrode surface to the fusion temperature; this time may be obtained from the following expression

$$\frac{1}{\sqrt{\frac{S_0}{f} + t_f}} \lg \frac{\sqrt{\frac{S_0}{f} + t_f + \gamma t_f}}{\sqrt{\frac{S_0}{f} + t_f - \gamma t_f}} = \frac{0.87}{P} f (\pi c \gamma \lambda)^{\frac{1}{2}} T_f.$$

where  $S_0$  and  $f$  are determined from figure 5;

$c$  and  $\gamma$  are the specific heat and thermal conductivity of the solid metal;

$T_f$  is the fusion temperature.

Relationships  $h_1(t)$  for pulse powers of 300 and 1,870 W, computed by means of these equations, are shown in figures 1 and 2. The relationships  $h_3(t)$  for mechanism No. 3 were computed in the same manner. In this case the values of  $c$ ,  $\gamma$  and  $\lambda$  are taken to correspond to the liquid metal, while  $T_f$  and  $t_f$  are replaced by  $T_k$ --evaporation temperature and  $t_k$ --the time corresponding to this temperature.

In these cases, the evaporation of the metal from the surface of the electrode begins after 11 and 25  $\mu$ sec. During this time the area of the source does not vary too much. Assuming that it has a constant value during this period of time, the variations  $h_4(t)$  were computed for mechanism No. 4.

All of these variations are shown in figures 1 and 2 and are numbered correspondingly.

The difference between the values  $h_1$  and  $h_3$  or  $h_4$  is very large and /80 lies outside the limits of possible errors in the calculations or in the measurements. This makes it possible to determine the metal ejection mechanism with sufficient reliability.

If we compare the theoretical and the experimental curves, we can draw the following conclusions. In figure 1, curves 4 and 5 differ within the limits of experimental error and calculation error and practically coincide. At the same time, curves 1 and 5 obviously do not coincide, even if we take into account the possible errors. The comparison of curves 3, 4 and 5 shows that with a pulse power of 300 W, the metal from the steel electrode is removed primarily through the mechanism of quiescent evaporation. The small layer of metal, which has been fused before the beginning of evaporation, is ejected in the course of the discharge or at the end of the discharge.

The situation is different when the power is 1,870 W (fig. 2). Neither the first, the second nor the fourth mechanism is clearly shown. The actual process takes an intermediate position. In the course of discharge, there is a gradual ejection of a portion of the metal as some fused layer is /81 accumulated. Therefore, the effectiveness of the process is less than would be produced by Mechanism No. 1, but greater than would be produced by Mechanism No. 4.

Curves 1 are computed on the assumption that 95 percent of the energy liberated in the discharge channel is transmitted to the electron, and that the energy is equally distributed between the electrodes. It is known that at the beginning of the discharge, the anode receives more energy than the cathode. Curve 6 in figure 2 is computed under the assumption that the anode receives 75 percent of the energy, while the cathode receives 25 percent. Under this assumption, during the first 100  $\mu$ sec curve 6 is in fairly good agreement with the experimental curve; apparently at the beginning of the discharge the metal is ejected in accordance with Mechanism No. 1, then the ejection of the metal takes place depending on the accumulations of a certain layer. It is possible that as the discharge is developed further, the decrease in erosion is produced by the redistribution of the energy between the electrodes. In this case the anode must receive approximately 3 times less energy than the cathode.

The experimental data which we have presented and their comparison with theoretical results confirm the dependence of the erosion mechanism on the pulse power. Indeed if the power is increased by a factor of 6, while the duration and other conditions are the same, the volume of the lune increases by a factor of 32, which is difficult to explain by the effect of power alone.

#### Investigations Carried Out by High-Speed Motion Picture Photography

To verify our conclusions and to obtain additional data, high-speed motion picture photography was applied to study the ejection of the metal from the electrodes during electric erosion.

During the motion picture photography, the metallic rod electrode was replaced with a graphite electrode, which was not destroyed in these experiments. The distance between the electrodes was increased to 40-50  $\mu$ .

Visual observations and color pictures showed that metal particles are ejected from the electrode during the discharge. These particles have a white color, which gradually becomes red as the particles move. In addition, there is a luminous zone which surrounds the discharge channel. This zone <sup>/82</sup> masks the tracks of particles which fly through it. However, if the prints are made with long exposures, the luminescence of the zone disappears and the picture shows the track of particles inside the zone. The rod electrode and the discharge channel also become visible. The diameter of the latter is several times less than the diameter of the electrode.

The particles which fly off the steel electrode have a spherical form. The diameter of most of the particles is less than 25  $\mu$ . To measure the particles, the discharge was surrounded with a cylinder in which the particles were collected and then measured. The velocity of ejected particles reached a value of 2,000 m/sec and more. The exposure during the photographing of the particle is equal to the ratio of its diameter to its velocity. Therefore, application of high-speed photography does not make it possible to record the ejected particles. The speed of photography was reduced to 4,000-2,000 frames per sec, and the duration of the discharge was increased to 5-10  $\mu$ sec.

The frames of the high-speed photographs for the ejection of metal from a steel electrode are shown in figure 6. The photographs show a continuous flow of particles. This picture is observed when the pulse power is 1,000 W or more. When the power is 300 W, the ejected particles are not observed in high-speed photographs. However, the investigation of the products of erosion shows that when the pulse duration is 50  $\mu$ sec, 20-30 particles with a diameter of 10 to 30-40  $\mu$  fly out of the electrode; for larger durations there are only 1 or 2 particles. The energy of such a pulse is 0.15 J. When the pulse energy is several tens of J (a power of 15,000-18,000 W), the number of particles with a diameter greater than 10  $\mu$  is of the order of several thousand. When the pulse energy is decreased from 22 to 3 J (power from 18,000 to 2500 W), the volume of all the ejected particles with a diameter greater than 25  $\mu$  is decreased by a factor of 24. For the case of high energy the volume of these particles is 55-65 percent of the lune volume and decreases to 30 percent when the energy is 3 J. At high energy the particles with a diameter greater than 70  $\mu$  constitute 1/2 or even 75 percent of the volume of ejected particles, while at smaller energies they constitute only 25 percent.

Thus high-speed photographs and the investigation of the products of erosion confirm the conclusion that the mechanism of metal ejection depends on the pulse power. At low powers the ejection mechanism is predominately <sup>/83</sup> vaporous (Nos. 3 and 4), while at high powers it is of the liquid-drop type (No. 1).

Figure 7 shows the frames for the ejection of metal from an aluminum electrode. The nature of the metal ejection is the same as in the case of the steel electrode. The same picture is observed in the case of copper electrodes and when the electrodes are made of heat resistant steel.

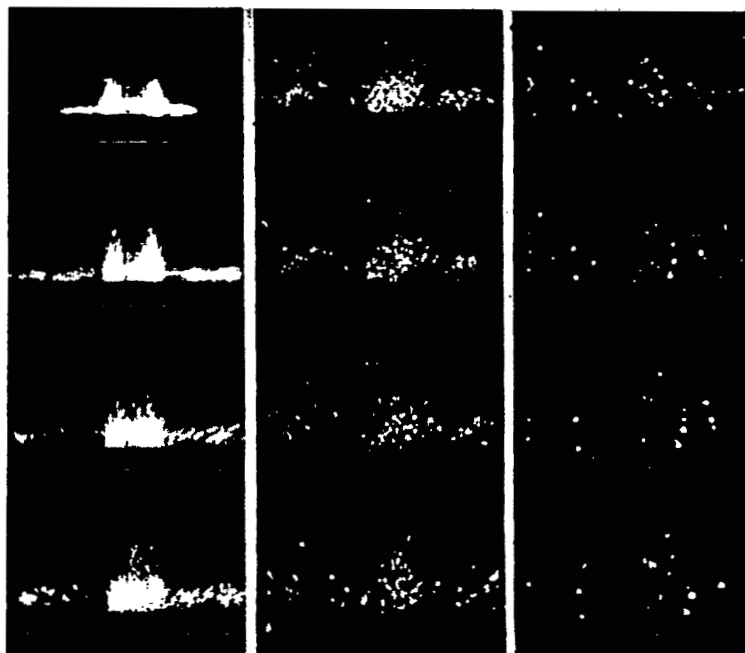


Figure 6. First 12 frames of high-speed motion picture photography showing process of metal ejection from steel electrode.

However, in the case of aluminum and copper electrodes, another picture is also observed: the particles do not fly in a continuous stream, but rather fly out episodically, piece by piece, at long intervals. The number of particles is substantially less, and their dimension is substantially larger.

The high-speed photographs make it possible to measure the velocity <sup>/85</sup> of ejected particles. If at least one of the electrodes has a conic form, the discharge zone is open and the particles fly out with velocities which exceed 2,000 m/sec. When both electrodes are flat, the velocity of the particles flying out of the gap are smaller by 1-2 orders. The photographs showed that before flying out of the inner electrode space the particles undergo multiple collisions and reflections from the electrodes. As a result, not only the velocity, but also the particle size decreases, because during collision the particles frequently break down into smaller particles. Sometimes the large particles temporarily short-circuit the space between the electrodes. As they fly out of the interelectrode space, most of the particles spontaneously break down into smaller particles in the air, thereby producing a bunch of tracks on the photographs.

The high speed photographs also show that, due to their collision and reflection, the particles are retained in the interelectrode space and can fly out of this space after the discharge has ceased. However, when the discharge zone is open, the flight of new particles sometimes ceases long before

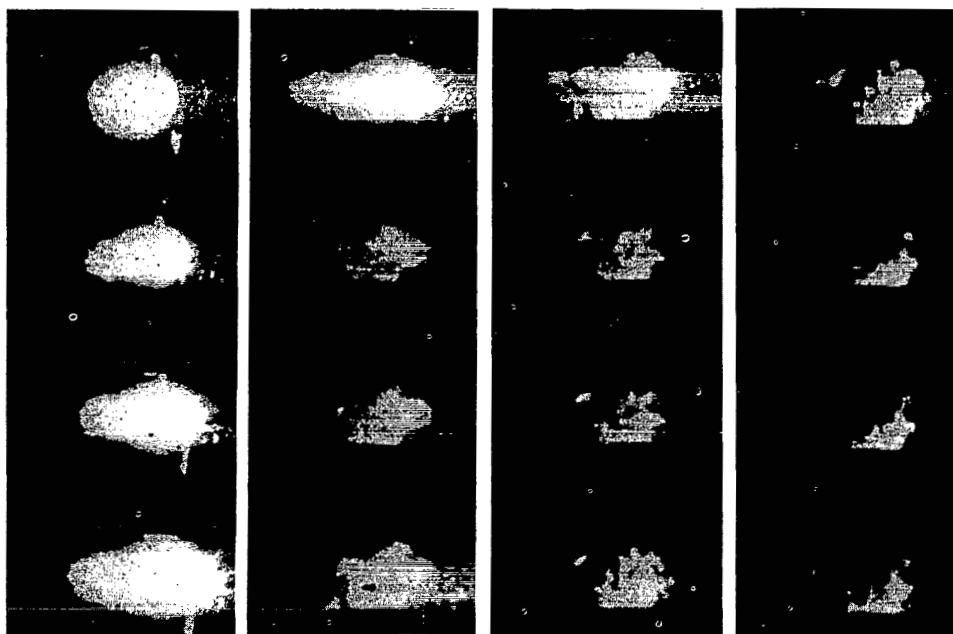


Figure 7. First 12 frames of high-speed motion picture photography showing process of metal ejection from aluminum electrode.

/84

the discharge terminates. This is observed with particular clarity when one electrode is flat and the other is conic. Figure 8 shows the profile of such an electrode and of the lune formed in the steel, when the pulse energy is 55 J. In this case, a bank is formed around the lune whose height is greater than the depth of the lune and the bank conceals the discharge zone. The discharge continues, the particles ejected from the lower electrode are reflected from the upper bank and remain inside the closed space. The volume of the bank achieves a value which is approximately 40 percent of the lune volume. Therefore, the mechanism of bank formation is of practical interest.

#### The Nature of the Forces Which Remove the Metal

The bank may be formed by means of a mechanism which is different from the ones enumerated above. There are facts which indicate that the bank is formed by the gradual continuous ejection of the liquid metal from the lune (this is shown by the wrinkles which exist on the bank slopes). There is a proposition that this pressure may be caused by the action of electrodynamic forces. The axial and radial components of the electrodynamic forces play a different role. The relationship between the components varies in the course of the discharge. At the beginning of the discharge, the axial component of the forces which eject the metal from the lune predominates. In steel electrodes during 15  $\mu\text{sec}$ , and in copper electrodes during 0.15  $\mu\text{sec}$ , the axial

/86



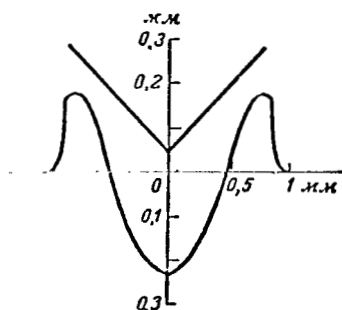


Figure 8. Profile of electrode and of lune in steel when pulse energy is 55 J. Lune is surrounded by high bank.

forces are high, but the volume of the fused metal is small. Toward the end of the discharge, when there is a large amount of fused metal, the axial forces decrease almost by two orders; at the same time the radial forces which inhibit the ejection of the metal increase by the same amount. Thus, it is difficult to explain the formation of the banks by the ejection of the metal produced by electrodynamic forces.

Experimental facts indicate that the role of electrodynamic forces in the ejection of metal is insignificant. This is confirmed by the absence of banks under some conditions and the presence of solidified metal drops along the edges of the lunes. The form of the solidified metal, which has been ejected, confirms the episodic and explosive nature of the forces. Controlled experiments were carried out in which the conditions were varied in such a way that the ejection of the metal did not take place, but the banks were still formed. This shows that the formation of the banks does not take place due to the gradual ejection of the metal.

Further high-speed photographs have made it possible to make the proposition that the banks consist of individual layers formed by the drops of liquid metal, which are reflected for the last time from the opposite electrode.

Thus, the basic mechanism for the ejection of the metal at high powers is of the liquid droplet type. The forces which eject the metal have an episodic and explosive nature, because it is improbable that any other explanation can be obtained for the high velocity of particles which exceeds 2,000 m/sec, when the particles fly out of the lune. This mechanism for the ejection of the metal and the nature of the forces which throw it out may be due to the microscopic heterogeneities. Due to such heterogeneities, the temperature field in the electrodes has a nonmonotonic nature. Due to a pressure which substantially exceeds atmospheric pressure, the metal in such nuclei is heated to a temperature which is substantially greater than the boiling temperature, which finally produces an explosion and an ejection of a small portion of the liquid metal, which is above the explosion nucleus. This nature of the forces which eject metal during electric erosion easily explains all observed experimental facts, such as, for example, the variation in particle size, the distribution of particles and their velocity as a function of pulse energy and power, etc.

#### REFERENCES

1. Zingerman, A. S., Livshits, A. L. and Sosenko, A. B. On The Physical Factors which Determine the Productivity of Electropulse Machining of Metals, in collected works "Electric Pulse and Electric Contact Method of Machining Metals" (O fizicheskikh faktorakh opredelyayushchikh proizvoditel'nost' elektroimpul'snoy obrabotki metallov, v sb. "Elektroimpul'snyy i elektrokontaktnyy sposoby obrabotki metallov"), No. 3, ENIMS, 1962.
2. Zingerman, A.S. The Thermal Theories of Electric Erosion of Metals (Teplovyye teorii elektricheskoy erozii metallov), Izvestiya VUZov, Elektromekhanika, No. 5, 1960.

## COMPUTING THE CONTACT AREAS OF STATIONARY AND SLIDING CONTACTS

I. V. Kragel'skiy, N. B. Demkin and N. N. Mikhin

The investigation performed earlier by the Friction Laboratory <sup>/87</sup> of the Institute of Metal Studies of the AN SSSR on the contact process between two solid bodies has made it possible to obtain design equations for determining the effective contact area of stationary contacts. The nature of contact making (ideal plastic contact, contact with hardening, elastic contact) <sup>/88</sup> determines the nature of the formulas which must be used in the calculations.

Therefore, the first problem in computing the contact area is to clarify the nature of the contact making.

The criteria for contact making may be the ratios of the penetration depth  $h$  to the radius of the roughness  $r$ . Approximate calculations show (ref. 1) that plastic contact occurs when  $h/r \geq 0.01$  for ferrous metals and when  $h/r \geq 0.0001$  for light metals.

Plastic contact predominates during the first loading of the surfaces which are not finished too well, and also when the surfaces slide as they are worn in.

Elastic contact takes place when any surface is loaded again with a force which does not exceed the initially applied force. This is true because during the first loading of well finished surfaces, and also during the sliding of the surfaces, the penetration depth decreases due to hardening. Therefore, we may assume that an elastic contact predominates.

In the case of the plastic contact, the relative contact area may be determined with sufficient accuracy from the equation of Bowden and Tabor (ref. 3).

$$\eta = \frac{q_c}{C\sigma_s}, \quad (1)$$

or, if we let  $C\sigma_s = H_B$  we obtain

$$\eta = \frac{q_c}{H_B}.$$

In this case the contact period does not depend on the roughness of the surface.

When we have an elastic contact of a rough surface with a smooth surface (ref. 2), we obtain the following expression for the relative contact surface.

$$\eta = \left(\frac{b}{2}\right)^{\frac{1}{2\nu+1}} \left(\frac{r}{h_{\max}}\right)^{\frac{\nu}{2\nu+1}} \left[\frac{2,35(1-\mu^2)q_c}{kE}\right]^{\frac{2\nu}{2\nu+1}}, \quad (2)$$

where  $\eta$  is the ratio of the effective contact area to the contour surface;  
 $r$  is the radius of curvature of the apexes of the projections; 89  
 $h_{\max}$  is the maximum height of the roughness;  
 $E$  is Young's modulus;  
 $\mu$  is the Poisson ratio;  
 $q_c$  is the contour pressure;  
 $b, \nu$  are constants which characterize the reference curve;  
 $k$  is the coefficient which depends on  $\nu$  and which is obtained by approximate integration.

The variations in  $k$  as a function of  $\nu$  are shown in table 1.

TABLE 1. TYPICAL VALUES OF  $k$  AS A FUNCTION OF  $\nu$ .

$\nu$	2	3	4	5	6
$k$	0,8	0,67	0,62	0,58	0,55

The contour area is formed by the elastic deformation of the base and may be computed by means of the Hertz equations.

Equation (2) remains valid for the relative contact area of two rough surfaces. In this case, the constants  $\nu$  and  $b$  are determined by means of constants  $\nu_1, \nu_2, b_1, b_2$  of the contact surfaces

$$\nu = \nu_1 + \nu_2; \quad (3)$$

$$b = \frac{k_1 b_1 b_2 (h_{1\max} + h_{2\max})^{\nu_1 + \nu_2}}{h_{1\max}^{\nu_1} h_{2\max}^{\nu_2}}, \quad (4)$$

where  $\nu_1, \nu_2, b_1, b_2$  are constants of the reference curve for the first and second surface;

$h_{1\max}, h_{2\max}$  are the maximum heights of the irregularities for the first and second surface;

$k_1$  is a coefficient which depends on  $\nu_1$ , and  $\nu_2$ .

For  $\nu_1 = 2$   $\nu_2 = 2$ ;  $k_1 = 0.16$ ;  
 for  $\nu_1 = 3$   $\nu_2 = 2$ ;  $k_1 = 0.1$ ;  
 for  $\nu_1 = 3$   $\nu_2 = 3$ ;  $k_1 = 0.05$ .

The value of  $r$  is determined from the following expression

$$r = \frac{r_1 r_2}{r_1 + r_2}, \quad (5)$$

while  $\frac{1 - \mu^2}{E}$  is determined from /90

$$\frac{1 - \mu^2}{E} = \frac{1 - \mu_1^2}{E_1} + \frac{1 - \mu_2^2}{E_2}. \quad (6)$$

The values of  $b$  and  $\nu$  are determined from the curve of the reference surface constructed from polygrams, which reflect the longitudinal and transverse roughness.

The initial part of the curve for the reference surface as a function of clearance is given by the following expression (ref. 4)

$$\eta = b\epsilon^\nu, \quad (7)$$

where  $\epsilon = h/h_{\max}$  is the relative clearance.

We determine  $\eta$  and  $\epsilon$  from expression (7) by substituting the values of  $b$  and  $\nu$  from the initial part of the curve for the reference surface.

Typical values of  $b$  and  $\nu$  for different finishes are shown in table 2.

TABLE 2. TYPICAL VALUES OF  $b$  AND  $\nu$ .

Type of finishing	$\nu$	$b$
Planing, grinding, milling	2	1-4
Polishing	3	4-6
Buffing	3	5-10

The radius of curvature of the roughness apexes is determined from the polygrams by means of the following equation

$$r = \frac{d^2}{8a}, \quad (8)$$

where  $d$  is the length of the protrusion cross section;  
 $a$  is its height.

The design radius of curvature  $r$  is determined from the equation

$$r = \sqrt{r_{\text{longitudinal}} r_{\text{transverse}}}, \quad (9)$$

where  $r_{\text{transverse}}$  and  $r_{\text{longitudinal}}$  are the radii of curvature of the roughness determined from the polygrams taken in the longitudinal and transverse directions with respect to the direction of the relative displacement. /91

The approximate values of the radii of curvature for different finishes are shown in table 3.

If we substitute the most typical values of  $b$ ,  $r$  and  $v$  in equation (2), we obtain the following expression for the approximate evaluation of the contact surface when two buffed surfaces make an elastic contact

$$\eta = 3.4 \left( \frac{q_c}{Eh_{\text{max}}} \right)^{10/11} \quad (10)$$

Since equation (2) contains several quantities which are determined experimentally, an error in their determination is inevitable. The effect of the error in the determination of  $b$ ,  $v$ ,  $h$  and  $r$  on the accuracy of determining the actual contact surface is shown in table 4.

TABLE 3. APPROXIMATE VALUES OF THE RADII.

Type of finishing	$r, \mu$
Polishing	30-40
Buffing	300-500
Finished with abrasive cloth	10-15

TABLE 4. THE EFFECT OF THE ERROR IN DETERMINING THE PARAMETERS.

Measured quantity	Measurement error, in %	Error in area $\frac{\Delta\eta}{\eta} \cdot 100\%$
$b$	30	4
$r$	30	12
$h$	30	12
$v$	30	15

The equations which we obtained determined the actual contact surface during static loading. We must now determine whether we can apply them when the surfaces slide. Obviously, they will be valid in the case when the effective contact area during sliding does not change significantly from the contact

area during the stationary state. However, there are different points of view concerning the relation between contact surfaces for sliding contacts and stationary contacts.

According to the investigations of L. S. Kokhan, during the elastic <sup>/92</sup> contact of a long cylinder with a plane surface the area of the effective contact, when normal and tangential forces are present, is actually determined only by the action of the normal forces

$$A = A_0(1 + 0.5f^2), \quad (12)$$

where  $A_0$  is the area of the contact which is subjected only to a normal load;  
 $f$  is the friction coefficient.

When  $f = 0.3$ , the area increases only by 5 percent.

Investigations for the same case carried out by Saverin (ref. 5) also showed that there was an insignificant increase in the contact surface.

In the case of a plastic contact, according to the opinion of a series of investigators (refs. 6 and 9), we should expect a substantial increase in the contact area during sliding compared with the area increase in the stationary state. Thus, Tabor (ref. 6) obtained the following relation between the touching surfaces

$$(1 + \alpha f^2) = (A/A_0)^2, \quad (13)$$

where  $\alpha$  is an empirical coefficient which has been assigned different values by various authors.

According to the experimental data of Tabor and McFarlan (ref. 6)  $\alpha = 3.3$ .

Courtney-Pratt and Eisner (ref. 7) assumed that

$$\alpha = 11.6.$$

For the axially symmetric model of unit roughness Tabor (ref. 8) obtained the value of  $\alpha = 25$ .

Aynbinder (ref. 9) obtained the value  $\alpha = 27$  theoretically.

When  $f = 0.3$ , we obtain a relation between the contact surfaces for different values of  $\alpha$ , which are shown in table 5.

We conducted investigations to clarify the variation in the effective contact area during sliding for the case of elastic and plastic contacts.

TABLE 5. THE EFFECT OF TANGENTIAL STRESS ON THE CONTACT AREA.

/93

Type of contact	Source	$\alpha$	$\frac{A}{A_0} \cdot 100\%$
Plastic Contact	According to the data of McFarlan and Tabor (ref. 6)	3.3	114
	According to the data of Courtney-Pratt (ref. 7)	11.6	143
	According to the data of Tabor (ref. 8)	25	180
Elastic Contact	According to the data of Aynbinder (ref. 9)	27	185
	The variation in the contact surface during elastic contact	$1 + 0.5f^2$	105

We should point out that in considering the relation between the contact surfaces for the sliding state and the stationary state, it is necessary to take into account the fact that during the initial stages of the friction process the surfaces are worn in, which changes their geometry, whereas in the case of surfaces which have already been worn in, the geometry remains unchanged. Therefore, for sliding contacts we must distinguish between two stages:

- (1) the sliding of surfaces which are not worn in when the microgeometry changes during the friction process;
- (2) the sliding of worn-in surfaces when the microgeometry does not change.

In the first case,  $A_r$  varies until a roughness is established which is typical for the given friction conditions. In this case the variation in the effective contact area is explained not only by the variation in the stressed state, but also by the variation in the temperature and the nature of micro-roughness destruction. In the second case, the microgeometry has become established, and the variation in the contact surface may occur only during displacement by a distance equal to the diameter of the contact spot. After this the single contact is destroyed and the formation and destruction of contacts is repeated.

Two special devices were constructed to investigate this phenomenon: the first was used to measure the contact area directly, the second was used to measure the contact area indirectly.

The first device, which measured the total contact area directly, used an optical method based on the disruption of the total internal reflection /94 of a glass prism at the point of contact with the rough surface. The schematic diagram of this device is shown in figure 1. A beam of light from source S falls on glass prism 6 and undergoes complete internal reflection at the horizontal boundary. After this it falls on photocell  $\phi$ , which is connected



to a photometric scheme. At the contact points, depending on the nature of the contact material, the light is completely or partially absorbed, so that these spots appear dark on a mirror background in the reflected light.

Sample 1 is secured in ring 2 which can rotate around the stand serving as its axis. Ring 2 can also be displaced along axis 4 from the top down. The tangential force is applied to flat spring 3, whose flexure shows the effect of the friction force. Thus sample 1 may be displaced without bending along prism 6 and be subjected to a normal load. The possible error in the vertical loading due to the bending of the coupling rod is less than 2 percent. At first, the sample was loaded only with a vertical force and the contact area was photographed; after this it was displaced slightly and a photograph was taken again. Then, as the load was increased, the contact area was measured by means of a planimeter. In determining the contact area of a rubber sphere, the variation in the contact area was obtained from the increase in the contour contact area. The results of the experiments for the elastic and plastic contacts are shown in table 6.

TABLE 6. THE EFFECT OF DISPLACEMENT ON THE CONTACT AREA.

/95

Type of sample	Test pair	Nature of contact	Displacement, in $\mu$	Vertical loading, in kg	Friction coefficient	Contact area, in $\text{mm}^2$		$A/A_0$
						Before displacement	After displacement	
Sphere	Rubber-glass	Elastic	30	0.538	0.6	60.5	66.3	1.09
				0.668	0.6	99.0	101	1.02
				0.856	14	141	144	1.02
Plane	Copper-glass	Plastic	30	40	0.2	4.00	4.45	1.12
				100	0.2	9.9	10.5	1.06

If we compare the contact area in the stationary state, when only vertical forces are acting, with the area when tangential and vertical forces act, we can see that the effective contact area during displacement by approximately the diameter of the contact spot is insignificantly greater than the area of

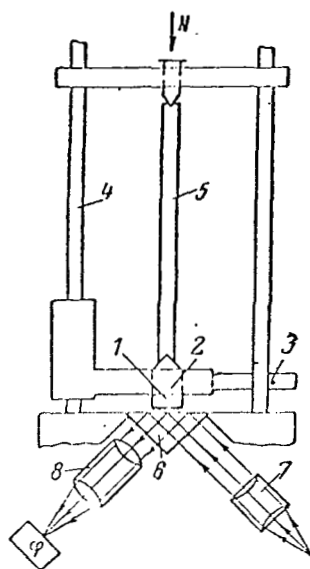


Figure 1. Diagram of device for direct measurement of contact surface.

1, sample; 2, ring; 3, flat spring; 4, stand; 5, coupling rod; 6, glass prism; 7, condenser; 8, lens.

the contact in the stationary state. Thus, for example, during elastic contact of rubber with the prism, when it slides under a load of 628 g ( $f = 0.6$ ), it increases only by 10 percent compared with the stationary state (figs. 2a and b).

In the case of a plastic contact, when a copper sample is displaced along the prism by the width of the contact spot and when it is subjected to a load of 20 kg/wt ( $f = 0.2$ ), the contact surface does not increase by more than 5 percent.

In order to determine the effect of displacement on the area of a single contact of two metallic surfaces, experiments were conducted to investigate the variations in the surface of a single irregularity.

The experiments were conducted by means of the setup shown in figure 3. The contact area of a single micro-irregularity of a copper surface in contact with the Ioganson plate 1 was measured. Ioganson plate 1 is secured in carriage 2, which can be displaced in guides 3 by means of a motor. The upper sample 4 is placed in frame 5, which is secured to flat screen 7. The frame has an area which holds the weights to produce a normal loading.

/97

Needle 8 is secured to the frame, and the graduation line on this needle is observed with the microscope. Movable carriage 2 also has a needle 9, whose end is placed in the same plane with needle 8, so that both needles can be observed simultaneously in the microscope. String 11 is used to apply a uniform load and is placed under tension by a Warren motor. The experiments were conducted in the following manner. Sample 4 was secured to frame 5 and a normal load was applied; after this the frame was removed and the contact area was photographed. Then the frame was installed again, the load was applied and carriage 2 with the Ioganson plate was displaced. By observing the displacement of the graduation lines on needles 8 and 9 from the scale of the optical micrometer of the microscope, it is possible to measure the relative displacement of samples 4 and 1 and to evaluate the deformation of spring 7 from the displacement of needle 8. Spring 7 is calibrated beforehand, and the effect of the friction force is established from its deformation. After the samples are displaced, the frame is removed and the contact area is again photographed. The dimension of the contact area is measured <sup>/98</sup> from the photograph by means of a planimeter. When the displacement was equal to the diameter of the contact area, the contact area increased by 3-7 percent. With additional sliding, the area again increased by a small amount. The increase in the area as a function of displacement is shown in figure 4.

The substantial increase in the contact area during additional sliding is apparently explained by the wearing-in of the micro-irregularity associated with reforming or elimination of the material.

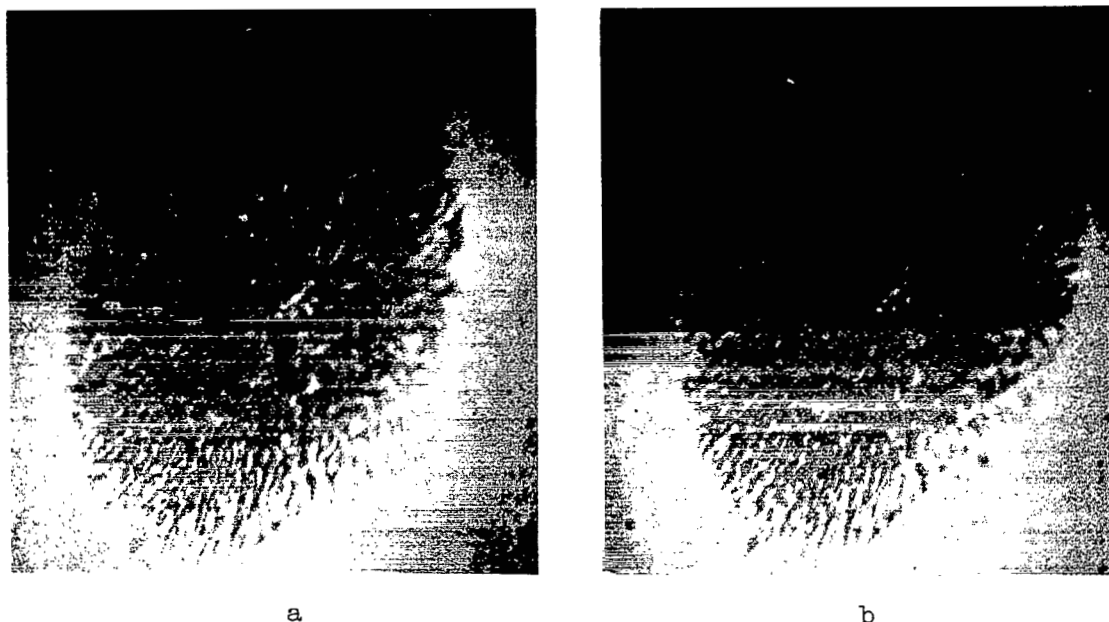


Figure 2. Contact of rubber with glass prism. a, before displacement; b, after displacement. Vertical load  $N = 628$  g/wt, friction coefficient  $f = 0.6$

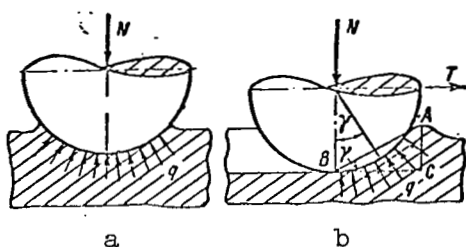


Figure 5. Diagram showing contact of single irregularity in stationary state (a) and in presence of slipping (b).

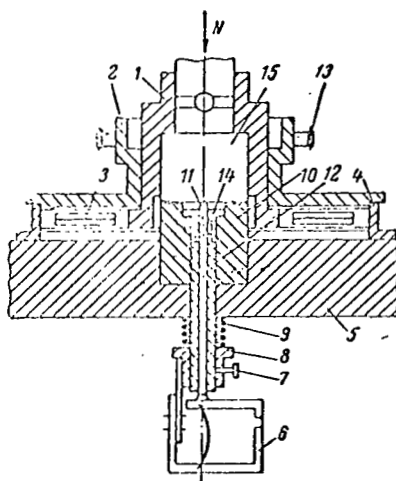


Figure 6. Diagram of device for measuring simultaneously approach and friction force. 1, cross-piece; 2, moving ring; 3, sensor for measuring friction force; 4, stationary ring; 5, base plate; 6, frame with sensors for measuring approach; 7, stop screw; 8, sliding cylinder with frame; 9, lower sample; 10, spiral spring; 11, pusher; 12, tube; 13, gear drive; 14, nut; 15, upper sample.

Rotation is imparted to the upper sample from the moving ring /101 through four plate springs 3, which contain the sensors for measuring the friction force. The load is applied to the upper sample by means of a dynamometer (not shown in the drawing) and can be varied from 200 g to 200 kg.

The approach was measured by means of pusher 11 and an elastic small beam with cemented sensors. In order to make calibration convenient, the small beam was inserted into frame 6.

TABLE 7.

Material	Vertical loading, in kg	Approach, determined experimentally		Theoretical approach during motion
		Static values	Experimental value during motion	
U-10 steel, 6th class of purity	20	1.7	1.97	2.4
Aluminum 6th class	40	2.43	2.50	2.76
	60	3.2	3.55	3.62
Magnesium, 6th class	20	1.8	2.05	2.3
	40	2.3	2.62	2.65
U-10 steel, 6th class	60	2.67	3.05	3.14

To eliminate the error produced by the deformation of the lower sample 10, which is installed on plate 5, the frame, attached by means of slipping cylinder 8 and bolt 7 on tube 12 containing nut 14 with a collar, was suspended on the lower sample. To eliminate the error produced by the clearance between the collar and the ring groove of the lower sample, the collar is held in the groove by the pressure of spiral spring 9. With this construction we can measure the approach with an accuracy of  $0.03 \mu$  and only measure the deformation of the surface.

The signals showing the friction and the approach are recorded /102 simultaneously on moving photographic paper. The experiments confirm the proposition that at the beginning of the displacement the approach must vary. During the time of this variation, there is a redistribution of elementary areas of contact in the contact zone.

A typical oscillogram showing the variation in approach during the displacement for contact of U-10 steel with aluminum at a load of 20 kg/wt is shown in figure 7.

Results obtained during the making of contacts between a hard material and a soft material: magnesium, cadmium, aluminum, Armco-iron, make it possible for us to assume that during the displacement of a plastic contact the increase in the contact surface should be insignificant (e.g., it should be of the order of 10-15 percent).

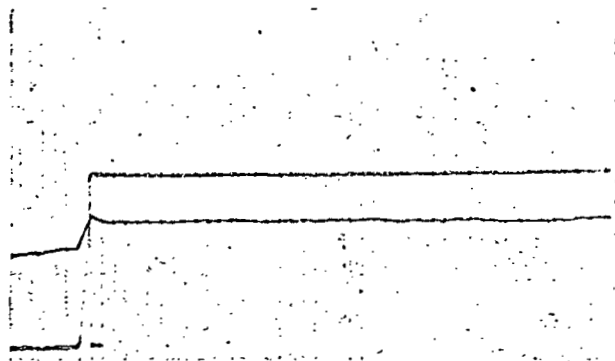


Figure 7. Variation in approach during displacement. Contact materials were: U-10 steel, heat treated to a hardness of  $H_B = 360 \text{ kg/wt/mm}^2$ , 6th class of purity;

aluminum, 6th class of purity ( $H_B = 30 \text{ kg/wt/mm}^2$ )

the vertical force was  $N = 40 \text{ kg/wt}$ , friction coefficient  $f = 0.28$ .

## Conclusions

1. Under actual conditions, in most cases, when contacts are well worn in, we have elastic contacting; in this case, for approximate calculations of stationary as well as sliding contacts we may use the following equation, which was obtained theoretically and confirmed experimentally

$$\eta = 3.4 \left( \frac{q_c}{Eh_{\max}} \right)^{10/11}.$$

2. For a plastic contact, we may use the equation derived by Bowden and Tabor

$$\eta = \frac{q_c}{H_B}.$$

## REFERENCES

1. Kragel'skiy, I. V. The Conditions of Material Deformation on Friction Surfaces, in collected works "Dry Friction" (Ob usloviyakh deformirovaniya materiala na poverkhnostyakh treniya, v sbornike "Sukhoeye treniye"). Izd-vo AN Litovsk SSR, 1961.

2. Demkin, N. B. The Actual Contact Area During Static Loading and During Start-Up (Fakticheskaya ploshchad' kasaniya pri staticheskom nagruzhении i pri trogании). Izvestiya VUZov, No. 4, 1962.
3. Bowden, F. P. and Tabor, D. Friction and Lubrication of Solids, Oxford, 1950.
4. Kragel'skiy, I. V. The Contact Area of Rough Surfaces, in collected works "Electric Contacts" (Ploshchad' kasaniya sherokhovatykh poverkhnostey, v sbornike "Elektricheskiye kontakty"). Gosenergoizdat, 1958, Demkin, N. B. and Kragel'skiy, I. V. The Effect of Roughness and Material Properties on the Contact Area during Elastic Contact, in collected works "Electric Contacts" (Vliyaniye sherokhovatosti i svoystv materiala na ploshchad' kasaniya pri uyrugom kontakte, v sbornike "Elektricheskiye kontakty"). Gosenergoizdat, 1960.
5. Saverin, M. M. The Contact Durability of Material Subjected Simultaneously to a Normal and Tangential Loading (Kontaktnaya prochnost' materiala v usloviyakh odnovremennogo deystviya normal'noy i kasatel'noy nagruzok). Vol. 1, Mashgiz, 1946.
6. McFarlan, A. and Tabor, D. Proc. Roy. Soc., Vol. 202, No. 1069, p. 244.
7. Courtney-Pratt, I. S. and Eisner, E., Proc. Roy. Soc., Vol. 238, No. 1215, p. 529.
8. Tabor, D. Proc. Roy. Soc., Vol. 251, No. 1266, p. 378.
9. Aynbinder, S. B. The Contact Area between Rubbing Surfaces (O ploshchadi kontakta mezhdu trushchimisya poverkhnostyami). Izv. AN SSSR, OTN, "Mekhanika i Mashinostroyeniye," No. 6, 1962.

# ENERGY LOSSES IN CLOSING CONTACTS MEASURED BY MEANS OF AN OSCILLOGRAPH

V. S. Pellinets

When a circuit containing a capacitor C and a load resistance R (fig. 1) is closed, part of the energy is liberated at the contacts 3. Energy losses in the contacts lower the efficiency of the circuit, limit the rate of energy introduction to the load and, what is most important, destroy the contacts. To evaluate these losses and to find a way of decreasing them, two series of oscillographic measurements were taken. The processing of experimental data obtained has made it possible to express the functions of the transitional resistance in the form of a hyperbola with constant coefficients obtained statistically. At the same time, several unusual phenomena were established, in particular the independence of losses as a function of contact material and contact finish. /103

## Experimental Methods

It is known from data published in the literature (refs. 1-3) that a series of phenomena takes place when electric contacts close: there is a normal or "short" arc, various forms of conductance through surface films, "spilling" resistance associated with the small area of actual contact and others. /104 The relative role of each process is not constant and depends on a large number of factors--initial voltage, presence of films on contact surfaces, switching rate, etc. For this reason, it was desirable to measure not the characteristics of individual processes, but the total value of the instantaneous relative losses of power  $p$  as a function of time

$$p(t) = \frac{n_c}{n}, \quad (1)$$

where  $n_c$  is the power dissipated at the contacts;

$n$  is the total power dissipated in the circuit.

The function  $p = p(t)$  makes it possible to find the equivalent transitional resistance (commutation function)

$$r_c(t) = R \frac{p}{1-p}, \quad (2)$$



which may characterize a given contact from the standpoint of energy loss when a capacitive circuit is closed. The losses were determined by taking oscillograms of voltage at the contacts and of the voltage at the load. Measurements were taken with periodically closing contacts and with single closing of the contacts. The schematic diagram of the setup used in the first case is shown in figure 2. Capacitor  $C$  is discharged periodically through contact 3 of the RP polarized relay through resistance  $R$  and is charged through resistance  $R_3$  from battery  $B$ .

The voltage curve is photographed from the screen of the IO-4 oscilloscope, which is connected successively to contacts 3 and resistance  $R$ .

The diagram of the setup used for single closing of the contacts (fig. 3) provides for simultaneous measurement of voltage across contacts  $K_3$  and load  $R$ . Capacitor  $C_5$  is charged through large resistance  $R_7$  and  $R_8$  from battery  $B$ . The closing of the contacts is accomplished by means of electromagnet  $EM_1$ , which is excited by auxiliary capacitors  $C_1$  and  $C_2$ .

The scan of the OK-15M oscilloscopes was triggered by the voltage from the contacts through short lines  $L_2, L_3$ ; the measured voltages were fed to the deflection plates through cable sections  $L_1, L_4$ , which produced a /105 delay of approximately  $1.3 \mu\text{sec}$ . The lines were not matched, because the reflected signal is substantially delayed and does not arrive until the process is over.

In each case the closing of the contacts was made at a new point on the surface of the electrodes.

The contacts were manufactured 6-8 months before the measurements were taken and were stored under room conditions.

Measurements were taken in the range 24 to 1,000 V with capacitors from 0.1 to 80 mfd, using contacts made of the following materials: silver, German silver, stainless steel, tin-plated brass. The purity of the surface finish varied from  $V_4$  to  $V_9$ , the load resistance varied from 0.1 to 25 ohms. The contact closing rate and the inductance of the circuit were also measured. Observation time varied from 0.5 to  $5 \mu\text{sec}$ .

The curves for  $p(t)$  and  $r_c(t)$  (fig. 4) were constructed from the oscillograms.

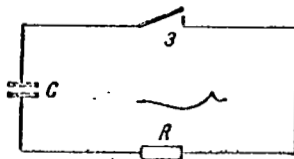


Figure 1. Diagram of capacitor circuit.

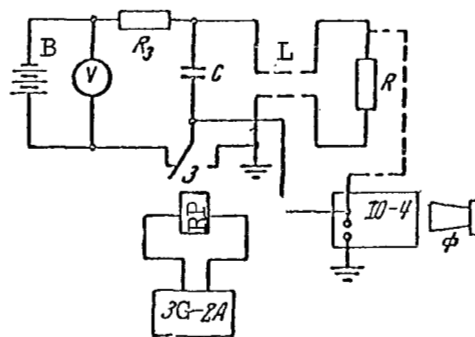


Figure 2. Oscilloscope measurements of energy loss in closing contacts.

#### Form of the Commutation Function and the Variation in the Transitional Resistance as a Function of Various Factors

The curves for the transitional resistance as a function of time, obtained in different experiments, have a substantial spread, which has made their analysis possible only with the aid of statistical methods. Nevertheless the shape of the curves in all cases makes it possible to approximate them by means of a hyperbola with a positive or negative constant component (in the latter case the approximation is valid in the range of positive values of  $r_c$ ). Thus, the commutation function has the following form /107

$$r_c = \frac{\beta'}{t} \pm \gamma, \quad (3)$$

where  $\beta'$  is the loss coefficient, microhenries ( $\mu H$ )  
 $t$  is the time;  
 $\gamma$  is a constant component.

To compare the results obtained in different cases, it was convenient to reduce expression (3) to the form

$$r_c = \frac{\beta}{t}, \quad (4)$$

where coefficient  $\beta$  is obtained from the values of  $\beta'$  and  $\gamma$  under conditions that the energy losses are equivalent over a certain period of time, when they are determined from equations (3) and (4).

The value of the transitional resistance depends substantially on the load resistance and the switching rate. The value of parameter  $\beta$  in the range /108



of switching velocities from 0.1 to 0.5 m/sec decreases on the average by a factor of 2.1. The variation  $\beta = \chi(R)$  is not regular; therefore, the qualitative data presented later pertain to values of R from 10 to 25 ohms.

In all cases the value of loss parameter  $\beta$  does not depend on the capacity or on the initial voltage in the specified range. However, the greatest paradox was the absence of a relationship between the losses and the electrode materials (of those mentioned before) and the purity of the surface finish. A repetition of the experiments using different combinations of a parameter confirmed the earlier results.

This unexplained phenomenon is apparently due to the special nature of the processes which take place when a capacitative circuit is closed.

When an inductance greater than 3-5  $\mu\text{H}$  was introduced into the circuit, there was a noticeable increase in perimeter  $\beta$ .

### The Quantitative Nature of the Losses

Parameter  $\beta$  may be evaluated quantitatively from experimental data for a circuit whose inductance is not greater than 3  $\mu\text{H}$ , whose closing rate is approximately 0.1 m/sec and whose load resistance varies from 10 to 25 ohms. The other parameters and states are in the range indicated above. For this case the distribution curve for the parameter may be expressed by the modified III Pearson function of the form

$$y \approx 3.6 \cdot 10^{16} x^{3.37} e^{-39.296 x^{\frac{1}{8}}}.$$

For convenience, limits of the quantity  $\beta$  in table 1 are presented for certain values of s (the probability that the value of  $\beta$  will not fall outside the stated limits).

By using the data given in table 1 and by using equation (4), we can find formulas for computing the basic energy characteristics of the capacitative circuit.

Thus the expression for energy  $W_\tau$ , liberated during time  $\tau$  in load R, may be obtained by substituting the value of  $r_c$  into the differential equation of the equivalent circuit (fig. 5), which is solved with respect to the energy /109

$$\begin{aligned} \frac{W_\tau}{CE^2/2} = & \frac{1}{\alpha-1} \left\langle (1+\delta)^{\alpha-1} e^{-\alpha\delta} [2(1+\delta) - \alpha\delta] - \right. \\ & - 2 + \left( \frac{e}{\alpha} \right)^\alpha \Gamma(\alpha+1) \{ P[2\alpha, 2(\alpha+1)] - \\ & \left. - P[2\alpha(1+\delta), 2(\alpha+1)] \} \right\rangle, \end{aligned} \quad (5)$$

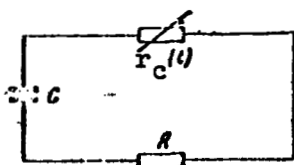


Figure 5. Equivalent scheme for carrying out calculations.

where  $\Gamma$  is the Gamma function;  
 $P$  is a probability function of two variables (the arguments are shown in square brackets);

$$\alpha = 2\beta/CR^2.$$

$$\delta = Rl/\beta.$$

In the same way we can find the expression for the relative energy losses during the time interval  $\tau$

$$\frac{W'_\tau}{W_\tau + W'_\tau} = \frac{1 + \alpha - (1 + \delta)^{\alpha-1} (1 + \alpha + \delta) - \left(\frac{e}{\alpha}\right)^\alpha \Gamma(\alpha + 1) \times}{(\alpha - 1) [1 - e^{-\alpha\delta} \times \dots \rightarrow} \quad (6)$$

$$\leftarrow \dots \times \{P[2\alpha, 2(\alpha + 1)] - P[2\alpha(1 + \delta), 2(\alpha + 1)]\} \times (1 + \delta)^\alpha,$$

where  $W'_\tau$  is the energy dissipated by the contacts during the time  $\tau$ .

TABLE 1.

Probability S	Value of $\beta$ in $\mu\text{H}$	
	Minimum	Maximum
0.5	0.88	0.88
0.9	4.3	0.16
0.99	15.0	0.035
0.999	35.0	0.012
0.9999	68	0.046
0.99999	120	0.0018

Although the experimental results were obtained for limited time intervals, the comparison of calculations, carried out by means of equations (5) and (6) with experimental data obtained when losses were measured during the period of the total capacitor discharge, show that equations (5) and (6) /110 may be used to compute the total relative losses within the limits of the approximation. In this case they can be transformed in the following manner

$$\frac{W'_{\infty}}{CE^2/2} = \left\{ 1 + a - \left( \frac{e}{a} \right)^a \Gamma(a+1) P[2a, 2(a+1)] \right\}. \quad (7)$$

For practical cases the total relative losses vary in the range 3-50 percent. When the rate of contact closure is higher than 10-20 m/sec, the losses are quite small.

## Conclusions

Experiments on the oscilloscope measurement of losses in closing contacts has helped us to find an expression for the commutation function, enabling us to evaluate the energy characteristics of specific circuits for a specified range of parameters and states.

The discrepancy in the values of the energy computed by means of equation (5) and experimental results in the range 25 to 1,000 V was not greater than 35 percent, which should be considered the characteristic error of the data presented above.

## REFERENCES

1. Holm, R. Electric Contacts (Elektricheskiye kontakty). Izd-vo I.L., 1961.
2. Yelinson, M. I. and Vasil'yev, G. F. Natural Electron Emission (Avtoelektronnaya emissiya). Fizmatgiz, 1958.
3. Atalla, M. M. Arcing of Electrical Contacts of Telephone Switching Circuits. Bell System Technical Journal, Vol. 32, Nos. 5 and 6, 1953; Vol. 33, No. 3, 1954; Vol. 34, Nos. 1 and 5, 1955.

## TRANSIENT CURRENTS AND VOLTAGES WHICH OCCUR IN BREAKING CONTACTS IN A LOW VOLTAGE dc INDUCTIVE CIRCUIT

B. Ye. Kravchuk

The transient process which occurs in a switched circuit and at the /111 contacts is characterized by transient current and transient voltage. The transient current and voltage at the contacts determine the nature of contact destruction.

A large number of factors affects the transient currents and voltages, including the nature of the gas discharge process occurring at the breaking contacts. Attempts have been made to solve such problems analytically. In these approaches the transitional resistance between the contacts was approximated by a suitable function of time (refs. 2, 5 and 6). However, these solutions have no significant practical value.

To date, the processes associated with the breaking arc can be studied objectively and in detail only by means of the physical experiment.

This report presents the results of investigating the effect of several factors on transient currents and voltages. We should point out that for a more or less detailed investigation of this problem the properties and characteristics of the test setup are of prime importance. Until quite recently such investigations were carried out by means of galvanometer oscillographs, which did not always have the necessary frequency characteristics. The results presented in this report were obtained in simple series dc inductive circuits (fig. 1) with 28 and 120 V, using standard switches. Various two-beam oscilloscopes were used to record currents and voltages. This provided recordings without substantial distortions.

Analysis of numerous current and voltage oscillograms has made it possible to establish their typical form (fig. 2). The process of voltage variation may be divided into 4 stages: I, II, III and IV (fig. 2). /112

During stages I, II and III, the current decreases to 0 and the circuit is discharged. Stage IV takes place when the circuit is disconnected and is associated with the reestablishment of the voltage at the open contacts. During the first stage the contacts open and all of the processes associated with the breakdown of the liquid bridges and the formation and elongation of the arc take place. This stage always takes place for any disconnected currents, inductances and switching equipment, etc. The physical picture of the processes which take place in the first stage has been investigated sufficiently well, and the results of these investigations are contained in the proceedings

of the two preceding conferences (refs. 9 and 10) and in other works (refs. 7 and 8). This stage of the transient process is associated with the time during which the contacts of the switching equipment come apart. It is known, for example, that for low voltage switches the time of contact separation /113 is of the order of 0.5-1  $\mu\text{sec}$ .

After the moving contacts stop and a maximum distance is established between the contacts, the second stage of voltage variation begins. We note that when the surrounding conditions are unchanged, the voltage at the beginning of the second stage is more or less constant for fixed voltages of the system. This stage is characterized by a sufficiently slow increase in voltage, which approximately follows the linear law. During this time the current continues to decrease. The duration of this stage is determined by the energy supply in the switched circuit, and varies when the latter varies. As we know, the energy supply in this case is determined by the inductance of the circuit and by the square of the current.

The third stage represents the final stage of arc quenching. In this stage the current breaks off and the processes which characterize the electric opening of the circuit are concluded. A further change in the voltage between the contacts is associated with the oscillations of the voltage in the load and with reestablishment of the voltage across the open contacts. Voltage oscillations occur due to the presence of inductance and distributed capacity in the load. After the current breaks off, the voltage continues to increase across the capacitance. The voltage reaches a maximum value, and the oscillatory process begins involving the drop in voltage to its nominal value.

Investigation of arc burning stability has shown that the arc is always quenched if the static volt-ampere characteristic is above the straight line  $U_b - iR$ .

By analyzing the photographs of many processes we arrive at the following conclusions:

(1) the inductance of the open circuit and the nominal current produce an effect on the nature of transient voltage variation;

(2) stage II is absent for currents up to  $i_L \leq 10-15$  A; when  $i > 15$  A, Stage II appears and is developed with time;

(3) lowering of the air pressure which surrounds the contacts causes the appearance of Stage II at smaller currents than stated above;

(4) as the value of the nominal current increases, a slight /114 decrease in the arc voltage is observed in the circuit;

(5) for a given contact gap and fixed conditions the duration of the electric breaking of the circuit does not depend on the displacement rate of the contacts.



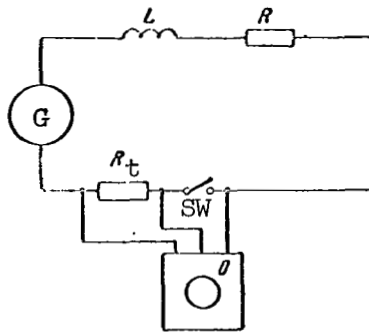


Figure 1. Diagram of circuit.  $L$ , inductance;  $R$ , circuit resistance;  $R_t$ , test resistance;  $O$ , oscilloscope;  $G$ , generator;  $SW$ , switch.

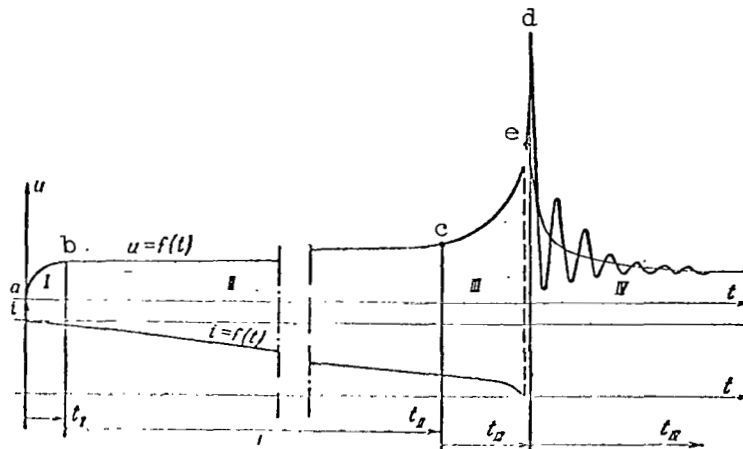


Figure 2. Typical pictures:  $i_d = f(t)$  and  $U_t = f(t)$ .

The duration of voltage variation over the first region  $t_I$  for the cases investigated is almost equal to the contact separation time  $t_{CS}$ . For currents  $i_L \leq 2 \text{ A}$   $t_I \approx 1 \text{ msec}$ . For  $i_L > 2-5 \text{ A}$   $t_I \approx 2-4 \text{ msec}$ . The duration of the second region is variable and its special evaluation is required in the future. The duration of the third region is sufficiently constant for many cases, and is equal to  $t_{III} \approx 4-8 \text{ msec}$ . When the currents are very small,  $t_{III}$  decreases. In this case it is more difficult to break the process down into the indicated regions.

The true (dynamic) volt-ampere characteristics of the arc differ substantially from the static characteristics (fig. 3). We should note that the presence of horizontal regions on these characteristics and their duration are determined not by the velocity of contact displacement, but by commutation conditions and apparently are determined first of all by conditions of heat transfer from the arc.

From this it follows that the total duration of the electric contact breaking process consists of the sum of the duration of each region

$$t_b = t_I + t_{II} + t_{III}. \quad (1)$$

By using a large amount of experimental data, we made an effort /115 to establish a relation between time  $t_b$  of circuit breaking and various factors.

For this purpose, we constructed graphs (fig. 4) which show the values of  $i_L$  plotted along the axis of the abscissas to a logarithmic scale and the values  $t_b / i_L^2$  along the axis of the ordinates. All experimental points are situated on straight lines, and these lines have different slopes for different nominal circuit voltages. In addition, when the inductance becomes larger, the curves move up. For different switches when the circuit inductances remain the same, the straight lines move down as the contact gap increases.

As a result of approximating the curves by straight lines, we can arrive at the following expression

$$\frac{\ln i_L}{a} + \frac{\ln t_b / i_L^2}{b} = 1 \quad (2)$$

and by carrying out an algebraic transformation, we obtain /116

$$t_b = e^{b/a} i_L^{2a/b} = k_t i_L^{\alpha_1}, \text{ sec.} \quad (3)$$

We see that the time of electric breaking is proportional to some coefficient  $k_t$  and to the nominal current raised to the power  $\alpha_1$ . With this expression it is simple to compute the duration of transient processes, the quantity of liberated energy in the contact gap, etc. Table 1 shows some values of these coefficients.

If we construct the function  $k_t = f(L)$  (fig. 5) from the existing data, as a first approximation for this coefficient we use expression

$$k_t = k_{t_0} + mL. \quad (4)$$

Then expression (3) may be rewritten in the following form

$$t_b = (k_{t_0} + mL) i_L^{\alpha_1}. \quad (5)$$

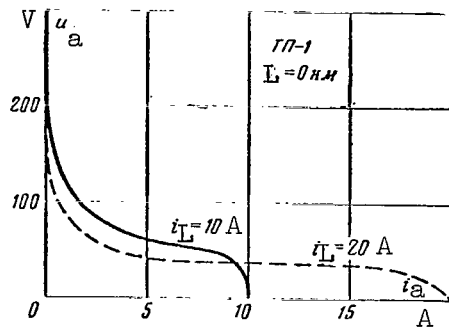
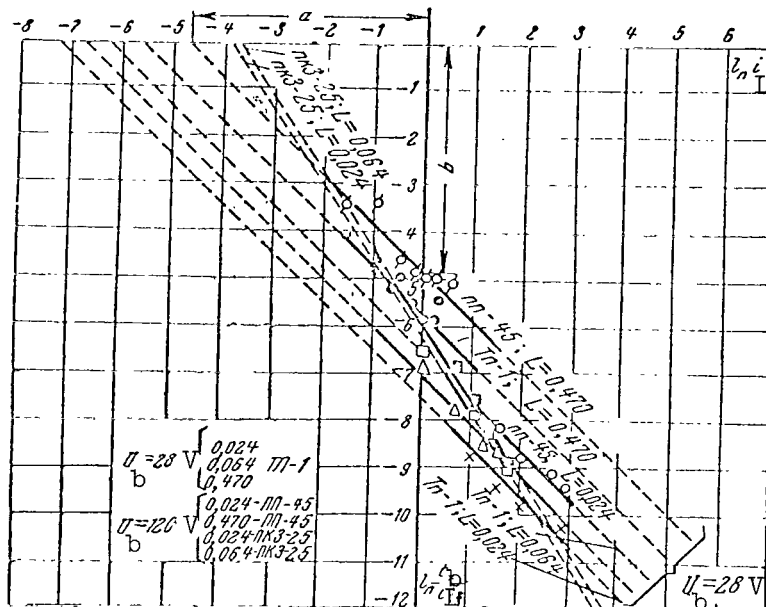


Figure 3. Dynamic arc.



Key to  
figures:

ПКЗ = PKZ

ПП = PP

ТП = TP

Figure 4. Graphs of  $\ln t_{br} / i_L^2 = f(\ln i_L)$ .

These expressions show that the duration of the breaking process also depends on the circuit inductance  $L$  and on the coefficients  $k_{to}$  and  $m$ . In addition to  $i_L$ , the quantities  $\alpha_1$ ,  $k_{to}$  also effect  $t_b$ ; only when the inductances are high is there a serious effect produced by the second term in expression (4). It is interesting to note that when the nominal circuit voltage increases, exponent  $\alpha_1$  decreases. In addition, in a system with  $U_b = \frac{117}{30}$  V,  $\alpha \approx 1$ . Figure 6 shows the graph to  $k_{to} = f(\delta)$ , where  $\delta$  is the air density.

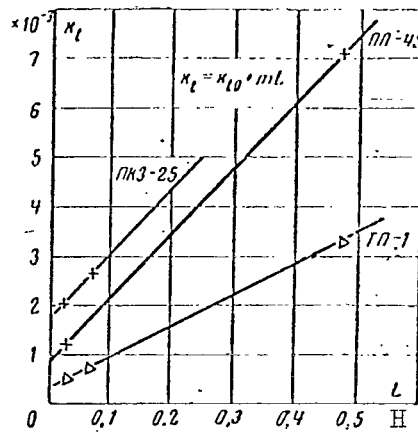


Figure 5. Function  $k_t = f(L)$ .

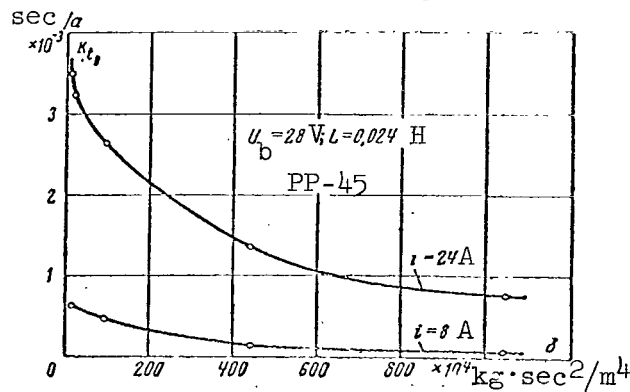


Figure 6. Graph of  $k_{t0} = f(\delta)$ .

TABLE 1.

Type of switch	Inductance in H	$\frac{2a-b}{a} = \alpha_1$	$k_t$ sec	Remarks
TP-1	0.024	1.0025	$0.46 \cdot 10^{-3}$	Line Voltage $U_b = 28$ V
TP-1	0.064	1.0028	$0.80 \cdot 10^{-3}$	
TP-1	0.470	1.0035	$3.22 \cdot 10^{-3}$	
PP-45	0.024	1.000	$1.21 \cdot 10^{-3}$	
TP-1	0.470	1.004	$7.1 \cdot 10^{-3}$	

We can see from figure 6 that when the air pressure is lowered the coefficient  $k_{t0}$  increases substantially, particularly at high currents. In this connection

we can make the following remarks. Any switch must transform a certain quantity of magnetic field energy into thermal energy. Obviously the rate of magnetic field energy transformation into thermal energy depends also on the conditions of heat transfer and on the arc. Apparently the coefficient  $k_{t0}$  characterizes the capacity of the switched equipment to transform electric energy of the arc into thermal energy. For this reason there apparently is a quadratic variation in  $k_{t0}$  as a function of  $(\delta)$ .

A large number of experimental data show that in low voltage /118  
dc circuits the variation in the transient current as a function of time may  
be approximated by

$$i_d = i_L [1 - (t/t_b)^n]. \quad (6)$$

Figure 7 shows the experimental curves  $i_d = f(t)$  plotted in relative  
coordination. The same figure shows curves computed by means of equation (6).  
As we can see, the coincidence of the curves is satisfactory. The same  
relationship was used by O. B. Bron for industrial dc networks with a voltage  
in excess of 500 V.

Exponent  $n$  apparently reflects the special features of the process. In  
this connection we constructed function  $n = f(A_M)$  (fig. 8). It follows from  
the results of the investigations that for  $A_M > 0.5$  J (where  $A_M = \frac{Li^2}{2-v}$ ) ex-  
ponent  $n$  remains constant and is close to unity in all cases. When the magnetic  
field energy is  $A_M < 0.5$  J and  $U_b = 28$  V, exponent  $n$  increases, but does not  
exceed 2-2.5.

Thus, we can assume that when  $A_M > 0.5$  J, exponent  $n$  does not depend on  
the value of current  $i_L$ , circuit inductance  $L$  and magnetic field energy  $A_M$ . For  
 $A_M < 0.5$  J, exponent  $n$  depends on  $i_L^2$ .

We note that at the end of the current variation process exponent  $n$   
becomes variable and increases, and therefore the value of the transient cur-  
rent given by expression (6) is only valid as a first approximation. It is  
more difficult to approximate the voltage curve by means of analytical func-  
tions. However, this can be done approximately if the variation in the tran-  
sient voltage as a function of time is broken into 4 stages, as was done  
earlier.

For the first stage this variation will be

$$u_I = a_I t; \quad (7)$$

For the second stage

$$u_{II} = u_{II0} + a_{II} t; \quad (8)$$

For the third stage

$$u_{III} = u_{III0} + a_{III} e^{b_{III} t}. \quad (9)$$

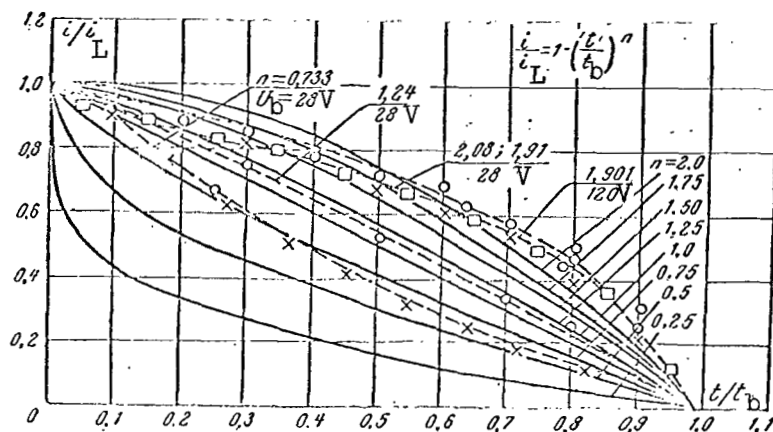


Figure 7. Graphs  $i_d = f(t)$ .

We can obtain numerical expressions for all coefficients by taking the average of a large number of measurements. It is interesting to note that  $\frac{120}{\text{exponent } b_{III}}$  is a function of nominal current  $i_L$ . A detailed investigation

of these processes has made it possible to establish their duration and the factors which affect them. The coefficients which have been obtained may be used to carry out tests for improving the quality of switches. It is then possible to give a more complete expression for the energy of the breaking arc and for its component parts and to show the validity of expression (5) derived for  $t_b$ . As we know, the equation of voltage balance for a simple series

circuit will have the form (fig. 1)

$$e = iR + L \frac{di}{dt} + u_D. \quad (10)$$

Multiplying both sides of the last equation by  $idt$  and integrating each term we obtain

$$\int_0^{t_b} u_D idt = \int_0^{t_b} e idt + \frac{L^2}{2} \left[ \frac{1}{L} + R \right] \int_0^{t_b} i^2 dt. \quad (11)$$

We designate the expression on the left by  $A_D$ , the first term of the right side by  $A_g$ , the second by  $A_M$  and the third by  $A_R$ . Depending on the properties of the regulator, we may assume (as a first approximation), that during switching the voltage at the generator will be expressed by the equation

$$u_b = e - \Delta e \left( \frac{t}{t_b} \right)^n, \quad (12)$$

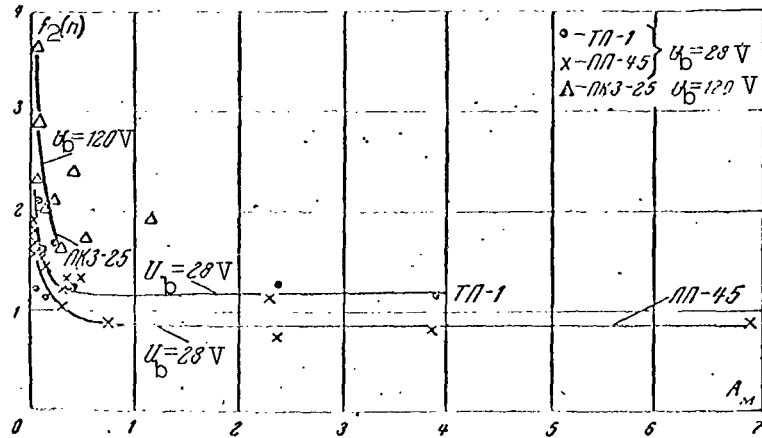


Figure 8. Variation  $n = f(A_M)$ .

while the emf of the generator will be given by

$$e = u_b + \Delta e \left( \frac{t}{t_b} \right)^n = u_b + \alpha_2 u_b \left( \frac{t}{t_b} \right)^n, \quad (13)$$

where

$$\frac{\Delta e}{u_b} = \alpha_2.$$

We substitute (6) and (13) into the expression for energy  $A_g$  supplied to the circuit by the generator and integrate the resulting equation. Then we have

/121

$$\begin{aligned} A_g &= \int_0^{t_b} e i dt = u_b i_L t_b \frac{n}{n+1} + u_b i_L t_b \frac{\alpha_2 n}{(n+1)(2n+1)} = \\ &= \frac{P_L t_b}{n+1} f_1(n) + \alpha_2 \frac{P_L t_b}{(n+1)(2n+1)} f_2(n) = \frac{U_b^2}{R} t_b f_1(n) + \alpha_2 \frac{U_b^2}{R} t_b f_2(n). \end{aligned}$$

Here

$$f_1(n) = \frac{n}{n+1}, \quad (15)$$

$$f_2(n) = \frac{n}{(n+1)(2n+1)}. \quad (16)$$

It follows from expression (14) that the energy supplied by the generator to the circuit during the switching time is determined by the nominal power of load  $P_L$  by time  $t_b$  and by coefficients  $f_1(n)$ ,  $f_2(n)$  and  $\alpha_2$ , or by the circuit

voltage  $u_b$ , current  $i_L$  and the same coefficients. The first two coefficients depend on the nature of current variation with time. The graph of the function  $f_1(n)$  is shown in figure 9, and the function  $f_2(n)$  is shown in figure 10. It follows from the graphs that  $f_1(n)$  does not exceed a value of 0.68-0.71, when  $n = 2-2.5$ .  $f_2(n)$  has a maximum when  $n = 1/\sqrt{2} = 0.706$ , which is equal to 0.17. Thus the coefficient  $f_1(n)$  for  $n = 1$  is approximately equal to 122 0.5, while the coefficient  $f_2(n)$  is approximately equal to 0.17. The values of the coefficient  $\alpha_2$  are determined by the magnitude of the load and by the properties of the generator. We can see from expression (14) that a more substantial role in the magnitude of the energy supplied by the generator is played by the first term of this expression.

As we can see from (14), the energy supplied by the generator to the circuit is proportional to the square of voltage  $u_b$ . An experimental graph, shown in one of the works of O. B. Bron and L. A. Rodshteyn (ref. 1) for industrial equipment constructed for different voltages, is in agreement with analytical expression (14). Apparently we can assume that energy  $A_g$  is proportional to the second degree of the nominal voltage  $u_b$ .

The magnitude of the energy which is dissipated in the load resistance  $A_R$  is determined by the corresponding integral from (11), after (6) is substituted into it. It has the following form

$$A_R = i_L^2 R t_b \frac{2n^2}{(n+1)(2n+1)} = P_L t_b f_3(n) = \frac{u_b^2}{R} t_b f_3(n). \quad (17)$$

The coefficient  $f_3(n)$  is a function only of exponent  $n$  (fig. 11).

For the values  $n = 1-3$   $f_3(n) = 0.35-0.7$ . As we can see from (17), the energy loss and the circuit resistances are determined by the power dissipated in the load, by the startup time of the arc and by the coefficient  $f_3(n)$ , which is given by the value of the nominal current.

By using expressions (14) and (15) we can determine the part of 123 the arc energy supplied by the generator

$$\begin{aligned} A_{g.a} &= A_g - A_R = u_b i_L t_b (\alpha_2 + 1) f_2(n) = \\ &= P_L t_b (\alpha_2 + 1) f_2(n) = \frac{u_b^2}{R} t_b (\alpha_2 + 1) f_2(n). \end{aligned} \quad (18)$$



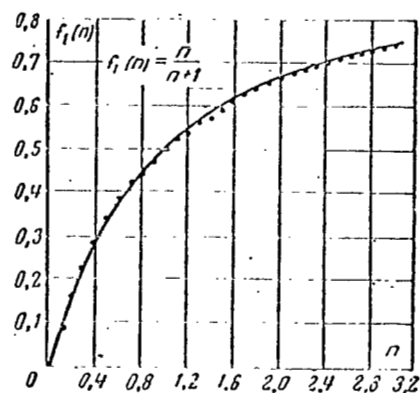


Figure 9. Variation of  $f_1(n)$ .

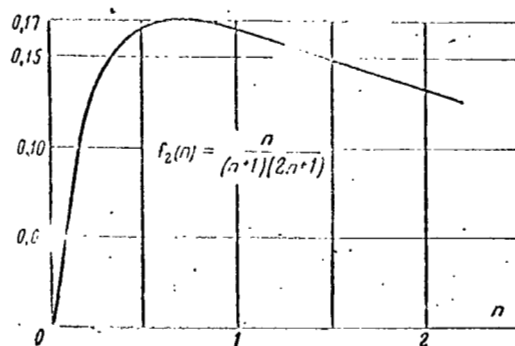


Figure 10. Variation of  $f_2(n)$

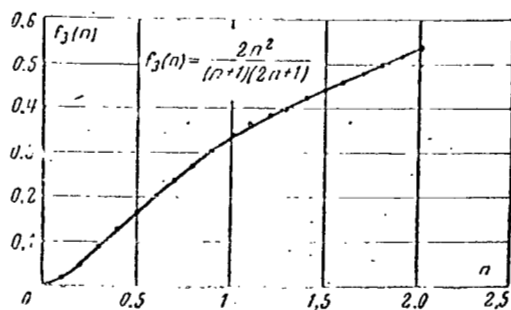


Figure 11. Variation of  $f_3(n)$ .

As we can see the energy supplied to the circuit by the generator  $A_g$  is dissipated primarily in the circuit resistances. The energy  $A_{g.a}$  begins to play a substantial role in the arc processes only when the power of the load is high, or when the burning time of the arc is great. If we assume that

$\alpha_2 = 0$  and  $n = 1$ , expression (18) coincides with the expression for the energy  $A_{g.a}$  derived by O. B. Bron (ref. 1). If we make use of the expressions for  $A_M$  and  $A_{g.a}$ , it is easy to determine the magnitude of the entire energy liberated in the arc:

$$\begin{aligned} A_{AT} &= A_M + A_{g.a} = \frac{Li_L^2}{2} + i_L t_b (\alpha_2 + 1) f_2(n) = \\ &= i_L \left[ \frac{T}{2} + t_b (\alpha_2 + 1) f_2(n) \right] = \\ &= P_L \frac{T}{2} + P_L t_b (\alpha_2 + 1) f_2(n). \end{aligned} \quad (19)$$

Here,  $T = L/R$  is the time constant of the switched circuit.

We can see that the energy dissipated in the arc consists of two components. The magnitude of the first component is determined by the power  $P_L$  dissipated in the load, or by the current  $i_L$  and the time constant  $T$ . The magnitude of the second component is determined by the power in the load  $P_L$ , by the circuit breaking time  $t_b$  and by the properties of the circuit and of the generator, which are determined by coefficients  $\alpha_2$  and  $f_2(n)$ . The latter expression is a certain generalization of known data (ref. 4). On the basis of expression (5) for  $t_b$ , which was introduced earlier, we can write this expression in the following form:

$$\begin{aligned} A_{AT} &= P_L \frac{T}{2} + i_L P_L (\alpha_2 + 1) (k_{t_0} + mL) f_2(n) = \\ &= \frac{L}{2} i_L^2 + i_L^3 R (\alpha_2 + 1) (k_{t_0} + mL) f_2(n), \end{aligned} \quad (20)$$

or

$$\frac{A_{AT}}{i_L^2} = \frac{L}{2} + i_L R (\alpha_2 + 1) (k_{t_0} + mL) f_2(n) = \frac{L}{2} + k_1 i_L. \quad (21)$$

Here

$$k_1 = R (\alpha_2 + 1) (k_{t_0} + mL) f_2(n). \quad (22)$$

In addition, it is assumed that  $\alpha_1 \approx 1$  in expressions (20) and (21).

As we can see from the graph in figure 12 for  $A_{AT}/i_L^2 = f(i_L)$  constructed

from experimental data, the axis of the ordinates intercepts segments which are close in value to  $L/2$ , while the angular coefficients of the straight lines are close to the values of  $k_1$  computed by means of equation (22). This confirms that the derived equations agree with the results of the experiments. We should remember that all of the expressions which have been obtained are valid for a free electric arc.

We have shown several special features of transient processes /125 which occur in low voltage inductive dc circuits. The analytical expressions and the coefficients which have been presented are associated with the breaking arc and make it possible to refine the calculations and investigations of switching equipment. By taking into account the increased requirements for the number of breaking cycles in switching equipment, the problem of developing theoretical and experimental concepts on the nature of transient processes is quite timely.

In conclusion we note that in addition to the basic process, which takes place during the breaking of the electric circuit, auxiliary processes take place, for example, overvoltage and oscillations of the reestablished voltage, which add a series of special features to the entire commutation process.

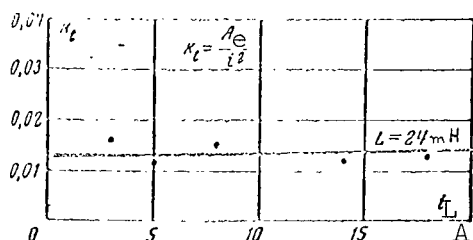


Figure 12. Graph of  $A_{AT}/i_L^2 = f(i_L)$ .

#### REFERENCES

1. Bron, O. B. and Rodshteyn, L. A. dc Contactor Breaking Frequency (Chastota otklyucheniya kontaktorov postoyannogo toka). Vestnik Elektromyshlennosti, No. 10, 1957.
2. Zalesskiy, A. M. High Voltage Electric Equipment (Elektricheskiye apparaty vysokogo napryazheniya). Gosenergoizdat, 1957.
3. Koblents, M. G. The Operation of dc Contactors in the Repetitive Short Term State (Rabota kontaktorov postoyannogo toka v povtorno-kratkovremennom rezhime). Vestnik Elektromyshlennosti, No. 2, 1960.

4. Krymskiy, G. A. Determination of the Electric Arc Energy in dc Switching-Off Equipment (Opredeleniye energii elektricheskoy dugi v otklyuchayushchikh apparatakh postoyannogo toka). Trudy Ufimskogo Aviatsionnogo Instituta, No. 3, 1957.
5. Kulebakin, V. S. Morozovskiy, V. G. and Sindeyev, P. M. The Electrical Equipment of Airplanes (Elektrosnabzheniye samoletov). Oborongiz, 1956.
6. Ryudenberg, R. Transient Processes in Electric Power Systems (Perekhodnyye protsessy v elektroenergeticheskikh sistemakh). Izd-vo I.L., 1955.
7. Usov, V. V. and Zaymovskiy, A. S. Metals and Alloys Used in Electrical Engineering, Vol. 3, "Semiconductor, Rheostat, and Contact Materials" (Metally i splavy v elektrotekhnike). Gosenergoizdat, 1957.
8. Holm, R. Electric Contacts (Elektricheskiye kontakty). Izd-vo I.L., 1961.
9. Electric Contacts, Proceedings of Conference, November 26-28, 1962. (Elektricheskiye kontakty, Trudy soveshchaniya, 26-28 noyabrya 1962). Gosenergoizdat, 1963.
10. Electric Contacts, Proceedings of Conference, July 1-6, 1958. (Elektricheskiye kontakty, Trudy soveshchaniya, 1-6 iyulya 1958). Gosenergoizdat, 1960.

## WELDING OF ELECTRIC CONTACTS AT HIGH CURRENTS

O. B. Bron and N. G. Myasnikova

### Scope of the Work

The maximum switching capacity of many modern devices is limited by the welding of their contacts at high currents. There are two complementary methods for preventing this welding. /126

First, the design is carried out in such a way as to prevent excessively large liberation of heat at the contacts, when the current is at its maximum value.

In the second place, an effort is made to select contact materials which do not weld at all or which will weld at extremely high currents.

The present work is concerned with the solution of the latter problem. At the present time cermet contacts are widely used. It is possible to vary the properties of these contacts over a wide range. For this reason, it is important to establish criteria for the capacity of contacts to resist welding. Such criteria, with other conditions being equal (pressure, contact shape), are the welding current and the force necessary to break welded contacts.

However, there are many values of currents capable of causing welding. One of these currents has a minimum value. In the future we shall call this the minimum welding current  $I_{\min}$ , and we shall use it as one of the criteria

for evaluating the properties of contact materials.

In the same way the force  $P$  necessary to break welded contacts has many values. It depends on the magnitude of the current which causes welding. The minimum value of the force  $P$  takes place when the contacts are welded with the minimum current  $I_{\min}$ . It is precisely this value of the force  $P$ , which should

be taken as the criterion for evaluating the capacity of contact materials to resist welding.

The testing of contact materials for welding, which consist of finding the minimum current  $I_{\min}$  and the corresponding force  $P$ , is associated /127

with a series of difficulties. The welding currents are usually very large, and their prolonged flow through the contacts is not permissible. It is necessary to use pulses of current.

However, the minimum current is unknown; therefore, it is necessary to conduct many experiments using current pulses of different magnitude, before it is possible to decide on the minimum current. In addition, the welding current depends on the pulse duration and on the current rise time. It is precisely this situation that frequently makes the comparison of results obtained by different investigators impossible.

The purpose of the present work was to find a method which would simplify the testing of contact materials for welding, and which would free the results of these tests from a series of quantities difficult to determine.

The second problem of the work was to establish characteristics for a series of well-known contact materials, which would make it possible to determine their capacity to resist welding.

To solve the first problem, it became necessary, first of all, to omit the testing of contacts with the current pulses and to proceed with tests conducted under a stationary thermal state.

In this case it is unnecessary to conduct a large number of experiments to determine the minimum value of the welding current, because it is determined during the first experiment. Furthermore, its value is not affected by the duration of the pulse or by the rate of change of the current. This method of testing was achieved by using water to cool the contacts. Under these conditions it was possible to pass very large currents through the contacts which did not produce excessive heating. At the same time it was noted that cooling with water does not affect the temperature of those contact areas where welding occurs.

#### Theoretical Assumptions

In considering the problem of contact heating, two temperatures are distinguished: the average temperature of the entire contact and the temperature of the "contact area." The welding of contacts starts with the fusion of metal of the "contact area." Therefore, the question concerning the temperature of this area is of prime significance in considering the welding process, while the average temperature of the contacts is apparently of secondary importance. For this reason, the question arose concerning the possibility of achieving contact welding, i.e., diffusion of metal at the contact area with a low average contact temperature. A positive answer to this question was obtained by using water cooling. /128

Let us consider the thermal field of contacts cooled with water. Figure 1 shows the diagram of such contacts with one contact area EF. Let us assume that the area has the form of a circle with radius  $a$ . We further assume that the surface of the contact area EF and the surfaces AB and CD cooled by water are isothermal. In the stationary state the current flux density lines are directed from the area EF, which is at the high temperature, to the surfaces AB and CD, which are at the lower temperature. The picture of thermal flux densities in this case may be determined by using the method of mirror reflexion. The entire

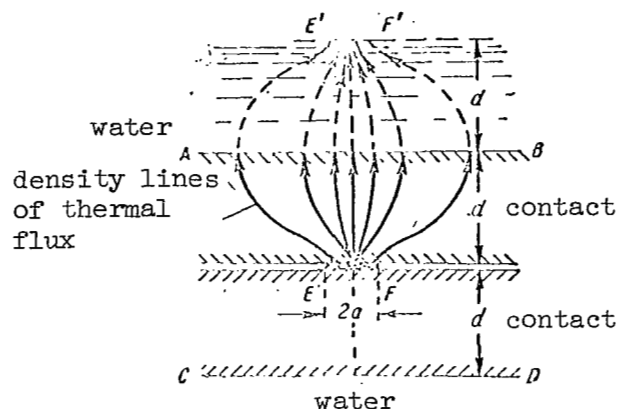


Figure 1. Heat flux in water cooled contacts.

process of heat transfer from the contact area to the cooling water by the surfaces takes place as if there were heat sinks on the other side of these surfaces at a distance  $d$ . One of such sinks  $E'F'$  is shown in figure 1. For a field such as this, the temperature difference between the contact area and the area cooled by the water may be determined from the following relationship (refs. 1 and 2).

$$\Delta\tau = \frac{1}{8} \frac{U_c^2}{\lambda_0} \left[ 1 - \frac{2}{\pi} \arcsin \frac{a}{\sqrt{(2d)^2 + a^2}} \right], \quad (1)$$

where  $U_c$  is the voltage drop at the contacts;

$\lambda$  is the heat conductivity;

$\rho$  is the specific resistance of the contact material.

When  $d = \infty$  the expression in the brackets becomes equal to unity and we have an equation for  $\Delta\tau$  which corresponds to the one obtained by Holm for a contact with forced cooling

$$\Delta\tau = \frac{1}{8} \cdot \frac{U_c^2}{\lambda \rho}.$$

Figure 2 shows the variation in  $\Delta\tau$  as a function of wall thickness for different values of pressure  $F$  on silver contacts with  $U_c = 60$  mV. These curves

show that when the thickness of the wall is  $d \geq 5$  cm, water cooling has practically no effect on the temperature of the contact area. This is true because the radius of the contact surface is usually small compared to the thickness of the heat conducting layer  $d$ . However, the effect of water cooling on the average temperature of the contact, which is measured with the thermometer, is very high.

From these considerations it was concluded that the application of water cooling makes it possible to achieve metal fusion temperatures on contact surfaces while the contacts themselves remain cold.

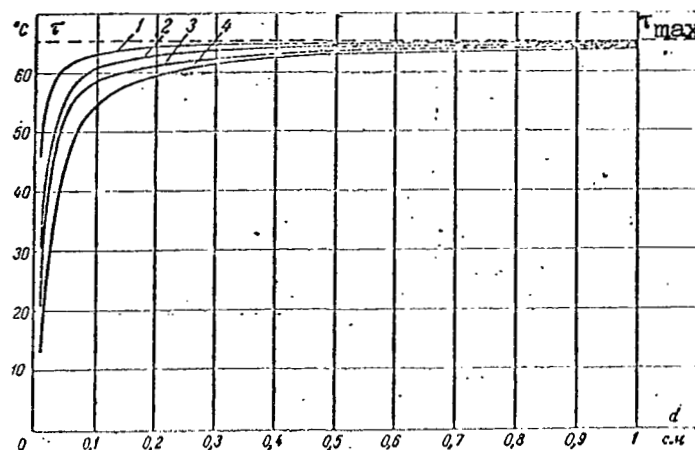


Figure 2. Variation in excess contact area temperature over temperature of surfaces cooled with water as function of wall thickness for different values of pressure between contacts. 1, 1 kg-wt; 2, 5 kg-wt; 3, 10 kg-wt; 4, 30 kg-wt.

#### Results of Experimental Verification

These considerations required experimental verification. To achieve this, the device shown in Figure 3 was designed.

Stationary hollow contacts 3 and 4 were welded to two hollow tubes 1 and 2. These contacts were connected to a movable contact 5. The movable contact 5 was pressed against the stationary contacts 3 and 4 with calibrated springs 6. The length of the springs was measured with a slide gage, between the feelers 8. Busbars from low voltage equipment supplying a dc current of 10,000 A were attached to the terminals. The magnitude of the current was controlled by means of a rheostat in the excitation winding of the generator. /131

Because we could not measure the temperature of the contact area, we observed the conditions during the experiments under which the contact became welded in the stationary state.

During the experiments, the following were measured:

- $I$ , the current in the contact;
- $U_c$ , the voltage drop at each contact;
- $\tau$ , the average overheating of each contact;
- $\tau_o$ , the temperature of the surrounding air;
- $\tau_{in}$ , the temperature of the water at the inlet;
- $\tau_{out}$ , the temperature of the water at the outlet;



Q, water consumption;  
F, contact pressure.

The experiments were conducted in the following order:

1. A definite pressure was established on the copper contacts, which were shielded beforehand.

2. The consumption of water was measured and remained unchanged for each experiment.

3. The current in the circuit was increased slowly, and the voltage drop across the contacts was observed. When welding occurred, the voltage drop decreased. This indicated that welding had taken place. At this point the quantities listed were recorded. For each pressure the experiment was repeated several times with a different rate of water consumption.

The results were used to plot the following curves:

(1) The variation in the contact welding current as a function of water consumption for different contact pressures (fig. 4);

(2) The variation in the average contact temperature (measured with thermocouples) as a function of water consumption; in this case the pressure was  $F = 5$  kg-wt, and the current was  $I = 4,000$  A. The same figure has a broken curve which shows the temperature of the water (fig. 5);

(3) The variation of the welding current as a function of contact pressure (fig. 6).

On the basis of these experiments, it was possible to make the following conclusions, which confirmed the accuracy of theoretical assumptions.

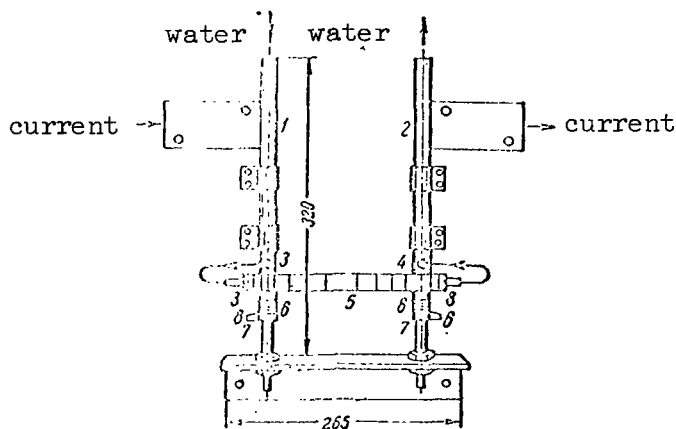


Figure 3. Device used in investigation of contacts for welding.

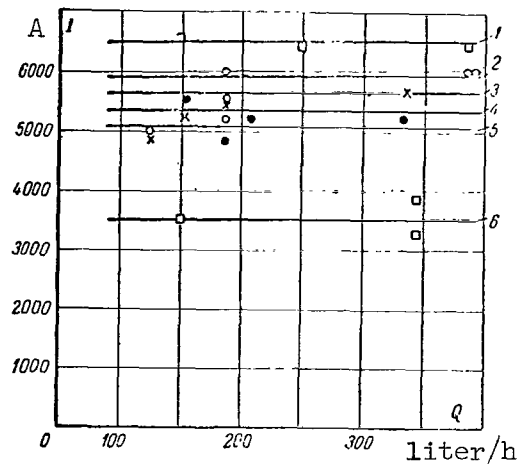


Figure 4. Variation in welding current as function of water consumption for various contact pressures: 1, 9.9 kg-wt; 2, 8.6 kg-wt; 3, 7.4 kg-wt; 4, 6.3 kg-wt; 5, 5 kg-wt; 6, 3.7 kg-wt.

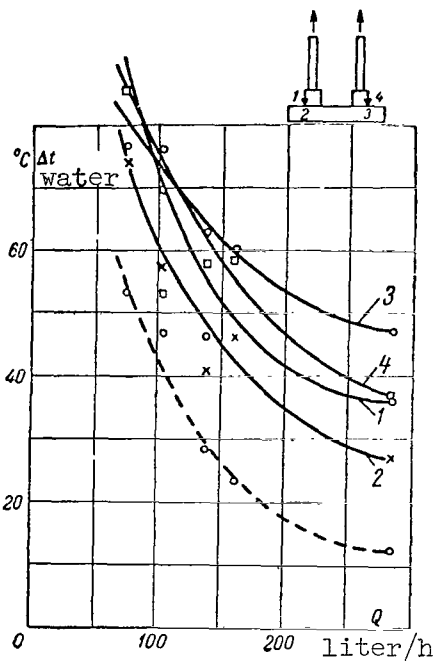


Figure 5. Variation in average contact temperature as function of water consumption. Numbers 1, 2, 3 and 4 indicate point where temperature was measured.

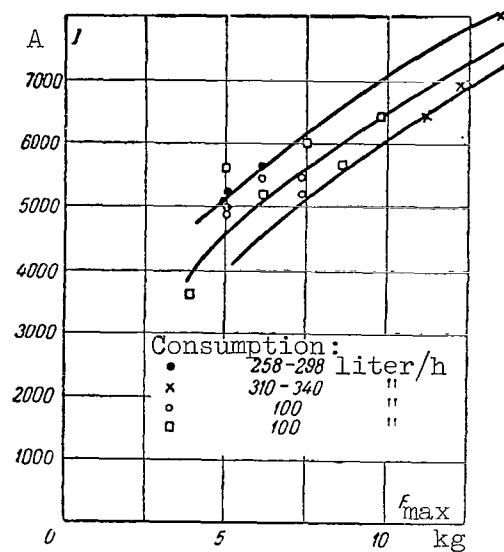


Figure 6. Variation in welding current as a function of contact pressure for different amounts of water consumption.

1. The welding current of the contacts is practically independent of the average contact temperature and is not affected by the intense water cooling. This conclusion is confirmed by the fact that the curves  $I = f(Q)$  in /132 figure 4 are parallel to the axis of the abscissas, although the average contact temperature in this case varies substantially (fig. 5).

2. This conclusion is also confirmed by the curves in figure 6, which shows the variation in the welding current as a function of pressure for different amounts of water consumption. Here all points lie in a narrow zone; their spread with respect to the average line is explained by the different value of contact resistances and not by the difference in water consumption.

3. The device which we have described makes it possible to observe contact welding in the stationary state without using pulses. Water cooling maintains a low average contact temperature at the time of their welding.

#### Further Development of the Method and the Properties of Various Materials

Our previous considerations were used as a basis for developing new equipment to test contact materials for welding (ref. 4).

This equipment is shown in figure 7. It consists of two hollow /134 cylindrical contact holders: stationary holder 1 and movable holder 2. The movable contact holder is connected to the lever system 3 and is free to rotate around the axis 4. Weight 5 can be displaced along the lever 3. When the weight is on the arm AB, the movable contact is pressed against the stationary contact.

When the weight is displaced, forces act on the arm AC separating the welded contacts from each other. Both movable and the stationary contact holders are cooled with water, which is supplied to them by means of tube 6, and which flows to the inner walls of the contact holders through the cavity between these tubes. The contact test material 7 is secured on the contact /135 holders by means of screw caps 8. The contacts have the form of two cylinders with radius  $r = 12$  mm intersecting at a right angle.

By using this equipment, we were able to determine the welding current of contacts with a prolonged flow of test current without danger of fusion and overheating of the contacts. The currents can be measured at different contact pressures, and it is possible to determine the force required to separate welded contacts.

The calculations and conclusions presented here are valid for the stationary thermal state in the region between the contact surface and the surface cooled by water. To satisfy these conditions, the increase of contact current during the experiment could be carried out only at a rate which does not exceed a certain value. For the equipment described here, this maximum rate was determined in the following manner: the contact welding currents  $I_b$  for

different rates of current variation  $di/dt$  were measured. It turned out that when  $di/dt \leq 4$  kA/sec, the welding current does not depend on  $di/dt$ . This means that the thermal state has enough time to become stationary. When the  $di/dt > 4$  kA/sec, the welding current increases slightly with an increase in the rate of change of the current. This means that the thermal state has not had enough time to become stationary.

All of the measurements described here were carried out with a rate of change of current less than 2 kA/sec.

During the tests an oscilloscope was used to record the current in the circuit and the voltage drop across the contacts. One of such oscillograms pertaining to the copper contact is shown in figure 8a.

The process of current and voltage variation, as we can see, takes place slowly and lasts for 10-15 sec. Under these conditions, the entire process may be observed by following the indicators of the meters. If recording ammeters and voltmeters are used, the oscilloscope is not required. We used the oscilloscope only because we did not have the necessary recorders. /136

By considering the diagram of current  $I$  and voltage  $U_c$  in figure 8a we can divide the entire process into 3 regions:

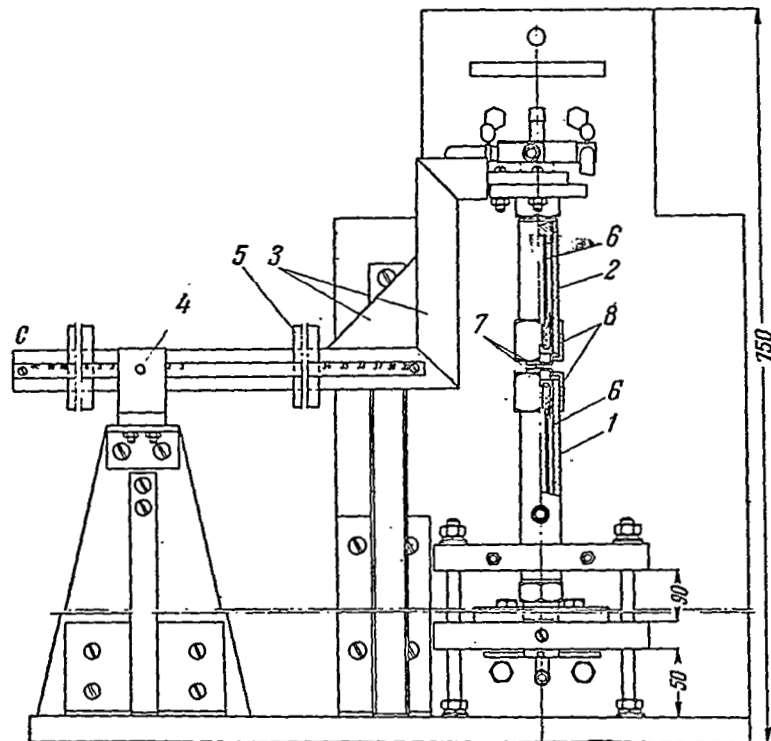


Figure 7. Equipment for testing welding of contacts.

Region 1, from point A to point B. Here the current  $I$  increases and the contact voltage  $U_c$  decreases. The contacts are heated.

Region 2, from point B to point C. Here the current continues to increase, while the voltage drop remains constant or decreases slightly. Point B corresponds to the maximum welding current  $I_{\max}$ . The entire region from B to C may be called the region of contact welding.

Region 3, from point C to point D. Here the current decreases and causes a decrease in the voltage drop. The contacts are cooled.

On the basis of the current and voltage diagrams we can compute the value of contact resistance  $r_c = U_c / I$  and can construct the variation in this resistance as a function of  $U_c$ . The corresponding diagram is shown in figure 8b.

Here we also see 3 regions. Along the region AB corresponding to the current increase, the contact resistance increases with an increase in voltage drop (and consequently with an increase in temperature) of the contact area. This agrees with the well-known expression (ref. 3)

$$r_c = r_{co} \left( 1 + \frac{2}{3} \alpha \tau \right),$$

according to which the contact resistance must increase with the temperature.

Apparently this is explained by the fact that as the temperature increases, the pressures which exist in our experiments cause an increase in the size of the contact areas, which leads to a lowering of the contact resistance.

At point B the contact area temperature reaches a value which causes the metal to fuse. At this point the contact resistance drops sharply (section BC) in spite of the current increase, which only expands the region occupied by the molten metal. The voltage drop in this region is almost constant or decreases.

The decrease in the resistance  $r_c$  and in the voltage drop  $U_c$  begins /137 at point C. Along the region CD the current decreases and the welded contacts cool.

Diagrams similar to those described have a definite characteristic form for each material. We have called them the welding characteristics.

Figure 9 shows the welding characteristics for silver contacts, while figure 10 shows them for cermet contacts made of the Ts G-1 composition (82 percent Ag plus 17 percent Zn O + 1 percent C). The minimum welding current  $I_{\min}$  depends on the pressure  $F$  between the contacts. It increases with increased pressure. Figure 11 shows the variation in  $I_{\min}$  as a function of pressure  $F$  for silver contacts (curve 1).

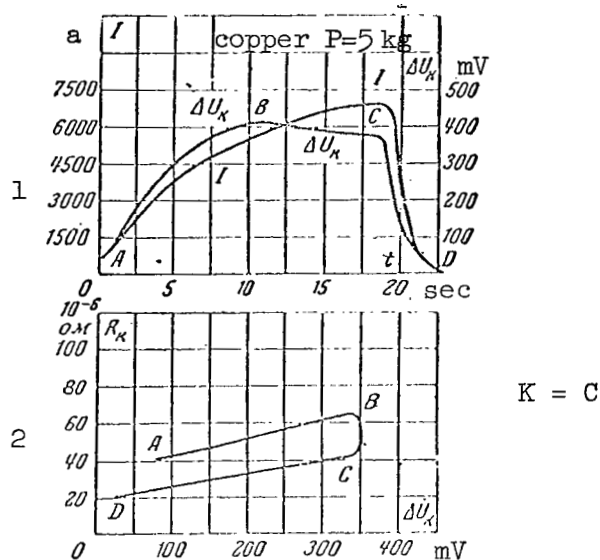


Figure 8. Characteristics of copper contacts. 1, oscillogram of current and voltage drop at contacts; 2, variation in contact resistance as function of voltage drop with contact pressure of 5 kg-wt.

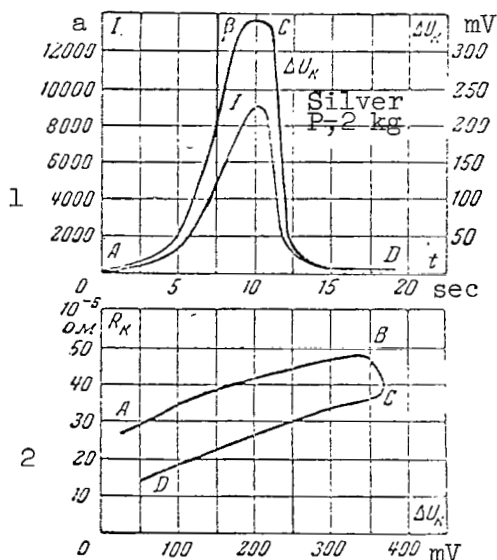


Figure 9. Characteristics of silver contacts. 1, oscillograms of current and voltage drop at contact; 2, variation in contact resistance as function of voltage drop with pressure of 7 kg-wt.

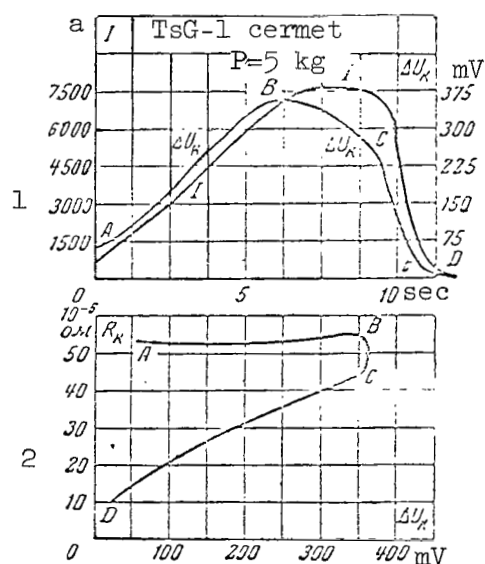


Figure 10. Welding characteristics of Ts G-1 cermet contacts. 1, oscillograms of current and voltage; 2, variation in contact resistance as function of voltage drop with pressure of 5 kg-wt.

As we have pointed out, in addition to the minimum current,  $I_{\min}$ , an important characteristic of contact weldability is the force  $P$ , which must be applied to separate the welded contacts. The value of this force also depends on the pressure between the contacts and increases with this pressure. Figure 11 shows curve 2. This curve shows the variation in the force  $P$  as a function of pressure  $F$  for silver contacts; however, the force  $P$  depends not only on the pressure  $F$ , but also on the value of the current  $I$  passing through the contacts, when this current is greater than  $I_{\min}$ . With currents less than  $I_{\min}$ , welding does not take place and the force  $P$  is equal to zero. With currents greater than  $I_{\min}$ , the force  $P$  increases with the increase in the difference  $I - I_{\min}$ . Figure 11, curve 2, shows the force  $P$  when  $I = I_{\min}$ . Thus this curve refers to the minimum value of the force  $P$ . The minimum current for various points of curve 2, i.e., for different pressures between the contacts  $F$ , is not the same. Its value is determined from figure 11, curve 1 for corresponding values of contact pressure  $F$ .

Using the method described in this work, a series of contact materials were tested for welding. The results of these tests, which make it possible to compare the capacity of these materials to resist welding, are shown in table 1.

TABLE 1.

Material	Composition	$I_{\min}, a$	$V_c, mV$	$I_m, a$	$P, kg-wt$
Copper	Cu	6 500	350	7 900	18
Silver	Ag	6 800	300	6 800	25
S2G12	78%Cu+10%Ta <sub>2</sub> O <sub>5</sub> + +10%S <sub>2</sub> CO <sub>3</sub> +2%C	1 900	400	2 200	5
S2G13	79%Cu+12%Ta <sub>2</sub> O <sub>5</sub> + +6%S <sub>2</sub> CO <sub>3</sub> +3%C	1 300	330	1 550	weak
Ts.G-1	82%Ag+17%ZnO+1%C	5 900	350	7 100	8
Ct-1	62%Ag+38%TaC	5 400	350	6 600	10
PTG-2	85%Ag+12%Ta <sub>2</sub> O <sub>5</sub> +3%C	6 600	370	7 400	10

Contact pressure  $F = 5 \text{ kg-wt}$ .

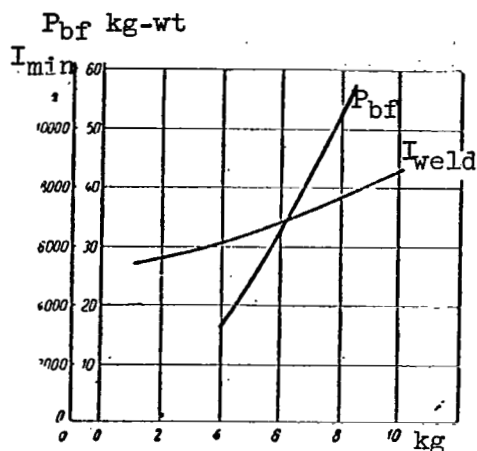


Figure 11. Variation in minimum welding current  $I_{weld}$  and breaking force of welded contacts  $P_{bf}$  as function of pressure  $F$ .

The table contains the following values:

$I_{min}$ , minimum welding currents;

$U_c$ , maximum value of voltage drop;

$I_m$ , maximum value of the current; the fact is that during the period of the experiments it was impossible to stop the increase in current when it reached the minimum value of  $I_{min}$ ; it continued to

increase for some time, as we can see from the oscillograms in figures 8, 9 and 10; the current  $I_m$  has an effect on the value

of the force  $P$ , which must therefore be referred to the current  $I_m$ ;

$P$  the force necessary to separate the welded contacts.

## Conclusions

1. During the testing of contact materials for welding, it is expedient to use water cooling for all current-carrying elements (contacts, contact holders, contact bridges). Under these conditions testing may be carried out with a prolonged flow of test current through the contacts without the danger of the latter melting or overheating. /141

2. Water cooling has practically no effect on the temperature of the contact area and consequently on the minimum welding current.



3. If we give up using current pulses and convert to testing in the stationary thermal state, it will be possible to (a) simplify the testing process; (b) improve its accuracy; (c) eliminate the effect of quantities which are difficult to measure, e.g., rate of increase of the current and the duration of the pulse.

4. The criteria for determining the capacity of contact materials to resist welding are the minimum current and force necessary to separate the welded contacts.

5. In addition to these criteria the special features of contact materials are characterized by the variation in contact resistance  $r_c$  as a function of voltage drop  $U_c$  (during the welding process). The proposed method of testing makes it very simple to obtain these relationships. They can be used not only to determine the minimum welding current, which can be done with great accuracy, but also to select the compositions for cermet contacts.

6. The work presents comparative characteristics of a whole series of contact materials obtained with this method.

#### REFERENCES

1. Bron, O. B. The Heating of Air-Cooled Contacts, in "Electric Contacts," Proceedings of a Conference (Nagrevaniye vodookhlazhdayemykh kontaktov), v sbornike "Elektricheskiye Kontakty", June 1-6, 1959, Gosenergoizdat, 1960.
2. Ollendorf, F. Currents in the Ground (Toki v zemle). Gosenergoizdat, 1932.
3. Holm, R. Electric Contacts (Elektricheskiye kontakty). Izd-vo I.L., 1961.
4. Bron, O. B. and Myasnikova, N. G. Equipment for Testing Contact Materials for Welding (Apparat dlya ispytaniya kontaktnykh materialov na privarivaniye). Author's Certificate (Soviet Patent) No. 129698, dated April 5, 1960.

# APPLICATION OF THE ADDITIVITY PRINCIPLE TO THE EROSION OF ELECTRODES IN PULSE DISCHARGES WITH LOW INTERELECTRODE GAPS

A. I. Kruglov

/142

Most of the experimental investigations concerned with the erosion of electrodes during pulse discharges have been carried out using single pulses, or a series of pulses separated by intervals of time several orders of magnitude greater than the duration of the pulses. In the latter case all processes produced by the preceding pulses are completed before the next pulse occurs. Under these conditions the processes which take place at the electrodes and in the gap, when one of the pulses of a series passes, are practically the same as the processes which occur when a single pulse passes.

We can now extend the rules obtained with single pulses to processes which occur when a train of pulses passes, and to consider the electrode erosion under these conditions as an additive process, determined by the simple addition of individual acts of erosion produced by individual pulses. This approach is valid when the duration of the transient processes in the switched circuits is quite small, compared with the time interval between commutations. However, in cases when the pulse repetition rate is such that the processes are not damped during the interval between pulses, the principle of erosion additivity requires an experimental verification.

The question concerning the limits of applicability of the additivity principle is particularly significant for the electroerosion machining of metals, because in this case it is directly connected with the problems of determining the optimum operating conditions of generation equipment. The latter situation was the determining factor in the selection of the parameter range for the discharge pulses and of the experimental conditions. /143

Investigations were carried out by using pulses with a duration of  $10^{-6}$ - $10^{-5}$   $\mu$ sec at 100-200 V. The gap between the electrodes did not exceed  $10^{-2}$  cm; the medium was kerosene and water.

In electroerosion machining the flow of discharge pulses leads to a series of perturbations in the interelectrode gap. These perturbations may be divided into two groups (refs. 1 and 2). The first group contains perturbations produced by the overall effect of a large number of pulses. Such perturbations include contamination of the gap with metallic electrode particles, filling of the interelectrode space with gaseous products produced by

the breakdown of the medium under the influence of the discharges, increase in the interelectrode gap due to the destruction of electrodes, etc. A special feature of these perturbations is their insignificant variation in time during the period of the pulse sequence. Indeed, when the area of the electrodes is sufficiently large, the extent of contamination of the interelectrode space by the erosion particles cannot substantially change when a single pulse acts. The same conclusions are made concerning the other perturbations. For this reason, the perturbations of this group may be called quasistatic. The degree of influence of quasistatic perturbations on erosion is determined by the conditions under which the particles and gases are removed from the gap.

In a stationary process the level of these perturbations over a sufficiently long period of time remains practically unchanged.

The second group of perturbations, called dynamic perturbations, refers to the processes which take place directly in the localized zone of action of each successive pulse. These perturbations are associated with the deionization processes in the discharge plasma, after the pulse passes through and after the movement of the gas bubble which surrounds the discharge zone, /144 etc. Unlike the quasistatic perturbations which are determined by the overall effect of the pulse series, the dynamic perturbations are characterized by their high damping rate, and their reaction time is comparable with the pulse repetition rate. Therefore, when investigating the effect of these perturbations, it is not necessary to take into account the action of the preceding pulses, and we can limit ourselves to the effect of one pulse on erosion produced by the pulse following the first.

To carry out the investigations, a generator was designed to produce a pair of pulses. The diagram of this generator is shown in figure 1. The generator produced two pulses with the same energy and duration, separated by an interval which could be regulated by complete overlapping of the pulses to 200  $\mu$ sec. The generation of twin pulses is accomplished by the sequential discharge of condensers  $C_1$  and  $C_2$  through the primary winding of the pulse

transformer Tr, whose secondary winding is connected to the spark gap. The condensers are discharged when the pulse thyratrons  $L_6$  and  $L_7$  are turned on by

positive pulses applied to their grids and developed by the circuit using tubes  $L_1 - L_5$ . The sinusoidal line voltage is fed to the grid of the thyatron

$L_1$ , which makes it possible to fire the thyatron with a frequency of 50 cps.

The signal from the cathode of the thyatron is fed to the cathode follower  $L_5$ , which develops the firing pulses fed to the grid of tube  $L_7$ . The firing

pulse is fed to the grid of the second powerful thyatron with a controlled delay produced by tubes  $L_2 - L_4$ . The delay control is achieved by means of

a variable resistance  $R_{10}$  in the grid circuit of the right half of tube  $L_2$ ,

which operates as a one-shot multivibrator.

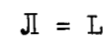


Figure 2 shows the variation in the magnitude of erosion produced by a pair of pulses as a function of the interval between the pulses for two values of pulse energy. The magnitude of the minimum permissible interval corresponds to the abscissa of the point where the curve passes from the inclined region to the horizontal region. We can see from the graph that when the pulse separation is  $n < 1$  the magnitude of erosion produced by the pair of pulses is maximum. Actually the condition  $n < 1$  means that the pulses overlap, so that actually a single pulse with double energy passes through the spark gap. The existence of the interval between pulses produces a decrease in the total energy. This can be explained by the fact that the repetitive pulses pass through gases and vapors which are formed by preceding pulses, and the deionization of vapors and gases does not have enough time to end before the next pulse occurs. As a result of this, the average current density at the anode and cathode discharge spots decreases, due to the high expansion of the discharge channel in the gas compared to that in the liquid medium. In view of this, the total energy entering the electrodes decreases and the magnitude of erosion also decreases. When the interval is increased and when the second pulse passes through, the regions of electrode surface subjected to the action of the preceding pulse are cooled due to the conduction of heat inside the electrodes; in view of this, the volume of metal fused by the second pulse decreases and the total magnitude of erosion is lowered.

A further increase in the interval produces an increase in the dielectric strength of the spark gap, and a part of the repetitive discharges passes through other regions of the interelectrode space filled with the medium. As the interval increases, the probability of the repetitive discharge increases, and the total erosion begins to increase. At the point where the curve for the total erosion goes over from the increasing region to the horizontal region, all repetitive discharges pass through the liquid medium.

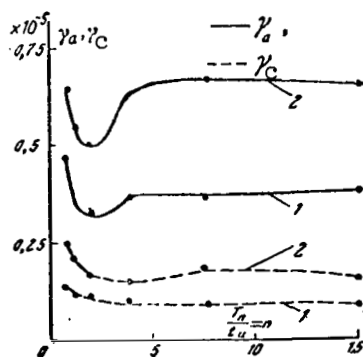


Figure 2. Variation in erosion produced by twin pulses as function of pulse repetition rate: a -  $W_n = 0.2$  J; b -  $W_n = 0.3$  J.

The abscissas of the transition point for the curves from the increasing region to the horizontal region determine the limiting values of pulse repetition rate for which the principle of erosion additivity is valid. From these graphs it follows that for pulses in the region of a few tenths of a

Joule, whose duration is of the order of  $10^{-5}$  sec, this limit is 4-5. /147

However, the erosion characteristic of twin pulses is not the only criterion for the frequency characteristics of the spark gap.

In some types of generators the interelectrode gap serves as a nonlinear element in the generating system and determines the parameters of the generated pulses as well as the generation process.

The quantitative characteristic of the frequency properties of the spark gap in this case is the curve for the repetitive ignition of the discharge. The curve for the repetitive ignitions determines the variation in the voltage necessary for the repetitive ignition of the discharge, as a function of time measured from the end of the current discharge pulse.

The experimental method of obtaining the curves for repetitive ignitions during pulse discharges consists of measuring the breakdown voltage of the gas discharge gap over different assigned intervals of time, after the current pulse has passed through. The breakdown voltage is measured by applying voltage pulses of different amplitude to the spark gap over controlled intervals of time (ref. 3). The same method was used in the present work.

Figure 3 shows the curves of repetitive ignitions for two different pulse energies with the same interelectrode distance. It follows from this graph that the rate of recovery for the breakdown strength decreases with an increase in the pulse energy.

These results make it possible to draw certain conclusions /148  
concerning the frequency characteristics of the spark gap.

It follows from the graphs that the curves of repetitive ignitions have two radically different regions. The first region is characterized by a relatively sharp rise in the curve, i.e., the recovery of the dielectric strength of the gap along this region takes place rather rapidly. This is followed by a region of complete recovery of breakdown voltage in time. This variation in the curve for repetitive ignitions makes it possible to conclude that there are different physical processes which determine the recovery mechanism for the dielectric strength of the discharge gap after the discharge. We can assume that the rather rapid increase in the breakdown voltage along the first region is associated with the processes of deionization of vapors and gases which fill the gas bubble formed by the discharge. The subsequent, slow increase in the breakdown voltage can hardly be explained by these processes. If this proposition is valid, it is impossible to explain the results obtained earlier during the investigation of erosion produced by twin pulses. Indeed, it follows from these results that the minimum permissible separation, above which the total erosion of the pulse pair no longer depends on the

separation, is equal to 4-5. This maximum pulse separation corresponds approximately to the transition point of the curve for repetitive ignitions from the region of sharp rise to the sloping region.

If we assume that the curve of repetitive ignitions along the sloping region of its rise determines the breakdown strength of the gap in the region filled with the gas bubble, the repetitive discharge will take place through the gas bubble. In this case, the magnitude of erosion produced by the action of the second pulse must differ substantially from the magnitude of erosion produced by the first pulse. However, actually this is not observed, and consequently the second discharge does not take place through the gas bubble, but rather through the liquid, even though the process of dielectric strength recovery of the spark gap has not been completed by this time.

To explain this result, it is necessary to take into account /149 that the discharge through the spark gap lowers the breakdown strength not only in the region where the discharge takes place due to the formation of ionized vapors and gases, but also leads to a lowering of the breakdown strength of the liquid medium in the zone surrounding the gas bubble.

The latter takes place due to the contamination of the liquid near the boundary of the gas bubble by finely dispersed products of erosion, which fly out of the discharge zone. The presence of suspended metallic particles in the liquid produces local heterogeneities of the electric field when the voltage is applied to the gap. The breakdown strength of the liquid at its boundary with the gas bubble is therefore lower. The presence of a high concentration of suspended particles in the liquid near the walls of the gas bubble was established by Zolotykh (ref. 4) by the method of shadow X-ray pulse photography.

The relatively slow processes of the scattering of these particles and their evacuation from the discharge zone may explain the slow increase in the breakdown voltage of the gap along the sloping region of the curve for the repetitive ignitions.

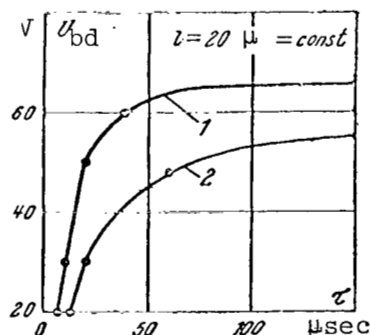


Figure 3. Curves showing recovery of dielectric strength of gap for different pulse energies: a -  $W_n = 0.3$  J; b -  $W_n = 0.03$  J.

Consequently, the maximum pulse repetition rate must be selected on the basis of the interval determined by the point of transition of the curve for repetitive ignitions from the region of rapid rise to the sloping region.

Information on the curves for repetitive ignitions makes it possible to determine the maximum pulse repetition rate for the generators as a function of the voltage variation of the unloaded generator after the discharge.

It follows from this that the process of electrode erosion under the action of a series of pulse discharges satisfies the additivity law, if the pulse separation is not less than some limiting value determined by the characteristics of pulses and by a series of other considered conditions.

In this connection a question has arisen as to whether this principle can be extended to the erosion process produced by a single pulse, i.e., as to whether the mechanism of erosion in the pulse discharge is additive.

The answer to this question is also of some interest because /150  
some investigators assume that the erosion process in the pulse discharge is additive. This applies to the hypotheses and theories for the erosion mechanism proposed by Williams (ref. 5), Nekrashevich and Bakuto (ref. 6), Dayvers (ref. 7). The common feature of these hypotheses is the concept of erosion in the pulse discharge as an overall effect produced by the elementary acts of erosion due to the continuously repeated pulses.

In spite of the different physical mechanisms used by these authors as a basis for explaining these "elementary acts" of erosion, it is assumed in all cases that the action of these mechanisms is independent of the time during which the process takes place.

A special laboratory setup was built to carry out the investigations. This setup included a pulse generator developed especially for these experiments. This generator formed pulses in the spark gap, whose form (fig. 4) consisted of a superposition of two trapezoidal pulses of different duration and amplitude. According to the relative duration of these pulses, they were called "long" and "short" pulses. The position of the "short" pulse with respect to the leading edge of the "long" pulse given by the time  $\tau_1$  could be varied from 0.5 to 100  $\mu\text{sec}$ .

The graph in figure 5 shows the variation in the erosion of a copper anode and cathode as a function of time displacement  $\tau_1$  "of the short" pulse relative to the leading edge of the "long" pulse. The duration of the "long" pulse was 20  $\mu\text{sec}$  and its amplitude was 60 A. The duration of the "short" pulse was 1.5  $\mu\text{sec}$  and its amplitude was 400 A. The axis of the ordinates shows the total value of electron erosion produced by  $96 \times 10^{-3}$  pulses. The working medium was kerosene. The amplitude of the voltage applied during the pulse interval was 200 V. We can see that, as the delay is increased /151/  
for the application of the "short" pulse, the erosion of the anode and of the cathode increases and reaches a maximum value when  $\tau_1 = 11 \mu\text{sec}$ . With further increase in delay the erosion is somewhat reduced.



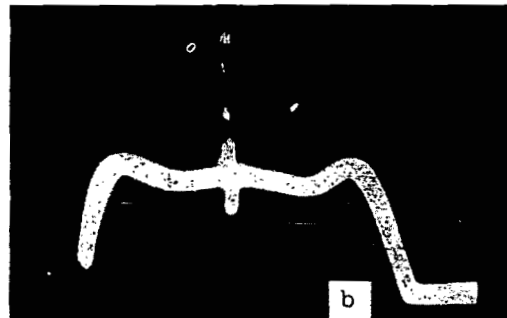
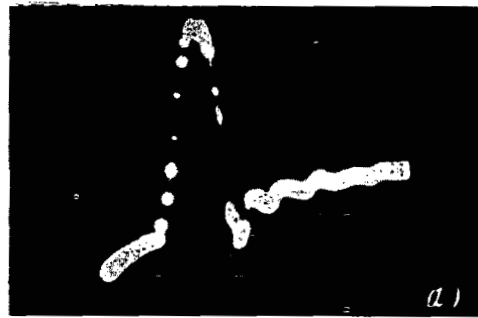


Figure 4. Oscillograms of current pulse with displaceable overshoot. a, overshoot at leading edge; b, overshoot at middle of pulse.

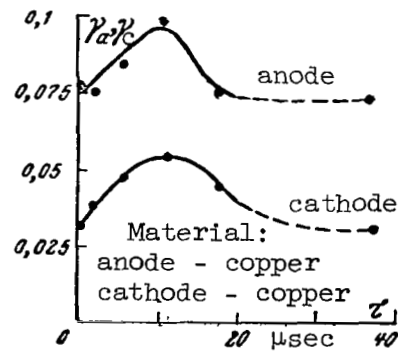


Figure 5. Variation in erosion of copper electrodes as function of "short" pulse position.

The same results were obtained with other electrode materials. Figure 6 shows the same variation for an anode made of T15K6 alloy and a cathode made from LS59 brass alloy. We note in this case that the erosion of the brass cathode is decreased, with an increase in the displacement of the "short"

pulse. The results which we obtained are interesting, primarily /152  
 from the point of view of their interpretation in the light of existing  
 theories and hypotheses on the erosion mechanism in a low voltage pulse dis-  
 charge with small gaps in a liquid dielectric medium.

One of the first conclusions which follows from the established ex-  
 perimental relationships is that it is impossible to explain them within the  
 framework of hypotheses based on the additive laws of material removal by  
 the action of a single pulse.

Thus, if we use the equation derived by I. G. Nekrashevich and I. A.  
 Bakuto to determine the value of the erosion (ref. 6) we obtain:

$$\gamma = A \frac{1}{t_{n1}} \int_0^{t_{n1}} [i_1(t) + i_2(t - \tau_1)]^2 dt, \quad (1)$$

where  $i_1(t)$  is the instantaneous current of the "long" pulse;

$i_2(t - \tau_1)$  is the instantaneous current of the "short" pulse.

It follows from (1) that

/153

$$\gamma = A \frac{1}{t_{n1}} \left[ \int_0^{t_{n1}} i_1^2(t) dt + 2 \int_0^{t_{n1}} i_1(t) i_2(t - \tau_1) dt + \right. \\ \left. + \int_0^{t_{n1}} i_2^2(t - \tau_1) dt \right]. \quad (2)$$

If we consider the displacement of the "short" pulse inside the interval  
 of the flat region of the "long" pulse, where

$$i_1(t) = I_1 = \text{const},$$

and substituting  $t' = t - \tau_1$  in the last two intervals, we obtain

$$\gamma = A \frac{1}{t_{n1}} \int_0^{t_{n1}} i_2^2(t') dt' + 2I_1 \int_0^{t_{n2}} i_2(t') dt' + \int_0^{t_{n2}} i_2^2(t') dt, \quad (3)$$

where  $t_{n2}$  is the duration of the "short" pulse, i.e., the magnitude of  
 erosion does not depend on the position of the "short" pulse.

The same result may be obtained by using the remaining hypotheses on  
 the erosion mechanism.

However, the results obtained may be interpreted quite simply on the  
 basis of the theory which explains erosion by the processes of heat propaga-  
 tion, caused by two-dimensional sources formed at the anode and at the cathode  
 due to the energy received from the discharge channel (ref. 8).

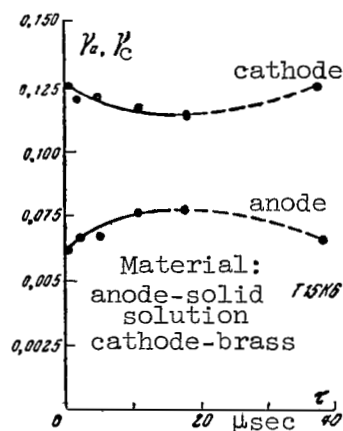


Figure 6. Variation in erosion of electrodes as function of "short" pulse position. Anode, TL5K6 solid solution, cathode, LS59 brass.

The variation in the value of erosion during the temporary variation of the "short" pulse position may be explained qualitatively by the change in the dimensions of these sources, and in the energy density flowing to the electrodes during the period of the pulse (ref. 9).

When the "short" pulse is applied at the initial stage of the discharge, i.e., when the value of  $\tau_1$  is small, the high rate of energy flow leads to

a sharp widening of the channel. As a result, after the "short" pulse has ceased to act, the density of the energy flowing to the electrodes due <sup>/154</sup> to the action of the "long" pulse is lowered in the subsequent stage of the discharge. As a result, the volume of molten and vaporized metal in this stage of the discharge turns out to be insignificant. When the "short" pulse is delayed in the initial stage of the discharge, the radial dimensions of the channel are small, due to the low rate of energy transmission into the channel. As a result, the density of the energy fed to the electrodes at this stage of the discharge is relatively large, and the specific weight of this discharge stage in the total balance of thermal pulse reaction is considerable. Therefore, we can observe an increase in erosion with an increase in the delay time of the "short" pulse. At the same time, the density of the thermal flux produced by the "short" pulse in turn depends on the time when it is applied to the discharge channel. When  $\tau_1$  increases the dimensions of the gas bubble formed during the preceding stage by the action of the "long" pulse increase. As a result of this when  $\tau_1$  increases, the density of the

thermal flux at the electrodes decreases. This thermal flux is formed by the action of the short pulse due to the rapid expansion of the channel in the gaseous medium. The latter explains the presence of a maximum on the curve  $\gamma = f(\tau_1)$ .

## REFERENCES

1. Zolotikh, B. N. The Physical Principles of Electrospark Machining (Fizicheskiye osnovy elektroiskrovoy obrabotki). Proceedings of the Third All-Union Conference on Electric and Ultrasonic Methods of Machining Materials (Doklady na III Vsesoyuznom soveshchanii po elektricheskim i ul'trazvukovym metodam obrabotki materialov), No. 2, 1958.
2. Kruglov, A. I. Pulse Generators for Electrospark Machining (Generatory impul'sov dlya elektroiskrovoy obrabotki). Proceedings of the Third All-Union Conference on Electric and Ultrasonic Methods of Machining Materials (Doklady na III Vsesoyuznom soveshchanii po elektricheskim i ul'trazvukovym metodam obrabotki materialov), No. 20, 1958.
3. Rubchinskiy, A. V. The Restoration of Breakdown Strength after the Spark Discharge, in collected works "Investigations in the Field of Electric Discharges and Gasses," (Vostanovleniye probivnoy prochnosti posle iskrovogo razryada, v sbornike "Issledovaniye v oblasti elektricheskogo razryada v gazakh"). Trudy VEI, Gosenergoizdat, 1958.
4. Zolotikh, B. N. The Basic Principles of Electrospark Machining of Metals in a Liquid Dielectric Medium, in collected works "Electroerosion Machining of Metals (Osnovnyye polozheniya elektroiskrovoy obrabotki metallov v zhidkoy dielektricheskoy srede, v sbornike "Elektroerozionnaya obrabotka metallov"). Izd-vo Moskovskogo Doma nauchno-tekhnicheskoy propagandy imeni F. E. Dzerzhinskogo, 1961.
5. Nekrashevich, I. G. and Bakuto, I. A. The Question of the Mechanism in the Electric Erosion of Metals, Collected Scientific Works of FTI AN BSSR, (K voprosu o mekhanizme elektricheskoy erozii metallov) Sbornik nauchnykh trudov, No. 2, 1955.
6. Zolotikh, B. N. The Effect of Pulse Duration on the Electric Erosion of Metals (Vliyaniye dlitel'nosti impul'sa na elektricheskuyu eroziyu metallov). Elektrichestvo, No. 8, 1956.
7. Zingerman, A. S. The Physical Principles of the Electroerosion Machining of Metals, Collected Works "New Methods of Electrical Machining of Metals," (Fizicheskiye osnovy tekhnologii elektroerozionnoy obrabotki metallov, sbornik "Novyye metody elektricheskoy obrabotki metallov"), Mashgiz, 1955.

## INVESTIGATION OF THE FINE TRANSFER OF MATERIAL ON SILVER CONTACTS

A. Khench

The breakdown of heavy duty contacts is frequently due to the change /155 in the form of the contacts produced by the electric arc during breaking and making. The change in the form of the contacts produced by the transfer of contact material from one electrode to the other produces a crater at the cathode and a point at the anode. Holm has called this the rough transfer of material particles at the contacts.

The transfer of material and the change in the form of the contacts is also observed in the case of weak currents, even when switching occurs in the regions which are below the boundary curve of the electric arc. In this case there is a transfer of material from the anode to the cathode, i.e., in a direction opposite to that which occurs when there is a rough transfer of material particles. In view of the small amount of transported material, this phenomenon has been called fine transfer by Holm. The change in the form of the contacts during fine transfer may be observed with the naked eye as a surface roughness, but it is necessary to use a microscope or a magnifying lens clearly to observe the craters at the anode and the protrusions at the cathode. Even though fine transfer produces a very small change in the form of the contacts, it is highly undesirable, because in some cases it leads to adhesion of the surfaces and thus impairs switching.

It is obvious that the magnitude of the fine transfer depends on the electrical parameters of the scheme: voltage, current, resistive, inductive and capacitive impedances, etc. It also depends on the special characteristics of switching (e.g., on the speed of motion), and also on the effect of the surrounding medium and the properties of contact materials.

In the past the phenomenon of fine transfer was explained by the Thomson effect and by other similar effects assuming that during the breaking of the contacts there is an asymmetric temperature distribution at the contact /156 point. According to Thomson, the region of the maximum temperature must be close to the anode. However, the measurement of the Thomson effect at high temperature does not always confirm this proposition; therefore to date there is no accurate explanation of the fine transfer. Recently the phenomenon of the fine transfer is frequently explained by the presence of "short" electric arcs, which occur during rapid switching. The anode material is vaporized by the electric discharge, is ionized and precipitated on the cathode. However, it is doubtful that this phenomenon completely explains the mechanism of fine transfer, particularly when the deposits are of different form. They can have the form of thin irregular peaks, wide circular domes, etc.

As an illustration, figure 1 shows pictures of the contacts (magnified 150 times). The left photograph shows the structure while the right one shows the form of the protrusion. The protrusion shown in the first picture was formed after  $10^6$  switchings of the circuit with a load of 2 A and 1  $\mu\text{H}$  at 10V. The height of the protrusion is approximately 0.1 mm and it appears to contain cracks. Small balls consisting of contact material form at its base; the external view of the protrusion seems to indicate that it consists entirely of a large number of such balls.

The second photograph shows a protrusion of large size (after  $0.5 \cdot 10^6$  switchings with a load of 4 A, 5  $\mu\text{H}$  at 6 V). Frequently a wedging of the contacts is observed, due to the hooked form of the protrusion. Both the structure of the protrusions as well as frequent cases of asymmetry point to the incorrectness of the theory which assumes the formation of protrusions only due to the condensation of material from the vapor state, and make it possible for us to conclude that the protrusions are also formed from the solidified particles. /157

The explanation of this phenomenon would have some basis, were it not for the fact that the measurement of erosion frequently produced questionable results. Data on the magnitude of erosion obtained from the literature vary considerably, even for the same contact material. This cannot be explained by different experimental conditions. The amount of transported material in

cubic centimeters for each making of the contacts is of the order of  $10^{-13}$ . This quantity is too insignificant to be measured by conventional means. It is necessary to add that this quantity is only of theoretical interest, because

a volume of  $10^{-13} \text{cm}^3$  does not interfere with the operation of the contacts. Therefore, it is customary to determine the amount of transported material

after  $10^3$ - $10^6$  commutation; in this case it is assumed that the quantity of contact material transported during each switching is superposed. However, the accurate measurement of the quantity of transported material is associated with definite difficulties.

There are three methods of taking measurements:

- (1) by weight;
- (2) by volume;
- (3) by using radioactive isotopes.

These methods were verified by using silver contacts.

The gravimetric method is the most descriptive one. It requires weighing with an accuracy of  $10^{-6}$ - $10^{-7}$  g. If we consider the losses at the anode and the weight increase at the cathode, the results of the measurements can be checked. However, it is difficult to realize this method in practice, because the contacts which weigh 20 mg are secured to holders which weigh several grams. The relatively large ballast weight has a negative effect on the accuracy of the measurements.

Therefore, when measurements of this type are made, the material transported to the cathode is removed with a razor blade and weighed. Results more accurate than those produced by direct weighing are achieved by converting the silver into dithio-ozonate. This experiment was first conducted by /158 G. Fisher and described by Ivaneyev. In this method the silver ions form a golden yellow residue with dithio-ozone, which is separated by means of tetrachloromethane; it can be separated very easily with a 462 type filter, and quantitative data may be obtained by comparison with standard data.

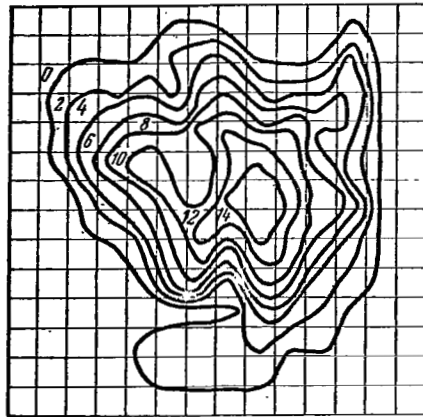
In the investigation of nonprecious metals this approach for measuring the transported material has the advantage that the result does not depend on the formation of oxides. By using this method we can show that on silver-platinum and silver-nickel contacts the transfer of particles does not take place. The basic disadvantage of this method is that not all of the transported particles can be determined. A large number of experiments have shown that only 10-20 percent of the results are reproducible.

Until recently the volumetric-analytic method was used most frequently. In this method a microscope is used to enlarge the image of the contact, and its volume is computed. In the calculations it is assumed that the deposits have the form of cones or cylinders, and that their position is more or less symmetric. This assumption is without sufficient basis. Even after examining the first photograph, the validity of these assumptions becomes questionable. A more accurate method of measuring protrusions is possible by using a special device. This device consists of a test rod with a diamond probe which examines (feels) the test surface. The variations in the position of the probe are magnified by means of an electromechanical induction transducer by a factor of 10,000 and are recorded on tape. From this tape data a topographic picture of the contact is obtained.

Figure 2 shows an example of such a picture. The width of the protrusion is 200  $\mu$ , while its height is 35  $\mu$ . The picture makes it possible to determine the asymmetry of the protrusion. Comparing these results with results obtained by means of a microscope we find that the latter are 10 percent higher. This discrepancy in the results may be explained by the inaccuracy of the reference surface. The accuracy is also affected by the diffuseness of the graduation lines of the microscope and cannot be completely /159 eliminated. The disadvantages of the volumetric-analytic method are particularly noticeable in the investigation of flat deposits, as we shall show later. The application of the volumetric-analytic method by using the device described is difficult in production testing.



Figure 1. "Fine" transfer on silver contacts.



Area: 10 mm - 20  $\mu$   
Height of one unit - 2.5  $\mu$

Figure 2. Topography of "fine" transfer on silver contacts.

The method of radioactive isotopes is particularly convenient for measuring the particles of transported material during electroerosion. In this method it is necessary that the anode be made of radioactive silver, while the cathode is made of ordinary silver. The active products transported from the anode to the cathode are counted with a counter. The higher the activity of the anode contacts, the greater is the accuracy which can be achieved in the measurements. However, the accuracy is limited first of all by the power of the neutron flux entering the counter, and then by the permissible dose of activity. Therefore, experiments of this type can only be conducted with low activity anodes. The maximum permissible anode activity is approximately 20 mCi. Experiments conducted with radioactive substances, whose activity /160 is several orders lower, are practically safe. By applying this method, it was possible to determine a mass of transported material of the order of  $10^{-9} \text{ cm}^3$ .

The physical principle, which is the basis of the measurements in this case, consists of the fact that normal silver has two components with at.wt 107 and 109. When the silver is bombarded with neutrons, the weight of the silver with at.wt 109 is the first to change. When a neutron attaches itself to this silver, it produces an unstable atom whose at.wt is equal to 110. Under the influence of radiation this atom changes into a cadmium atom, whose at.wt is equal to 110 and whose half-life is equal to 270 days. As a result, before equilibrium is achieved, the cadmium atom develops unstable products accompanied by  $\gamma$ -rays, which in turn are used to determine the amount of transported silver particles.

Figure 3 shows the variation in the transfer of the silver contacts obtained by the three methods; in all three methods the same type of contacts were used with 2 A, 4 mH at 10V. The magnitude of electroerosion was determined in the interval between  $0.5 \cdot 10^6$  and  $3 \cdot 10^6$  commutations. To simplify the measurements, a large number of commutations was selected; in addition, the inductance of the circuit was purposely selected to be high, to /161



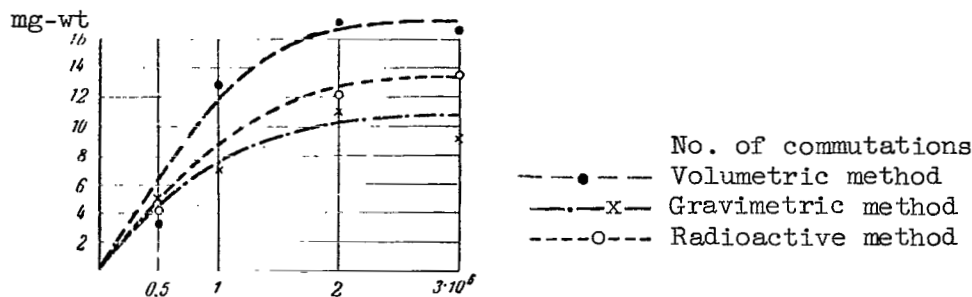


Figure 3. Magnitude of "fine" transfer of silver contacts measured by three methods.

increase the amount of transferred material. By examining this figure we can see that the nature of the curves is the same. The volumetric-analytic method gives relatively high values, while the gravimetric method gives slightly lower values. The method of radioactive isotopes gives intermediate values. The values shown on the curves are the average of a series of measurements. When the number of commutations is increased, the spread increases. It also follows from the curves that the assumption concerning the linear increase in the amount of transferred material is incorrect when the number of commuta-

tions is approximately  $10^6$  and higher. This is true regardless of the method of measurement. We can assume that with a large number of commutations, the thin sharp protrusions are partially broken down; this is confirmed by photographs made with the aid of a microscope (fig. 1). It is desirable, therefore, to measure the transferred material by the method of radioactive isotopes, using the lowest number of commutations.

When the number of commutations is less than  $0.5 \cdot 10^6$  the curves in figure 3 do not confirm a linear relationship between the number of commutations and the quantity of transferred material. Therefore, the amount of transferred material in the range of 500-30,000 commutations is determined by the method of radioactive isotopes. The results of these measurements are shown in figure 4. It follows from this that the linear relationship <sup>/162</sup> between the magnitude of erosion and the number of commutations exists only up

to 4,000 commutations. This corresponds to  $10^{-7}$  cm<sup>3</sup> or  $10^{-6}$  g of eroded silver. We can assume that for an arbitrary number of commutations the upper limit can best be determined from the amount of transferred material (in the range

$10^{-6}$  to  $10^{-7}$  g), rather than from the number of commutations. The results of the measurements question the earlier investigations of erosion which obtain the specific erosion as the ratio of the total magnitude of erosion to the number of commutations.

Another reason for questioning the accepted methods of measurement is the insufficient attention paid to the parameters of the switched circuit, when there is a sudden change in current. We should remember that overvoltages occur, which are affected to a large degree by the value of the circuit inductance. Therefore, it is first necessary to select experimental data which correspond to minimum inductance ( $\sim 0.5$   $\mu$ H). However, we should remember that in practice the inductance is much higher.

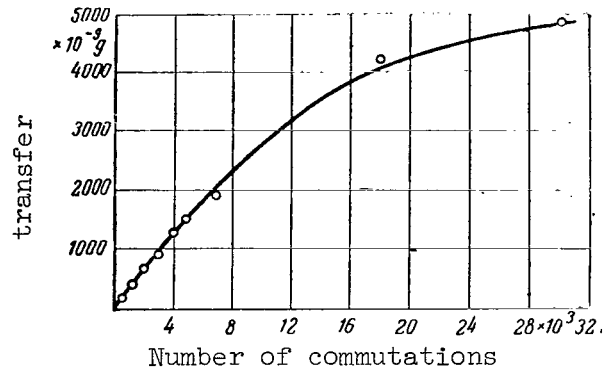


Figure 4. "Thin" transfer on silver contacts as function of number of commutations (measured by method of radioactive isotopes).

Figure 5 shows the profile of worn silver cathodes when the inductance of the circuit is 0.5, 5 and 100  $\mu\text{H}$ . Next to these are photographs of the surfaces of the corresponding anodes. We can see from the photographs that when the inductance increases the protrusion also increases. With an inductance of 100  $\mu\text{H}$  (view from the side), the protrusion is hardly noticeable. /163 The volumetric-analytic method in this case would show that the transfer of material has decreased. However, the photograph of the anode shows the distortion of its form.

Figure 6 shows the variation in the amount of transferred material as a function of circuit inductance with a current of 4 A at 6 V. The maximum value of the transported material is observed at 50  $\mu\text{H}$ . The profiles of the contacts (figure 5) at 100  $\mu\text{H}$  prove that the application of the method of radioactive isotopes is more expedient than the application of the volumetric-analytic method. As a check, a second series of experiments was conducted, in which only the cathodes were activated. This made it possible to determine the random transfer of material from the cathode to the anode.

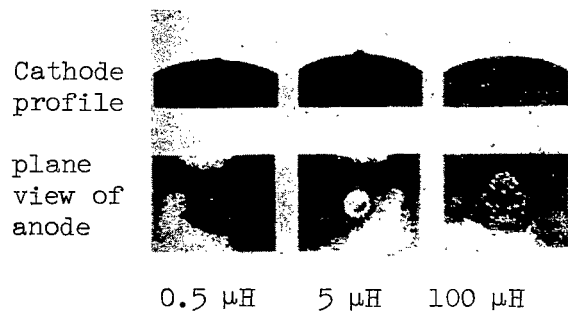


Figure 5. Form of cathode and anode wear for different values of load inductance.

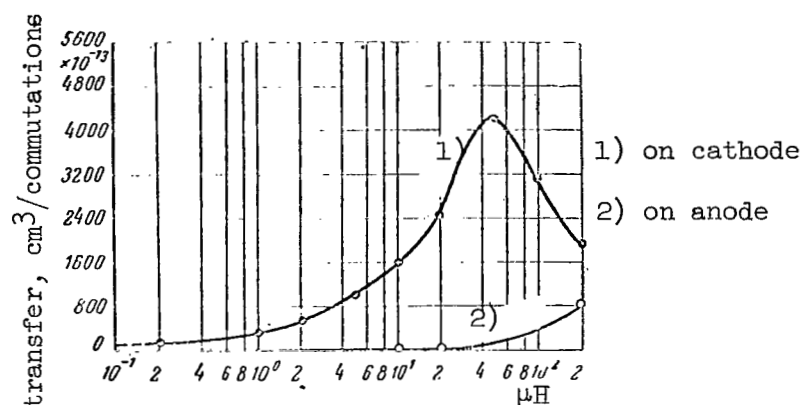


Figure 6. "Fine" transfer on silver contacts as function of circuit inductance.

The lower curve in figure 6 reflects these results. Thus there is a transfer of material from the cathode to the anode. It increases with increased inductance. We can also show that the transfer of material to the cathode or the anode depends on the stage of the commutation process. Thus, the application of the method of radioactive isotopes for investigating the transfer of material is more expedient than the application of the gravimetric and volumetric methods.

The disadvantage of this method is that it permits only the determination of the transfer at the contact, while the amount of the splashed and evaporated substance cannot be determined.

## PART II. CONSTRUCTION AND APPLICATION

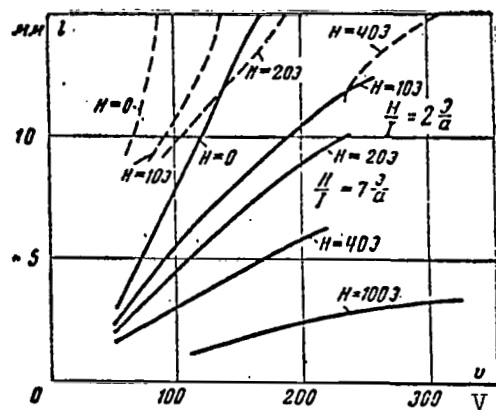
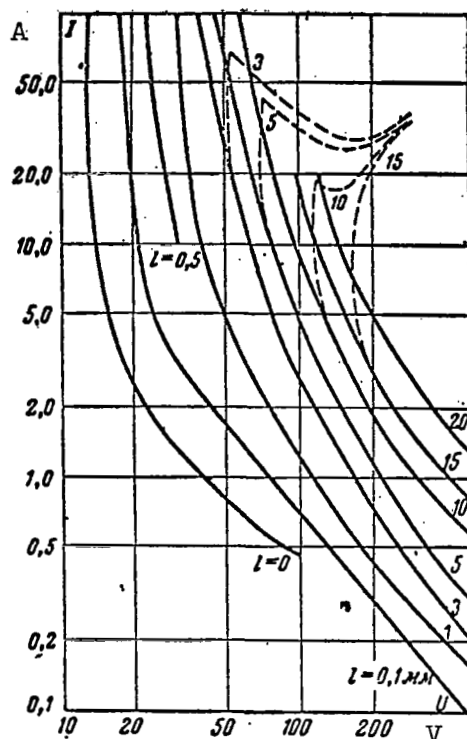
### ARC QUENCHING AT CRITICAL dc CURRENT VALUES

R. S. Kuznetsov, P. M. Zemskov and V. A. D'yachkova

We consider a free dc arc at atmospheric pressure confined to the interelectrode space when electrodes are fabricated from silver, copper, silver-cadmium oxide composition and similar materials not producing substantial thermionic emission. To quench this arc in a period which does not exceed 0.1 sec, when the circuit time constant  $T = L/R$  is not greater than 0.01 sec, it is necessary and sufficient that the points which characterize the voltage  $U$  between the contacts, after the current is turned off, and the points which characterize the current in the closed contacts  $I$ , lie below the solid curves shown in figure 1. If the voltage exceeds the quantities determined by these curves for various distances  $\iota$  between the contacts by 10 percent, a prolonged arc may appear. If there are several breaks connected in series, we must assume that each break carries a voltage which is equal to the line voltage divided by the number of breaks in the circuit. /164

Usually, when the currents are above 5 A, a large effect on the quenching of the arc is produced by electrodynamic forces which occur between the arc and the adjoining current-carrying members, as well as by the motion produced by the heated air. In the conventional constructions with finger contacts, the arc moves to the arms from the region between the contacts. In this case, the quenching of the arc under these conditions (contact material, circuit time constant, burning time) will be determined by the broken curves shown in figure 1. We can see that for every given voltage and contact separation distance there is an interval of currents for which the arc is not quenched. These currents are known as critical currents. For example, poorer conditions for the quenching of the arc when the gap is  $\iota = 15$  mm will take place with a current of  $I = 10$  A. In this case, when the voltage is less than 170 V, the arc is quenched and if the voltage is higher than this, it is not quenched. /166

For each voltage  $U$ , there is a minimum contact gap  $\iota$  for which there are no critical currents. When there is no external arc quenching magnetic field and when the time constant of the circuit is greater than 0.01 sec, the corresponding relationship is shown in figure 2 by the solid curve  $H = 0$ .



## Magnetic Quenching

If we have a constant external magnetic field, where the intensity does not depend on the current in the principal circuit, and if this field is perpendicular to the arc, the quenching of the arc during critical currents (under specified conditions) is characterized by the solid curves  $H = 10, 20, 40$  and  $100$  Oe. The field intensity  $H$  was measured when there was no current in the arc.

If we have an external magnetic field produced by the arc quenching coil connected in series with the current circuit, then, if saturation is absent, the field intensity will be proportional to the current in the principal circuit. In this case, under these conditions, the quenching of the critical currents is characterized by solid curves  $H/I = 2$  Oe/A and  $H/I = 7$  Oe/A.

The field intensity  $H$  was also measured when there was no current  $I$  in the loop and when there was current only in the arc quenching coil.

## Circuit Inductance

Inductance in the circuit increases the burning time of the arc because it decreases the rate of change of the current. If in the case of a highly inductive load, (e.g.,  $L/R = 0.1$  sec) the burning time of the arc is equal to  $0.1$  sec; this does not necessarily mean that a slight increase in the voltage will cause the arc to extend as in the case of resistive load (see above). However, we think that in switches normally used in control circuits the arc must be quenched for a period of time not exceeding  $0.1$  sec, when the circuits have high inductance, because in the contrary case there /167 will be excessive burning of the contacts and a decrease in the accuracy of actuators, due to prolonged switching of the current. This requirement obviously does not pertain to the automatic devices for quenching the field, which disconnect the excitation windings of electric machines.

During the burning of the arc, the emf of self-inductance is added to the circuit voltage  $U$ . If we assume that, when the current  $I$  is switched off, the rate of change of the current during arc burning time  $t_{\text{arc}}$  is constant,

the emf of self-inductance will be equal to

$$e = L \frac{I}{t_{\text{arc}}} = \frac{LU}{Rt_{\text{arc}}} = U \frac{T}{t_{\text{arc}}},$$

where  $T$  is the circuit time constant.

Therefore, we may assume that in a circuit with inductance, as well as in a circuit without an inductive load, the quenching of the arc takes place at a voltage greater than the voltage of the circuit with an inductive load by a factor of  $(1 + T/t_{\text{arc}})$ . The broken lines in figure 2 show the variation in the

gap of the contacts as a function of line voltage for  $T = 0.1$  sec. At this

voltage the arc is always quenched in less than 0.1 sec, when  $H = 0, 10, 20$  and 40 Oe. A comparison of these curves with the corresponding solid curves, which refer to the case  $T < 0.01$  sec, shows that the arc is extinguished in the period of time  $t_{\text{arc}} < 0.1$  sec for a high inductance load with  $T = 0.1$  sec,

when the voltage is approximately twice as small as in the case of a low inductance load with  $T = 0-0.01$  sec. This confirms the results presented above, and makes it possible to determine the conditions for the quenching of the arc in circuits with an inductive load.

In conclusion we should note that the form of the broken curves in figure 1 may appear contradictory. For example, with a contact gap of 3 mm and a current of 50 A (before the appearance of the arc), the arc is not quenched (during the period 0.1 sec) at 60 V, but is quenched at 300 V. This is explained as follows: at relatively low voltages the introduction of resistance by an arc 3 mm long lowers the current so much that the electrodynamic force is insufficient to move the arc out of the space between the electrodes.

With somewhat larger voltages and smaller decreases in the current, the arc leaves the space between the electrodes, is extended and is /168 quenched. Consequently, the inductance may facilitate the quenching of the arc for some currents, because during the breaking of the contacts it momentarily sustains the current at a level necessary to move the arc to the arms. This should be borne in mind in testing. The solid curves in figure 1 refer to the most difficult conditions of quenching, which occur in the circuit when  $T = 0$  or 0.01 sec.

## QUENCHING OF AN ELECTRIC ARC WHEN SWITCHING OFF CURRENTS OF 5-150 A AT 660 V

V. A. Kleymenov and N. I. Korbal'

At the present time there is a plan to convert to 660 V line power <sup>/168</sup> in a series of industries such as the coal industry, the oil industry and the chemical industry. This conversion is proposed because it is not possible to break down the substations and move the transformers closer to the loads, etc. Under these conditions an increase in voltage produces a positive economic effect. At the same time, the electrical industry is not entirely ready to introduce 660 V. The design and production of electrical equipment operating at 660 V is one of the most important problems of the electrical industry at the present time.

This article presents the results of investigations on the quenching of an electric arc during the commutation of circuits operating at a nominal voltage of 660 V, when switching off currents of 5-150 A. It is necessary to investigate the switching off of small currents, because the increase of voltage to 660 V may lead to the occurrence of prolonged or extended arcs during the commutation of current. This phenomenon is highly undesirable, and it is necessary to know the conditions under which it can occur.

Investigations were carried out using actual equipment designed for application in 500 V circuits with the most characteristic arc quenching systems: KI-150 (closed type chamber with a steel frame (fig. 1a) or Deion screens (fig. 1b); two-stage break per phase); KT-5023 (chamber with a longitudinal <sup>/169</sup> slot, single-stage break per phase, electromagnetic blowing); KTV-34 (chamber with Deion screen, single-stage break per phase). The nominal current of all the contactors is equal to 150 A. The effect of the breaking speed of contacts was investigated, using a type KT-5023 contactor with an altered kinematic arrangement. The effect of magnetic field intensity in the quenching zone of the arc was investigated by means of the type KT-5013 contactor with a modified electromagnetic arc system. Investigations were carried out at 690-700 V. The power source was a type TS-320/10 transformer; the loads consisted of air reactors, coils of electromagnets (without iron) and resistance boxes. The current, power factor and duration of arc burning were measured by means of oscillograms. Figures 2-6 show the curves constructed from the results of the experiments. These curves give the variation in the duration of arc burning as a function of the parameters of the switched-off load and of the switching equipment.





Figure 1. Chamber of KI-150 contactor.  
a, with brackets; b, with Deion screens.

The variations in the duration of arc burning as a function of the switched-off current (fig. 2) for the investigated arc quenching systems have the same nature. When contactors with a single-stage break per phase, /170 switch off currents from 12 to 16 A, and when contactors with a two-stage break per phase switch currents from 30-35 A, the duration of the arc is a maximum. When currents less than these are switched off, the arc is extinguished during the first passage of the current through the zero value. When switching currents greater than the ones specified, the duration of the arc burning decreases compared with its maximum value.

The variation in the duration of arc burning as a function of the load power factor (fig. 3) for contactors with a single-stage break per phase differ from the analogous variations for contacts with two-stage break per phase. For contactors with a single-stage break per phase the duration of the arc burning is constant when the load factors are not greater than 0.5-0.6. As the load factor increases above 0.6, the duration of the arc decreases monotonically and becomes equal to 0.01 sec when a resistive load is switched off. For contactors with a two-stage break per phase the range of the power coefficient may be broken down into two regions: /171

$$0 \leq \cos \varphi \leq 0.5-0.6; 0.6 < \cos \varphi \leq 1.$$

In both regions the duration of the arc is independent of the power factor of the load. However, in the first region we have arcs of long duration, while in the second region the arc is extinguished during the first passage of the current through its zero value, regardless of whether the chamber contains a checking device or a Deion screen.

The variation in the duration of the arc as a function of contact opening is shown in figure 4. For contactors with a single break per phase the range of investigated contact openings may be divided into two regions:  $\delta \leq 7$  mm and  $\delta > 7$  mm. In the first region the decrease in the contact opening produces an increase in the duration of the arc, except when currents greater than 60 A are switched off by contactors with electromagnetic blowing, in which case the duration of the arc remains constant when the openings are decreased to 3 mm. In the second region the duration of the arc does not depend on the /172 opening between the contacts. For contactors with a two-stage break per phase the duration of the arc does not change when the opening of the contacts is varied from 5-14 mm.

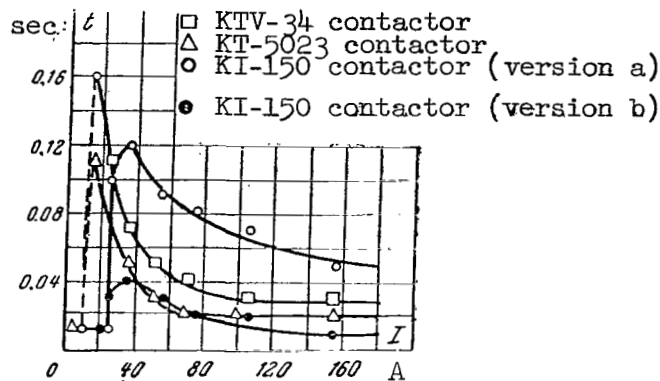


Figure 2. Variation in arc duration as function of current switched off. Power factor of load is 0.3-0.4.

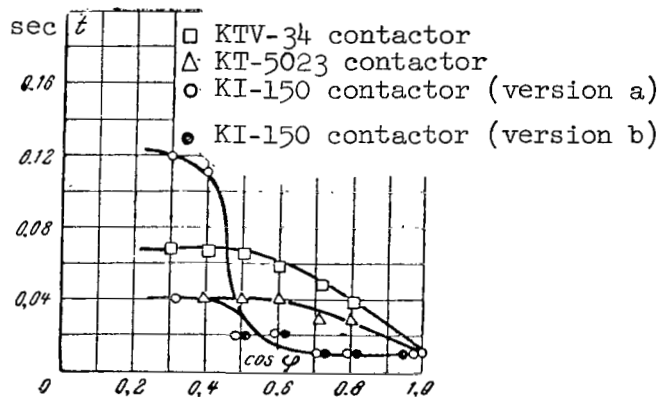


Figure 3. Variation in duration of arc burning as function of power factor of the switched-off load. Switching off current 32-36 A.

The variation in the duration of the arc as a function of the contact breaking rate is shown in figure 5. When electromagnetic blowing is present, the variation of the contact-breaking rate in the range 0.2-1.5 m/sec does not produce a change in the duration of the arc. When magnetic blowing is absent, the increase in the contact-breaking rate in the range 0.2-0.6 m/sec somewhat lowers the duration of the arc; at higher rates the duration of the arc remains constant.

The variation in the duration of the arc as a function of magnetic field intensity in the region of arc quenching is shown in figure 6. When currents less than 50 A are switched off, even a small magnetic field intensity produces a sharp decrease in the duration of the arc. Thus, for example, if the external field is absent, a current of 15 A will produce a prolonged arc. However, when the magnetic field with an intensity of 10 A/cm is present, the

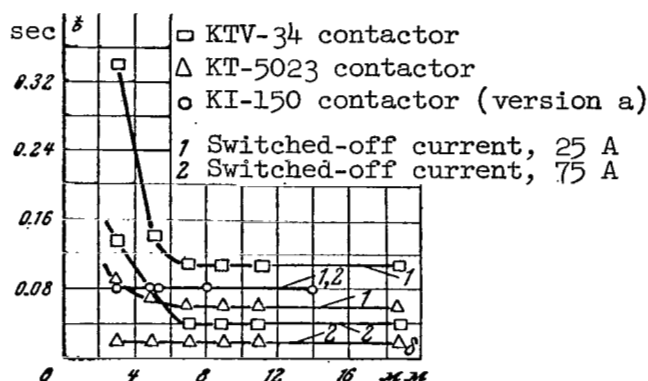


Figure 4. Variation in duration of arc burning as function of contact opening. Power factor of load is 0.3-0.4.

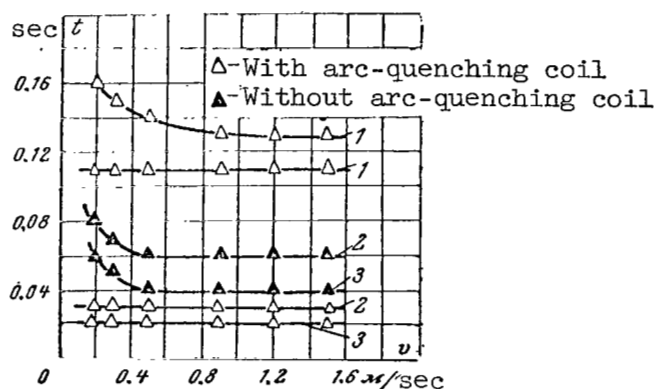


Figure 5. Variation in duration of arc as function of velocity of contact breaking. KT-5023 contactor. Power factor of load is 0.3-0.4. 1, 15 A; 2, 50 A; 3, 105 A.

arc is extinguished; in this case the duration of the arc is 0.24 sec. With a current of 25 A an increase in the magnetic field intensity from 0-10 A/cm produces a decrease in the duration of the arc from 0.31-0.14 sec. With currents greater than 50 A, the increase in the magnetic field intensity reduces the duration of the arc to a much lesser degree.

Before proceeding with the analysis of these results, we recall the basic assumptions for the process of ac arc quenching. The quenching of an ac arc is reduced in essence to the prevention of repetitive ignitions of the arc after the current has passed through its zero value. The probability of repetitive ignitions is determined by the relation between the restoring strength of the arc gap and the restored voltage ( $U_{res}$ ) over the same interval.

If at any instant of time after the current has passed through its zero value

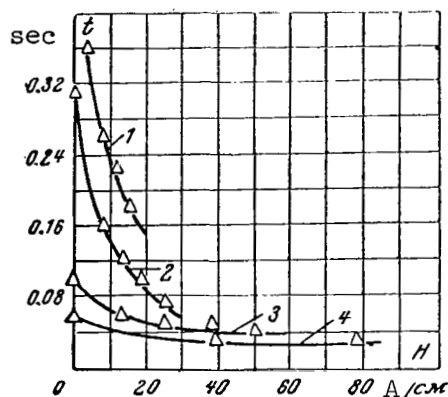


Figure 6. Variation in duration of arc as function of magnetic field intensity. KT-5013 contactor. Power factor of load is 0.3-0.4. 1, 15 A; 2, 25 A; 3, 50 A; 4, 105 A.

the restoring strength exceeds the restored voltage, the arc is extinguished. If, however, at some instant of time the restored voltage exceeds the restoring strength of the gap, a repetitive ignition of the arc will take place and the duration of the arc will increase by at least one more half-period. /173

The recovery voltage at the arc gap is determined by the line voltage, by the power factor of the load, by the number of breaks per phase, by the distributed parameters  $L$  and  $C$  of the load and by the resistance of the arc column.

The restoring strength of the arc gap consists of the sum of the initial restoring strength, determined by the contact material and the switched current and by the strength of the arc column which increases in time with velocity, depending on the value of the switched current and the structural parameters of the arc quenching chamber. In the case of a freely quenched arc, it also depends on the length.

On the basis of this approach to the mechanism of arc quenching, the variation in the duration of the arc as a function of the load parameters and of the switching equipment may be explained in the following manner.

**The Effect of the Switched-off Current.** For small values of current, the restoring strength of the arc gap after the first passage of the current through its zero value exceeds the restoring voltage, and the arc is extinguished during a period of time not exceeding 0.01 sec. At a certain value of the current the restoring strength of the arc gap after the first passage of the current through its zero value turns out to be inadequate; in order to quench the arc, it is necessary to extend it to a sufficient length or to use an arc-quenching device; therefore, the duration of the arc in this case will exceed 0.01 sec. As the switched-off current increases in value, the electromagnetic forces which act on the arc increase, and therefore the time

required for the arc to achieve the necessary length or the time for the arc-quenching device to operate decreases; consequently, the duration of the arc also decreases.

The Effect of the Load Power Factor. When inductive loads are switched off by means of contactors with a single-stage break per phase, the restoring strength of the arc gap is insufficient to quench the arc during the first passage of the current through its zero value, and the arc is quenched /174 either in an arc-quenching device (in this case the duration of the arc at constant current remains constant), or it takes place when the arc reaches the necessary length. When the restoring voltage decreases, the arc length necessary for quenching decreases, so that the duration of the arc must also decrease when the power factor of the load is increased. The restoring voltage at the arc gap for contactors with a two-stage break per phase, when all other conditions are equal, is half of that for contactors with a single-stage break per phase; therefore, with loads of low inertia (power factor greater than 0.5-0.6) the restoring strength of the arc gap after the first passage of the current through its zero value turns out to be greater than the restoring voltage, and the arc is quenched. At high inductive loads the restoring strength of the arc gap turns out to be insufficient, and in these cases the arc is extinguished in the arc-quenching device, which provides for the constant duration of the arc when the power factor of the load is varied.

The Effect of Contact Opening. For small openings of the contact with a single-stage break per phase, the length of the arc between the contacts and the electrodynamic force acting on it are small. This produces a situation where the arc is not immediately blown out from the contacts, but is blown out after some period of time. The increase in the contact opening by several millimeters (and also the application of electromagnetic blowing) causes the arc to move out of the contacts under its own or external magnetic field. It is extended by this field to the necessary length and quenched.

The Effect of Contact Breaking Speed. At low contact-breaking speeds, the length of the arc is small during several half-periods (from the time the contacts separate), and this produces an increase in arc duration, compared with the case when the contacts break at the rate greater than 0.6 m/sec, when the opening of the contacts during the first passage of the current through its zero value is sufficient for the arc to be blown out by the /175 magnetic field. The duration of the arc in this case is determined only by the time necessary for the arc to achieve the necessary length, or by the reaction time of the arc-quenching device.

The Effect of Magnetic Field Intensity in the Zone of Arc Motion. As the magnetic field intensity is increased in the zone of arc motion, its velocity increases, due to the increase in the aerodynamic forces which act on it. This decreases the time required for the arc to achieve the necessary length, or for the arc-quenching device to operate. When currents greater than

50 A are switched off, the natural magnetic field of the arc is sufficiently strong. Therefore, the increase in the external magnetic field produces a smaller decrease in arc duration than in the case when low currents are switched off.

Figure 7 shows the variation in the arc duration as a function of the switched-off current for the KTV-34 contactor, when switching currents at a voltage of 530 V (according to the data of O. B. Bron) and 690 V (according to the data of the present investigators). The coincidence of the arc duration at currents greater than 60 A may be explained by the fact that in this case the arc is quenched in the arc-quenching device (Deion screen). Since the time that it takes the arc to reach the Deion screen, and consequently its duration, are determined only by the switched-off current, the duration of the arc must not depend on the voltage. When smaller currents are switched off, the quenching of the arc occurs when it achieves a definite length determined by the circuit voltage. Therefore, in switching off circuits with a voltage of 530 V, the duration of the arc must be less than /176 when switching off circuits with a voltage of 690 V.

Figure 8 shows the results of all experiments conducted by us. The axis of the ordinates shows the instantaneous values of the recovered voltage for one break of the phase in which the current has reached its zero value, before it has reached it in the other phases. It is given by the expression

$$U_{\text{inst}} = \frac{\sqrt{2} \frac{U}{\sqrt{3}} \sin \varphi}{n},$$

where U is the linear voltage of the line;  
 $\varphi$  is the phase shift between the current and the voltage;  
 n is the number of breaks per phase.

For each pair of values ( $U_{\text{inst}}$ , I) we have one of the following /177 cases:

(a) the arc is quenched during the first passage of the current through its zero value for each of a series of breaks;

(b) the arc is quenched either during the first, during the second or during the subsequent passages of the current through its zero value.

We can see from figure 8 that the quenching of the arc during the first passage of the current through its zero value is affected very little by the arc-quenching device, by the magnetic field intensity, by the rate of contact separation, by the opening of the contacts or by the type of arc-quenching device. These factors affect primarily the duration of the arc. This makes it possible to introduce a curve in figure 8, which separates the points ( $U_{\text{inst}}$ , I) corresponding to the quenching of the arc during the first, second

or subsequent passages of the current through its zero value. This curve makes it possible to determine simply the cases in which the switching off of currents up to 150 A causes the arc to be quenched during the first passage of the current through its zero value.

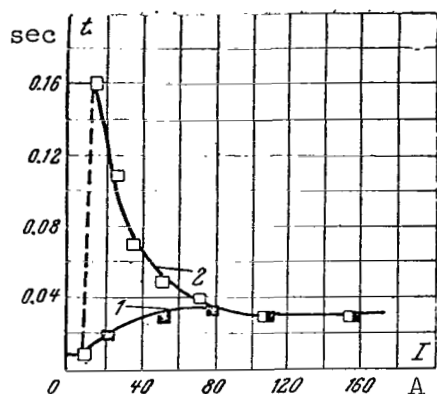


Figure 7. Variation in arc duration as function of switched-off current. KTV-34 contactor. 1, according to data of O. B. Bron ( $U = 530$  V,  $\cos \varphi = 0.38$ ); 2, according to data of author ( $U = 690$  V,  $\cos \varphi = 0.3-0.4$ ).

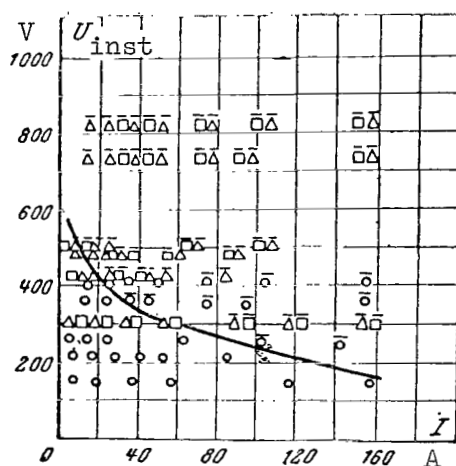


Figure 8. Variation in instantaneous value of recovered voltage for which arc is quenched during first passage of current through zero value as function of switched-off current. Points with bars correspond to arc-burning time no greater than 0.01 sec; points without bars correspond to quenching of arc during first passage of current through zero value.

Let us compare our results with those obtained by I. S. Tayev. In figure 9 the data of I. S. Tayev are used to construct the variations in the restoring strength of the arc gap as a function of current for the instant of time  $t=12.5$  and  $50 \mu\text{sec}$ , which corresponds to the large (40 kc) and small (10 kc) values of

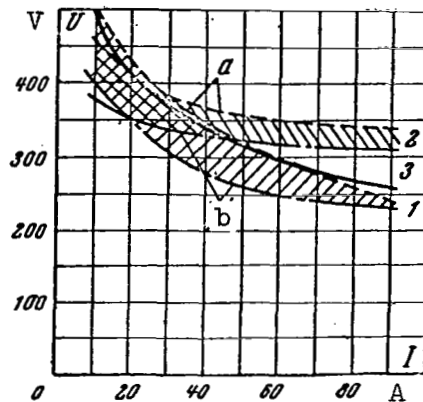


Figure 9. Comparison of data obtained by present investigators (curve 3) with data obtained by I. S. Tayev (curves 1, 2). a, strength of arc gap after  $t = 12.5 \mu\text{sec}$  ( $f_0 = 40,000$  cps); b, strength of the arc gap after  $t = 50 \mu\text{sec}$  ( $f_0 = 10,000$  cps). 1, copper contacts; 2, brass contacts; 3, curve shown in figure 8.

the frequency of natural oscillations of the circuit which took place in our experiments. The voltage supplied from the line to the arc gap at the time  $t = 1/2 f_0$  may in general be equal to or greater than  $U_{\text{inst}}$ , depending /178

on the distributed parameters  $L$  and  $C$  of the circuit and the resistance of the arc gap. According to the investigations of I. S. Tayev, in practical cases the amplitude coefficient of the restoring voltage is close to unity. Therefore,  $U_{\text{inst}}$  shown in figure 8 must be close to the value of  $U_{\text{rec}}$ . A

comparison of the data obtained by I. S. Tayev with the data obtained by the present investigators essentially confirms this. In this case we should compare the values of  $U_{\text{inst}}$  with the values of  $U_{\text{rec}}$  in the upper part of the

shaded region, when currents are small, and in the lower part, when they are large.

The following conclusions can be made from the investigations.

1. In a series of cases when switching circuits with a voltage of 660 V, the arc burns for a period greater than 0.01 sec. The maximum duration of the arc takes place when the currents are 15-40 A.

2. In equipments with single-stage breaking per phase, when the contact opening is increased to 7 mm, the duration of the arc decreases. An increase in the opening above 7 mm does not shorten the duration of the arc.



In equipments with two-stage breaking per phase, without electromagnetic blowing, the magnitude of the contact opening in the range 5-14 mm has no effect on the duration of the arc.

3. In equipments with a single breaking per phase, when the magnetic field is present, the rate of contact separation in the range 0.2-1.5 m/sec has almost no effect on the duration of the arc; when the magnetic field is absent, the increase in the contact-breaking rate lowers the duration of the arc slightly.

4. When the magnetic field intensity is increased, the duration of the arc decreases.

5. The variation in the instantaneous value of the restoring voltage, at which the quenching of the arc does not take place during the first passage of the current through its zero value, as a function of current (fig. 8) may be used to design electrical equipments.

## SILVER CONTACTS AT ELEVATED TEMPERATURE WITH PROLONGED LOADING

O. B. Bron and M. Ye. Yevseyev

### Formulation of the Problem

The norms which are currently in effect for the heating of current-carrying elements of electrical equipment (GOST 403-41) provide for a maximum temperature increase of  $85^{\circ}\text{C}$  (when the ambient temperature is  $35^{\circ}\text{C}$ ) for the case of intermittent prolonged operation of massive sliding and butt contacts with silver inserts. These norms were developed in our country in the 30's without sufficient experimental verification.

In recent years, investigations in a series of countries have suggested that the temperature of silver contacts may be increased considerably. This suggestion was reflected in the preparation of norms by the International Electrical Engineering Commission, according to which the temperature of silver and silver-plated contacts is limited only by the allowable heating of current carrying parts adjoining the contacts.

If this were true, the nominal currents of many electrical equipments with silver contacts which satisfy the present norms could be increased substantially.

The present work was carried out to clarify such possibilities.

### Methods of Investigation

To clarify these claims, experiments were conducted using contacts of type V switches with a nominal current of 1,000 A containing 4 roller contacts connected in parallel.

The diagram showing the contact part of these switches is shown in figure 1. The movable principal contacts have the form of rollers with silver rims. When the equipment is turned on, these rollers are moved into the gap between the stationary principal contacts and close them, as shown in figure 1. The number of contact rollers may vary, depending on the nominal current of the switch.

The arc-quenching contacts are connected in parallel with the principal contacts. The equipment is designed in such a way that the arc-quenching contacts make first when the equipment is turned on, while when the equipment is turned off, they break after the principal contacts. Thus, the principal

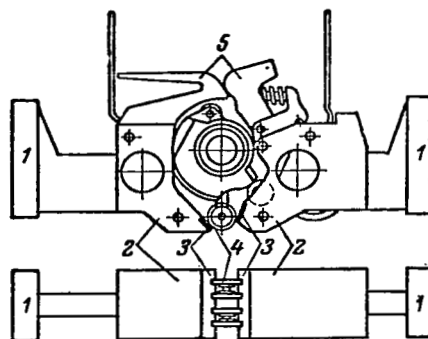


Figure 1. Contact part of type V switch.  
1, terminals; 2, stationary principal contacts; 3, silver plate; 4, movable principal contacts; 5, arc-quenching contacts.

contacts are protected from burning produced by the electric arc. The principal contacts were the basic subject of the present investigation. The arc-quenching contacts were insulated and current did not pass through them. Eight of the contacts described were tested (A, B, C, D, E, F, G and H, fig. 2). They were connected in series, and a current of 1,000 A was passed through them. However, switches G and H had 4 contacts which were switched on, while switches E and F had 3, switches C and D had 2 and switches A and B had only 1 principal roller contact.

In switches G and H, each roller carried 250 A.							
"	"	E	"	F	"	"	333 "
"	"	C	"	D	"	"	500 "
"	"	A	"	B	"	"	1000 "

All contacts of switches G and H were operated close to the nominal load, while the contacts of switches E and F were overloaded with current by a 181 factor of 1.33, contacts C and D were overloaded by a factor of 2 and A and B were overloaded by a factor of 4.

All equipments carried a current of 1,000 A continuously for a period of 220 days (5,280 h). During the investigations the temperature of the various components and the voltage drop at the contacts were measured.

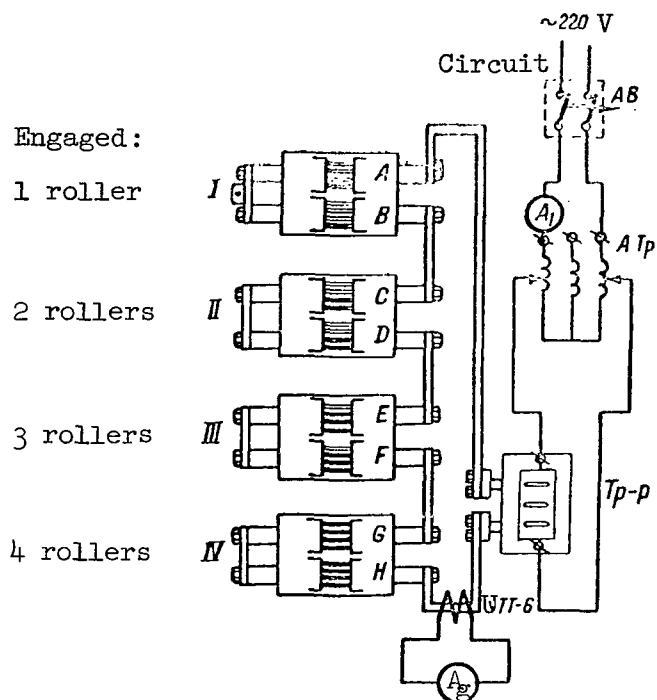


Figure 2. Diagram showing arrangement of type B switches during tests.

### Overheating and Voltage Drop

The basic results of the observations are expressed by curves in figures 3 and 4.

Figure 3 presents curves which show the variation in the excess temperature of the principal silver contacts as a function of the time during which they carried currents with different loads.

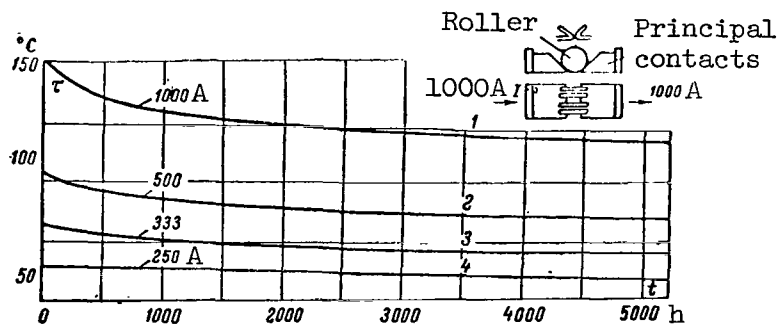


Figure 3. Variation in excess temperature of contact rollers with different current loading as function of time.

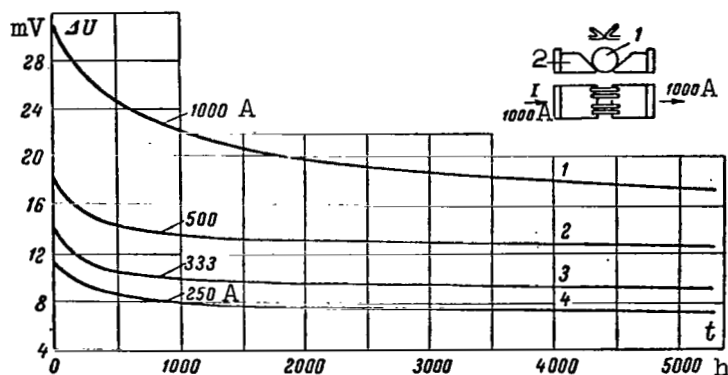


Figure 4. Variation in voltage drop at silver contacts as function of time (for different current values).

The most important conclusion from these observations is that the /182 overheating of all silver contacts used in the experiments did not increase (as was the case for copper contacts) and did not remain constant (as one might expect), but decreased.

This decrease in overheating was more pronounced in contacts with a smaller load. For roller contacts carrying a current of 1,000 A (curve 1) the temperature rise during the test period dropped from 142 to 105°C. For contact rollers with a current of 250 A (curve 4) the temperature rise decreased from 55 to 48°C during the tests.

Observations of the contact voltage drop were in agreement with /183 observations of the heating of silver contacts (fig. 4).

The voltage drop for all experimental silver contacts decreased rather than increased over a period of time. This decrease in voltage drop and consequently in contact resistance is most pronounced in contacts which are highly heated (curve 1) and less in contacts which have a lower temperature (curve 4).

#### Contact Surfaces

After tests for prolonged current flow the contacts of the test equipment were disassembled and carefully examined.

Figure 5 shows the photographs of the contacts which had the highest temperature during the tests. The number I designates the rollers, while the number II designates the stationary silver contacts with the rollers. A current of 1,000 A was passed only through the roller designated with the number 4. Mica plates were placed under rollers 1, 2 and 3 and current did not pass through these.

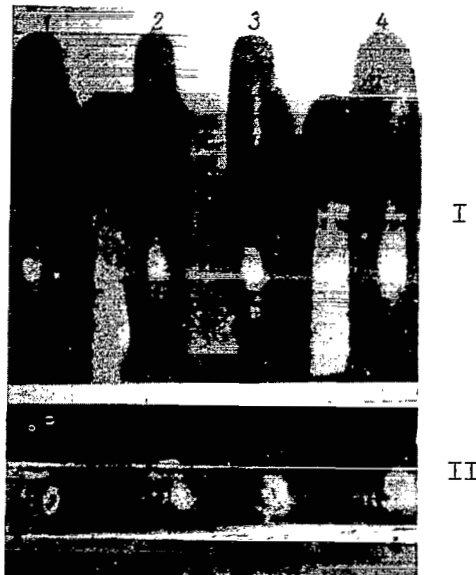


Figure 5. Contacts of type B switch. I, rollers; II, stationary contact. Current of 1,000 A passed through roller 4 and through contact area with same number for period of 220 days (5,280 h). Rollers 1, 2 and 3 and contact areas with same numbers on stationary contact were insulated from each other during this time, and current did not pass through them.

/184

Both the surface of the rollers and the silver plates of stationary contacts contained a dark gray layer of silver oxides. However, those regions where contact was made were completely free of oxides.

The contact areas which rested on the mica plates (rollers 1, 2 and 3) were also not oxidized. Apparently in this case the pressure on the contact areas protected them from oxidation.

The contact surface most free from oxides was on roller 4 and on the portion of the stationary contact coupled with it (designated by the number 4). Current passed precisely through these areas.

In addition, these contact areas free from oxides had light hollows on the surface of the silver. These hollows indicate that during the process of prolonged heating, the contact areas increased due to plastic deformation. Apparently this plastic deformation was one of the reasons for the decrease in the contact resistance in the course of the test period.

The pressure on the contact areas between the roller and the stationary contact was approximately 10 kg-wt and remained constant during the entire period of time, while the equipment carried current.

#### Phenomena Occurring During the Repetitive Making of Contacts

As we have pointed out, the external appearance of the contact surface (fig. 5) differs radically from the appearance of the roller surface. This raised the question concerning the behavior of such a contact during the repetitive switching of the equipment. In this case contact may take place at the oxidized areas due to prolonged heating of the contacts.

To answer this question, experiments were carried out on the repetitive switching of silver contacts. After the roller carried a current for 5,000 h, the equipments were turned off and again turned on, so that the silver contacts would touch through surfaces which have become oxidized as a result of the preceding heating. After this, the equipment again carried the current for the period of 2,000 h. The results showing the overheating  $\tau$  and the voltage drop  $U_c$  in these contacts are shown in figure 6. /185

As we can see from the curves, in this case the voltage drop  $U_c$  and the overheating  $\tau$  increased sharply and then began to drop as in the experiments described previously. This shows that the silver oxides are broken down when they are heated again, and the contacts are again warped due to prolonged heating.

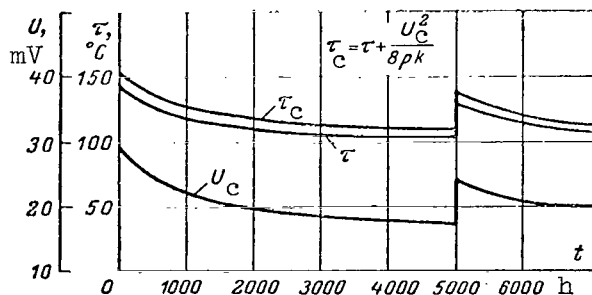


Figure 6. Variation in overheating and voltage drop for silver contacts switched on for second time.

## Overheating of Contact Areas

The overheating of the contact area is of considerable interest. We can assume that the observed deformation of the contacts during prolonged loading is produced by the excessive heating of the contact areas, which is different from the average overheating of the contacts  $\tau$ . The average temperature rise of the silver contacts during the tests was measured with thermometers.

The excessive heating of the contact area  $\tau_c$  may be computed by using a relationship given in (refs. 1 and 2) /186

$$\tau_c = \tau + \frac{U_c^2}{8\rho\lambda} \quad (1)$$

where  $U_c$  is the voltage drop at the contact;

$\rho$  is the specific resistance of contact material;

for silver  $\rho = 1.65 \cdot 10^{-6} \text{ cm} \cdot \Omega$ ;

$\lambda$  is the heat conductivity of the contact material;

for silver  $\lambda = 4.17 \text{ W/cm} \cdot \text{deg}$ .

In our case, when the voltage dropped from 30 to 20 mV, the excess temperature of the contact area above the average contact temperature was only 8 to 16°C.

In figure 6, next to the curve of  $\tau$  showing the average excess heating of the contacts, we introduce the curve for  $\tau_c$ , which characterizes the excess heating of the contact area.

Thus, within the limits of experimental error, the excess heating of the contact area differs little from the average excess heating of the entire contact and cannot produce a substantial effect on this phenomenon.

## Variation in Contact Resistance as a Function of Temperature

By observing the variation in the voltage drop of the contacts and in their temperature during these experiments, we were able to determine the variation in contact resistance as a function of temperature at different instants of time. These variations are shown in figure 7.

It turned out that after silver contacts carry current for a prolonged period of time, their contact resistance  $r_c$  does not increase with temperature, as we might expect from the well-known relationship (ref. 1)

$$r_c = r_0 \left( 1 + \frac{2}{3} \alpha \tau \right) \quad (2)$$



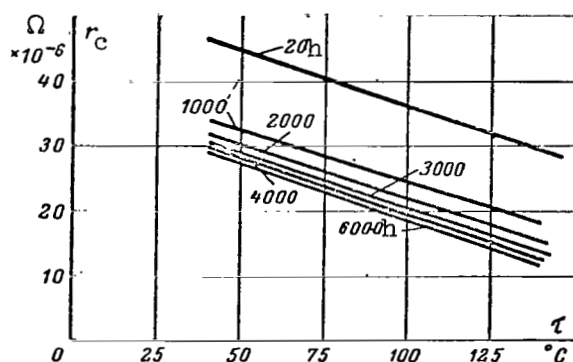


Figure 7. Variation in resistance of silver contacts as function of temperature for different instants of time.

but drops according to a linear law with temperature increase. This nature of the variation is retained during the entire period of time, while the contacts are carrying a current.

In each contact the magnitude of the resistance  $r_c$  decreased with /187 time, while the nature of the variation  $r_c = f(\tau)$  remained the same.

We should note that when the excess temperature varied from 50 to 140°C at the beginning of the experiments (curve 1, fig. 7), the resistance of the contact decreased by a factor of 1.5, while after 5000 h (fig. 7) it had decreased by a factor of two.

The deviation from expression (2), which we have described, is apparently explained by the fact that during the derivation of expression (2) the plastic deformation of the contact material due to prolonged heating was not taken into account.

#### Dimensions of the Contact Areas

As we have pointed out (fig. 6), the examination of contacts after 5,000 h of operation under current revealed darkened contact areas free of oxides. By using magnification it was possible to measure their areas with a high degree of accuracy. The results of these measurements showing the variation in the size of the contact area, free of oxides, as a function of excess temperature are shown in figure 8. It turned out that the dimensions of the area increase sharply with excess temperature.

The magnitude of the contact area of a purely metallic contact, as /188 we know (refs. 1 and 2), may be computed from the relationship

$$r_c = \rho/2a, \quad (3)$$

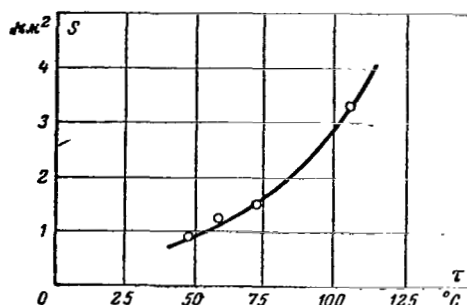


Figure 8. Variation in magnitude of contact area as function of excess temperature (after 5,000 h of operation with current).

where  $r_c$  is the contact resistance;

$\rho$  is the specific resistance of the contact material;

$a$  is the contact area radius (it is assumed that the contact area is circular).

Proceeding from (3) and taking into account the variation in the specific resistance  $\rho$  as a function of temperature, we obtain an expression for the contact area

$$S = \pi a^2 = \pi \frac{\rho^2}{4r_c^2} (1 + \alpha\tau)^2. \quad (4)$$

If we substitute the values of  $r_c$  and  $\tau$  into this expression, we obtain an area  $S$  which is less than that measured directly.

After 5,000 h of operation with a current, the resistance of contacts in equipments where a current of 1,000 A passes through one roller was equal to

$r_c = 17.5 \cdot 10^{-6} \Omega$ , while the temperature was  $\tau = 125^\circ\text{C}$ .

Substituting these quantities into equation (4), we obtain

$$\begin{aligned} S &= 3.14 \frac{1.65^2 \cdot 10^{-12}}{4 \cdot 17.5^2 \cdot 10^{-12}} (1 + 0.0036 \cdot 125)^2 = \\ &= 1.45 \cdot 10^{-3} \text{ cm}^2 = 1.45 \text{ mm}^2. \end{aligned}$$

Direct measurements give a value of  $S = 3.3 \text{ mm}^2$ , i.e., there is a discrepancy by a factor of 2. The discrepancy is of the same order for other points on the curves in figure 8.

/189

What produces this discrepancy?

We can make the following hypotheses:

(a) We measured the entire surface free from oxides. It is possible that only part of the surface participates in the transmission of current from one contact to the other.

(b) Expression (3) is the basis of the calculation which assumes that the dimensions of the contact area are much smaller than the cross section of the contact itself. In our case, as we can see from figure 5, the dimensions of the area free of oxides are comparable with the width of the contact roller. This produces an increase in resistance  $r_c$  and a decrease in the contact area computed by means of expression (4).

By using a coefficient determined experimentally in expression (4) and taking its value close to two, we can construct the curves (fig. 9) which show the variation in the contact area as a function of time for contacts with different current loadings.

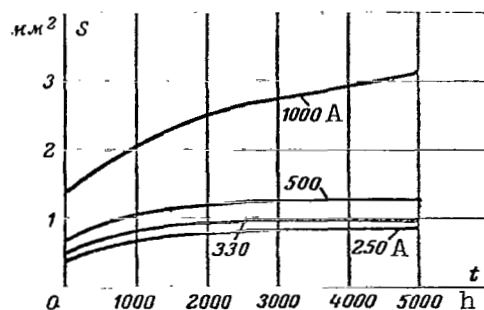


Figure 9. Variation in size of contact areas as function of time for different current loads.

These curves show that contact areas increase rapidly at first and then their rate of increase slows down. This takes place because the specific pressure on the contact area decreases as the area increases.

## Conclusions

(a) The electrical resistance of silver contacts during excessive heating (above the temperature allowed by the norms) and prolonged operation does not increase, but has a tendency to decrease. /190

This tendency increases with contact temperature.

(b) The resistance of silver contacts at high excess temperatures drops with temperature. This is associated with a slow growth in the residual deformation of the heated contacts.

(c) The excess temperatures of silver contacts for a series of electrical equipments may be increased substantially over values allowed by the present norms. For this reason the norms for the currents in a series of equipments operating with silver contacts may be increased.

(d) A need has arisen for the reexamination of existing norms for the heating of silver contacts.

#### REFERENCES

1. Holm, T. Electric Contacts (Elektricheskiye kontakty). Izd-vo I. L., 1961.
2. Merl, V. Electric Contact (Elektricheskiy kontakt). Gosenergoizdat, 1962.
3. Keil, A. Materials for Electric Contacts (Werkstoffe für elektrische Kontakte). Berlin, 1960.

THE DETERIORATION OF CONTACTS DURING THE SWITCHING OF  
LOW VOLTAGE (UP TO 220 V) dc AND ac CURRENTS

V. T. Nezhdanov and B. A. Vasil'yev

Introduction

The electric deterioration of contacts is observed both during the opening and closing of dc and ac electric circuits and depends on the following factors: /190

(1) operating conditions:

- (a) type of current (dc or ac);
- (b) value of current and voltage;
- (c) nature of the load (when dc current is turned on, the wear is greater at lower load inductance; in all other cases, when the inductance of the switched circuit is increased, the deterioration of the contacts increases); /191
- (d) the number of cycles (makes and breaks) per hour, if this produces an excess heating of the contact;
- (e) the media in which the current is commutated by the contacts;

(2) the structural parameters of the equipment:

- (a) the duration of the arc at the contacts;
- (b) the time and amplitude of contact vibrations during making, which depend substantially on the initial contact pressure, on the speed of contact movement at the instant of making, on the mass of contacts with the contact holders, on the rigidity of contact springs and on the shocks produced by the magnetic system;
- (c) contact materials, their dimensions, shape, purity and smoothness of the contacting surface as well as the homogeneity of the structure;
- (d) the magnitude and direction of the magnetic field in the arc-quenching zone;
- (e) the speed of separation of the contacts during breaking.

The electric deterioration of contactor contacts under heavy duty conditions is 10 to 20 times less than their mechanical durability, and at a frequency of 1200 commutations per hour the contacts must be replaced quite frequently, which is difficult to do under operating conditions. It takes a long time to develop new contactors and put them into production. New heavy duty

contactors of the KPV-600 and KT-5000 series have the same shortcomings. Therefore, a need has arisen to produce contact systems which resist wear and which can be placed into production with minimum design changes. The simplest solutions to this problem are as follows:

- (1) the replacement of contact material with one more resistant to wear;
- (2) the selection of a more rational value for the magnetic field in the arc-quenching zone;
- (3) the selection of contact separation rate during breaking.

Investigations were conducted at VNIIEM to determine the variation <sup>/192</sup> in the electric wear of contacts as a function of contact material and the value of the magnetic field in the arc-quenching zone when dc current is switched off, and also as a function of contact separation speed when ac current is turned off.

#### The Effect of Material and Magnetic Field Intensity on the Wear of Contacts when Switching Off dc Current

It was established (ref. 1) that during the switching off of a dc current of 600 A at 220 V with copper contacts, the wear of these contacts increased when the magnetic field intensity in the contact zone was increased.

SOK15, SN-40, SV-70 and also SOM8 cermet contacts made by oxidation of German silver were investigated at VNIIEM. For comparison purposes, copper contacts were also tested.

The tests were conducted under the same conditions using the same type KP-505 contactors (nominal current of 600 A), manufactured by the Cheboksarsk plant for electrical equipment and designed for heavy duty operation. The contacts have the form of cover plates with the following dimensions: 30 x 30 x 2 mm for SOK15, SN-40, SOM8 and 34 x 25 x 2 mm for SV-70, which were soldered to the copper contact holders with No. 287 solid solder.

To produce an externally controlled magnetic field in the arc-quenching zone, two shunting coils were installed on the contactors in order to maintain a definite external magnetic field intensity. This field was controlled at 50, 250 and 500 Oe.

The power was fed to the circuit by a type PN-1750 dc generator with a power of 130 kW and a nominal voltage of 230 V.

The load consisted of type YaS-2 resistance boxes and type PB concrete reactors. The time constant of the circuit which was switched off was equal to 0.014 sec. The contacts of the test contactors were turned on without current in the main circuit; 50,000-75,000 breaks were performed for each type of contact and for each value of the external magnetic field intensity (50, 250 and 500 Oe).

The magnitude of the contact's cover plate wear was determined from /193 the loss in their weight and from the decrease in depression. Measurements were made before the tests were started and after every 25,000 breaks. The breaking frequency was 600 per hour with PV = 40 percent. The duration of the arc when a current of 600 A was turned off with a recovery voltage of 230 V and an external magnetic field intensity of 50 Oe was 14 msec; for 250 Oe it was 9 msec and for 500 Oe it was 6 msec. As we can see, in this contactor the arc duration, when the magnetic field intensity in the arc-quenching zone is 500 Oe, is almost half of the value when the external magnetic field intensity is 50 Oe. The total weight loss produced by the wear of the contact pair as a function of the number of breaks is shown in figures 1 and 2.

We can see from figures 1 and 2 that when a dc current of 600 A is switched off, and when the external magnetic field intensity in the arc-quenching zone is 50-500 Oe, the contact materials may be placed in the following order of decreasing electric wear resistance: SB-70, SOK15, SOM8, copper (M-1), SN-40, their wear is directly proportional to the number of breaks.

The wear according to change in weight and contact depression of one pair of contacts (stationary and fixed) as a function of external magnetic field intensity during one switching of dc current at 600 A is shown in the table and in figures 3 and 4.

Wear	Magnetic field intensity in Oe	Wear of a pair of contacts from various materials during one switching at different magnetic field intensity				
		SV-70	SOM8	SOK15	SN-40	Copper (M-1)
According to change in weight, g	50	$4.4 \cdot 10^{-5}$	$2.6 \cdot 10^{-5}$	$3 \cdot 10^{-5}$	$16 \cdot 10^{-5}$	$8.4 \cdot 10^{-5}$
	250	$5.6 \cdot 10^{-5}$	-	$3.2 \cdot 10^{-5}$	$10.4 \cdot 10^{-5}$	-
	500	$1.8 \cdot 10^{-5}$	$5.6 \cdot 10^{-5}$	$3.4 \cdot 10^{-5}$	$11 \cdot 10^{-5}$	$10.8 \cdot 10^{-5}$
According to change in gap depression, mm	50	$1.8 \cdot 10^{-6}$	$3 \cdot 10^{-6}$	$2.6 \cdot 10^{-6}$	$22 \cdot 10^{-6}$	
	250	$4.4 \cdot 10^{-6}$	-	-	$16 \cdot 10^{-6}$	
	500	$1.4 \cdot 10^{-6}$	$11 \cdot 10^{-6}$	$6 \cdot 10^{-6}$	$14 \cdot 10^{-6}$	

As we can see from figures 3 and 4, the wear of copper contacts, SOM8 contacts and the SOK15 cermet contacts, when a current of 600 A is switched off, increases both in weight and in gap depression when the magnetic field intensity in the arc-quenching zone increases from 50 to 500 Oe; in each case it follows the same law established for the copper contacts (ref. 1). In the SOK15 contacts, the weight loss is small, while the change in the depression increases substantially with an increase in the magnetic field intensity. /194 This phenomenon is associated with the ejection of liquid bridges from the operating surface of the contacts to its edge in the direction of arc motion. /195

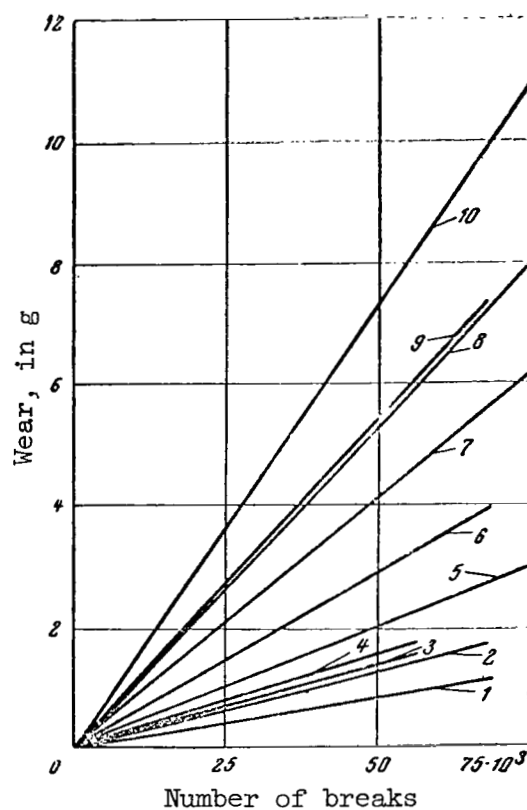


Figure 1. Variation in total wear by weight of contact pair as function of number of times current of 600 A is turned off, when the external magnetic field intensity is 50 and 500 Oe.

1, SB-70,  $H = 500$  Oe; 2, SOM8,  $H = 50$  Oe; 3, SOK15,  $H = 50$  Oe; 4, SOK15,  $H = 500$  Oe; 5, SB-70,  $H = 50$  Oe; 6, SOM8,  $H = 500$  Oe; 7, copper (M-1),  $H = 50$  Oe; 8, copper (M-1),  $H = 500$  Oe; 9, SN-40,  $H = 500$  Oe; 10, SN-40,  $H = 50$  Oe.

The electric wear of the SN-40 contacts when a dc current of 600 A is turned off decreases sharply in weight and in contact depression, when the external magnetic field intensity in the arc-quenching zone increases from 50 to 250 Oe; when the field is further increased to 500 Oe, the wear of the contacts increases slightly. This may be explained by the fact that when the 196 magnetic field intensity is increased to 250 Oe, the duration of the arc at the contacts and the volume of the bridges decrease. A further increase in field intensity to 500 Oe leads to the ejection of liquid bridges and metal vapors beyond the contacts. The nature of the wear of the SN-40 contacts is the same as that of the copper contacts when currents of lower value are switched off (ref. 1). The electric wear of contacts with the SV-70 high-melting components, both from the standpoint of weight and contact depression, increases slightly with an increase in magnetic field intensity to 250 Oe.



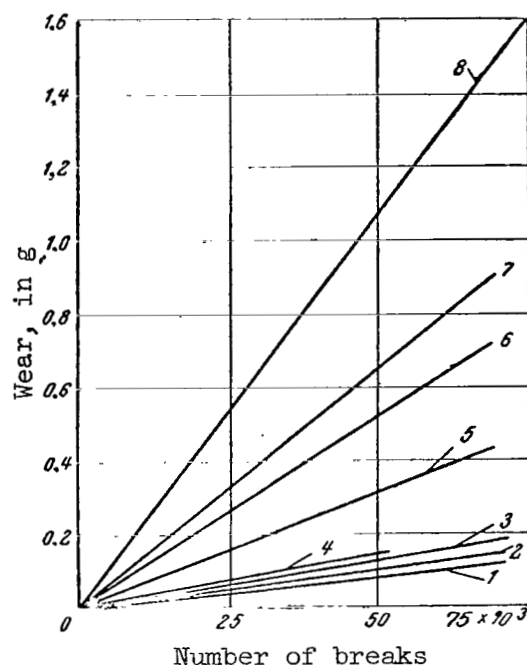


Figure 2. Variation in change of contact depression as function of number of times that 600 A current is turned off, when the external magnetic field intensity is 50 and 500 Oe.

1, SB-70,  $H = 500$  Oe; 2, SB-70,  $H = 50$  Oe; 3, SOK15,  $H = 50$  Oe; 4, SOM8,  $H = 50$  Oe; 5, SOK15,  $H = 500$  Oe; 6, SOM8,  $H = 500$  Oe; 7, SN-40,  $H = 500$  Oe; 8, SN-40,  $H = 50$  Oe.

However, when the magnetic field intensity is increased further to 500 Oe, it decreases sharply. Apparently, this is associated with the fact that in contacts with high-melting components, when the duration of the arc decreases /197 (associated with the increase of the magnetic field in the arc-quenching zone), the volume of liquid bridges and their ejection beyond the limits of the contacts sharply decrease at high magnetic field intensities.

The electric wear of the SV-70 contacts at a magnetic field intensity of 50-250 Oe is greater in weight and smaller in contact depression than that of contacts fabricated from SOK15 and SOM8. This is explained by the fact that the specific weight of the SV-70 contact is equal to  $14 \text{ g/cm}^3$ , while that of SOK15 and SOM8 is  $9.6 \text{ g/cm}^3$ .

As we can see from figures 3 and 4, the electric wear of the SB-70 contacts, under equal conditions, particularly when the external magnetic field intensity in the arc-quenching zone is 500 Oe, is 4-5 times less than that /198 of copper (M-1) contacts which are presently used in the KPV-500 contactors. It is 2-10 times less than that of the SOM8, SOK15 and SN-40 contacts, respectively.

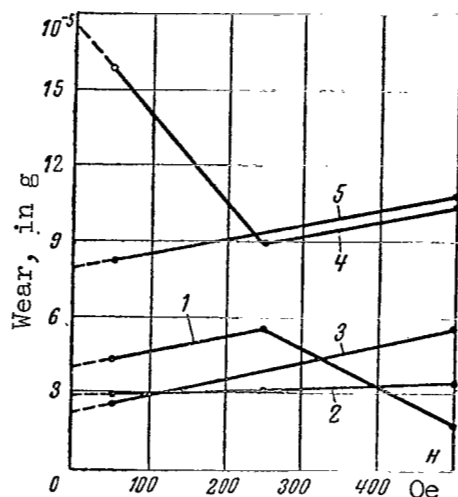


Figure 3. Variation in contact wear (in weight of contact pair) as function of magnetic field intensity produced by shunt coils during one break of 600 A current.

1, SB-70; 2, SOK15; 3, SOM8; 4, SN-40; 5, copper (M-1).

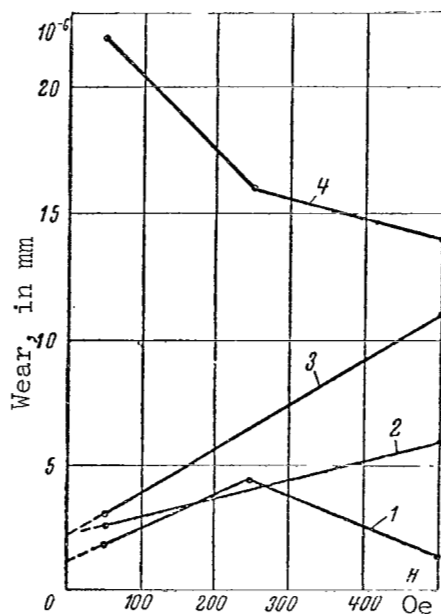


Figure 4. Variation in contact wear (change in contact depression) as function of magnetic field intensity produced by shunting coil during single break of current of 600 A.

1, SB-70; 2, SOK15; 3, SOM8; 4, SN-40.

However, it should be remembered that the generation of strong external magnetic fields in equipment will require a considerable expenditure of material and will also increase the electric losses in the equipment and cause it to heat more.

Since the investigations were conducted using one sample, it is desirable to check the results by using a large number of contactor samples.

#### The Variation in the Wear of Contacts as a Function of Their Separation Speed when a 50 cps ac Current is Switched Off

The variations in the wear of contacts as a function of their separation speed and magnitude of contact gap were determined when currents up to 380 A at 220 V were switched off in the case of a resistive load. Investigations were carried out, using a setup which provided for the displacement of the contacts in the axial direction without arc-quenching devices (the arc was extended and quenched in the gap) with contact gaps of 2 and 6 mm and a single-stage breaking of the circuit. The contact plates were fabricated from a silver bar with a diameter of 25 mm. The contact separation speed was varied from 0.05 to 0.55 m/sec. The current source was a TS-320 transformer, while the load consisted of the YaS-2 resistance boxes. The contacts switched on and switched off currents of 50, 100, 150, 270 and 380 A with a frequency of 60-180 cph. The arc was quenched during the first passage of the current through its zero value.

For each value of contact separation and separation speed 200-400,000 cycles were carried out. The results of the investigation are shown in figures 5 and 6.

As we can see from figures 5 and 6, the electric wear of the contactors decreases 6-12 times with contact separation from 2-6 mm, when the separation speed is in the range from 0.55-0.05 m/sec. This pertains to currents from 50 to 380 A, which are switched off at 220 V when the load is purely resistive.

When the contact separation speed is decreased from 0.55 to 0.1-0.2 /199 m/sec, the wear of the contacts decreases very little, but when the speed is decreased further, it drops sharply. When the contact gap is increased from 2-6 mm under the same conditions, the wear of the contacts in the region of the arc increases.

This is explained by the fact that when the contact separation distance is increased, the arc voltage increases until the first passage of the current through its zero value, due to the high voltage drop in the arc column, which increases the power dissipated in the arc. As a result, fusion, burning /200 and vaporization of the contact material increases; in the case of a long arc, the metal vapors together with the arc column are ejected beyond the contacts, while in the case of a short arc they are condensed on the same surface of the contacts. The small increase in wear during the increase of the contact separation speed to 0.1-0.2 m/sec and above may be explained by the fact

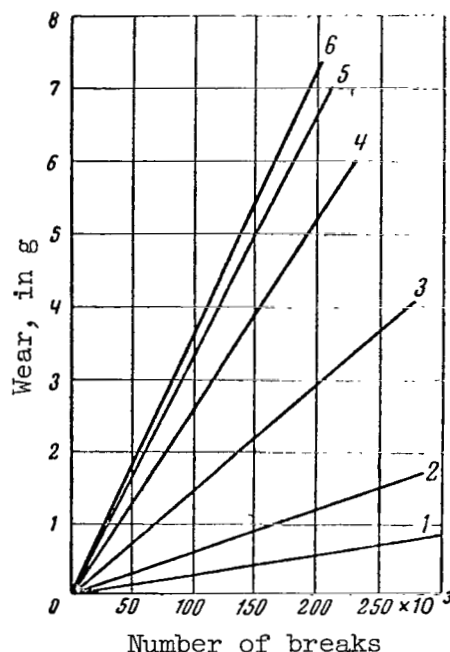


Figure 5. Variation in contact wear as function of number of current breaks at 380 A with different contact separation speeds and different gaps.

1,  $\delta = 2$  mm,  $v = 0.05$  m/sec; 2,  $\delta = 6$  mm,  $v = 0.14$  m/sec; 3,  $\delta = 2$  mm,  $v = 0.11$  m/sec; 4,  $\delta = 2$  mm,  $v = 0.55$  m/sec; 5,  $\delta = 6$  mm,  $v = 0.2$  m/sec; 6,  $\delta = 6$  mm,  $v = 0.55$  m/sec.

that at these speeds the contacts separate by 1-2 mm during one half period of the current, and apparently, in most cases, the arc has time to be quenched, while at larger contact gaps the arc is quenched less frequently.

When an ac current with any inductive load is switched off and the arc is quenched during the first passage of the current through its zero value, apparently the variation in contact wear as a function of their speed of separation will have the same nature as when the ac current of a purely resistive load is turned off.

These conclusions may be used to assist in the modernization of existing equipments and the development of new equipments. It is well known that when the speed of movable contacts during making is decreased (when all other conditions are equal), contact vibration decreases and consequently contact wear decreases. Therefore, with low voltage 50 cps ac equipment at 220 V (with a single break per pole) and at 380 V (with two breaks per pole), when the arc is quenched during the first passage of the current through its zero value, it

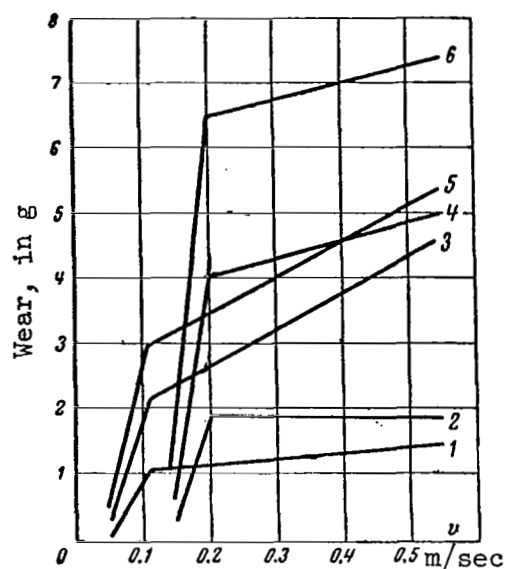


Figure 6. Variation in contact wear as function of contact separation speed and different gaps  $\delta$ .

1,  $\delta = 2$  mm,  $I = 150$  A; 2,  $\delta = 6$  mm,  $I = 150$  A;  
 3,  $\delta = 2$  mm,  $I = 270$  A; 4,  $\delta = 6$  mm,  $I = 270$  A;  
 5,  $\delta = 2$  mm,  $I = 380$  A; 6,  $\delta = 6$  mm,  $I = 380$  A.

is recommended that the speed of the contacts be reduced both when they make and when they break, and that the contact gap also be reduced to 2-3 mm.

#### REFERENCE

1. Bron, O. B. The Electric Arc in Control Equipment (Elektricheskaya duga v apparatakh upravleniya). Gosenergoizdat, 1954.

## RESISTANCE OF CONTACT MATERIALS TO ELECTRIC WEAR

O. F. Gayday

The resistance to electric wear of contacts used in contactors is /201 determined to a large extent by the properties of contact materials. In recent years extensive work has been done to develop various monometallic and cermet compositions for use in contacts of contactors. For this reason it has become necessary to evaluate these contact materials from the standpoint of their capacity to resist wear and to select systems which have maximum resistance to wear. In recent years a large number of materials have been investigated at the Leningrad affiliate of the VNIIEM at the "Elektrosila" plant. This article presents the results of these investigations.

### Methods of Investigation

At the present time there is no standard procedure for testing the /202 resistance of contact materials to wear. For this reason, instead of testing materials for wear, we investigated the wear of contacts made from various materials and used in the KM-2000 contactors produced by the plant. These contactors are designed for a nominal current up to 300 A dc and up to 150 A ac. The total wear produced by the making and breaking of contacts was investigated.

The operating conditions for the test were selected on the basis of the following considerations. A contactor is used most frequently to turn on a stationary motor and to turn off a motor which has attained full operating speed and which carries a nominal load. This means that when an asynchronous motor is turned on, a current equal to 6-7 times the nominal value must pass through the contacts of the contactor. The amplitude of the first half wave may even exceed the nominal current by 10-11 times. When the loaded electric motor is turned off, the current flowing through the contacts is of nominal value, while the voltage is only 0.15-0.2 of the nominal line voltage.

When a dc motor is turned on, the current through the contacts of the contactor is equal to 2.5-4 of the nominal value. The loaded motor is turned off at the nominal current and at a voltage equal to 0.1-0.2 of the nominal value.

During testing of the contacts special provisions were made so that their wear was produced under precisely these conditions.

The simulation is difficult, because it is difficult to select a motor with the necessary parameters for each contactor. In addition, testing of contacts for wear requires a long period of time. To accelerate the test process

it is necessary to turn on and turn off the contactors at a higher frequency (up to 150 commutations per hour). Under these conditions the electric motor overheats, and for this reason it is necessary to use artificial schemes.

Figures 1 and 2 show the arrangements used to test ac and dc contact pairs for electric wear at the equipment laboratory of the Leningrad affiliate of VNIIEM.

The resistive load consisted of type SN resistance boxes, using a constantan ribbon or wire (for currents of 25-150 A), and YaS type resistance boxes, using cast iron or the SN type using Nichrome (for current of 300-600 A).

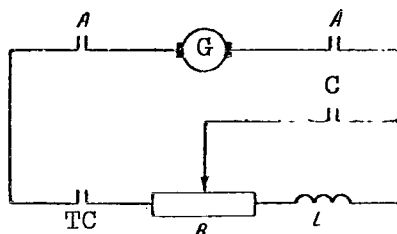


Figure 1. Diagram of test setup for measuring dc contactor wear.

G, generator; TC, test contactor; C, auxiliary contactor; A, automatic device; R, resistance; L, inductance.

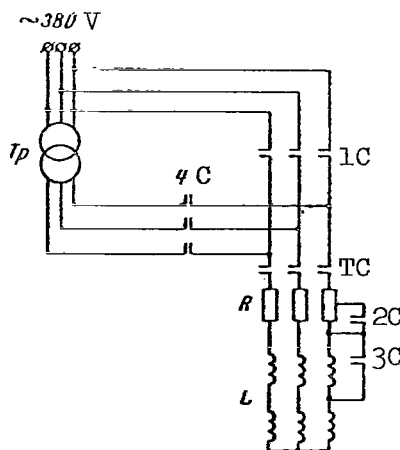


Figure 2. Diagram of equipment used to test wear of ac contactors.

TC, test contactor; R, resistance; L, inductance; 1C, 2C, 3C, 4C, auxiliary contactors.

The inductive load for ac operation consisted of coils without cores connected in series. The construction of such a reactor makes it possible to control its inductance in steps. The inductances of the reactors are computed by means of the following equation (ref. 1)

$$L = 10.5n^2D \left( \frac{1}{\frac{2h}{D} + \frac{2b}{D}} \right)^x \cdot 10^{-6} \text{ mH},$$

where n is the number of turns;  
 D is the average diameter in cm;  
 b is the radial width of the winding in cm;  
 h is the axial length of the winding in cm;

$x = 0.75$  for the case when  $0.3 < \frac{1}{\frac{2h}{D} + \frac{2b}{D}} \leq 1$ ;

$x = 0.5$  for the case when  $1 < \frac{1}{\frac{2h}{D} + \frac{2b}{D}} \leq 3$ .

Experience has shown that the deviation of the reactor inductance from its calculated value does not exceed  $\pm 10$  percent.

The inductive loads in dc schemes consisted of chokes, except when contactors were tested at a nominal current of 600 A, in which case air reactors were used.

The scheme shown in figure 2 was used to test contacts at nominal currents of 25-150 A.

The scheme shown in figure 3 was used to test ac contacts at nominal currents of 300 and 600 A. Power was supplied by the GPM-1000-750 type generator producing 830 kVA at 460 V and 1030 A.

The test and auxiliary equipments were controlled by means of cam controllers. Experience has shown that these are more reliable than relays and provide for a stable cycle.

The contact materials were tested by means of dc contactors 5 of the KM2000 series with a nominal current of 300 A.

Contacts whose dimensions were 19 x 13 x 3 mm (16 x 13 x 3 mm for SOK15) were soldered to copper contact holders using No. 287 solder (fig. 4).

The test contacts were used to switch on a current equal to 4 times its nominal value at 220 V and to switch off a nominal current at 110 V fed to an inductive load of 2 mH. The making and breaking frequency was 600 operations per hour with PV = 40 percent. The equivalent current per cycle was equal to the nominal current of the contactor. The magnitude of the current was measured by means of an oscilloscope.



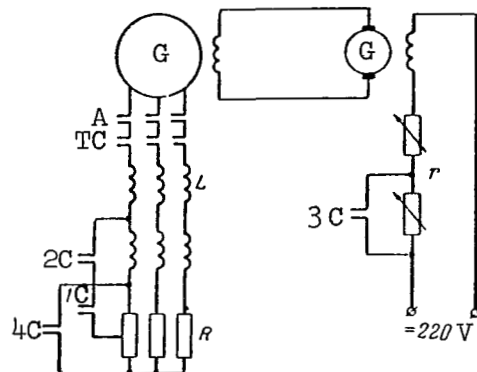


Figure 3. Diagram of test setup for measuring wear of ac contactors.  
G, generator; A, automatic device; TC, test contactors; L, inductance; R, resistance; r, regular rheostat; 1C, 2C, 3C, 4C, auxiliary contactors.

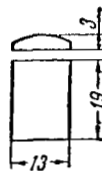


Figure 4. Form of soldered contact plate.

The criterion for evaluating the wear of contacts was the variation in the total thickness of the contact pair and the variation in the weight of each of the contacts measured at the beginning and at the end of the tests. The wear by weight per operation was determined by dividing the total weight loss of all the contacts by the number of breaks and by the number of total operations. /205

The value of the specific weight loss (the weight wear per operation) makes it possible to compare the results with those published in the literature. In addition, the degree of contact destruction under the action of erosion was examined. Tests were stopped under the following conditions:

- (1) when the depression of the contacts reached a value equal to 0.15-0.2 of its initial value;
- (2) when at least one of the soldered contacts was worn so that the copper of the contact holder began to show;
- (3) when contacts were welded.

In the course of the tests the voltage drop at the contacts and their temperature were periodically measured.

The physical properties of the test contact materials and the results of the test are shown in table 1.

TABLE 1. PHYSICAL PROPERTIES OF CONTACT MATERIALS AND RESULTS OF THE TESTS

Material	Composition	Vickers hardness, kg-wt/mm <sup>2</sup>	Density g/cm <sup>3</sup>	Specific Electrical Resistance, $\Omega \cdot \text{mm}^2/\text{m}$	Maximum change in contact depression, mm	Specific weight loss, g	Number of Operations in thousands
Silver	99.9% Ag	26	10.5	0.0161	1.15	0.102	200
SOM15	95% Ag, 5% CuO	40	9.9	0.0195	3.1	0.42	80*
SOM10	90% Ag, 10% CuO	63	9.8	0.0243	2.25	0.17	247
SOM15	85% Ag, 15% CuO	56	9.1	—	2.25	0.202	168*
SOK15	85% Ag, 15% CdO	30—60	10.1	0.029	1.1	0.163	117
MZS37Mo	60% Mo, 37% Ag, 3% Cu	160	10.1	0.0423	3.0	2.55	28*
SKV30	70% Ag, 30% Wc	90	10.6	0.0268	3.5	1.07	34*
Kd5KV10	65% Ag, 20% Ni, 10% Wc, 5% Cd	80	9.9	0.0515	2.0	1.76	6*
SNZK	64% Ag, 30% Ni, 5% Cd, 1%C	70	9.0	0.056	2.7	0.75	50
SNChK	54% Ag, 40% Ni, 5% Cd, 1%C	80	9.1	0.0595	1.15	0.6	31*
SM40	60% Ag, 40% Mo No	90	—	0.0342	1.9	2.22	10*
SV50	50% Ag, 50% W	115	13	0.0318	1.55	3.26	11
Copper	—	35	8.89	0.0175	3.65	0.477	60
MV20	80% Cu, 20% W	100	9.8	0.0242	0.75	0.715	27*
CuCd2	98% Cu, 2% Cd	120	8.7	0.0187	2.85	0.525	78
CuCd Ag 4	92.8% Cu, 2.1% Cd, 5.1% Ag	110	8.8	0.0203	—	1.45	36*
CuCd Ag 5	90.7% Cu, 4.3% Cd, 5% Ag	110	8.8	0.0213	1.75	0.583	40*

\*Contacts became welded.

The operation of the contacts was also investigated with ac current. These tests were conducted with the KM-2000 contactor with a nominal current of 150 A.

The investigation covered silver contacts and SOM cermet contacts (with copper oxide content from 5 to 25 percent) as well as SOK15 contacts.

The test contacts were used to switch on a current equal to 6 times the nominal value with  $\cos \varphi = 0.4$  and to switch off a nominal current with  $\cos \varphi = 0.4-0.5$  at 50 V. The equivalent current per cycle was equal to the nominal current of the contactor. The switching frequency was 1320 operations per hours with  $PV = 40$  percent. The initial contact pressure was 2.3 kg weights, contact depression 3.5-4.0 mm and a contact gap of 8-8.5 mm. The results of the tests are shown in table 2.

TABLE 2. WEAR OF DIFFERENT CONTACT MATERIALS

Contact material	Maximum variation in depression of contacts, mm	Specific weight loss, $\text{g} \cdot 10^{-4}$	Number of operations in thousands
Silver	1.75	1.18	52*
SOM5	2.6	-	45
SOM10	2.6	0.1	136**
SOM15	3.4	0.1	271
SOM20	2.25	0.9	31*
SOM25	2.4	2.57	9*
SOK15	-	-	206

\*The contact became welded.

\*\*Tests were stopped because the contacts became unwelded from the contact holder.

### Results and Conclusions

1. The relative evaluation of different contact materials tested in dc contactors showed that under test conditions the best contacts were those made of silver and of the SOM10 and SOK15 cermets. They sustained the largest number of operations.

2. The least wear by weight was exhibited by silver contacts. In SOM10 and SOK15 cermet contacts the wear by weight was 1.6-1.7 times greater than for silver.

3. During the testing there was a transfer of metal from the anode to the cathode in all of the above contacts. This phenomenon is most pronounced in silver where the depth of the depression on the contact reached a value /208 of 2 mm, but is less pronounced in SOK15 and even less in SOM10.

4. These results have induced us to settle for the SOM10 and SOK15 materials for the KM-2000 contactors operating with nominal dc currents up to 300 A.

5. The analysis of contact materials tested in ac contactors shows that the maximum number of operations was sustained by contacts made from cermet compositions, SOM15, SOK15 and SOM10.

6. In the investigation of contacts made from SOM cermet with a copper oxide content of 5-25 percent, the best results were obtained with SOM10 and SOM15 contacts. The specific wear by weight in these compositions is practically the same.

7. From these results, in selecting the material for the contacts of the KM-2000 contactors operating with ac currents up to 150 A, we settled for the cermet compositions SOM10, SOM15 and SOK15.

#### REFERENCES

1. Mikhaylov, V. V. The Design of High Voltage Equipment (Raschet i konstruirovaniye vysokovol'tnoy apparatury). Gosenergoizdat, 1951.
2. Bron, O. B. The Electric Arc in Control Equipment (Elektricheskaya duga v apparatakh upravleniya). Gosenergoizdat, 1954.
3. Balagurov, V. A., Galteyev, F. F., Gordon, A. V. and Larionov, A. N. The Design of Electric Equipment Used in Aircraft (Proektirovaniye elektricheskikh apparatov aviatsionnogo elektrooborudovaniya). Oborongiz, 1962.
4. Kuznetsov, R. S. On the Wear of Contacts in Low Voltage Electric Equipment (Ob iznose kontaktov nizkovol'tnykh elektricheskikh apparatov). Vestnik Elektropromyshlennosti, No. 5, 1959.

## A PHENOMENON AT THE CONTACTS OF A SEALED RELAY

A. V. Gordon, V. N. Gimmel'brodskiy and O. N. Mikheyeva

1. The development of various automatic control systems and the in-crease in the number of relays used in these systems have substantially raised the requirements for their reliability. At the same time, the operating conditions of relays are frequently quite severe. This is particularly true of relays used in mobile equipment. At the present time almost all relays used for these purposes are sealed, which protects them from mechanical damage, contamination and direct contact with water and other liquids. To prevent the penetration of dust inside the relay, the cases are tightly fitted and are sometimes sealed. /208  
/209

The TKE type relay (fig. 1), widely used in automation at the present time, has a solid cover which is tightly fitted and rolled on. This construction protects the relay quite well from external effects, but does not seal it hermetically. Therefore, there is a restrained exchange between the inner cavity of the relay and the external atmosphere. It has been established that the latter situation leads to one substantial disadvantage. /210

2. The TKE type relays were produced in large quantities for many years, and no peculiarities were noted in the operation of their contacts. After the "hermetic" sealing of the relays was improved by fitting the case more closely and cementing it in place, one group of relays was condemned due to the adhesion of normally closed contacts.

One of the operations during the checking of finished relays consists of heating a relay for a period of 30-45 min by passing current through its winding. In the course of this test the lamps in the circuit of the normally closed contacts (fig. 2) became lit for some of the relays which were supposed to be open at this time. After the cover was removed from the relay for visual inspection of the relay contacts, this phenomenon did not repeat itself. To investigate the behavior of the relay, a special version of the relay was constructed, whose case had glass inspection windows (fig. 3).

3. Observation through these windows revealed the following. Soon after the windings of the relay are energized, dew begins to precipitate on the stationary small busbar of the normally closed contacts. The dew gradually forms small droplets of water, which gradually build up into a large droplet. The latter hangs down from the busbar and fills the gap between the contacts, forming a water bridge between them. Since the water is distilled, no noticeable flow of current appears at the initial instant. However, the difference of /211

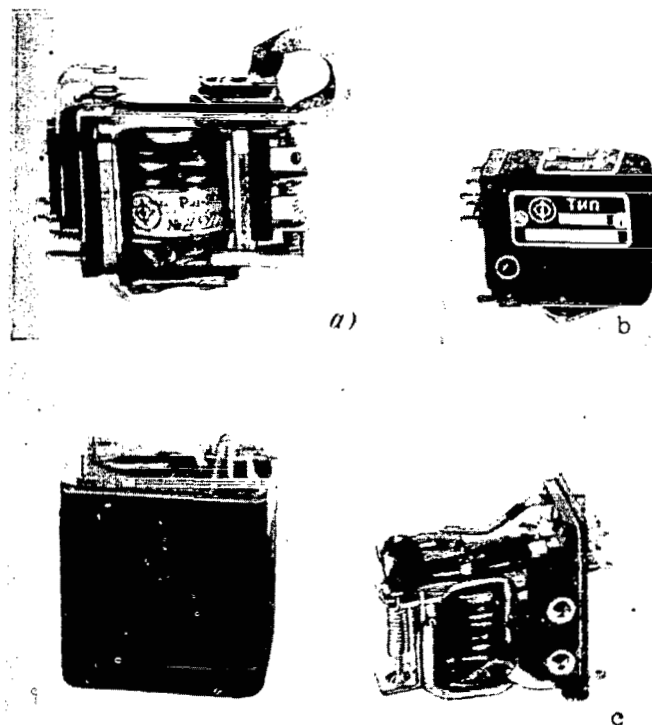


Figure 1. Three methods of packaging electromagnetic switching relays.  
a, open; b, protected from mechanical damage; c, protected from dust.

potential between the two contacts causes the water to break down into oxygen and hydrogen. The active hydrogen liberated in this manner combines with the silver of the contacts and forms silver hydride  $\text{AgH}$ . The latter is oxidized and forms a conducting solution of silver oxide  $\text{Ag}_2\text{O}$  in water. As a result, a current path develops between the open contacts and the signal light goes on.

Initially, the current-carrying region has a relatively large cross section and is filled with a grey loose mass (fig. 4a). As the mass dries under the influence of the passing current, it constricts and becomes denser (fig. 4b) and finally forms a thin, dense, fragile current-carrying bridge (fig. 4c).

4. In a state of rest this "bridge" can be retained for a long period of time. When subjected to an impact, it breaks down. Vibrations (within the limits allowable for the relay) do not break it down. The bridges do not /212 form when the relay is vibrating, because the moisture is unable to collect on the relay contacts in sufficient quantity to breach them.

For dc current the "bridges" on silver contacts are formed when the potential difference between the contacts is 2 V or more.

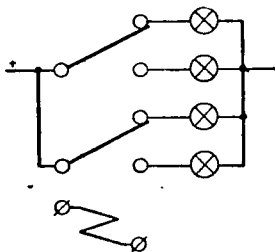


Figure 2. Diagram showing connection of signal lamps.

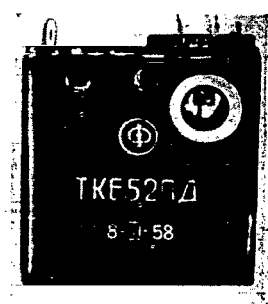


Figure 3. Case with windows for visual observation.

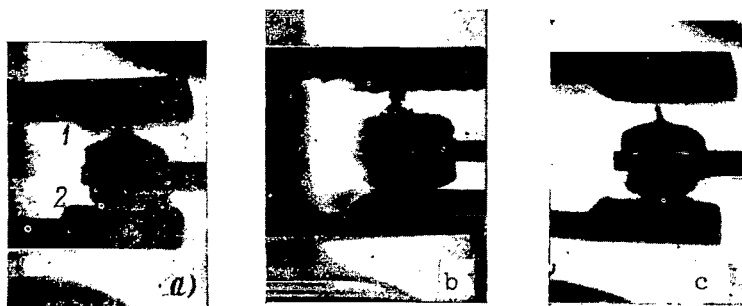


Figure 4. Current-carrying bridges.

In the case of an ac current with a frequency of 50 cps, the formation of bridges on silver contacts takes place approximately at 60 V.

When the gap between the silver contacts is 0.56-0.7 mm, the resistance of the current-carrying bridge at the instant of its formation is approximately 200  $\Omega$ , while at the end of the process it is 0.4-0.5  $\Omega$ .

The current-carrying bridge between the silver contacts is capable of carrying a current of 2-2.5 A for a prolonged period of time. When the current is 5 A, the bridge burns up in a period of 0.5-30 sec.

After the bridge has burned up or is mechanically destroyed, a characteristic gray deposit remains on the contacts and slightly exceeds the transitional resistance between them. As a result, the voltage drop across closed contacts may exceed the allowable limit of 90 mV for this type of relay.

5. The formation of current-carrying bridges across the open contacts was first observed on the TKE52PD relay with silver contacts. This relay is designed to work at an ambient temperature up to +60°C and a winding temperature of +160°C. Therefore, the construction of the relay coil and of other components, which are not made of metallic materials, utilizes textolite, lacquered

silk, cotton threads, silk mantles and compressed materials with ligneous fillers.

Subsequently, the formation of current-carrying bridges across open contacts during their operation under normal conditions was observed also in other similar relays whose contacts were made of silver or of materials which contain silver as a component, specifically: SOM8, OK-12, SRPD-20 and others.

High-temperature relays (TKE52PDT and others), designed for operation in an ambient temperature up to  $+100^{\circ}\text{C}$  with allowable winding temperature to 213  $190-210^{\circ}\text{C}$ , did not develop current-carrying bridges when subjected to the temperature cycle.

In these relays the insulating materials consist of the following: glass textolite, teflon, lacquered glass fibers, glass mantles, and the AG-4 pressed material with glass filler.

In these relays current-carrying bridges were observed only after they remained for a prolonged period of time in a medium with increased humidity, or when moisture was forced into them (evacuation of air from the relay and the injection of humid air).

Since the construction and dimensions of "high-temperature" and "conventional" relays are the same, the difference in their behavior is obviously determined by the difference in the capacity of the materials to absorb water.

The table presents the corresponding data for the TKE52PD and TKE52PDT relays after 48 hours in a humidity chamber with a relative humidity of 98 percent at a temperature of  $+20^{\circ}\text{C}$ .

The amount of moisture absorbed or adsorbed in various parts of the relay is shown in figure 5.

The data show that the conventional relay, when all other conditions are equal, collects approximately 3 times as much moisture as the high-temperature relay (0.147 g or approximately 5 drops instead of 0.047 g or 1.5 drops).

Therefore, the high-temperature relay under normal atmospheric conditions did not form current-carrying bridges, while the conventional relay formed bridges across 20 to 30 percent of the contacts.

The insulation of the coil and the insulating mantles have a different capacity to absorb and adsorb water.

For example, the LSh-2 material collects 25 times more moisture than the LSK-7 material. The silk mantle collects water 6.5 times more than the glass one, etc. The lacquered internal surface of the cap accumulates twice as much moisture (0.0103 g) than the surface which is not lacquered (0.0055 g). Although in the relay which uses the least amount of water-absorbing and adsorbing materials, the danger of current-carrying bridges is substantially reduced, it is not entirely excluded.



THE CAPACITY OF INDIVIDUAL COMPONENTS OF THE HIGH-TEMPERATURE  
RELAY AND THE CONVENTIONAL RELAY TO ABSORB AND ADSORB WATER

/214

Name of component or part	Weight when delivered, g	Weight after drying, g	Weight after 48 hours in humidity chamber, g	Weight of moisture on component parts, g	Moisture content %
TKE52PDT (relay without cover)	69.2278	69.184	69.231	0.047	0.068
TKE52PD (relay without cover)	62.2154	62.1546	62.291	0.1464	0.22
TKE52PDT coil (AG-4 flanges, F-4 and LSK-7 insulation, glass fiber, EK-1 impregnation, PETK4-1 wire)	20.2045	20.2034	20.2253	0.0219	0.11
TKE52PD coil (type A sheet textolite flanges, LSh-2 insulation, sewing thread, 2F-95 lacquer, PEV-1 wire)	20.7456	20.7255	20.798	0.0755	0.36
TKE52PDT contact panel (AG-4 pressed material)	18.3372	18.2858	18.316	0.0222	0.12
TKE52PD contact panel (K-21-22 pressed material)	14.519	14.4516	14.499	0.0474	0.325
TKE52PDT small cable insulation (glass mantle and glass thread)	1.01	1.0984	1.1018	0.0034	0.003
TKE52PD small cable insulation (silk mantle and conventional thread)	1.0236	1.0192	1.041	0.0218	0.021
TKE52PDT coil insulation (LSK-7)	0.8926	0.885	0.8902	0.0012	0.14
TKE52PD coil insulation (LSh-2)	0.507	0.5039	0.5372	0.0333	6.2
TKE52PD and TKE52PDT case:					
a) lacquered	18.4151	18.3860	18.4066	0.0206	0.112
b) not lacquered	17.759	17.7496	17.7654	0.0158	0.09

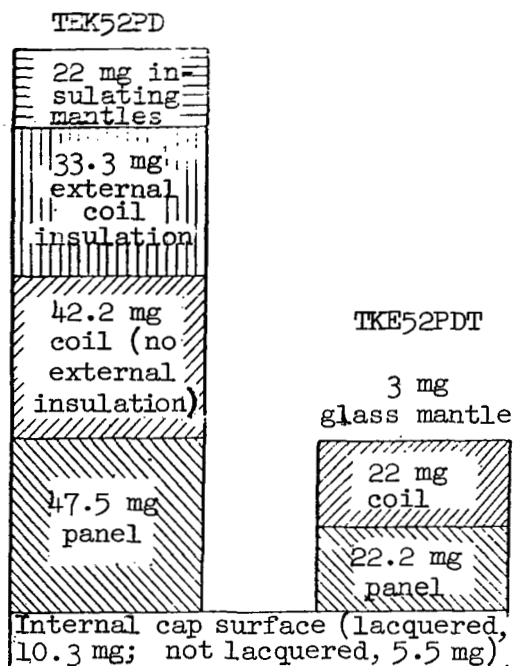


Figure 5. Capacity of relay components to absorb and adsorb water.

Therefore, further attempts were made to eliminate this shortcoming /215 by thermally insulating the leads of the stationary contacts and the contacts themselves. This was accomplished by:

- (a) thermally insulating the external leads with cotton;
- (b) thermally insulating the external leads by means of tubes made from silicon rubber;
- (c) thermally insulating with plastic baffle plates on the stationary contacts.

In all cases the tendency to form current-carrying bridges was lowered, but not to a sufficient degree. Since the effect of current-carrying bridges was most pronounced in the relay with a tightly closed cover and was not observed in relays whose covers had slots, it was decided to provide for the ventilation of the internal space in addition to using favorable insulating materials. For this purpose, a ventilating hole with an area of 0.6 cm<sup>2</sup> was made in the case and was covered with three layers of No. 0063 screen (GOST 3584-53; 7700 meshes per 1 cm<sup>2</sup>). Such a construction provides for an effective protection against penetration of dust into the inner cavity of the relay. /216

The volume occupied by the electromagnetic and relay contact system was equal to  $20 \text{ cm}^3$ , the volume of the air inside the relay was equal to  $25 \text{ cm}^3$ . Thus, the ratio of the filled volume to the unfilled volume is approximately 0.45, and the ratio of the screen area to the air volume is approximately  $0.024 \text{ l/cm}$ . The construction of the relay is shown in figure 6.

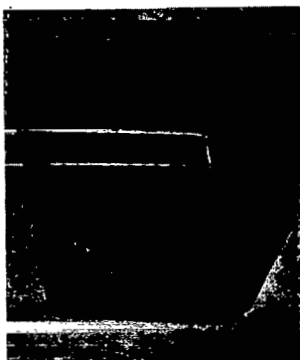


Figure 6. Relay with ventilating windows.

In the course of the preceding investigations it was established that the following conditions are very severe from the standpoint of moisture accumulation inside the relay: the presence of the relay in the humidity chamber for a definite period of time, followed by cooling to  $-70^{\circ}\text{C}$  during a period of 20-30 min, and a second placement into the humidity chamber until dew appears.

Relays with screens (with a total number of 40 contact groups) were subjected to such tests. After 48 hours in the humidity chamber and 5 temperature cycles, current-carrying bridges did not appear. The same results were obtained when the tests were repeated.

Only after the relays were in the humidity chamber for 120 hours, followed by 5 temperature cycles, was there a formation of bridges in 7 percent of the contacts. Under the same conditions, relays without screens and with unstable materials formed bridges in 80-90 percent of the contact pairs.

Icing tests showed that relays with ventilation openings are also less susceptible to the loss of contacting than relays with solid covers. Apparently the introduction of ventilation is responsible for the elimination of volatile substances which are liberated by the components into the relay cavity, and consequently this ventilation decreases the probability of insulating films forming on the contacts.

The investigations which were carried out permit the following conclusions:

(a) The relay either must be vacuum-sealed or must be ventilated. The relay must not be sealed in such a way that exchange with the outer medium is difficult, but not completely eliminated.

/217

(b) The complete elimination of the effect of humidity on the operation of the contact system may be achieved only in a hermetically sealed relay.

Ventilated designs eliminate the formation of moisture in the relay volume, reduce the danger of current-carrying bridges and reduce the icing of contacts and the formation of insulating films on these contacts due to the precipitation of volatile substances given off by the components of the relay.

(c) The materials used in relays must have a minimum capacity to absorb and adsorb water.

# EFFECT OF MOISTURE ON THE FORMATION OF CURRENT-CARRYING BRIDGES ACROSS ELECTRIC CONTACTS MADE OF DIFFERENT MATERIALS

G. N. Volosevich

The purpose of the present work is to investigate the tendency of different contact materials to form current-carrying bridges in the presence of moisture. /217

As shown in reference 1, the open silver contacts of switching relays which carry a dc voltage may form current-carrying bridges in the presence of moisture, which short-circuit the contact gap and produce false operation of circuits.

Because silver is widely used as contact material, all initial experiments were carried out using silver contacts.

In order to carry out in detail the investigation of the conditions for the formation of current-carrying bridges across contacts of various materials, a device was built which made it possible to install removable contacts and to control the contact gap (fig. 1). /218

To simulate the precipitation of moisture and the conditions under which a current-carrying bridge is formed, a drop of distilled water was introduced into the contact gap and the necessary voltage was applied to the contacts. The circuit diagram of this device is shown in figure 2.



Figure 1. Device for studying formation of current-carrying bridges.

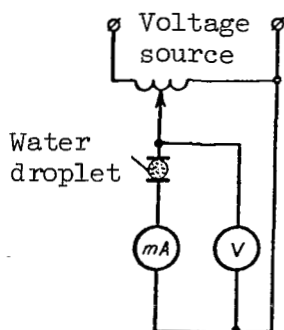


Figure 2. Circuit diagram for the device shown in figure 1.

It is well known that pure distilled water has a low electrical conductivity ( $0.043 \cdot 10^{-6} \Omega^{-1} \cdot \text{cm}^{-1}$ ). These properties are retained only when water is completely isolated from air. Water which is in contact with air contains dissolved gases (carbon dioxide), which form carbonic acid and increase its electrical conductivity by a factor of several tens (ref. 2). Thus, distilled water by itself is a very weak electrolyte, i.e., is only partially dissociated into ions. Under the action of applied voltage, a drop of distilled water introduced into the contact gap is saturated to some extent by the metal oxide of the contact material and its electrical resistance decreases, so that it forms a current-carrying bridge.

#### The Effect of dc Voltage and Contact Gap on the Formation of Current-Carrying Bridges on Silver Contacts

The tendency of contact material to form current-carrying bridges is /219 determined by the leakage current and by the electric resistance of the contact gap short-circuited with a drop of distilled water.

The effects of dc voltage and of the size of the contact gap on leakage currents and on the electric resistance of the contact gap were determined for silver contacts with a diameter of 6 mm at dc voltages of 1.5, 2, 3 and 5 V with contact gaps of 0.3, 0.5 and 0.7 mm.<sup>1</sup> Table 1 shows the average data on the variation of the leakage current between silver contacts as a function of time. We should note that the formation of the current-carrying bridge under the action of applied voltage is an unstable process, and its electric resistance fluctuates over a rather wide range. Table 2 presents the data on the variation of the electric resistance of the contact gap. It follows from the table that the time when the formation of the current-carrying bridge starts depends on the values of the voltage and of the gap. It decreases with increased applied voltage and decreased gap.

<sup>1</sup>A. P. Goryachev, V. T. Gerasimov and V. P. Simonov participated in the work.

TABLE 1. VARIATION IN THE VALUES OF LEAKAGE CURRENTS OF SILVER CONTACTS FOR dc OPERATION, IN mA

Time	Voltage between contacts, in V									
	1.5	2			3			5		
	Contact gap, in mm									
	0.3	0.3	0.5	0.7	0.3	0.5	0.7	0.3	0.5	0.7
0	0	0	0	0	0	0	0	0	0	0
15 sec	0	2	0	0	40	0	0	225	17	0
30 sec	0	20	0	0	450	0	0	1100	70	5
45 sec	0.7	70	0	0	750	5	0	1600	475	25
1 min	5	150	10	0	1000	15	10	2500	750	90
1.5 min	43	500	50	0	2000	100	100	Bridge burned up	Bridge burned up	750
2.0 min	140	2000	150	10	Bridge burned up	750	250			Bridge burned up
2.5 min	300	3500	300	30		Bridge burned up	650			
3.0 min	400	Bridge burned up	900	50			1200			
3.5 min	800		1500	75			1500			
4.0 min	1200		3000	100			Bridge burned up			
	Bridge burned up		Bridge burned up							
5 min				300						
10 min				2200						

TABLE 2. VARIATION IN THE MAGNITUDE OF THE ELECTRIC RESISTANCE OF THE CONTACT GAP OF SILVER CONTACTS SHORT-CIRCUITED WITH A DROP OF DISTILLED WATER IN THE CASE OF dc CURRENT, IN  $\Omega$

Time	Voltage between contacts, in V									
	1.5		2		3			5		
	Contact gap, in mm									
	0.3	0.3	0.5	0.7	0.3	0.5	0.7	0.3	0.5	0.7
0 sec										
15 "		1 000			75			22	294	
30 "		100			6.7			4.5	71	1 000
45 "	2 100	29			4.0	600		3.1	11	500
1 min	300	13	200		3.0	200	300	2.0	6.7	55
1.5 "	35	4.0	40		1.5	30	30			6.7
2.0 "	10.7	1.0	13.3	200		4.0	12			
2.5 "	5.0	0.6	6.7	67			4.6			
3.0 "	3.7		2.2	40			2.5			
3.5 "	1.9		1.3	26.6			2.0			
4.0 "	1.2		0.7	20						
5.0 "				6.7						
10.0 "				0.9						

The intensity of increase in leakage currents (rate of change of the resistance) also depends on these parameters. As far as the minimum resistance of the bridge is concerned, this quantity in the final analysis depends little on the magnitude of the voltage and of the gap, and on the average is reduced to 0.5-1.5  $\Omega$ . However, if we note that as the contact gap is increased, a larger amount of moisture and a longer time will be required to short-circuit the contacts under operating conditions, and that the conditions for the retention of the bridge in this case become more difficult, such an increase in the contact gap may decrease the number of relay failures under operating conditions.

For a given contact gap, some minimum value of applied voltage is necessary for the formation of a current-carrying bridge. For silver con- /221  
tacts with a gap of 0.3 mm, this voltage lies in the range 0.7-0.9 V, while with a gap of 0.5 mm it lies in the range of 0.9-1.1 V, and with a gap of 0.7 mm the range is 1.1-1.3 V. As we have already stated, the time at which the current-carrying bridge forms depends on the magnitude of the applied voltage and of the gap. For silver contacts operating with a dc current, this time has values shown in table 3.

The burning of the current-carrying bridge, as we can see from /222  
table 1, takes place with a current of 0.75-3.5 A. As the voltage between the contacts is increased, the power dissipated in the contact gap also increases, and therefore the time during which the current-carrying bridge burns up decreases.



TABLE 3. AVERAGE TIME WHEN FORMATION OF THE CURRENT-CARRYING BRIDGE STARTS

Contact gap, in mm	Voltage between contacts, in V					
	1	1.5	3	5	10	25
0.3	10 min	1.5 min	25 sec	12 sec	3 sec	0.5 sec
0.5	-	4 min	1 min	25 sec	6 sec	1 sec
0.7	-	9 min	1.5 min	50 sec	12 sec	2 sec

#### Effect of Voltage and ac Frequency on the Formation of Current-Carrying Bridges across Silver Contacts

To determine the effect of voltage and ac current frequency on the formation of current-carrying bridges, the leakage currents were measured, and the electrical resistances of the contact gap were computed for the case of silver contacts at a frequency of 50 cps and 400 cps and at different voltages. These quantities were determined with contact gaps of 0.3, 0.5 and 0.7 mm and are presented in tables 4-9.

TABLE 4. VARIATION IN THE LEAKAGE CURRENTS OF SILVER CONTACTS OPERATING WITH A 50 cps ac CURRENT, IN mA

Time in min	Voltage between contacts, in V									
	3		5		10		25			
	Contact gap, in mm									
	0.3	0.3	0.5	0.7	0.3	0.5	0.7	0.3	0.5	0.7
0	0.25	0.55	0.36	0.30	1.0	0.55	0.55	3.5	2.0	1.60
0.5	0.45	0.75	0.40	0.32	1.48	0.93	0.65	4.4	2.77	2.56
1.0	0.52	0.80	0.42	0.32	1.55	1.04	0.73	4.5	2.90	3.00
1.5	0.56	0.80	0.45	0.36	1.65	1.06	0.75	4.6	2.95	3.05
2.0	0.59	0.82	0.45	0.38	1.65	1.08	0.80	4.7	3.00	3.10
2.5	0.60	0.82	0.45	0.38	1.68	1.10	0.82	4.8	3.10	3.20
3.0	0.60	0.84	0.45	0.39	1.70	1.10	0.82	5.0	3.10	3.25

It would seem that with a symmetric ac current there should be no precipitation of the metal on the contacts, since the alternation of the process of solution and precipitation of the metal must be mutually compensated when the direction of the current changes. Data which have been obtained on the variation of the electric resistance of a drop of distilled water on silver contacts under the action of an ac current show that although the process of electrolysis is made more difficult in this case, it nevertheless takes place. /223

TABLE 5. VARIATION IN THE LEAKAGE CURRENTS OF SILVER CONTACTS IN THE CASE OF 400 cps ac CURRENT, IN mA

Time in min	Voltage between contacts, in V									
	3		5		10		25			
	Contact gap, in mm									
	0.7	0.3	0.5	0.7	0.3	0.5	0.7	0.3	0.5	0.7
0	0.15	0.45	0.32	0.30	1.18	0.73	0.61	2.80	1.75	1.65
0.5	0.15	0.46	0.37	0.32	1.35	0.84	0.68	3.20	2.48	2.45
1.0	0.15	0.46	0.38	0.32	1.41	0.89	0.80	3.60	2.52	2.62
1.5	0.15	0.46	0.38	0.32	1.44	0.93	0.84	3.90	2.53	2.57
2.0	0.15	0.46	0.38	0.32	1.50	0.95	0.86	4.20	2.54	2.57
2.5	0.15	0.46	0.38	0.32	1.51	0.96	0.90	4.50	2.54	2.57
3.0	0.15	0.47	0.39	0.32	1.54	0.97	0.92	4.70	2.54	2.58

TABLE 6. VARIATION IN THE VALUES OF THE ELECTRICAL RESISTANCE OF THE CONTACT GAP OF SILVER CONTACTS WHICH ARE SHORT-CIRCUITED WITH A DROP OF WATER IN THE CASE OF 50 cps ac CURRENT, IN  $\Omega$

Time in min	Voltage between contacts, in V									
	3		5		10		25			
	Contact gap, in mm									
	0.3	0.3	0.3	0.7	0.3	0.3	0.7	0.3	0.5	0.7
0	12 000	9 100	13 900	15 600	10 000	18 200	18 200	7 130	12 500	15 600
0.5	6 770	6 770	12 500	15 600	6 750	10 700	15 400	5 600	9 300	9 760
1.0	5 770	6 260	12 400	11 280	6 450	9 600	13 700	5 500	8 620	8 350
1.5	5 360	6 260	11 100	13 880	6 050	9 450	13 300	5 430	8 480	8 200
2.0	5 100	6 110	11 100	13 100	6 050	9 260	12 500	5 320	8 300	8 070
2.5	5 000	6 100	11 100	13 100	5 950	9 100	12 200	5 200	8 050	7 820
3.0	5 000	5 050	11 100	12 800	5 880	9 100	12 200	5 000	8 070	7 700

TABLE 7. VARIATION IN THE ELECTRIC RESISTANCE OF THE CONTACT GAP OF SILVER CONTACTS SHORT-CIRCUITED WITH A DROP OF DISTILLED WATER IN THE CASE OF 400 cps ac CURRENT, IN  $\Omega$

Time in min.	Voltage between contacts, in V									
	3	5			10			25		
	Contact gap, in mm									
	0.7	0.3	0.5	0.7	0.3	0.5	0.7	0.3	0.5	0.7
0	20 000	11 100	15 650	16 670	8 470	13 700	16 400	8 950	14 300	15 150
0.5	20 000	10 900	13 500	15 600	7 200	11 900	14 700	7 800	10 100	10 200
1.0	20 000	10 900	13 150	15 600	7 100	11 250	12 500	6 910	9 900	9 700
1.5	20 000	10 900	13 150	15 600	6 950	10 800	11 900	6 400	9 870	9 700
2.0	20 000	10 900	13 150	15 600	6 670	10 500	11 610	5 950	9 860	9 700
2.5	20 000	10 900	13 150	15 600	6 630	10 400	11 100	5 550	9 860	9 700
3.0	20 000	10 900	12 730	15 600	6 500	10 300	10 850	5 300	9 860	9 700

TABLE 8. AVERAGE VARIATION IN THE MAGNITUDES OF THE LEAKAGE CURRENT OF SILVER CONTACTS WITH A CONTACT GAP OF 0.3 mm FOR THE CASE OF ac CURRENT, IN mA

Time, sec	Frequency of 50 cps		Frequency of 400 cps
	127 V	220 V	200 V
0	80	140	330
5	90	90	200
10	90	Bridge burned up	Bridge burned up after 7 sec
15	80		
20	70		
25	50		
30	Bridge burned up		

TABLE 9. AVERAGE VARIATION IN THE VALUES OF THE ELECTRIC RESISTANCE OF THE CONTACT GAP OF SILVER CONTACTS (0.3 mm) SHORT-CIRCUITED BY A DROP OF DISTILLED WATER IN THE CASE OF ac CURRENT, IN  $\Omega$

Time, sec	Frequency of 50 cps		Frequency of 400 cps
	127 V	220 V	200 V
0	1590	1570	600
5	1410	2440	1000
10	1410	Bridge burned up	Bridge burned up after 7 sec
15	1590		
20	1810		
25	2540		
30	Bridge burned up		

This phenomenon may be explained if we take into account the rectifying action during the electrolysis of a series of metals, including silver, copper, nickel, tungsten and others (ref. 3). The rectifying action occurs when /224 cathode and anode polarization are not the same, in which case the electric resistance at the boundary between the metal and the electrolyte will not be the same in both directions.

If, in the case of dc operation, the formation of the current-carrying bridge between silver contacts is accompanied by a very sharp decrease in /225 the electric resistance, and if on the average it has a value of  $1\ \Omega$ , then in the case of ac operation, the magnitude of electric resistance is many times greater than for the dc case ( $1000$ - $10,000\ \Omega$ ).

The nature of the increase in the leakage current for ac operation is not the same as for dc operation. In the case of dc operation, a definite period of time is required before the current-conducting bridge starts to form, and this time depends strongly on the magnitude of the applied voltage (table 3). In the case of ac operation, this time is very short and practically does not depend on the value of the applied voltage.

The minimum electric resistance of the bridge during ac operation depends to a large degree on the magnitude of the voltage and on the frequency: for small voltages (up to  $25\text{ V}$ ) it is  $5000$ - $10,000\ \Omega$ ; for large voltages ( $127$ - $222\text{ V}$ ) it is  $1000\ \Omega$ . The increase in frequency from  $50$  to  $400\text{ cps}$  decreases this resistance by a factor of  $2$ , on the average.

Figures 3 and 4 show the oscillograms for the variation in the leakage current at  $220\text{ V}$ ,  $50\text{ cps}$  and  $200\text{ V}$ ,  $400\text{ cps}$ .

When the voltage is turned on, the leakage current reaches its maxi- /226 mum value very quickly and then decreases gradually. The current is disrupted when the bridge burns up.



Figure 3. Oscillogram showing variation in leakage currents at  $220\text{ V}$ ,  $50\text{ cps}$ .

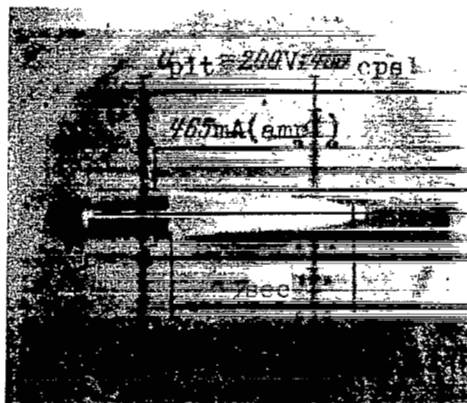


Figure 4. Oscillogram showing variation in leakage currents at  $200\text{ V}$ ,  $400\text{ cps}$ .

#### Tendency of Different Contact Materials to Form Current-Carrying Bridges

The tendency of various contact materials to form current-carrying /227 bridges, as in the case of silver contacts, was checked by measuring the

leakage current and the electrical resistance of the contact gap short-circuited with a drop of distilled water. All the leakage currents were measured with a single contact gap of 0.3 mm at a dc voltage of 5, 10 and 25 V. The results of the measurements are shown in tables 10-13.

TABLE 10. VARIATION IN THE LEAKAGE CURRENTS THROUGH CONTACTS MADE OF DIFFERENT MATERIALS WITH A CONTACT GAP OF 0.3 mm AND 5 V dc, IN mA /228

Contact material	Time, min							
	0	0.5	1.0	1.5	1.0	2.5	3.0	5.0
Silver		1100	2500	Bridge burned up	Short circuit			
Rhenium-silver	200	3500	4500					
Rhenium	200	3000	Short circuit					
Copper		4	50	70	150	300	400	500
SrPd-20	1	150	200	500	1100	1600	Bridge burned up	1500
ANS-70	1	150	500	550	600	650	700	
APDS-70	1	3-30	10-50	10-80	10-100	15-140	20-160	
APDNS-70	0.5	1-4	4-20	5-35	5-70	6-110	8-150	
Platinum	14	15	15	15	15	15	14	
PLI-10	0.7	0.8	0.9	0.9	0.9	1.1	1.2	
Palladium	2	2	2.2	3	3	3	3	
PdI-18	1	2	2	2	2	2	2	
SrPd-40	1	1.5	1.5	1.5	1.5	2.5	3	
PdI-10	0.5	0.5	0.44	0.40	0.40	0.38	0.36	
Gold	1	1	1	1	1	1	1	
Nickel	1.4	0.60	0.46	0.40	0.36	0.32	0.30	

As we can see from these data, silver, rhenium, copper and the SrPd-20 and ANS-70 alloys have a tendency to form current-carrying bridges.

There is a particularly sharp drop in the resistance of the contact gap when contacts are made from rhenium and from a rhenium-silver alloy. The leakage current jumps to 200 mA when the voltage is turned on and then increases rapidly to reach a value of 3-4.5 A. We should point out that while with silver contacts the current-carrying bridge burns up at high currents and breaks the electric circuit, with rhenium and with rhenium-silver alloys this bridge sinters into a solid mass and produces a short circuit. Contacts made of the APDS-70 and APDNS-70 are less susceptible to this, although the leakage currents after a 3-min exposure to a voltage of 5 V reach a value of 150-160 mA.

TABLE 11. VARIATION IN THE VALUES OF THE LEAKAGE CURRENT THROUGH THE CONTACTS MADE OF DIFFERENT MATERIALS WITH A CONTACT GAP OF 0.3 mm AT 10 V dc, IN mA

Contact material	Time, min						
	0	0.5	1.0	1.5	2.0	2.5	3.0
Platinum	56	50	35	35	40	40	40
PLI-10	1.5	2.0	3.0	6.0	9	10	16
Palladium	2	5	5	7	7	8	8
PdI-18	4	5	5	5	5	5	5
SrPd-40	1.5	2.0	2.5	5	7	9	10
PdI-10	0.8	0.8	0.8	0.8	1.0	1.3	1.5
Gold	2	3	3	3	3	3	3
Nickel	1.3	0.7	0.55	0.46	0.42	0.36	0.34

TABLE 12. VARIATION IN THE VALUES OF THE LEAKAGE CURRENT AS A FUNCTION OF TIME THROUGH CONTACTS OF VARIOUS MATERIALS WITH A CONTACT GAP OF 0.3 mm AT 25 V dc, IN mA

Contact material	Time, min						
	0	0.5	1.0	1.5	2.0	2.5	3.0
Platinum	100	70	85	100	90	100	130
PLI-10	3	4	5	6	7	10	20
Palladium	6	7	8	9	10	11	14
PdI-18	15	15	15	15	16	16	16
SrPd-40	3	4	4	5	8	9	10
PdI-10	2	3	4	5	6	7	7
Gold	7	8	9	10	9	9	9
Nickel	1.6	1.4	0.8	0.6	0.52	0.46	0.46

It should be pointed out that the leakage currents through APDS-70 and APDNS-70 are unstable. In a series of cases, even with 25 V dc, they fluctuate over a wide range from 10 to 200 mA. This instability most probably is explained by the fact that these contact materials do not constitute an alloy, but a cermet composition of silver and palladium, where each component (silver and palladium) may appear in its individual (pure) form.

Tables 11 and 12 show the leakage currents for 10 and 25 V dc for only eight materials with lower leakage currents.

Of the tested materials, the best were nickel, gold, PdI-10, SrPd-40, PdI-18, palladium, PLI-10 and platinum.

TABLE 13. AVERAGE ELECTRIC RESISTANCE OF A CONTACT GAP OF 0.3 mm SHORT-CIRCUITED WITH A DROP OF DISTILLED WATER, AND OPERATING WITH dc CURRENT FOR DIFFERENT CONTACT MATERIALS

Contact material	Resistance, $\Omega$	
Silver	1	
Rhenium-Silver	1	Residue is stable and short-circuits the contacts
Rhenium	1	
Copper	10	
SrPd-20	30	
ANS-70	30	
APDS-70	30	
APDNS-70	50-5000	
Platinum	200	
PLI-10	500-5000	
Palladium	1000-1500	
PdI-18	1000-2500	
SrPd-40	1000-5000	
PdI-10	1000-5000	
Gold	2500-5000	
Nickel	10,000-15,000	Resistance increases with time

We should point out that the lowest tendency to form current-carrying bridges was exhibited by nickel. The leakage currents for nickel do not increase with time, as do the currents for all other materials, but rather tend to decrease (3-4 times in a period of 3 min). This decrease apparently is explained by the formation of a surface oxide film which inhibits the passage of an electric current. Since nickel in its pure form is not very suitable for contact material due to its low resistance to electric wear, the greater interest is in investigating alloys containing nickel and their capacity to form current-carrying bridges under conditions of moisture. /229

The testing of contact pairs made of two different materials has shown that during dc operation, the tendency of a contact pair to form current-carrying bridges is determined primarily by the material at the anode (+). Thus, for example, the contact pair consisting of silver and nickel has shown the following electric resistance of the contact gap when the polarity was changed: anode (+) silver, cathode (-) nickel--5  $\Omega$ , anode nickel, cathode silver--5000  $\Omega$ . /230

## Conclusions

The investigations which have been carried out to determine the tendency of various contact materials to form current-carrying bridges in the presence of moisture have shown that the tendency of different materials is different. Silver, rhenium, copper and compositions with a large content of /231

these metals are strongly susceptible to this phenomenon. Nickel, gold, palladium, platinum and their alloys are most resistant to the formation of current-carrying bridges.

The form of the current plays a determining role in the formation of current-carrying bridges. The most intense formation of current-carrying bridges takes place with a dc current. The electric resistance of the contact gap is much greater for ac current than for dc current (by a factor of 100-1000). In the case of the dc current, the value of the electric resistance of the contact gap depends little on the magnitude of the voltage and of the gap. However, the time at which the formation of the bridge begins is closely dependent on the value of the voltage and the gap. When the voltage is increased and the contact gap is decreased, this time decreases sharply.

For ac current, the minimum electric resistance of the contact gap depends to a large degree on the voltage. As the voltage is increased, the resistance decreases by several factors. The time for formation of the current-carrying bridge in the case of ac current is very small and practically does not depend on the applied voltage.

On the basis of what we have presented, we can conclude that in selecting contact materials for electric switching equipment, it is necessary to take into account their tendency to form current-carrying bridges when moisture is present.

#### REFERENCES

1. Gordon, A. V., Gimmel'brodskiy, V. N. and Mikheyeva, O. N. A Phenomenon at the Contacts of a Sealed Relay (Ob odnom yavlenii na kontaktakh rele zakrytogo ispolneniya). This volume, p. 185.
2. Skorшелletti, V. V. Theoretical Electrochemistry (Teoreticheskaya elektrokimiya). Khimizdat, Leningrad, 1959.
3. Vagramyan, A. T. and Solov'yev, Z. A. Methods of Investigating the Electrodeposition of Metals (Metody issledovaniya elektroosazhdeniya metallov). Izd-vo AN SSSR, 1955.



## INVESTIGATION OF CAM CONTACTS OF PUNCHED CARD MACHINES

V. Dauknis, I. Mayauskas, G. Prantskyavichyus  
and V. Ryauka

The purpose of investigating the cam contacts of punched card machines was to obtain information on the special features associated with their operation and also on their useful life. /232

The construction of cam contacts of punched card machines is shown schematically in figure 1. The cam disk usually has 1-12 recesses and rotates with a velocity of 120 rpm and consequently can produce 120-1440 contact makes per minute. The static force on the contact varies from 1.5-8.0 g-wt. The contacts are made of tungsten rod with a diameter of 4 mm; the irregularities of the initial surface are of the order of  $0.8-3.5 \mu$ , which corresponds to the 7-9th class of purity. The contacts switch a circuit at 100 V dc carrying a current of 0.02-0.04 A. The inductance of the circuit may carry from 0.5 to 10 H, and the resistance may vary from 2.7 to 6.0 k $\Omega$ .

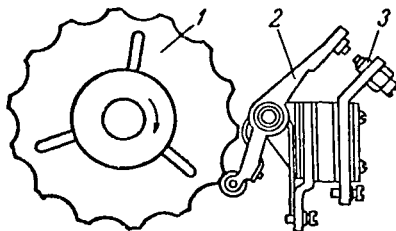


Figure 1. Schematic representation of the cam contacts of punched card machine. 1, cam disk; 2, movable contact; 3, stationary contact.

As the contacts make and break, electric oscillations take place in the circuit accompanied by the sparking of the contacts. It has been determined experimentally that when a spark-quenching scheme is absent, the duration of the electric oscillations (the time from their appearance to their total damping) is 200 to 1600  $\mu$ sec. In this case there is a linear relationship between the duration of the electric oscillations and the inductance of the circuit. In addition, it has been established that the increase in voltage or a decrease in the circuit resistance produces an increase in the duration of the oscillations and, consequently, in the duration of sparking.

During making, mechanical vibrations of the contacts take place. /233  
Their number depends on the static pressure and when the latter is increased to 2.5 N and higher, the number of spring-backs decreases to one. The time during which the contact is open due to vibration is 50  $\mu$ sec, when the pressure is greater than 2.50 N. This time is insignificant compared with the duration of the electric oscillations and, therefore, when the pressure is greater than 2.5 N, the effect of mechanical vibrations on the life of the contacts operating without a spark-quenching scheme is insignificant.

The application of a spark-quenching scheme decreases the duration of sparking during the breaking of the contacts by a factor of 1000 (down to 2-5  $\mu$ sec). Under the investigated operating conditions, the duration of sparking depends little on the inductance of the circuit and constitutes only 2-5  $\mu$ sec. When spark-quenching schemes are present, the duration of mechanical vibrations produces a substantial effect on the duration of sparking when the contacts make. Thus, for example, when the contacts make at the initial instant, the duration of the sparking is 8-10  $\mu$ sec; during the first rebound it is 25-40  $\mu$ sec and during the second rebound it is 10-20  $\mu$ sec. The duration of sparking depends on the gap between the open contacts, on the speed developed by the movable contact under the action of the spring and on the impact force of the contacts.

To investigate the useful life of tungsten contacts, a special stand was built where the contacts operated under conditions close to true operations. The effect of circuit parameters on the life of the contacts was investigated, i.e., the inductance and resistance as well as the capacity of the spark-quenching network, contact pressure and the degree of wear of the cam disk profile. The behavior of 6-12 cam contacts was investigated under each operating condition.

In the investigation of the contact operation, it was assumed that the contact operates normally if a current sufficient to actuate the relay mechanisms enters the circuit.

The condition of the contacts was checked by two methods: first, by periodically measuring the contact resistance (using an ammeter and a voltmeter), then by determining the instant of time for each contact when it begins to conduct a current which is insufficient for the operation of the relay. This was achieved by using the circuit shown in figure 2. In this circuit a constant negative bias was supplied to the grid of the TG01/1.3 thyatron through the resistance  $R_1$  from the battery. /234

During the normal operation of the contacts, a pulse voltage with an exponential rise and decay (broken curve, fig. 3) is fed to the grid through resistance  $R_2$ . As a result of this, the potential of the grid increases, but

does not reach a value at which the thyatron fires. The zone of potential values for which the thyatrons are fired is shaded in figure 3. /235  
During a single contact failure, the period of voltage increase is doubled, and the grid potential has time to reach a value so that the thyatron necessarily fires (solid curve, fig. 3). It remains in this state until the voltage

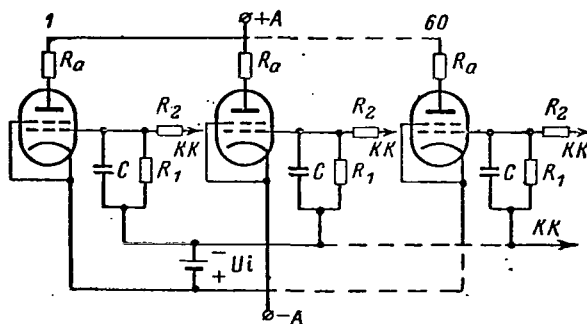


Figure 2. Circuit for determining contact failures.

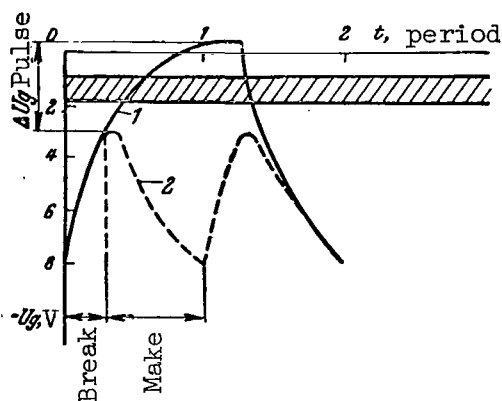


Figure 3. Variation in voltage at grid of thyatron.

is removed from the anode of the thyatron to place it in its initial state. The parameters of the failure control circuit were selected separately for all of the investigations, taking into account the characteristics of the power circuit.

This checking of the contact failures was carried out every  $5 \cdot 10^5$  commutations, and the resistance was measured every  $10^6$  commutations. The data which were obtained showed that transitional resistance of the contacts during their operation varies chaotically. It is not possible to determine from the value of the transitional resistance whether the contacts have failed. This is obvious from the curves shown in figure 4, which represent the variation in contact resistance as a function of the number of commutations. The recording scheme determined the time when the contacts failed; the measurement of the contact resistance did not do this. Apparently the interval of time during which the contact failed was not long.

The useful life of the contacts with a resistance of 3 and 5 kΩ was determined as a function of circuit inductance. In each case, the inductance

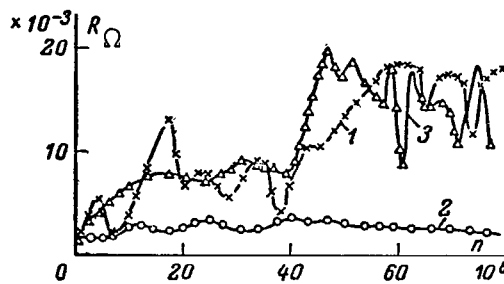


Figure 4. Variation in contact resistance as function of number of commutations.

was measured in the range from 0.5 to 10 H. The useful life of the contacts was recorded as the number of commutations performed by the contact before its first failure (ref. 3). The variation in the average useful life of the contacts as a function of circuit inductance is shown in figure 5. The curve has a maximum at 5 H. /236

In the region of small inductances, sparking is slow when the contacts are broken; however, when they are made, very high temperatures occur at the contact points, and these temperatures are large when circuit inductances are small. When the circuit inductances are high, strong sparking occurs when the contacts are broken, which also reduces the useful life of the contacts. The maximum on the curve pertains to the most favorable combination of parameters for both processes.

Experiments to clarify the effect of a resistive circuit load on the operating time of the contacts were carried out with circuit inductances of 0.5, 5 and 10 H. In each case, the resistance of the circuit was varied from 3 to 6 k $\Omega$ . The results which were obtained are shown in figure 6.

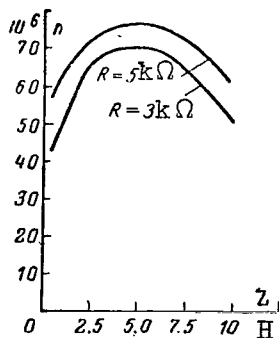


Figure 5. Variation in failure-free operation as function of circuit inductance.

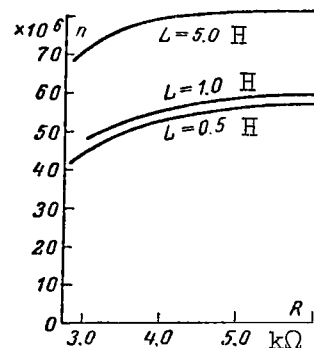


Figure 6. Variation in failure-free operation as function of current in circuit with resistive load.

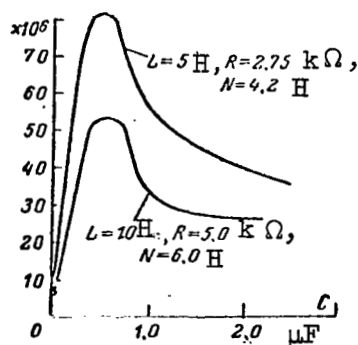


Figure 7. Variation in failure-free operation as function of spark-quenching circuit capacity.

As we can see from the curves, an increase in the resistive load, i.e., a decrease in the contact current, leads to an increase in the operating time of the contacts.

Investigations on the effect of capacity in the spark-quenching circuit on the duration of contact operation showed that this variation has a maximum (fig. 7). When the contact is broken, larger capacities produce a more intense quenching of the spark. When the contact is made, smaller capacities are better, because the energy supplied in this case is less. The results are analogous to the data obtained by R. Holm (ref. 4).

In addition, it was established that a resistive load of 100-200  $\Omega$  is most favorable for the spark-quenching scheme. Therefore, in all experiments to determine the reliable life the contacts were protected with spark-quenching schemes, whose parameters were as follows: resistance of 140  $\Omega$  and a capacity of 0.5  $\mu\text{F}$ .

When the force produced by the spring on the movable contact is increased, the speed of contact approach as well as the impact force increase. The increase in the approach speed must lead to a decrease in the sparking time during the making of the contacts, while an increase in the impact force should lead to a more intense mechanical destruction of the contact. The tests which were carried out and whose results are shown in figure 8 showed that an increase in the contact pressure decreases the period of failure-free operation of the contacts.

During making and breaking, the approach speed is substantially affected by the profile of the cams which undergo intense wear; the profile changes substantially. It was established that their volumetric wear is directly proportional to the number of revolutions of the cam disk and to the static pressure on the roller. The approach speed during making and the speed of contact breaking is substantially less for worn cams than for new cams.

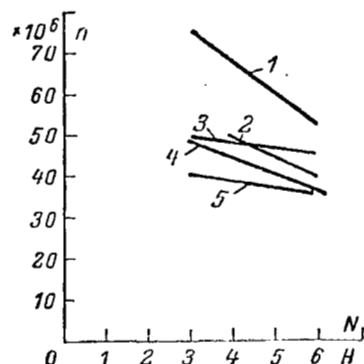


Figure 8. Variation in spark operation time as function of contact pressure.  
 1,  $R = 3 \text{ k}\Omega$ ,  $L = 1.0 \text{ H}$ , new cams; 2,  $R = 3 \text{ k}\Omega$ ,  $L = 1.0 \text{ H}$ , cams of average life;  
 3,  $R = 3 \text{ k}\Omega$ ,  $L = 1.0 \text{ H}$ , worn out cams; 4,  $R = 5 \text{ k}\Omega$ ,  $L = 10 \text{ H}$ , new cams; 5,  $R = 5 \text{ k}\Omega$ ,  $L = 10 \text{ H}$ , worn out cams.

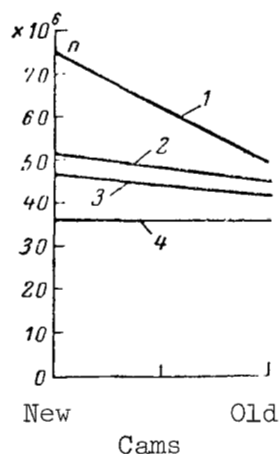


Figure 9. Variation in failure-free life as function of cam wear.  
 1,  $L = 1 \text{ H}$ ,  $R = 3 \text{ k}\Omega$ ,  $N = 3 \text{ N}$ ; 2,  $L = 1 \text{ H}$ ,  $R = 3 \text{ k}\Omega$ ,  $N = 6 \text{ N}$ ; 3,  $L = 10 \text{ H}$ ,  $R = 5 \text{ k}\Omega$ ,  $N = 3 \text{ N}$ ; 4,  $L = 10 \text{ H}$ ,  $R = 5 \text{ k}\Omega$ ,  $N = 6 \text{ N}$ .

The testing of cams having a different degree of wear showed that the wear of the cam profile decreases the failure-free life of the contacts (fig. 9).

We should point out that there was a large spread in experimental data. This should be attributed to the difference in the contact areas due to the irregularities in contact surface. Therefore, in the design and fabrication of cam contacts, special efforts should be made to keep the contact surfaces parallel. /238

#### REFERENCES

1. Electric Contacts, Proceedings of 26-28 October, 1956 Conference (Elektricheskiye kontakty, Trudy soveshchaniya (26-28 oktyabrya 1956g.)). Gosenergoizdat, 1958.
2. Electric Contacts, Proceedings of 1-6 June, 1959 Conference (Elektricheskiye kontakty, Trudy soveshchaniya (1-6 iyunya 1959g.)). Gosenergoizdat, 1960.
3. Malikov, I. M., Polovko, A. M., Romanov, N. A. and Chukreyev, P. A. The Theory and Calculation of Reliability (Osnovy teorii i rascheta nadezhnosti). Sudpromgiz, 1960.
4. Holm, R. Electric Contacts (Elektricheskiye kontakty). I. L., 1961.

## INVESTIGATION OF NEW CONTACT SYSTEMS FOR MINIATURE HIGH-FREQUENCY SWITCHES

I. G. Mordukhovich and N. P. Barshteyn

High-frequency wafer switches (fig. 1) are important commutating elements of electronic equipment. They have a rather wide and diverse application.

/239

The use of wafer switches permits such operations as the switching of individual networks and radio equipment stages, alternate switching of similar circuit networks with different component values or the alternate switching of different circuits and stages, etc.

The important requirements which must be satisfied by the switch include high reliability of contacting, small value of transitional resistance and stability during operation.

In the case of high-frequency operation, the requirements for the transitional resistance and the interelectrode capacities and inductances are even more stringent.

A small value of the transitional resistance characterizes the reliability of making contact, while a large value of the transitional resistance, even though allowable under certain circuit conditions, is, nevertheless, undesirable, because it shows that the contact is unreliable and unstable during operation.

/240

For contacts operating in high-frequency circuits, it is desirable to have the lowest possible and the most stable transitional resistance for any value



Figure 1. High-frequency wafer switch.



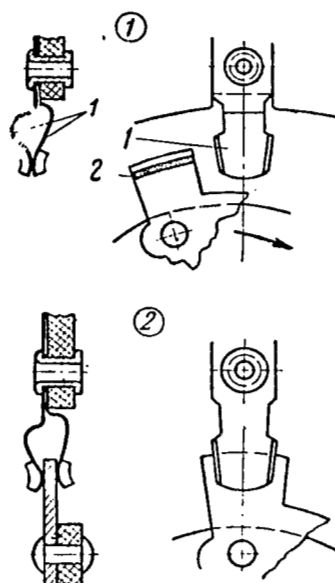


Figure 2. Operation of contacts in wafer switch.

of current and voltage and under any environmental conditions and mechanical loads. In these circuits, when a transitional contact resistance is unstable, it may produce various interferences (rustling, crackling, noise), which exceed the level of the main signal. At these frequencies an increase in the transitional resistance also produces a sharp decrease in the quality factor of the high-frequency input circuits. In heterodyne circuits and in master oscillators an increase and instability of the transitional resistance may introduce additional damping, which decreases their stability and excitation.

Experience has shown that the best operation of such contacts takes place when the transitional resistance does not vary more than 25 percent.

By using existing designs of high-frequency switches it is not possible to obtain a low and stable transitional resistance, which would provide for a prolonged and reliable operation of the switched circuits. We can see this from the following considerations. Existing switches use sliding contacts, as shown in figure 2. The operation of these switches is influenced considerably by the sliding friction between the stationary contacts 1 and the moving contact 2 producing rapid wear. Another disadvantage of these contacts is the instability of their position during the instant of switching and the presence of different paths for the current passing between two points of the contact field. This produces a change in the resistive and reactive impedance in the high frequency circuit.

Experience has shown that the largest number of failures occurring in high-frequency contacts are due to the unreliability of the contact elements.

It is obvious that the production of miniature high-frequency switches, which satisfy the given requirements, is first associated with the correct selection of contact designs and materials.

The miniaturization of wafer switches is usually accomplished by a direct decrease in the geometric dimensions of existing designs. This accentuates the disadvantages of sliding contacts even further.

#### Selection of New Contact Systems for Switches

It is known that the coefficient of rolling friction is at least ten times less than the coefficient of sliding friction. This situation was used as a basis for the design of contacts for wafer switches; this also provided for the shortest current path when any electric circuit was switched on. The design was achieved by connecting the circuit with two stationary contacts situated in different planes and a movable roller (or ball) contact which closed them.

Figure 3 shows the contact systems and their elements. Designs I and II are based on rolling friction (the moving roller contact rotates around /242

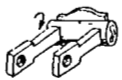
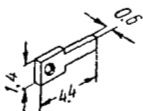
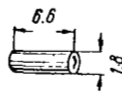
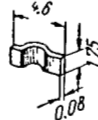

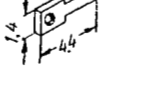
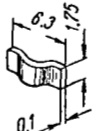
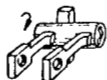
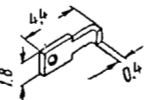
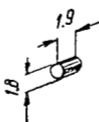
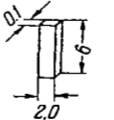

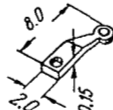

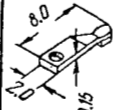
No.	General view	Stationary contact (leaf)	Moving contact	Contact spring
I				
				
II				
III				
IV				

Figure 3. Contact systems and their elements.

its axis), while designs III and IV (for comparison purposes) are based on sliding friction (the moving roller contact is rigidly attached to the rotor).

The table shows the materials selected for the contacts.

The selection of the best design and of the best material for the contact pair was based on the results of investigations carried out using the /243 following methods:

No. of design	Material	
	of leaf	of contact
I	1. L-62 brass-plated with 10 $\mu$ of silver and 5 $\mu$ of palladium	Silver +4% Pt SrNM-2-20
	2. L-62 brass-plated with 10 $\mu$ of silver and 1-2 $\mu$ of rhodium	SrNM-2-20
II	1. L-62 brass-plated with 10 $\mu$ of silver and 1-2 $\mu$ of rhodium	SrNM-2-20 PdSr-80
	2. Bimetal SrNM-2-20 silver-nickel-copper alloy and L-62 brass	SrNM-2-20 APdNS-70
	3. Bimetal of Sr999 silver and L-62 brass	
III	1. BNT-1.9 bronze-plated with 10 $\mu$ of silver and 5 $\mu$ of palladium	SrNM-20
	2. BNT-1.9 bronze-plated with 10 $\mu$ of silver and 1-2 $\mu$ of rhodium	SrNM-2-20
IV	1. BNT-1.9 bronze with welded Sr999 silver contacts	Sr999
	2. BNT-1.9 bronze with welded SrNM-2-20 contacts	SrNM-2-20

The transitional resistances of the contacts were measured under static and dynamic conditions with contact pressures of 10, 25, 35, 45, 70 and 90 g-wt, with currents of 50, 150, 250 and 350 mA and temperatures of 18, 80, 120 and 150°C under conditions of normal tropical humidity.

The setup used in the tests consisted of a model of a single wafer switch (fig. 4). The necessary contact pressure was achieved by adjusting the control screw. The magnitude of the contact pressure was checked by hanging a weight at the contact point.

The ammeter-voltmeter method was used to measure the transitional /244 resistance of contacts in all cases.

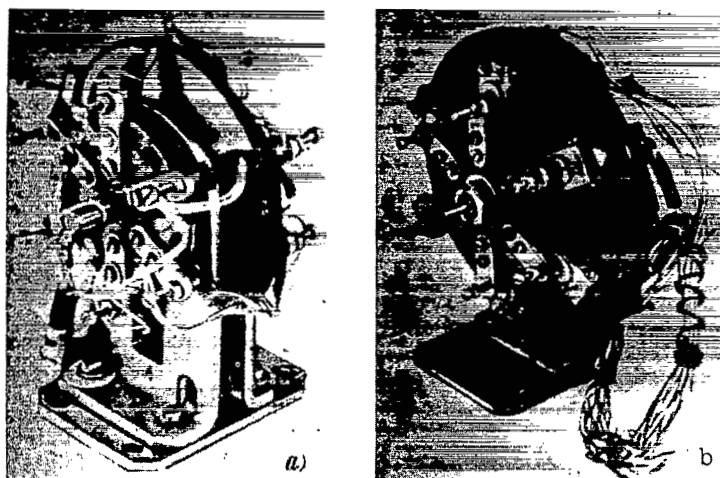


Figure 4. Setup for testing designs under static conditions.  
a, for III and IV contacts; b, for I and II contacts.

The contact pairs which produced the best results under normal static and dynamic conditions were used to measure the transitional resistance at elevated temperatures.

In all designs a constant pressure of 70 g-wt was established between the leaves and the contact. The contacts were tested with a dc current from 50 to 300 mA at 250 V and with an ac current of 180 mA at 28 mc/sec and 12 V.

The transitional resistance was measured after 0, 1, 3, 5, 10, 15, 20, 25, and 30 thousand commutations.

#### Results of the Investigations

Figures 5, 6 and 7 show the variation in the transitional resistances of contacts as a function of contact pressure under static conditions. /245

As we can see from the figures, the nature of the variation in the contact resistance, as the contact pressure is increased, does not depend on the contact system design or on the materials.

Measurements conducted at an ambient temperature of 150°C showed that the increase in transitional resistance was insignificant.

Figures 8-11 show the results of the investigations of the magnitude and the variation in the contact resistance as a function of contact design, material, number of commutations and the value of the commutated current during operation.

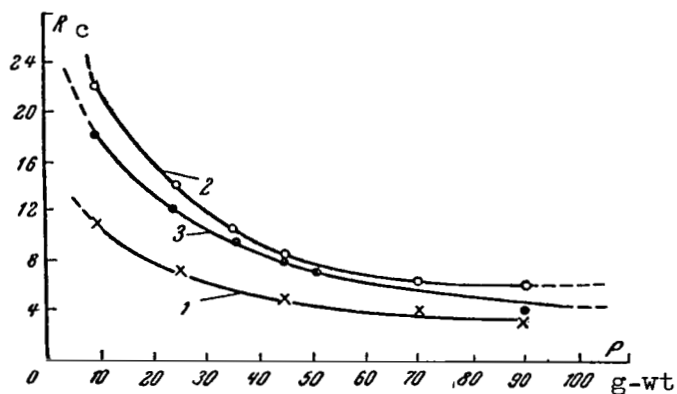


Figure 5. Variation in transitional contact resistance for design I as function of contact pressure under static conditions.

1, leaf - brass + 10  $\mu$  Ag + 1  $\mu$  Rd, contact SrNM-2-20; 2, leaf - brass + 10  $\mu$  Ag + 5  $\mu$  Pd, contact SrNM-2-20; 3, leaf - brass + 10  $\mu$  Ag + 5  $\mu$  Pd, contact Ag + 4% Pt.

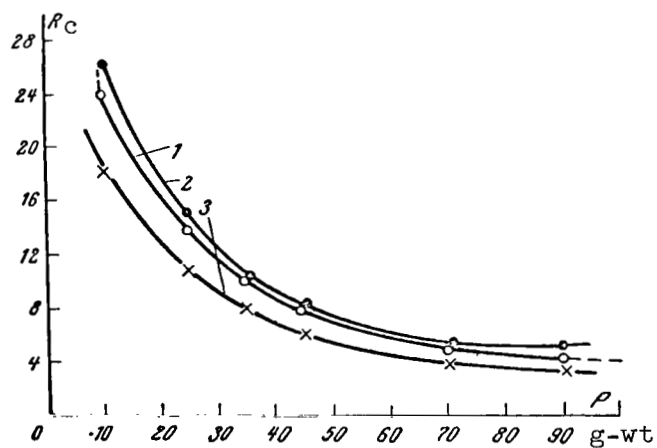


Figure 6. Variation in transitional contact resistance of design II as function of contact pressure under static conditions.

1, leaf - bimetallic silver, contact APdNS-70; 2, leaf - SrNM-2-20 bimetallic, contact SrNM-2-20; 3, leaf - brass + 10  $\mu$  Ag + 1  $\mu$  Rd, contact SrNM-2-20.

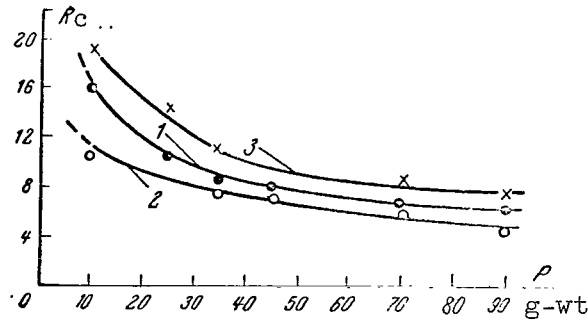


Figure 7. Variation in transitional contact resistance of designs III and IV as function of contact pressure under static conditions.

1, design IV: leaf - bronze + SrNM-2-20, contact SrNM-2-20; 2, design III: leaf - bronze + 10  $\mu$  Ag + 1  $\mu$  Rd, contact SrNM-2-20; 3, design III: leaf - bronze + 10  $\mu$  Ag + 5  $\mu$  Pd, contact SrNM-2-20.

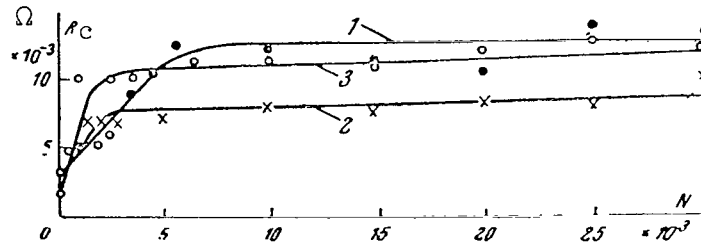


Figure 8. Variation in transitional contact resistance of design I as function of number of commutations with dc current of 0.3 A at 250 V

Operating conditions:  $U = 250$  V;  $I = 300$  mA;  $P = 70$  g-wt.

1, leaf - brass + 10  $\mu$  Ag + 5  $\mu$  Pd, contact Ag + 4% Pt; 2, leaf - brass + 10  $\mu$  Ag + 1  $\mu$  Rd, contact SrNM-2-20; 3, leaf - brass + 10  $\mu$  Ag + 5  $\mu$  Pd, contact SrNM-2-20.

For all materials which were used to fabricate I and II contact pairs, the nature of the variation in the transitional resistance with the number of commutations is approximately the same.

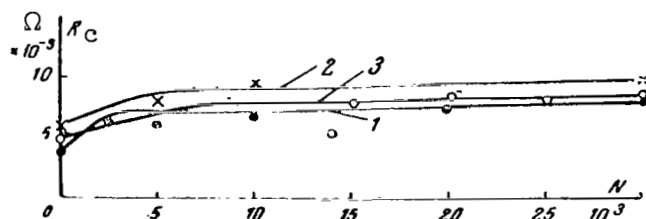


Figure 9. Variation in transitional resistance of contacts I as function of number of commutations when operating with dc current of 0.05 A at 250 V. Operating conditions:  $U = 250$  V;  $I = 50$  mA;  $P = 70$  g-wt. 1, leaf - brass +  $10 \mu$  Ag +  $1 \mu$  Rd, contact SrNM-2-20; 2, leaf - brass +  $10 \mu$  Ag +  $5 \mu$  Pd, contact SrNM-2-20; 3, leaf - brass +  $10 \mu$  Ag +  $5 \mu$  Pd, contact Ag + 4% Pt.

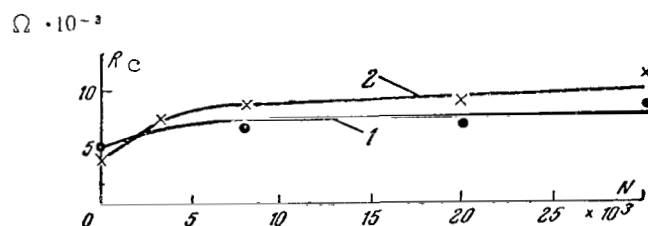


Figure 10. Variation in transitional resistance of contacts I and II as number of commutations at temperature of  $120^{\circ}\text{C}$  with dc current of 0.3 A at 250 V. Operating conditions:  $I = 300$  mA;  $U = 250$  V;  $P = 70$  g-wt. 1, design II: leaf - brass +  $10 \mu$  Ag +  $1 \mu$  Rd, contact SrNM-2-20; 2, design I: leaf - brass +  $10 \mu$  Ag +  $1 \mu$  Rd, contact SrNM-2-20.

The transitional resistance after 5000 commutations for contacts of the same material is two times greater for design I than for design II.

The lowest variation in the transitional resistance for design I was observed in the case of the contact pair whose leaves were made of brass plated with  $10 \mu$  of silver and  $1-2 \mu$  of rhodium and in the case of contacts from SrNM-2-20. The insignificant variation in the transitional resistance during operation is due to the low coefficient of friction between these materials (fig. 8).

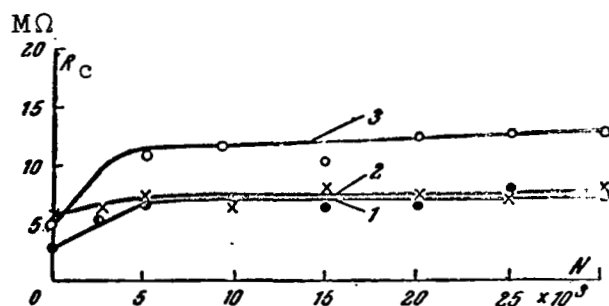


Figure 11. Variation in transitional resistance of contacts I and II as function of number of commutations at frequency of 28 mc/sec with current of 0.18 A at 12 V.

Operating conditions: frequency 28 mc/sec; I = 180 mA; U = 12 V; P = 70 g-wt. 1, design I: leaf - brass + 10  $\mu$  Ag + 1  $\mu$  Rd, contact SrNM-2-20; 2, design II: leaf - brass + 10  $\mu$  Ag + 1  $\mu$  Rd, contact SrNM-2-20; 3, design II: leaf - SrNM-2-20 bimetallic, contact SrNM-2-20.

The decrease in the value of the switched current from 300 to 50 mA does not change the qualitative nature of the curves for the transitional resistance (fig. 9).

Thus, the testing of contact pairs at constant current under room temperature has shown that the minimum transitional resistance and maximum stability of operation is best achieved by contact pairs of designs I and II, in which the leaves are made of L-62 brass-plated with 10  $\mu$  of silver and 1-2  $\mu$  of rhodium, and in which the contacts are made from SrNM-2-20.

Therefore, the effect of 120°C temperature on the variation of the transitional resistance during operation was established by using contact pairs of designs I and II, which were fabricated from these materials. /247

When operation takes place at a temperature of 120°C there is an insignificant increase in the transitional resistance (fig. 10).

The effect of high-frequency currents on the variation in the transitional resistance during operation was also studied by using contact pairs of designs I and II with leaves fabricated from brass and plated with 10  $\mu$  of silver and 1-2  $\mu$  of rhodium and with contacts made of SrNM-2-20. /248

It follows from figure 11 that the curves, which show the variation in the contact resistance at high frequency, do not differ qualitatively from the



curves for dc operation. However, the magnitude of these variations is somewhat less than that for dc current.

The wear of contacts after 30,000 commutations is different for different designs. /249

The wear of contacts of design I is somewhat greater than the wear of contacts of design II.

In the case of design II, the maximum wear is observed when the contacts are made of the same material. The increase in the transitional resistance during operation is also maximum in this case.

The contacts which commute high-frequency currents had substantially less wear. However, in this case the wear of contact pairs of design I was somewhat greater than that of design II.

The results obtained for the wear of contacts agree well with data on the variation of the transitional resistance during operation.

Thus, tests conducted with new designs confirm the desirability of using designs which utilize rolling friction instead of sliding friction.

Based on the results of these investigations, miniature high-frequency wafer switches were designed. These were tested by the government and /250 produced better results than earlier designs. In addition to improvement in other characteristics, the transitional resistance of the contacts decreased by a factor of 4-5 and the stability of switching was substantially increased.

#### REFERENCES

1. Holm, R. Electric Contacts (Elektricheskiye kontakty). Izd-vo Inostran-  
noy literatury, 1961.
2. Pestryakov, V. B. and Sachkov, D. D. Design of Radio Components and Cir-  
cuits (Konstruirovaniye detaley i uzlov radioapparatury). Gosenergoiz-  
dat, 1948.
3. Khorinskiy, A. L. Principles of Radio Components Design (Osnovy konstrui-  
rovaniya elementov radioapparatury). Gosenergoizdat, 1959.

## INVESTIGATION OF PLUG-TYPE CONNECTORS OPERATING WITH MICROCURRENTS AT MICROVOLTS

A. I. Fedorov and G. Z. Zakirov

The trend in modern electronics is towards the reception and processing of lower level signals. There is an increased application of connectors in low level circuits, and these connectors must operate with stability under different environmental conditions and provide an effective connection of circuits under mechanical loads without losses at the points of contact. /250

It is of particular practical interest to determine and study the reasons which produce unstable conductance of electric contacts at microvoltages. It is known that the electrical conductivity of contacts depends on the materials of the contact pair, their plating, purity of finish and on the condition of the contact surfaces as well as on the contact pressure. Usually the contacting surface is partially covered with insulating films and, therefore, only a part of it has a metallic or a quasimetallic contact.

The contact surface of cylindrical contacts which have palladium, gold, silver and nickel plating, due to the high contact pressure which breaks down the films of various chemical compositions, continues to conduct current even after being subjected to aggressive media containing hydrogen sulfide. /251

However, when contact pairs are investigated for the prolonged passage of a current of the order of a fraction of a  $\mu\text{A}$  at a contact voltage of 2-3  $\mu\text{V}$  under normal atmospheric conditions, cases are observed when the current in the contact circuit decreases, disappears and then is completely restored. This phenomenon described in domestic and foreign literature has been explained by the presence of "dry circuits" or "dry connections" associated with the electric contacts.

We are interested in the reasons for the disappearance and spontaneous restoration of the current in a low-power circuit utilizing electric contacts. The investigations of basic electric characteristics of contact pairs have clarified this phenomenon.

### Experimental Investigations

The contact surface of electric contacts is usually covered with insulating films. In the course of operation under the influence of different climatic conditions, aggressive media, plating wear and other phenomena which age

the contacts, the contact surface becomes covered with films of different chemical compositions and the conductivity of contacts deteriorates. The investigation of contact conductivity during artificial aging is of practical interest when contacts are to be used in low-power circuits. By determining the variation in the transitional resistance as a function of different factors it is possible to find the limiting voltage at which cylindrical contacts lose their capacity to conduct a current.

With this in mind the volt-ampere characteristics of contact pairs were investigated. The contacts had a diameter of 1 mm (fig. 1) and were made of the brass-bronze alloys and brass-Kovar alloy with silver, gold, palladium and nickel plating.

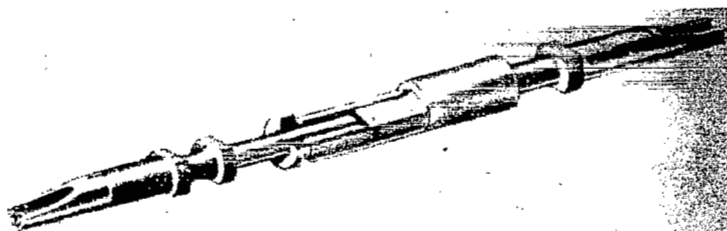


Figure 1. General view of contact pair with diameter of 1 mm.

The contact pairs were investigated in the state in which they were delivered and also after they were subjected to the following: a mixture of air with 0.1 percent hydrogen sulfide ( $H_2S$ ) for a period of 4-6 h; in a medium with normal humidity at a temperature of  $150^{\circ}C$  and in a medium with increased relative humidity of 95-98 percent at a temperature of  $40^{\circ}C$ , after 500 connections couplings during a period of 30 days. A total of 600 contact pairs was investigated.

The volt-ampere characteristics were investigated in the voltage range from 0.4  $\mu V$  - 1 mV with a load resistance of 0.2, 100  $\Omega$  and 40 k $\Omega$  in the contact circuit.

When the conductivity of the contacts was determined, the effect of the thermo-emf on the nature of the volt-ampere characteristics was established. The application of the compensation method for measuring the voltage drop across the calibration resistance (load resistance), when determining the current  $I_{cc}$  in the contact circuit, has made it possible to take into account the

value of the thermo-emf and to compute the true value of the current with a sufficient degree of accuracy by using the expression

$$I_{cc} = \frac{U_1 - (\pm U_2)}{R_c},$$

where  $U_1$  is the voltage drop across the calibrated resistance (load resistance) produced by the given emf and the thermo-emf of the contact pair; /253  
 $U_2$  is the voltage drop across the calibrated resistance produced by the thermo-emf;  
 $R_c$  is the calibrated resistance (load resistance) equal to 0.2  $\Omega$ , 100  $\Omega$  or 40 k $\Omega$ .

The volt-ampere characteristics of contact pairs with different platings (figs. 2 and 3), which have been maintained for a period of six hours in an aggressive medium containing hydrogen sulfide ( $H_2S$ ), are represented by straight lines over the entire range of voltage variation (from 0.4  $\mu V$  - 1 mV) and show the normal conductivity of contacts.

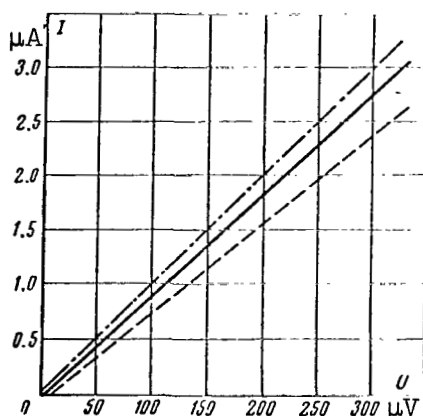


Figure 2. Current in contact circuit as function of applied voltage. Material of contact pair is brass-bronze. Solid line shows curve for gold-gold plating; dot-dash line for palladium-palladium plating; broken line for silver-silver.

The same nature is exhibited by the relationship  $I = F(U)$  for contact pairs subjected to other factors which produce artificial aging.

The investigation of the variation in the transitional resistance of the contact as a function of voltage is as important as the investigation of the volt-ampere characteristics, because, in the general case, we encounter circuits with rather low voltages and with currents of the order of a few tenths of a  $\mu A$ . In such circuits the variation in the contact transitional resistance is quite important. /254

The nature of the variation in  $R_{trans} = F(U)$  was investigated in the applied voltage range from 4  $\mu V$  to 1 mV. A total of 200 contact pairs was investigated.

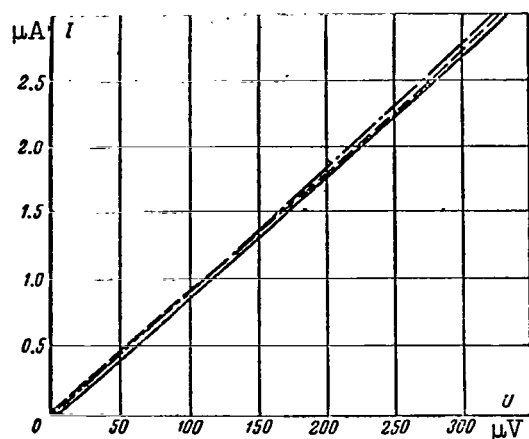


Figure 3. Variation in current of contact circuit as function of applied voltage. Material of contact pair is brass-Kovar. Plating: dot-dash line, palladium-nickel; broken line, gold-nickel; solid line, silver-nickel.

Figures 4 and 5 show the graphs of  $R_{trans} = F(U)$ , constructed from experimental data. These curves show that the transitional resistance of contact pairs decreases with increase in the voltage applied to the contact circuit. This behavior of the curves may be explained by the presence of films on the contact surface, which produce an additional resistance to the passage of current at low values of applied voltage.

Experimental investigations on the conductivity of contact pairs subjected to artificial aging have shown that a certain increase in the transitional resistance of contact pairs at low voltages of 4  $\mu V$  and higher does not disrupt the operation of the circuit.

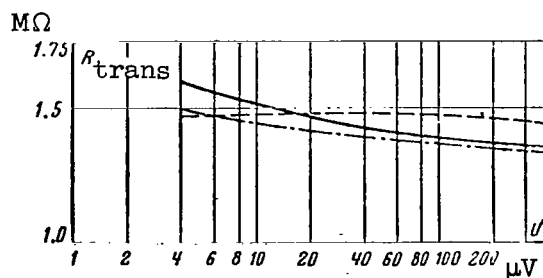


Figure 4. Variation in transitional resistance of contact pairs as function of applied voltage. Material: solid line, palladium; broken line, gold; dot-dash line, silver.

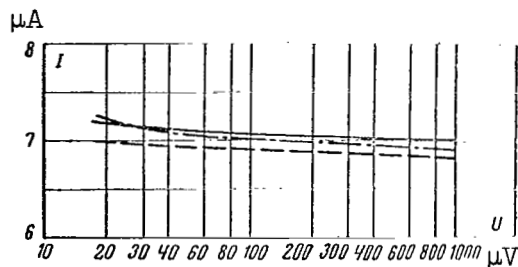


Figure 5. Variation in transitional resistance of contact pairs as function of applied voltage. Platings: solid line, palladium-nickel; dot-dash line, gold-nickel; broken line, silver-nickel.

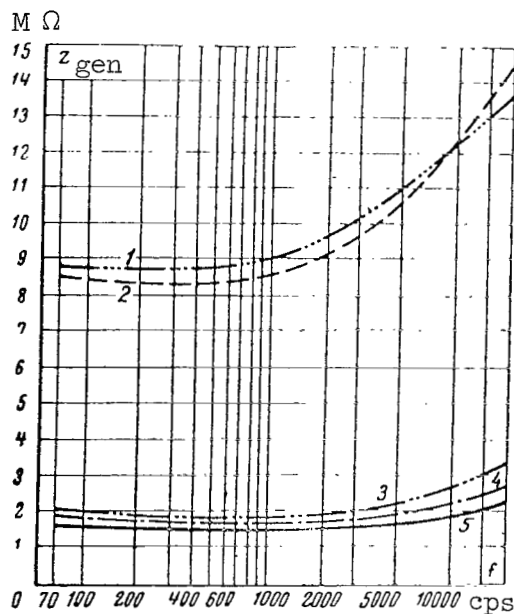


Figure 6. Variation in total resistance of contact pairs with different platings as function of frequency when voltage applied to contact circuit is 10  $\mu$ V. Plating material: 1, nickel-gold; 2, nickel-silver; 3, gold-gold; 4, palladium-palladium; 5, silver-silver.

To determine the upper frequency limit at which cylindrical contact pairs could be used, the characteristics  $R_{trans} = F(f)$  were determined and investigated. Investigations were conducted with frequencies in the range from 70 cps to 20 kc with contact voltages of 5, 10, 20 and 30  $\mu$ V. Figure 6 shows the graphs for the relationship  $R_{trans} = F(f)$ .

We see from the graphs that as the frequency of the applied voltage is increased, the values of the total resistances of the contact pair increase and at 20 kc they are twice as large as the transitional resistances measured with dc current. The increase in the common resistance of contact pairs with the frequency of applied voltage may be explained by the presence of an inductive component of contact pair impedance, because the contact pair, like any conductor in a closed circuit, has inductance.

In conventional circuits the transitional contact resistance decreases as the contact pressure is increased. This phenomenon is valid up to a certain value of the pressure force  $P$ . After this point, an increase in contact pressure does not change the transitional resistance, which remains almost constant. /257

The phenomena are similar in low-power circuit with cylindrical contact pairs, subjected to artificial aging. This becomes clear if we consider table 2, which shows the values of  $R_{trans} = F(P)$ , in which the voltage across the

contacts is 20  $\mu V$ . We can see from the table that the transitional resistance of the contact pairs, which were tested as they were delivered, is almost independent of contact pressure variation from 50 g to 5 kg. The contact resistance of contact pairs measured after they are subjected to an aggressive medium containing  $H_2S$  decreases with an increase in contact pressure. This

mechanism is due to oxide films on the contacting surfaces, whose conductivity varies with contact pressure.

The presence of vibration and shock loads does not disrupt the electric contact when the electric load in the contact circuit is equal to  $1 \cdot 10^{-11}$  A at 25 mV.

It has been established that after the presence of shock loads the transitional resistance of the contact pair varies up to 10 percent of its initial value.

The investigation of electric contact stability during the action of mechanical loads, when the voltage in the contact circuit is less than 25 mV, is not possible, because there is no test equipment which can measure the pulse current variation in the contact circuit with a duration of the order of 1 hundredth of a msec.

The variation in the thermo-emf of the contact pairs as a function of the temperature difference between the stems of the plug and of the jack was determined during the investigations.

When two dissimilar metals touch a contact, emf develops between them. This emf does not depend on the shape or on the dimensions of the touching metals, but depends only on the nature of the metals and on the temperature at their contact point. /258

TABLE 2. THE VARIATION IN THE TRANSITIONAL RESISTANCE OF CONTACT PAIRS MADE OF BRASS-BRONZE ALLOYS WITH DIFFERENT PLATINGS AS A FUNCTION OF CONTACT PRESSURE WHEN THE CONTACT CIRCUIT OPERATES AT 20  $\mu$ V

Contact pressure in g-wt	Value of the transitional resistance of contact pairs, in M $\Omega$					
	Silver		Gold		Palladium	
	As delivered	Held in hydrogen-sulfide for 6 h	As delivered	Held in hydrogen-sulfide for 6 h	As delivered	Held in hydrogen-sulfide for 6 h
50	2.1	2.74	1.98	3.6	2.86	3.43
100	2.16	2.66	1.95	3.5	2.82	3.5
200	2.06	2.49	1.88	3.3	2.76	2.93
300	1.93	2.36	1.95	3.46	2.79	2.98
400	2.06	2.31	1.95	2.88	2.78	2.98
500	1.91	2.27	1.88	2.8	2.74	2.84
600	1.93	2.21	1.88	2.88	2.74	2.74
700	1.8	2.17	1.8	2.86	2.5	2.70
800	1.8	2.13	1.95	2.77	2.56	2.67
900	1.84	1.88	1.95	2.6	2.44	2.61
1000	1.55	1.95	1.88	2.56	2.3	2.58
2000	1.61	1.83	1.88	2.46	2.35	2.55
3000	1.61	1.85	1.5	2.44	2.02	2.54
4000	1.74	1.75	1.5	2.40	2.02	2.50
5000	1.74	1.68	1.5	2.38	1.88	2.45

During the determination of the volt-ampere characteristics and the useful life of contact pairs with a microcurrent load, it was established that contact pairs made of the same material and having the same plating develop a thermo-emf equal to 2  $\mu$ V even at normal temperatures.

The investigation of electric contacts with platings from the standpoint of generated thermo-emf makes it possible to gain a deeper understanding of "dry circuits" or "dry connections."

Before the relationship  $E_{\text{TEMP}} = F(\theta)$  was determined, the values of the thermo-emf of contact pairs made of heterogeneous materials and having different platings were measured under different atmospheric conditions (table 3). /259

In order to establish the lower limit of voltages for the operation of the contact pairs of the 2RM connector, the variation in the thermo-emf of contact pairs made of alloys brass-brass, brass-bronze and brass-Kovar plated with silver, gold, palladium and nickel was determined experimentally as a function of the temperature drop between the stems of the plug and the jack. From these, the values of the specific thermo-emf were determined (table 4).



TABLE 3. THE VALUES OF THERMO-emf OF CONTACT PAIRS UNDER DIFFERENT ATMOSPHERIC CONDITIONS

Contact pairs and platings	Value of thermo-emf, $\mu\text{V}$			
	Under normal conditions	With a relative humidity of 95-98%	At temperature of $150^{\circ}\text{C}$	In vacuum
Silver over brass and bronze	1.5	1.3	41.4	0
Silver over brass and nickel over Kovar	4	4.3	166.2	0
Gold on brass and nickel on Kovar	4	4.2	270	0
Palladium over brass and nickel over Kovar	4	8.5	162	0

TABLE 4. AVERAGE VALUES OF THE SPECIFIC THERMO-emf OF CYLINDRICAL CONTACT PAIRS

Contact pair materials and plating materials		Average value of specific thermo-emf, $\text{V/deg}$
Brass-brass	Without plating	$2.6 \cdot 10^{-6}$
	Silver-silver	$2.97 \cdot 10^{-6}$
	Gold-gold	$1.945 \cdot 10^{-6}$
	Palladium-palladium	$3.55 \cdot 10^{-6}$
	Silver-palladium	$2.577 \cdot 10^{-6}$
	Gold-palladium	$2.612 \cdot 10^{-6}$
Brass-bronze	Without plating	$2.95 \cdot 10^{-6}$
	Silver-silver	$3.112 \cdot 10^{-6}$
	Gold-gold	$2.596 \cdot 10^{-6}$
	Palladium-palladium	$3.366 \cdot 10^{-6}$
	Silver-palladium	$2.126 \cdot 10^{-6}$
	Gold-palladium	$2.136 \cdot 10^{-6}$
Brass-Kovar	Without plating	$2.54 \cdot 10^{-5}$
	Silver-nickel	$2.69 \cdot 10^{-5}$
	Gold-nickel	$2.434 \cdot 10^{-5}$
	Palladium-nickel	$2.202 \cdot 10^{-5}$

Figure 7 presents the combined graph showing the variation in the thermo-emf of contact pairs as a function of temperature drop between the stems of the plug and the jack; we find from the graph that the maximum value of the

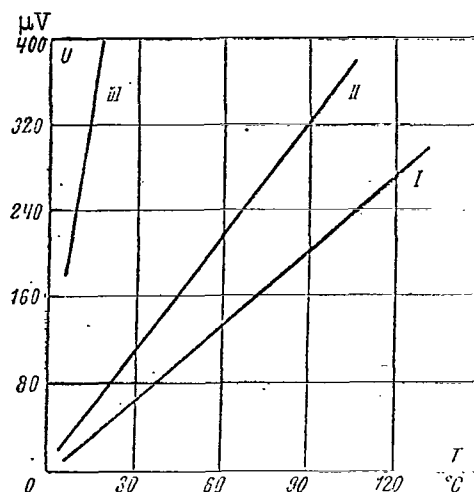


Figure 7. Combined graph for variation of thermo-emf of contact pair as function of temperature difference between stems of plug and jack. Material: I, brass-brass; II, brass-bronze; III, brass-Kovar (without plating).

thermo-emf occurs in the case of contact pairs made of the brass-Kovar alloy, while the minimum value occurs in the case when contacts are made from the brass-brass alloys.

For the same combination of materials used in contact pairs, the maximum value of the thermo-emf occurs in contacts plated with silver and palladium. The use of connector contact pairs in circuits with microcurrents at microvoltages, taking into account the generated thermo-emf, makes it possible to expand their range of application and exclude the possibility of contact failure in low-power circuits. /260

Under normal operating conditions the contact pairs may remain under a load for a prolonged period of time, and their reliability is an important factor.

If several dozen identical contact pairs are hooked up in series so that the total thermo-emf is the sum of the emf's of individual contact pairs, and if this arrangement is connected to a microvoltmeter, we can observe the variation in the thermo-emf of contact pairs as a function of time under normal atmospheric conditions. An experiment of this type was conducted with contact pairs made of the brass-Kovar alloy with gold-plated jacks and nickel-plated plugs. Eighty-four contact pairs were soldered in series and left under normal conditions. /261

For several hours a microvoltmeter measured the variation in the thermo-emf as a function of time. Figure 8 shows this variation in the total thermo-emf.

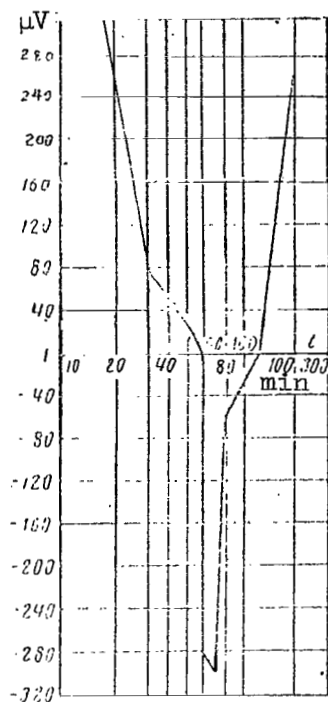


Figure 8. Variation in total thermo-emf generated at contact pairs as function of time. Material of contact pairs is brass-Kovar. There are 84 contact pairs. Temperature of surrounding medium is  $+20^{\circ}\text{C}$ .

We can see from the graph that the thermo-emf of the contact pair does not remain constant in magnitude or sign, but changes with time. This change is not regular. A large number of contact pairs was used to achieve accuracy and to make it convenient to measure the thermo-emf. At the same time, it was necessary to establish whether the polarity of the total thermo-emf would change in time if its value is greater than  $300\text{ }\mu\text{V}$ . The variation in the total thermo-emf as a function of time shown in the graph may be reliably referred to each individual contact pair. /262

The variation in the magnitude and sign of the contact thermo-emf was established during the determination of the prolonged useful life of the contact pair operating at microvoltages under normal atmospheric conditions and at a temperature of  $100^{\circ}\text{C}$ . The contact pair made of brass-Kovar alloys and plated with gold-nickel was placed in a thermostat, where the temperature was maintained at  $100^{\circ}\text{C}$ . After this its thermo-emf was measured, and the contact pair was connected to a circuit containing a voltage opposite to that resulting from the contact thermo-emf and exceeding the latter by  $2\text{--}3\text{ }\mu\text{V}$ . Pulse counters contained in the circuit recorded the number of galvanometer deflections from its initial position, both in magnitude as well as in sign. When the galvanometer

needle was deflected from its assigned position, the value of the thermo-emf and the value of the voltage applied to the circuit were measured.

Investigations of this type were carried out, using contacts made from homogeneous and heterogeneous materials and having different platings. It was established experimentally that "dry circuits" or "dry connections" do not exist in the contact pairs of the 2RM connectors. However, a contact thermo-emf does exist and changes in magnitude and in sign and produces a change in the direction of the current in the circuit or a total disappearance of the current followed by its spontaneous restoration. /263

In view of the special importance of providing reliable operation of contact pairs carrying microcurrents at microvoltages, a special electric circuit scheme was developed for automatically recording the current in the contact circuit. This scheme is shown in figure 9. The operation of the scheme is based on the automatic recording of the deviation in the current of the contact circuit from a definite preassigned value.

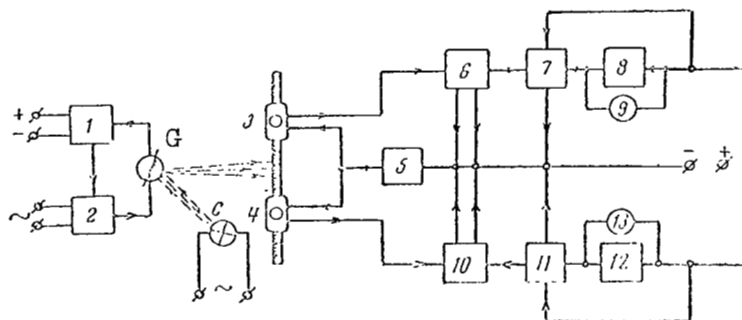


Figure 9. Functional diagram of automatic system for measuring current in contact circuit with microcurrent loads at microvolts during prolonged operation of contact circuit.

The voltage from divider 1 is transmitted to the contact circuit, consisting of a contact pair placed in thermostat 2 and galvanometer G placed in a chamber isolated from mechanical and electric noise and from light. The galvanometer is illuminated by light source C. The current in the contact circuit is set in such a way that the beam of light reflected from the galvanometer mirror is at the geometrically neutral point between photocells 3 and 4, which serve as electric switches controlling electronic amplifiers 6 and 10.

The photocells are connected to a source of dc 5. Let us assume that photocell 3 reacts to a decrease, while photocell 4 reacts to an increase in the current of the contact circuit. A decrease of the current in the contact circuit produced, for example, by an increase in the value of thermo-emf /264 of the contact pair which opposes the given emf in the contact circuit, will

cause the frame of the galvanometer to rotate and move the beam of light towards photocell 3. When photocell 3 is illuminated, the plate current in amplifier 6 increases to a value required to operate relay 7, which controls counter 8. Counter 8 records one deviation in the value of the current in the direction of decrease. An optical or acoustic signaling system 9 is connected parallel to the counter.

When the value of the current increases in the contact circuit, the second symmetric half of the scheme begins to operate, and counter 12 records the deviation of the current from a given value in the direction of increase.

The above scheme makes it possible to carry out the following investigations:

(a) continuously to determine in electric circuits, with contacts of any design and form made of various materials, the effectiveness of circuit connections during operation with microcurrents and microvoltages for a period of many days or months under conditions of a preset temperature difference and increased relative humidity;

(b) to determine the interval of contact thermo-emf fluctuations under definite climatic and atmospheric conditions.

## Conclusions

The investigations have made it possible to extend the application of connector contacts and to establish the lower limit of dc and ac currents equal to  $1 \cdot 10^{-11}$  A with a frequency up to 20 kc.

The lower limit of dc voltage is established, taking into account the specific values of thermo-emf, and the temperature differences between the stems of the plug and the jack.

The lower limit of ac voltage with a frequency up to 20 kc is established by taking into account the optimum signal-to-noise ratio, but is not below 10  $\mu$ V.

### PART III. CONTACT MATERIALS

#### HEAVY DUTY CERMET SWITCHING CONTACTS

I. P. Melashenko and K. V. Gubar'

The investigation of physical, mechanical and electric properties of cermet contacts as a function of structure dispersion, carried out during the last few years at VNIIEM, NIIelektro and IPM AN UkSSR have shown that it is practical to utilize contacts with a powdered structure. /265

The physical, mechanical and electric properties of finely dispersed cermet contacts, whose average particle size is less than one micron, are better than those of contacts with the conventional structure whose average particle size is of the order of 50 microns. The comparative electric tests of SOK 15 contacts for endurance carried out at different times by different organizations have shown that contacts of finely dispersed materials are 2 to 3.5 times better.

There are many methods of obtaining contacts with a finely dispersed structure, and some of these were used by VNIIEM, since 1950: the wet mixing of oxides in ball mills with subsequent pressing and heat treatment in air or in a controlled atmosphere; preparation of a fine silver powder by precipitation from a water solution of silver nitrate by means of hydroquinone; the diffusion annealing of metallurgic alloys of the silver-cadmium, silver-copper types and others until compositions of silver-cadmium oxide, silver-copper oxide are obtained; the combined precipitation of components in the form of thermally unstable carbonates and hydrates<sup>1</sup> with their subsequent firing or reduction; the combined precipitation with ultrasonic agitation; liquid mixing with simultaneous grinding in vibrating mills, etc. /266

If we consider these methods from the standpoint of mass production, from our point of view the precipitation of salts in the form of carbonates or hydrates is the most suitable method. The works of VNIIEM (1961 - 1962) were carried out in accordance with a program to investigate the laws which would permit a rational development of an industrial production method for finely dispersed mixtures of the SOK 15m type (15 percent CdO, 85 percent Ag) and of contacts from this material as the final product.

---

<sup>1</sup>The work of V. V. Usov, Ye. M. Murav'yeva and others; VNIIEM, 1955.

Since 1957 the work conducted at VNIIEM included the preparation of laboratory samples of most of the cermet electrical contact compositions of a finely dispersed structure which are known in engineering. However, the organization of their mass production in each case requires a substantial number of additional investigations.

Before considering the basic factors which affect the properties of finely dispersed compositions in the production process, we consider the general laws of electrical wear associated with the powdered structure. As an example, we consider the SOK 15 type composition.

Six variations of the SOK 15 type contacts were specially prepared and tested. The degree of dispersion in the structure of these samples varied from 300 to 0.5 microns (based on the average diameter of silver grains). The photograph of the microstructure of the SOK 15 type contacts with various dispersions (300 - 200 - 150 - 50 - 0.5 microns), which were tested for electric durability and hardness is shown in figure 1. The variation in electric wear and hardness of the SOK 15 type contacts as a function of the average silver grain diameter is shown in figure 2. As dispersion increases, the hardness of the SOK 15 contacts increases approximately along a parabolic curve and changes its value from 40  $H_B$  (dispersion of 300 microns) to 85  $H_B$  (dis-

/267

persion of 0.5 microns). It is of prime interest to compare the hardness at two boundary points of the left part of the curve because contacts with silver grains whose diameter is 50 microns are of the industrial type widely used at the present time in instrument design. Compared with these contacts which have a hardness of 58  $H_B$  in the annealed state, the hardness of finely dispersed con-

tacts increases almost by 50 percent, which has a very beneficial effect on their operation characteristics.

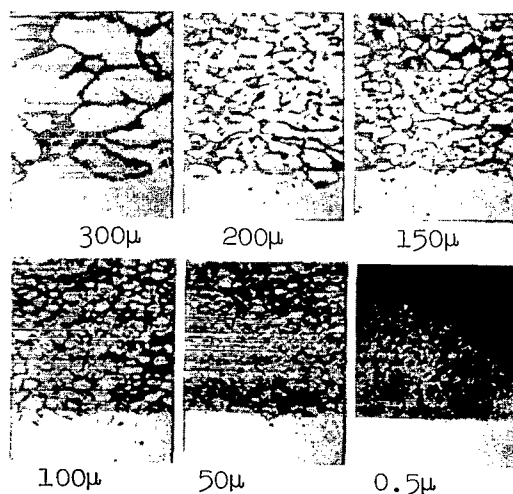


Figure 1. The microstructure of the SOK 15 contacts of various dispersions.

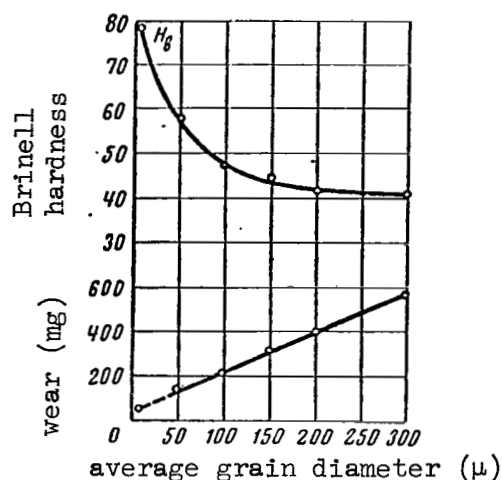


Figure 2. The electric wear and hardness of the SOK 15 contacts as a function of structure dispersion.

The latter is illustrated by the electrical wear of the SOK 15 contacts depending on the degree of dispersion of the structure. We should note that this relationship has a rectilinear nature and a substantial slope with respect to the axis of the abscissas, which shows that the dispersion of the structure is one of the most significant methods of increasing the durability of cermet contacts. /268

The linear relation between the wear of SOK 15 contacts and the degree of structure dispersion shows that work should be done to increase the degree of structure dispersion to improve the durability of future contacts.

Electric tests were carried out by means of a special laboratory setup of the electromagnetic type using ac current of 60 V, contact current of 120 A, contact pressure of 0.5 kg-wt and a make-break frequency of 1200 cycles per hour. The load was resistive; contact dimensions were  $\phi 8 \times 2.2$  mm with a spherical operating surface. The vibration time of the contacts was 4-7 m/sec (measured by means of a millisecond stopwatch of the MS-1 type and periodically checked by means of an oscillograph). When the vibration departed from the assigned value, the equipment was readjusted. The high vibration level increased the wear of the test contacts and decreased the test time. The current-carrying elements of the equipment were cooled with flowing water.

Each point on the curve in figure 2 is constructed from the average wear of 6-8 pairs of contacts after 50,000 test cycles. An exception to this is the boundary point at the left, which represents the wear of finely dispersed contacts and which was obtained in a different manner. The testing of finely dispersed contacts was carried out by using industrial samples of the KTF 5043 ( $I_{\text{nom}} = 100$  A) and KM 2300 ( $I_{\text{nom}} = 100$  A) ac contactors under conditions encountered in their actual exploitation. Contacts with a conventional structure (50μ) /269



were tested in parallel with the finely dispersed SOK 15m contacts (average grain diameter  $0.5 \mu$ ). Contacts of the KTF 5043 contactors were investigated at NIIelektro,<sup>1</sup> of the KM2300 contactors at VNIPTI of the "DINAMO" plant. The following comparative results were obtained: the wear of finely dispersed SOK 15m contacts of the KTF 5043 contactors was 3.1 times less than of conventional contacts; in the KM 2300 contactors the wear of finely dispersed contacts was 2.1 and 3.6 times less. Thus, from the available data, the average coefficient for the decrease in the wear of finely dispersed contacts with respect to conventional contacts is approximately 2.9. For the sake of reliability, this coefficient was somewhat decreased. The point in figure 2 corresponding to the average grain size of  $0.5 \mu$  was introduced to show a wear of 2.5 times less than for a contact with an average grain diameter of  $50 \mu$ . The section of the straight line between these two points is broken.

Considering the general nature of the graph showing the SOK 15 contact wear as a function of structure dispersion we note that when the average diameter of the silver grains decreases from 300 to  $0.5 \mu$ , the electric wear decreases approximately by a factor of 6. When the circuit parameters are different, the slope of the wear line will be different.

Below we present the results of investigations carried out to develop methods for the industrial production of finely dispersed SOK 15m compositions and of contacts made from these compositions. The dimensions of SOK 15m particles were investigated. These were obtained by a combined precipitation of carbonates from solutions of nitrate salts of silver and cadmium using equal amounts of saturated solutions of sodium bicarbonate. The dimensions of the particles were studied as a function of precipitation reaction time, temperature of the precipitating agent, concentration of initial solutions and the intensity of their mixing. The chemical composition was continuously controlled. The process was continued until the composition did not deviate by more than  $\pm 0.5$  percent.

The size of the composition particles was determined indirectly using the Deryagin method. In this method the magnitude of the external specific powder surface was first determined and then the average diameter of the particles was determined from the formula.<sup>2</sup> This method is based on measuring the resistance exhibited by a porous body (a tablet pressed from the powder) to the flow of rarefied air. /270

Curves showing the variation in particle size of the SOK 15m powder as a function of precipitation reaction time, precipitating agent temperature and concentration of initial solutions are shown in figure 3. The solutions were mixed with a mechanical agitator of the vane type with vanes turning in one direction

---

<sup>1</sup>Contacts were also manufactured at NIIelektro.

<sup>2</sup>Measurements using the Deryagin method were carried out by T. V. Peregudova.

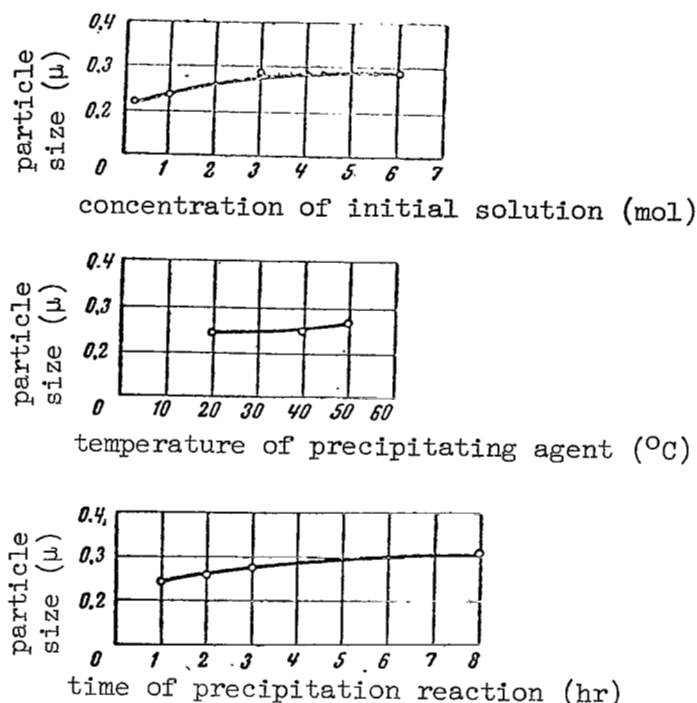


Figure 3. The variation in the particle size of the SOK 15m powder as a function of the precipitating agent temperature, the precipitation reaction time and the concentration of initial solutions.

(the vanes were constructed in the form of a frame). The mechanical agitation of the salt solution and of the precipitating agent was carried out for a 271 period of one hour. After this the precipitating reaction took place without agitation. When the reaction time was increased from one to eight hours there was an insignificant increase in the average dimension of the particles.

To obtain a minimum particle size, the precipitation operation should be carried out as rapidly as possible. The requirements for the completeness of the precipitation reaction are exactly opposite and require an increase in the reaction time. After one hour of exposure, the content of silver ions in the filtrate is equal to 0.21 g/liter, i.e., the reaction for the formation of the carbonates is not complete. The microstructure of a contact fabricated from this mixture is unsatisfactory (fig. 4). The analysis of the filtrate after a two-hour precipitation shows traces of silver which indicates that the reaction is complete. The same is observed after a precipitation time of 3, 4, 6, and 8 hours. Thus the optimum precipitation time is two hours.

The variation in the particle size as a function of precipitating temperature with a constant precipitating reaction time was considered at temperatures of 20, 40 and 50 $^{\circ}\text{C}$ . Higher temperatures are not permissible due to the breakdown of the precipitating agent--a saturated solution of sodium bicarbonate. Sodium bicarbonate was dissolved in warm water so that the following question arises even under industrial production conditions: is it possible



Figure 4. The microstructure of SOK 15m contacts fabricated from a mixture precipitated in a period of one hour.

to operate with a warm precipitating agent or should it be cooled? Experiments have shown (see fig. 3) that an increase in the temperature of the precipitating agent has very little effect on the variation of the powder particle size and, in practice, it is possible to operate with a warm precipitating agent.

The problem concerning the effect of initial solution concentration on particle size is also quite important. This problem is directly associated with the productivity of the process, the volumes of the reaction vessels for precipitation and with the production surfaces. The variation in the size of SOK 15m composition particles as a function of the concentration of initial solutions was investigated by using 0.1M, 1M, 3M and 6M concentration of silver and cadmium nitrate salts. Investigations showed (fig. 3) that the most dispersive material corresponds to the decimolar concentration. When the concentration of the solution is increased to a 3-molar value, there is some increase in particle size which is retarded with a further increase in concentration. We should note that the variation in particle size as a function of initial solution concentration takes place in a narrow interval between 0.2 and 0.3  $\mu$ . /272

Thus, the industrial process of cooling carbonates may be carried out at high concentration of initial solutions, for example, at 3-molar concentrations.

The photographs showing the microstructure of the SOK 15m contacts as a function of the initial solution concentration are shown in figure 5.<sup>1</sup>

<sup>1</sup>Metallographic investigations were carried out by V. N. Sorokina and T. V. Peregodova.

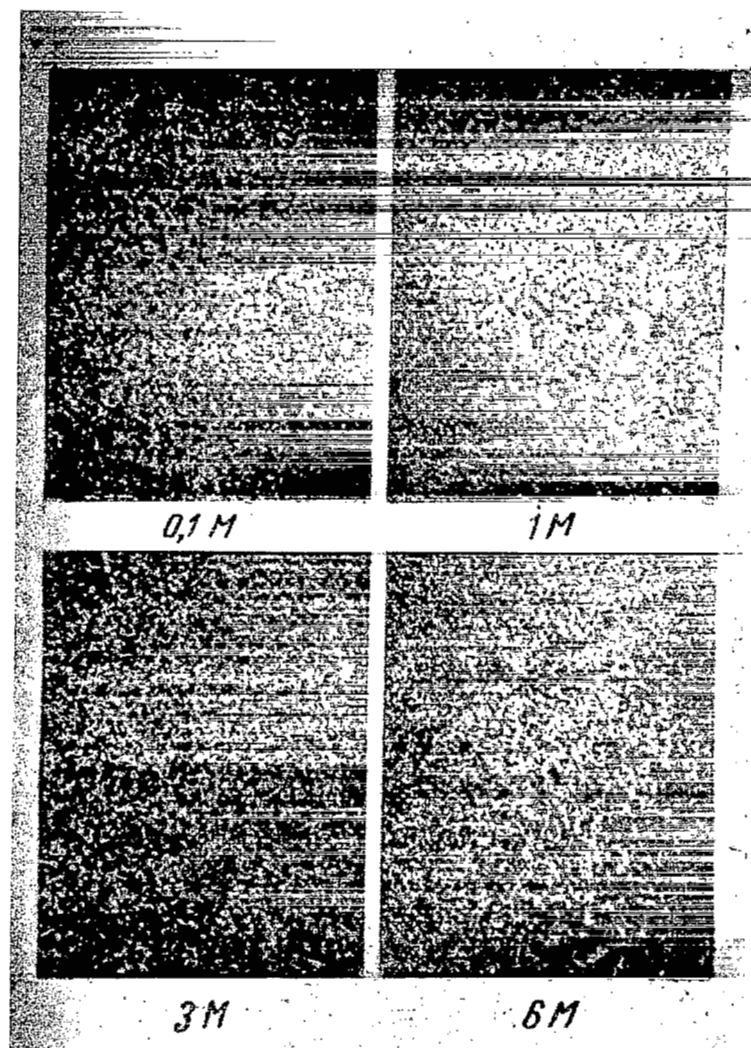


Figure 5. The microstructure of the SOK 15m contacts as a function of initial solution concentration.

The intensity of agitation during the precipitation process has some effect on the dispersion of the powders. However, the existing construction of the agitator did not make it possible to control the intensity of agitation over wide limits. The minimum particle size was obtained when the angular velocity of the agitator was 90 rpm, which was assumed to be optimum. A further increase in the rpm produced a decrease in the intensity of agitation because the entire volume of the liquid began to rotate.

The investigation of this problem should be continued by using different methods of mixing the solutions.

Thus, an optimum variation of the technology for the finely dispersed SOK 15m mixtures was contemplated, which takes into account all the

considerations expressed above: the concentration of the initial solutions of silver and cadmium salts is 3M, the temperature of the precipitating agent is 40°C and the reaction time is two hours.

As the dimensions of the particles of powders were determined by means /274 of the Deryagin method, they were simultaneously investigated by means of an electron microscope.<sup>1</sup>

The method of analysis by means of an electron microscope consisted of the following. The surface of a plate (~15.15 mm) cut from an aluminum wrapping foil was covered with a thin layer of the powder. For this purpose, one side of the foil was dipped into the loose powder and then the excess powder was removed by shaking the foil vigorously. This left a thin layer of powder on the foil in an amount sufficient for investigation.

After this, the foil with the powder was placed into a vacuum bell of the UVR installation. After this, carbon electrodes were used to deposit a thin carbon film of thickness 300-400 Å on the surface of the foil with the adhering powder by the method of thermal diffusion.

The sample obtained in this manner was cut into sections of approximately 3.3 mm which were carefully placed on the surface of a mixture of acids (70 percent hydrochloric acid and 30 percent nitric acid) with the aluminum side down. The pieces floated until the aluminum was dissolved.

After the aluminum foil was dissolved, the remaining carbon films with the attached powder were quickly removed by means of a thin metallic screen, were washed in water, dried and examined under the electron microscope.

Figure 6 shows the granulometric composition in the form of frequency graphs of finely dispersed SOK 15m powder, PS1 (GOST 9724-61), of electrolytic silver powder, used in the production of cermet contacts and of the industrial SOK 15 mixture from the PS1 silver powder and cadmium oxide powder. The frequency curves are constructed on the basis of data from 1000 measurements of particles from each powder under the electron microscope with a magnification of 10,000.

We should point out that the finely dispersed SOK 15m powder (1) obtained by the combined precipitation and the so-called "conventional" SOK 15 powders (3) and Ag (2) are materials whose particle sizes are of the same order of /275 magnitude. The frequency maximum for SOK 15m corresponds to 0.2 - 0.3 μ while for SOK 15 it corresponds to 0.4 - 0.5 μ and for Ag to 0.8 - 0.9. The cadmium oxide powder is also a finely dispersed material whose prevalent particle size is of the order of 0.2-0.3 μ as we can see from the electron microscope picture taken with a magnification of 10,000 (figure 7).

Nevertheless the microstructures of ready-made contacts from the SOK 15m and SOK 15 mixtures are substantially different (see fig. 1). The silver

---

<sup>1</sup>Performed by Ye. V. Mileschin.

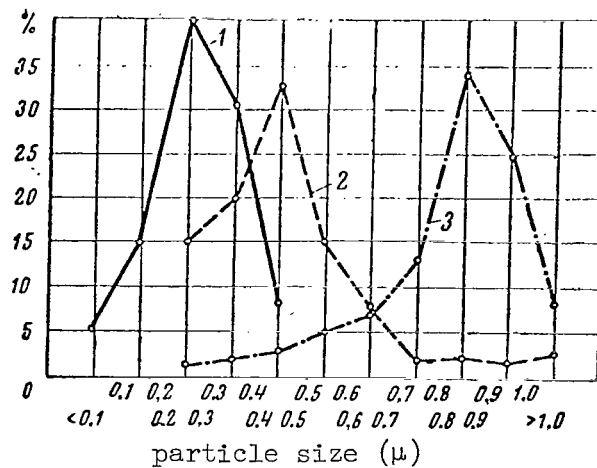


Figure 6. The frequency graphs of the SOK 15m powders (1), SOK 15 (2) and electrolytic silver (3) from electron microscope analysis data (1000 samples of each powder were measured with a magnification of 10,000).

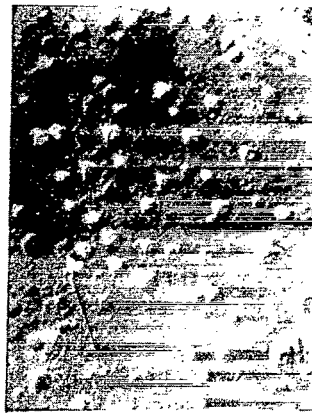


Figure 7. Carbon replica of cadmium oxide powder particles magnified 10,000 times.

particle size in a fired SOK 15m contact is two orders of magnitude smaller than in the same contact made from SOK 15 (0.5  $\mu$  instead of 50  $\mu$ ). Apparently this is explained by the fact that in the SOK 15m mixture each particle of the powder is a composition of silver and cadmium oxide which cannot be divided /277 mechanically. When this mixture is used, there are no changes during the pressing and firing of contacts fabricated from it. The situation is different with the SOK 15 mixture. Here the silver and cadmium oxide particles are isolated but an ideal distribution is not observed. During the mixing process and later during pressing and firing, they are conglomerated and form larger particles than the initial silver powder particles or cadmium oxide particles in the mixture.

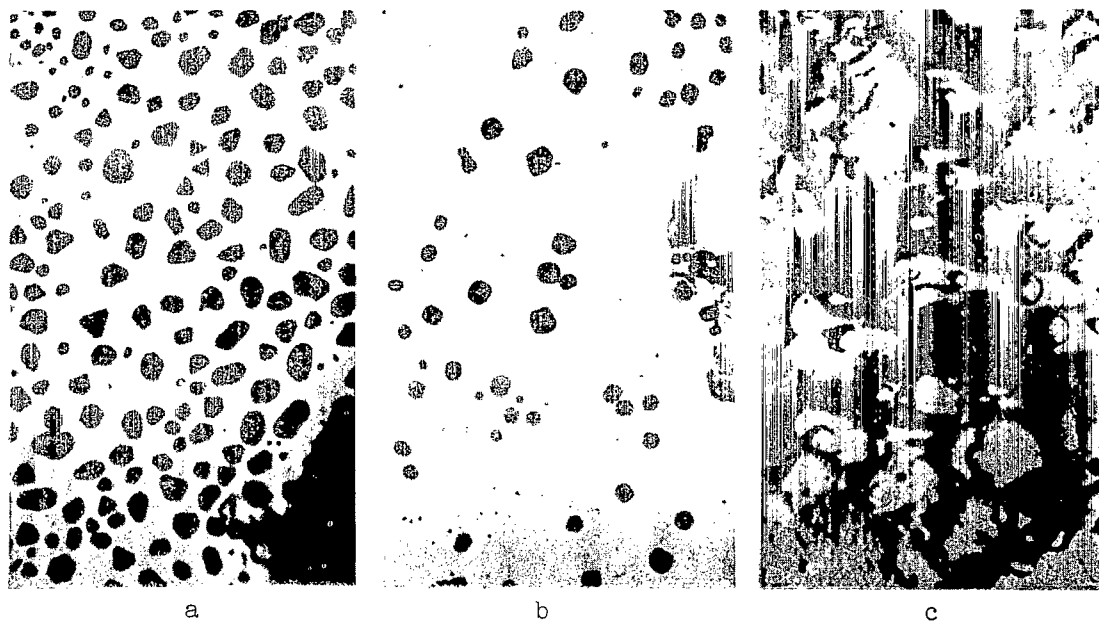


Figure 8. Particles of the SOK 15m powder on a carbon film without shading (a, b) and with chromium shading (c).

The form of the particles of finely dispersed SOK 15m powder approaches a spherical shape (fig. 8). This is beneficial for the accurate measurement of the average particle size by using the Deryagin method, which is based on the assumption that all of the particles are spherical. For this reason there is good agreement in the present work between the dimensions of SOK 15m powder particles measured by the Deryagin method, the electron microscope, which presents a direct picture and the direct measurement of dimensions by means of the replicas (see figs. 3 and 6). This increases the reliability of our results.

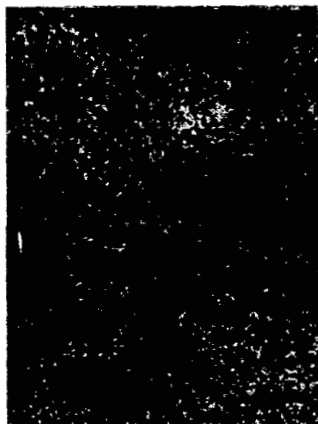


Figure 9. The microstructure of the SOK 15m contact manufactured from an experimental powder prepared by the VDM plant.

Figure 9 shows the microstructure of the SOK 15m contact fabricated from an experimental powder prepared under production conditions at the Moscow plant for the secondary precious metals. The microstructure is exceptionally uniform, does not contain foreign inclusions and pores, and indicates that the contact is of high quality.

The finely dispersed mixtures, including SOK 15m, have a poured weight which is several times less than that of conventional mixtures and a substantially worse viscosity which makes it difficult to automatically press the contacts (particularly small contacts) by means of high speed automatic presses.

One of the solutions to this problem consists of a preliminary granulation of finely dispersed powders to obtain sufficiently stable conglomerates of particles with a diameter of 100-300  $\mu$ . /278

Investigations in the region of cermet contacts with finely dispersed structures are most promising. There is reason to expect that the development of work in the direction of a further dispersion of structures will make it possible to obtain compositions which will have qualitatively new properties, most valuable for low duty electric equipments which primarily use contacts made of pure precious metals or their alloys.



## DEVELOPMENT AND INVESTIGATION OF HEAVY DUTY FINELY DISPERSED CONTACTS

N. N. Smaga, B. A. Yudin and Ye. V. Markov

During the conference held at Yerevan in 1961 on electric cermet com- /278  
ponents, a report was presented on finely dispersed SOK 15 contacts. The  
new simple method proposed by us for obtaining a finely dispersed batch for  
these contacts by chemical means provided for a homogeneous and particularly  
fine contact structure. Tests on contacts made from such a batch were carried  
out by using contactors which switched three phase currents of 100-700 A at  
400 V and by using automatic equipment with currents up to 30-40 kilo amperes  
and  $\cos \varphi = 0.4-0.5$ . These tests showed that contacts made from the new mate-  
rials are three times more durable than normal contacts used in these equip-  
ments: in the first case SOK 15 and in the second case SN 30. This substan-  
tial improvement in quality should be explained by the transition from a  
coarsely dispersed to a finely dispersed homogeneous contact structure.

Since the time of the conference, we and other organizations have tested  
finely dispersed contacts fabricated from SOK 15 under other operating con-  
ditions and in other equipments (table 1).

In all cases, the durability of finely dispersed contacts of SOK 15 was  
substantially greater than the durability of normal contacts manufactured  
from an alloy of the same composition or from silver. The transportation of  
metal from one contact to the other during dc operation was substantially /279  
less in finely dispersed contacts than in silver-plated contacts. Thus  
the finely dispersed contacts of SOK 15 showed a rather high resistance to wear  
in the entire range of switching currents from one ampere to tens of thousands  
of amperes both for dc and ac. The other properties of these contacts (sta-  
bility of contact resistance, resistance to welding) are also better than in  
normal contacts of SOK 15.

At the present time development work has been completed on three more  
finely dispersed compositions for contacts silver-copper oxide (SOM 15),  
silver-chromium oxide (SOKh 5 and SOKh 10) and silver-nickel SN 30.

The experimental finely dispersed compositions were tested for elec-  
trical wear by means of mass produced automatic AZ 120 switches when this  
equipment handled short circuits up to 40 kiloamperes with  $\cos \varphi = 0.4$  and  
when this equipment performed multiple switching of nominal currents of 100 A  
with  $\cos \varphi = 0.7$  with three phase current of 380 volts.

TABLE 1

Type of Equipment	Switching Parameters		
	Current (A)	Voltage (V)	Cos $\varphi$
PKT-560 Contactor	300-500	20	0
RP-1 Relay	2	380	0.4
KT-5000 Contactor	100 makes }	380	0.3
	10 breaks }		
	25 makes }	220	1
	1 break }		

<sup>1</sup>For  $\tau = 0.05$  sec.

The durability of all these contacts was substantially greater than that of normal contact SN 30 used in these equipments. In addition to this, from the standpoint of durability, the finely dispersed contacts SOM 15 and SOM 8 were superior to SOM 10 contacts which were obtained by the oxidation of /280 silver-copper alloy.

We should point out that the majority of the developed compositions as well as the normal contacts SN 30 of these automatic switches tend to weld when they switch short-circuited currents. Therefore, as a rule they cannot be used in switches where the switching pairs are made of the same material. Therefore, under these operating conditions such contacts are usually used in pairs with normal contacts of silver-graphite (SG 5). However, the latter release a considerable quantity of soot when switching high currents. As a result of this the insulation resistance as well as the electric strength is lowered. The advantage of the newly developed silver-chromium oxide SOKh 5 contacts compared with SG 5 contacts is that they release less current-conducting soot and have better resistance to wear when switching nominal currents and approximately the same resistance to wear when switching short-circuited currents.

The dimensions of the test contacts were 13·12·2.4 mm. The weight of the silver underlayer for the silver-metal oxide contacts was 0.15 grams.

To obtain finely dispersed mixtures by the method of combined precipitation from solutions, it is necessary that all of the metals which are contained in a given composition produce practically insoluble and thermally unstable salts (carbonates, oxalates, or formates). The initial substances must be easily soluble salts (nitrates), because the resulting precipitates are easily cleansed of nitrate ions by water.

The technological process of obtaining finely dispersed batches by the chemical method proposed by us--the method of combined precipitation of thermally unstable salts--is, in general, the same for contacts of all compositions indicated above. Let us consider this method by using, for example, the preparation of a finely dispersed batch of the SOM 15 composition of silver-copper oxide.

A salt mixture from a two-molar solution of silver nitrate and copper nitrate is obtained at room temperature (solution 1). The precipitating agent--sodium bicarbonate--is prepared separately as a saturated solution (solution 2).

If the solutions are prepared at a temperature of 50-60°C, a batch with the larger grain size is obtained. /281

Small portions of solution 1 are added to solution 2 while the mechanical agitator is used to continuously stir the solution. After the precipitation has formed, its completeness is checked. If the solubility of salts obtained in the precipitation differs by several orders of magnitudes, it is necessary to take an excess of the precipitating agent so that several components precipitate from the solution simultaneously.

The precipitation is washed with distilled water using a diphenylamine indicator. It is then washed with alcohol and dried in an oven at a temperature of 110-120°C for a period of two hours. If the precipitation is not washed with alcohol, it forms lumps after it is dry. The dried precipitation is broken down for a period of thirty minutes at a temperature of 420-450°C in air. The decomposition temperature of the precipitation is determined by the Kurnakov pyrometer.

After decomposition, the batch is ready for use. The dimension of the particles in the batch does not exceed 0.1 micron.

The salt solution for the composition silver-chromium oxide and silver-nickel should be decomposed in hydrogen.

The preparation of contacts from the finely dispersed batch is basically the same as the preparation from a normal roughly dispersed batch.

The microstructure of finely dispersed SOK 15m contacts is shown in figure 1, and that of the normal SOK 15 is shown in figure 2. It follows from these figures that the structure of the developed contacts is finely dispersed and is homogeneous. The dimensions of the particles in the finished contact do not exceed one  $\mu$ . In contacts with rough dispersion there are individual distributions of the components.

The characteristics of finely dispersed contacts and certain technological data are presented in table 2.

It follows from the data in the table that, for the case of finely dispersed contacts the flexural strength, hardness, density and specific conductivity are higher than for contacts with rough dispersion.

Thermographic investigations have shown that the decomposition of the mixture for batches of above compositions ceases at a temperature up to 400°C. To compare the tendency of the mixtures to sinter, the kinetics of the sintering process was investigated. For this purpose, samples of square cross sections 3.3 mm and of length 30 mm were prepared with the same initial /282

TABLE 2

Type of Contacts	Pressing	Sintering		Repeated pressing	Annealing		Physical characteristics			
	Pressure (tons/cm <sup>2</sup> )	Temperature (°C)	Time (min)	Pressure (tons/cm <sup>2</sup> )	Temperature (°C)	Time (min)	Density (g/cm <sup>3</sup> )	Specific resistance ohms·mm <sup>2</sup> /m	Brinell hardness (kg-wt/mm <sup>2</sup> )	Flexural strength (kg-wt/mm <sup>2</sup> )
Finely dispersed SOK 15	4	800	60	8	450	30	9.86	0.0250	79.9	45.6
Roughly dispersed SOK 15	4	900	60	8	450	30	9.6	0.0289	59.9	10.5
Finely dispersed SOM 15	4	800	60	8	450	30	9.58	0.0361	75.0	45.0
Finely dispersed SOM 8	4	800	60	8	450	30	9.85	0.0263	62.0	83.0
Finely dispersed SOKh 5	4	800	60	8	450	30	9.6	-	52.0	-
Finely dispersed SN 30	2	800	60	8	450	30	9.9	0.0248	72.0	56.0
Roughly dispersed SN 30	2	860	120	8	450	30	9.7	0.0267	55.0	41.0

porosity. The samples were sintered in  $10^{-2}$  mm Hg at  $800^{\circ}\text{C}$  and after a definite period of time were removed from the oven and cooled together with the quartz test tube. After this, their linear dimensions were measured by means of an optical indicator. Figure 3 shows the variation in the /283 relative linear shrinkage as a function of sintering time for samples prepared from a carbonate mixture decomposed at a temperature of  $400^{\circ}\text{C}$  (curve 5),  $500^{\circ}\text{C}$  (4),  $600^{\circ}\text{C}$  (3) and for samples pressed from mechanical mixtures (curves 1 and 2). Investigation has shown that the tendency of the mixtures which have /284 been obtained by the decomposition of precipitated carbonates, to sinter is rather high and depends on the decomposition temperature of the mixtures decreasing when the latter increases. The samples prepared from a mechanical mixture which have been held at a temperature of  $800^{\circ}\text{C}$  for one hour showed very little shrinkage. Their final porosity was practically unchanged from the initial value whereas the porosity of samples from carbonate mixtures was decreased almost by 2 during the sintering time.

In addition to the above compositions, other compositions were developed and tested, such as silver-boron carbonate (5 percent), silver-barium carbonate (10 percent), silver-indium oxide (10 percent), silver-nickel-boron nitride (29-1 percent), silver-calcium (75 percent), silver-silicon carbide (5 percent) and others. Contacts made of these compositions are very durable at high currents; however, when shorting currents of the order of 45 kilo amperes at 400 V were turned off, the last three compositions exhibited a high transitional resistance. In the case of the silver-baron carbide (5 percent) contacts, a large transitional resistance was recorded after nominal currents were turned off.

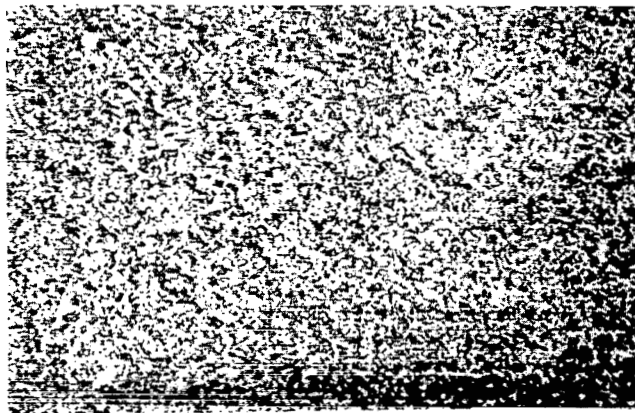


Figure 1. The microstructure of finely dispersed SOK 15 contact magnified 130 times.

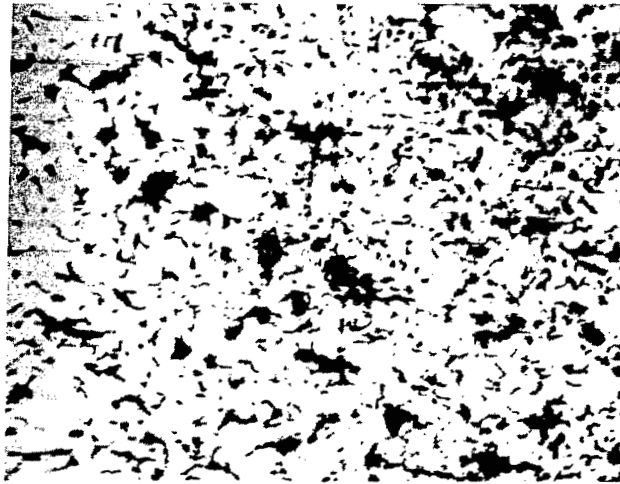


Figure 2. The microstructure of roughly dispersed SOK 15 contact magnified 130 times.

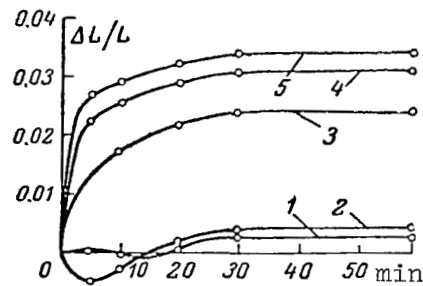


Figure 3. The variation in the relative linear shrinkage as a function of sintering time for samples of carbonate mixtures which were decomposed at 400°C (5), 500°C (4), 600°C (3); and samples of mechanical mixtures KhELZ (2) and KhEMZ (1).

## Conclusions

As a result of our work, we obtained, by chemical means, a batch for contacts of various compositions. The investigations which we have described have shown that contacts made of this batch have a rather finely dispersed and homogeneous structure and, as a result of this, their useful life and other properties, as a rule, are greater than in contacts of the same composition which have a rough dispersion.

Considering the relative simplicity of this method of obtaining batches for contacts, the substantially lower price of the batch and higher contact

qualities prepared from it, the proposed technology should be considered as an advanced one compared with the technology used in powder metallurgy.

The transition to the production of batches for contacts using the proposed method, initially for contacts SOK 15, SN 30, SN 40, SOM 10, SOM 15, will provide for an economy of material and will increase the quality of produced contacts.

## Cu-Cd AND Ag-Cd CERMET CONTACTS

A. B. Al'tman and E. S. Bystrova

In the production of silver and copper alloys with cadmium, metallurgical practice produces a loss of cadmium in burning which is equal to several tens percent. This makes it difficult to obtain cast alloys of stable composition and increases the harmful effects of production. Due to the volatilization of cadmium, substantial difficulties also arise in the preparation of cadmium alloys by means of conventional cermet technology involving the pressing and firing of metallic powders. /285

We present a brief description of the method for preparing Cu-Cd and Ag-Cd cermet alloys without a cadmium loss. We also present the results of investigating Cu-Cd and Ag-Cd breaking electric contacts and Cu-Cd collector plates.

In the proposed method, the Cu-Cd cermet alloys are prepared by mixing copper powders and metallic cadmium in ratios necessary to obtain a given chemical composition (ref. 1). The mixture of powders is pressed and then fired in an atmosphere of protective gas at high pressure in a charge consisting of a mixture of high melting metallic oxide powders and cadmium oxide (or metallic cadmium).

The excess pressure of the gaseous medium during heating, soaking and cooling of the sintered articles is maintained at a value not less than 2-3 atm. The charge contains from 1 to 20 percent cadmium oxide or from 0.5 to 10 percent metallic cadmium; the remainder of the charge consists of aluminum oxide or titanium dioxide. The exact limits of cadmium component contents in the charge are selected experimentally, depending on the required amount of cadmium in the alloy and depending on the heating cycle. Sintering is achieved in a hermetically sealed vessel whose gaseous medium is not rejuvenated. /286

In the present work, the samples were fired in an argon atmosphere in a charge consisting of a mixture of cadmium oxide (or metallic cadmium) and aluminum oxide.

Table 1 shows the magnitude of cadmium loss during the firing of Cu-Cd as a function of charge composition. The addition of 1 percent CdO to aluminum oxide in the charge lowers the cadmium losses to 5 percent (of the cadmium content in the batch). The increase in cadmium oxide content in the charge to 2-3 percent produces the deposition of cadmium on the surface of the sintered articles. These data pertain to the initial sintering pressure of 2 atm.



TABLE 1. VARIATION IN CADMIUM CONTENT OF Cu-Cd CERMET ALLOYS (99 PERCENT Cu, 1 PERCENT Cd) AFTER SINTERING AT 900°C IN DIFFERENT CHARGES

Composition of charge, in percent		Initial pressure of sintering atmosphere in atm	Variation in cadmium content in percent*
Al <sub>2</sub> O <sub>3</sub>	CdO		
-**	-**	2	-60
100	-	2	-25
99	1	2	- 5
98	2	2	+14
97	3	2	+40
-**	-**	25	-50

\*The sign "-" means a decrease, while the sign "+" means an increase in cadmium content.

\*\*The samples were fired without a charge.

Thus, sintering in the charge consisting of 98-99 percent Al<sub>2</sub>O<sub>3</sub> and 2-1 percent

CdO makes it possible to obtain a sintered material of almost constant chemical composition without cadmium loss. Sintering in a charge consisting of 100 percent Al<sub>2</sub>O<sub>3</sub> and the increase of initial pressure to 25 atm (when heating without

a charge) also lowers cadmium losses. The properties of cadmium copper (bronze) both cermet and metallurgical, and also of pure copper (without an admixture of cadmium) are compared in table 2. Cadmium copper is used in collector /287 plates and contact rings of electrical equipment and also for the breaking contacts of contactors and other low voltage electric equipment (refs. 2 and 3).

Cermet cadmium copper (99 percent Cu, 1 percent Cd) was used to manufacture collector plates, and a collector was assembled for the DK656B motor of the electrical trolley system. At the same time a motor was tested with a collector manufactured from M-1 copper. The collectors were assembled at the "Dinamo" plant; the tests were conducted by the central laboratory of VNIPTI at the "Dinamo" plant.

The basic technical specifications of the DK656B motor are as follows:  
 $U = 550 \text{ V}$ ;  $I = 5.3 \text{ A}$ ;  $n = 1700 \text{ rpm}$ ;  $P_2 = 2 \text{ kW}$ ;  $PV = 100 \text{ percent}$ . Brushes were

of the EG2A type and were covered electrically with graphite. The results of tests on the durability of the collectors after the motor operated for a period of 527 hours are shown in table 3. The temperature of the motor during the testing of the collectors was in the range 65-70°C. The wear of collectors

TABLE 2. PROPERTIES OF CERMET CADMIUM COPPER (99 PERCENT Cu, 1 PERCENT Cd), OF CADMIUM COPPER USED IN COLLECTORS (0.9-1.2 PERCENT Cd REMAINDER-Cu) AND OF THE M-1 COPPER.

Material	Nature of processing	Hardness $H_B$	Rupture strength in tension kg-wt/mm <sup>2</sup>	Specific electrical resistance $\Omega \cdot \text{mm}^2/\text{m}$
Cermet cadmium copper	Final pressing, annealing	55- 65	16-20	0.0230
	Final pressing	95-105	26-31	-
Metallurgical cadmium copper	In soft state	60	25-28	0.0207
	After 50 percent deformation	95-115	40-60	-
Metallurgical M-1 copper	Without deformation	44	20-24	0.0178
	with deformation	90	40-50	-

from cermet cadmium copper and from collector M-1 copper was almost the same in this case; however, the wear of brushes on the collector manufactured from cermet cadmium copper was approximately two times smaller than that of the brushes on the collector manufactured from the M-1 copper. /288

Breaking electric contacts made of cermet cadmium copper (of the same chemical composition) were tested at the "Dinamo" plant in the KPD-113 dc contactors with a voltage of 110 V, and an active load with a frequency of 600 makes per hour and a PV = 5-6 percent with current of 150, 300 and 560 A. The electrical wear of the contacts was determined after 120,000 makes-breaks (with a current of 300 and 560 A). The tests showed that under these conditions, the contacts of cermet cadmium copper are approximately 1.5-2 times better from the standpoint of wear than the contacts from rolled M-1 copper (table 4). The same wear ratio was determined earlier when contacts of M-1 copper were compared with collector cadmium copper (GOST 4134-48) (ref. 3).

TABLE 3. RESULTS OF TESTING COLLECTORS MADE OF CERMET CADMIUM COPPER AND M-1 COPPER.

Collector material	Decrease in brush height, mm*	Decrease in brush weight, g*	Decrease in collector diameter, mm
Cermet cadmium copper	6.1	1.6150	0.0535
M-1 copper	11.3	2.9935	0.0580

\* EG2A brushes

The following method (ref. 4) was proposed for the fabrication of cermet alloys of silver and cadmium. Silver powder and cadmium oxide powder are mixed in a ratio necessary to obtain the required chemical properties. The required forms are pressed from the mixture. The pressings are sintered in an oxidizing atmosphere at a relatively high temperature (to obtain high mechanical strength). When sintering takes place under these conditions, the cadmium oxide loss is insufficient (fig. 1).

The sintered samples are heated the second time at a lower temperature in a reducing atmosphere to reduce cadmium oxide and obtain a solid Ag-Cd solution. When the sintered samples are heated in hydrogen up to 400-450°C, the change in the weight of the samples, for all practical purposes, does not exceed the value of the losses due to the total reduction of cadmium oxide to metallic cadmium (fig. 2). At a temperature above 500°C the losses /289  
/290

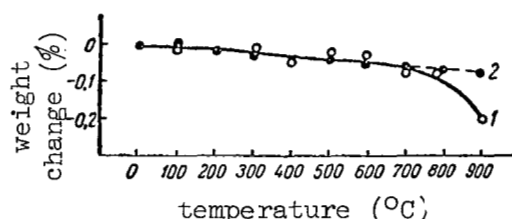


Figure 1. Variation in weight of samples pressed from cadmium oxide (100 percent CdO) and silver (100 percent Ag) as function of sintering temperature. Samples were sintered in air. 1, samples of CdO; 2, samples of Ag.

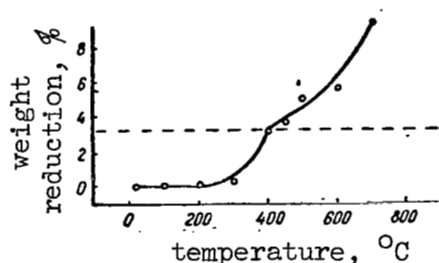


Figure 2. Variation in the weight of Ag-CdO samples (73 percent Ag, 27 percent CdO) as function of heating temperature in hydrogen; broken line shows computed value of weight variation in samples when cadmium oxide is entirely reduced to metallic cadmium.

TABLE 4. WEAR OF BREAKING ELECTRIC CONTACTS FABRICATED FROM CERMET CADMIUM COPPER (1) AND FROM ROLLED M-1 COPPER (2) WHEN dc CURRENT OF 150-560 A IS TURNED ON AND OFF.\*

Material	Current in A	Specific wear in milligrams**		
		Moving contact	Stationary contact	Contact pair
1	150	5.3	9.5	14.8
2	150	14.6	15.8	30.4
1	300	6.9	36.4	43.3
2	300	26.7	48.3	77.4
1	560	6.4	115.7	122.0
2	560	42.0	106.8	148.8

\*110 V, 600 cycles per hour, duration of switched-on position 5-6 percent resistive load.

\*\*For one cycle (make-break).

increase radically due to the evaporation of cadmium. With subsequent final pressing and annealing we obtain durable dense articles from the Ag-Cd alloy with a stable structure and stable properties.

Cermet technology is used to fabricate breaking electric contacts for voltage regulators in diesel-electric generators from the alloy based on the system Ag-Cd (76.5 percent, 22 percent Cd, 1 percent Ni, 0.5 percent Fe). The contacts operate in a dc circuit with a current of 8 A and a voltage of 75 V. Experience obtained during the operation of these contacts for a period greater than ten years has shown that they are stable against burning and provide for stable voltage within the limits of  $\pm 1$  V. Under the same conditions, contacts made of silver and a silver-cadmium oxide composition (12 percent CdO) were found unsuitable.

#### REFERENCES

1. Al'tman, A. B. and Bystrova, E. S. Method of Preparing Copper or Silver Alloys with 0.1-30 percent Cadmium by Using the Cermet Method (Sposob izgotovleniya splavov medi ili serebra s 0.1-30% kadmiya metallokeramicheskim sposobom). Byulleten' Izobreteniy, Vol. 2, No. 135, 222, 1961.
2. Pasynkov, V. V. A Part in the Handbook on Electrical Materials (Razdel v spravochnike po elektrotekhnicheskim materialom). Gosenergoizdat, Vol. 2, 1960.
3. Al'tman, A. B. and Bystrova, E. S. Cadmium Bronze as a Material for Breaking Electric Contacts, in collected works "Electric Contacts" (Kadmiyeva bronza kak material dlya razryvnykh elektricheskikh kontaktov v sb.: Elektricheskiye kontakty). Gosenergoizdat, 1960.
4. --- Method of Obtaining Alloys for Electric Contacts (Sposob polucheniya splavov dlya elektricheskikh kontaktov). Byulleten' Izobreteniy, Vol. 1, 1958, Soviet Patent No. 110996.

## INVESTIGATION OF ELECTRIC CONTACT EROSION OF TUNGSTEN-RHENIUM ELECTRODES<sup>1</sup>

M. I. Tishkevich

The electric contact erosion was studied to obtain erosion diagrams /291 for tungsten-rhenium electrodes. Such diagrams constructed for various metals and their alloys may be used as a basis for developing theoretical concepts regarding the effect of various structural parameters on the magnitude of erosion.

Investigations were made of the erosion stability of cermet samples made of pure tungsten, supplied by two different suppliers, and also of tungsten-rhenium composition: WRe-5 (tungsten plus 5 percent rhenium), WRe-10, WRe-15, WRe-20. Judging from the phase diagram,<sup>2</sup> these compounds represent the  $\alpha$ -phase.

The erosion of electrodes in contact systems is due to the action of the current during making and breaking of contacts. To achieve a deeper understanding of the reasons for electric erosion, the experiments were conducted using an experimental setup to measure erosion independently for breaking and making of electrodes.

The samples had the shape of a cylinder with the end of the working surface having diameter  $d = 4$  mm. The working surface of the samples was polished until bright (the absence of scratches and roughness was observed visually). Experiments were conducted with a switching frequency of 11-12 cps and a contact time

of the order of  $10^{-2}$  sec. The dc voltage in the circuit was 12 V and the average current  $I_{av} = 3$  A. The erosion of eight contacts was determined simul-

taneously by weighing them; the average erosion of a single contact pair was also determined.

Since the circuit contained no capacity or inductance (neglecting the feeder lines) and since the voltage and current were relatively small, a noticeable

---

<sup>1</sup>The work was carried out in collaboration with the Scientific Research Institute of Automatic Instruments.

<sup>2</sup>Ye. M. Savitskiy, M. A. Tylkina, L. L. Shishkina, Izvestiya AN SSSR, OTN, "Metallurgiya i Toplivo," No. 3, 1959.

erosion on one pair of contacts could be obtained only after  $20-25 \cdot 10^6$  makes, which corresponded to 70 hours of operation time.

/292

The illustration shows the average value of contact erosion for each make as a function of rhenium percentage; it also shows the values for pure tungsten of the "T" series (lower point) and of group 155 (upper point). The solid line shows the values of cathode erosion during making (CM) and breaking (CB). The broken line shows the erosion of the anode during making (AM) and breaking (AB) of the contact.

The table presents data on the total erosion during making and breaking of one contact pair of electrodes (cathode plus anode) during a single contact and during one hour of operation.

From the data which we have obtained we can make the following conclusions:

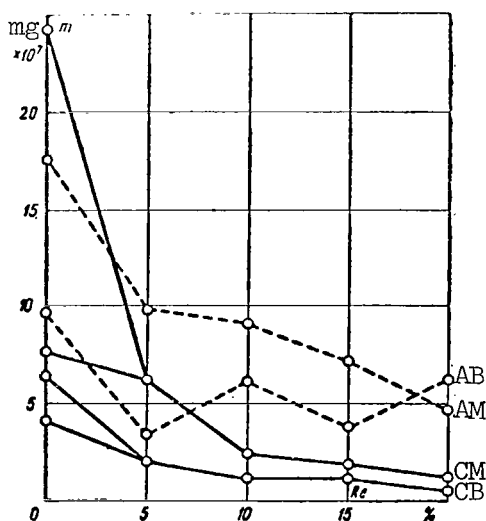
1. Tungsten of the "T" series is more resistant to erosion than tungsten of the 155 group.

2. The erosion of electrodes decreases as the amount of rhenium in the sample increases.

/293

3. The cathode has 2 to 4 times less resistance to erosion compared with the anode.

4. The erosion of the anode and of the cathode during the making of electrodes is greater than during their breaking.



Average value of erosion per contact during one make as function of rhenium content in sample.

# Erosion of Electrodes (mg)

Electrode composition	During breaking of contacts		During making of contacts	
	During one contact	During one hour of operation	During one contact	During one hour of operation
W, of the "T" series	$8.1 \cdot 10^{-7}$	$45.47 \cdot 10^{-3}$	$14.36 \cdot 10^{-7}$	$80.23 \cdot 10^{-3}$
W, of the 155 group	$14.2 \cdot 10^{-7}$	$79.51 \cdot 10^{-3}$	$41.69 \cdot 10^{-7}$	$233.57 \cdot 10^{-3}$
WRe-5	$5.26 \cdot 10^{-7}$	$29.52 \cdot 10^{-3}$	$17.2 \cdot 10^{-7}$	$96.18 \cdot 10^{-3}$
WRe-10	$7.35 \cdot 10^{-7}$	$41.19 \cdot 10^{-3}$	$11.6 \cdot 10^{-7}$	$65.23 \cdot 10^{-3}$
WRe-15	$5.00 \cdot 10^{-7}$	$28.09 \cdot 10^{-3}$	$9.00 \cdot 10^{-7}$	$50.71 \cdot 10^{-3}$
WRe-20	$6.71 \cdot 10^{-7}$	$37.61 \cdot 10^{-3}$	$5.45 \cdot 10^{-7}$	$30.47 \cdot 10^{-3}$



## INVESTIGATION OF BREAKING CONTACTS FOR IGNITION ASSEMBLIES

Z. S. Kirillova and A. G. Morozova

At the present time the contacts for ignition assemblies of engines /293 which operate at high altitudes are fabricated from an alloy of platinum with 25 percent iridium. In spite of its high contact properties, this alloy does not satisfy the increasing technical requirements for ignition systems from the standpoint of reliability, accuracy and useful life. Therefore, a series of alloys were tested which could perform better as contacts of ignition systems than the alloy of platinum with 25 percent iridium.

The performance of breaking contacts under definite electric circuit parameters are determined by physical and chemical properties of the selected material.

The contact material must have a high resistance to erosion during the action of the arc and of the spark, it must have a constant transitional contact resistance in time and it must not weld during its operation.

The following alloys and compositions were selected for the /294 investigations: alloys of platinum and iridium of the following brands PII-10, PII-20, PII-25, PII-40, PII-60; alloys of palladium and iridium of the following brands PDI-10, PDI-18, PDI-20, PDI-22, PDI-30; various alloys of palladium with rhenium, tungsten, silver; SrNM-2-20 and SOM silver alloys, and also cermet compositions of tungsten and rhenium.

It is known that the contacts of the breaking mechanism of an ignition system operate under rather severe conditions and are subjected to spark and arc erosion (ref. 1). The physical processes which accompany these forms of erosion are entirely different; in the case of the arc there is bombardment and destruction of the cathode by heavy positive ions while, in case of the spark, there is bombardment of the anode with electrons and its destruction.

The magnitude of erosion for arc processes and spark processes, when other conditions are equal, depends to a large degree on the properties of a contact material, and the same material may have a different resistance to spark erosion and arc erosion.

The testing of contact materials under conditions of spark formation and arc formation were carried out separately by using special experimental setups

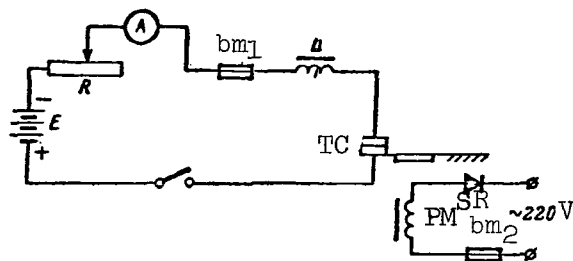


Figure 1. Electric scheme of arc erosion setup. E, dc current source 27 V  $\pm$  10 percent; R, variable resistance; L, inductance 0.0037 henries; TC, test contacts; PM, coil of the breaking mechanism; SR, selenium rectifier (bm = breaking mechanism).

which simulated the operation of contacts in a true assembly: the LZ-36 arc erosion installation and the LZ-42 spark erosion installation.

The electrical schematic of the arc erosion setup is shown in figure 1.

/295

Test contacts had a diameter 4-5 mm and a thickness of 0.8-1 mm; the pressure between the contacts was adjusted so that it was equal to 150 g-wt. The breaking frequency was 50 breaks per sec, the magnitude of the current in the closed circuit was 6 A and the test time was one hour. When the circuit was broken, an arc appeared at the contacts producing their erosion.

The electric circuit diagram of the setup for testing the stability of contacts to spark erosion is shown in figure 2. When the condenser  $C_2$  discharges, a spark escapes through the gap between the contacts (50 discharges per sec), and produces their erosion. The voltage across the contact gap is set equal to 3 kV and the test time is 2 hours.

The contacts were weighed before and after they were tested for stability to spark erosion, with an accuracy of 0.0001 g, because the variation in the weight of the contacts in percentage of their initial weight, is the basic characteristic of contact erosion stability.

In addition, when the contacts were tested for stability to arc erosion, their performance was evaluated by means of an oscillograph whose input was fed with the voltage from the contacts. The performance of the contacts was also evaluated from the value of transitional resistance between contacts before and after their operation.

The basic results of the investigation are shown in the table.

EROSION STABILITY OF ALLOYS

Contact Material	Arc erosion percent	Spark erosion percent	Transitional resistance (ohms)		Vickers hardness	Remarks
			Before operation	After operation		
Platinum + 10 percent iridium	13.4	4.7	0.10	0.10	188-197	Welding on some contacts
Platinum + 25 percent iridium	15.2	4.1	0.14	0.16	385-395	The same
Platinum + 25 percent iridium (mass-produced)	13.7	-	0.12	0.15	340-360	Weldings on the large part of the contacts
Platinum + 40 percent iridium	12.6	4.6	0.10	0.16	480-495	Welding on some contacts
Platinum + 60 percent iridium	9.1	3.4	0.16	0.20	430-445	No weldings
Palladium + 10 percent iridium	13.6	15.2	0.06	0.08	110-120	Weldings. Welding to the fullest extent is present in almost all of the contacts. The surface of the contacts is fused.
Palladium + 18 percent iridium	13.8	15.9	0.06	0.08	340-370	Weldings. Welding before the termination of the complete useful life.
Palladium + 20 percent iridium	14.6	15.8	0.06	0.08	380-430	The same
Palladium + 22 percent iridium	15.0	17.3	0.07	0.09	400-480	" "
Palladium + 30 percent iridium	15.6	14.1	0.07	0.09	510-530	" "
Palladium + 40 percent silver	24.0	15.0	0.01	0.01	165-178	Frequent weldings. Contact surface is fused and flattened.
Palladium + 80 percent silver	7.7	27.5	0.02	0.02	136-142	No weldings. Contact surface is fused and flattened.
Palladium + 35 percent silver + 5 percent cobalt	32.8	40.2	0.02	0.02	206-214	Weldings. Contact surface is fused and flattened.

Table (continued).

Argadur (78 percent silver + 20 percent copper + 2 percent nickel)	19.0	9.0	0.02	0.10	180	Frequent weldings. Contact surface is fused and flattened.
SOM-8	5.8	8.2	0.02	0.03	103-108	Weldings. Contact surface is insignificantly fused.
Palladium + 3 percent rhenium	14.2	14.4	0.15	0.17	152-160	No weldings. Contact surface is fused and flattened.
Palladium + 10 percent	17.2	12.9	0.15	0.17	229-236	The same
Palladium + 5 percent tungsten	8.1	-	0.05	0.05	225-232	No weldings.
Palladium + 10 percent tungsten	6.5	-	0.01	0.01	240-246	Weldings
Palladium + 15 percent tungsten	6.0	8.2	0.02	0.02	274-285	Weldings. Contact surface is fused and flattened.
Tungsten + 15 percent rhenium	5.2	1.4	0.20	3.5	502-566	No weldings. Uniform wear.
Tungsten + 16 percent rhenium	5.6	-	0.20	2.00	447-516	The same
Tungsten + 20 percent rhenium	4.6	-	0.20	2.00	480-530	" "
Tungsten + 20 percent rhenium (contacts were annealed at a temperature of 1800°C for a period of 30 min )	5.3	1.9	0.20	0.20	440-465	" "
Rhenium	30.2	7.7	0.05	0.06	362-386	" "
Tungsten	3.1	1.2	0.50		494-516	" "

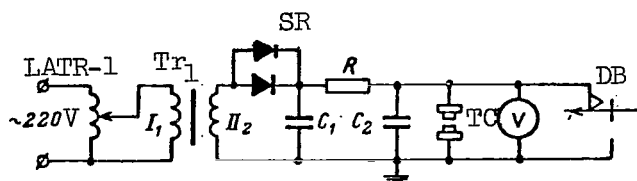


Figure 2. Schematic diagram of spark erosion setup. LATR-1, laboratory autotransformer; Tr, step-up transformer; SR, selenium rectifier; R, resistance of 18 kilo-ohms;  $C_1$ , capacitor of 1 mf;  $C_2$ , capacitor of 0.5 mfd; TC, test contact; DB, discharge button.

The alloys of the platinum-iridium system were tested for erosion stability as a function of iridium content, type of heat treatment, and in the case of the PLI-25 alloy also as a function of the cold-working of the material (20, 40, 50 and 80 percent deformation). Alloys of the platinum-iridium system pertain to dispersion-hardening alloys; therefore, various stages of heat treatment were conducted for these. /298

The first stage was dispersion-hardening at a temperature of 750°C during a period of two hours.

The second stage was dispersion-hardening at a temperature of 750°C with subsequent quenching at a temperature of 1100°C.

The third stage was dispersion-hardening at a temperature of 750°C, quenching at 1100°C and another dispersion-hardening at 750°C for two hours.

Under production conditions, the contacts were welded to contact holders at a temperature of 1100°C, i.e., at a temperature higher than the temperature of dispersion-hardening of these alloys. To clarify the effect of this technological operation on electrical wear of contacts, a second stage of heat treatment was carried out. The third stage was designed to increase the hardness of the contacts which had been welded to the contact holders.

The results of the test to determine hardness during different stages of heat treatment are shown in figure 3. It follows from the curves that of all investigated platinum-iridium alloys, only the alloy with 40 percent iridium has maximum hardness.

The dispersion-hardening of cold-worked samples of alloys increases the hardness by 40-60 units of the Vickers scale; quenching at 1100°C produces a recrystallization of the alloy and a substantial decrease in hardness; repeated dispersion-hardening increases the hardness insignificantly.

The erosion of the cathode during arc testing for alloys PII-10, PII-25 and PII-40 with various stages of heat treatment has a substantial value equal, on the average, to 12-15 percent of the contact weight. The PII-60 alloy has a smaller value of cathode erosion, equal approximately to 9 percent of the contact weight.

The erosion of all four platinum-iridium alloys during spark testing /299 is approximately the same and is 3-5 percent of the contact weight.

The welding of the contacts was observed most of all for the PII-25 alloy, regardless of the nature of heat treatment and of the degree of cold-working. For cold-worked contacts, from PII-10 and PII-40 alloys, weldings were observed during testing; after heat treatment, the contacts operated without weldings. Contacts from the PII-60 alloys did not weld at all during the entire test cycle. After the testing, the surfaces of all alloys had craters on the cathode and a protuberance on the anode, i.e., the transport of material was nonuniform over the surface of the contact.

The transitional resistances for all platinum-iridium alloys have a small value which varies little during operation.

Six groups of mass-produced contacts made from the PII-25 alloy showed a wide spread in erosion during the testing and substantial weldability.

The system of palladium-iridium alloys of types PDI-10, PDI-18, PDI-20, PDI-22 and PDI-30 was investigated for stability to arc and spark erosion /300 as a function of dispersion-hardening time (10-300 hours at a temperature of 700°C). In spite of a substantial increase in hardness due to dispersion hardening (fig. 4), all alloys of this system turned out to be completely unsuitable as contacts for the specified operating conditions. During tests for stability against arc erosion, only an insignificant part of the contacts operated for the entire required operating time (one hour). A large part of the contacts became welded substantially before the end of the operation cycle.

The magnitude of erosion of the contacts, which operated for the required period of time, is 12-15 percent of the contact weight. The erosion stability of palladium-iridium alloys during the spark test is also very poor: the surfaces of the contacts are fused and flattened out. The transitional resistances are small (0.05-0.20 ohm) and vary little during operation.

The alloys of palladium with silver (PSD-40 and PDS-80) with rhenium (PDR-3 and PDR-10) and tungsten (PDV-5, PDV-10 and PDV-15) and also silver alloys of the Argadur type and the SOM type also turned out to be unsuitable for operation under the test conditions.

Alloys of palladium with rhenium worked better than other alloys, and did not produce welds during the test process, but their erosion was substantial (17 percent of the contact weight). The transitional resistances of the /301 alloys of the group are small in value and remain almost unchanged during the test.

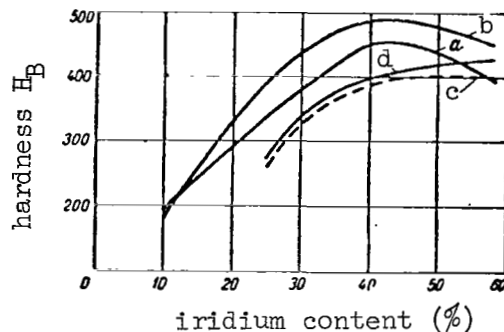


Figure 3. Variation in hardness of platinum-iridium alloys as function of iridium content and heat treatment. a, in the initial state; b, after dispersion-hardening at 750°C for two hours; c, after dispersion-hardening at 750°C for two hours and quenching at 1100°C; d, after dispersion-hardening at 750°C for two hours, quenching at 1100°C and repeated dispersion-hardening at 750°C for two hours.

Good results were obtained with alloys VR-16 and VR-20 of tungsten with rhenium. These alloys, which represent a homogeneous solid solution of two high melting metals, are produced by the powder metallurgy method. The addition of rhenium to tungsten substantially increases the corrosion properties of the alloy compared with tungsten. Tests were made with alloys of tungsten with rhenium which had been processed in different ways; alloys which are not subjected to annealing have a fine grain structure, alloys subjected to high temperature annealing (1500-2000°C) have a structure with larger grains.

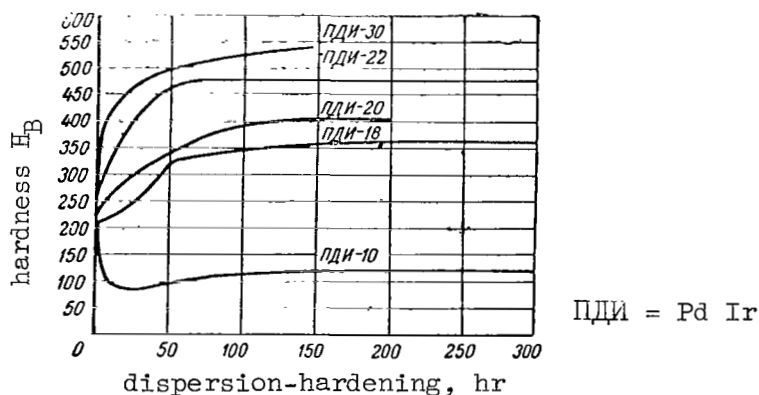


Figure 4. Variation in hardness of palladium-iridium alloys as function of dispersion-hardening time and temperature of 700°C.

All of the tested groups of tungsten and rhenium alloys showed high erosion stability when tested for arcing and sparking. Their erosion has an entirely different nature than that of alloys with a precious metal base. When the platinum and palladium alloys were tested for stability to arc erosion, the losses were carried by the cathode (the cathode material is transported to the anode), while few contacts made of tungsten and rhenium alloy show a weight loss both in the anode and the cathode, and the anode loses more material than the cathode. This is explained by the oxidation of the alloy at the high temperatures which take place when the arc burns.

The anode losses during the testing of the contacts for arcing are 4-6 percent of the initial contact weight and, a factor of particular importance, the wear over the entire surface of the contact is uniform.

When the contacts from the tungsten and rhenium alloy were tested for arc stability, there was not a single case of contact welding. Their spark erosion stability also turned out to be better than that of the platinum-iridium contacts. A substantial disadvantage of the VR type alloys is the considerable increase in the transitional resistance after testing.

It was established in the course of investigation that the contacts annealed at a temperature of 1800°C for a period of 30 min provide for the stability of transitional resistance during testing.

Tests undertaken to compare pure rhenium and pure tungsten showed that the transitional resistance of pure rhenium after operation remains completely unchanged, while tungsten loses its conductivity completely, but the erosion stability of tungsten (cathode losses of 3.1 with respect to the contact weight) is substantially higher than the stability of rhenium (30 percent losses) both for arc and spark erosion test. /302  
/303

Figures 5 and 6 show contacts made of the PII-25 alloy which are used at the present time and contacts from PII-60 and VR-20 alloys, which produce better results in stability tests for arc and spark erosion. /304

On the basis of our investigations we make the following conclusions:

1. Of the four investigated alloys of the platinum-iridium system, the best contact properties--erosion stability, total absence of welding and uniform wear--were exhibited by the PII-60 alloy.
2. The mass-produced contacts made from the PII-25 alloy undergo substantial erosion and have many welds during the test process.
3. All of the palladium alloys exhibited poor erosion stability, even though the hardness was increased by a factor of 2-2.5 after dispersion-hardening.
4. The alloy of tungsten with 20 percent rhenium (VR-20) exhibited substantially better contact properties than the alloy of platinum with 25 percent



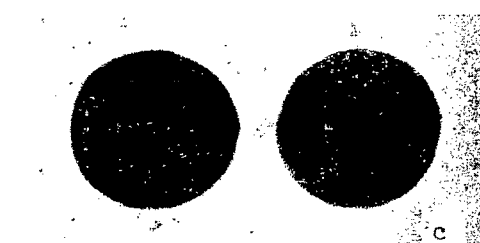
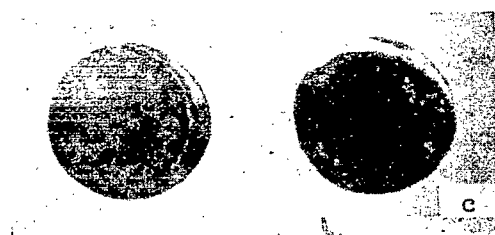
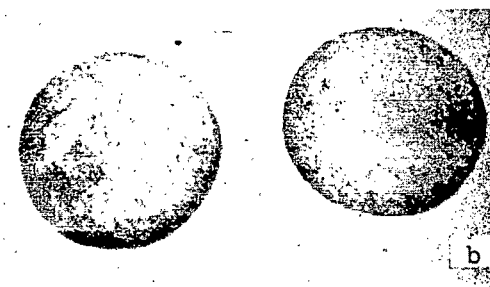
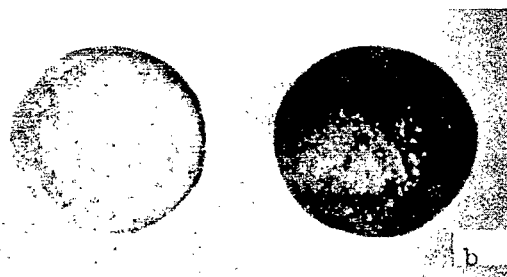
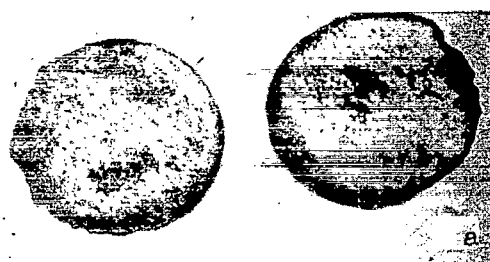
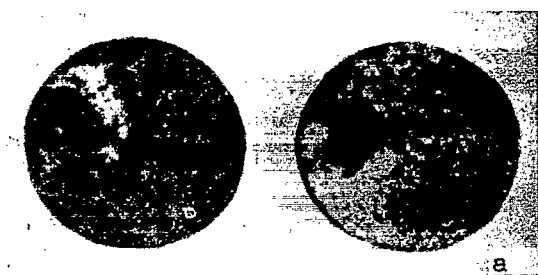


Figure 5. External view of contacts after testing for erosion stability in arc. a, PII-25 alloy; b, PII-60 alloy; c, VR-20 alloy.

Figure 6. External appearance of contacts after erosion stability tests using spark. a, PII-25 alloy; b, PII-60 alloy; c, VR-20 alloy.

iridium. The VR-20 alloy has high stability with respect to arc and spark erosion, produces no welds during operation and has uniform wear over the entire surface of the contacts.

The PII-60 and VR-20 alloys, which have better contact properties, are recommended for further tests in ignition systems.

#### REFERENCE

1. Usov, V. V. and Zamoyskiy, V. S., Conductor, Rheostat and Contact Materials (Provodnikovyye, reostatnyye i kontaktnyye materialy). Gosenergoizdat, 1957.

## THE POSSIBILITY OF USING CERMETS TO REPLACE TUNGSTEN

G. A. Bugayev

Relays of the REV 300 series are used in the control of electric drives primarily for the vibration control of electric drive current in the transient states. /304

Since vibratory relays have a high operating frequency (up to 8 cycles per sec), their contacts are made of tungsten to provide for the necessary resistance to wear.

In the intervals between the periods of the vibratory state of operation, tungsten contacts, which remain for a more or less extended period of time in an open state are covered with an oxide film which lowers the reliability of contacting. Since the intensity of oxidization increases sharply with humidity, this phenomenon is particularly dangerous for relays operating in tropical climates and at locations with high humidity. After relays designed for tropical use were tested for stability to humidity, cases were observed when the oxide film was not punctured during the first switching of the relay, even when the voltage was several tens of volts. /305

In view of this, work was carried out at ChETNII to study the possibility of replacing tungsten with some other material which is more resistant to corrosion and which, at the same time, has sufficient resistance to wear and other characteristics necessary for contacts.

The REV 300 contact system of the finger type has a single break; the gap between the contacts may be decreased to 1.5 mm by adjusting the relay. The relay must provide for the switching of dc current of 0.6 A at 110 V and 0.3 A at 220 V when the load is inductive.

The Institute of Powder Metallurgy of the Academy of Sciences of the Ukrainian SSR recommended the AVS-50 and ANS-70 compositions for testing under the specified operating conditions. Samples of contacts made from these compositions were compared with the tungsten contacts.

The following contact parameters were checked during the tests:<sup>1</sup>

---

<sup>1</sup>Tests were conducted by N. I. Donskoy.

- (1) switching capability;
- (2) resistance to electric wear;
- (3) reliability of contacting.

### Switching Capability

The maximum switching capacity was determined with a contact gap of 1.5 mm in a dc circuit with an inductive load consisting of the KP503 contactor coil with an engaged armature.

The values of the maximum currents which were switched off are shown /306 in table 1 where, for comparison purposes, the same quantities are given for silver and for the OK-15 cermet. As we can see from the table, the application of the AVS-50 and ANS-70 compositions instead of tungsten substantially lowers the switching capacity of the relay, particularly at 220 V when it is decreased by more than a factor of 2. This means that the relay cannot satisfy the specifications.

Table 1

Contact material	Maximum switched-off current, A	
	110 V	220 V
Tungsten	1.6	0.96
AVS-50	1.12	0.32(0.4)
ANS-70	1.12	0.32
OK-15	1.28	0.32
Silver	0.96	-

### Resistance to Electric Wear

Tests for resistance to electric wear were carried out at 220 V and 0.16 A (KR503 contactor coil); the contact gap was 1.5 mm. The values of the contact weight loss are shown in the drawing and were used to prepare table 2. The table also contains data on the testing of OK-15 contacts under the same operating conditions.

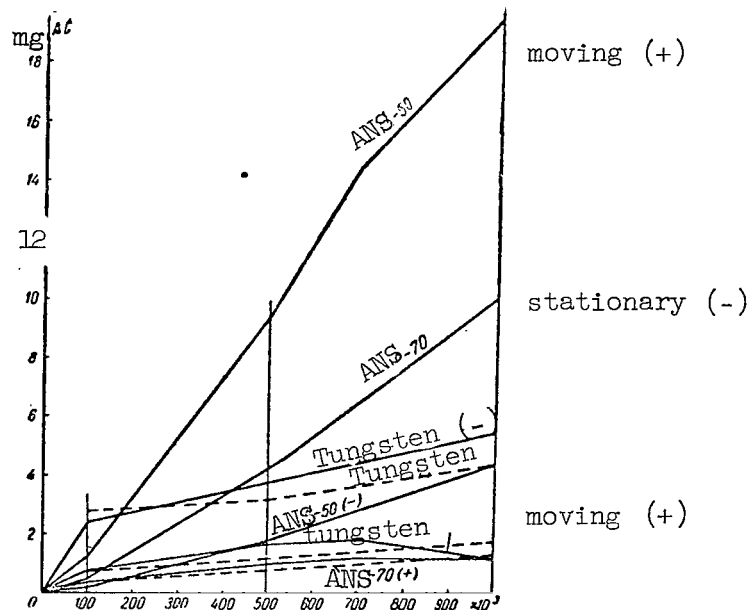
/307

From these data it follows that the maximum wear is approximately 5.5 for AVS-50, while for ANS-70 it is 3 times greater than for tungsten and has the same order of magnitude as OK-15. From the absolute value of the wear, all of the tested materials may be considered satisfactory because they provide for the required relay life of 10 million cycles (the contact weight is 0.4-0.6 g).

TABLE 2

Contact material	Weight loss during 1 million cycles,* in mg	
	Anode	Cathode
Tungsten	-0.6	3.4
AVS-50	19.2	4.4
ANS-70	-0.2	10
OK-15	1.8	14.8

\*The data in the table are obtained by rectifying the corresponding wear graphs and extrapolating them to the axis of the ordinates to eliminate the effect of the wear-in period. The values of the anode wear are corrected, taking into account the mechanical wear (1.2 mg) of the associated rear contact which did not switch the current. The minus sign is used to indicate that the contact weight has increased. For the OK-15 contacts, this processing of the data was not carried out.



Decrease in contact weight during electric wear. Broken line shows characteristics for stationary contacts which do not switch current.

### Reliability of Contacting

The contacting reliability was evaluated from the value of the transitional resistance and its stability under the action of high humidity, electric erosion and variation in contact pressure within operating limits for the relay. /308

The relay was held in the hygrostat for a period of 2 24-hour cycles (6 hours at + 40°C and 18 hours of cooling) with a relative humidity of  $95 \pm 3$  percent.

The effect of erosion was taken into account by measurements before and after the tests for electric wear resistance.

The measurement of the transitional resistance for different contact pressures has made it possible to determine the reliability of contacting, not only from the absolute value of the transitional resistance, but also from the degree of its dependence on contact pressure.

The values of the transitional resistance (in ohms) are shown in table 3. As we can see, in the initial state the contacts made from the AVS-50 and ANS-70 compositions provide for reliable contacting (including contacting in the humid medium) to the same extent as silver contacts, i.e., much better contacting than in the case of tungsten contacts. However, due to electric erosion which takes place during the operation of the contacts, the surface layer of cermet contacts apparently lose silver and the contacts, which become covered with the products of erosion, increase their transitional resistance radically and lower contacting reliability; this pertains primarily to the AVS-50 composition contacts whose contacting reliability after one million cycles was as low as the reliability of tungsten contacts. Erosion does not produce as 309 severe an effect on the contacts made from the ANS-70 composition; their reliability after one million cycles remains at a higher level than that of the tungsten contacts in the initial state.

This statement is particularly well illustrated by the results of tests in the hygrostat following the wear tests. The effect of humidity on eroded contacts made of tungsten and of AVS-50 produces an intense growth of the oxide film, which leads to almost complete loss of contacting reliability (the dielectric strength of the film is of the order of tens of volts); such a growth in the oxide film is not observed in the ANS-70 contacts, and the transitional resistance after the hygrostat even drops sharply, apparently due to the mechanical weakness of the products of erosion.

## Conclusions

The following conclusions can be made from the results of the work.

(1) Since the properties of the surface layer of cermets undergoes a substantial change during the operation of the breaking contacts, a comparison of cermet contacts in terms of their parameters in the initial state is an insufficient basis for evaluating their operating properties, particularly such properties as contacting reliability and transitional resistance. These 310 properties must be checked on contacts which are subjected to erosion during operation and also to humidity.

TABLE 3

Condition of the contacts						
Material	Before testing for electric wear					
	Before hygrostat (protected)			After hygrostat		
Pressure in g/wt	50	100	150	50	100	150
Tungsten	0.9	0.5	0.16	4	1.6	0.23
AVS-50	$3.3 \cdot 10^{-3}$	$2.73 \cdot 10^{-3}$	$2.35 \cdot 10^{-3}$	$3.2 \cdot 10^{-3}$	$2.5 \cdot 10^{-3}$	$2.3 \cdot 10^{-3}$
ANS-70	$3.5 \cdot 10^{-3}$	$2 \cdot 10^{-3}$	$2.7 \cdot 10^{-3}$	$6 \cdot 10^{-3}$	$4.3 \cdot 10^{-3}$	$2.7 \cdot 10^{-3}$
OK-15	--	$2.8 \cdot 10^{-3}$	--	--	$16.4 \cdot 10^{-3}$	--
Silver	--	$3.7 \cdot 10^{-3}$	--	--	$3 \cdot 10^{-3}$	--

Condition of the contacts						
Material	After testing for electric wear					
	Before hygrostat (unprotected)			After hygrostat		
Pressure in g/wt	50	100	150	50	100	150
Tungsten	5.7-21	2.4-15	4-7.9	$U_{op} = 50-100$ V		
AVS-50	3.3-15	0.53-1.3	0.3-1.4	$U_{op} = 10-20$ V		
ANS-70	0.24-0.47	0.12-0.15	0.05-0.07	$20 \cdot 10^{-3}$	$11 \cdot 10^{-3}$	$4.4 \cdot 10^{-3}$
OK-15	--	--	--	--	--	--
Silver	--	--	--	--	--	--

op = operating limits

(2) The AVS-50 composition is characterized by a sharp increase in transitional resistance during current switching operation and by a decrease in the reliability of contacting to the tungsten level; at the same time its electric wear resistance is substantially lower. The application of AVS-50 in place of tungsten also has a negative effect on the switching capability. Based on the results of the present work, the application of the AVS-50 composition to breaking contacts is not desirable.

(3) The ANS-70 composition is also subject to an increase in the transitional resistance during switching; however, under the test conditions, this increase was not substantial enough for us to conclude that the decrease in contacting reliability is inadmissible. Furthermore, the action of humidity did not produce a noticeable negative effect on contacting reliability.

Judging from the data published in the literature, the silver-nickel composition provides for wear-resistance which is several times greater than that of silver. This is confirmed indirectly by the data of the present work. Therefore this composition should be used.

(4) The special feature of tungsten is that it provides for a large number of switching cycles with currents from several tenths to one ampere, as a rule with small contact gaps. Based on the data of the present work, we can conclude that for voltages of the order of 6-12 V the replacement of tungsten by the ANS-70 composition should not substantially decrease the switching properties of the contacts in cases when a three-fold decrease in wear resistance is permissible. The replacement of tungsten with this composition may be expedient, because this will make it possible substantially to increase the contacting reliability, even with a simultaneous decrease in contact pressure.

However, at 110 V and particularly at 220 V, the switching capability is lowered substantially, which further limits the feasibility of replacing tungsten.

(5) The drop in the switching capability of the REV 300 relay /311 considered in the present work is the principal obstacle to the replacement of tungsten by the ANS-70 composition.

Judging from the fact that both AVS-50 and OK-15 give a switching capability of the same order as ANS-70, we may assume definitely that none of the known compositions containing silver can provide a commutation capability under the given conditions which is close to the commutation capability of tungsten contacts. For this reason, the replacement of tungsten with cermets does not appear feasible for the REV 300 relay.

In order to carry out a further search for methods of increasing the contacting reliability of this relay, the possibility of using an alloy of tungsten with rhenium or pure rhenium should be verified; judging from the data contained in the literature, these materials can provide a positive solution to this problem.

## SPECIAL FEATURES OF SWITCHING LOW LEVEL CURRENTS AND VOLTAGES BY MEANS OF CONTACTS

T. K. Shtremberg and D. V. Gayevskaya

Among the huge diversity of electric circuits which are switched by contacts, there are those in which the contacts themselves do not switch the current, but only prepare the circuit for switching by other contacts.

In electronic equipment, electric contacts frequently switch low level currents and voltages: from tens of microamperes and millivolts to hundredths of a microampere and several microvolts.

Such circuits and contacts which operate without currents or at low voltages and currents are called "dry" circuits and "dry" contacts. It is known that the switching conditions of "dry" circuits are very unfavorable for contacts.

Indeed, due to the chemical interaction of the contact metal with gases and vapors of the surrounding medium, films of chemical compounds form on contact surfaces--oxides, sulfides, hydrides, carbides, chlorides, etc. Also, the contact surfaces may become covered with organic deposits or with dust of various composition. These films and deposits may be conductive or may have insulating or semiconductor properties and may stop the flow of current in the circuit or distort the magnitude and form of the current curve. During the operation of the contacts, the insulation strength of the coatings (films or deposits), which depends both on the chemical composition and on their thickness, may be disrupted mechanically or electrically, and then the conductivity of the contacts is again reestablished. /312

To destroy films and deposits mechanically, it is necessary to have a sufficient static contact pressure, such as produced by the wearing-in or by the impact force of contacts against each other during their making.

The electric destruction of films and deposits is produced by their electric breakdown if the voltage supplied to the contacts when they are open is greater than the breakdown voltage of the films. The breakdown voltage of some films and deposits of precious metals and their alloys may reach a value of tens of volts or higher.

However, if the value of the current switched by the contacts is sufficient to produce their erosion, the resulting high temperatures at the contact points



may break down the chemical compounds of metals, for example, oxides, while the films and deposits of organic nature may burn up. Thus, the switching of heavy currents cleans the contacts from insulating coatings and reestablishes their conductivity.

It is quite obvious that the probability of destroying films and deposits on contacts which switch "dry" circuits is substantially lower and, consequently, the probability of failure is higher than in contacts which switch normal loads. Therefore, the contacts of "dry" circuits should use materials with a /313 minimum chemical activity and a sufficiently low sensitivity to the vapors of organic compounds.

The present work considers the results of an investigation of relay contacts which switch a non-reactive circuit of 5  $\mu$ A and 50 mV at a switching rate of 5 pulses/sec. In such a circuit, the contact potential difference and the thermo-emf, as a rule, do not exceed a fraction of 1 mV, and consequently are not significant from the standpoint of switching reliability.

In the course of the tests, the loss of contacting was recorded by means of a special device with a counter which made it possible to establish the total number of complete and "partial" disruptions in contacting.

The term "partial" disruption is used here for one of the following phenomena:

- (a) the switched circuit is not closed immediately, but with some delay with respect to the time of physical contact;
- (b) the circuit is not open completely, but there is an increase in the transitional resistance of the contact circuit above some limit which lowers the switched current by 20-40 percent.

We note that for contacts which switch low level currents and voltages, in most cases intermittent disruptions (complete or partial) which eliminate themselves after several switchings, are common.

The method of recording complete or partial disruptions of contacting is based on the following considerations:

1. It is assumed that the probability of a simultaneous disruption of the electric contact in a breaking and making pair of the same contact group is so small that it can be neglected.
2. To obtain high accuracies, and also to provide for a minimum wear of the recorder, the failures must be recorded by the latter directly, and not as the difference between the total number of commutations and the number of reliable connections.
3. The attachment of a device to the switching contacts for recording breakdowns does not change the parameters of the circuit and does not /314 introduce additional inductance or capacity.

Figure 1 shows the scheme for recording the disruption of contacting. The principle of operation of this system is as follows: when the contact group is operating normally, the current in the circuit which it switches ceases only during the time when the moving contact flies between the stationary contacts. This time is small compared with the time of the closed state of the contacts. Consequently, the pulses are fed to the amplifier with very short breaks (fig. 2a), so that the meter connected to the output of the amplifier does not have enough time to react to them.

If the interval between the current pulses at the input is increased in time due to the total (fig. 2b) or partial (fig. 2c), stoppage of current in one of the two contact pairs, or if the amplitude of one of the pulses decreases to some preset value due to an excessive increase in the transitional resistance of the corresponding contact pair (fig. 2d), the meter records this event.

The failures were registered by means of two SB-IM/100 meters connected in series. By connecting nonreactive resistances  $r_w$  in parallel to the windings of the meters, the time parameters of the latter were controlled, so that one of them reacted well to breaks whose duration was 40-50 msec and higher, while the second reacted to breaks with a duration of 60-80 msec and higher.

The reliability of the setup was checked periodically by means of 315 key K and, if necessary, a readjustment was made by increasing the plate voltage of the amplifier. The switching of the key K lever into one of the extreme positions made it possible to produce an artificial stoppage of current in the circuit of breaking or making contact pairs. The accuracy of the count was achieved because each pulse fed to the winding of the test relay was registered by both meters.

Amplifier A is a special three-stage dc pulse amplifier with stabilized plate voltage. Resistances  $r_1$  and  $r_2$  are used to maintain a voltage of 50 mV and a current of 5  $\mu$ A in the contact circuit. To control the current in the contact circuit, a microammeter is connected in series.

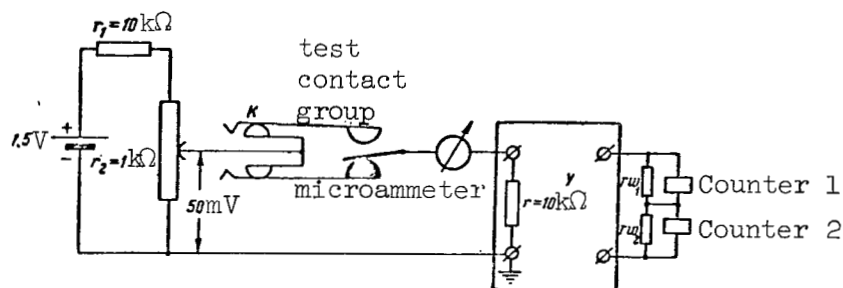


Figure 1. Schematic diagram for recording contact breakdown.

The following contacts made from the PII-10 alloy were tested at 5  $\mu$ A and 50 mV, taking into account intermittent breakdowns: RES-8 type relays filled with nitrogen (48 contact groups), RES-9 type relays (20 contact groups), RES-10 type relays encapsulated with epoxy (20 contact groups) and rolled-/316 in (24 contact groups), and RES-15 type relays (60 contact groups). In addition to this, the RES-6 relay was tested with non-standard contacts made of pure platinum (12 contact groups). Up to  $2 \cdot 10^5$  commutations were carried out.

The results of the test are shown in figures 3, 4, 5 and 6. In these figures and in subsequent ones, the following designations are used:

- N -- is the number of commutations performed by the relay;
- n -- is the number of contact disruptions (intermittent breakdowns);
- m -- the number of contact groups which showed intermittent breakdowns;
- M -- the total number of tested contact groups.

The graph in figure 3 shows the increase in the number of breakdowns, n, with the increase in the number of commutations. These graphs are useful for approximate evaluation of the contact reliability of different types of relays. For example, the curve pertaining to RES-10 with epoxy shows that with  $10^7$  commutations, only 10 percent of the contact groups performed without failure and only 19 percent produced less than 10 breakdowns, the remaining 81 percent showed 10 or more breakdowns.

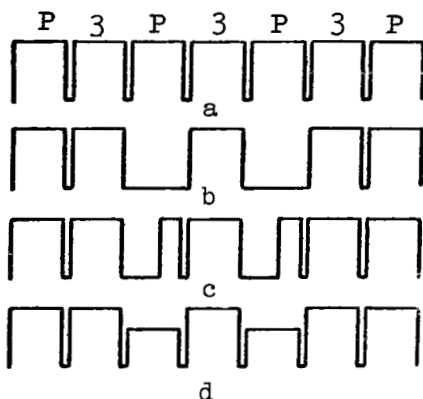
Under the same conditions, 67 percent of the contact groups of /317 relay RES-6 operated without failure, while 92 percent of the contact groups operated with less than 10 failures, i.e., only 8 percent (one contact group of 12) produced more than 10 breakdowns.

For illustration, the ordinates of the curves in figure 3 for  $N = 10^5$  are shown in the form of columns in figure 4. The relative number of contact groups which operated without failure corresponds to the height of the shaded column while the total height of the column shows operation with less than 10 breakdowns.

The slopes of the curves in figure 3 may also be used to characterize the rate of increase in contact groups which produce breakdowns or the intensity of breakdown occurrence,  $\lambda$ . Table 1 shows the approximate values of the latter within the limits of  $10^4$  commutations. They are shown for one commutation for a single contact group.

From figure 4 and table 1 we can see that the reliability of switching small currents and voltage depends to a substantial degree on the construction of the relay. The RES-6 relay is the most reliable one, while the RES-10 relay with epoxy is least reliable. The remaining types of relays are distributed in order of their numbers in table 1.

The characteristics shown in figures 3 and 4 show only the number of contact groups which operated without failure or with less than 10 breakdowns, and give no information concerning the total number of breakdowns which can occur in one contact group within the limits of the given number of commutations. Therefore, figure 5 shows curves for the relative number of contact



Operation of contacts without failure.

Total stoppage of current in breaking contacts during process of two commutations.

Partial (in time) stoppage of current in breaking contacts during process of two commutations (closing of circuit with delay).

Decrease of current in breaking contacts during process of two commutations due to excessive increase in transitional resistance of contacts.

Figure 2. Current oscillograms at relay contacts.

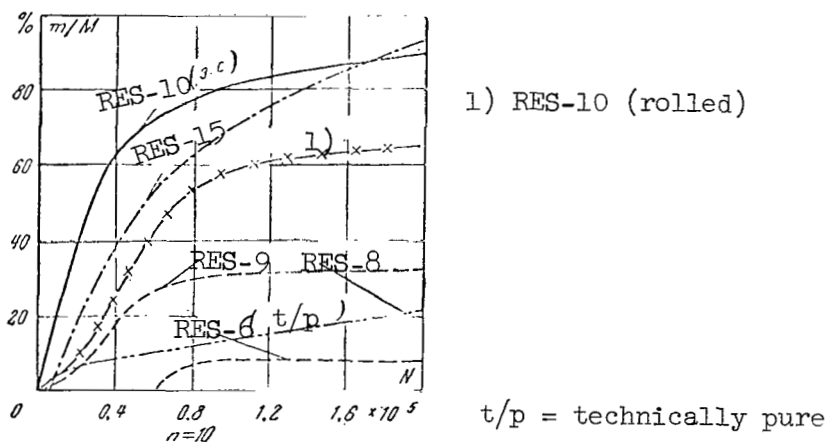
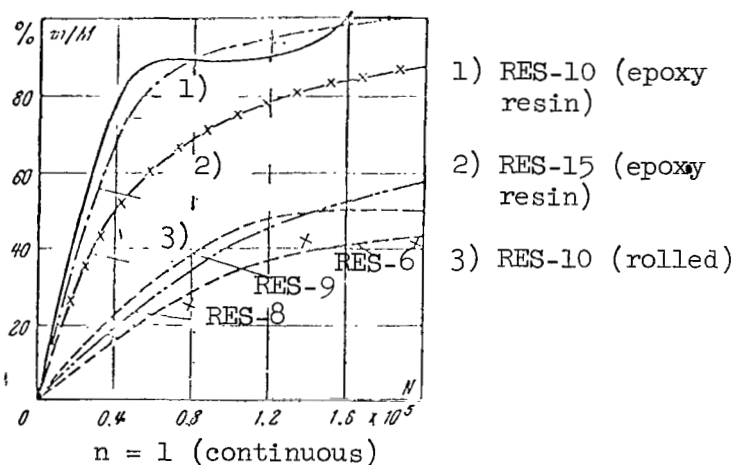


Figure 3. Distribution of number of commutations until nth breakdown.

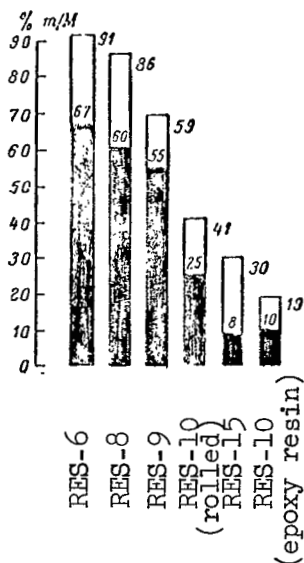


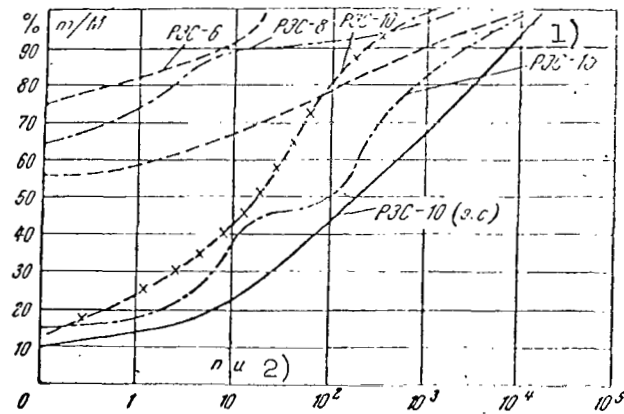
Figure 4. Diagram showing operation of contacts of various types of relays made from PlI-10 alloy when switching circuit of  $5 \mu\text{A}$  and  $50 \text{ mV}$  within limits of  $10^5$  commutations.

groups which produced  $n$  or less breakdowns within the limits of  $10^5$  and  $2 \cdot 10^5$  commutations. For example, the curve corresponding to relay RES-10 with epoxy (fig. 5a) shows that 100 and more breakdowns were produced by 43 tested 318 contact groups and over 200 breakdowns were produced by 50 percent of the groups. Under the same conditions an RES-6 relay exhibited not more than one breakdown in 82 percent of the contact groups and more than 10 breakdowns in only 8 percent of the contact groups. For the RES-6 relay, not a single contact group exhibited more than 20 breakdowns.

We can see from figure 5 that the arrangement of relay types according to the number of failures is the same as according to the reliability characteristics. We note that in all types except RES-6 there is a rather large spread in the quantity of breakdowns for some contact groups compared with others. Indeed, RES-8 and rolled-in RES-10 have from 0 to several thousand breakdowns, while RES-9, RES-15 and RES-10 with epoxy have more than  $10^4$  breakdowns.

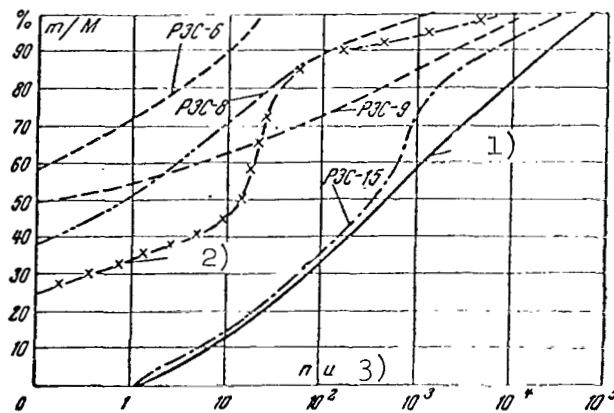
TABLE 1.

Relay type	$\lambda$ within the limits of $10^4$ commutations.
	$10^{-6}$ ————— 1 commutations. contact groups
RES- 6	3.8-3.9
RES- 8	4.8-5
RES- 9	6.5-7
RES-10	15-18
Rolled-in RES-15	18-22
RES-10 with epoxy	23-30



- 1) RES-9  
(rolled)  
2) lower breakdown

At  $N = 2 \cdot 10^5$  commutation limits



- 1) RES-10  
epoxy resin  
2) RES-10  
(rolled)  
PJC = RES  
3) lower breakdown

At  $N = 2 \cdot 10^5$  commutation limits

Figure 5. Distribution of breakdowns.

The curves in figure 6 show the increase in the average number of breakdowns when the number of commutations is increased. In most relay types, this relation is nonlinear. For the RES-10 and the RES-15 relays, they approach straight lines over a substantial region when plotted to the logarithmic scale, i.e., they follow the exponential law

$$\bar{n} = aN^{\alpha},$$

where  $\alpha = 2-3$ .

The rate of increase in the number of breakdowns can also be shown by the numerical ratio of the average number of breakdowns to the number of /319 commutations (table 2), which represents the average percentage of unperformed commutations.

From the table we can see that up to  $N = 10^5$ ,  $n_{av}/N$  percent increases for all relay types except RES-6. This shows that the breakdowns are not random, but are subject to causality. The number of breakdowns is directly related to the number of commutations.

From figure 6 and table 2 we see that the distribution of the /320 relays, according to the value of  $n_{av}/N$  percent, is the same order as in curves 3-5 in table 1, i.e., the most favorable values correspond to RES-6 and the least favorable to RES-10 with epoxy.

In order to increase switching reliability for low currents and voltages, similar tests were conducted on RES-9 and RES-10 relay types with contacts from 21 different precious metals and alloys. Relay RES-6 was fabricated with 12 contact materials, while relay RES-8 used contacts of gold and silver of industrial purity.

The results of all tests are presented in the form of graphs, similar to those shown in figures 4-6. We shall consider the results of these tests (figs. 7, 8, 9 and 10) as they apply only to the RES 10 relay with epoxy, since this relay was the most unreliable one of all those considered.

Among the 21 new contact materials the following were tested:

- (1) technically pure platinum and its alloys with rhodium (PlRd-10), osmium (PlOs-7) and ruthenium (PlRut-5);
- (2) technically pure rhodium and iridium;
- (3) technically pure palladium and its alloys with platinum (PdPl-50), rhodium (PdRd-10), iridium (PdIr-10), Osmium (PdOs-10), ruthenium (PdRut-5), silver (PdSr-30) and copper (PdM-40);
- (4) 999-th test silver; /321

TABLE 2.

Relay type	Ratio of average number break-downs to number of commutations $n_{av}/N$ percent					
	$N=2 \cdot 10^4$	$N=4 \cdot 10^4$	$N=6 \cdot 10^4$	$N=8 \cdot 10^4$	$N=10^5$	$N=2 \cdot 10^5$
RES-6	0	0.003	0.004	0.003	0.003	0.0015
RES-8	—	0.06	0.06	0.07	0.09	0.15
RES-10	0.01	0.06	0.09	0.10	0.095	0.06
Rolled in RES-15	0.08	0.20	0.4	0.6	0.9	1.3
RES-10 with epoxy encapsulation	0.60	1.10	1.8	2.3	2.7	3.8

(5) technically pure gold and its alloys with platinum (ZlPl-7), palladium (ZlPd-16), silver (ZlSr-40), nickel (ZlN-5) and zirconium (ZlTsr-3).

From figures 7 and 8 we can see that platinum, rhodium, iridium and their alloys with each other and with other metals of the platinum group--osmium and ruthenium--produced results which are close to those obtained for the PlI-10 alloy considered before. There are certain advantages in palladium and its alloys which are well illustrated in figure 8.

Within the limits of  $10^5$  and  $2 \cdot 10^5$  commutations, the columns corresponding to silver, gold and its alloys stand out. The best results correspond to technically pure gold. Of its alloys, the most reliable one is the alloy with nickel.

The upper left part of figure 9 shows curves which correspond to technically pure gold and to the ZlN-5 alloy. Slightly below this, we have other alloys of gold and silver. The area to the right and below is occupied by platinum, iridium, rhodium and platinum alloys.

In figure 10 the axis of the ordinates of the left graph starts with a value 2 orders of magnitude greater than that of the right graph. The left graph contains platinum and all of its five alloys, rhodium, iridium and several palladium alloys. The right graph contains the gold group and its alloys, silver and some alloys of palladium. /326

As in the case of the PlI-10 curves, the curves corresponding to the metals and alloys of the platinum group follow the exponential law approximately with  $\alpha = 2-3$  (with the exception of PdM-40). The curve corresponding to gold stands out in the right graphs; it is practically parallel to the axis of the ordinates. This means that the reason for the occurrence of break-downs in gold contacts has a different origin from the one for contacts manufactured from the materials of the platinum group. We should point out that in all relay types, contacts made of gold gave the best results and the break-downs in these as a rule are isolated, apparently being produced by the presence of the products of wear of the armature at the contact points or by the



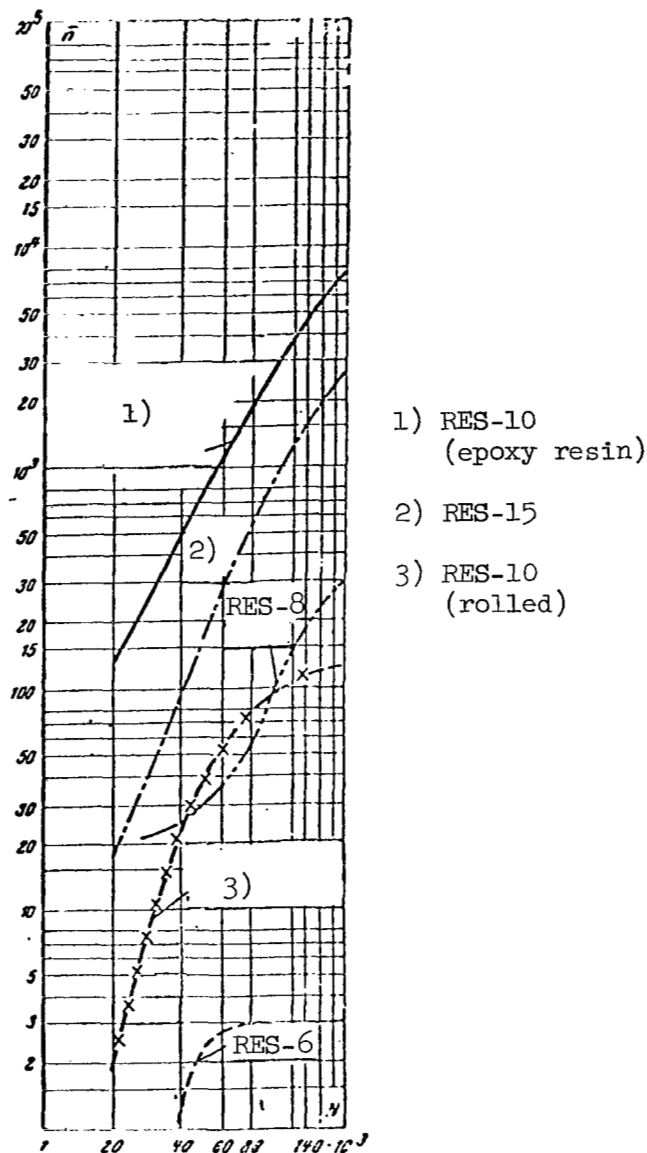
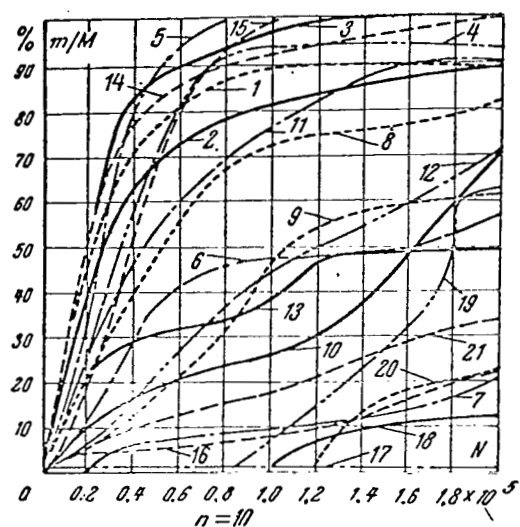
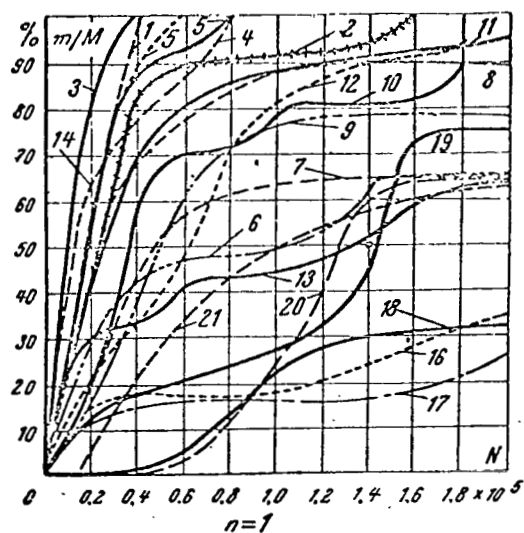


Figure 6. Average number of breakdowns  $\bar{n}$  for each contact group as function of number of switching cycles.

presence of foreign particles from the space surrounding the contacts. Thus, of the 36 contact groups of the RES-8 relay only one group exhibited one series of 31 breakdowns, which can be explained only by accidental contamination.



No.	Material	M
1	Pl t/p*	15
2	PI-10	20
3	PlR-10	18
4	PlOs-7	15
5	PlRut-5	18
6	PlPd-50	17
7	Pd t/p	18
8	PdI-10	18
9	PdR-10	13
10	PdOs-10	10
11	PdRut-5	20
12	PdS-30	18
13	PdM-40	19
14	Ir t/p	9
15	Rd t/p	11
16	Sr-999	30
17	Zl t/p	19
18	ZlN-5	15
19	ZlPl-7	13
20	ZlTsr-3	8
21	ZlRd-16	21

Figure 7. Distribution of number of commutations until n-th breakdown for RES-10 relay with epoxy under normal climatic conditions.

\*t/p = technically pure

/322

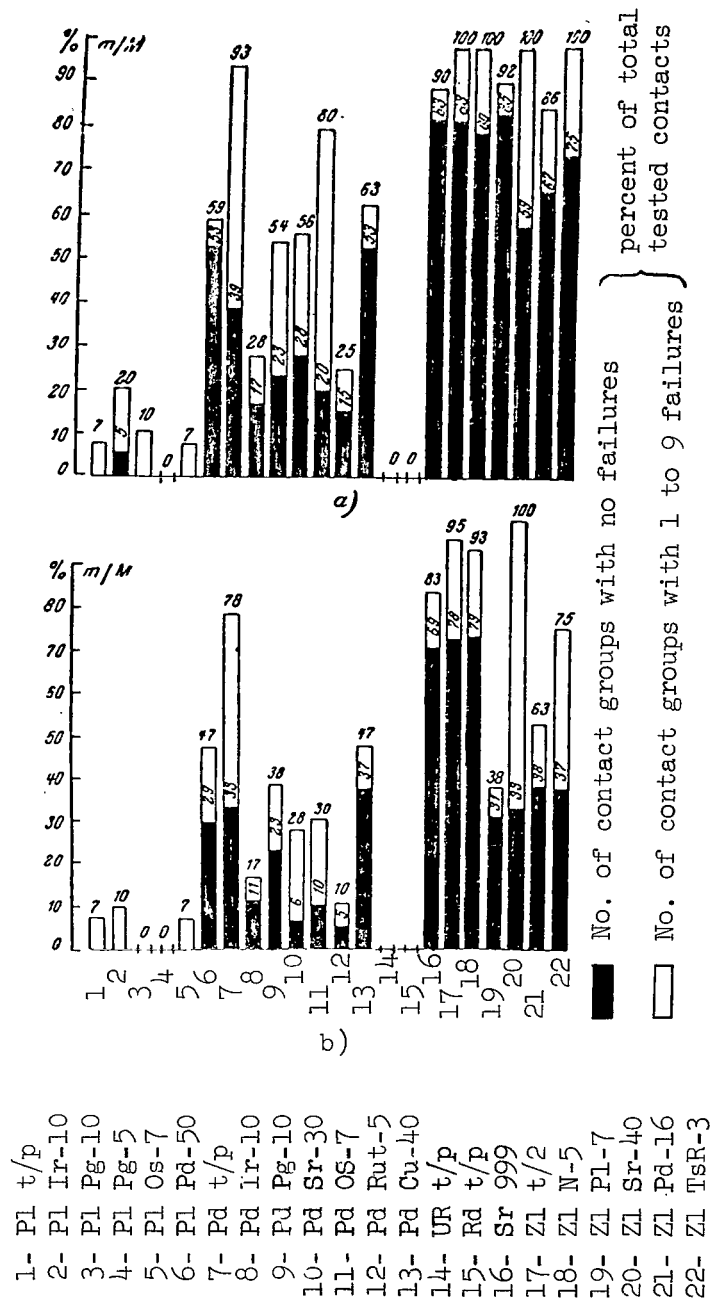


Figure 8. Diagram showing operation of RES-10 relay with epoxy with contacts made of different materials while switching a circuit with  $5 \mu\text{A}$  and  $50 \text{ mV}$ . a, within limits of  $10^5$  commutations; b, within limits of  $2 \cdot 10^5$  commutations.

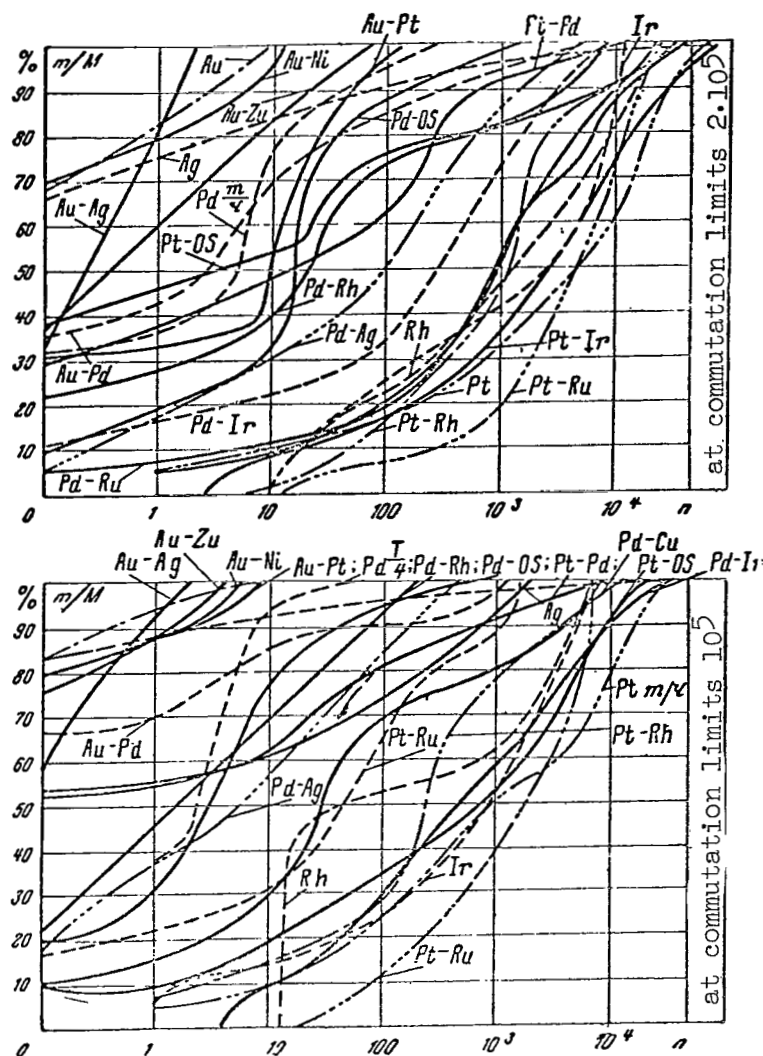


Figure 9. Distribution of number of contact break-downs for relay RES-10 with epoxy under normal climatic conditions.

The curves in figures 11-15 show the variation in the resistances of relay RES-10 and RES-9 contacts, which were broken in without a load, as a function of the number of commutations. Measurements were carried out with a current 0.1 A. In these drawings, the heavy lines correspond to the average values of contact resistance, while the thin lines show the minimum and maximum values. The shaded region shows the degree of spread in contact resistances.

We can easily observe (figs. 11 and 12) the advantages of gold and silver and even of gold alloys with nickel compared with palladium and the PII-10 alloy. The latter exhibit a high average contact resistance, which is several hundredths of times greater, and exhibit a larger spread which is at least 2 to

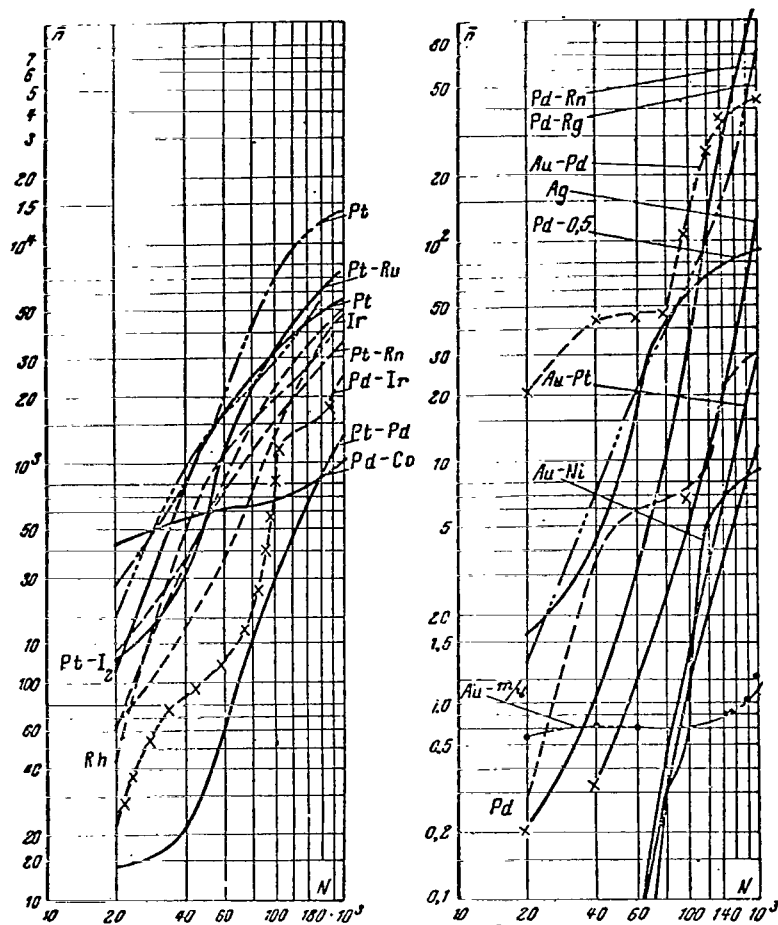


Figure 10. Average number of breakdowns which occur in one contact group as function of number of commutations of RES-10 relay with epoxy under normal climatic conditions.

3 orders of magnitude greater, if we take into account that the scale of the graphs for palladium and the PtI-10 alloy is 100 times greater than the scale of the graphs for silver, gold, and the Z1N-5 alloy. /332

Both figures also show that from the standpoint of contact resistance the Z1N-5 alloy is not as good as pure gold and silver.

The characteristics in figures 13 and 14 show the advantage of silver with respect to the PtI-10 alloy in RES-9 contacts. For comparison purposes, figure 15 also shows the curves for RES-10. The rise in the curves in figure 13 after  $3 \cdot 10^5$  is due to the wear of the supports (a drop in contact pressure

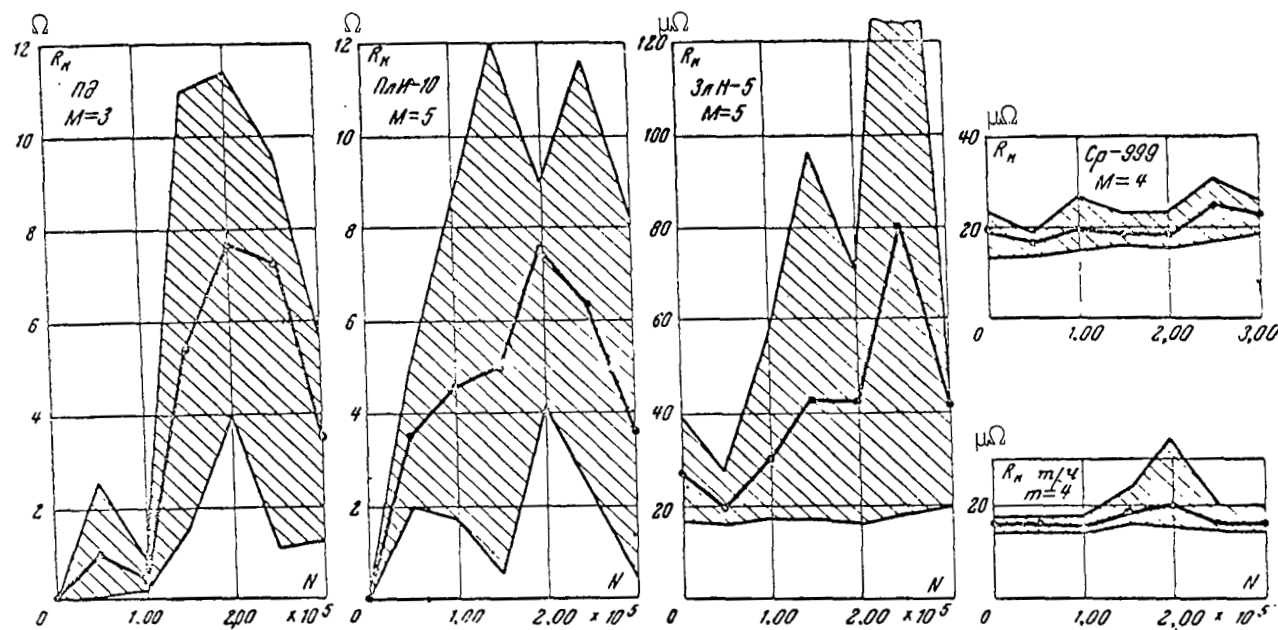


Figure 11. Resistance of relay RES-10 breaking contacts as function of number of commutations without failure (measured with current of 0.1 A).

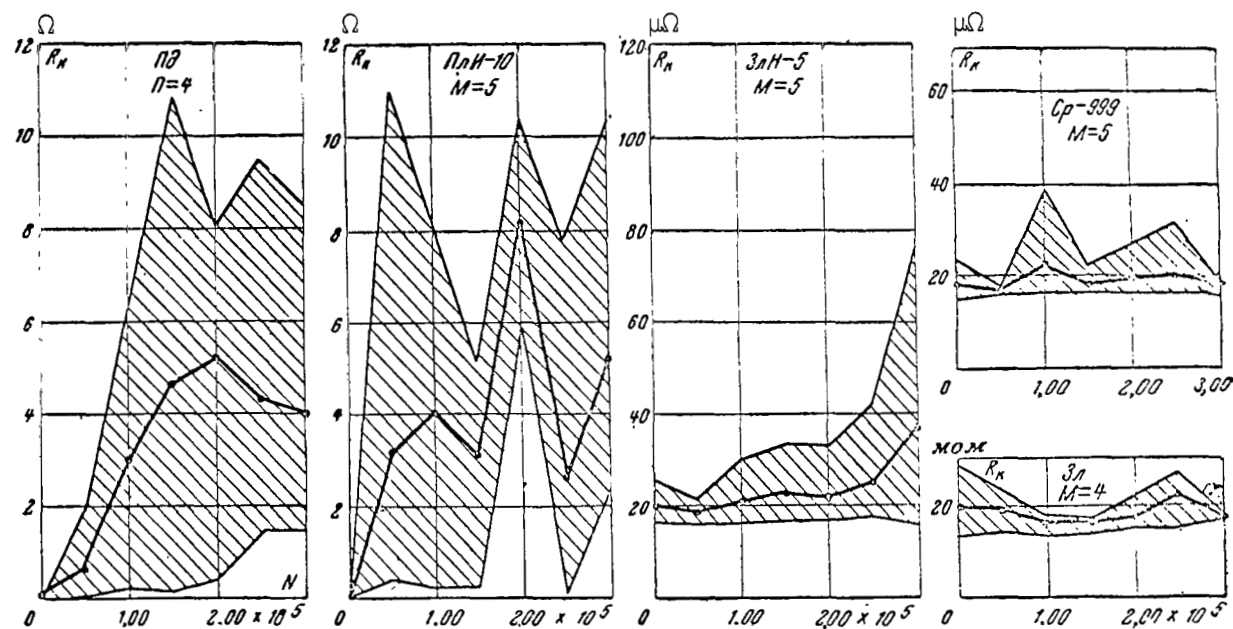


Figure 12. Resistance of RES-10 relay closing contacts as function of number of commutations without failure (measured with current of 0.1 A).

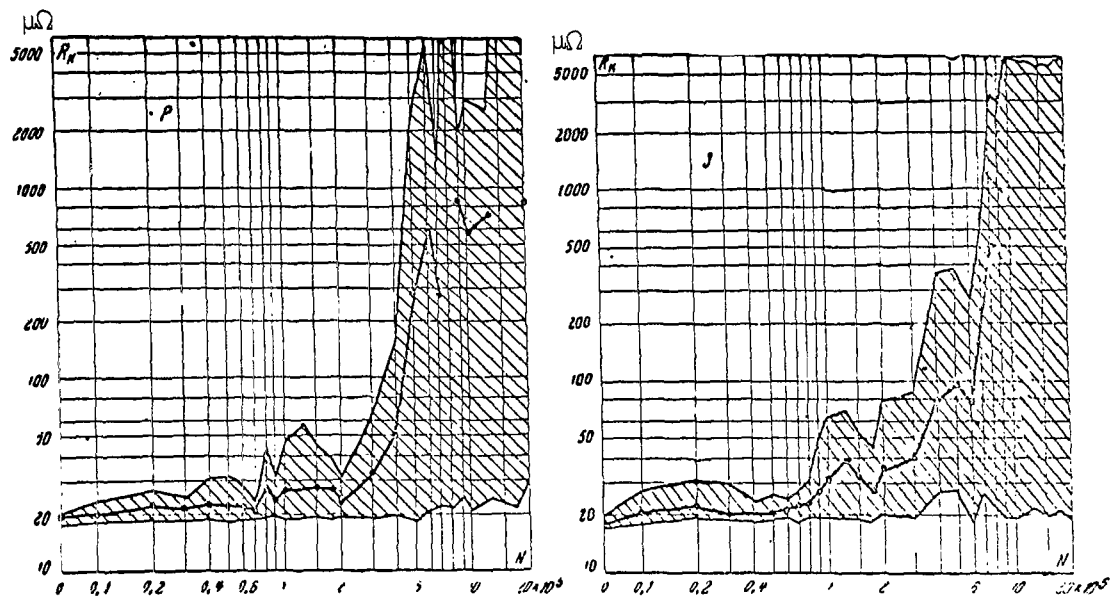


Figure 13. Resistance of RES-9 (Sr-999) contacts as function of number of commutations without failure (measured with current of 0.1 A,  $M = 10$ ).



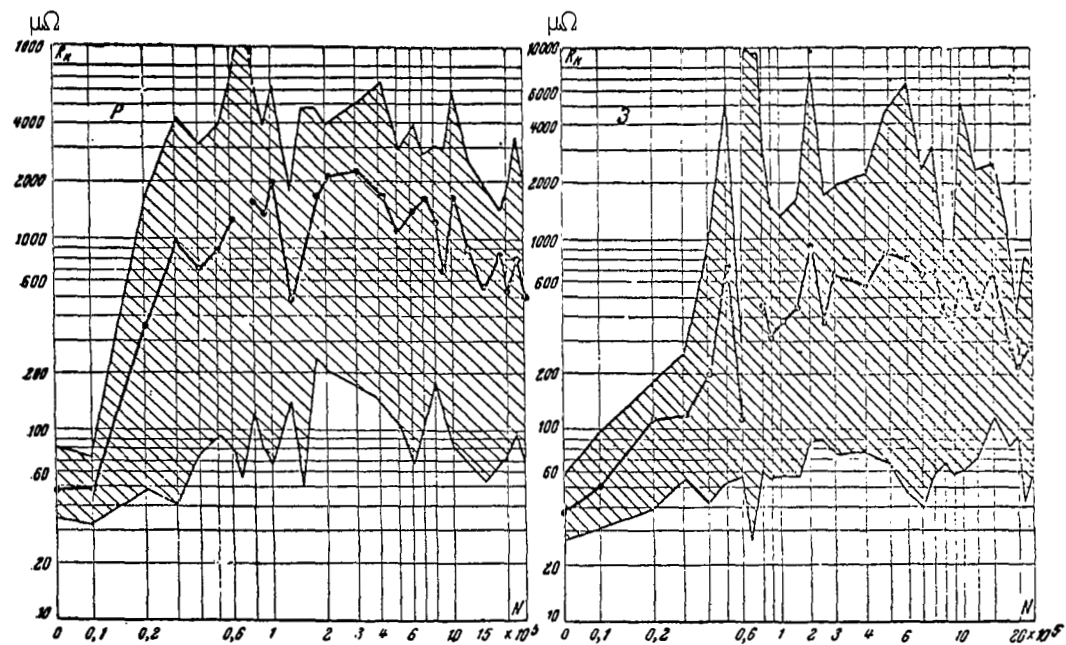


Figure 14. Resistance of RES-9 (PlI-10), relay contacts as function of number of commutations without failure (measured with current of 0.1 A,  $M = 12$ ).

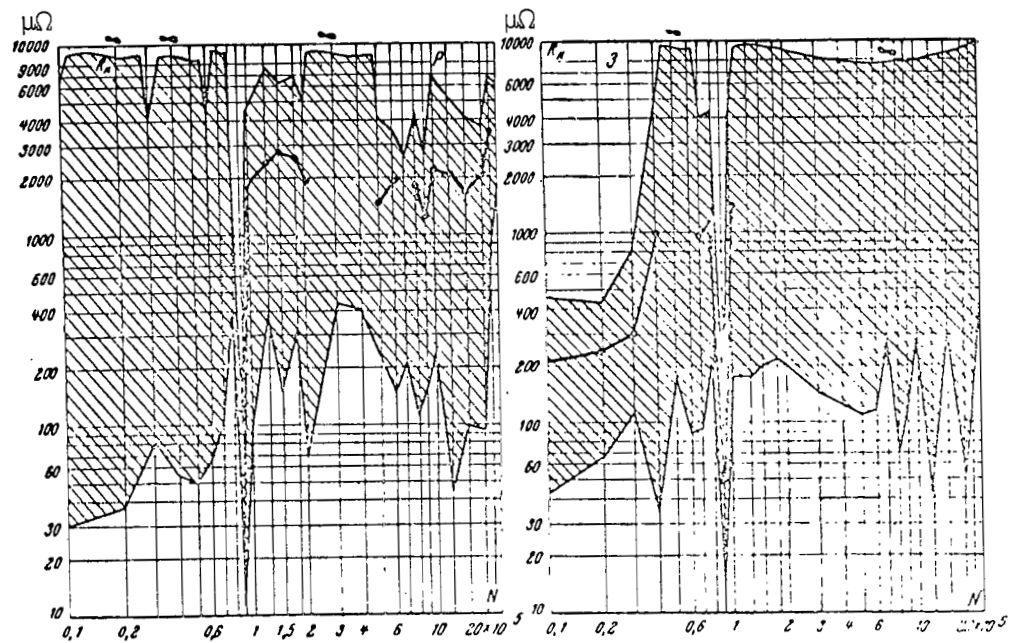


Figure 15. Resistance of RES-10 (PlI-10) relay contacts as function of number of commutations without failure (measured with current of 0.1 A,  $M = 10$ ).

and the contamination of contacts with the products of wear). Breaks in the curves at high numbers of commutation in figures 13, 14 and 15 show that the current does not pass through.

In order to establish the reasons for the different behavior of contacts from metal of the platinum group and contacts from gold and silver, samples of RES-9 and RES-10 relays which underwent  $2 \cdot 10^5$  commutations with a current of  $5 \mu\text{A}$  were opened and examined. Careful examination of contact surfaces under the microscope revealed the presence of a dark powder material on all contacts made from metal of the platinum group. In most cases the powder-like substance has the form of a rim around the operating area of the contacts, and grains of powder are observed beyond this rim and sometimes inside it. This powder-like substance is easily wiped off from the surface of the contacts with any soft object and leaves no spots on the contacts. After this, the surface of the contacts clearly shows a small area or lune produced by the mechanical wear of the operating surfaces. It is significant that, for contacts made from metals of the platinum group, this powder is deposited in the form of dense concentrations while on contacts made of gold, there is only a small trace of this powder in the form of small rims or specks of dust. On silver contacts, after  $2 \cdot 10^5$  commutations, the powder is almost absent. It is more noticeable on gold alloys: there are light rims and fine dust which are more pronounced for the ZlPl-7 and Zld-16 alloys than for the ZlN-5 alloy. Apparently, in the former, it is due to alloying with metals of the platinum group.

It is obvious that the amount of powder depends directly on the /333  
number of commutations. Therefore, the RES-10 relays with contacts made of silver, gold and the PII-10 alloy were broken-in with up to  $10^6$  commutations without a load in order to obtain a better comparison of individual contact materials. An examination of the contacts of these relays under the microscope showed that after a long period of operation, the powder-like substance is observed in all materials, but, for the case of silver and gold, it exists in small quantities, while for the PII-10 alloy, it achieves the form of dense abundant masses.

Figure 16 shows the photographs of the contacts after  $2 \cdot 10^5$  and  $5 \cdot 10^6$  commutations. Unfortunately, they cannot fully illustrate everything observed under the microscope; however, dark rings can be observed on these photographs. The dark rings surround a light spot corresponding to the working area of the contacts which has been subjected to mechanical wear.

We note that no strict rule has been observed between the number of failures and the quantity of liberated powder-like material on the contacts. Frequently contacts which produced relatively good results did not show less powder than contacts with a large number of failures. This is explained by the fact that the appearance of powder at the contact points is a random phenomenon which depends on many reasons associated with the process of contact making and breaking, specifically: on the impact force of the contacts, on the oscillation of the contact spring, on the rebound of the contacts, on the rocking of the armature in its suspension, on the degree of contact sliding during making and on other phenomena which cause the shaking and displacement of powder particles to the operating points of the contacts.

The mechanism which forms the powder-like substance is not completely understood. In foreign literature (refs. 1 and 2) its appearance is explained by the formation of polymerization products of vapors of organic substances which are evaporated from the components of the relay. The products of polymerization consist of thin transparent films on the surface of the contacts. In the course of contact operation, they are gathered around the operating areas in the form of dark powder. The special feature associated with the formation of this powder is that it appears only on contacts which are in operation. It is not detected on contacts which have remained in a state of rest. The formation of powder-like coatings on contacts is particularly noticeable in hermetically sealed constructions because in these, the concentration of organic vapors is increased. The test of RES-9 and RES-10 relays with open cases confirmed this: 8 tested contact groups of the RES-9 relay performed almost without failure, and the number of failures in relay RES-10 was radically reduced compared with the number of failures in sealed relays. Similar results were obtained for other contact materials of the platinum group. In the case of contacts from silver, gold and its alloys which showed a relatively small number of breakdowns in closed form, the opposite phenomenon is observed--the number of breakdowns in an open relay either remains unchanged or tends to increase. This may be explained by the fact that poorly conducting particles fall on the contacts of the open relay from the surrounding space. In the case of contacts made from metals of the platinum group, this is not noticeable. We should like to point out that all of the contacts which were used in the open form exhibited a greater mechanical wear of contact surfaces than the contacts of the sealed relays. Apparently because it has sufficient plasticity, the powder-like material serves as a type of lubricant which decreases contact friction during sliding. /335

Thus, the basic reason for the large number of breakdowns of contacts made of metals and alloys of the platinum group is due to the fact that during the operation of these contacts, deposits with a high resistance are formed on their surfaces due to the action of organic vapors.

Now we can explain the different behavior of PLI-10 alloy used in contacts of different types of relays (figs. 3-8 and table 1).

From the standpoint of organic vapor concentration, the most unfavorable conditions take place in the RES-10 and RES-15 relays encapsulated in epoxy because these relays are almost hermetically sealed, are small in size and the epoxy serves as an additional source of organic vapors. These two types of relays exhibited the minimum reliability at low currents.

The relatively high performance of the RES 8 hermetically sealed relay should be attributed to the high contact pressure and large volume and also to the small number of components made from organic substances. The superior results obtained with RES-9 compared with rolled RES-10 and also with RES-15 compared with RES-10 encapsulated with epoxy, are explained by the lower concentration of organic vapors because these relays have rolled cases. Finally, the RES-6 relay has a removable cover. Because of this, and because the relay has double contacts, this relay has the highest reliability of its type compared with others. /337



Figure 16. Photographs of RES-10 relay contacts made of PlI-10 after  $2 \cdot 10^5$  and  $5 \cdot 10^6$  commutations.

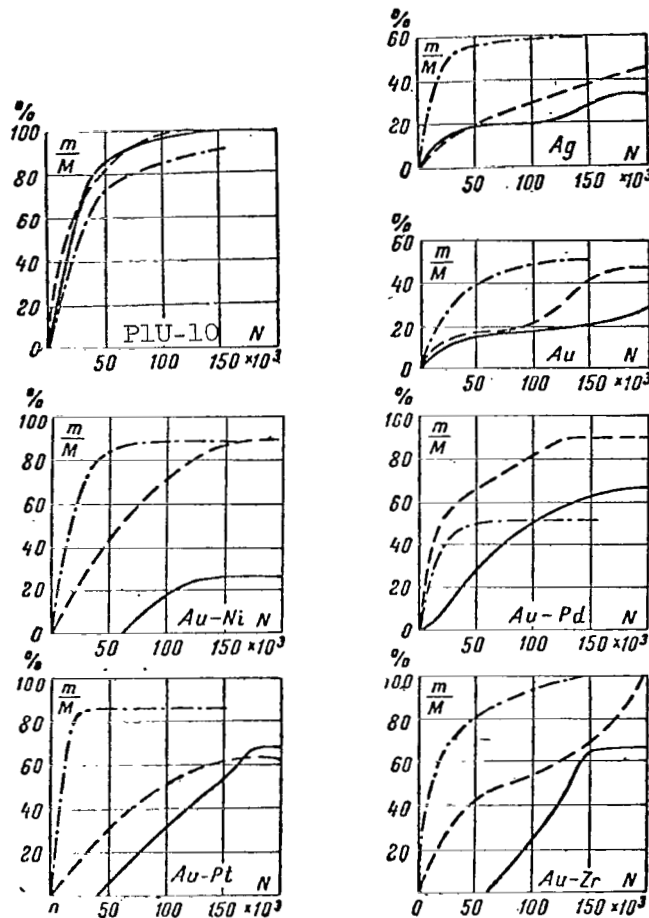


Figure 17. Distribution of number of commutations up to  $n$ -th breakdown of R-10 relay encapsulated in epoxy.

— normal conditions; - - - +  $125^{\circ}\text{C}$ ;  
- . - . -  $60^{\circ}\text{C}$ .

The less favorable test results obtained with the RES-10 relay with epoxy compared to relay RES-15 and also with RES-10 with rolled cases compared with RES-9 may be explained by the fact that during the making of contacts in RES-10, there is more sliding. Although this sliding is useful from the standpoint of wiping chemical compound films, it becomes detrimental when a large amount of powder-like substance is liberated, because this moves the powder into the operating region of the contacts.

The large spread in the number of breakdowns for contacts of different samples may be explained by the following: (a) the difference in vapor concentrations inside them, because one of them is hermetically sealed immediately after assembly with fresh materials and fresh lacquers, while the others are exposed for a while, which produces a partial evaporation of the organic substances from relay components; (b) different probability for the arrival of powder particles at contact points, which in turn depends on the amount of liberated material and on the special features of making and breaking mechanisms which we have discussed.

Generalizing the results obtained in the investigation of contacts which switch low currents and voltages, we can make the following general conclusions:

1. Metals of the platinum group and their alloys with each other and with other metals are entirely unsuitable for the switching of low level voltages and currents, because the organic vapors form powder-like deposits with high electric resistance on the contacts made of these materials.

2. The most suitable material for this purpose is technically /338 pure gold. The replacement of the PII-10 alloy, which is currently used, with gold will make it possible to increase substantially the reliability of low current and voltage commutation.

3. Gold alloys, in this respect, are not as good as gold, both under normal climatic conditions and at high temperatures and humidities (fig. 16).

4. Under normal climatic condition, silver produces results comparable with that of gold; however, it cannot be considered suitable, because it changes its performance radically under conditions of high temperature and humidity and particularly when it is used in the medium containing sulfurous compounds.

5. Since the commutation of low currents and voltages does not subject the contacts to erosion, there is no point in making them entirely out of gold. It is recommended instead that gold-plating be used with a thickness selected only from considerations of mechanical wear, which are determined by the required useful life, contact pressure and the mechanism of contact making and breaking--lapping, shock, etc. For relays with a small contact pressure (up to 15 g-wt), the necessary thickness of the plating need only be 3-5  $\mu$ .<sup>1</sup> In this case it is necessary to provide for adequate purity, density and binding

---

<sup>1</sup>Investigations have shown that the optimum thickness of gold plating is 3-5  $\mu$ .

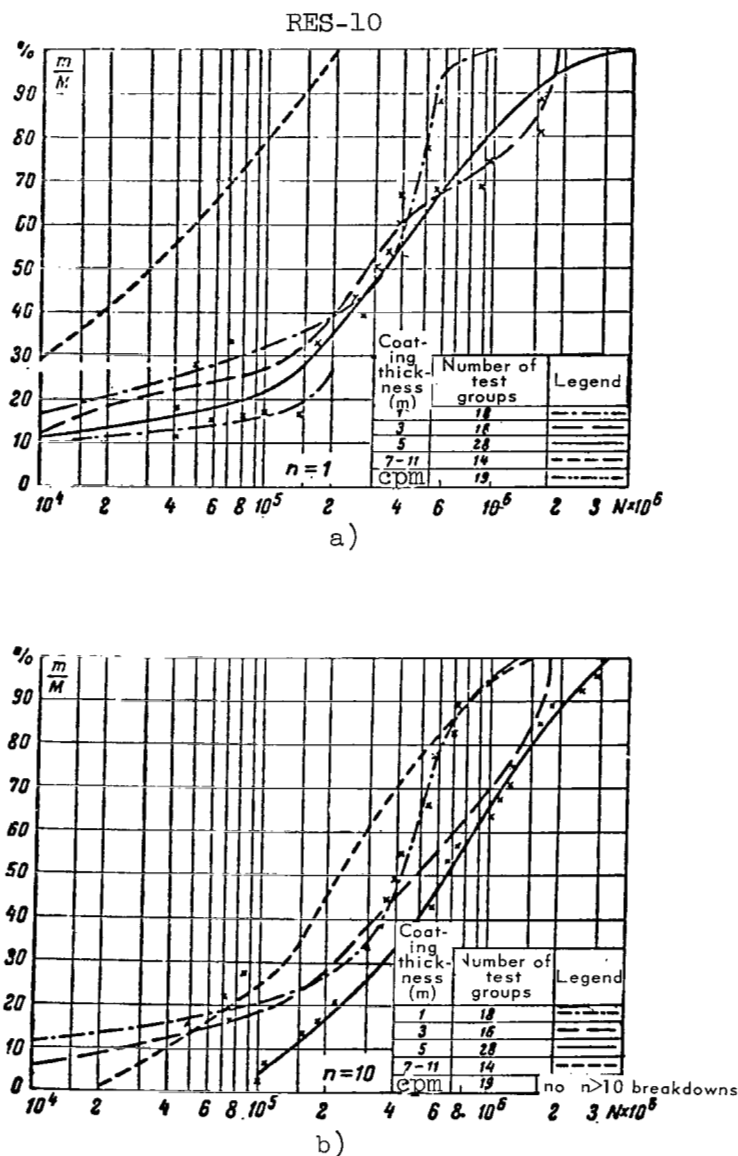


Figure 18. Distribution of number of commutations up to  $n$ -th breakdown of RES-10 relay contacts encapsulated in epoxy and gold-plated.

of the plating to the basic metal, and also a good finish for the plated surfaces of the contacts which must not have scratches, nicks or burrs.

6. Experiments have shown that even when gold contacts are used, breakdown is not completely eliminated, because products resulting from the wear of the armature fall on contact points together with foreign particles from the surrounding space; therefore, when assembling relays designed for the commutation of low currents and voltages, it is very important to exercise strict

control over the finish of individual parts of the armature. This will /339 make it possible to reduce the amount of products of wear during the operation of the relay. The components of the relay must be thoroughly washed and cleaned--the presence of dirt and particularly of oils is entirely inadmissible for relays designed to switch low currents. The relays must be assembled in a sterile atmosphere with conditioned air and with minimum humidity. The components must be dried and decontaminated before they are hermetically sealed or before the covers are put on to eliminate the initial vaporization of organic materials from the fresh relay components.

7. It is also recommended that the contacts be doubled, which substantially improves the commutation reliability.

#### REFERENCES

1. Hermance, H. W. and Egan T. F. Organic Deposits on Precious Metal Contacts, BSTJ, Vol. 37, No. 3, 1958.
2. Keefer, H. J. and Gumley, R. H. Relay Contact Behavior under Noneroding Circuit Condition, BSTJ, Vol. 37, No. 3, 1958.



CONTACTS OF RELAY-TYPE ELEMENTS AND MICROSWITCHES  
WHICH COMMUTATE LOW LEVEL SIGNALS

S. F. Solov'yeva, I. I. Sigachev, N. A. Surkova  
and Ye. V. Kogteva

The wide application of switching elements such as relays and microswitches in devices which perform logical, mathematical and tactical operations places substantial demands on their reliability in switching low level signals.

Until quite recently, not enough attention was devoted to the problem of contact behavior during the switching of low currents and voltages. The application of conventional switching elements to switch low level signals in equipment operating under rigid climatic and atmospheric conditions and stored for a prolonged period in warehouses and under field conditions, has led to the problem of the "dry" contact. /340

The first sign of a "dry" contact is the sharp decrease or complete disappearance of current in the switched network, followed by a rapid recovery and normal operation.

The nature of this phenomenon is not constant and it is difficult to isolate its principal cause.

However, a series of firms in the USA developed magnetically controlled reed relays whose contacts are placed in a medium of inert gas and are, therefore, completely isolated from external substances. This has made it possible to increase sharply the commutation reliability and to eliminate almost completely the phenomenon of "dry contact." This gives us a basis to assume that the basic reason for the occurrence of the "dry contact" is the sharp increase in the transitional resistance of the contacts, due to the formation of films on their surface which prevents the formation of a metallic contact. The effect of films will be most pronounced in designs with low contact pressure, which is now required due to a trend towards microminiaturization.

The films may be divided into four basic groups:

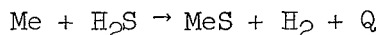
- (1) chemical (sulfides, oxides);
- (2) organic (carbon deposits);
- (3) absorbed or liquid (oil, water);
- (4) loose or solid contamination (dust, solder fluxes, etc.).

Obviously, in the design of reliable elements which switch low level signals when it is impossible to place the contacts in a vacuum or in an inert medium, it is necessary to have a contact pair whose transitional resistance, regardless of external factors, remains low and stable, even at low contact pressures.

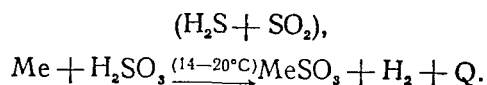
### The Effect of Prolonged Storage

The purpose of the present work was to find contact materials which could be used in designs with breaking contacts which are not hermetically sealed, but which would provide for reliable current switching in the range  $1 \cdot 10^{-6}$ -0.5 A with voltages from 0.5 to 30 V after prolonged storage in warehouses or in the field. /341

The atmosphere of industrial centers is highly contaminated with various gases. The most common impurities are the following:  $\text{SO}_2$  (sulfide dioxide) up to  $25 \text{ mg/m}^3$  and  $\text{H}_2\text{S}$  (hydrogen sulfide) up to  $5 \text{ mg/m}^3$  (ref. 1). Experiments have shown that hydrogen sulfide  $\text{H}_2\text{S}$  in humid air is most dangerous, particularly for precious metals, because the reaction for the formation of the sulfide



is more probable than the reaction for the formation of the sulfate



The last reaction is possible only for nonprecious metals, for silver and for some of its alloys.

Also, unlike  $\text{MeS}$ ,  $\text{MeSO}_3$  are clearly defined salts, which do not form a continuous film capable of disrupting the circuit during the making of contacts.

Therefore, the most dangerous gaseous impurity in humid air is  $\text{H}_2\text{S}$  which forms a sulfide film on the surface of all metals ( $\text{MeS}$ ).

Various experiments conducted by us and by others, and information on the value of the transitional resistance of silver contacts which were stored in unheated warehouses for a period of 5-7 years, have made it possible to select conditions for the accelerated tests of contact materials which are sufficiently close to actual conditions. The test contact materials in the form of specially prepared samples were processed in a corrosion chamber with flowing humid hydrogen sulfide having a concentration of three  $\text{mg/l}$ , a temperature of  $T = 25 \pm 3^\circ\text{C}$ , relative humidity of  $95 \pm 3$  percent and a volumetric gas flow of 10-15  $\text{ml/min}$ . /342

The duration of the tests was 2 days.

The following groups of alloys based on precious metals were selected for the investigations:

- (1) silver and alloys of Ag-Pd;
- (2) gold and alloys of Au-Pd, Au-Ni, Au-Zr;
- (3) platinum and alloys of Pt-Ni, Pt-Rh, Pt-Pd;
- (4) palladium and alloys of Pd-Ag.

#### Methods of Investigating the Electric and Physical Properties of Surface Films Formed on Contact Materials

A large number of measurements of the characteristics were made to carry out an extensive and intensive investigation of the electric and physical properties of surface films which are formed on contact materials due to interaction with an aggressive medium.

Each measurement was made several times.

Special attention was given to the preparation of sample surfaces to eliminate any possible flaws. The samples were supplied by the plants in semi-finished form.

In spite of great difficulties, it was possible to develop special methods for determining accurately the basic properties of surface films appearing on various contact materials.

All of the delivered alloys were in a cold-rolled state. They were used in this state without heat treatment to simulate true conditions.

Measurements were taken with the special setup (fig. 1), involving the contacting of a spherical surface with a flat surface.

Contacting was accomplished by means of the PMT-3 device designed for measuring the microhardness of materials. The diamond indenter of this 343 device was replaced with a spherical contact. The test materials were used to fabricate flat contacts of standard form. All samples were placed into special holders (fig. 2), fabricated from insulating material, and these holders were used to polish the samples and to process them in the corrosion chamber.

In order to make the comparison of results possible, all measurements were carried out with a spherical contact fabricated from the PII-25 alloy not subjected to corrosion treatment. The diagram showing the position of the contacts is shown in figure 3.

A special sliding carriage was mounted on a movable table of the PMT-3 device, which held the block with the test samples (flat contacts) and was secured in such a way that the required sample was under the spherical contact.

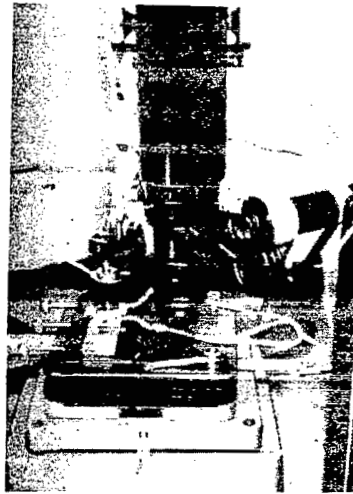


Figure 1. Contact assembly unit.

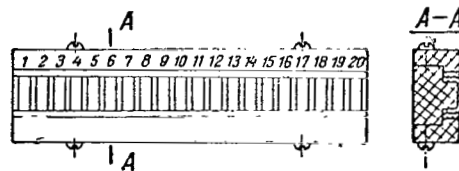


Figure 2. Holder with samples of test materials.

This device made it possible to carry out all of the measurements and to vary the contact pressure quite simply from 0.5 to 200 g-wt. In addition, the microscope of the PMT-3 device made it possible to control the condition /344 of the surface at the more important points of contacting. In order to provide for stable results, the entire setup consisting of PMT-3 and of the electrical system was thermostatically controlled (fig. 4). The effect of the temperature of the operator's hands was eliminated by means of wool gloves built into the protective screen to perform the required manipulations inside the box.

The films were investigated by means of a scheme shown in figure 5.

The voltage drop across the contacts under different operating conditions was measured by means of two devices: the F-16 photocompensating amplifier in conjunction with an N-16 recorder and a microvolt microammeter with a Herz light indicator (Austria). The F-16 device measures voltages over the range of  $(2-4-10-20-40-100) \cdot 10^{-8}$  V/mm.

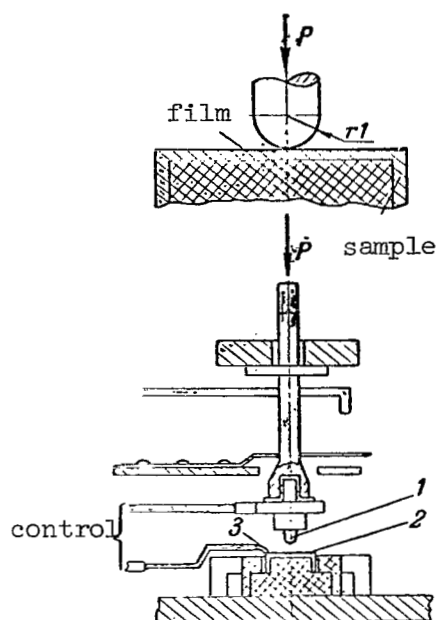


Figure 3. Diagram showing position of contacts. 1, spherical contact; 2, flat contact--test material; 3, leads to the control equipment.

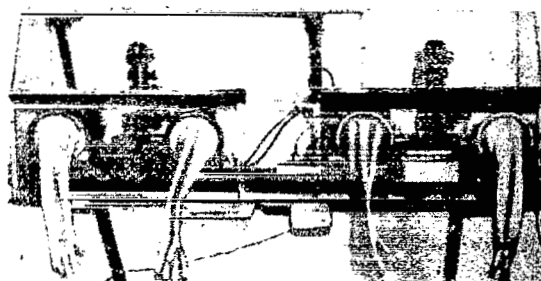


Figure 4. External view of test chamber.

The current through the contactor was adjusted by means of special resistance chains. To prevent interference, the entire system was screened.

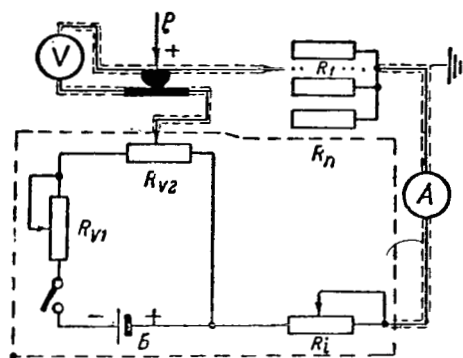


Figure 5. Diagram of setup for investigating contact resistance of films.

The holder with the test samples was installed and secured to the table of the PMT-3 device. Next the system was balanced in such a way that the point of contact of the sample with the sphere was at the crosshairs of the microscope eyepiece when the table was rotated by  $180^\circ$ .

The sample was carefully examined under the microscope with a magnification factor of 130 and regions were selected which were more or less identical in appearance, and measurements were made at these points. /345

The contact points were changed by displacing the sample into mutually perpendicular directions by means of micrometer screws on the table.

Pressure was established by means of the PMT-3 loading mechanism. The zero pressure at the contacts was taken as the one produced by a load of 0.5 g placed on the loading mechanism; with this load, a current must pass through the contact pair. When this load is removed, the current in the circuit must cease.

The weights on the loading mechanism were always changed by lifting the spherical contact. Then, the stop lever was moved uniformly to lower the spherical contact on the test sample which provided for a definite pressure between the contact plane and the sphere. The voltage across the open contacts was maintained at 50 mV. This value was selected to prevent the breakdown of the film. The current was measured from  $1 \cdot 10^{-6}$  to  $1 \cdot 10^{-1}$  A. /346

#### Contact Resistance

In order to evaluate the magnitude of the transitional resistance of the films formed on the surface of the test metals and to determine its variation as a function of current, voltage and contact pressure, the following relations were recorded:

$$R_0 = f(P); R_s = f(P) \text{ when } I = \text{const};$$

$$R_0 = f(I); R_s = f(I) \text{ when } P = \text{const},$$

where P is the contact pressure;

$R_0$  is the contact resistance of pure metal;

$R_s$  is the contact resistance after damp hydrogen sulfide has acted on the contacts in the corrosion chamber;

I is the current passing through the contacts.

Table 1 gives the values of the contact resistances  $R_{ot}$  computed for a contact pressure of 5 and 15 g-wt by means of the well-known equation

$$R_{ot} = \frac{\rho_1 + \rho_2}{2} \sqrt{\frac{H}{P}},$$

where H is the hardness of the softer contact material;

$\rho$  is the specific resistance of the contacts.

We can see that these values are close to the experimental values which have been obtained (table 1).

Some of the deviations can be explained by experimental error and by the presence of unstable films which were formed when the surfaces were prepared.

Although the measurements were preceded by a careful preparation of the contact surface, including buffing, degreasing and dehydration, our results 347 were still affected by the rapid formation of new surface films and by incompletely removed old films. This was particularly noticeable in such materials as silver and its alloys with palladium (20 to 60 percent Pd), whose value of  $R_0$  compared with  $R_{ot}$  is somewhat greater than for other materials.

It follows from the equation that  $R_{ot}$  is proportional to the sum  $\rho_1 + \rho_2$  of the contact test materials.

The analysis of test data shows that basically they agree with this relationship.

The characteristics  $R_0 = f(P)$  of the test materials for currents of 0.001-10 mA are shown in figures 6-11 and table 1, 2 and 3.

The methods described in this paper and also the utilization of the F-16 device permit us to measure the function  $R_0 = f(P)$  over new ranges--even with current of 1-10  $\mu$ A. It follows from our measurements (table 1) that the contact resistance remains constant when the current varies from 1  $\mu$ A to 10  $\mu$ A, excluding the spread apparently due to experimental errors.

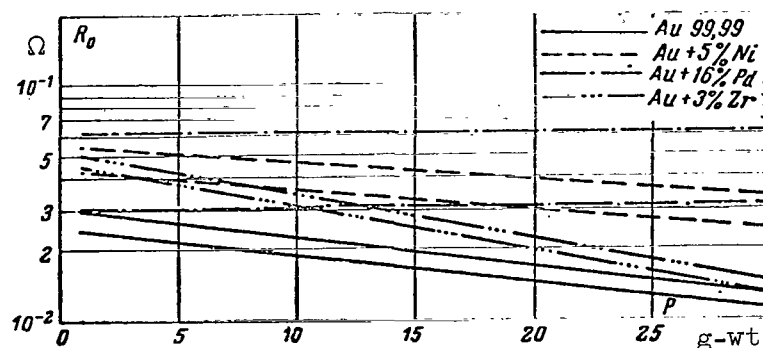


Figure 6.  $R_0 = f(P)$  when  $I = 1 \mu A$  for initial samples.

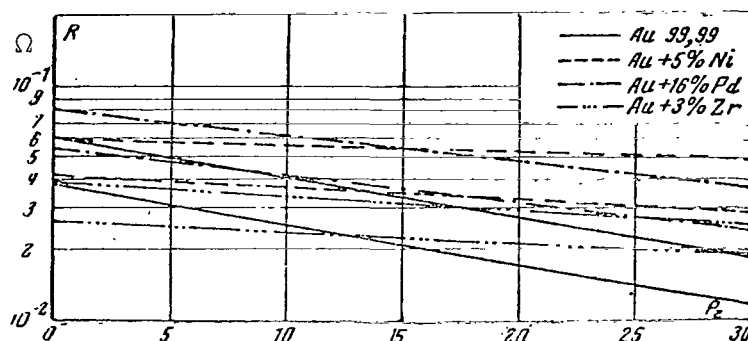


Figure 7.  $R_0 = f(P)$  when  $I = 10 \text{ mA}$  for initial samples.

The relations  $R_s = f(P)$ , i.e., the values of  $R$  after the contact materials have been processed in flowing damp hydrogen sulfide with currents of  $1 \mu A$  and  $10 \text{ mA}$  are shown in figures 12-17. /352

We present the relative value  $R_s/R_0$ , which can be used to compute the resistance of the contact after it is subject to  $H_2S$ .

Table 1 shows the values of  $R_s/R_0$  for contact pressures 5 and 15 g-wt and current of  $1 \mu A$  and  $10 \text{ mA}$ . As expected, pure silver shows the least resistance and its  $R_s$  increases sharply compared with  $R_0$ , which makes it impossible to use silver as contact material under these conditions with currents of  $10 \text{ mA}$  and contact pressures up to 30 g-wt; the  $R_s$  of silver alloys with palladium (Ag+20 percent Pd and Ag+60 percent Pd) also varies substantially and is /354



TABLE 1

Material	Density in g/cm <sup>3</sup>	Specific resistance $\Omega \cdot \text{cm} \cdot 10^{-8}$	Hardness, kg-wt/mm <sup>2</sup> (microhardness)	P = 5 g-wt						P = 15 g-wt						No. in the graphs figs. 18 and 19		
				$R_{0.5}$ , $\Omega \cdot 10^{-3}$	I = 1 $\mu\text{A}$		I = 10 mA		$R_{0.5}$ , $\Omega \cdot 10^{-3}$	I = 1 $\mu\text{A}$		I = 10 mA						
					$R_0$ , $\Omega \cdot 10^{-3}$	$R_S$ , $\Omega \cdot 10^{-3}$	$\frac{R_S}{R_0}$	$R_0$ , $\Omega \cdot 10^{-3}$		$R_S$ , $\Omega \cdot 10^{-3}$	$\frac{R_S}{R_0}$	$R_0$ , $\Omega \cdot 10^{-3}$	$R_S$ , $\Omega \cdot 10^{-3}$	$\frac{R_S}{R_0}$				
Au99.99	19.3	2.2	61	1.91	2.3	34	14.7	2.3	3.0	1.3	1.12	1.9	30	15.7	1.9	2.8	1.47	1
Au+16%Pd	16.8	25	162	5.2	4.8	8.0	1.69	4.8	8.0	1.66	3	4.8	6.0	1.25	4.8	6.0	1.25	2
Au+5%Ni	18.3	12.3	185	4.35	4.6	150	32.6	4.6	9.0	1.95	2.5	3.8	120	31.6	3.8	6.0	1.6	3
Au+3%Zr	18.3	20	147	4.55	4.0	42	10.5	4.0	10	2.5	2.64	2.6	42	16.2	2.6	8.0	3.08	4
Pt99.99	21.3-21.4	10.5	127	3.46	4.0	70	17.5	4.0	13	3.2	2	3.0	65	21.7	3.2	10.0	3.15	5
Pt+4.5%Ni	20.6	27	283	7.15	7.5	90	12	7.5	40	5.34	4.2	5.1	85	16.6	5.1	30	5.9	6
Pt+10%Rh			171		10	90	9	10	30	3		5	75	15	5	20	4	7
Pt+10%Pd	20.4	22	185	5.32	6	75	12.5	6	20	3.3	3.14	5	65	13	5	15	3	8
Ag+60%Pd	11	42	202	7.45	4.8	140	29.2	4.8	35	7.3	4.3	4.0	60	15	4	35	8.75	9
Ag+20%Pd	10.7	10.1	143	3.4	9	400	44.5	9	42	4.67	1.96	7.0	150	21.4	7.0	32	4.56	10
Ag99.99	10.5	1.6	89-96	2.3	2.8	3.5-10 <sup>3</sup>	1.2-10 <sup>4</sup>	2.8	2-10 <sup>4</sup>	0.7-10 <sup>4</sup>	1.33	2.4	1.5-10 <sup>3</sup>	0.6-10 <sup>3</sup>	2.4	0.3-10 <sup>3</sup>	0.12-10 <sup>4</sup>	11
Pd99.99	11.9-12	10.7	133	3.55	3.5	16	4.57	3.5	9	2.57	2.06	2.9	16	5.5	2.9	5	1.72	12
Pt+25%Ir	21.7	33	288															13

<sup>1</sup>Hardness was measured with materials in the delivered state.

TABLE 2

Materials	P = 5 g-wt, I = 1 $\mu$ A								P = 25 g-wt, I = $\mu$ A								Nos. in figs. 25-41
	Initial $R_I$ $\Omega \cdot 10^{-2}$	AG-4C		PCT		K-211-3		$\Phi$ П-4		Initial $R_I$ $\Omega \cdot 10^{-2}$	AG-4C		PCT		K-211-3		
		$R_n \cdot \Omega \cdot 10^{-3}$	$\frac{R_n}{R_n}$	$R_n \cdot \Omega \cdot 10^{-3}$	$\frac{R_n}{R_n}$	$R_n \cdot \Omega \cdot 10^{-3}$	$\frac{R_n}{R_n}$	$R_n \cdot \Omega \cdot 10^{-3}$	$\frac{R_n}{R_n}$		$R_n \cdot \Omega \cdot 10^{-3}$	$\frac{R_n}{R_n}$	$R_n \cdot \Omega \cdot 10^{-3}$	$\frac{R_n}{R_n}$	$R_n \cdot \Omega \cdot 10^{-3}$	$\frac{R_n}{R_n}$	
Au 99,99	35	—	—	90	2,57	—	—	—	—	33	—	—	90	2,72	—	—	1
Au+3% Zr	65	18	0,27	15	0,23	110	1,69	9,8	0,15	50	12	0,24	15	0,3	70	1,4	2
Au+16% Pd	530	—	—	550	1,04	—	—	—	—	380	—	—	350	0,92	—	—	3
Au+5% Ni	4000	1500	0,37	860	0,21	—	—	—	—	2900	1200	0,41	850	0,29	—	—	4
Ag 99,99	28	100	3,7	160	5,72	108	3,86	65	2,32	10,7	47	4,4	75	7,0	66	6,2	5
Ag+60% Pd	4500	—	—	2000	0,45	—	—	900	0,2	3700	—	—	1400	0,38	—	—	7
Ag+20% Pd	400	—	—	270	0,68	900	2,25	1000	2,5	320	—	—	220	0,69	525	1,64	6
Pt	600	45	0,08	230	0,38	—	—	—	—	430	35	8,1	200	0,46	—	—	12
Pt+10% Rh	40	—	—	115	2,88	43	1,07	—	—	9,8	—	—	100	10,4	32	3,27	13
Pt+10% Ir	450	—	—	390	0,87	650	1,44	—	—	107	—	—	250	2,3	225	2,1	8
Pt+10% Pd	180	—	—	45	0,25	—	—	—	—	102	—	—	43	0,42	—	—	10
Pd	800	—	—	430	0,54	380	0,48	450	0,56	720	—	—	375	0,52	325	0,45	11

TABLE 3

Materials	P = 5 g-wt, I = 10 mA								P = 25 g-wt, I = 10 mA								Nos. in figs. 25-41
	Initial $R_I$ $\Omega \cdot 10^{-2}$	AG-4C		PCT		K-211-3		$\Phi$ П-4		Initial $R_I$ $\Omega \cdot 10^{-2}$	AG-4C		PCT		K-211-3		
		$R_n \cdot \Omega \cdot 10^{-3}$	$\frac{R_n}{R_n}$	$R_n \cdot \Omega \cdot 10^{-3}$	$\frac{R_n}{R_n}$	$R_n \cdot \Omega \cdot 10^{-3}$	$\frac{R_n}{R_n}$	$R_n \cdot \Omega \cdot 10^{-3}$	$\frac{R_n}{R_n}$		$R_n \cdot \Omega \cdot 10^{-3}$	$\frac{R_n}{R_n}$	$R_n \cdot \Omega \cdot 10^{-3}$	$\frac{R_n}{R_n}$	$R_n \cdot \Omega \cdot 10^{-3}$	$\frac{R_n}{R_n}$	
Au 99,99	0,3	—	—	3,9	13,0	—	—	—	—	0,14	—	—	2,2	15,7	—	—	1
Au+3% Zr	2,8	2,8	1,0	4,25	1,52	5,0	1,79	2,0	0,72	1,78	2,2	1,23	2,75	1,54	2,2	1,23	2
Au+16% Pd	1,0	—	—	1,0	1,0	—	—	—	—	0,85	—	—	0,95	1,12	—	—	3
Au+5% Ni	1,8	2,4	1,3	3,7	2,06	—	—	—	—	0,76	1,72	2,24	3,6	4,73	—	—	4
Ag 99,99	0,65	0,6	1,0	4,5	6,9	6,5	10	3,9	6,0	0,6	0,5	2,87	3,2	5,35	4,5	7,5	5
Ag+60% Pd	4,0	—	—	3,2	0,8	—	—	12	3,0	3,3	—	—	2,2	0,67	—	—	7
Ag+20% Pd	1,2	—	—	1,6	1,33	1,4	1,17	7	5,8	0,93	—	—	0,72	0,77	0,8	0,86	6
Pt 99,99	1,9	3,2	1,68	2,25	1,18	—	—	—	—	1,4	2,3	1,64	1,85	1,32	—	—	12
Pt+10% Rh	5,3	—	—	7,0	1,32	6,0	1,13	—	—	3,8	—	—	5,4	1,42	4,3	1,13	13
Pt+10% Ir	6,5	—	—	1,1	0,17	12	1,85	—	—	4,8	—	—	0,62	0,13	9,8	2,04	8
Pt+10% Pd	6,0	—	—	1,8	0,3	—	—	—	—	3,3	—	—	0,86	0,26	—	—	10
Pd 99,99	1,5	—	—	1,5	1,0	1,5	1,0	24	16	0,7	—	—	0,68	0,97	0,65	0,93	11

 $\Pi = P$ ;  $\mu = I$

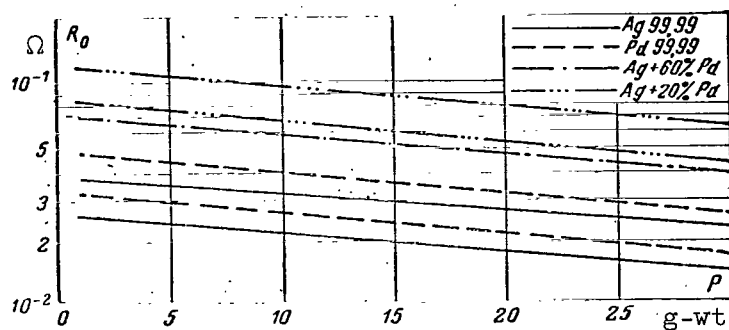


Figure 8.  $R_0 = f(P)$  when  $I = 1 \mu A$  for initial samples.

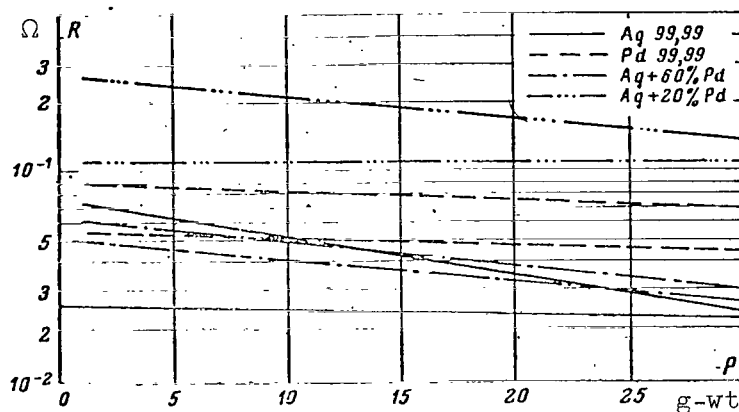


Figure 9.  $R_0 = f(P)$  when  $I = 10 \text{ mA}$  for initial samples.

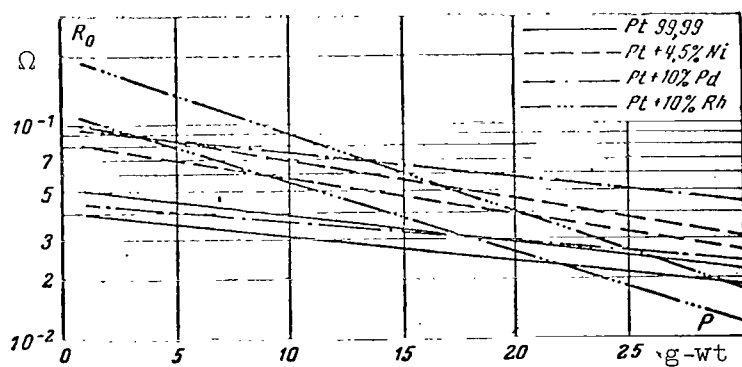


Figure 10.  $R_0 = f(P)$  when  $I = 1 \mu A$  for initial samples.

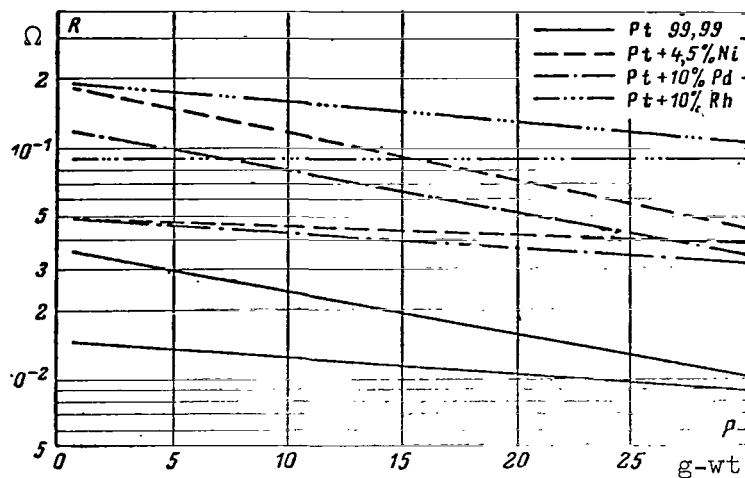


Figure 11.  $R_0 = f(P)$  when  $I = 100 \mu A$  for initial samples.

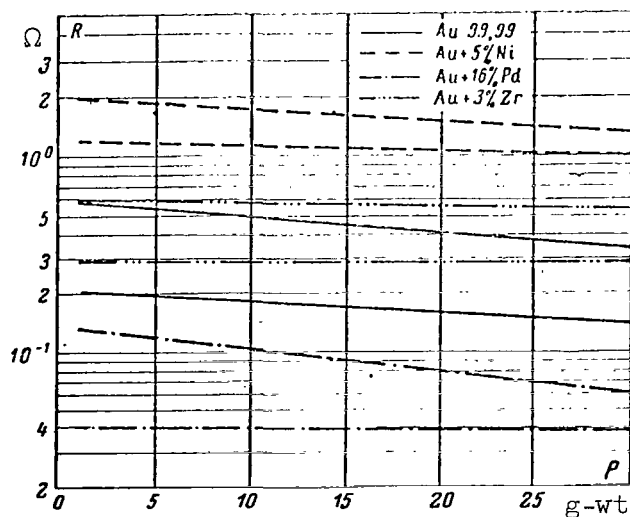


Figure 12.  $R_s = f(P)$  when  $I = 1 \mu A$ .

After the action of  $H_2S$  for a period of 2 days.

less for the Ag+60 percent Pd alloy than for the Ag+20 percent Pd alloy. However, the resistance  $R_s$  of the Ag+60 percent Pd alloy is unstable; it varies considerably depending on the contact pressure and the current.

/355

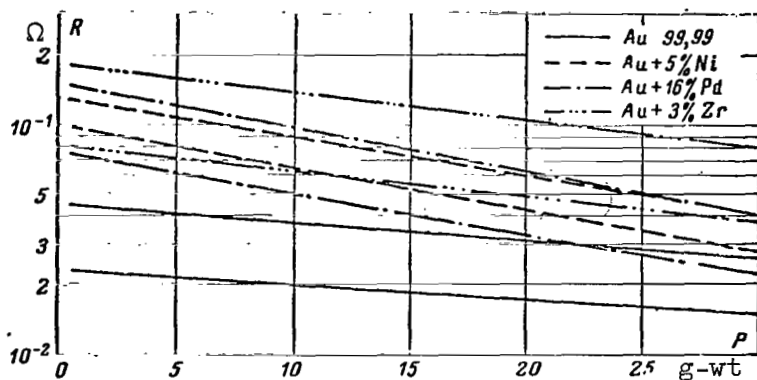


Figure 13.  $R_s = f(P)$  when  $I = 10 \mu A$ . After the action of  $H_2S$  for a period of two days.

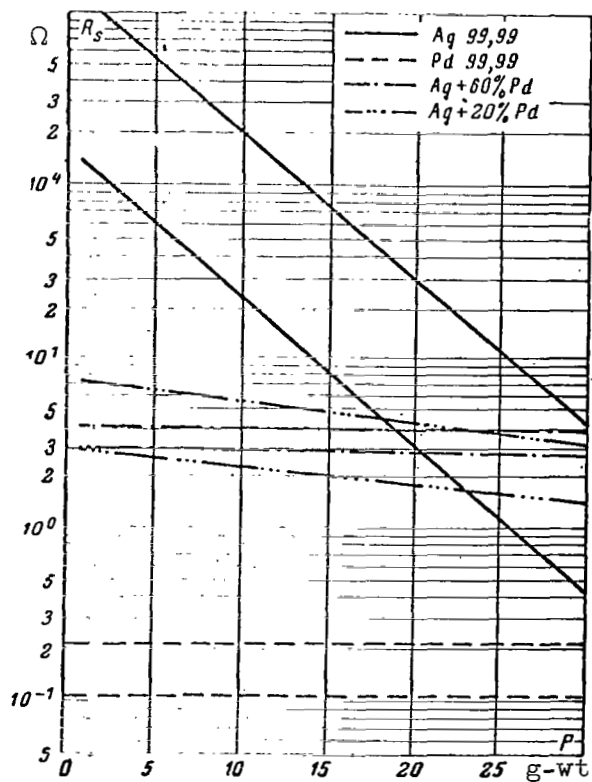


Figure 14.  $R_s = f(P)$  when  $I = 1 \mu A$ . After the action of  $H_2S$  for a period of two days.

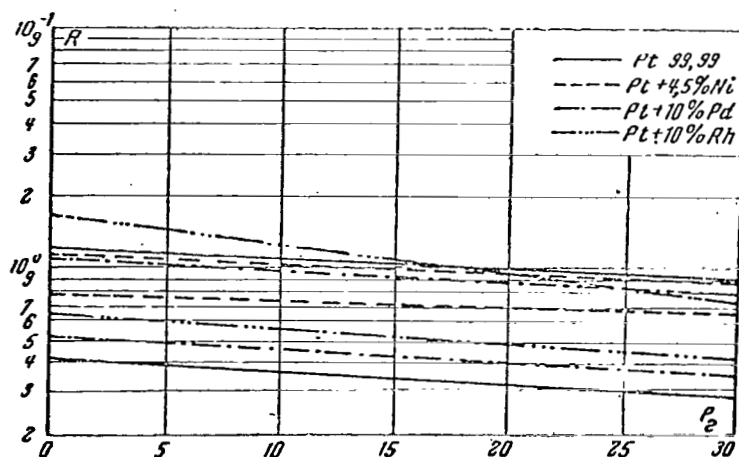


Figure 15.  $R_s = f(P)$  when  $I = 1 \mu A$ . After the action of  $H_2S$  for a period of two days.

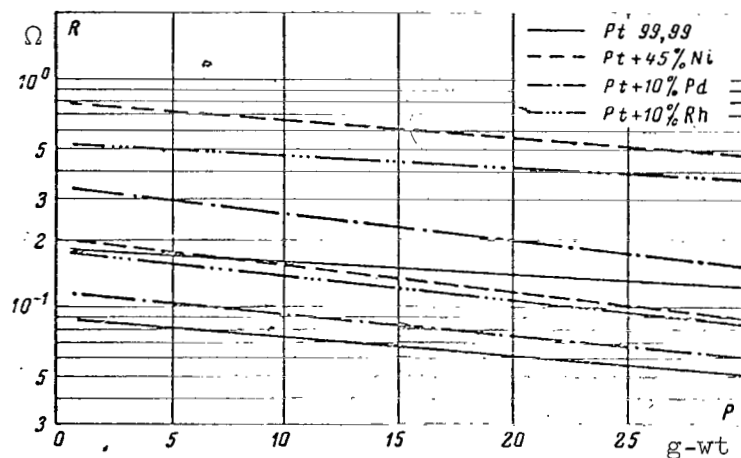


Figure 16.  $R_s = f(P)$  when  $I = 10 \text{ mA}$ . After the action of  $H_2S$  for a period of two days.

For pure palladium Pd, pure platinum Pt, alloys of platinum with nickel Pd+4.5 percent Ni, and platinum with palladium Pt+10 percent Pd, there is a sharp decrease in the value of  $R_s$  when the contact pressure is increased. /356

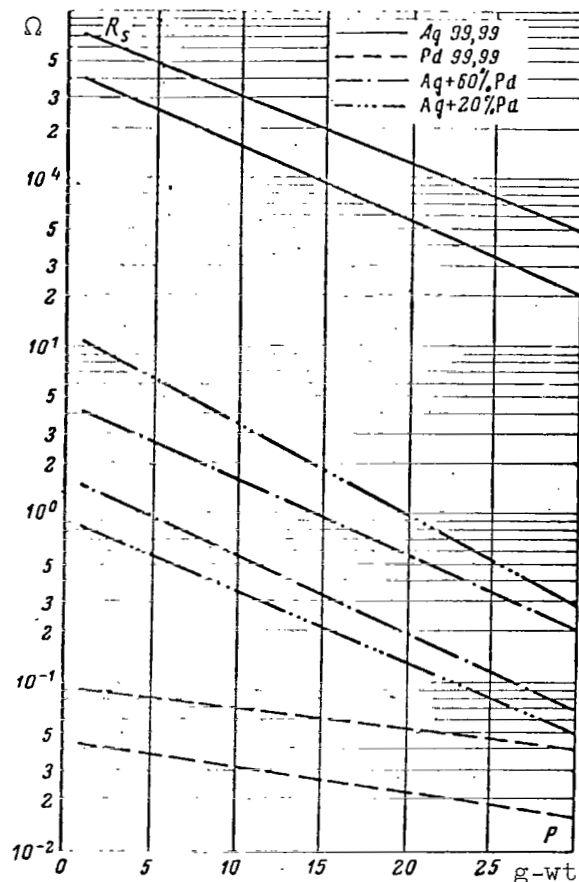


Figure 17.  $R_s = f(P)$  when  $I = 10$  mA.

After action of  $H_2S$  for two-day period.

Unlike these materials,  $R_s$  for the alloy of platinum with rhodium (Pt + 10 percent Rh) is quite stable and depends little on the variation of contact pressure in the range 2-30 g-wt. Apparently this can be explained by the great hardness of the alloy and the high plasticity of the film which is formed on this surface.

Experiments have shown that pure gold (Au 99.99) and its alloys /357  
with palladium, nickel and zirconium (Au + 16 percent Pd, Au + 4.5 percent Ni, Au + 3 percent Zr) are affected less by the action of hydrogen sulfide. The most promising is the alloy of gold with palladium (Au + 16 percent Pd) from the standpoint of contact resistance and stability.

As we can see from table 1, the ratio  $R_s/R_0$  for this alloy is close to unity.

For pure gold the quantity  $R_s/R_0$  is also close to unity; however, resistance  $R_s$  does not have high stability when contact pressure changes, which apparently is associated with the low hardness of this metal. The resistance  $R_s$  of contacts fabricated from an alloy of gold and nickel (Au + 4.5 percent Ni) and of gold and zirconium (Au + 3 percent Zr) is substantially more stable than that of gold contacts (although not to the same degree as for alloy Au + 15 percent Pd).

The function  $R_s = f(I)$  for  $P = \text{const}$  is shown in figures 18 and 19. As we can see from these figures, gold and its alloys, particularly the alloy of gold with palladium (Au + 16 percent Pd) are particularly stable with respect to the value of the contact resistance. The function  $R_s = f(I)$  for gold, for gold-zirconium and for gold-nickel has a slight drop between one and 10  $\mu\text{A}$ ; when the current is increased further, the contact resistance becomes relatively stable.

For pure palladium, pure platinum and its alloys, the magnitude of  $R_s$  decreases when the current increases and becomes stable at currents 1-10

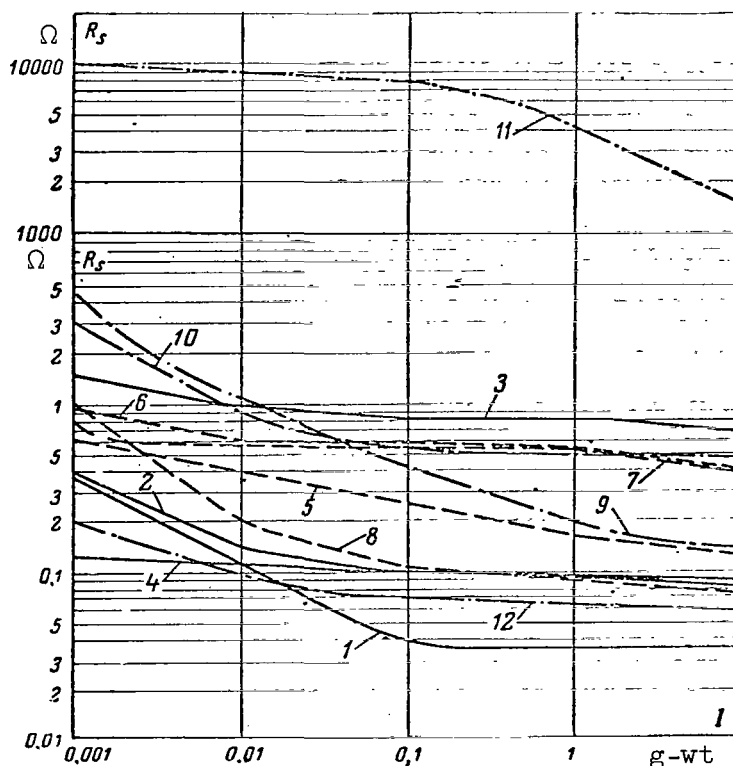


Figure 18.  $R_s = f(I)$  for  $P = 5 \text{ g-wt}$  after action of  $\text{H}_2\text{S}$  for two-day period.



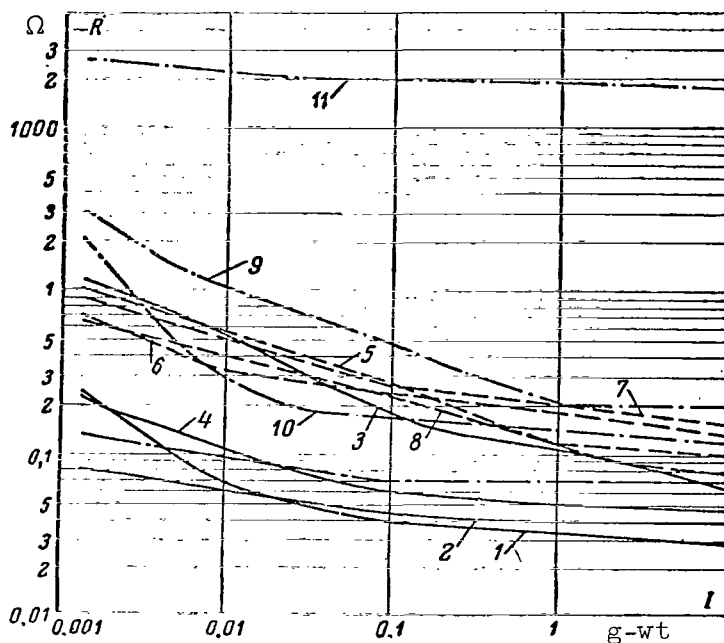


Figure 19.  $R_s = f(I)$  for  $P = 15$  g-wt after action of  $H_2S$  for two-day period.

mA. An exception to this is the alloy of platinum with Rhodium (Pt + 10 percent Rh) whose  $R_s$  becomes stable at currents  $< 10 \mu A$ .

The resistance  $R_s$  of silver alloys (Ag 99.99) and the function  $R_s = f(I)$  for currents 0.001-1 mA, in spite of their large value, are sufficiently stable which is apparently explained by the heavy thickness of the film. A further increase in the current leads to an insignificant decrease in  $R_s$ .

## Conclusions

1. Investigations were carried out with twelve different contact materials in their initial state and after exposure to an atmosphere of flowing humid hydrogen sulfide with concentrations of three mg/l for a period of two days. It was established that contacts which switch low level signals can use only alloys of gold and platinum.

2. The most promising alloy was that of gold with palladium (Au + 16 percent Pd), whose contact resistance remained almost unchanged after it was exposed in the corrosion chamber for a period of two days.

3. Of the gold alloys, that of gold with nickel (Au + 5 percent Ni) and that of gold with zirconium (Au + 3 percent Zr) deserve to be investigated further.

4. Of the platinum alloys, we can recommend the alloy of platinum with rhodium (Pt + 10 percent Rh); however, the contact resistance of this alloy after exposure to the  $H_2S$  medium for a period of two days is almost four times greater than that of the Au + 16 percent Pd alloy.

5. Silver alloys (the system Ag - Pd) and pure silver are entirely unsuitable.

#### The Effect of Organic Vapors in Hermetically Sealed Designs

The problem of the "dry" contact during the switching of  $\mu W$  power circuits has made it necessary to seal the contacts hermetically to protect them from the effects of the surrounding medium. /360

However, hermetic sealing has produced new problems. It has been discovered that prolonged storage and also a cyclic variation of the ambient temperature from a maximum to a minimum produce the degasification of many organic insulating materials which are used in the conventional construction of switching elements. The liberated gaseous by-products and also water vapor, produce harmful concentrations inside the hermetically sealed case which are collected on the surface of the contacts and form insulating polymer films. The transitional resistance of such contacts when they switch currents less than 0.5 A and have a contact pressure of less than 30 g-wt sometimes reaches a value of several  $M\Omega$ , which completely opens the switched circuit.

This defect is eliminated only when the contacts are placed in a completely isolated volume. This solution is possible when new switching elements are designed. The necessity of improving the reliability of designs developed earlier requires a search for a combination of contact and insulating materials which do not introduce these defects.

Investigations were carried out using the contact materials listed above in conjunction with the most widely applied plastics:

- 1) AG-4S OMTU 431-57 plastic
- 2) RST VTUP-121-58 plastic;
- 3) K-211-3 TUMKh P-1386-47 plastic;
- 4) 4 TU 810-59 fluorethylene.

Investigations were carried out in line with operational requirements which involve operation for 1000 hours at the maximum permissible temperature for each plastic material.

Since the 1000 hour tests would be too long, a special method for accelerated thermal aging was developed. The insulating materials listed below can be operated at the specified temperatures: /361

AG-4S (-60 to + 200°C) -- 500 hours at 200°C and 50 hours at 250°C;

K-211-3 and RST (-60 to + 150°C) -- 1000 hours at 150°C and 400 hours at 175°C;

FP-4 (-60 to + 280°C) -- over 1000 hours at 280°C.

The temperature for the accelerated thermal aging was selected so that it did not exceed the permissible short period temperature for a given insulating material.

Because under our conditions the insulating materials must retain their operational reliability for a period of 1000 hours, the following permissible operating temperatures were selected:

AG-4S 175°C;

K-211-3 and RST 150°C;

FP-4 250°C.

Tests were conducted for a period of 178 hours.

The test time was computed by means of the following equation

$$T_0 = T_1 \cdot 2^{\frac{t_1 - t_2}{10}},$$

where  $T_0$  is the useful life of the device in hours;

$T_1$  is the time of accelerated aging, in hours.

$t_1$  is the temperature of the accelerated aging in degrees C;

$t_2$  is the permissible operating temperature, in degrees C.

Plastic test samples were of standard form, were subjected to initial degasification and dehydration by heat treatment and then were placed together with the sample of the contact material into a hermetically sealed volume and subjected to thermal aging.

The ratio of the plastic volume to the volume of air in the hermetically sealed volume was selected as 2.5 based on the construction of the RPS-5 type relay.

Accelerated aging for 178 hours consisted of four cycles. During each cycle the sample was held at the respective permissible temperature for a period of 48 hours and was cooled to room temperature.

In these tests it was determined that the AG-4S, K-211-3 and RST plastics liberate a certain amount of liquid and that AG-4S and K-211-3 plastics liberate substantially more liquid than RST. Fluorethylene-4 did not liberate a noticeable amount of liquid. /362

In the visual inspection of contact material surfaces, it was established that after thermal aging with insulating materials, most of them develop dark spots which can be removed only by mechanical means and by wiping with alcohol. The characteristic forms of the spots on some of the contact materials are shown in figures 21-24. For comparison purposes, figure 20 shows the surface of the initial contact material.

Materials which were aged with the RST plastic developed small light spots which had no effect on the transitional resistance.

The transitional contact resistance of the plane-sphere pair were /363 carried out by means of methods described earlier with the exception that in this case, the spherical contact was made of the same material as the flat test material sample. Variations in the transitional resistance as a function of contact pressure were made with loads from 1 to 30 g-wt and currents from 1 to 100  $\mu$ A and 10 to 500 mA.

Figures 25-29 show the variation in the transitional resistance of the initial test samples  $R_i = f(P)$  and  $R_i = f(I)$ . As we can see, the transitional

resistance of the initial samples is practically independent of the variation in contact pressure in the range 5-30 g-wt. At the same time, a variation in the current from 1  $\mu$ A to 10 mA at constant pressure produces a decrease in the transitional resistance by a factor of 1-2. /364

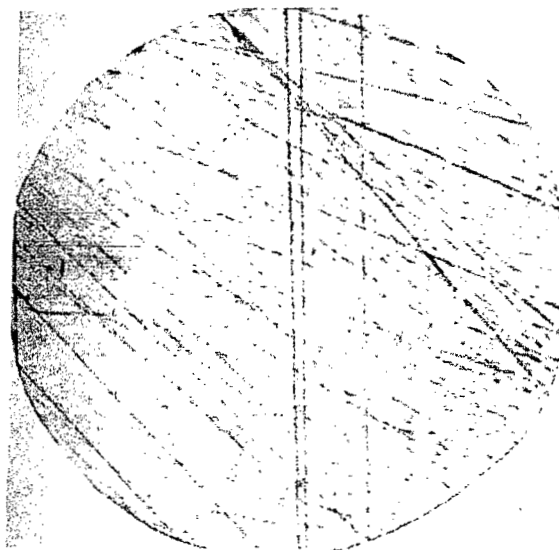


Figure 20. Surface of the initial contact material sample (X 150).

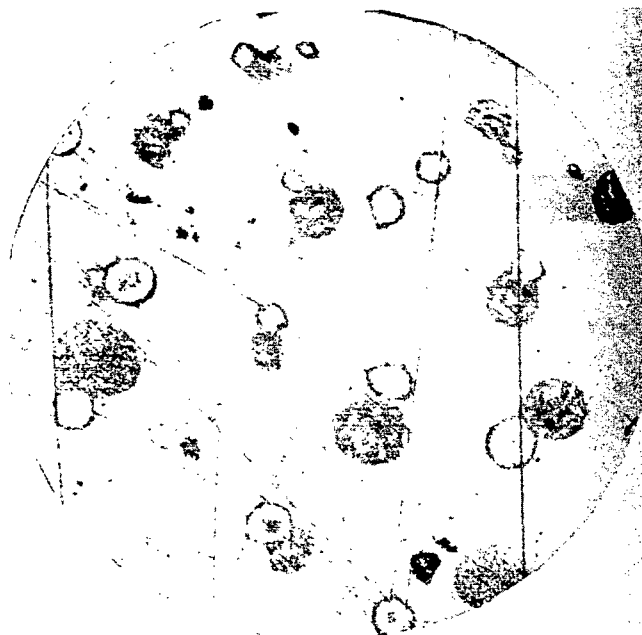


Figure 21. Contact surface of Au + 5 percent Ni after aging with FP-4 (X 150).

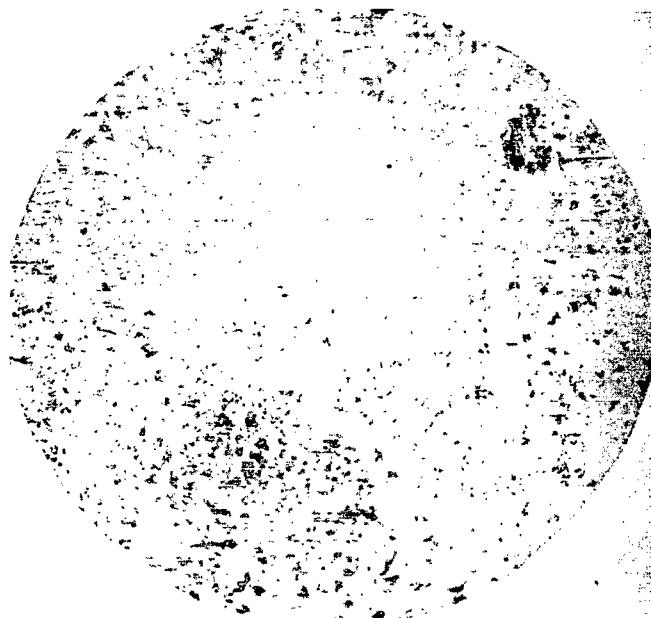


Figure 22. Contact surface of Ag after aging with RST (X150).

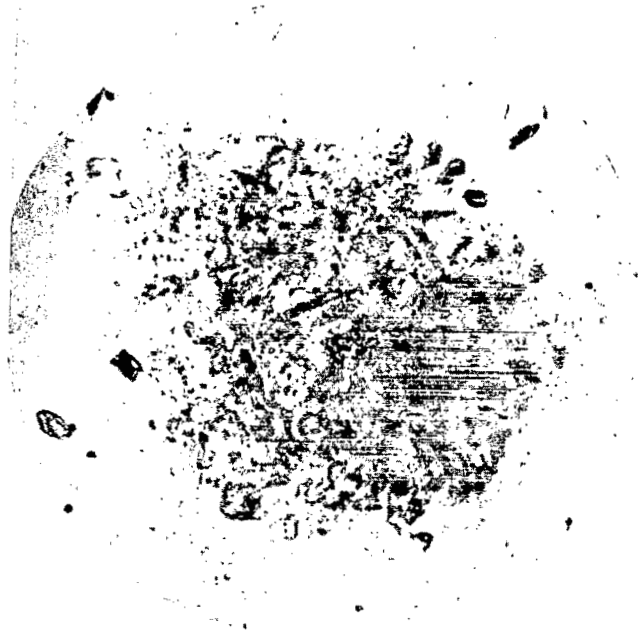


Figure 23. Contact surface of Ag + 60 percent Pd after aging with AG-4 (X 150).

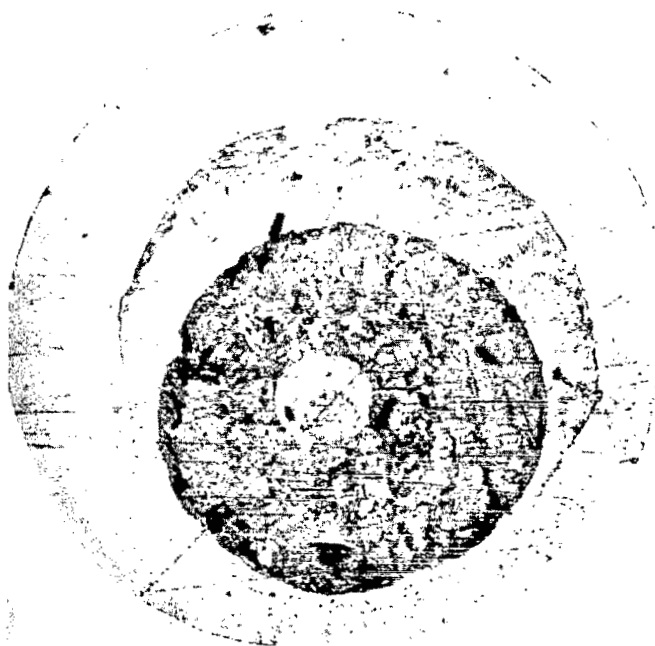


Figure 24. Contact surface of Au + 16 percent Pd after aging with K-211-3 (X 150).

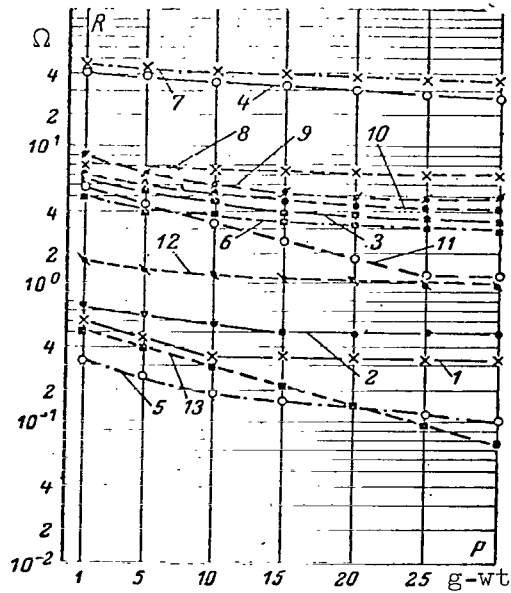


Figure 25.  $R_i = f(P)$  when  $I = 1 \mu A$ .

/367

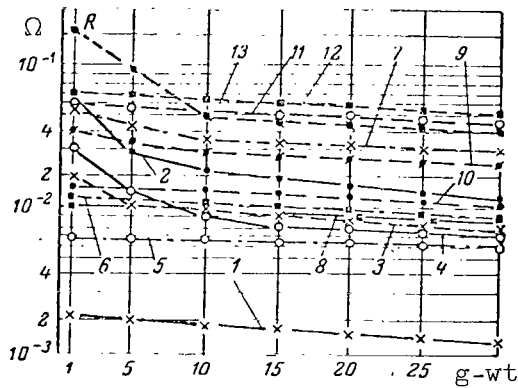


Figure 26.  $R_i = f(P)$  when  $I = 10 \text{ mA}$ .

Tables 2 and 3 show the results produced by volatile materials on the transitional resistance of the contact material. If the resistance of the contact material is greater than one  $M\Omega$ , the table contains a bar.

Figures 30-37 and 38-41 show the graphs of the functions  $R_t = f(P)$  and  $R_t = f(I)$  respectively and the numerical values of transitional resistances for contact materials which developed light spots after thermal aging but

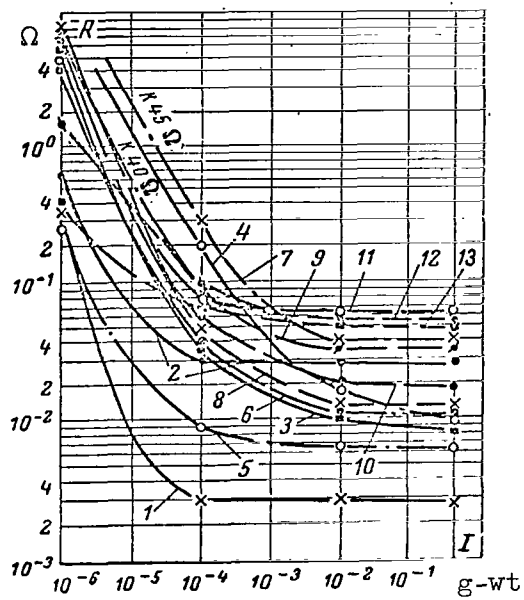


Figure 27.  $R_i = f(I)$  when  $P = 5$  g-wt.

/368

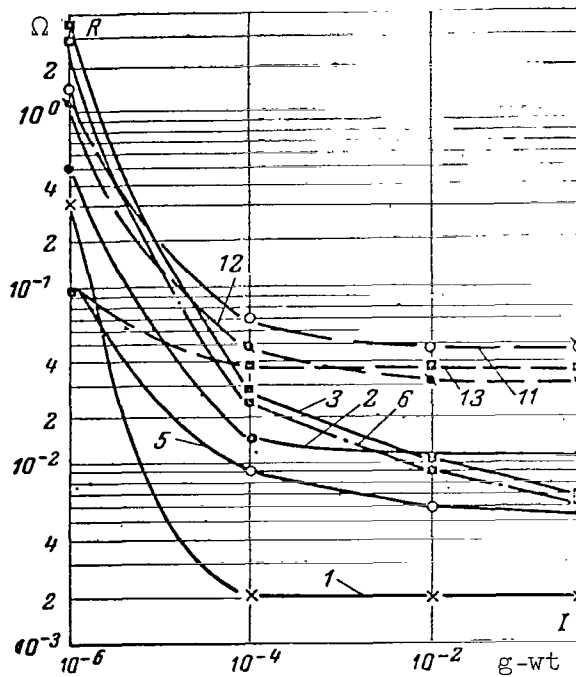


Figure 28.  $R_i = f(I)$  when  $P = 25$  g-wt.



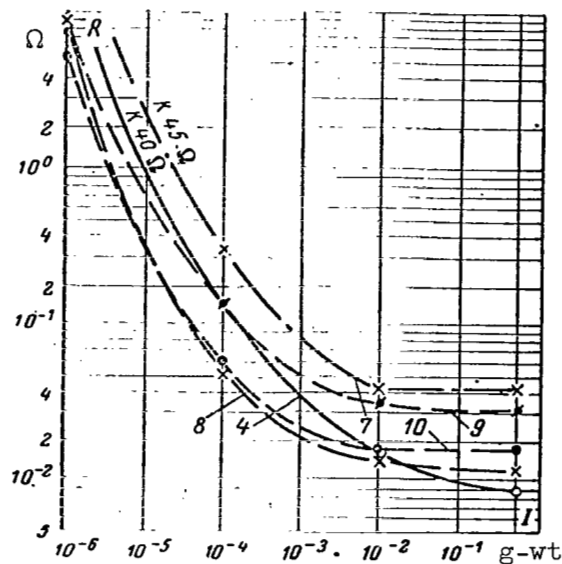


Figure 29.  $R_t = f(I)$  when  $P = 25$  g-wt.

/369

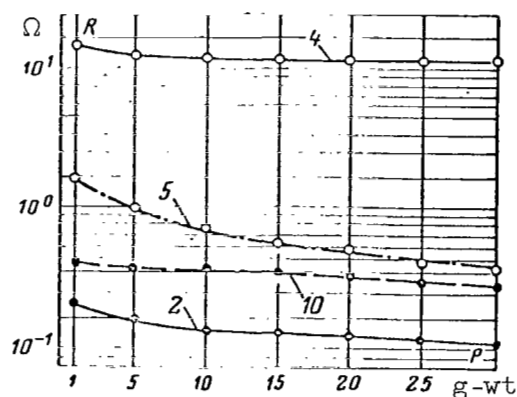


Figure 30.  $R_t = f(I)$  after thermal aging  
with AG-4 with  $I = 1 \mu A$ .

that did not exhibit a substantial variation in the magnitude of the transitional resistance ( $R_t$  is the transitional resistance of the contact material after thermal aging with insulating materials).

From the analysis of functions  $R_t = f(P)$  and  $R_t = f(I)$  we can see

/365

that the minimum transitional resistance (of the order of a fraction of an ohm) with pressures in the range 5-30 g-wt exist for the following contact materials:

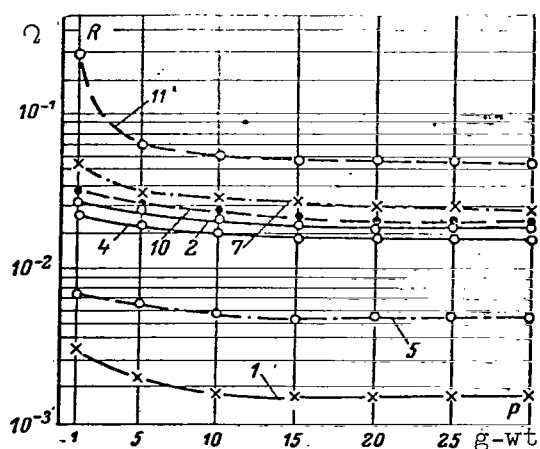


Figure 31.  $R_t = f(P)$  after thermal aging  
with AG-4 when  $I = 10$  mA.

/370

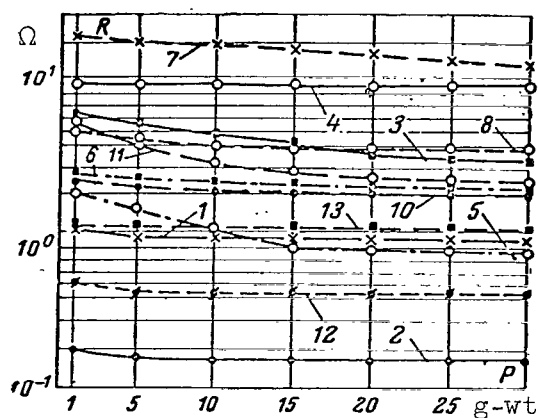


Figure 32.  $R_t = f(P)$  after thermal aging  
with RST when  $I = 1 \mu A$ .

with a current of  $1 \mu A$  after aging with the AG-4C plastic: gold + 3 percent zirconium, silver, platinum;

after aging with RST plastic: gold + 3 percent zirconium; gold + 16 percent palladium; silver; silver + 20 percent palladium; palladium; platinum; platinum + 10 percent iridium; platinum + 10 percent palladium; platinum + 10 percent rhodium;

after aging with the K-211-3 plastic; gold + 3 percent zirconium; silver; platinum + 10 percent rhodium;

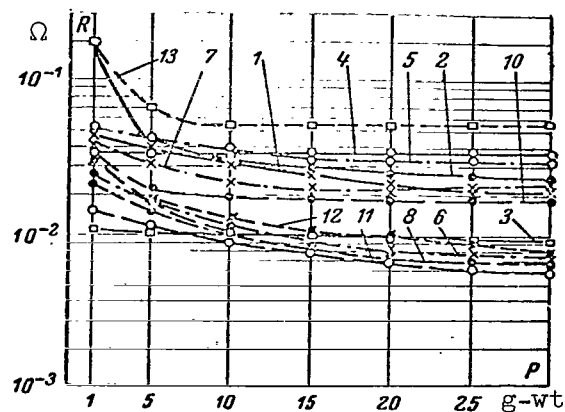


Figure 33.  $R_t = f(P)$  after thermal aging with RST with  $I = 10$  mA.

/371

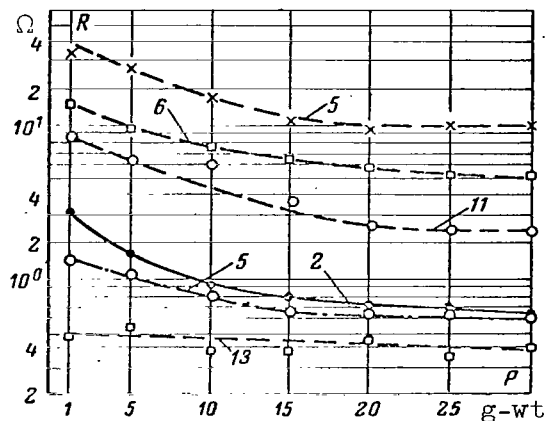


Figure 34.  $R_t = f(P)$  after thermal aging with K-211-3 when  $I = 1 \mu A$ .

after aging with FP-4: gold + 3 percent zirconium; silver;

with a current of 10 mA--all of the above combinations and also silver + 60 percent palladium and silver + 20 percent palladium after aging with K-211-3 and FP-4.

The transitional resistance of the contact pairs of all materials in the region of the spots corresponded to several and even tens of  $M\Omega$  regardless of the value of contact pressure and current. The occurrence of these spots on contacts surfaces is apparently explained by the fact that during the heating of organic insulating materials there is a sublimation of low molecular

/366

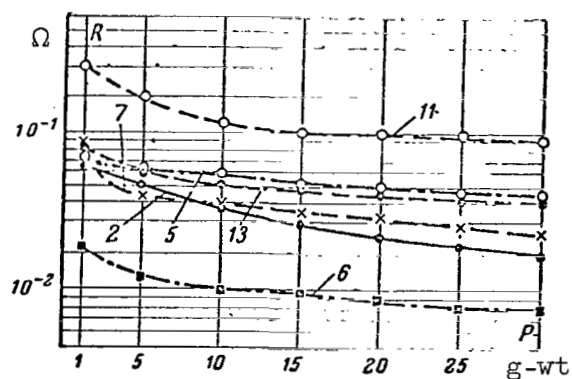


Figure 35.  $R_t = f(P)$  after thermal aging with K-211-3 when  $I = 10 \text{ mA}$ .

/372

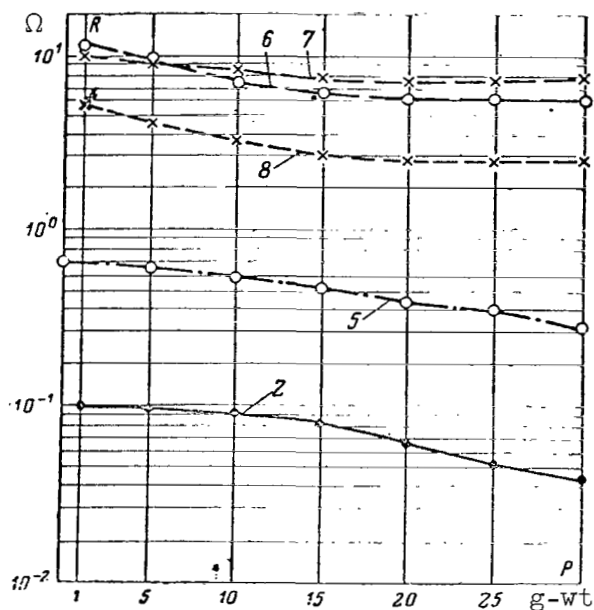


Figure 36.  $R_t = f(P)$  after thermal aging with FP-4 when  $I = 1 \mu\text{A}$ .

compounds and their sorption by the contact materials. Each insulating material produces a definite concentration of volatile substances.

The sorption increases with concentration or pressure and decreases with temperature. When the vapor and gas concentration reach saturation, the products of sublimation begin to condense.

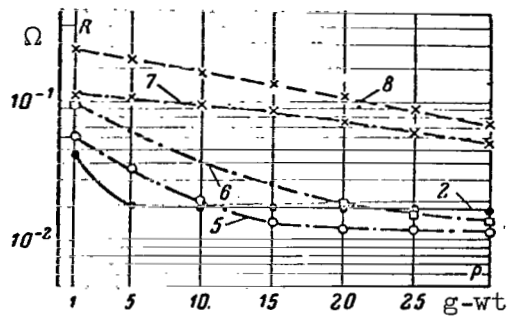


Figure 37.  $R_t = f(P)$  after thermal aging with FP-4 when  $I = 10$  mA.

/373

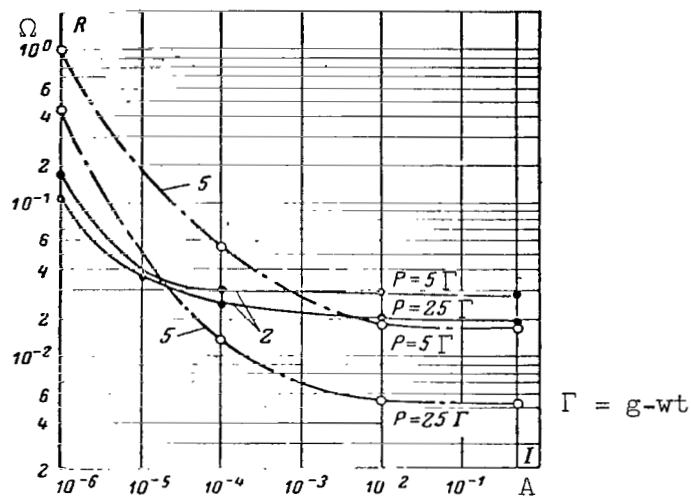


Figure 38.  $R_t = f(I)$  after thermal aging with AG-4.

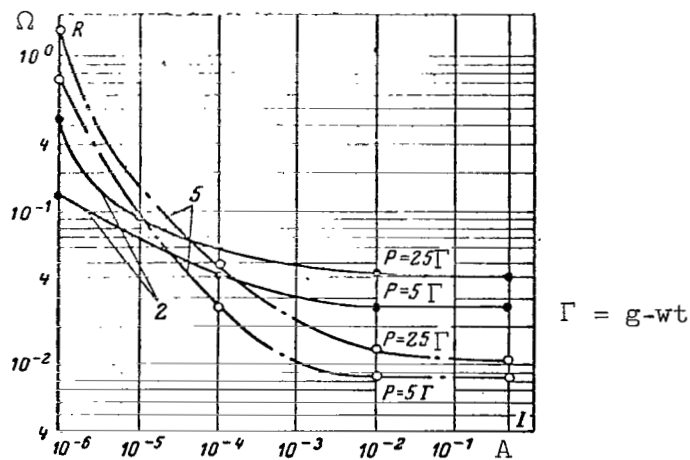


Figure 39.  $R_t = f(I)$  after thermal aging with RST.

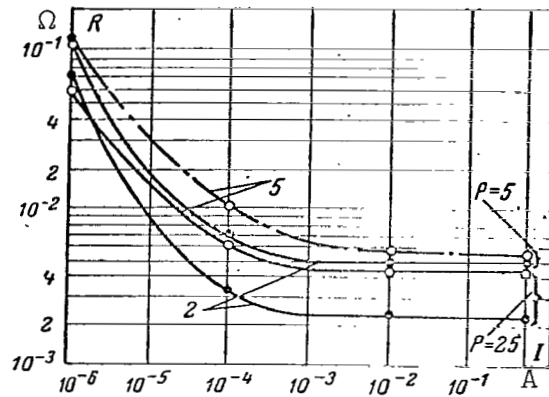


Figure 40.  $R_t = f(I)$  after thermal aging with K-211-3.

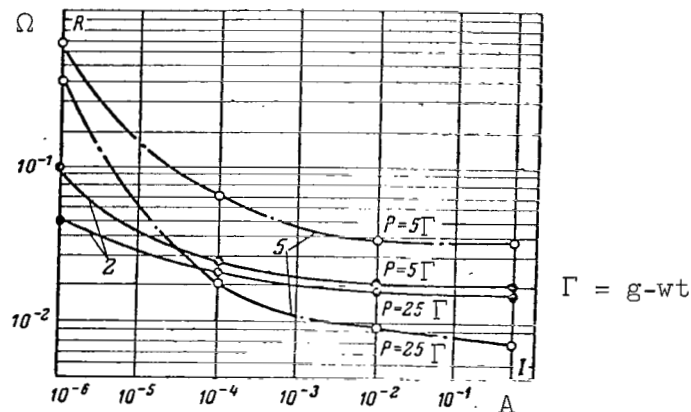


Figure 41.  $R_t = f(I)$  after thermal aging with FP-4.

In addition to this, sorption is determined by the structure and magnitude of the contact material free energy. Consequently, each contact material has definite sorption with respect to a definite gaseous product liberated when the insulating material is heated. /375

On the one hand, the variation in sorption as a function of volatile product concentration may explain the formation of small light spots on the surface of almost all contact materials which are aged with the RST plastic.

On the other hand, the absence of spots on such materials as silver and gold + 3 percent zirconium after thermal aging with almost all the insulating materials may be explained by the lowering of the sorption of these contact materials with respect to the sublimation products.

## Conclusions

1. Insulating materials AG-4C, K-211-3, RST and FP-4 liberate volatile products during aging and during the cyclic action of temperature. In hermetic constructions, these products are sorbed on the surface of the contacts.

2. The surfaces of some contacts retain polymer deposits in the form of individual spots whose transitional resistance reaches several tens of megohms. /376

3. In the case of contact materials made of silver and gold + 3 percent zirconium used in conjunction with the insulating materials, thin films are formed whose transitional resistance is not greater than a few tenths of an ohm. They can be recommended for switching elements.

## REFERENCES

1. Ryazanov, V. A. (ed.) The Maximum Permissible Concentration of Atmospheric Contaminations (Predel'no dopustimaya kontsentratsiya atmosferykh zagryazneniy) No. 3, Medgiz, 1957.
2. Astaf'yev, A. V. The Surrounding Medium and the Reliability of Radio Equipment (Okruzhayushchaya sreda i nadezhnost' radiotekhnicheskoy apparatury). Gosenergoizdat, 1959.
3. Rudnitskiy, A. A. Thermo-electric Properties of Precious Metals and Their Alloys (Termoelektricheskiye svoystva blagorodnykh metallov i ikh splavov) Izd-vo AN SSSR, 1956.
4. Troitskiy, V. S. The Theory of Measuring Small Signals (K teorii izmereniya malykh signalov) Izd-vo AN SSSR, 1951.
5. Howard, O. M. Fontana, V. J. Miniature Multiple-sided Capsules for Switching (Miniatyurnaya mnogostoronnyaya kapsula dlya pereklyucheniya). Transactions of the Conference on Electronic Components, Philadelphia, 1959.
6. Holm, T. Electric Contacts (Elektricheskiye kontakty) I. L. 1961.
7. Savel, J. Translation of a Czechoslovakian article appearing in the Journal "Slaboproudny obzor" 1954, Vsesoyuznyy Institut Nauchnoy i Tekhnicheskoy Informatsii (VINITI), 1958.

## ELECTROPLATING OF SWITCHING CONTACTS

S. Ya. Grilikhes and D. S. Isakova

The reliability of switching devices used in communications equipment is determined primarily by the quality of contact pairs. The resistance to wear, the magnitude and the stability of the transitional resistance are associated with the construction and materials of the contacts and with operating conditions. In relay engineering, contacts are made primarily of metallurgical alloys or cermet compositions based on the platinum group of metals. In other cases, for example in the case of switches, contacts are made of light metals and are covered with a plating of precious metals, primarily silver. However, the possibilities and achievements in the field of plating make its wider application feasible. /376

Along with its positive properties, first of all low specific and transitional electric resistance, silver has a series of disadvantages. These include low resistance to wear and an affinity for sulphur compounds. The latter produces a sulfide film on the metal which increases the transitional resistance. Gold is most resistant to corrosion but this metal, in addition to its high cost, is soft and has low resistance to wear.

Metals of the platinum group--palladium, rhodium and ruthenium--have better mechanical properties. The first two of them have been used in recent years as plating materials for the contacts of certain types of switches while ruthenium has not yet found a practical application.

In addition to these metals, their alloys can be separated electrolytically. This makes it possible to obtain plating with good mechanical properties and to simultaneously decrease the consumption of precious metals.

The recommendations published in the literature on the methods of plating with precious metals are concerned primarily with technological problems associated with the formation of smooth, dense deposits. The selection of the electrolysis conditions is not associated with the mechanical and electric properties of the deposits which are most significant for the operation of the contacts. This problem has received attention in the literature only quite recently.

The present work considers the refinement of the technology for plating contact elements with precious metals and considers some of their electric and mechanical properties.



## Methods Used in the Present Work

Samples were plated and subsequently tested for resistance to wear and for the value of the transitional resistance. The thickness of the plating in all cases, unless otherwise specified, was three microns.

The transitional resistance was determined as the resistance of /378 a point contact of two brass rods with a diameter of 1.2 mm operating at 6 V and carrying a current of 25 mA. Figure 1 shows the schematic diagram of the device used for measuring the transitional resistance. The brass rods which were plated were placed perpendicular to each other and had free contact at a point. The ends of the rods were secured in the holders of the device. Pressure at the contact point was achieved by a weight and was controlled with a grammer. The voltage drop across the samples and the reference resistance was measured with a PPTN-1 potentiometer.

A special setup was designed and constructed for testing the platings for resistance to wear.<sup>1</sup> Brass rods with a 2 mm diameter and plated upper surfaces were fixed in the upper and lower holders such that the rubbing pair made a point contact. The upper holder was subjected to reciprocating motion at an angle of 30 degrees. The resistance to wear was determined by the duration of abrasion process until the base metal was exposed. This was determined by means of a color chemical marker. The platings were subject to abrasion without any current passing through them, i.e., under conditions of pure mechanical wear and also by using dc and ac currents of various values. Another series of experiments was conducted with samples displaced in a step-like manner, i.e., the making and breaking of contacts was simulated.

## Plating with Silver and its Alloys

Silver electroplating may be obtained by means of cyanide, iodide /379 and iron cyanide electrolytes. The composition of the electrolytes has little effect on the electric properties of the platings. At low contact pressures there is a slight difference in the transitional resistance which decreases when the contact pressure is increased.

As is well known, silver is a rather soft metal and its resistance to wear is small, which produces a negative effect on the operation of the contacts. To increase the hardness and wear resistance of silver platings, the cyanide, electrolytes contain additions of antimony, palladium, cadmium and nickel (refs. 1 and 2). These metals are included in the deposit and change its properties. A large amount of the alloying component substantially increases the hardness of the alloy but also increases its specific and transitional resistance, which is undesirable for contacts. Some additions (double cyanide of potassium and nickel, cobalt nitrate, molybdic acid, lithium sulfate, etc.) increase the microhardness of silverplating but their action is unstable and, after a short

---

<sup>1</sup>The setup for testing platings for resistance to wear was designed by I. I. Filippovich.

period of time, the microhardness decreases (ref. 3). Obviously such additions are unsuitable for the silverplating of contacts.

In our experiments we used cyanide electrolytes for silver plating which contained additions of antimony, palladium and tellurium in such quantities so that they would have the least effect on the electrical properties of the deposits. The following solutions and electroplating conditions were used:

I.	Silver (converted to metal)	20 g/liter
	Potassium antimonate	10 "
	Potassium cyanide (free)	25 "
	Potassium hydroxide	3 "
	Potassium carbonate	10 "

Current density 0.25-0.5 A/dm<sup>2</sup>, electrolyte temperature 18-25°C.

II.	Silver (converted to metal)	30 g/liter
	Potassium cyanide (free)	35 "
	Potassium carbonate	40 "
	Potassium tellurite (converted to tellurium)	0.6 "

Current density 0.5-3 A/dm<sup>2</sup>, electrolyte temperature 18-25°C.

III.	Silver (converted to metal)	18 g/liter	<u>/380</u>
	Potassium cyanide (free)	20 "	
	Ammonium chloride	16 "	
	Palladium chloride	1.8 "	

Current density 0.5-1.0 A/dm<sup>2</sup>, electrolyte temperature 18-25°C.

The introduction of the above additives produces an increase in the microhardness of the electrolytic deposits. Silver precipitated from a cyanide electrolyte has a microhardness of 85 kg-wt/mm<sup>2</sup>. Deposits obtained with the above silverplating electrolytes with antimony had a microhardness of 165-204 kg-wt/mm<sup>2</sup> with an addition of tellurium they had a hardness of 110-136 kg-wt/mm<sup>2</sup> and with an addition of palladium they had a microhardness of 109-120 kg-wt/mm<sup>2</sup>. In each electrolyte the current density cannot be increased because it produces a dark loose plating.

From figure 2 we can see that the transitional resistance of platings obtained by means of electrolytes with palladium and tellurium is almost the same as the transitional resistance of silverplatings. The addition of antimony to the electrolyte produces an increase in the transitional resistance of the deposits.

The comparative testing for mechanical wear of platings obtained /381 by means of electrolytes containing antimony, palladium and tellurium has shown that, in the first case compared with the usual silverplating, the resistance to wear is increased by approximately a factor of two. The deposits were dense and semibright. The addition of palladium and tellurium produces a slight increase in resistance to wear.

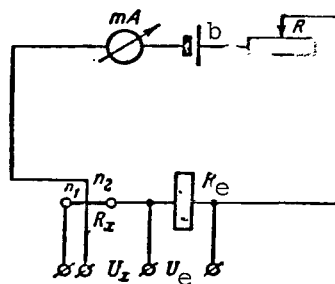


Figure 1. Schematic showing measurement of transitional resistance of electroplatings.

b, battery; mA, milliammeter;  $R_s$ , reference resistance; R, rheostat;  $n_1$ ,  $n_2$ , test sample;  $R_x$ , transitional resistance;  $U_e$ , voltage drop across  $R_e$ ;  $U_x$ ,

voltage drop across the contacts.

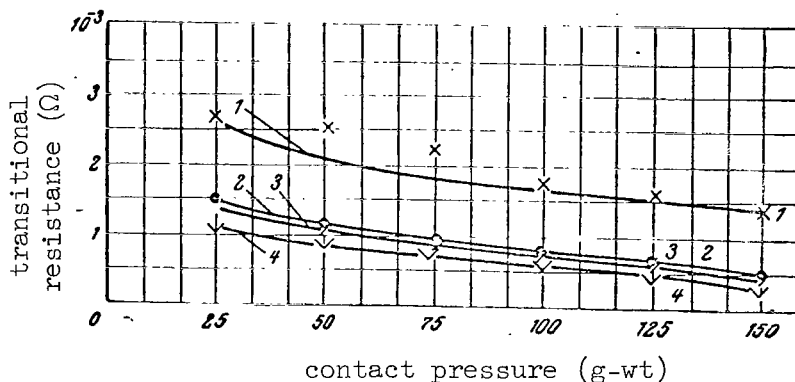


Figure 2. Variation in the transitional resistance of silverplated contacts as a function of contact pressure.

1, Silverplating obtained by means of an electrolyte with an addition of antimony; 2, silverplating obtained by means of an electrolyte with a palladium additive; 3, silverplating obtained by means of electrolyte without additive; 4, silverplating obtained by means of an electrolyte with tellurium.

### Plating with Gold and its Alloys

Gold platings achieved by means of conventional cyanide baths are characterized by low hardness and by resistance to wear. The thickness of the platings affects their quality. If the thickness is greater than  $2 \mu$ , the platings have a loose surface and must be hardened. If they are rubbed with special buffing tools they become dense and bright and their behavior under operating

conditions improves. However, this additional processing does not produce a substantial effect on the mechanical properties of gold plating. Better results are obtained by introducing additives into the electrolyte which are deposited, together with gold, and affect the structure and the composition of the platings. The addition of copper to the cyanide electrolyte produces alloy deposits whose composition may be varied over a wide range. This process has been developed and its application in industry poses no great difficulties.

Gold-copper platings are obtained by using an electrolyte of the following composition (g/liter):

Gold cyanide (converted to metal)	1.5-4.0
Copper cyanide (converted to metal)	3.0-5.5
Potassium cyanide (free)	8-12

Current density 1.5-1 A/dm<sup>2</sup>, electrolyte temperature 45-50°C.

The introduction of even a small quantity of copper into the gold deposit increases the microhardness. For a gold plating the microhardness is 90-100 kg-wt/mm<sup>2</sup>. When the coating contains 10 percent copper it is 190 kg-wt/mm<sup>2</sup>; with 25 percent copper it is 240 kg-wt/mm<sup>2</sup> and with 40 percent copper it is 270 kg-wt/mm<sup>2</sup>. Simultaneously, transitional resistance increases (fig. 3).

Gold-copper alloy plating was used in samples of relays without armatures which were filled with a gas and which operated with a noninductive load. Table 2 shows the comparative results obtained in testing the above platings and also palladium and rhodium platings. These results showed that, under conditions of an inert medium and erosion wear, alloys containing 60 percent gold and 40 percent copper have good stability with low transitional resistance. Relay contacts plated with these alloys were able to perform 10 million operations (ref. 13).

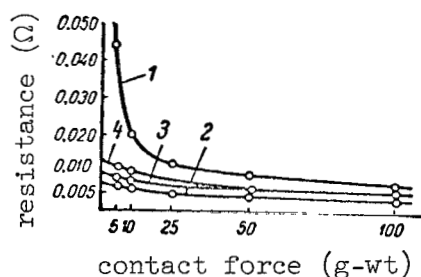


Figure 3. Variation in the transitional resistance of a gold plating and plating of gold copper alloy as a function contact pressure. 1, alloy consisting of 60 percent gold and 40 percent copper; 2, gold; 3, alloy consisting of 90 percent gold and 10 percent copper; 4, alloy consisting of 75 percent gold and 25 percent copper.

## Plating with Palladium and its Alloys

Phosphates and aminochloride electrolytes are used most commonly in industry to deposit palladium. Both solutions make it possible to obtain dense platings and additives make it possible to obtain bright surfaces. At the present time the quality of electrolytic platings made under industrial conditions is determined by their external appearance and thickness. Therefore, there is no information as to which electrolyte should be preferred in the palladium plating of contacts if we want to obtain platings with the best mechanical and electrical properties.

We investigated the microhardness, resistance to wear and transitional resistance of palladium platings obtained from aminochloride and phosphate electrolytes of the following composition:

1.	Palladium chloride	8-12 g/liter	
	Di-derivative sodium phosphate	100-120	"
	Di-derivative ammonium phosphate	20-24	"
	Benzoic acid	2.5-3	"
	Acidity of pH = 6.5-7.5 solution		
2.	Palladium (converted to metal)	18-20 g/liter	<u>/383</u>
	Ammonium chloride	8-10	"
	Ammonia	28-30	"
	Protalbinic acid	0.2-0.4	"
	Acidity of pH = 9.0-9.5		

The phosphate electrolyte was used with a current density of 0.5-0.6 A/dm<sup>2</sup> and a temperature of 70-80°C to obtain platings. If the current density is increased or if the temperature is lowered, the quality of the deposits becomes inferior.

The deposition of palladium from aminochloride electrolyte was carried out with a current density of 0.6-0.8 A/dm<sup>2</sup> and a temperature of 18-20°C. Under these conditions, the current yield is 100 percent, which cannot be achieved with the phosphate electrolyte.

When the aminochloride solution is used, the anode liberates chlorine as well as oxygen which deteriorates the operation of the bath. To eliminate this phenomenon, the anode and cathode spaces were divided by a porous ceramic diaphragm. This stabilized the operation of the electrolyte and deposits of heavy thickness were obtained in it.

A comparison of the properties of the platings obtained with different electrolytes has shown that they are quite diverse. The microhardness of palladium deposits with a thickness of 12-15 μ from the aminochloride solution is 229 kg-wt/mm<sup>2</sup> while from the phosphate solution it is equal to 378 kg-wt/mm<sup>2</sup>. This difference may be associated with the structure of the plating and the internal stresses in it. The internal stresses which occurred during the deposition of palladium in the aminochloride electrolyte were determined by means of a contactometer. The magnitude of the stresses was characterized by the deflection of the horizontally placed cathode which was recorded with an

optical device. It was established that the internal stresses increase with current density, palladium concentration in the solution and the thickness of the plating. One of the characteristic variations is shown in figure 4.

Calculations of the internal stresses in palladium deposits from amino-chloride electrolyte showed that their values are 2000-4000 kg-wt/cm<sup>2</sup>. This is substantially less than the internal stresses in deposits from phosphate electrolyte which, according to data published in the literature, are equal <sup>/384</sup> to 7000 kg-wt/cm<sup>2</sup> (ref. 4). Apparently this situation explains the relatively low microhardness of platings made with aminochloride electrolyte. It also explains the difference in the resistance to wear of palladium platings obtained with the above electrolytes. It is known that when the deposits crystallize with lower internal stresses it is possible to produce platings of substantial thickness. This proposition was confirmed in our case. In the aminochloride electrolyte, heavy platings with a thickness of 25  $\mu$  were obtained.

The PdM-40 palladium-copper alloy has shown good results in relay technology when used for contacts. Information published in the literature (ref. 12) pertains only to the deposition of these alloys in powder form which, of course, is unsuitable for the fabrication of contacts. A combined deposition of palladium and copper is difficult due to the large difference of potentials for the liberation of these metals from solutions of their simple salts. To make the precipitation potentials close in value, solutions of complex metal compounds were used. Dense deposits of palladium-copper alloys were obtained under laboratory conditions from phosphate-pyrophosphate solutions.<sup>1</sup> Depending

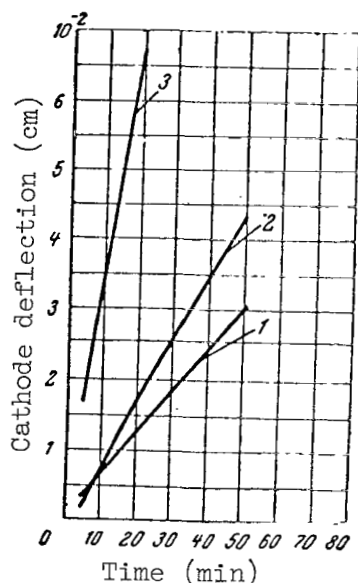


Figure 4. The effect of electrolysis duration on the deflection of the palladium cathode in an aminochloride electrolyte. Current density: 1, 0.5; 2, 0.7; 3, 1.0 A/dm<sup>2</sup>.

<sup>1</sup>Work to obtain platings of the palladium-copper alloy was carried out by L. I. Kulikova.

on the ratio of electrolyte components and the state of the electrolyte, the platings contained up to 50 percent copper. The increase of copper content in the deposit from 20 to 50 percent increases its microhardness from 360 to 432

kg-wt/mm<sup>2</sup>.

### Rhodium Plating

Thin rhodium plating with a thickness up to two  $\mu$  is used to protect /385 silver from tarnishing, to improve the reflective properties of the components, and to increase resistance to wear. Thin plating is unsuitable for contacts operating for a long period of time under high loads or under conditions when mechanical wear is accompanied by erosion wear.

It is difficult to obtain heavy rhodium platings because of the high internal stresses which occur in them and which cause the deposits to crack. In order to lower the internal forces, it has been proposed to introduce selenic acid (ref. 5 and 6), magnesium sulphate (ref. 7) and other special additives into the sulfate electrolyte for plating with rhodium. Reid (ref. 8) showed that when selenic acid is added to the sulfate electrolyte, tensile stresses first occur in the rhodium deposits which then decrease and are transformed into compressional stresses and approach a zero value at a definite plating thickness. When the internal stresses are at a minimum, dense platings of heavy thickness without cracks are obtained. V. I. Layner (ref. 9) notes that the beneficial action of selenic acid is more pronounced at high concentrations in the solution of rhodium and sulphuric acid.

When the rhodium electrolyte is prepared and used, impurities consisting of chlorine, copper, zinc, tin and iron ions may fall into it. Our experiments have shown that even if traces of chlorine are present in the solution, the platings become of the large crystal type, brittle and with cracks. Concentration of copper, zinc and iron make the electrolyte inoperative. The current yield is reduced, the deposits become dark with a brown shade and brittle. To prevent chlorine from entering the solution, it is necessary to wash rhodium hydrozides thoroughly when the electrolyte is being prepared. The pickling of components before plating should be carried out only in diluted sulphuric acid.

If a substantial amount of metal impurities is accumulated in the solution, it is necessary to regenerate the electrolyte completely and to reduce rhodium to its metallic state.

In our efforts to obtain thick rhodium platings we tried the following solutions: /386

I. Rhodium (converted to metal)	8-10 g/liter
Sulphuric acid	100-150 "
Magnesium sulphate	40-50 "

Current density 0.2-0.5 A/dm<sup>2</sup>, temperature of electrolyte 55-60°C.

II. Rhodium (converted to metal)	3-20 g/liter
Sulphuric acid	80-150 "
Selenic acid	2-7.5 "

Current density from 0.3 to 1.0 A/dm<sup>2</sup>, temperature of electrolyte 55-60°C.

Electrolyte I produced bright rhodium platings with a thickness up to 10 μ. Their microhardness was 600-700 kg-wt/mm<sup>2</sup>.

In electrolyte II, with increased current density and increased rhodium concentration, the current yield decreased. The introduction of selenic acid increased the current yield. The platings made with electrolytes containing selenic acid are of fine crystalline structure, and are light and less brittle. An electrolyte containing 15-20 g/liter of rhodium and 2-5 g/liter of selenic acid produced deposits with a thickness up to 25 μ.

#### Ruthenium Plating

The physical and mechanical properties of ruthenium are as good as those of palladium and rhodium and some of its chemical properties are better. However, there is almost no information on the industrial application of ruthenium platings. Patent literature (ref. 10 and 11) on ruthenium plating recommends electrolytes based on ruthenium nitrosohydroxide which make it possible to obtain platings with a thickness of 0.1-2 μ, which is quite suitable for contacts. The above references give no information on the method of preparing the electrolyte solutions, which makes it impossible to obtain and apply these platings. The absence of available soluble compounds of ruthenium necessitates the use of metallic ruthenium for preparing the electrolyte which makes the problem even more complex.

In our experiments to convert ruthenium into soluble form, it was fused with alkali hydroxide and potassium nitrate. The ruthenates obtained in this manner were processed in a special chemical manner and converted into 387 ruthenium hydroxide or ruthenium nitrosohydroxide, which was used to prepare the electrolytes.

We prepared the nitrosochloride electrolyte recommended in the literature and a new sulphate electrolyte which we developed for ruthenium plating:

I. Ruthenium nitrosotrichloride (converted to metallic ruthenium)	4-8 g/liter
Sulphuric acid	15-25 "
II. Ruthenium (converted to metal)	3-6 g/liter
Sulphuric acid	100-150 "

In electrolyte I, the current density was 1-1.5 A/dm<sup>2</sup>, while in electrolyte II, it was 2-2.5 A/dm<sup>2</sup>. In both cases, the temperature of the solutions was 60-70°C.



From the standpoint of industrial ruthenium plating, the advantages of the sulphate electrolyte should be considered. It permits easier-to-prepare, higher current densities.

The above electrolytes were used to obtain ruthenium deposits with a thickness up to  $6\ \mu$ . When the thickness is  $3\ \mu$ , the platings are bright and have a high reflective capacity, they do not tarnish during prolonged exposure to air but, as we shall see below, show no advantages in mechanical properties compared with palladium and rhodium.

#### Transitional Resistance and Durability of Platings

The curves in figure 5 show the variation in the transitional resistance of silver, palladium, rhodium and ruthenium platings. In all cases, the transitional resistance of the platinum group is higher than that of silver. This difference is particularly pronounced at small contact pressures and decreases when the contact pressures increase. The transitional resistance of ruthenium has some advantage over that of rhodium, which has the highest transitional resistance of all investigated metals.

We should pay special attention to the fact that the transitional resistance of palladium platings obtained from the aminochloride electrolyte are lower than those of platings obtained with the phosphate electrolyte. This difference, which decreases in magnitude, is retained during the entire wide range of contact pressures. This shows that even when pure metals are separated, their electric properties depend on the conditions of electrolysis.

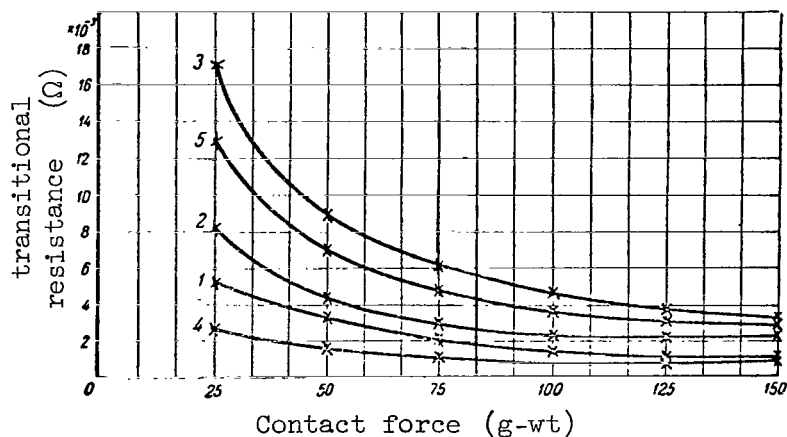


Figure 5. Variation in the transitional resistance of silver, palladium, rhodium, and ruthenium platings as a function of contact pressure. 1, palladium from aminochloride electrolyte; 2, palladium from phosphate electrolyte; 3, rhodium; 4, silver; 5, ruthenium.

Table 1 shows the test results on the durability of palladium and rhodium platings with a thickness of  $3\ \mu$  when the contact pressure is 100 g. Under these conditions, silver platings of the same thickness wear out in 15-30 min. Tests were carried out with making and breaking contacts. The data in table 1 show that electrolytic platings with metals of the platinum group are many times more durable than silver platings. When current is present, the wear of the plating becomes more intense compared with purely mechanical wear, and increases with the current. The most durable plating was of palladium obtained from the aminochloride electrolyte. Platings from the phosphate electrolyte are not quite as good. This situation, together with the data <sup>/389</sup> presented above on the transitional resistance, confirm that the electrolysis conditions have a significant effect on the properties of platings.

TABLE 1 THE DURABILITY OF ELECTROLYTIC PLATINGS UNDER VARIOUS PLATING CONDITIONS

Time of exposure of the basic metal, (hrs)							
ac current							
Type plating	500 mA 125 V 62.5 W	280 mA 75 V 21 W	170 mA 35 V 5.95 W	100 mA 20 V 2 W	50 mA 150 V 7.5 W	175 mA 150 V 26.25 W	Without current
Palladium (from phosphate electrolyte)	2	20	60	120	97	-	240
Palladium (from aminochloride electrolyte)	2	30	100	280	100	73	300
Rhodium (from sulfate electrolyte)	1.5	8	20	65	75	60	-
dc current							
	600 mA, 110 V, 66 W		330 mA, 110 V, 33 W		125 mA, 25 V, 3.325 W		
	anode	cathode	anode	cathode	anode	cathode	
Palladium (from phosphate electrolyte)	0.5	0.5	6.5	7.2	60	120	
Palladium (from aminochloride electrolyte)	0.5	0.5	9.5	18	120	120	
Rhodium (from sulfate electrolyte)	0.5	0.5	2	5	6	23	

Ruthenium platings obtained from the nitrosochloride electrolyte are less durable than rhodium platings. The addition of selenic acid to the sulphate electrolyte for rhodium plating increased the durability of rhodium platings.

Switches with contacts plated with palladium and having a thickness of  $5\text{ }\mu$  were tested together with these samples. With currents 150 V and 100 mA, the contacts lasted for 100,000 switchings while at 250 V and 50 mA they performed 50,000 switchings. The transitional resistance was quite stable. /390

In selecting platings for the gas-filled relay without an armature, as stated above, gold alloys of gold and copper, palladium and rhodium platings of  $5\text{ }\mu$  thickness were tested (ref. 13). Tests were conducted in a nitrogen atmosphere, an AC current of 0.1 A, a power of 2.4 W and with a current of 0.4 A and a power of 9.6 W with making and breaking contacts.

The test results shown in table 2 points to the high stability of platings of rhodium, palladium and alloys of gold-copper containing 60 percent gold. From the standpoint of purely erosion wear, the contacts plated with palladium and rhodium had a higher transitional resistance. The rhodium platings exhibited insufficient stability of the transitional resistance during testing. It is necessary to consider that because the tests were conducted in an inert medium, the surfaces of the contacts were not oxidized. In a conventional atmosphere, oxide films may form on alloys with a large percentage of copper under severe electric operating conditions. In this case it is desirable to use gold or its alloy with a small percentage of copper.

TABLE 2 THE STABILITY OF PLATINGS MADE WITH DIFFERENT CURRENT LOADS UNDER CONDITIONS OF EROSION WEAR

Type plating	Number of operations until a sharp variation in the transitional resistance occurs, in millions of cycles	
	Current loading 2.4 W	Current loading 9.6 W
Gold	8-10	-
Alloy, 90 percent gold + 10 percent copper	12-14	-
Alloy, 75 percent gold + 25 percent copper	14-16	-
Alloy, 60 percent gold + 40 percent copper	15-17	-
Palladium (from aminochloride electrolyte)	10-18	5-8
Rhodium (from sulfate electrolyte)	16-20	8-10

## The Effect of the Surrounding Medium on the Transitional Resistance of the Platings

The medium in which electric contacts operate has an effect on /391  
their transitional resistance. The degree of this effect is determined by the composition of the medium, its temperature, the duration of the contacts in the medium, contact materials and their operating conditions.

We investigated the effect of climatic conditions on gold and palladium platings (98 percent relative humidity at 40°C for a period of 96 h) and also the effect of several organic materials: vapors of the BF-4 cermet, bakelite lacquer, perchlorovinyl resin, 624a nitroenamel (for a period of 1500 h at room temperature).

Increased humidity leads to an insignificant increase in the transitional resistance when the contact pressures are low (fig. 6). Palladium platings obtained from the aminochloride and phosphate electrolytes in this respect behave identically.

Of the organic materials, the 624a nitroenamel, bakelite lacquer and perchlorovinyl resin produce the highest effect. The longer the sample remains in some medium, the greater is the change in its transitional resistance (figs. 7 and 8). The uncompressed gold platings, due to their highly developed surface, have increased susceptibility to the action of the surrounding medium. Therefore, gold coatings must be compressed by special /393  
buffing.

The results of our experiments confirm the high sensitivity of the transitional resistance to the formation of films on the surface of the metal. The electric resistance and mechanical strength of the films depend on the composition of the surrounding medium and on the interaction of the plating material with this medium. Gold has high chemical stability, does not react with organic materials and the layers which form on it due to the condensation of vapors do not have a stable bond with the metal. Palladium, due to its high catalytic activity, may, in some media, produce undesirable reactions and the formation of films on the metal which are more stable. The effect of the operating medium on the transitional resistance of contacts must be taken into account in designing equipment, particularly in the case of hermetically sealed semifinished components.

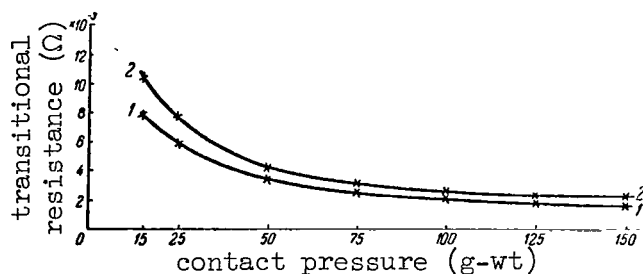


Figure 6. Effect of humidity on transitional resistance of palladium plating. 1, before tests; 2, after spending 96 hours in medium with 98 percent relative humidity.

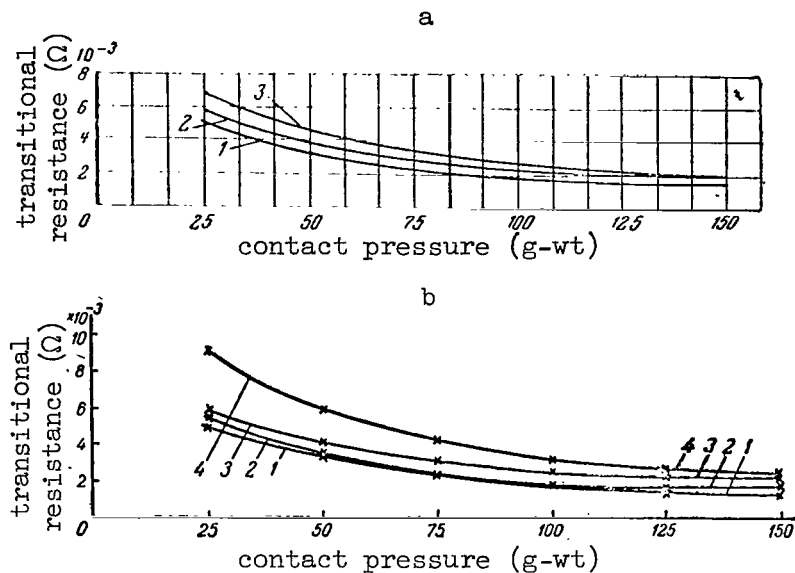


Figure 7. Effect of operating medium on transitional resistance of palladium plating. a, operating medium - bakelite lacquer vapors; 1, before testing; 2, after 130 h of testing; 3, after 1,500 h of testing; b, operating medium - vapors of 624a nitroenamel; 1, before testing; 2, after 130 h of testing; 3, after 237 h of testing; 4, after 1,500 h of testing.

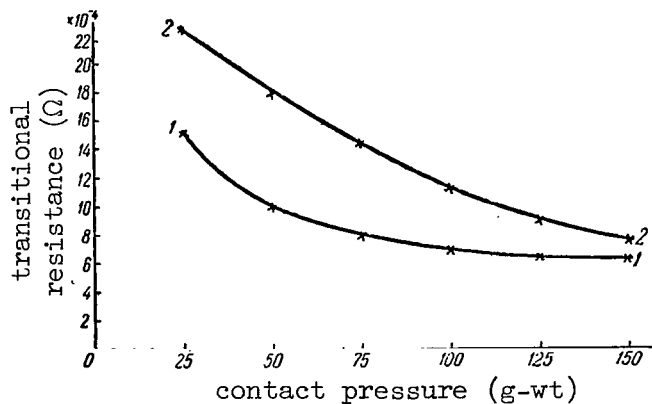


Figure 8. Effect of operating medium on transitional resistance of gold platings. Operating medium, bakelite lacquer vapor. 1, before testing; 2, after 1,500 h of testing.

## Conclusions

1. To increase the operating characteristics of contacts which switch circuits, it is necessary to replace silver platings with platings of the platinum group of metals, which are most stable mechanically and chemically. If we consider operating conditions, economic and engineering factors, palladium will find the greatest application of the platinum group metals.
2. The conditions of electroplating affect the mechanical and electric properties. With this in mind, the palladium plating of contacts should be carried out in an aminochloride electrolyte, because the platings obtained in this case have a higher resistance to wear and have a smaller transitional resistance than deposits from the phosphate electrolyte.
3. In cases when operating conditions prevent the replacement of silvered contacts with others, these should be obtained from electrolytes containing additives which increase the microhardness and the durability of the platings. Antimony may be used as an additive of this type in the cyanide electrolyte.
4. Gold platings, in view of their high chemical stability, should /394 be used in those cases when the contact pressure is low, when the voltage is low and a high reliability of making contacts is required after the contacts have been open for a long period of time. When greater durability is required, the contacts should be plated with an alloy of gold and silver.

## REFERENCES

1. Fedot'yev, N. P., Bibikov, N. N., Vyacheslavov, P. M. and Grilikhes, S. Ya. Electrolytic Alloys (Elektroliticheskiye splavy). Mashgiz, 1962.
2. Vyacheslavov, P. M. Electroplating with Alloys (Gal'vanicheskiye pokrytiya splavami). Mashgiz, 1961.
3. Zimmer, W. Sportleder Ingeborg, Neue Erkenntnisse der galvanischen Hart, Elektrik, 14, No. 8, 1960.
4. Ostroumov, V. V. Mechanical Stresses in the Electrolytic Deposition of Palladium (Mekhanicheskiye napryazheniya v elektroliticheskikh osadkakh palladiya). Zhurnal Fizicheskoy Khimii. Vol. 31, No. 8, 1812, 1957.
5. Reid, F. H. Trans. Inst. Met. Finish, 33, 106, 1957.
6. Fischer J. Galvanische Edelmetallueberzüge, Verlag Galvanotechnik, 1960.
7. U.S. Patent No. 2895889 and 2895890, dated July 21, 1959.

8. Reid F. H. Trans. Inst. Met. Finish, 36, 7430, 1959.
9. Layner, V. I. and Velichko, Yu. A. Electrolytic Deposition of Rhodium, in the Series "Advanced Scientific Technical and Industrial Experience," Protection of Metals from Corrosion, Durable and Decorative Platings (Elektroliticheskoye osazhdeniye rodiya, v serii "Peredovoy nauchno-tekhnicheskoy i proizvodstvennyy opyt," Zashchita metallov ot korrozii, iznosostoykiye, i dekorativnyye pokrytiya). No. 14, Theme 16, No. N-62-131/14 GOSINTI, 1962.
10. U. S. Patent No. 2057638, dated October 1937.
11. French Patent 799251, dated June 1936.
12. Karpova, R. A. Tverdovskiy, I. P. Hydrogen Excess in Dispersed Alloys of Palladium and Copper (Perenapryazheniye vodoroda na dispersnykh splavakh palladiy-med'). Works of GIPKh, No. 42, 1959.
13. Grilikhes, S. Ya., Yevgenova, I. N. and Baykova, I. G. Electrolytic Plating of Contacts, in the Series "Advanced Scientific Technical and Industrial Experience" Protection of Metals from Corrosion, Durable Anti-friction and Decorative Platings (Gal'vanicheskiye pokrytiya kontaktov, v serii "Peredovoy nauchno-tekhnicheskoy i proizvodstvennyy opyt," Zashchita metallov ot korrozii, iznosostoykiye anti-friktsionnyye i dekorativnyye pokrytiya). No. 8, No. M-60-96/8, TsITEIN, 1960.

## ALLOYS OF PALLADIUM WITH TUNGSTEN, RHENIUM, OSMIUM AND IRIDIUM

Ye. M. Savitskiy, M. A. Tylkina, V. P. Polyakova,  
I. A. Tsyganova and Ch. V. Kopetskiy

Alloys of the platinum metals, (platinum, palladium, rhodium, /395  
iridium, osmium and ruthenium) with transitional metals of the V - VIII group attract more and more attention as materials with special physical properties. Their basic positive properties are as follows: high melting temperature, resistance to corrosion in aggressive media, high specific electric resistance and its low temperature coefficient, stability of electric characteristics and good machinability. Among the platinum metals, one of the more interesting and promising ones is palladium. According to the Bulletin of Platinum Metals of the USA, palladium occupies the second place next to platinum in the amount mined. However, it is four to five times cheaper than platinum. Up to the present time, due to insufficient investigation of its alloy properties and the absence of structural diagrams, palladium has not been widely used. However, some alloys of palladium with copper, gold, silver, platinum and iridium are well known and are used in contact, potentiometer and current carrying materials.

In the laboratory of rare metals and alloys of the A. A. Baykov Institute of Metallurgy, investigations have been carried out on the physical and chemical interaction of palladium with the transitional metals of the VI - VIII group of the III long period. Four double structural diagrams have been constructed: palladium-tungsten, palladium-rhenium, palladium-osmium, palladium-iridium, part of a triple diagram palladium-tungsten-rhenium; and certain properties of these alloys have been investigated.

According to modern concepts, the basic factors which determine the interaction of metals are their position in the periodic system, the isomorphism of the crystalline structures, the difference in the values of atomic diameters and in their electronegative properties and difference in melting temperature. The combination of all these factors during the interaction of palladium /396  
with metals of the third long period produces conditions under which a rather wide range of solid solutions with a palladium base are formed.

The structural diagrams of palladium with tungsten, rhenium, osmium, iridium and tungsten-rhenium were first constructed by us using the method of physical and chemical analysis, and are shown in figures 1 and 2. With all four



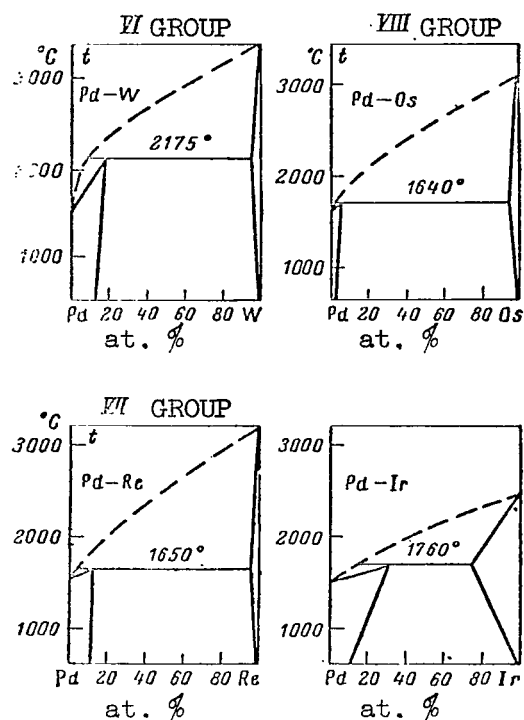


Figure 1. Structural diagrams of palladium with tungsten, rhenium, osmium and iridium.

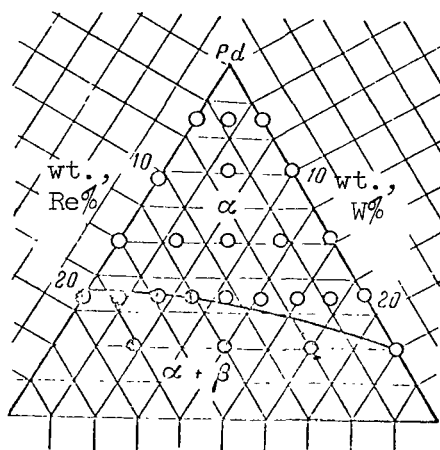


Figure 2. Phase diagram of palladium-tungsten-rhenium system.

investigated metals, palladium forms diagrams of the simplest type with two limited solid solutions. Chemical compounds have not been detected in these systems. All investigated metals increase the melting temperature of palladium. A solid solution with a palladium base is formed directly from the fused mixture and, according to the peritectic reaction  $Zh + \beta \rightarrow \alpha$ , where  $\beta$  is

397

the primary solid solution based on the high melting metal (tungsten, rhenium, osmium, iridium). Tungsten produces the greatest rise in the melting temperature of palladium. Thus, with a 20 percent tungsten content by weight, the melting temperature of the alloy reaches 2,000°C; the temperature of the peritectic reaction in the palladium-tungsten system is 2,175°C.

At temperatures close to temperatures of peritectic reactions of the corresponding systems, we should expect a sufficiently wide region of solid solutions with a palladium base, and the solubility of cubic metals--tungsten and iridium--in palladium (18.5 and 27 percent, respectively, by at.wt) is substantially higher than the solubility of hexagonal osmium and rhenium (1.13 and 12.5 percent by at.wt respectively). According to phase analysis, the region of triple solid solution, palladium-tungsten-rhenium, which are rich in palladium, is narrowed from 25 percent by weight from the palladium-tungsten side to 20 percent by weight from the palladium-rhenium side (fig. 2).

We investigated certain mechanical and electric properties of double and triple system alloys with a palladium base in the region of solid solutions in cast and deformed state. All investigated alloys in the range of solid solutions have sufficient plasticity, which makes it possible to deform them at room temperature. Using the methods of cold-rolling and drawing with intermediate heat treatments, wires with diameters up to 40  $\mu$  were obtained from a series of alloys. We should point out that as palladium is alloyed with high-melting elements of the VI - VIII group, the working of palladium in the cold state becomes difficult. In this respect, the action of hexagonal rhenium is most pronounced, which distorts the cubic lattice of palladium more than the cubic metals, tungsten and iridium. Two phase solutions of these systems are practically impossible to work in the cold state. An exception to this are the alloys of palladium and osmium where the low solubility of osmium produces a negligible hardening of palladium, and the presence of the second phase--solid solution with an osmium base in the form of small inclusions--makes it possible to cold-work the metal and obtain wire with a diameter of 60  $\mu$  by the method of cold-drawing, when there is 20 percent osmium by weight. /398

Solid solutions of palladium with high-melting metals are characterized by the dendrite structure in the cast state (fig. 3b). The diffusion processes take place very slowly in these alloys, and to transform the cast alloys into a homogenous state requires prolonged annealing at sufficiently high temperatures (not less than 500 h at 1,000°C). We should point out that all alloying additives investigated by us produce a decrease in the grain size of palladium. In this respect, the effect of hexagonal metals of osmium and rhenium is particularly pronounced (figs. 3 e and d). Twinings in alloys of palladium with iridium are observed in the annealed state (fig. 3e).

The alloying of palladium with tungsten, rhenium, osmium, iridium and tungsten-rhenium produces a substantial increase in hardness as the amount of additive is increased in the alloy (fig. 4). Maximum hardness occurs in alloys of palladium with rhenium. There is also a sharp increase of hardness in alloys of palladium with osmium. The increase of hardness in alloys of palladium with iridium and tungsten, as the percentage of alloying additive is increased, takes place monotonically and achieves a value of /399

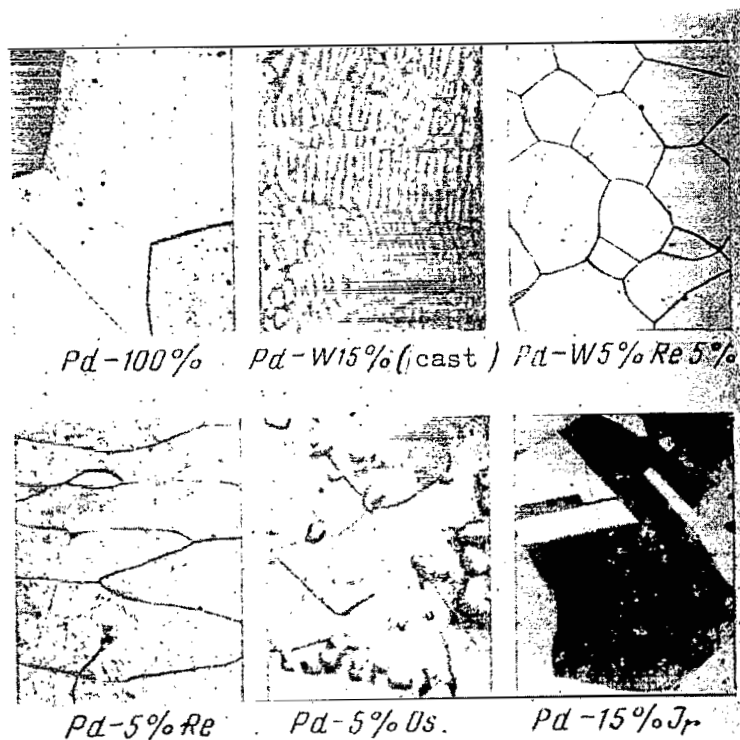


Figure 3. Microstructure of alloys (X 200).  
a, 100 percent palladium; b, 85 percent palladium, 15 percent tungsten, cast,  $\alpha$ ; c, 90 percent palladium, 5 percent tungsten 5 percent rhenium,  $\alpha$ ; d, 95 percent palladium, 5 percent rhenium,  $\alpha$ ; e, 95 percent palladium, 5 percent osmium,  $\alpha + \beta$ ; f, 85 percent palladium, 15 percent iridium,  $\alpha$ .

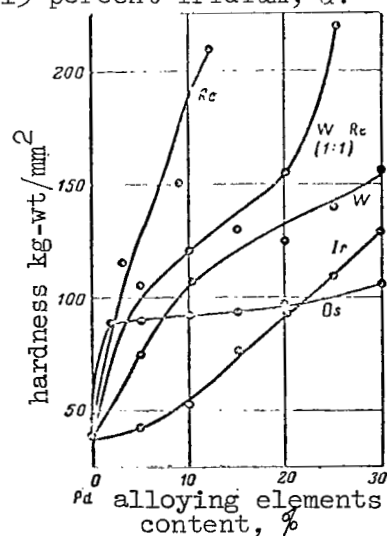


Figure 4. Effect of alloying additives on hardness of palladium.

approximately 120-150 kg-wt/mm<sup>2</sup> at the limits of the solubility of high-melting metals in palladium. Tungsten increases the hardness of palladium more than iridium. In the palladium-iridium system, investigations have shown a substantial variation in the hardness of alloys as a function of heat treatment temperature. Figure 5 shows the variation in the hardness of alloys as a function of quenching temperature. Due to the lowering of the quenching 401 temperature, the hardness of alloys containing 20 and 30 percent by weight of iridium is increased by a factor of 1.5-2. Such variations in hardness are associated with the variations in the solubility of iridium and palladium and with the occurrence of the second phase.

The strength of alloys of palladium with high-melting additives was measured by means of wires with a diameter of 0.2 mm (fig. 6). We should point out that the variation in the tensile strength as a function of the percentage of additive has the same nature as the variation in hardness. The variations in the strength of alloys of palladium with iridium and with tungsten have a more monotonic nature, and the alloying of palladium with tungsten and iridium produces a substantial increase in  $\delta_B$  only when there is a large amount of alloying additive (98 kg-wt/mm<sup>2</sup> with an iridium content of 20 percent by weight).

The alloying of palladium with high-melting metals lowers its plasticity considerably. Thus, with relatively small additions of rhenium and osmium, the relative elongation of these alloys drops sharply compared with pure palladium. However, in alloys of palladium with tungsten, the relative elongation remains sufficiently high--30 percent when the tungsten content is 20 percent by weight. A sharp increase in strength and a decrease in plasticity is observed in alloys of palladium with hexagonal metals.

The introduction of rhenium into palladium radically increases the 402 temperature at which it begins to recrystallize. Figure 7 shows the microstructures of palladium alloys with rhenium which illustrate the processes taking place in the deformed alloys during annealing. As we can see, the fibrous structure corresponding to the deformed state is retained in unalloyed palladium up to 400°C; as the amount of rhenium is increased, the fibrous structure is retained at higher temperatures (with 3.4 percent by weight of rhenium, the temperature is 800°C; with 8.74 percent by weight of 403 rhenium, it is 1000°C). The increase in the content of the alloying element in the alloy slows down the increase in the size of the recrystallized grains. Thus, the size of pure palladium grains after annealing at 800°C is approximately 60  $\mu$ , while in alloys with 3.4 percent rhenium annealed at 1,000°C, it is twice as small, i.e., approximately 30  $\mu$ , while in an alloy with 8.74 percent rhenium it is 18-20  $\mu$ .

The specific electrical resistance (fig. 8) was measured at temperatures of 25 and 100°C, and its temperature coefficient was computed in this interval. We should note that all alloying additives substantially increase the specific electrical resistance of palladium. In the region of solid solutions, the strongest effect is produced by tungsten metal of the VI A group. These results confirm data on the effect of the elements of group VI A on the 404

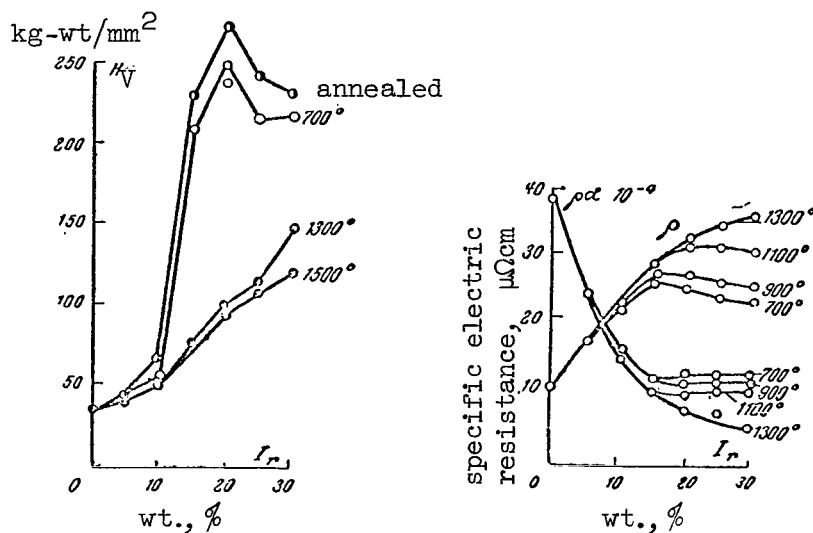


Figure 5. Effect of heat treatment on properties of palladium-iridium alloys.

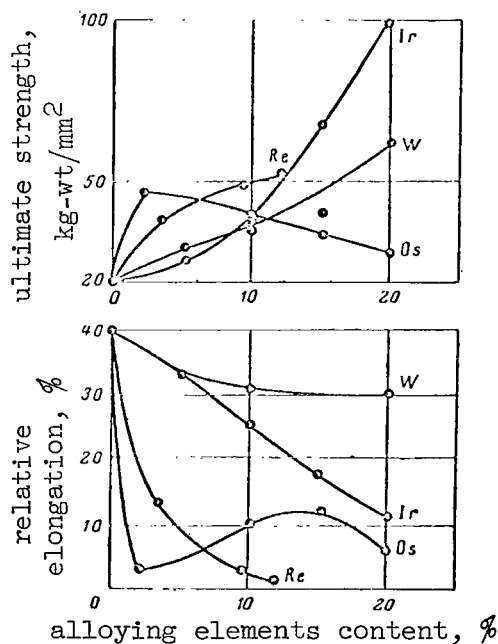


Figure 6. Effect of alloying additives on ultimate strength and relative elongation during tension of palladium.

electrical resistance of palladium, which are known for the first and second long periods. The maximum value of electrical resistance for these alloys is observed in the alloy of palladium with 20 percent tungsten ( $107-110 \mu\Omega\cdot\text{cm}$  with a temperature coefficient  $(4.5-7) \cdot 10^{-5}$ ). The value of the specific

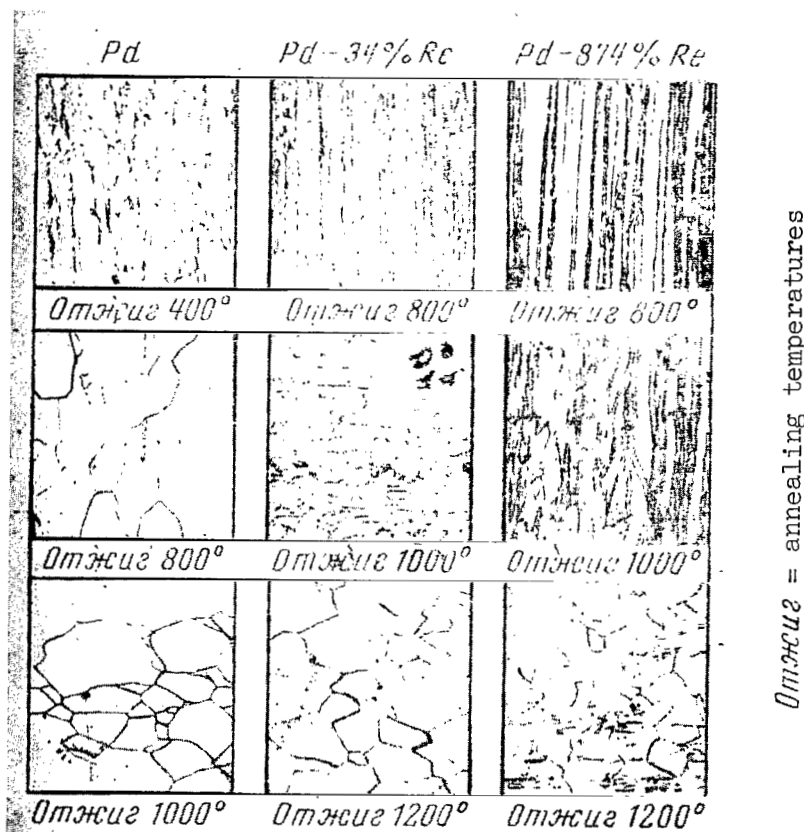


Figure 7. Recrystallization of palladium-rhenium alloys.

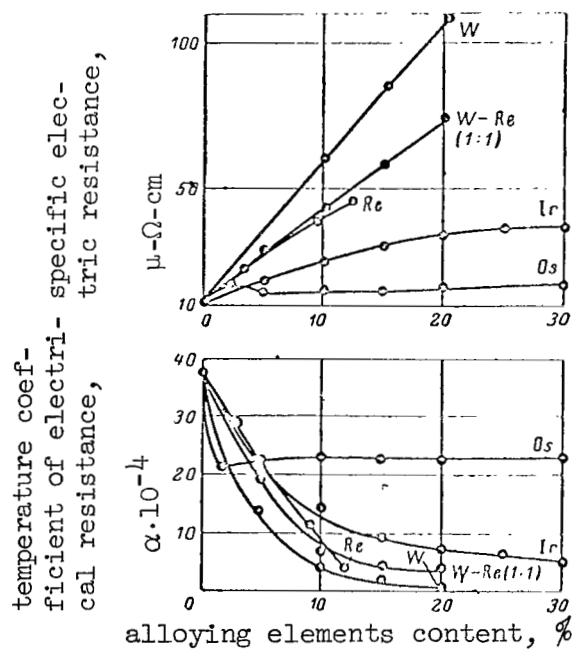


Figure 8. Effect of alloying additives on electrical resistance of palladium.

electric resistance as a function of alloying additive increases gradually. The alloying of palladium with 2 percent osmium produces some increase in the specific electrical resistance and a drop in its temperature coefficient. A further increase in the amount of osmium in the alloys does not produce a change in the electrical characteristics up to 30 percent osmium. This is associated with the presence of the second phase in the alloys and with the low solubility of osmium in palladium. In alloys of palladium with iridium there is a variation in the specific electrical resistance and in its temperature coefficient as a function of temperature (fig. 5). The separation of the second phase in alloys during the lowering of the heat treatment temperature is accompanied by a decrease in the electrical resistance and an increase in its temperature coefficient. Consequently, within the limits of these measurements, the value of electrical properties may be controlled by heat treatment.

The alloying of palladium with high-melting metals of the III long period produces a change in the sign of the absolute thermo-emf in a palladium-copper thermocouple (fig. 9). In alloys of palladium with tungsten and iridium, the maximum thermo-emf is achieved with 15 percent of iridium by 405 weight, while in alloys with rhenium it is achieved with 5 percent rhenium by weight. After this, the thermo-emf decreases. This decrease is particularly effective in the palladium-tungsten system where, in alloys of palladium with 30 percent tungsten, the absolute thermo-emf reaches a value of  $1.8 \mu\text{V}/\text{deg}$ . For alloys of palladium with osmium we should note that there is a sharp increase in the value of the thermo-emf. With 2 percent osmium, the value of the thermo-emf reaches  $2 \mu\text{V}/\text{deg}$ . In the two-phase region (up to 30 percent osmium) the value of the thermo-emf remains constant and is the lowest of all the thermo-emf's of the investigated alloys.

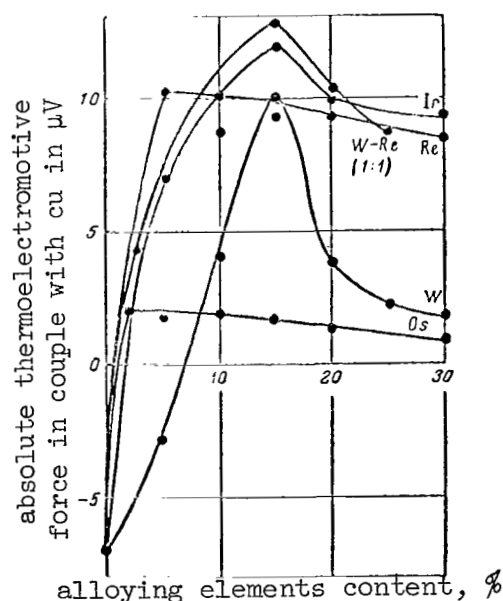


Figure 9. Effect of alloying additives on absolute thermo-emf of palladium and copper pair.

With the mutual alloying of palladium by tungsten and rhenium, alloys in the range of solid solutions have intermediate properties with respect to the boundary two-component systems. We should note that the addition of rhenium to the alloys of palladium-tungsten in the region of solid solutions lowers the melting temperature and the specific electrical resistance and increases the hardness and the temperature coefficient.

The table shows some mechanical and electrical properties of ribbons with a width of  $108\ \mu$  and a thickness of  $15\ \mu$  which were obtained by us in collaboration with Z. A. Timofeyeva (the "Vibrator" plant).

alloy content	% pressing	H kg-wt/mm <sup>2</sup>	$\sigma_B$ kg-wt/mm <sup>2</sup>	E kg-wt/mm <sup>2</sup>	$\rho$ $\mu\Omega\cdot\text{cm}$	Temp $\mu\text{V}/\text{deg}$
Pd+5%W	99.8	91	43	8 985	40	—
Pd+10%W	99.8	154	99.3	15 475	70	—
Pd+15%W	99.8	172	92	17 970	—	—
Pd+20%W	96.8	150—168	—	—	96	+3.4
Pd+15%W+5%Re	96.8	194—199	133	17 472	—	—
Pd+5%Os	99.8	80	50	13 000	15	+3.1
Pd+15%Os	99.8	75	50	13 000	14	+3.1
Pd+20%Os	99.8	85	55	14 200	15	+3.1
Pd+8.7%Re	96.8	126—132	—	—	39.8	+11.5
Pd+5%Re	99.8	90—95	—	—	20.6	+5.11

One of the alloys which is of great interest in modern instrument construction is the high-resistance corrosion resistant PdV-20 alloy of palladium with tungsten (fig. 10). This alloy has high resistance (of the order of  $100\ \text{M}\Omega\cdot\text{cm}$ ) with a rather low temperature coefficient  $(4-5)\cdot 10^{-5}$ , its thermo-emf when paired with copper is  $3.9\ \mu\text{V}/\text{deg}$ ; the transitional resistance of the alloy when paired with silver is  $0.006\ \Omega$  at a pressure of 200 g-wt. The mechanical properties of the alloy are very high: the ultimate strength is  $65\ \text{kg-wt}/\text{mm}^2$  with an elongation up to 30 percent. The alloy has a high resistance to corrosion in a series of aggressive media: ammonia, sulfur dioxide, sea water and others. A slide wire wound with PdV-20 alloy has been operating in an aggressive medium, containing 0.05-0.13 mg of carbon bisulfide, for almost one year without cleaning and contact disruption, whereas the conventional slide wires with manganin windings, operating under the same conditions, require daily cleaning due to the disruption of the contact. The new slide wires increase the operational reliability of the entire device. The high resistance to wear of this alloy provides for a useful life of 10 million cycles, whereas the useful life of the devices using other alloys varies from 60 thousand to 3 million cycles. Some of the properties of this alloy are as good as and some are better than those of the imported "Gera-610" alloy produced by GEREUS (Federated German Republic).





Figure 10. Wire manufactured from PdV-20 alloy and its microstructure.

## Conclusions

This article has considered the physical and chemical inter actions of palladium with the transitional metals of the III long period (tungsten, rhenium, osmium and iridium). With all these metals, palladium forms structural diagrams of the peritectic type with two restricted solid solutions. Chemical compounds were not detected in the systems. The effect of alloying palladium with tungsten, rhenium, osmium and iridium on its properties--hardness, ultimate strength, relative elongation during tension, recrystallization, and specific electric resistance and its temperature coefficient, the absolute thermo-emf when paired with copper, has been considered.

## STABILITY OF ELASTIC ELEMENTS OF COMMUNICATIONS EQUIPMENT AT ELEVATED TEMPERATURES

R. I. Mishkevich

The development of instrument construction and particularly of radio electronics in our nation is closely associated with the utilization of reliable elastic elements, many of which, in addition to high elastic properties, must have a high electrical conductivity. In view of increased severity of environmental conditions in which the devices operate (increased temperature, operation in aggressive media, etc.), the requirements levied on elastic elements have increased sharply. In view of this, the known spring alloys applied for many years have been augmented with new materials based on nickel and on other high-melting elements, which must be used to produce modern instruments. /407

Although spring materials such as brass and bronze have been used for a long time, the literature still contains no data characterizing the stability of their properties during prolonged operation at high temperatures and the possibility of improving these by heat treatment. Maximum operating temperatures for different spring alloys have also not been established. /408 Therefore, random, unsystematic data are used in the design of instruments, including the results of short-term tests, which are frequently carried out under different conditions. In order to establish the possibility of using some alloy for current-conducting contact springs, in relays and switches, etc., it is necessary to have data on its relaxation stability<sup>1</sup> with time and at elevated temperatures, together with data on other properties, and to compare these data with the design requirement.

At the present time the following requirements must be satisfied by current-carrying springs designed for application in new equipment:

(1) high relaxation stability over a wide temperature range (the relaxation of stresses must not be greater than 10 percent at temperatures from -60 to +500°C during 300 h with an initial bending stress up to 50 kg-wt/mm<sup>2</sup>);

(2) low specific resistance (not greater than 0.30  $\Omega \cdot \text{mm}^2/\text{m}$ ); a temperature coefficient not greater than 0.001;

(3) stability of mechanical properties ( $\delta_{\text{stab}}$ ) over prolonged time under the action of a cyclic load ( $N = 10^7$  or more cps) at extreme temperatures;

<sup>1</sup>Relaxation is the change in the magnitude of stress, when the total deformation remains fixed.

- (4) resistance to corrosion;
- (5) freedom from magnetic properties;
- (6) good machinability;
- (7) good soldering properties.

The requirement which is most difficult to satisfy is the high relaxation stability at elevated temperatures involving an insignificant drop in initial stress.

Carbon and alloy steels and also some alloys of light metals, which until recently have been used as basic spring materials, do not satisfy all of these requirements. The new alloys must have very high resistance to heat. The 409 problem of resistance is one of the most urgent problems of modern metallurgy. This problem has been considered for a long period of time, so that there is a large amount of experimental material available giving a sufficiently clear picture of the capabilities of heat resistant alloys with different bases (ref. 1). Thus, the metal bases may be arranged in the following series according to the resistance of their alloys to heat:

Mg-Al-Cu-Ti-Fe-Ni-Co-Mo-W-Nb.

To obtain a heat-resistant spring alloy, it is necessary to select the corresponding base and to alloy it with high-melting elements; the presence of high-melting elements in turn produces an increase in electric resistance and in mechanical strength. When mechanical strength becomes high, machining becomes more difficult. For this reason, and for a series of other reasons, it is difficult to have all of the necessary physical and mechanical properties in the same material.

At the present time, industry produces spring materials which can be used for contact current-carrying springs operating up to a maximum temperature of 350-400°. Developments in technology require that the operating temperature be above 400°C. The search for new alloys must proceed in this direction.

The increase in the reliability of devices using elastic elements depends substantially on whether the stability of these elements can be increased. The stability of elastic elements may be increased by decreasing the magnitude of the active stresses, which is quite difficult because it requires a design change, or new materials, or new methods for heat treatment and mechanical processing.

To solve the problem of using new materials, it is necessary first of all to determine those changes which occur in elastic elements, in particular in relay contact springs due to the application of the load.

It is known that during the operation of springs their characteristics /410 change, the tightness decreases and the contact pressure decreases. The relaxation process is of great practical significance.

It has been determined that the crushing and turning of the units takes place during the relaxation process, i.e., the same processes take place as in the case of small plastic deformation. From the standpoint of dislocation theory, the redistribution of internal energy between the microvolumes leads to the displacement of single dislocations, which overcome the corresponding barriers. If the dislocations do not return to the initial position, irreversible deformation may occur.

Thus, in order to increase the relaxation stability of alloys, it is necessary to create such barriers for the movement of dislocations, which could not be overcome under given conditions. In addition, it is necessary to increase the binding force in the lattice, which increases the friction for retarding the motion of dislocations and also the diffusion activation energy, which hinders the process of dislocations absorption near the grain boundaries.

Work at the present time is being carried out in these directions for the purpose of creating new alloys and new methods of thermal and thermomechanical treatment.

#### Methods of Investigation

In the present work we investigated alloys with a copper base (brass, bronze, German silver) and alloys with a nickel base and a molybdenum base.

The increase in the elastic properties of alloys with a copper base is obtained, as a rule, by plastic deformation (rolling, drawing, etc.); therefore, the alloys are used primarily in a solid state which corresponds to deformation with a 50-60 percent reduction in area. At the same time the elastic properties of brass, bronze and German silver, as shown in a series of works (refs. 2 and 3), are insufficiently high for many applications.

In addition, the elastic properties are characterized by sharp /411 anisotropy, i.e., they depend to a large extent on the direction assumed in punching out members from a sheet, or a ribbon.

At the same time brass and bronze in their deformed (hard) state have an additional capacity for hardening, which may be realized only when heat treatment involves annealing before recrystallization. It has been established that after additional annealing of the deformed alloys, the elastic limit is sharply increased, the magnitude of the residual stresses is decreased and relaxation stability occurs both at normal temperature and when heated. In addition, anisotropy decreases sharply due to heat treatment. Therefore, the investigation of relaxation at elevated temperatures was carried out in the present work using alloys with a copper base, both in the deformed state and in the heat-treated state.

Since these states were unknown, we investigated the effect of temperature and soaking in the course of low temperature annealing on the elastic properties of the alloys (Young's modulus and elastic limit), determined at room temperature (using equipment furnished by MVTU), and the effects of temperature on relaxation stability at elevated temperatures. From this work the optimum low temperature annealing states were established.

As a rule, alloys with a nickel base are subject to precipitation-hardening. Their advantage is that after quenching they are in a plastic state and can be cut and bent, etc.; after being subjected to additional tempering for precipitating-hardening, they achieve considerable hardness together with high elastic properties. Springs made of these alloys were investigated after tempering for precipitation-hardening.

Until recently, the processes of stress relaxation have been studied with samples of large cross section (refs. 4 and 5). The trend towards miniaturization makes it necessary to test samples of small cross section.

We developed a rather simple method for testing thin springs for relaxation under conditions of cantilever bending, which are close to the operating conditions of contact springs in relays. The relaxation of the initial <sup>412</sup> bending stress was fixed in time by calculations based on the decreasing contact pressure. The contact pressure was measured by means of a grammeter. Springs stamped along the longitudinal direction from ribbon with a working surface  $20.3 \times 0.3$  mm were rigidly attached on one side to special plates. The position of the free end was fixed by means of a bolt which provided the required contact pressure. Five to ten springs were tested at each pressure. For convenience the grammeter was fixed on a special stand and the plate with the springs could be displaced in the groove of this stand. During measurements, the plate with the springs was in a vertical position.

The accuracy of measuring contact pressure, which was usually done visually when the gap occurred at the point where the spring came in contact with the needle of the grammeter, may be increased substantially by recording the metallic sound which occurs following the dull sound produced by the finger hitting the springs. By using this method we achieved an accuracy of 0.5 percent.

Tests were carried out with springs having a thickness of 0.15-0.3 mm with initial loads from 10 to 120 g-wt. When converted to the initial bending stress, this is equal to 5-55 kg-wt/mm<sup>2</sup>.

The contact pressure was measured in the static state depending on the duration of soaking (from 30 min to 300 h) at temperatures from -60 to +400°C (at elevated temperatures the interval was 50°C). The contact pressure was measured periodically after each soaking using the same springs and the same isothermal curve, which has been experimentally justified (ref. 5). The magnitude of the contact pressure was measured after each soaking of 5-10 springs, was averaged out and computed as a percentage of the initial value assumed to be 100 percent.

To establish the effect of temperature on the measurement of contact pressure, a special device was built which made it possible to carry out the measurements directly while heating in the thermostat, and which was based on the same principle of measuring pressure from the quality of sound described above. Contact pressure measurements in this case were somewhat more /413 complicated, but the results became sufficiently accurate and reproducible after some experience.

The results of measurements conducted directly at the test temperatures showed that the value of the contact pressure in this case is 3-4 percent lower than that obtained after cooling (for the same conditions and for the same material). In the direct measurement of contact pressure in the thermostat it was possible to test up to ten springs. Since the test required a larger number of samples, all future measurements were made after cooling to room temperature and correcting for the temperature.

The effect of cold working was studied under the same conditions, i.e., after soaking the springs under stress ( $\delta_0 = 8-15 \text{ kg-wt/mm}^2$ ) in the heat chamber for a period of 0.5, 1, 5, 10 and 100 h, after which they were removed and brought to room temperature, and the contact pressure was measured.

Turning to the method of determining the elastic properties of the spring materials, we should point out that at the present time there is no universally accepted method for doing this. It is for this reason that handbooks on spring materials present only data on short-term strength, relative elongation and hardness. Information on the values of the modulus and the elastic limit providing for a closely specified residual deformation, as a rule, is not available. At the same time, in a series of recent works (ref. 6) it has been determined that although the theoretical method of designing springs is based on Hooke's law, the latter can be used only with certain assumptions during the initial loading of real materials. Actually, there are systematic deviations from Hooke's law, which are caused by the heterogeneity of material structure and which are detected by residual deformation.

The magnitude of residual deformation may increase very rapidly when loading takes place above the conditional elastic limit measured with low accuracy, and may be quite insignificant when loading is below the conditional elastic limit.

The higher the limit of elasticity with small residual deformation, /414 the greater will be the initial stresses with which the elastic element can operate without residual deformation.

For contact springs, the tolerance for residual deformation is taken as 0.002 percent.

Because the limit of elasticity for a closely specified residual deformation is the most important characteristic of alloys, which are used for elastic elements, it was necessary to have equipment and methods for determining the elastic properties.

In our work we used the instruments and methods developed by the Bauman MTU (ref. 7), which are available to any industrial laboratory and which have an accuracy of approximately 2 percent.

In the course of the work it was established that the methods used justified themselves and could be utilized to determine the elastic properties of spring materials.

The states of heat treatment of investigated spring alloys, which are very significant for obtaining high relaxation stability, were assigned according to the maximum value of the elastic limit for a closely specified residual deformation, after which they were checked for prolonged relaxation at elevated temperatures.

#### Investigation of Stress Relaxation in Alloys with a Copper Base

Alloys with a copper base were tested for relaxation primarily at temperatures of 100-250°C. Samples of the following alloys were selected for the test: L-62, BrA7, BrKMts3-1, BrOF-6.5-0.15MNTs15-20, BrB-2.5, BNT-1.9.

The L-62 brass is widely used in the electronics industry as a reinforcing material. Recently it has become known (ref. 3) that this brass subjected to low-temperature annealing at 200°C after cold-rolling, acquires high elastic properties so that it can be used as a spring material. Consequently, the L-62 brass was included in the tests at elevated temperatures. /415

The BrOF6, 5-0.15 and KMts3-1 bronzes are used to manufacture contact springs which operate under normal conditions; for elevated temperatures there are no data on the relaxation of these materials.

The BrA7 aluminum bronze is used less frequently due to soldering difficulties, but is interesting from the standpoint of its thermal stability.

The MNTs15-20 German silver is widely used in radio electronics and has a series of advantages compared with other materials; therefore, it was necessary to determine accurately the maximum operating temperature of this alloy.

The BrB-2.5 and BNT-1.9 beryllium bronzes are high strength spring materials; however, data on their relaxation stability at elevated temperatures is not available. Springs made of this bronze were stamped in the quenched state after which they were subjected to precipitation-hardening in a vacuum at a temperature of 300°C for a period of 2.5 h. This produced an increase in their strength and elastic properties.

The relaxation curves shown in figures 1 and 2 for L-62 brass with  $\delta_0 = 5$  and 15 kg-wt/mm<sup>2</sup> show that as the temperature is increased from 100 to 250°C, there is an intense increase in relaxation. The effect of initial stress

is less pronounced. From these figures it is also clear that it is advantageous to have low temperature annealing whose effect is lost at 250°C.

The use of L-62 as spring material must be limited to a temperature of 100°C (even when annealing is used) and to low stresses: not greater than 5 kg-wt/mm<sup>2</sup> (fig. 3).

The use of L-62 in a cold-worked state produces an increase in the relaxation coefficient by 30 percent under the same conditions (fig. 4).

The effect of annealing temperature on mechanical and elastic properties of L-62 is shown in figure 5. The curves for the conditional limits of elasticity have maxima, while  $\tau_p$  decreases and  $\delta$  increases. The hardness after annealing at a temperature > 250°C decreases, which shows that the process of softening has started.

When the temperature is lowered (-60°C), the relaxation of stresses takes place more slowly than at the high temperature (fig. 6). /418

The variation in the microhardness is noticeable only at the initial moment after which it is stabilized. This is characteristic of the relaxation process (fig. 7) and was confirmed for a series of other materials.

The A7 bronze is more stable from the standpoint of relaxation than the L-62 brass. The application of low-temperature annealing at 275°C for 30 min, to achieve a maximum value for the limit of elasticity, leads to an increase in relaxation stability (fig. 8). Annealing at a temperature 20°C higher than the test temperature was less effective. The curves (figs. 9 and 10) show the effect of initial stresses and of the test temperature on the relaxation coefficient, as well as the effect produced by heat-treatment.

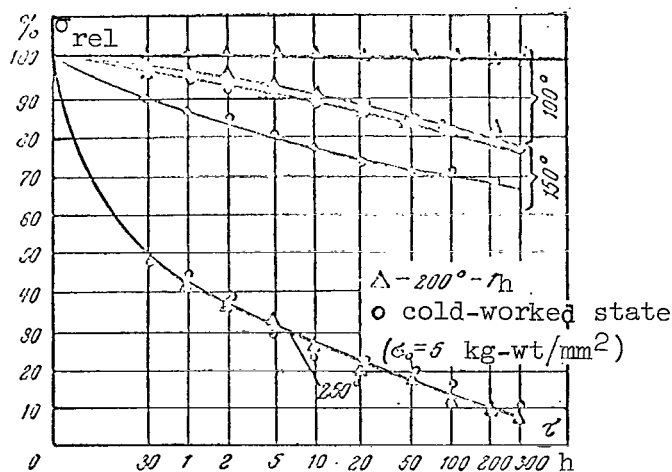


Figure 1. Relaxation of stresses in L-62 brass at temperatures 100-

250°C with  $\sigma_0 = 5$  kg-wt/mm<sup>2</sup>. /416



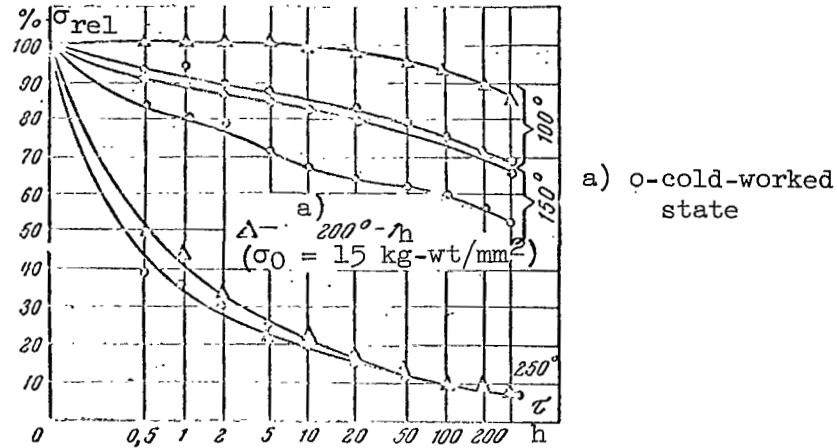


Figure 2. Same with  $\delta_0 = 15$   
kg-wt/mm<sup>2</sup>.

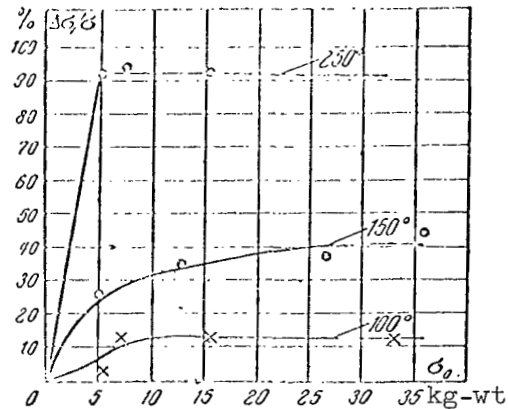


Figure 3. Effect of initial stress on variation in relaxation coefficient of L-62 at temperatures 100-250°C ( $\tau = 300 \text{ h}$ ; preliminary annealing at 220°C for 1 h).

We can recommend the application of A7 bronze up to 100°C with

/420

$\delta_0$  up to 35 kg-wt/mm<sup>2</sup>. When springs from the A7 bronze remained in the cold, this did not lead to substantial relaxation as in the case of a series of other materials. Figures 11 and 12 show the curves for the relaxation coefficients of springs made from BrOF6.5-0.15 in cold-worked and in heat-treated state as a function of initial stress. The increase in the temperature from 100-150°C produces an intense increase in relaxation, which cannot be stopped even when annealing is carried out under optimum conditions (320°C for 1 h).

/421

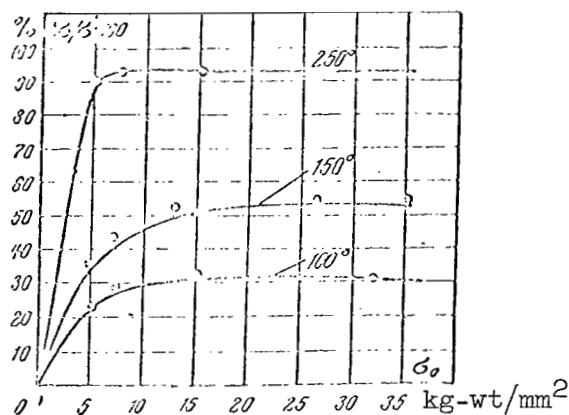


Figure 4. Effect of initial stress on variation of relaxation coefficient of L-62 at temperatures 100-250°C;  $\tau = 300$  h (in a cold-worked state).

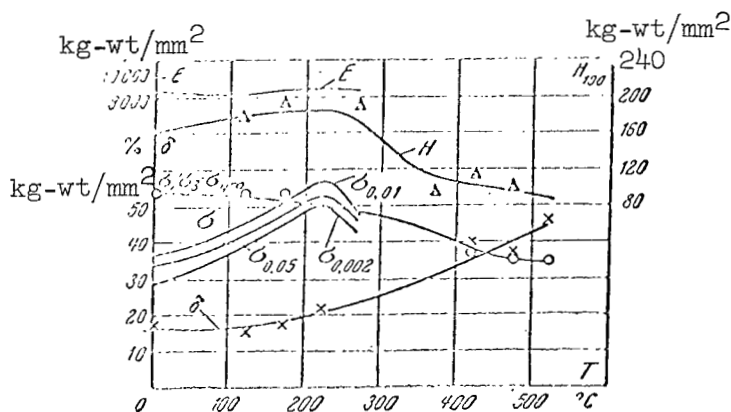


Figure 5. Effect of annealing temperature on mechanical properties of L-62 ( $\tau = 5$  h).

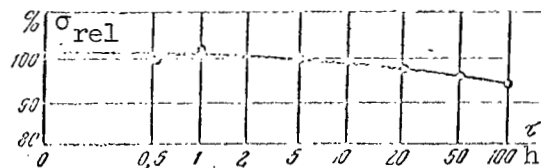


Figure 6. Relaxation of stresses in L-62 at temperature of -60°C (cold-worked state).

The KMtsZ-1 bronze is close in thermal stability to BrA7 and BrOF6. 5-0.15 described previously.

It can be recommended only for use up to a temperature of 100°C (when low temperature annealing is carried out at 275°C for 30 min).

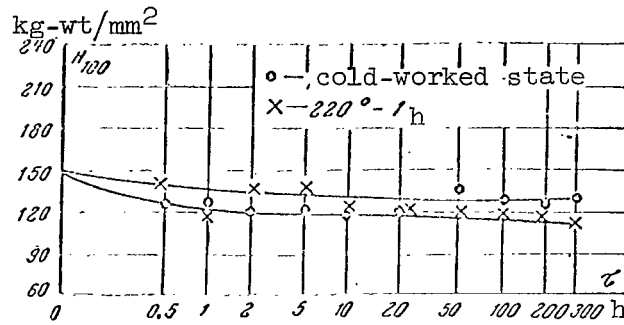


Figure 7. Variation in microhardness of L-62 during relaxation process at temperature of 100°C.

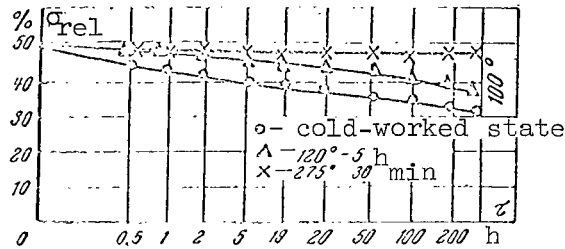


Figure 8. Relaxation of stresses in A7 bronze at temperature of 100°C.

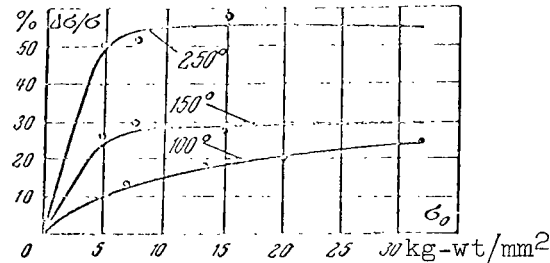


Figure 9. Effect of initial stress on variation of relaxation coefficient of BrA7 in cold-worked state at temperatures of 100-250°C ( $\tau = 300$  h).

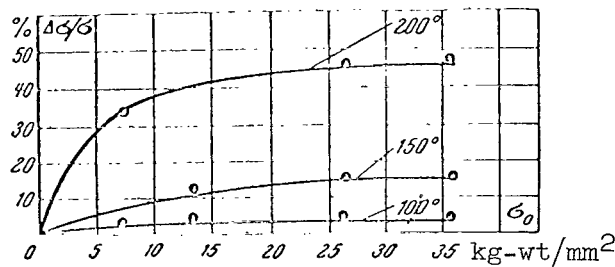


Figure 10. Effect of initial stress on variation of relaxation coefficient of BrA7 (after annealing at 275°C for 30 min) at temperatures of 100-200°C (300 h).

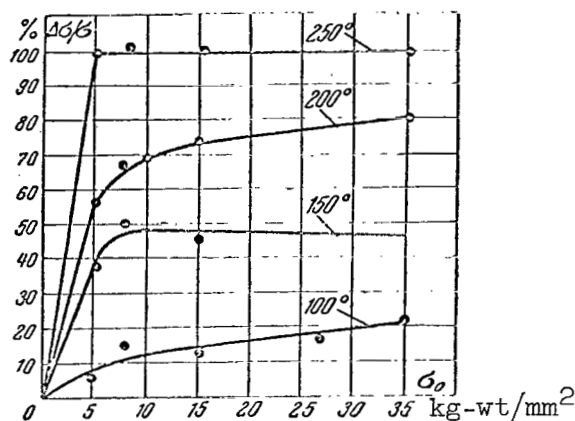


Figure 11. Effect of initial stress on variation of relaxation coefficient of BrOF6.5-0.15 in cold-worked state at temperatures of 100-250°C ( $\tau = 300$  h).

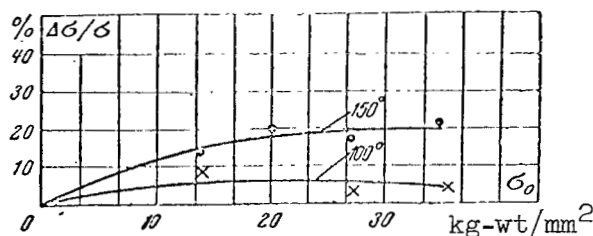


Figure 12. Effect of initial stress on variation of relaxation coefficient of BrOF6.5-0.15 (after annealing at 320°C for 1 h) at temperatures of 100-150°C ( $\tau = 300$  h).

The MNTs-15-20 alloy, unlike the preceding materials, has a higher relaxation stability. It can be recommended for use at temperatures below 200°C (fig. 13), when it is annealed at 300°C for 4 h. Above 200°C, relaxation increases (fig. 14).

Beryllium bronze is strong and has good elastic properties at room temperature; however, above 150°C, it rapidly loses its relaxation stability even at low stresses (fig. 15).

This alloy is also sensitive to overloading: even at a temperature of 150°C it can be used only with stresses up to  $\sigma_0 = 15$ -20 kg-wt/mm<sup>2</sup>.

The BNT-1.9 alloy behaves in the same way and has a slightly lower relaxation stability than BrD-2.5.

The investigation of the microstructure of spring materials during relaxation process is of theoretical interest from the point of view of clarifying its nature, and also is of practical interest to establish the microstructures which characterize the alloys with relaxation stability.

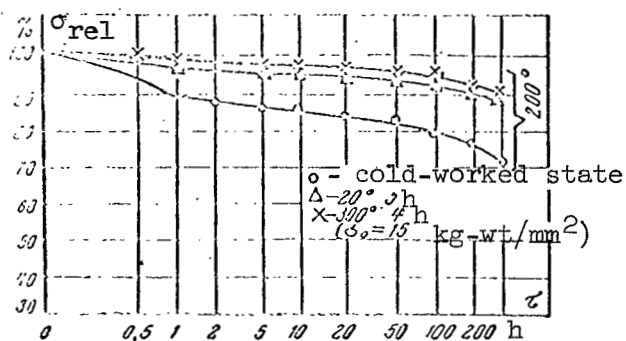


Figure 13. Relaxation of stresses in MNTs-15-20 alloy at temperature of 200°C.

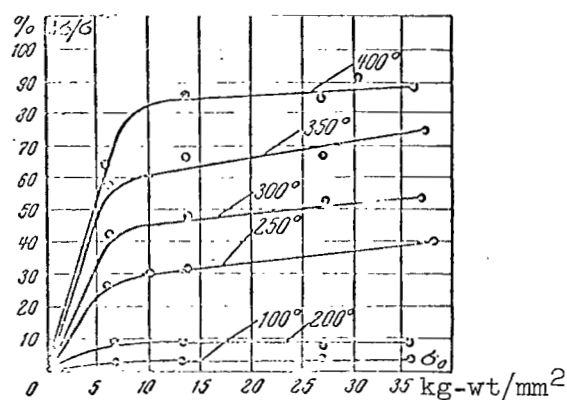


Figure 14. Effect of initial stress on relaxation coefficient of MNTs-15-20 after annealing at 300°C for 4 h (at temperatures of 100-400°C;  $\tau = 300 \text{ h}$ ).

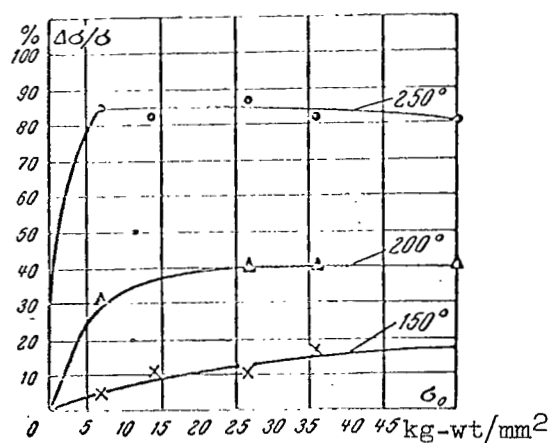


Figure 15. Effect of initial stress on relaxation coefficient of BrD-2.5 alloy at temperatures of 150-250°C.

There are published works on the investigation of the microstructure /423 of steel after relaxation (stainless steel and others). However, there is no information of this type for alloys with a copper and a nickel base. We have tried to solve this problem in our work. Since, in the tests, the springs were secured in a cantilever fashion, the maximum bending stresses were concentrated at the fixed point. Therefore, if the section is taken in the region which is situated far away from the fixed point, it is impossible to find differences in the microstructure as a function of soaking or of the temperature during the relaxation process. Also, it is impossible to obtain the expected effect with samples which are heated without being stressed.

The cross section is prepared using a sample at the built-in point. Figures 16 and 17 show the microstructure of the MNTs-15-20 samples, after they have been tested for relaxation for a period of 300 h at temperatures of 100-350°C.

Figure 16a shows the microstructure of MNTs-15-20 in the initial state after cold-rolling. The picture shows grains oriented in a different manner, whose slip bands have their own directions with respect to each grain. /425

Figures 16b, c, d and e show the microstructures after the relaxation testing of cold-worked German silver at 150, 200, 250 and 350°C, while Figures 17a, b, c and d show heat-treated German silver at temperatures of 100, 200, 250 and 350°C. By comparing these microstructures, we can see that during the relaxation process of cold-worked German silver, even at 150°C, the slip bands inside the grains straighten out and move from one grain to another in a definite direction (fig. 16b).

Furthermore, when the temperature is increased to 220°C, the formation of the slip bands increases (fig. 16c), and new units appear. When the temperature reaches 250-350°C, the slip bands come closer together and occupy a large area (fig. 16e). /426

By examining the microstructures of heat-treated German silver after testing under the same conditions, and comparing them with microstructures of cold-worked German silver we can see that the process of slip band formation after heat treatment is retarded: rebuilding takes place inside the microvolumes and a fine structure is formed. Under these conditions relaxation takes place at a slow rate (fig. 17b) and only when the temperature is raised to 250-350°C and the heat treatment loses its effect does the process of oriented slip bands formation start (figs. 17c and d).

In this way it was shown experimentally how the microstructure changes during the process of the hot relaxation of German silver, and the role of heat treatment as a retarding factor was established.

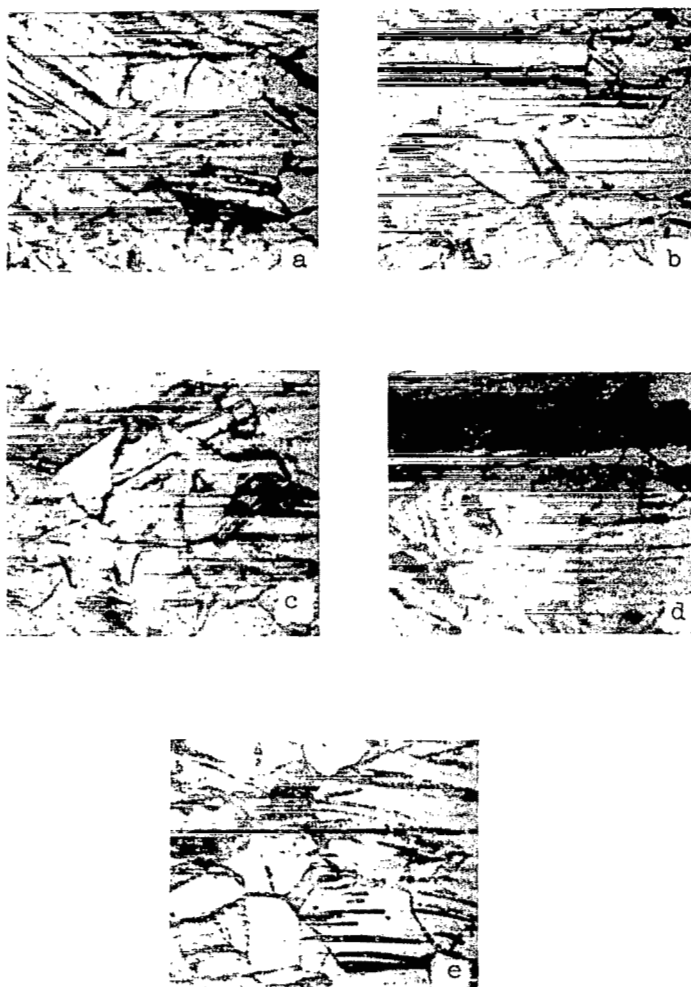


Figure 16. a, microstructure of MNTs-15-20 in initial state after cold-working; b, c, d, e, microstructure of cold-worked German silver after testing for relaxation at temperatures of 150, 200, 250 and 350°C for period of 300 h.

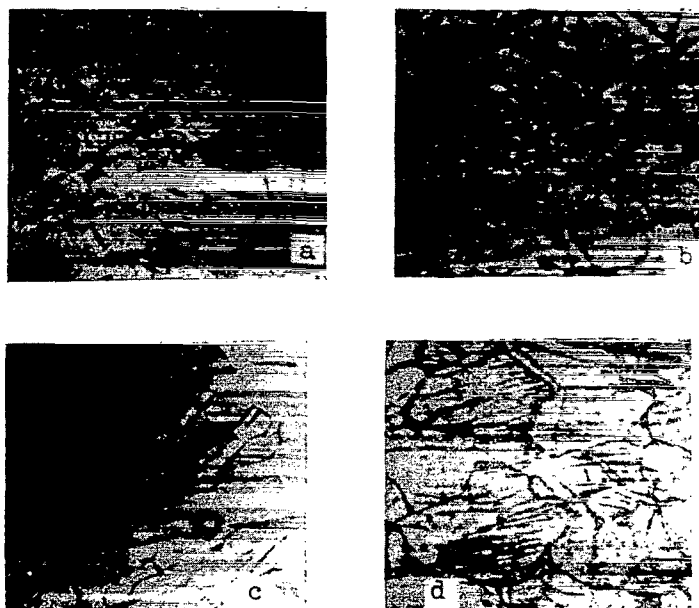


Figure 17. Microstructure of heat-treated German silver after testing for relaxation at temperatures of 100, 200, 250 and 350°C for period of 300 h.

#### The Investigation of Stress Relaxation in Alloys with a Nickel Base

Alloys with a nickel base and with Be, Mo and W additives have sufficient plasticity in quenched state which makes it possible to machine them. After precipitation-hardening is performed on completed parts, the alloys acquire high strength. Initially, these alloys were recommended for elastic elements designed to operate at a temperature of 250°C.

Recently, with transition to vacuum melting, the technology has been improved, and it has therefore been possible to run tests at temperatures of 300-400°C. Unfortunately, these alloys have been taken out of production at the present time due to their high toxicity, although technical specifications have already been published guaranteeing the required properties, including a low electrical resistance of  $0.25-0.30\Omega\cdot\text{mm}^2/\text{m}$ .

The TAN-5-2-1 (Ni-Ti-Al-Nb) alloy developed by the State Design and Planning Scientific Research Institute for Working of Nonferrous Metals (TU TSMO OZ No. 27-62), underwent extensive testing for relaxation. Even at the beginning of the investigations it was established that it is very stable with respect to contact pressure at elevated temperature. Its disadvantage is the relatively high specific electric resistance ( $0.45\Omega\cdot\text{mm}^2/\text{m}$ ). However, if we take into account the series of valuable properties: high relaxation stability, resistance to oxidation, etc., the TAN-5-2-1 alloy deserves special attention. The TAN-5-2-1 alloy is stable and can be used up to a temperature of 350°C with stresses up to 55 kg-wt/mm<sup>2</sup>. /427



Additional tests were carried out on alloys with a nickel base developed by the Institute of Precision Alloys TsNII ChM.

Of particular interest in this group of alloys is alloy No. 7234, containing Ni-Ti-Al-Re. In spite of its high relaxation stability, it has a serious disadvantage--and extremely high electrical resistance ( $0.65\Omega\cdot\text{mm}^2/\text{m}$ ).

The number 400 alloy developed at the Bauman MVTU has  $\rho = 0.35\Omega\cdot\text{mm}^2/\text{m}$ . It was tested for relaxation at temperatures of 350-400°C. The relative characteristics of relaxation stability for all investigated alloys after soaking for 300 h are shown in figure 18.

The behavior of the parabolic curves, which characterize the variation in the stress relaxation of various materials as a function of temperature, shows that their relaxation stability increases when the copper base is replaced with a nickel base, and that it is associated with the alloying of the base. The following alloys have a relaxation which is not greater than 10 percent: at a temperature of 100°C, Br KMts 3-1; BrOF 6.5-0.15; Br BNT-1.9; at 150°C, Br2.5; at 200°C MNTs-15-20, kunmal' B; at 250°C TN-3; at 300°C Mo; at 350°C EI996, TAN-5-2-1. Alloy 7234 has most resistance to heat and its stress relaxation at  $T = 350^\circ\text{C}$  over a period of 300 was only 3 percent.

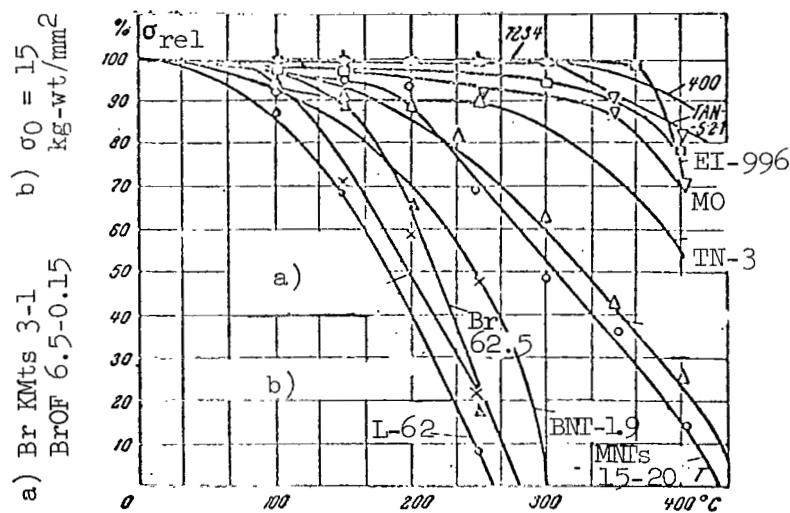


Figure 18. Comparative characteristics of relaxation stability of alloys.

## Conclusions and Recommendations

1. The stress relaxation of 18 spring materials has been investigated with  $\delta_0 = 5-55 \text{ kg-wt/mm}^2$  and at temperatures in the range 100-400°C for a period of 300 h and at  $T = 60^\circ\text{C}$  for a period of 100 h. The positive effect of low-temperature annealing has been proven. This annealing increases the limits of elasticity and retards the processes of relaxation.

2. Since the stress relaxation of spring materials lowers the stability of contact springs, when selecting a particular material for springs it is necessary to remember that the test results were obtained for the static state, specifically:

Temperature °C	Alloy
100	L-62
100-125	BrA7 BrKMts3-1 BrOF 6.5-0.15
150	BrB2.5
200	MNTs-15-20
300	EI996, Mo (Mo only in hermetically sealed relays)
350	TAN-5-2-1 "400"

These materials may be used only when they are subjected to heat treatment as recommended.

3. An effort was made to study the microstructure of MNTs-15-20 in connection with the relaxation processes. In this case, the kinetics of slip band displacement was established as well as the displacement of units inside the grains and at their boundaries due to the relaxation process. The retarding action of heat treatment leading to the formation of a fine structure has also been established.

## REFERENCES

1. Rakhshadt, A. G. and Shur, L. M. Heat Treatment and the Strength of Materials and Alloys, in collected works "Works of the Bauman MVTU" (Termicheskaya obrabotka i prochnost' materialov i splavov, v sbornike "Trudy MVTU imeni Baumana"), 1958.
2. Tsobkallo, S. O. and Vashchenko, Z. A. Some Problems of the Solid Body (Nekotoryye problemy tverdogo tela). Izd-vo AN SSSR, 1959.
3. Rakhshadt, A. G., Rogel'berg, I. L., Vorob'yeva, L. P. and Puchkov, B. I. "Metal Studies and Heat Treatment of Metals" ("Metallovedeniye i termicheskaya obrabotka metallov"). No. 2, 1960.
4. Gintsburg, Ya. S. Stress Relaxation in Metals (Relaksatsiya napryazheniy v metallakh). Mashgiz, 1957.

5. Oding, I. A. Relaxation and Creep in Metals (Relaksatsiya i polzuchest' v metallakh). Vestnik Mashinostroyeniya, Nos. 5-10, 1946.
6. Handbook of Metal Studies and Heat Treatment of Steel and Cast Iron, (Metallovedeniye i termicheskaya obrabotka stali i chuguna) Metallurg-izdat, 1961.
7. Rakhshtadt, A. G. and Shtremel', M. A. Zavodskaya Laboratoriya, No. 6, 1960.

## PART IV. RELIABILITY OF CONTACTS

### THE RELIABILITY OF THE ELECTRIC CONTACT

B. S. Sotskov and I. Ye. Dekabrun

Switching contacts are widely used in electrical circuits. Frequently <sup>/430</sup> it is assumed that they are the most unreliable components, and determine to a large extent the unreliability of relay circuits.

This is true if the operating conditions of a contact are improperly selected. However, when the operating conditions of contacts are properly selected, their reliability is of the same order as the reliability of other components.

In considering the reliability of switching contacts, we should bear in mind that it depends on the operating conditions of the circuits and on the load parameters. The latter is particularly true in cases when the load consists of a relay member.

The reliability of a contact is determined by its ability to operate properly during all of its four stages: open, closed, make and break.

#### Reliability of the Open Circuit

We begin by considering the open circuit. Figure 1 shows the connection of a contact used to control the load  $R_L$ .

As characteristics of the load we select the average values of the operate currents  $\bar{I}_{av}$  and release currents  $\bar{I}_{re}$  and their root-mean-square values  $\Delta$  and  $\Delta'$ .

The variability factors for the operate and the release currents, i.e., <sup>/431</sup> the ratios  $\Delta/\bar{I}_{av}$  and  $\Delta'/\bar{I}_{re}$  are sufficiently constant for each type of relay.

For weak current relays, they lie within the limits

$$\frac{\Delta}{\bar{I}_{av}} = 0.03 - 0.13 \quad \text{and} \quad \frac{\Delta'}{\bar{I}_{re}} = 0.05 - 0.25.$$

We have the insulation resistance parallel to the open contact, i.e., resistance to leakage currents between contacts  $R_{i0}$  and insulation resistances between each of the contacts and grounds  $R_{i1}$  and  $R_{i2}$ . Usually  $R_{i1} \approx R_{i2} \approx R_i$ .

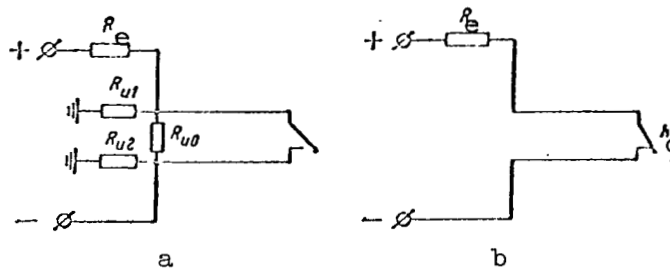


Figure 1. Schematic diagram showing a contact connection: a, open state; b, closed state.

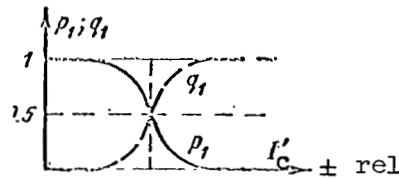


Figure 2. Probability of failures  $q_1$  and reliability of relay release  $p_1$  when closed circuit is being opened.

Thus, when the contacts are open the following current flows in the circuit.

$$I'_x = \frac{E}{R_e + \frac{R_i \cdot 2R_1}{R_1 + 2R_1}} = \frac{E}{R_i + R_{ieq}}$$

The ratio of the current when contacts  $I_x$  are closed to the current 432 when contacts  $I'_x$  are open determines the so-called load multiplication factor

$$k = \frac{I_x}{I'_x} = \frac{E}{R_i + R_e} \cdot \frac{1}{\frac{E}{R_i + \frac{R_i \cdot 2R_1}{R_1 + 2R_1}}} = \frac{R_i + R_{ieq}}{R_e + R_e} = \frac{1 + \frac{R_i}{R_e}}{1 + \frac{R_e}{R_e}} = \frac{1 + \frac{R_i}{R_e}}{2}$$

The value of current  $I'_x$ , which is frequently called the quiescent current, must be substantially less than the value of the release current so that the relay can be released when it operates as a load.

The probability of relay failure during release  $q_1$  is determined by the normal distribution law

$$q_1 = \frac{1}{\sqrt{2\pi} \Delta'} \int_{-\infty}^{I'_x} e^{-\frac{(I'_x - \bar{I}_{re})^2}{2\Delta'^2}} dI'_x.$$

Consequently, the reliability of the load being disconnected when the contacts open will be

$$p_1 = 1 - q_1 = 1 - \frac{1}{\sqrt{2\pi} \Delta'} \int_{-\infty}^{I'_x} e^{-\frac{(I'_x - \bar{I}_{re})^2}{2\Delta'^2}} dI'_x.$$

We should point out that when we connect  $r_c$ , parallel to the contact for spark quenching, the quiescent current  $I'_x$  increases to a value

$$I'_x = \frac{E}{R_i + r_c},$$

which decreases the reliability of switching off the load when the contact is broken. From this point of view, it is desirable to connect the spark quenching resistance parallel to the load and not parallel to the contacts.

#### Reliability of Contact Closure

/433.

If the probability that the elementary contact on the surface of two adjacent bodies does not close is equal to  $q_0$ , the probability that these contacts do not close will be given by the expression

$$q_2 = q_0^m,$$

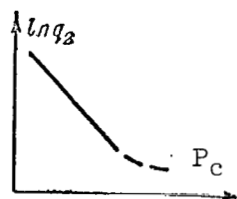


Figure 3. Failure of contact  $q_2$  to close as a function of contact pressure.

where  $m$  is the number of elementary contacts on the contact area  $s$  between the bodies.

Since  $M = sm$  and  $m = kp$ , where  $p$  is the average value of the specific contact pressure, we have

$$q_2 = q_0^M = q_0^{sm} = q_0^{skp} = q^{kP_c},$$

where  $P_c$  is the contact pressure.

This relationship is confirmed experimentally. Figure 3 shows the experimental curve  $q_2 = \varphi(P_c)$ , which satisfies the equation

$$\ln q_2 = -kP_c.$$

The probability that the contacts close is equal to

$$p_2 = 1 - q_2 = 1 - q_0^{kP_c} = 1 - e^{\ln q_0^{kP_c}} = 1 - e^{-k_1 P_c}.$$

As the contact wears, its reliability decreases. It follows from theoretical considerations which have been verified experimentally, that the variation in the volume of the contact is proportional to the number of operating cycles  $N$ . Therefore,

$$\Delta G = gN,$$

where  $g$  is the change in the volume during one operating cycle (make-break), which depends on the operating conditions, i.e., on the voltage  $E$ , the current  $I$ , the time constant of the load circuit  $\tau$  and the material of the contact /434 ( $\gamma_1 a_1 \alpha_1 I_{00}$ ). We may assume

$$g \approx \{U_0 / \tau\} \cdot a (I - I_{00}^2).$$

The change in the volume of the contacts produces a decrease in the contact pressure

$$\Delta P_c = c \Delta G = cgN = c_1 N,$$

which leads to a change in the probability of contact failure during their closure

$$\begin{aligned} q_2 &= e^{-k_1(P_c + \Delta P_c)} \approx 1 - [k_1 P_c + k_1 c_1 N] = \\ &= (1 - k_1 P_c) + k_1 c_1 N = q_{2c} + c_2 N \approx (\lambda + \lambda' f) t, \end{aligned}$$

where

$$\lambda \approx \frac{q_{2c} k}{t}; \quad f = \frac{N}{t}; \quad c_2 = \lambda'.$$

The reliability of a contact when it makes may be expressed as

$$p_2 = 1 - q_2 \approx 1 - (\lambda + \lambda')t \approx e^{-(\lambda + \lambda')t}.$$

If we assume that the reliability of the contact when it makes is equal to  $p_2 = p_{20}$ , and if we make and break the contacts  $N$  times during the period  $t_0 = N/\bar{t}$ , we find that

$$p_0 + \lambda t_0 = -cN,$$

or

$$\ln [-(\ln p_0 + \lambda t_0)] = \ln c + \ln N.$$

When the arc is absent, i.e.,  $U < U_0$  and  $I \gg I_{00}$ , we have  $g \approx aI^\alpha$  and, consequently,

$$c_2 = k_1 c g = k_1 c a I^\alpha = a_0 I^\alpha.$$

We let  $-(\ln p_0 + \lambda t_0) = A$ ; then

$$A = a_0 I_{x1}^\alpha N_1 = a_0 I_{x2}^\alpha N_2 = \dots,$$

or

$$\left( \frac{I_{x1}}{I_{x2}} \right)^\alpha = \frac{N_2}{N_1}.$$

If we know the value  $N_1$  for some current  $I_{x1}$ , we can use this expression to find another value  $N_2$  corresponding to the current  $I_{x2}$ .

#### The Reliability of Contact Release

/435

The reliability of contact release is determined by its resistance to stable welding. Experimental investigations have shown that when the contacts begin to weld, it is necessary to have a definite pressure  $P_w$  to release them.

There is an empirical relation between the magnitude of this pressure and the current which passes through the contacts when they are welded. This relation has the form

$$P_w = c_0 I_w^2.$$

These relations may also be obtained by examining an approximate model of the welding process. If we assume that during the initial period of time  $\Delta t$  which has elapsed from the beginning of the contact, heat is liberated which melts the metal at the contact point, we obtain

$$cV(\theta_{\text{melt}}^0 - \theta_0^0) + LV = I^2 R_c \Delta t,$$

where  $c$  is the specific heat;

$L$  is the latent heat of fusion;

$V_0$  is the volume of the fused metal;

$\theta_m^0$  and  $\theta_0^0$  are the fusing temperature and the temperature of the contact before



it is made, respectively;

$R_c$  is the resistance of the contact:

$$R_c = \frac{\rho}{2r}$$

( $r$  is the radius of the contact surface;  $r = a_0 P^{1/3}_c$ ).

We assume that  $\Delta t = \frac{\Delta y}{v_{av}}$ ,

where  $v_{av} = \frac{v_{max}}{2}$  is the average velocity of contact surface warping;

$\Delta y$  is the magnitude of contact warping, which according to Hertz is equal to

$$\Delta y = k \sqrt[3]{P_c} r.$$

The volume of the melted part of the contact is given by

$$V = \frac{4}{3} \pi r^3.$$

The contact area may be expressed as

/436

$$s_a = \pi r^2 = \frac{3}{2} a_0 [r (v_W^0 - v_0^0) + L] \frac{1}{v_{av}} I^2 = c_0 \frac{I^2}{v_{av}}.$$

If the voltage necessary to break the contacts at their normal temperature is equal to  $\sigma_0$ , the pressure necessary to break the welded contacts is given by

$$P_W = \sigma_0 s_a = c_0 \frac{I^2}{v_{av}} = c_{00} I^2.$$

Let us assume that the relation

$$P_W = c_{00} I_W^2$$

is known; it is obtained experimentally or computed by using an approximate model of the welding process.

Let us assume that the actual value of the welding current is equal to  $I_x$ . A welding pressure will correspond to this current

$$P_x = P_W = c_{00} I_x^2.$$

The true pressure for breaking the contacts which is determined by the mechanical characteristics of the relay will be designated by  $P_m$ ; corresponding to this pressure we have a welding current

$$I_W = \sqrt{\frac{P_m}{c_{00}}}.$$

Let us take the ratio  $k = P_x/P_m$ ; then:

for  $P_x$  when  $P_c/P_m = k = 0$ , we have  $\ln k = -\infty$ ;

for  $P_x = P_m$  when  $P_c/P_m = k = 1$ , we have  $\ln k = 0$ ;

for  $P_x = \infty$ , when  $P_c/P_m = k = \infty$ , we have  $\ln k = \infty$ .

These relations are satisfied by the normal logarithmic distribution for 437 the probability of failure due to welding

$$q_3 = \frac{1}{\sqrt{2\pi}\Delta_{\ln k}} \int_{-\infty}^{\ln k} e^{-\frac{(\ln k - \overline{\ln k})^2}{2\Delta_{\ln k}^2}} d(\ln k) =$$

$$= \frac{1}{\sqrt{2\pi}\Delta_{\ln k}} \int_{-\infty}^{\ln k} e^{-\frac{\left(\frac{I_x^2}{I^2} - \frac{\overline{I_x^2}}{I^2}\right)^2}{2\Delta_{\ln k}^2}} d\left(\frac{I_x^2}{I^2}\right).$$

The reliability of the contact from the standpoint of resistance to welding is determined (fig. 4) as

$$p_3 = 1 - q_3 = 1 - \frac{1}{\sqrt{2\pi}\Delta_{\ln k}} \int_{-\infty}^{\ln k} e^{-\frac{(\ln k - \overline{\ln k})^2}{2\Delta_{\ln k}^2}} d(\ln k).$$

The Reliability of a Closed Circuit

In order that the closed state of the load circuit be maintained with reliability, we must have a current in the circuit such that

$$I_x \gg I_{op},$$

where  $I_{op}$  is the operate current of the load, a;

$$I_x = \frac{E}{R_1 + R_c}.$$

The reliability of the contact when the circuit is closed (fig. 6) 438 is given by

$$p_4 = \frac{1}{\sqrt{2\pi}\Delta} \int_{-\infty}^{I_x} e^{-\frac{(I_x - \overline{I_{av}})^2}{2\Delta^2}} dI_x.$$

Frequently it is necessary to close a load circuit which has some resistance

$$R_{\min} < R_n < R_{\max},$$

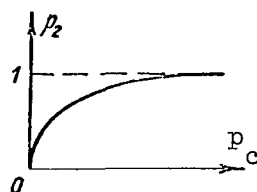


Figure 4. The variation in the reliability of contact closure  $p_2$  as a function of contact pressure.

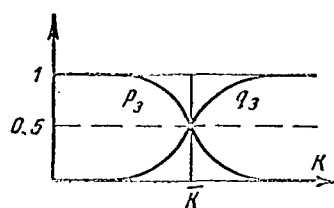


Figure 5. The probability of failures  $q_3$  and reliability  $p_3$  of contact closure.

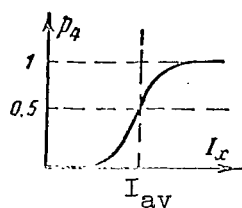


Figure 6. Reliability  $p_4$  of the circuit breaking.

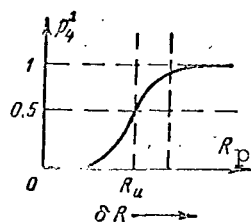


Figure 7. The probability of retaining the contact resistance  $p_4^1$  within given limits.

and it is necessary that the error in the resistance of the circuit, including the resistance of the contacts, be less than a given allowable relative error  $\delta$ ; in this case we have

$$R_z = R_{\min} + R_c = R_{\min} \left( 1 + \frac{R_c}{R_{\min}} \right)$$

and

$$\delta \geq \frac{R_c}{R_{\min}},$$

or

$$R_c \leq \delta R_{\min}$$

The reliability of operation of the contacts, i.e., the probability that the requirement  $R_c < \delta R_{\min}$  be satisfied, is determined by assuming a normal

distribution law for the resistance of the contact (fig. 7),

/439

$$p_4^1 = \frac{1}{\sqrt{2\pi} \Delta R_c} \int_{-\infty}^{R_c} e^{-\frac{(R_n - \bar{R}_c)^2}{2\Delta^2 R_n}} d(R_n).$$

The resulting reliability of contact operation in a given circuit is determined as

$$p_z = p_1 p_2 p_3 p_4 = \prod_{j=1}^4 p_j.$$

# THE RELIABILITY OF ELECTROMAGNETIC RELAY CONTACTS ACCORDING TO OPERATIONAL DATA

G. Ya. Rybin

The relay is used in very large quantities in various electronic equipments. With the advent of automation and equipment complexity, the number of relays used continues to grow. On the average, in 1961 there were 270 relays in one piece of equipment, i.e., approximately 1,100 electric circuits were switched by means of contact relays.

When a relay fails, the entire piece of equipment usually fails. It usually takes a long time to trouble-shoot and replace a defective relay (on the average up to 3 hr). This is not always permissible if we consider modern requirements for reliability. At the present time, a great deal of work is being conducted to collect, generalize and analyze information on relay failures under operating conditions. The results of these investigations have shown that in more than 60 percent of the cases, failures are caused by relay contacts (the entire contact system), up to 27 percent of the failures are due to failures in the windings and approximately 13 percent of the failures are due to defects in the moving system of a relay and to the mechanical failure of individual components. The basic causes of failure and their relative number (150 relays) are shown in table 1.

TABLE 1

DISTRIBUTION OF RELAY FAILURES ACCORDING TO CAUSES

Point of Failure	Reason for Failure	Percentage of Total Failure
Contacts	Disruption of Control	28.8
	Burning of Contacts	19.7
	Welding of Contacts	6.8
	Insulation Breakdown	5.3
Winding	Short circuit	14
	Break	10
	Insulation Breakdown	3.3
Defects in Relay Construction	Sticking of the Armature	2.3
	Mechanical Failure of Individual Components	6.8
	Others	3

The basic reason for the disruption of contact adjustment is the recurring deformation of contact blades and their displacement in contact packs.

This was confirmed by an examination of the relay whose contacts did not close. In this case, when the winding was in working order, there was no noticeable wear on the contacts, the contact surfaces were clean, but when the armature was moved up and down the contact springs did not bend. When external pressure was applied to the contact springs, the contacts operated properly. In individual cases a gap was observed between contacts which were supposed to be closed, and when pressure was applied to the contact packs, the contact springs were displaced.

The burning of contacts is manifested by the presence of soot on the contacts and a substantial change in their configuration (due to the formation of pits on one of the contacts and craters on the other, or due to the spattering of contact material). The failures are because oxide films form on the surface of the contacts or because the contacts are worn and do not close. The burning of contacts is observed primarily in relays which switch reactive loads at currents in excess of 0.1 amperes. /441

The welding of contacts is not a typical reason for the failure of an electromagnetic relay. Most frequently, welding occurs when the current passing through the contacts is substantially in excess of the allowable value. For example, in many contact spring relays which fail due to the welding of contacts, the iridescent tarnish colors are observed which could not be formed by normal currents. However, in some relays which have low contact pressure and low breaking force (less than 10 grams), the sintering of contacts as well as point welding of the contacts was observed when switching currents were 1 to 2 amperes. Therefore in relays which have low contact pressure and consequently, a large transient contact resistance and low breaking force, we should expect a much larger number of failures due to contact welding than shown in table 1.

The breakdown of insulation between the contact plates and also between the contact plates and the case are usually due to manufacturing defects. When high quality insulating materials are used, failure due to breakdown will be less frequent because the insulated components have a large factor of safety with respect to their electrical strength.

A further generalization of table 1 shows that all contact failures may be divided into two classes: the "short circuit" failure, i.e., when the switched circuit is not open or is short-circuited to the case and "break" failures, i.e., when the switched circuit does not close.

Of a total of 100 percent of failures about 80 percent are of the "break" type while 20 percent of the failures are of the "short circuit" type.

The ratio between the break failures and the short circuit failures may change, depending on the magnitude of the load and the nature of the switching network.

With a decrease in the switched current, the number of "break" failures increased and when the current increased there were more "short circuit" failures.

It should be pointed out that when the switched current was increased, /442 the total number of failures also increased. Thus, when the currents were from  $0.7 I_1$  to  $I_1$  there were approximately twice as many failures as for others values of the current.

When low currents are switched (less than 50 ma) and the voltage is less than 6 volts, in addition to complete the failure of contacts, there were quite a few cases when the relay developed intermittent trouble, i.e., there were isolated cases when the current did not pass through the contacts due to the presence of oxide films on the surface of the contacts or due to insulating particles which became lodged between the contacts. These insulating particles were frequently the products of combustion or of organic evaporations.

It was not possible to completely clarify the effect of the load on the reliability of contacts. However, when the load was inductive, there were approximately 2.5 times more failures than when the load was resistive. The reliability of these data is not very great because purely resistive loads are not encountered very frequently. Of the total number of loads, only 7 percent have a resistive nature while 31 and 62 percent are capacitive and inductive loads respectively.

The largest number of failures (up to 90 percent) takes place during the first 1,000 - 1,200 hr of operation. The reasons for most of these failures are concealed manufacturing defects, the misalignment of the contact system which must also be attributed to manufacturing defects. Then, the number of failures decreases by a factor of 15 - 20 and remains relatively constant for a period of 5,000 - 6,000 hr.

The subsequent increase in the number of failures is due primarily to the burning of contacts and to their wear.

On the basis of the material which we have presented, we can make the following conclusions pertinent to increasing the reliability of contacts:

1) it is recommended that relay contacts be reserved, in which case by considering the relation between break failures and short circuit failures it is possible to design the most rational schemes;

2) it is rational to utilize the contacts of a relay for switching the currents of a resistive load which do not exceed  $0.7 I_1$ ,

3) in switching loads which have a reactive nature, the switched currents should be decreased by a factor of not less than 2 - 4 with respect to the /443 nominal value;

4) in switching small currents and voltages, it is recommended that gold or gold-plated contacts be used.

## THE USEFUL LIFE OF PLATINI-IRIDIUM RELAY CONTACTS AS A FUNCTION OF LOAD CURRENT

T. K. Shtremberg and N. A. Belozerova

The reliability of electric contacts is determined both by their corrosion and erosion while their useful life is determined primarily by their erosion.

The erosion of electrical contacts depends on a rather large number of conditions, specifically:

- 1) on the parameters of the switched network and on the switching conditions (the type of power source, the nature and magnitude of the load parameters, the value of the current and the voltage, frequency of switching, etc.);
- 2) on the physical and chemical properties of contact material (melting and boiling temperature, heat conductivity, hardness, structure, arc parameters, etc.);
- 3) on the conditions of the surrounding medium in which the contacts operate (chemical composition, temperature, humidity, pressure, extent of contamination by foreign substances -- the presence of dust, smoke, organic vapors, etc.);
- 4) on the dimensions, shape and construction (single or double contacts) and on the condition of the contact surface (cleanliness and type of finish);
- 5) on the properties of the mechanism which operates the contacts: on the contact pressure and the extent of its variation during the switching process, on the static gap between the contacts, on the velocities of making and breaking, on the presence and degree of chattering, on the form of contact operation -- perpendicular to the working surface or with a tangential component (with slipping).

Because it is difficult to take into account all these conditions, the analytical methods for computing the useful life of contacts covered in the 444 literature (refs. 1 and 2) cannot give sufficiently accurate results, particularly because they require information on a series of empirical factors which, at the present time, are known only for a limited number of contact materials and external factors.

It is known that for most of the loads which are encountered in weak current contacts utilizing precious metals and their alloys these contacts wear out unevenly over the entire surface: their erosion as a rule takes the form of a crater on one of the contacts and a pip on the other.



The existing analytical methods for computing the erosion of contacts in the best case only give us the volume of the material transported to the opposite electrode but make it impossible to determine accurately the height of the pips which are usually responsible for limiting the useful life of contacts because they wedge in the craters of the opposite electrode or weld to its walls.

Taking this into account we must admit that the useful life of a contact device, even if we have an analytical expression for it, must be determined accurately by the experimental investigation of contacts in a given device under specific loading conditions.

The present work considers the results of experimental investigations to determine the useful life of platinum-iridium contacts of miniature relays RES-9 and RES-10 for nonreactive loads with a current from 1 to 5 amperes and a voltage 30 to 32 volts. These loads are of interest because they are typical and are recorded in the technical specifications of most of the domestic weak current relays and in the catalogs of many foreign relays.

As a criterion of useful life, the present work utilizes the number of cycles which a relay undergoes until systematic failures occur.

The failure of contacts is described as any disruption of their operation, i.e., both the lack of connection in a switched network when the contacts close (failure of the first kind), as well as failure to open a circuit when the contacts break (failure of the second kind).

Systematic failures are failures of the same group of contacts which are repeated after short intervals of time. /445

Complete failures, i.e., inability to switch, in the present work are compared with systematic failures.

Misalignment or temporary individual breakdowns after which the contact pair operates properly for a long time were taken into account in the investigation but were not considered when the data were analyzed.

Failure of the first kind, in which the contacts do not make an electric connection, occurs for the following reasons:

- a) the formation of a poorly conducting film or the presence of foreign insulating particles at the contact point;
- b) a decrease in contact pressure due to a high degree of contact erosion or due to the deformation of the spring;
- c) mechanical damage to contacts or contact springs.

Failures of the second kind, in which the contacts do not open, are illustrated by the following examples:

- a) the welding of the contact pair;
- b) the wedging of the pips of one electrode in the crater of the opposite electrode;
- c) the nonquenching of the arc in the interval of time between contacts supported by the ionization of the gaseous medium;
- d) the breakdown of insulation between contacts.

Failures of the first kind are usually characteristic of contacts which offer weak resistance to erosion or which are worn to a point where there is a sharp drop in contact pressure.

Contacts made of precious metals and their alloys, which have been subjected to erosion but which retain sufficient contact pressure, are usually not subject to failures of the first kind. This is so because the insulated particles which fall on the contacts are burned up while the poorly conducting chemical films are broken down.

Failures of the second kind, as a rule, are caused by the erosion of contacts; however, short-term welding is possible in contacts which are not worn when the contact pressure is low due to the presence of roughness on the surface of the contacts or due to the random presence of metallic particles between the electrodes. These metallic particles are produced by the wear of the moving parts of the relay. /446

When the loads exceed the limits of arc forming but are below the point of the second erosion inversion (ref. 3), failures of the second kind are most probable. In this case, failures of the first kind can occur only when there is a sharp drop in contact pressure due to the sudden break of the pips, due to auxiliary members with worn supports or due to the thermal deformation of contact springs.

#### Methods of Determining the Useful Life of Contacts

The investigation of contact life in the present work was conducted by recording and analyzing the reasons for all the failures shown in figure 1. The basis of this method has been the comparison of the operation of two contact pairs when the probability of simultaneous failure is so small that it can be neglected. The failures were recorded by means of a conventional subscriber's meter. The characteristics of this meter are such that it does not operate when we have short pulses produced by a difference in the make and break time of two contact pairs (but is reliable for pulses of longer duration).

Figure 1 shows two variations for connecting the meter to the load circuit of the contacts: the lower version has one while the upper version has two windings. In both cases the meter is connected in parallel not to the entire load  $R + r$  but only to its small part  $r$  with a resistance sufficient

Key:

KJ1 = KL  
 H = N  
 HP = NR  
 3B = ZV  
 CJ1 = SL  
 P = R  
 H3 = NZ

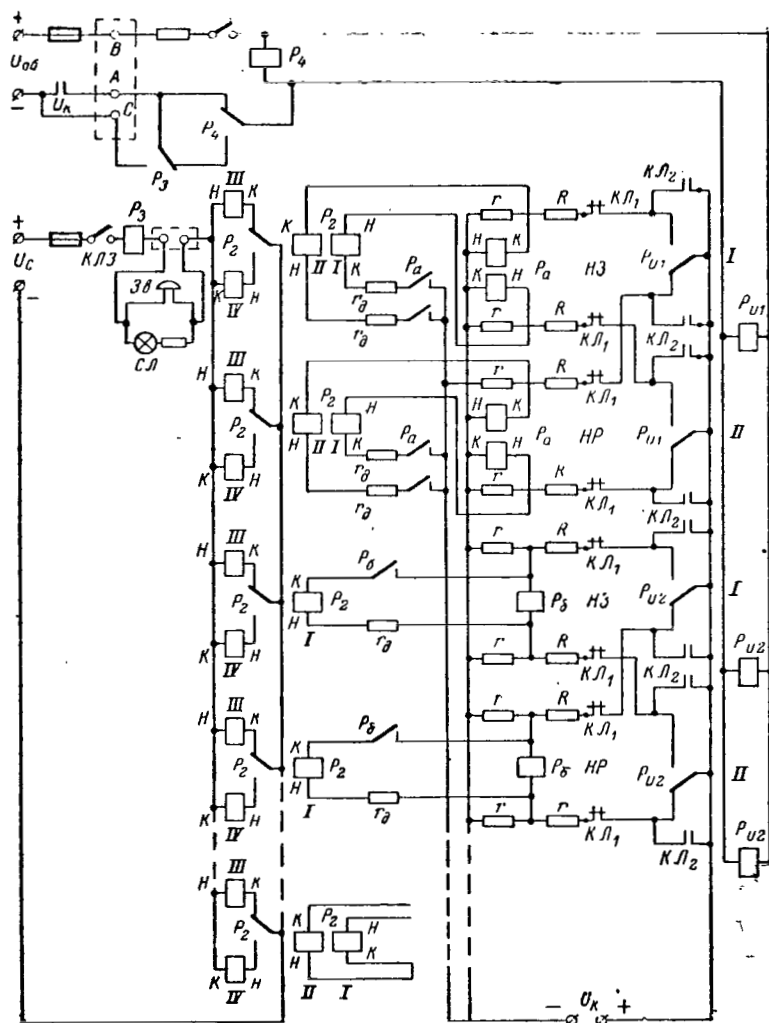


Figure 1. Registration of types I and II control failure with automatic commutation stop at failure.

for the reliable operation of the meter. This is done in order to reduce to a minimum the coupling between the circuits of the two contact pairs which are serviced by one meter.

In this circuit, when any failure occurs, switching is stopped automatically and a sound signal is produced. This is achieved by means of a polarized relay of the RP-5 type whose windings are in parallel with the windings of the meter. Relay  $R_2$  operates when there is a failure and is locked through its own contacts by winding III, or IV. At the same time it closes the alarm circuit (bell) and relay  $R_3$ , which is of the RP-7 type. The latter's contacts shunt the pulse /448 contact PC of the pulse generator, which is connected in series with the windings of the test relays  $R_t$ , and the switching of these relays ceases. In order that the relay remain in the position in which the failure occurred, an auxiliary relay  $R_4$  of the same type is used. This relay has the same winding as the test relay  $R_t$ . If failure has occurred in the contacts which open, the windings of the test relays  $R_t$  are disconnected by the opening of the make contacts of relay  $R_4$ . If failure has occurred in the make contacts, the windings of the test relays are connected to the power source through the make contacts of the auxiliary relay  $R_4$  and the contacts of relay  $R_3$  are shunted by the pulse contact.

The relay pair which has failed and the nature of the failure are determined by the direction in which relay  $R_2$  operates and by the position of the armature of the auxiliary relay  $R_4$ . The possible variations are shown in table 1 which is convenient to use.

The winding of relay  $R_2$ , which is of the RP-5 type, is connected to the winding of the meter through contact pairs  $R_a$  or  $R_b$  which make when the latter operates. This is done to avoid the useless operation of relay  $R_2$  when it reacts to the difference in the make and break time of the test pairs or to vibration.

The two switching keys  $Key_1$  and  $Key_2$  are provided to check the operation of the system.

The operation of the normally closed contacts  $Key_1$  simulates the failure of the first kind while the operation of the normally open contacts  $Key_2$

TABLE 1

Sequence number	Manner of operation of $R_2$		Position of the armature	Nature of failure
	contacts normally closed. $R_1$	contacts normally open. $R_1$		
1	←	-	Release	Normally closed contact did not close, I Group
2	←	-	Operate	Normally open contact did not close, II
3	→	-	Release	Normally closed contact did not close, II
4	→	-	Operate	Normally open contact did not close, I
5	-	←	Release	Normally open contact did not open, II
6	-	←	Operate	Normally closed contact did not open, I
7	-	→	Release	Normally open contact did not open, I
8	-	→	Operate	Normally closed contact did not open, II
9	←	→	Release	Normally open contact did not open I. Welding or clinching.
10	←	→	Operate	Normally closed contact did not close } I.- Did not open;
				Normally closed contact did not open } II. Welding or clinching.
11	→	←	Release	Normally open contact did not close } II.- Did not close;
				Normally open contact did not open } II Welding or clinching.
12	→	←	Operate	Normally closed contact did not close } II.- Did not open;
				Normally closed contact did not open } I. Welding or clinching.
				Normally open contact did not close } I.- Did not close.

simulates failure of the second kind. During the checking operation in each case, the meter must count each pulse which enters the winding of the test relay.

Key<sub>3</sub> is used to clear the system (to stop switching after recording and determining the nature of the failure).

#### Life Tests and Establishment of Norms

Because the erosion of contacts depends on many factors, the useful life of a relay depends on its construction. Also, there is a large spread of the useful life of individual relays and in the contact groups of the same relay. /450

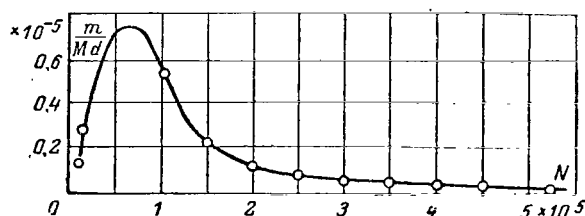


Figure 2. The distribution of useful life for relay RES-10 contacts when switching a network with  $U_c = 30-32$  volts and  $I_c = 2$  amperes ( $M = 123$ ).

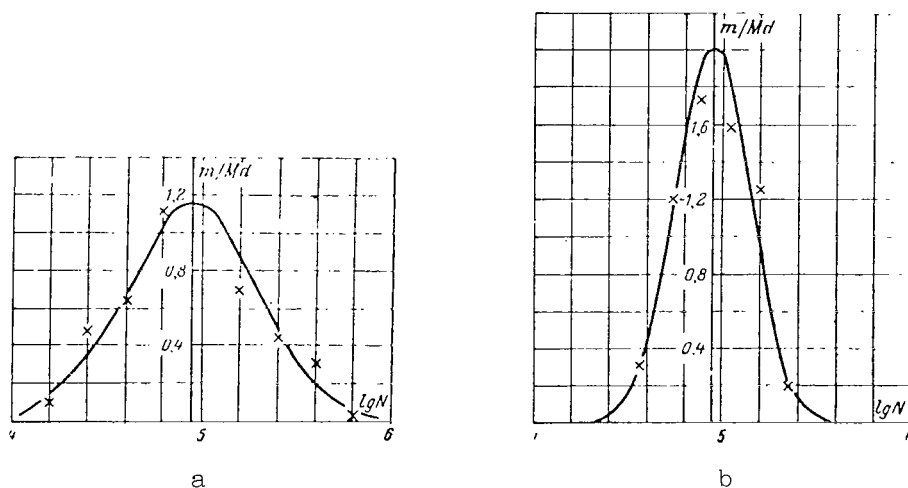


Figure 3. Distribution curves showing the logarithm of the useful contact life for the RES-10 relay which switches a circuit with  $U_c = 30-32$  volts and  $I_c = 2$  amperes. a, relay encapsulated with epoxy resin ( $M = 122$ ); b, relay with a rolled case ( $M = 83$ ).

It is necessary to point out that there is an interaction of these factors. For example: a) the lowering of the contact pressure during a switching process increases erosion which, as a rule, is associated with a decrease in the breaking speed of the contacts when the relay pulls in, and this in turn increases the duration of the arc during closing, leading to an increase in erosion; b) the wear of auxiliary members, for example of the supports, leads to the formation of soot on the contacts which increases the intensity of the arc and also increases the erosion of the contacts, etc.

Apparently this situation is responsible for the spread in the useful life of contacts which does not satisfy the normal law. As we know, this law is valid when the large number of minor factors are independent and produce an equal effect.

The testing of a relatively large number of contacts used in RES-9 and RES-10 relays loaded with 2 amperes and 30-32 volts has made it possible to establish the distribution of useful life for these contacts. This distribution law was later confirmed by the results of testing the contacts of other types of relays with different loads.

Figure 2 shows the differential distribution curve for the useful life of 122 samples of the RES-10 relay, obtained by grouping the points of the 451 histogram over 11 intervals.

Figures 3 and 4 show the differential and integral distribution curves for the logarithm of the useful life for contacts of the RES-10 relay with a typical load of 2 amperes, while figures 5 and 6 show these curves for the RES-9 relay with a load of 1 and 2 amperes.<sup>1</sup>

From figure 2 we can see that the distribution of the useful life of contacts does not follow a normal law. However, as we can see from figures 3 and 5, the logarithm of the useful life does satisfy this law. Indeed, the crosses and points which correspond to experimental data, lie close to the bell-shaped theoretical curves which are constructed from the statistical distribution parameters obtained by processing the experimental data. Some of the deviations may be explained by insufficient amount of statistical material, i.e., by the limited number of test samples.

The integral distribution curves constructed on the basis of ungrouped 452 data on probability graph paper (figs. 4 and 6), are close to straight lines which shows that the distribution is close to normal. Some deviations from a straight line were noted at the beginning of the curve. This is due to the unavoidable presence of samples with short life due to concealed defects. For this reason, these points were dropped. The deviation from the straight line at the end is due to the truncation of the distribution curve which takes place

---

<sup>1</sup>The technical specifications for the RES-9 relay provide for a contact current of 0.8 amperes when contacts are made from the PLI-10 alloy and for 2 amperes when the contacts are made of silver.

because the useful life of any group of contacts is limited.

/453

It is quite important to establish the distribution law for the useful life of contacts. If we know this law and test a small quantity of samples, we can establish the operating characteristics of relay contacts for a given production run and we can also establish the effect of design and production changes, and changes in the materials of the contacts. We can compare relays of different construction and also determine the useful life of new designs, etc.

/454

Indeed, if the distribution law is known, we can use equations (2) and (3) to determine the numerical values of the parameters of this distribution, i.e., the distribution center, which gives us the most probable useful life and of the root-mean-square deviation from the distribution center which characterizes the stability of useful life.

In addition to this, if we know the distribution of the useful life, we can establish norms which could be included in the technical specifications. To accomplish this it is sufficient to use the simple law  $k_{\sigma}$  and

/455

determine the boundary value for the logarithm of the useful life from the following equation<sup>1</sup>

$$(\lg N)_{\min} = \overline{\lg N} - k(1 + q_{\sigma})\sigma_{\lg}^1, \quad (1)$$

where  $\overline{\lg N}$  is the average value of the logarithm for the useful life  $s$  of the tested samples

$$\overline{\lg N} = \frac{\sum_{s=1}^M \lg N_s}{M}, \quad (2)$$

where  $M$  is the number of tested contact groups;

$S$  is the number of the sample in the contact group;

$\sigma_{\lg}$  is the root-mean-square deviation of the logarithm of useful life:

---

<sup>1</sup>Here the confidence interval of the distribution center  $\overline{\lg N}$  is not taken into account. This is justified by the fact that the confidence probability  $\alpha_1$  of the quantity  $(\lg N)_{\min}$ , which is computed from the confidence boundaries  $\lg N$  and  $\sigma_{\lg}$ , which, in turn, are established with a confidence probability  $\alpha$ , will turn out to be greater than the latter.

The question of the confidence probability  $\alpha$  necessary to determine the boundaries of  $\lg N$  and  $\sigma_{\lg}$ , so that their substitution into equation (1) provides for a given confidence boundary in the value of  $(\lg N)_{\min}$ , is not solved at the present time.



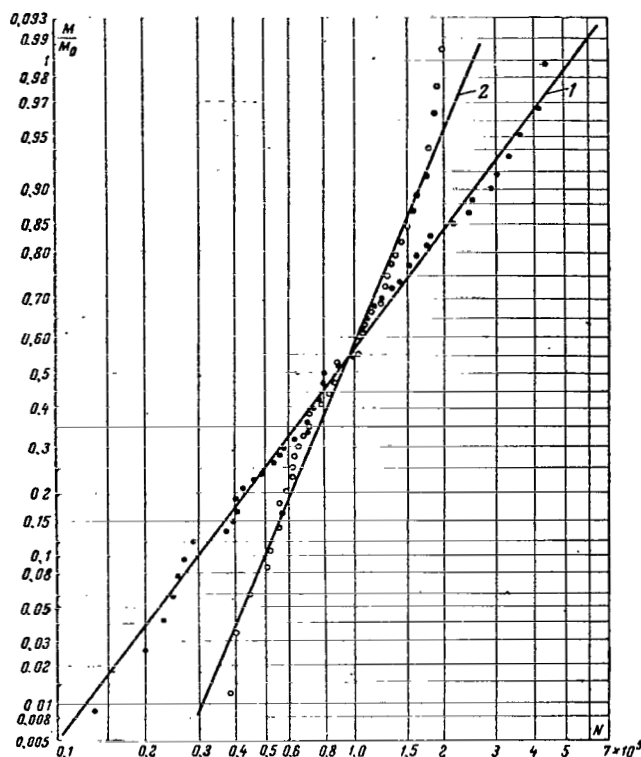


Figure 4. The integral distribution curves for the logarithm of the useful life of relay RES-10 contacts when the load is 2 amperes and 30-32 volts. 1, with epoxy resin ( $M_0 = 122$ ); 2, rolled case

( $M_0 = 83$ ).

$$\sigma_{lg} = \sqrt{\frac{\sum_{s=1}^M (\lg NS - \overline{\lg N})^2}{M-1}}, \quad (3)$$

$q_{\sigma}$  is a coefficient which takes into account the confidence limit of the root-mean-square deviation (ref. 4), which can be obtained from the distribution tables of  $\alpha(q_{\sigma}, M-1)$  depending on the number of tested contacts in group  $M$  and the given confidence probability  $\alpha$  (ref. 4); usually it is assumed that  $\alpha = 0.9-0.95$ ;

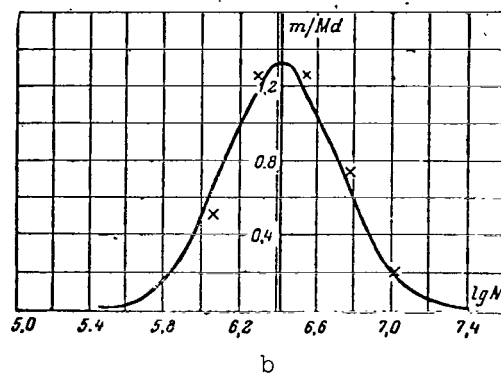
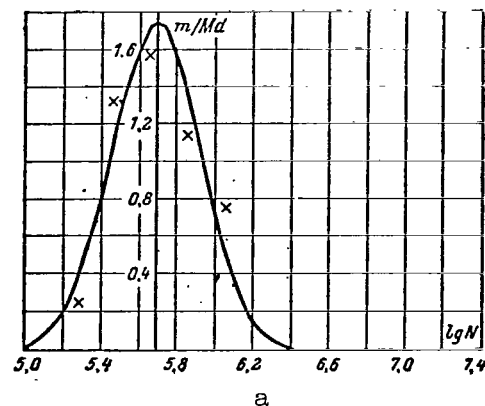


Figure 5. Distribution curves for the logarithm of the useful contact life of the RES-9 relay when  $U_c = 30-32$  volts. a, silver contacts;  $I_c = 2$  amperes; b, PLI-10 contacts,  $I_c = 1$  ampere.

$k$  is the coefficient which determines the boundary of the useful life <sup>/456</sup> which contains  $R$  percent of contacts for a given relay type; for values of  $R$  from 99.0 to 99.9 percent  $k = 2.33 - 3.09$  and is obtained from the tables giving the quantiles of normal distribution (ref. 5).

The antilogarithm of the quantity obtained by means of equation (1) will give the value of the norm for the useful life of the contacts  $N_{\min}$ .

Table 2 lists the values of the distribution parameters  $\overline{\lg N}$  and  $\sigma_{\lg}$

obtained from experimental data (see figs. 3-6) and computed by means of equation (1). The value of the minimum useful life for  $k = 2.33$  and  $q_\sigma = 0$ ,

(i.e., without taking into account the confidence limit)  $N$  is the antilogarithm of  $\lg N$  and determines the most probable useful life.

The ratio  $\frac{\sigma_{\text{unit}}}{\lg N}$  is a convenient quantity for determining the degree of spread in the useful life when undertaking quality control in a given production run.

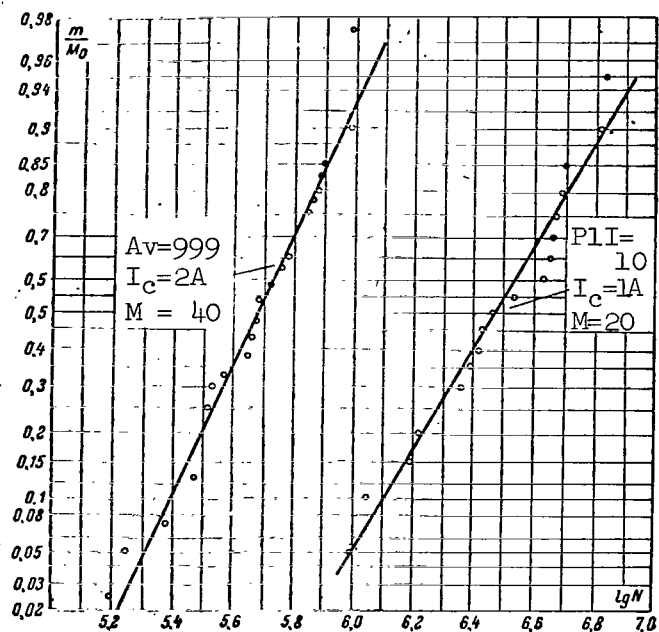


Figure 6. Integral distribution curves for the logarithm of useful life for relay RES-9 contacts when  $U_c = 30-32$  volts.

TABLE 2

Relay type	Contact Material	M	Load		$\overline{\lg N}$	$\sigma_{\lg}$	$\frac{\sigma_{\lg}}{\overline{\lg N}}, \bar{N}$	$\lg N_{\min}$	$\sim N \cdot 10^5$	$N_{\min} \cdot 10^5$
			U, c	I, a						
RES-9	PLI-10	20	30-32	1	6.44	0.292	4.5	5.76	27.6	5.75
RES-9	Av.999	40	30-32	2	5.68	0.225	4.0	5.16	4.8	1.45
RES-10 epoxy resin	PLI-10	122	30-32	2	49.4	0.356	7.2	4.11	0.87	0.13
RES-10 rolled	PLI-10	83	30-32	2	4.95	0.199	4.0	4.49	0.89	0.31

The data in Table 2 show that when the load is two amperes: a) the minimum useful life of the RES-9 and RES-10 relays is substantially less than given in the technical specification; b) the useful life of the RES-9 relay with silver contacts is 4.5 times greater than that of the RES-10 relay with rolled case and with contacts made from the PLI-10 alloy; c) the replacement of the epoxy encapsulation with the rolled case in the RES-10 relay did not change the probable value of useful life but has made it possible to stabilize it (has made it possible to reduce the value of  $\frac{\sigma_{lg}}{lgN}$  by almost a factor of 2), as a result of which the useful life increased almost by a factor of 2.5.

#### Variation in the Useful Life of the PLI-10 Alloy Contacts as a Function of 457 Contact Current

The results of determining the useful life of platini-iridium contacts of the RES-10 relay (with epoxy resin) and the RES-9 relay at 30 volts and different load currents are shown in figures 7 and 8 in the form of differential curves for logarithmic distribution of the limiting useful life for each of the contact currents I.

From figures 7 and 8 we can see that for both types of relays, the distribution parameters  $lgN$  and  $\sigma_{lg}$  are linear functions of the contact current logarithm (see the reduced graphs at the right) i.e.,

$$\overline{lg N} = \overline{lg N_1} - a \lg I; \quad (4)$$

$$\sigma_{lg} = \sigma_{lg1} - b \lg I, \quad (5)$$

where I is the average contact current

a and b are coefficients which characterize the rate of decrease respectively of the average and the root-mean-square deviation in the values of the logarithm of the useful life when the contact curve increases;

$\overline{lg N_1}$  and  $\sigma_{lg1}$  are the average and the root-mean-square deviation of the logarithm of useful life when the contact current is 1 ampere.

From (4) it follows that the most probable useful life for platini-iridium contacts which switch a nonreactive load in the limits 0.8 - 5 amperes, may be represented by the following equation

$$\tilde{N} = \frac{\tilde{N_1}}{I^a}, \quad (6)$$

where  $\tilde{N}$  is the antilogarithm of the average value of the logarithm of useful life for any contact current I;

$\tilde{N_1}$  is the same when the contact current is 1 ampere.

The coefficients  $\overline{\lg N_1}$  and  $\sigma_{\lg 1}$  are constants when the voltage of the control circuit, the material of the contacts and the construction of the relay are fixed. Coefficients a and b for the RES-9 and RES-10 relays are the same. We may, therefore, assume that they are determined by the voltage in the control circuit and by the contact material. Substituting (4) and (5) into (1) we find an expression for the minimum contact life /459

$$N_{\min} = \frac{\tilde{N}_1 \cdot 10^{-k\hat{\sigma}_{\lg 1}}}{I^{a-kb}} = \frac{N_{\min 1}}{I^{a-kb}}, \quad (7)$$

where

$$N_{\min 1} = \tilde{N}_1 \cdot 10^{-k\hat{\sigma}_{\lg 1}} \quad (8)$$

and is the antilogarithm of the quantity

$$(\lg N)_{\min 1} = \overline{(\lg N)_1} - k\hat{\sigma}_{\lg 1}, \quad (9)$$

$\hat{\sigma}_{\lg 1} = (1 + q_\sigma)\sigma_{\lg 1}$  is the upper confidence group of the root-mean-square deviation in the useful life when the contact current is 1 A. /460

If we do not take into account the confidence interval of the root-mean-square deviation in equation (6),  $\hat{\sigma}_{\lg 1} = \sigma_{\lg 1}$ .

The broken lines in figures 7 and 8 show the minimum useful life as a function of contact current for  $k = 2.33$ , i.e., for a reliability of  $p = 99$  percent, without taking into account the confidence interval  $q_\sigma = 0$ .

Table 3 shows the values of coefficients  $\tilde{N}_1$ ,  $\sigma_{\lg 1}$ , a and b, obtained from the graphs in figures 8 and 7, as well as the value of  $N_{\min 1}$ .

TABLE 3

Relay type	Contact material	$\lg N_1$	$\sigma_{\lg 1}$	a	b	$\tilde{N}_1$	$N_{\min 1}$	$\frac{\sigma_{\lg 1}}{\lg N_1} \%$
RES-9	PLI-10	6.5	0.3	2.6	0.16	$3.16 \cdot 10^6$	$6.2 \cdot 10^5$	4.6
RES-10	PLI-10	5.6	0.37	2.6	0.16	$4 \cdot 10^5$	$5.5 \cdot 10^5$	6.6
(epoxy resin)								
RES-10	PLI-10	5.7	0.247	2.6	0.16	$5.43 \cdot 10^5$	$1.4 \cdot 10^5$	4.3
(rolled)								

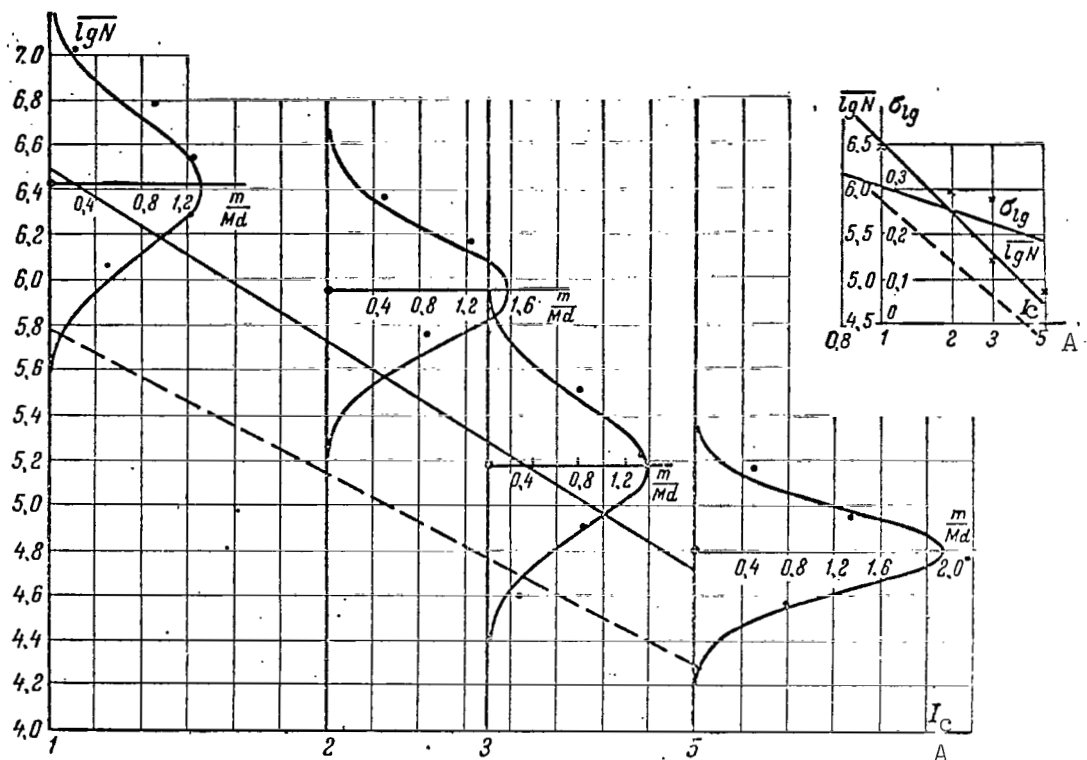


Figure 7. Logarithmic distribution curves for useful life of RES-9 relay contacts as function of contact current when  $U_c = 30-32$  V.

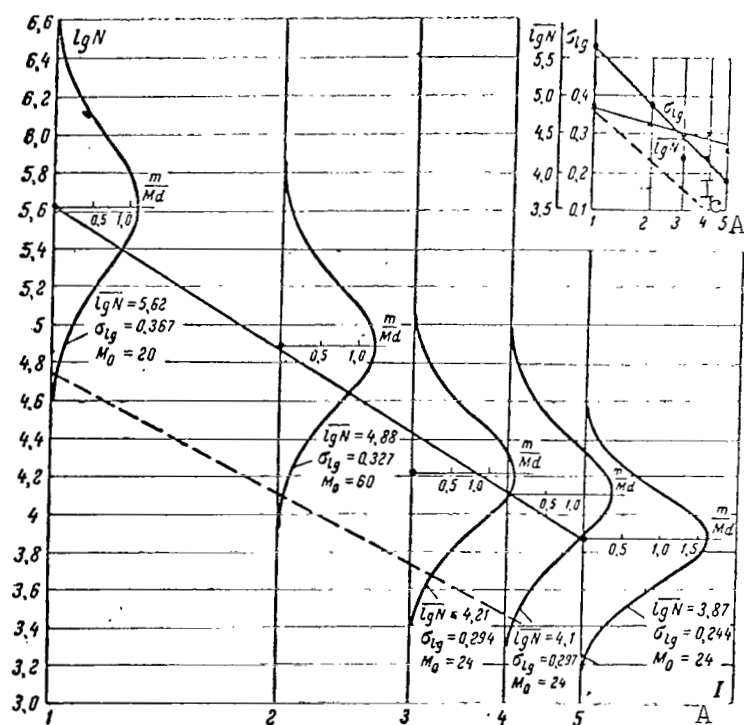


Figure 8. Logarithmic distribution curves for useful life of RES-10 relay contacts as function of contact current when  $U_c = 30-32$  V.

By comparing the values of coefficients  $\tilde{N}_1$  in table 3 it is clear that the most probable useful life of platini-iridium contacts for any contact current at 30 volts in the range 0.8 to 5 amperes is 8 times greater for the RES-9 relay than for the RES-10 relay with the epoxy resin and  $\sigma$  times greater than for the RES-10 relays with rolled cases.

The ratio of the coefficients  $N_{min1}$  which determines the minimum useful life with respect to RES-10 with epoxy resin shows an even greater difference. Specifically, the difference is equal to a factor of 11 because the spread in the useful life of these types is not the same. If we represent the latter by the ratio  $\sigma_{lg}/\sqrt{lgN}$  (table 3) we see that for the RES-10 relays with epoxy resin it is almost twice as large as for the RES-9 relay due to the effect of hermetic sealing and of the epoxy resin vapors on the erosion of contacts. For the rolled RES-10 relay, the spread is approximately the same as for RES-9 relay.

Let us assume that the coefficients a and b do not depend on the type 461 of relay.<sup>1</sup> Then, to establish the useful life of any type of relay with platini-iridium contacts when the contact curve varies from 1 to 5 amperes it is sufficient to have the distribution parameters for some one contact current i. Then, the coefficient  $\tilde{N}_1$  may be obtained from equation (6)

$$\tilde{N}_1 = \tilde{N}_i i^a, \quad (10)$$

while the coefficient  $\sigma_{lg1}$ , may be obtained from equation (5)

$$\sigma_{lg1} = \sigma_{lg i} + b \lg i. \quad (11)$$

If we use the data on the distribution parameters of the useful life for the RES-10 relay with the rolled case and a contact current of  $i = 2$  amperes (see figures 3 and 4), we find and record in table 3 the corresponding coefficients  $\tilde{N}_1$  and  $\sigma_{lg1}$ , and also the design value  $N_{min1}$ .

Substituting the values given by table 3 into equation (7) we determine the minimum useful life of contacts for all the types of relays whose contact currents are recorded in the technical specifications for  $p = 99$  percent (table 4).

---

<sup>1</sup>However, this should be verified by running a test with any two loads.

TABLE 4

Relay type	I, A technical specifications	$N_{ts}$	$N_{min}$
RES-9	0.8	$10^6$	$1.01 \cdot 10^6$
RES-10 (epoxy resin)	2	$10^5$	$1.17 \cdot 10^4$
RES-10 (rolled)	2	$10^5$	$3.04 \cdot 10^4$

We can see from table 4 that the minimum useful life of the RES-9 relay when the contact current is 0.8 amperes is close to the one recorded in the technical specifications, while for the RES-10 relay with a contact current of 2 amperes it is substantially less than the value recorded in the technical specifications. To provide a reliability of  $p = 0.99$  it must be decreased to  $1.2 \cdot 10^4$  for the relay with the epoxy resin and to  $3 \cdot 10^4$  for the relay with the rolled case.

By obtaining the variation in the useful life of contacts as a function of contact current, we can accelerate the testing of relay contacts. Indeed, if we determine the values of the distribution parameters  $\lg N_f$  and  $\sigma \lg_f$  for forced loading, we can use them and equation (1) to determine the value  $N_{minf}$ . Then it is easy to determine the minimum useful life for other values of the contact current  $I$  by using the expression

$$N_{min} = N_{minf} \frac{I_f}{I}^{a-kb}. \quad (12)$$

For  $k = 2.33$

$$N_{min} = N_{minf} \frac{I_f}{I}^{2.33}. \quad (13)$$

In conclusion, let us consider the failures of PLI-10 contacts operating with the load specified above.

The analysis of failures has shown that approximately 90 percent are due to the wedging of pips on one electrode in the craters of the opposite electrode or due to the welding of the electrodes. An exception is the RES-10 relay operating with a current of 1 ampere for which only 65 percent of the contacts failed by not opening. Apparently in this case there was a greater sliding of the contacts during closure compared with RES-9. This slipping either prevented the formation of large pips or was responsible for their breaking,



because when the current is 1 ampere, the latter usually have the shape of thin needles.

By considering the principal reasons for the failure of platini-iridium contacts under considered loads, it must be admitted that to increase their usual life it is necessary to find contact materials with a lesser tendency to form needle-like pips.

## Conclusions

1. A schematic diagram of a test setup has been presented for recording failures of contacts incorporating an automatic termination of switching in the event of any failure and with a device which makes it possible to determine the nature of the failure and to identify it with one of two contact pairs, handled by one recording mechanism.

2. The operation of this test setup to determine the useful life of contacts has made it possible to collect statistical data and to determine the distribution law for the life of contacts. It was shown that the latter satisfies the normal logarithmic law. The question of establishing a norm for the useful life of contacts and the incorporation of this information in the technical specifications was considered. Norms for the useful life of contacts were established for a series of miniature relays for certain loads.

3. The variation in the limiting useful life of platini-iridium contacts as a function of current in nonreactive loads was established for the range 0.8 - 5 amperes and 30 - 32 volts. These are typical loads recorded in the technical specifications for most light-duty relays manufactured in the USSR and for relays described in the catalogs of foreign nations. Empirical equations were obtained showing the variation in the limiting useful life of platini-iridium contacts as a function of contact current. This made it possible to determine the approximate life of platini-iridium contacts for any contact currents in the range 0.8 - 0.5 amperes based on the testing of contacts at any one of two loads. It has been shown that when the variation in the useful life of contacts is established as a function of contact current, it is possible to carry out accelerated tests for quality control in production runs.

## REFERENCES

1. Sotskov, B. S., The Design of Relay Contacts, "Electric Contacts", Proceedings of a Conference (Voprosy rascheta kontaktov rele, "Elektricheskiye kontakty") Gosenergoizdat, 1956.
2. Holm, P., Electric Contacts, (Elektricheskiye kontakty), I. L., 1961.
3. Sotskov, B. S., The Element of Automatic and Remote Control Equipment (Elementy avtomaticheskoy i telemekhanicheskoy apparatury). Gosenergoizdat, 1950.

4. Venttsel', Ye. S., The Theory of Probability (Teoriya veroyatnostey) Fizmatgiz, 1956.
5. Shor, Ya. B., Statistical Methods of Analysis in Quality Control (Staticheskiye metody analiza i kontrolya kachestva i nadezhnosti) Izd-vo Sovetskoye Radio, 1962.

## DETERMINING NORMS FROM THE BASIC ELECTRIC PARAMETERS OF CONNECTOR CONTACTS

V. S. Savchenko

/464

### Formulation of the Problem

One of the key problems facing modern radio electronics is to provide reliable operation of electronic equipment under severe operating conditions. One solution to this problem is to provide highly reliable components, including highly reliable connectors.

To solve this problem, industry is currently conducting periodic and continuous reliability tests which will substantially improve the quality of production.

In the course of this testing program, complete and partial failures of components are observed. We use the term partial failure when a device is still capable of operating but when its characteristics no longer conform with the technical specifications, i.e., when there is a deviation of electric parameters from the norm.

Since any deviation from the norm is classified as a failure, this deviation must produce a deterioration in the operation of a contact device or it must make it possible to forecast its complete failure.

In other words, the norms for electrical parameters of contacts must be such that the results of reliability tests are objective and reflect the potential of some contact device. For this reason, a correct selection of norms for the electrical parameters of contacts is of prime importance.

In a series of cases, the norms which are contained in the technical specifications for contact devices do not satisfy these requirements.

On the one hand, there are cases when during inspection reliable components are selected together with those which have potential defects. Such potential defects manifest themselves when the device is in operation. This situation is encountered in cases when the lowering of the norms is without basis.

/465

This is so because the physical and chemical phenomena in contacts have not served as a basis for establishing norms in regard to electrical parameters. Up to the present time there has been an insufficient exchange of information between those concerned with the theory of contacts and those concerned with their practical construction and exploitation.

Therefore, it has become necessary to find a way for determining norms on the basis of electrical parameters of contacts and to present a method for computing them. The present work attempts to do this by analyzing the thermal states of contact devices.

Experience has shown that a large percentage of failures in the operation of contact devices takes place due to an increase in the temperature above its optimum value. This leads to the oxidation of contact surfaces, burning, and finally, to the loss of electrical contact, i.e., to complete failure. Also, when normal temperatures are exceeded, there is a deterioration in the physical properties of the dielectric which surrounds the contact. As a result, there is a decrease in the insulation resistance, in mechanical strength and also in the breakdown voltage.

Thus, since the thermal state of the contact is determined to some degree by its electrical characteristics, the norms for the basic electric parameters of contacts may also be determined by proceeding from the condition that the temperature during operation must not exceed a certain value.

#### The Transitional Resistance of the Contact

In the region where current passes from one body of the contact to another we encounter resistance which is known as the transitional resistance of the contact. The Joule heat which is dissipated in the transition zone determines the temperature state of the transition zone. We should distinguish between "local overheating" of the constriction region and overheating of the "apparent" contact surface.

The temperature of local overheating may be determined from an expression given in reference 1

$$\theta_1 = \frac{U_c^2}{8\sigma_k} = \frac{I^2 R^2_{tr}(t)}{8\sigma k}, \quad (1)$$

where  $U_c$  is the voltage drop across the contact resistance;

$\sigma$  is the specific electrical conductivity of the contact (plating) material;

$k$  is the specific thermal conductivity of the contact (plating) material.

To determine the excess temperature of an apparent contact surface  $\theta_2$  we consider a cylindrical contact represented by an equivalent scheme in figure 1.

In the steady state, the excess heat flowing into element  $dx$  over that which is removed is compensated for by heat loss through the surface  $\pi D_c dx$ , i.e.,

$$k_1 \frac{\pi D_c^2}{4} \cdot \frac{d^2 \theta}{dx^2} - k^* \theta = 0,$$

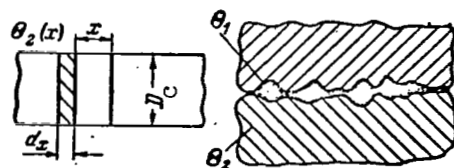


Figure 1. Equivalent scheme of a cylindrical contact.

where  $k_l$  is the thermal conductivity of the contact material;

$D_c$  is the diameter of the contact;

$k^*$  is the coefficient of heat transfer from the surface of the contact whose length is 1 cm;

1467

$\theta$  is the instantaneous value of the excess temperature.

The boundary condition assumes that, at the junction point, half of the total heat liberated in the transitional resistance of the contact  $R_{tr}$  is removed into each part of the contact, i.e.,

$$-k_l \frac{\pi D_c^2}{4} \left[ \frac{d\theta}{dx} \right]_{x=0} = \frac{1}{2} I^2 R_{tr}(t).$$

The coefficient of the heat transfer coefficient  $k^*$  depends on the specific conditions of heat transfer, i.e., on the magnitude of the thermal resistance to the thermal flux from the surface of the contact.

Thus, in analyzing the temperature state of the operating contact, it is not permissible to consider the latter independently from the rest of the device.

As an example, let us consider a single-contact cylindrical connector whose diameter is much smaller than its length (fig. 2).

In this case we can reduce the solution of our problem to the solution of heat liberation by a rod of infinite length (ref. 2)

$$\theta_2(x) = \frac{\frac{1}{2} I^2 R_{tr}(t)}{\sqrt{0.25 k_l k^* \pi D_c^2}} e^{-\frac{x \sqrt{k^*}}{\sqrt{0.25 k_l \pi D_c^2}}}; \quad (2)$$

$$\theta_1 = \frac{\frac{1}{2} I^2 R_{tr}(t)}{\sqrt{k_l k^* \frac{\pi D_c^2}{4}}}.$$

where

$$k^* = \frac{2\pi a}{\frac{2}{h \frac{D_1}{2}} + \frac{1}{\lambda_1} \ln \frac{D_2}{D_c} + \frac{1}{\lambda_2} \ln \frac{D_1}{D_2}}, \text{ watts/cm} \cdot \text{degree};$$

$h$  is the coefficient of heat transfer to the surrounding air;

$\lambda_1$  is the thermal conductivity of the dielectric;

/468

$\lambda_2$  is the thermal conductivity of the connector housing;

$D_1$  is the external diameter of the connector case;

$D_2$  is the internal diameter of the connector case;

$a$  is a correction coefficient which takes into account the deviation of contact configuration from a cylindrical form.

Thus, both the temperature of the local hot spot and the temperature of the apparent contact surface are determined by the value of the electrical current which passes through the contact and by the value of its transitional resistance, i.e., to prevent the exceeding of a given temperature state for a given value of current, it is necessary that the value of the transitional contact resistance be less than some allowable value. It is known that the magnitude of the transitional resistance depends on the temperature while we are interested in the allowable value of the transitional resistance which is reduced to normal conditions, i.e., to values which we obtain when we take measurements at room temperature with low currents.

The variation in the transitional resistance as a function of the temperature of the surrounding medium is the same as that in any conductor

$$R_{\text{trans}}(t_2) = R_{\text{trans}}(\theta_1)(1 + \alpha t_2).$$

Here the term surrounding temperature means the temperature on the apparent contact surface.

The variation in the transitional resistance as a function of the temperature of the hot spot is somewhat different

$$R_{\text{trans}}(\theta_1) \approx R_{\text{trans}}(0) \left(1 + \frac{2}{3} \alpha \theta_1\right).$$

However, this relationship is valid when the plating material satisfies the Wiedmann-Lorentz law.

If we take into account the temperature variation of the transitional resistance, we obtain an expression for its allowable value, reduced to normal conditions:

$$R_{\text{trans allow}}(0) = \frac{\sqrt{L} T_2}{I} \arccos \frac{T_2}{T_2 + \Theta_1}, \quad (3)$$

where  $L$  is the Wiedmann-Lorentz coefficient ( $L = 2.4 \cdot 10^{-8}$  volts<sup>2</sup>/degree);  
 $I$  is the current;  
 $T_2$  is the value of the maximum permissible temperature of the apparent contact surface in degrees Kelvin;  
 $\Theta_1$  is the allowable value of the hot spot temperature.

Expression (3) determines the allowable value of the transitional resistance for a given hot spot temperature.

In the same way, for a given temperature of the apparent contact surface, there is a definite allowable value for the transitional resistance.

$$R_{\text{trans allow}}(0) = \frac{2\Theta_2 \sqrt{k_1 k^* \frac{\pi D^2}{4}}}{I^2 (1 + \alpha t_2) \left(1 + \frac{2}{3} \alpha \Theta_1\right)}, \quad (4)$$

where  $\Theta_2$  is the allowable temperature of the apparent contact surface.

Thus, the allowable transitional resistance may be determined from the given temperature of the hot spot and the given temperature of the apparent contact surface. Therefore, it is interesting to determine which of these temperature states is significant. For this purpose let us construct the functions  $\Theta_1 = f(I)$  and  $\Theta_2 = f(I)$ , assuming that  $R_{\text{trans}}(0) = 0.2 \cdot 10^{-3}$  ohm;

$\alpha = 4 \cdot 10^{-3}$  1/degree;  $k_1 = 3.8$  watts/cm.degree;  $k^* = 3 \cdot 10^{-4}$  watts/cm.degree  
 (fig. 3).

The allowable temperature of the constriction region is selected to prevent the adherence and welding of contacts as well as the oxidation of the contact plating when such a temperature prevails for a prolonged period of time.

The allowable value of the contact body temperature is selected from the thermal stability of the dielectric which surrounds the contact. As a result, the temperature of the hot spot usually lies in the limits 100 - 300°C while the allowable temperature of the apparent contact surface lies in the range

10 - 50°C.

/470

From the graphs shown in figure 3 we can see that the thermal state in the region of constriction has a significant value only when the currents are large and when the diameters of the contacts are large. Therefore, in the

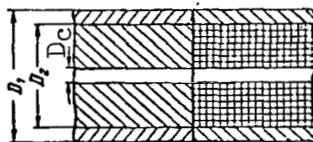


Figure 2. Equivalent scheme of a cylindrical single-contact connector.

future we shall assume that the allowable value of the transitional resistance for the case of light-duty contacts is determined only by the given excess temperatures of the apparent contact surface. In this case, by analyzing expression (4) we may also conclude that to provide for a constant excess temperature of the apparent contact surface for contacts of various diameters it is necessary to satisfy the following condition

$$\frac{D_c}{I^2 R_{\text{trans allow}}(0)} = A = \text{const.} \quad (5)$$

Now let us see how this condition is satisfied in practice.

472

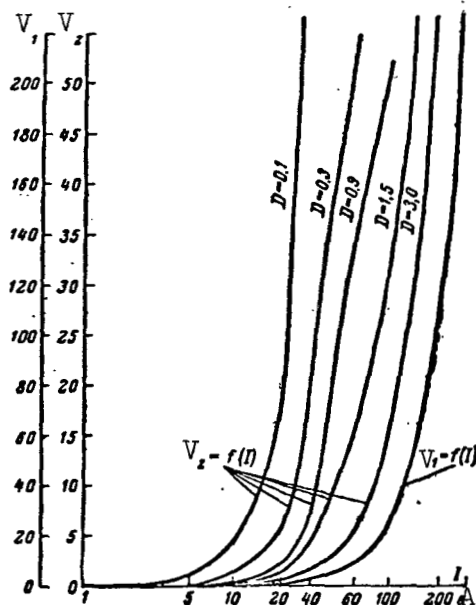


Figure 3. The variation in the excess temperatures as a function of current.



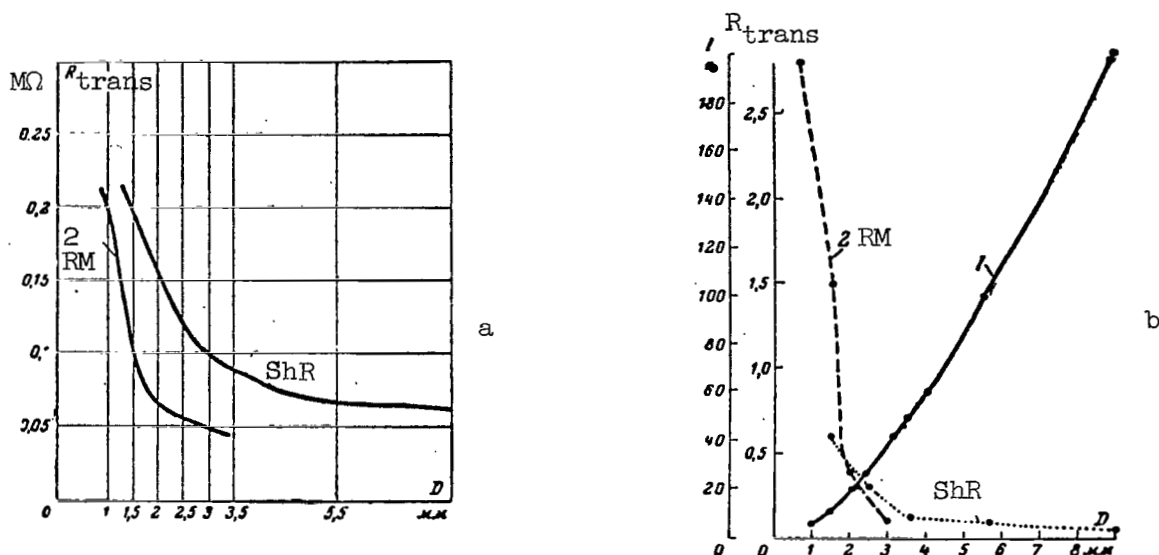


Figure 4. Variation in  $R_{trans}$  as a function of the contact diameter of the ShR and 2RM connectors. a, measured values; b, computed values.

Figure 4 represents the relationship  $R_{trans} = f(D_c)$  for the measured values of contact  $R_{trans}$  when delivered, and also for the values  $R_{trans}$  computed from the norms for the value  $R_{contact}$  which are contained in the technical specifications for the ShR, 2RM connectors. Figure 4 also shows the functions  $I = f(D_c)$ .

On the basis of these values, the function  $A = f(D_c)$  (fig. 5) is constructed for different contact diameters.

As we can see from figure 5, the parameter  $A$  is not constant for various values of  $D_c$ . Therefore, we may assume that the values of the load currents for connectors of the ShR and 2RM type are selected improperly for existing values of  $R_{trans}$ .

This proposition is confirmed by the results of tests conducted with these connectors which indicated that the norms for the allowable values of load current should be reexamined.

Thus, the example which we have cited illustrates once more the importance of determining the norms on the basis of the transitional contact resistance. We can solve this problem by analyzing the thermal states of contact operation.

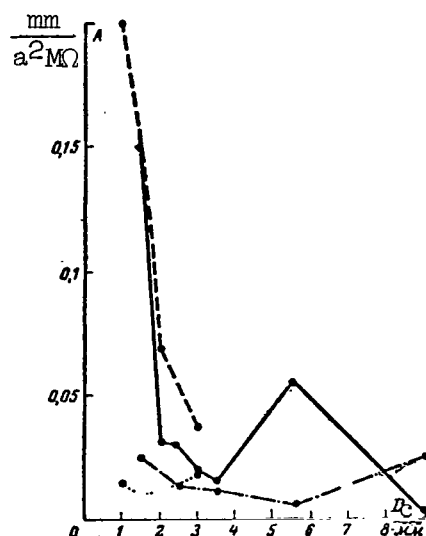


Figure 5. Variation in the parameter A as a function of the contact diameter of connectors ShR and RM.

#### The Norm for the Value of the Transitional Contact Resistance

It is known that the transitional contact resistance may vary sharply during operation. Therefore, the norm for the magnitude of the transitional resistance must be selected in such a way that, under any operating condition, /473 it does not exceed its allowable value for a given temperature state of contact operation.

In this case, the norm for the value of the transitional contact resistance is determined from the following equation

$$R_{\text{trans norm}}^{(0)} = \frac{R_{\text{trans allow}}^{(0)}}{\eta_1 \eta_2 \eta_3 \eta_4}, \quad (6)$$

- where  $\eta_1$  is the safety factor which takes into account the possible variations in the transitional contact resistance during multiple switching;  
 $\eta_2$  is the safety factor which takes into account the possible variations in the transitional resistance when mechanical loads are present (vibration, shock);  
 $\eta_3$  is a safety factor which takes into account the possible variations in the transitional resistance under the influence of climatological factors and prolonged storage;  
 $\eta_4$  is the safety factor which takes into account the possible deviations in the production of the contacts and also the allowable level of contact current overloads.

Let us consider these safety factors in greater detail. It is known that when a connector is coupled or decoupled, its transitional resistance varies and in the case of defective contacts this variation may take place over a very wide range of values (fig. 6).

To characterize the level of variation in the value of the transitional contact resistance in the course of multiple switching, we introduce a non-stability parameter for the transitional resistance in the static state, whose value is determined from the following expression

$$\frac{\Delta R_{st}}{R} = \frac{R_{trans \max}(0) - R_{trans \min}(0)}{R_{trans \text{ av}}(0)} \cdot 100\%. \quad (7)$$

To determine accurately the limits of variation in the transitional resistance, it is necessary to carry out a very large number of measurements, which is impossible in most cases. Therefore, it is desirable to find these limits, even approximately, by using only 3 to 5 measurements. /474

It has been determined that usually the distribution of transitional resistance values during multiple switching satisfies the normal law for which the following inequalities are valid

$$R_{trans \text{ av}}(0) - t_{\alpha} \frac{s}{\sqrt{n}} \leq R_{trans}(0) \leq R_{trans \text{ av}}(0) + t_{\alpha} \frac{s}{\sqrt{n}}, \quad (8)$$

where  $R_{trans \text{ av}}(0) = \frac{1}{n} \sum_{i=1}^n R_i$  is the average value of the transitional contact

resistance determined from  $n$  measurements;  
 $t_{\alpha}$  is the quantile of the Student distribution, which is a function of  $(n-1)$  and  $p$  (the confidence probability);

$s = \sqrt{\frac{1}{n-1} \sum_{i=1}^n (R_i - R_{trans \text{ av}})^2}$  is the root-mean-square deviation of the

instantaneous value of the transitional contact resistance from its average value.

Inequality (8) shows the possible limits for the variation in the value of the transitional resistance which may exist during multiple switching of the contact. In this case, the factor of safety  $\eta_1$  will be equal to

$$\eta_1 = \frac{R_{trans \text{ av}}(0) + t_{\alpha} \frac{s}{\sqrt{n}}}{R_{trans \text{ av}}(0)} \approx 1 + \left( \frac{\Delta R}{R} s i \right) \cdot \frac{t_{\alpha}}{\sqrt{3n}}, \quad (9)$$

where  $\frac{\Delta R}{R} \text{ si}$  is the norm for the instability of the transitional resistance in the static state.

Thus, the norm for the transitional resistance is directly associated with the norm for the value of its instability.

When mechanical loads act on the contact, its transitional resistance also changes. During vibration and shaking it is possible to have continuous variations in the contact pressure and a displacement of the adjoining surfaces which form the contact. This, obviously, produces a variation in the transitional contact resistance and makes it variable, depending on the nature of the vibrations.

Because a snap connector or a vacuum tube panel represents a multiple-resonant system, the variation in the transitional resistance (the instability of transitional resistance) depends both on the value of the acceleration as well as on the frequency of vibrations (fig. 7).

In the dynamic state, the norm for the instability of the transitional contact resistance is established on the basis of the allowable level of vibration noise and is usually refined when the contact device is developed

$$\frac{\Delta R}{R} \text{ di} = \frac{R_{\text{trans max}}(0) - R_{\text{trans min}}(0)}{R_{\text{trans norm}}(0)} \cdot 100\%. \quad /476$$

On the basis of this the safety factor will be equal to

$$\eta_2 = 1 + \frac{\Delta R}{R} \text{ di}. \quad (10)$$

When various climatological factors affect the contact, its transitional resistance may increase. The degree to which the transitional resistance increases depends basically on the stability of the contact plating material to the action of these factors. Also, when the contacts are stored for a prolonged period of time, various aging processes take place which also tend to increase the transitional resistance. Investigation has shown that when the contacts are plated with precious metals, the value of the factor of safety  $\eta_3$  lies within the limits 1.5-2.0.

The value of the safety factor  $\eta_4$ , which takes into account the production variation of contacts as well as the allowable level of excess contact currents, lies in the limits 2.0-2.5.

Thus, the expression giving the norm for transitional contact resistance has the form

$$R_{\text{contact norm}}(0) = \frac{(0.2 - 0.35) \theta_2 D \sqrt{\pi k_1 k^*}}{1^2 (1 + \alpha t_2) \left(1 + \frac{2}{3} \alpha \theta_1\right) \left(1 + \frac{\Delta R}{R} \text{ di}\right) \left(1 + \frac{t_a}{3} \cdot \frac{\Delta R}{R} \text{ si}\right)}. \quad (11)$$

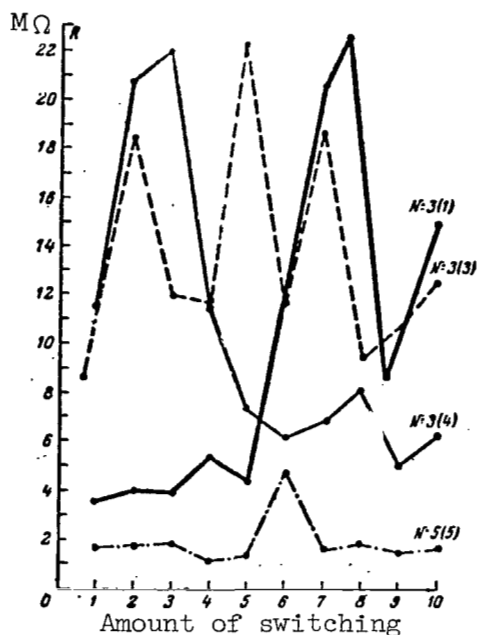


Figure 6. Transitional resistance of ring-type contacts during multiple switching.

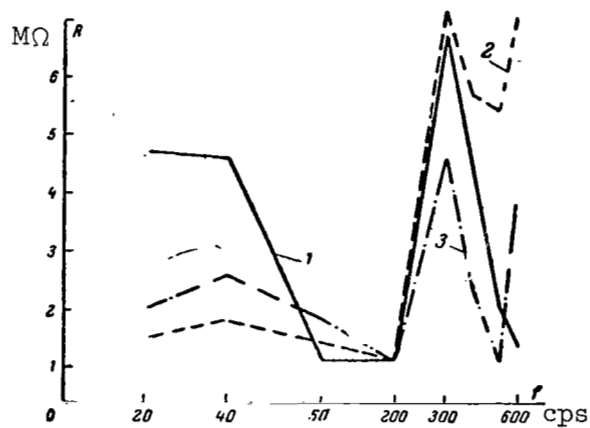


Figure 7. The variation in the ac component of the transitional contact resistance of a simple triangular area as a function of vibration frequency during acceleration.

## The Norm for the Value of the Contact Resistance

In practice the value of transitional resistance is not covered in the technical specifications because there is no method for measuring this parameter. The parameter used to check the quality of the contact is the so-called "contact resistance" (unfortunately in technical documentation this parameter is erroneously called the transitional resistance). The contact resistance represents the following sum

$$R_{\text{contact}} = R_{\text{trans}} + R_{\text{pin}} + R_{\text{soc}} + R_{\text{sol}},$$

where  $R_{\text{trans}}$  is the transitional contact resistance;

$R_{\text{pin}}$  is the resistance of the working part of the pin;

$R_{\text{soc}}$  is the resistance of the socket;

$R_{\text{sol}}$  is the resistance of the solder connection.

Resistances  $R_{\text{pin}}$ ,  $R_{\text{soc}}$  and  $R_{\text{sol}}$  may be assumed, with some approximation, to be constant for a given contact construction. Therefore, the value of the contact resistance is determined by the transitional contact resistance.

As a result of this, the norm for the value of the contact resistance depends on the norm for the value of the transitional resistance

$$R_{\text{contact norm}}(0) = R_{\text{trans norm}}(0) + R_{\text{arm norm}}(0). \quad (12)$$

The contact resistance determines the operating temperature of the contact. The temperature of the body of the contact (for the case of a single-contact cylindrical connector) is equal to

$$t_2 = t_{\text{sm}} + \Theta_2 + \Theta_3, \quad (13)$$

where  $t_{\text{sm}}$  is the temperature of the surrounding medium;

- $\Theta_2$  is the excess temperature of the apparent contact surface without taking into account the Joule heat liberated by  $R_{\text{arm}}$ ; /478  
 $\Theta_3$  is the excess temperature of the contact body without taking into account the Joule heat liberated by the transitional resistance.

The value of the excess temperature  $\Theta_3$  is determined by the resistance  $R_{\text{arm}}$ . For the case of a single-contact cylindrical connector, the operating temperature state of the contact, if we do not take into account the Joule heat liberated by the transitional resistance, is given by the following equation

$$\pi k^* D_c \theta_3 dx - I^2 dR_{\text{arm}}(t) = 0,$$

or

$$\pi k^* D_c \theta_3 dx - I^2 \frac{4\sigma(t)}{\pi D_c^2} dx = 0.$$

Solving this equation we obtain

$$\theta_3 = \frac{I^2 R_{\text{arm}}(t)}{\pi k^* D_c l} = \frac{4I^2 \sigma(t)}{\pi^2 D_c^3 k^*}, \quad (14)$$

where  $l$  is the length of the contact.

It follows from this that the norm for the value of the resistance  $R_{\text{arm norm}}(0)$  will be equal to

$$R_{\text{arm norm}} = \frac{(0.4 - 0.5) \pi k^* l D_c \theta_3}{I^2 (1 + \alpha t_2)}, \quad (15)$$

while the norm for the value of the contact resistance will be equal to

$$R_{\text{arm norm}}(0) = \frac{D_c}{I^2} \left\{ \frac{(0.2 - 0.35) \sqrt{\pi k^*} \times}{(1 + \alpha t_2) \left(1 + \frac{2}{3} \alpha \theta_1\right) \times} \right. \\ \left. \frac{\times \left[ \theta_2 \sqrt{k_1} + 2\theta_1 \sqrt{\pi k^* l} \left(1 + \frac{2}{3} \alpha \theta_1\right) \left(1 + \frac{\Delta R}{R} d_1\right) \times \right.}{\times \left(1 + \frac{t_a}{3} \cdot \frac{\Delta R}{R} s_1\right) \times} \right.} \\ \left. \frac{\times \left(1 + \frac{t_a}{3} \cdot \frac{\Delta R}{R} s_1\right) \right]}{\times \left(1 + \frac{\Delta R}{R} d_1\right)} \right\}. \quad (16)$$

Consequently, to provide an identical thermal state for a contact of 479 any diameter, the following condition must be satisfied

$$\frac{I^2 R_{\text{cont norm}}(0)}{D_c} = B = \text{const}, \quad (17)$$

which unfortunately is not considered in establishing norms for the value of the contact resistance (figs. 8 and 9).

In determining  $R_{\text{cont norm}}(0)$  in most cases it is easier to use the total value of contact body temperature excess in place of its individual components.

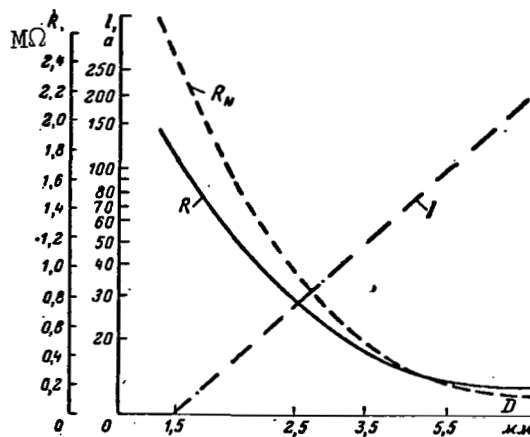


Figure 8. The variation in the contact resistance as a function of contact diameter;  $R_N$ , resistance according to norms

published in the technical specifications;  $R$ , measured resistance;  $I$ , allowable contact current according to technical specifications.

Then

$$R_{\text{cont norm}}(0) = \frac{(0.2 - 0.35)}{\pi D_C^2} \times \quad (18)$$

$$\times \left\{ \frac{\sqrt{k_1} (\theta_2 + \theta_3) \pi^2 D_C^3 k^2 - 4 I^2 \sigma_0 (1 + \alpha t_2)}{\sqrt{\pi k^* I^2 (1 + \alpha t_2)} \left( 1 + \frac{2}{3} \alpha \theta_1 \right) \left( 1 + \frac{\Delta R}{R} \right) \left( 1 + \frac{t_2}{3} \frac{\Delta R}{R} \right)} \right\} \cdot \left\{ 2 \sigma_0 I \right\}.$$

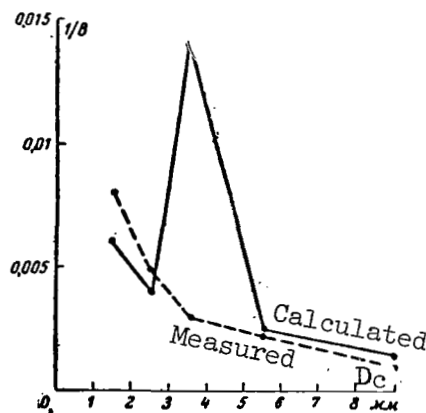


Figure 9. Variation in the parameter B as a function of the contact diameter in connector ShR.



Thus the norm for the value of the contact resistance depends on /480  
the contact diameter, on the contact current, on the assigned value for the  
instability of the transitional contact resistance both in the static as well  
as the dynamic state, on the contact material, on the surrounding temperature  
and on the specific conditions of heat transfer in the equipment itself, i.e.,  
the norm for the value of the contact resistance cannot be determined without  
taking into account the construction of the entire device, the physical prop-  
erties of the dielectric, which surrounds the contact, thermal effects pro-  
duced by adjoining contacts.

### The Thermal State of the Multiple-Contact Snap Connector

The question considered above on the thermal operating state of a con-  
tact pertained to the case of a single contact in a snap connector, i.e.,  
we considered only the liberation of Joule heat in this contact.

In the case of a multiple-contact connector, the thermal operating state  
of each contact is determined by the liberation of Joule heat in this contact  
as well as by the thermal effect of other contacts. Also, in this case, not  
all the contacts operate under the same temperature conditions. From the  
standpoint of severe thermal conditions, the contacts in question are at the  
center of the connector.

The value of the total excess temperature of the central contacts must  
be such that the temperature in the body of these contacts is always less  
than the maximum working temperature of the dielectric which surrounds the  
contacts, i.e.,

$$t_{cb} = t_{sm} + \Theta_2 + \Theta_3 + \Theta_4 + \Theta_5 \leq t_{mwd}, \quad (19)$$

where  $t_{cb}$  is the temperature in the body of the cylindrical contact;

$t_{sm}$  is the temperature of the surrounding medium;

$t_{mwd}$  is the maximum working temperature of the dielectric;

$\Theta_4$  is the excess temperature at the center of the connector due to  
liberation of Joule heat by the adjoining contact;

$\Theta_5$  is the excess temperature of the external surface of the connector.

Let us determine the value of the excess temperature at the center of  
the connector  $\Theta_4$ . To do this, let us consider the equivalent scheme of a  
multi-contact cylindrical snap connector shown in figure 10.

The excess temperature at the center of the connector is equal to

$$\theta_4 = \sum_{i=1}^n \theta_{4,i}.$$

where  $\Theta_{4i}$  is the excess temperature at the center of the connector due to the thermal effect of one of the adjacent contacts.

To determine the values  $\Theta_{4i}$  we consider the temperature field inside the connector due to the liberation of heat at the contact which is placed eccentrically in the circular insulation. The external surface of the insulation has the same temperature of all points equal to  $t_{sm} + \Theta_{5i}$ , i.e., it is isothermal.

The surface of a cylinder with diameter  $\frac{2SD_2}{D_2 + 2S}$ , passing through the center of the connector, is also isothermal. The temperature at all points of the surface is equal to  $t_{sm} + \Theta_{5i} + \Theta_{4i}$ .

Because the same thermal flux passes through these surfaces we can write the following equality /482

$$\frac{\Theta'_{2i} + \Theta'_{3i} - \Theta_{4i}}{R^*_{trc}} = \frac{\Theta'_{2i} + \Theta'_{3i}}{R^*_{t\ diel}}$$

where  $\Theta'_{2i} + \Theta'_{3i}$  is the excess temperature of the contact body placed eccentrically in the connector;

$R^*_{t\ diel}$  is the thermal resistance of the connector insulation to the thermal flux, produced by the liberation of Joule heat in the contact which is placed eccentrically;

$R^*_{trc}$  is the thermal resistance of a cylinder with  $\frac{2SD_2}{D_2 + 2S}$ ,

diameter whose side surface passes through the center of the connector.

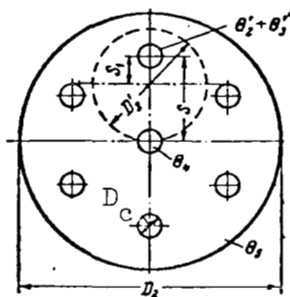


Figure 10. The schematic of a multi-contact snap connector.

If we make some rough approximations, calculations show that in this case  $(\theta'_{2i} + \theta'_{3i}) \approx (\theta_{2i} + \theta_{3i})$ , i.e., the excess temperature of the contact body placed eccentrically in the connector is the same as the temperature which would occur if it (the contact body) were to be situated at the center of the connector.

Then

$$\theta_{ii} = \frac{(\theta_{2i} + \theta_{3i})(R^*_{\text{diel}} - R^*_{\text{trc}})}{R^*_{\text{diel}}} \quad (20)$$

where

$$\begin{aligned} R^*_{\text{diel}} &= \frac{1}{2\pi\lambda_1 l} \times \\ &\times \ln \frac{\sqrt{\left(\frac{D_2}{2} + \frac{D_c}{2}\right)^2 - S^2} + \sqrt{\left(\frac{D_2}{2} - \frac{D_c}{2}\right)^2 - S^2}}{\sqrt{\left(\frac{D_2}{2} + \frac{D_c}{2}\right)^2 - S^2} - \sqrt{\left(\frac{D_2}{2} - \frac{D_c}{2}\right)^2 - S^2}}; \\ R^*_{\text{trc}} &= \frac{1}{2\pi\lambda_1 l} \times \\ &\times \ln \frac{\sqrt{\left(\frac{D'_2}{2} + \frac{D_c}{2}\right)^2 - S_1^2} + \sqrt{\left(\frac{D'_2}{2} - \frac{D_c}{2}\right)^2 - S_1^2}}{\sqrt{\left(\frac{D'_2}{2} + \frac{D_c}{2}\right)^2 - S_1^2} - \sqrt{\left(\frac{D'_2}{2} - \frac{D_c}{2}\right)^2 - S_1^2}}; \\ D'_2 &= \frac{2SD_2}{D_2 + 2S}; \quad S_1 = \frac{2S^2}{D_2 + 2S}. \end{aligned}$$

To provide for identical temperature conditions in the connectors, /483  
regardless of the number of contacts, it is necessary that

$$\theta_2 + \theta_3 + \theta_4 + \theta_5 = \text{const},$$

or

$$\begin{aligned} &(\theta_2 + \theta_3) + \sum_{i=1}^n (\theta_{2i} + \theta_{3i}) \left(1 - \frac{R^*_{\text{trc}}}{R^*_{\text{diel}}}\right) + \\ &+ \sum_{i=1}^n (\theta_{2i} + \theta_{3i}) \frac{\frac{1}{\pi D_1 l h}}{R^*_{\text{diel}} + \frac{1}{\pi D_1 l h}} = \text{const}. \end{aligned} \quad (21)$$

Thus, if equality (21) is to be satisfied, it is necessary to introduce a load current coefficient whose magnitude is computed by means of the following equation

$$x^2 = \frac{(\theta_2 + \theta_3 + \theta_4 + \theta_5) \times}{I^2 [(3-5) R_{\text{cont norm}}(0) \sqrt{\pi k^* b} - 2\sigma_0 l \sqrt{\pi k^* b} + 4\sigma_0 (1 + \alpha t_2)] \times} \times \frac{\pi^2 \sqrt{k_1 D_c^3 k^*}}{R_{\text{diel}}^* + \frac{1}{\pi D_1 l h}} \times \left[ 1 + n \left( 1 - \frac{R_{\text{trc}}^*}{R_{\text{diel}}^*} \right) + \frac{\frac{n}{\pi D_1 l h}}{R_{\text{diel}}^* + \frac{1}{\pi D_1 l h}} \right], \quad (22)$$

where  $n$  is the number of contacts in the connector

$$b = (1 + \alpha t_2) \left( 1 + \frac{2}{3} \alpha \theta_1 \right) \left( 1 + \frac{t_a}{3} \cdot \frac{\Delta R_s}{R} \right) \left( 1 + \frac{\Delta R_d}{R} \right).$$

Thus, when the diameter of the connector and the number of contacts increase, the values of the operating currents must be lowered in accordance with the load current coefficient  $\kappa$ .

## Conclusions

- a) The establishment of substantiated norms for the electrical contact parameters will make it possible to improve the quality control of units produced at the factories. This, in turn, will make it possible to improve the reliability of these devices.
- b) The norms for the value of the transitional contact resistance /484 and for the contact resistance are determined by the allowable operating temperatures of the contacts. Therefore, one way of determining these norms is to carry out thermal calculations for the contacts.
- c) The norms for the value of the transitional resistance depend on the values of the assigned operating currents and on the excess temperature of the apparent contact surface.
- d) The norm for the value of the contact resistance depends on the assigned values of operating currents and the excess temperature of the contact body.
- e) Both the norm for the value of the contact resistance and the norm for the value of the transitional resistance depend directly on the norm for the instability of the transitional resistance in the static and dynamic state.
- f) To provide for an identical temperature state for various contact diameters, the following condition must be satisfied

$$\frac{I^2 R_{\text{trans norm}}(0)}{D_c} = \text{const}; \quad \frac{I^2 R_{\text{cont norm}}(0)}{D_c} = \text{const}.$$

- g) The norm for the value of the contact resistance is expressed as the norm for the average value of the contact resistance (the average is taken from three readings).

h) The norm for the value of the contact resistance is determined for a connector of definite diameter and for the case of a single-contact snap connector.

i) To provide for an identical temperature operating state of the central contact in a multiple-contact snap connector, it is necessary to introduce the load current coefficient whose value depends on the diameter of the connector and on the number of contacts.

#### REFERENCES

1. Holm, R. Electric Contacts (Elektricheskiye kontakty), I. L., 1961.
2. Kutateladze, S. S. The Theory of Heat Transfer, (Osnovy teorii teploobmena) Mashgiz, 1962.

A. Yu. Gorodetskiy

Contacts are one of the principal sources which affect the reliability of a relay. According to operational data, the failure of contacts represents 60 percent of all relay failures. One of the reasons for this is that there is an absence of adequate information on the switching possibilities of contacts. As a result of this, they are quite frequently used improperly and are required to perform tasks for which they are not designed.

Until quite recently, the reliability of contacts was established in an indirect way. For operating states which do not produce electrical wear, the evaluations were made by varying the adjustable parameters. For operating conditions which produce electrical wear, the nature and magnitude of the latter was evaluated. However, these evaluations were of a qualitative nature.

The visual methods of controlling the operation of the contacts which involve the use of light bulbs connected in parallel with the load cannot be considered satisfactory. Only by using special systems which make it possible to record and qualify failures, is it possible to evaluate the reliability of contacts. It is also necessary to record transitional failures which may disappear by themselves and not recur for a long period of time.

These systems must satisfy the following requirements: they must supply complete information on the type of failure (failure to close or failure to release), they must have the necessary sensitivity, optimum time characteristics, maximum flexibility and minimum effect on the operation of the contacts which are being tested.

The systems which control the operation of contacts may be constructed to compare the operation of two or more test contacts of the same relay (ref. 1) or to control the operation of the test relay with that of a reference contact which does not switch the load currents. In the first case it is assumed that a simultaneous failure of two test contacts is of low probability; this is confirmed by experiment, especially when testing is done under normal conditions. In the second case, the reference contact is selected so that it is reliable; it switches only the control circuits of the system, and its probability of failure is very small. /486

The systems for recording failures may be divided into two types, depending on the method used to connect the load circuits. In the first system, the input consists of the voltage drop across the compared networks (the "linear systems"), in the second, the input of the system is connected to the equipotential points of two networks being compared (the so-called transverse systems which react to voltage appearing at the input of the system).

Usually when life tests are run, the type of failure is not known beforehand; to determine the type of failure, it is necessary to determine which contact of the relay has failed and also what its position is. In cases when the type of failure is known beforehand, as in mass testing, and the detailed distribution of failures with time is not acquired, it is rational to add the failures which occur over a period of time by means of a counter.

The operate time of the system for recording failures must be adjusted so that there is no interference from relay chatter or from the operate time difference between the contacts under test. On the other hand, if the type of failure is not known beforehand, the total operate time must be set within the time during which the test relay is drawing current or not drawing current. This is necessary to fix the position of the relay during failure. In this case, it is possible to stop the operation of the entire system and investigate the failed contact or to identify the failed contact and its position without stopping the system. Below we shall consider systems which stop operating when a contact fails.

The required sensitivity for systems which record failures is determined by the range of possible loads. Most of the systems for detecting failures use electromagnetic relays.

The limited sensitivity of neutral electromagnetic relays decreases the range of their application. The windings of the relay which control the operation of the contacts are connected in parallel with the load resistance. In this case it is impossible to produce a purely resistive load or to produce inductive loads with definite parameters. Systems which use the RP-5 /487 polarized relays are more sensitive. The short operate time of the RP relay (several milliseconds) makes it difficult to adjust it so that there is no interference from relay chatter and from the operate time difference between the contacts under test. Therefore, the use of these relays may lead to false signals.

The electronic systems for recording failures are free from these disadvantages. By using vacuum tubes with the output electromagnetic relays, it is possible to obtain the desired sensitivity over a large range of loads such that the effect of the control circuits on the operation of the test contacts is insignificant.

Let us consider some relay systems and electronic systems for recording failures.

#### dc Operation

Figure 1 shows a relay system for recording failures in the dc range. In this system, the operation of the test contacts is compared with the operation of the reference contact. In the normal operation of the test contacts, both windings of the control relay are connected so that they oppose each other. They either carry a current or do not carry a current, in which case the relay does not operate. When some test contact does not make or break, the corresponding

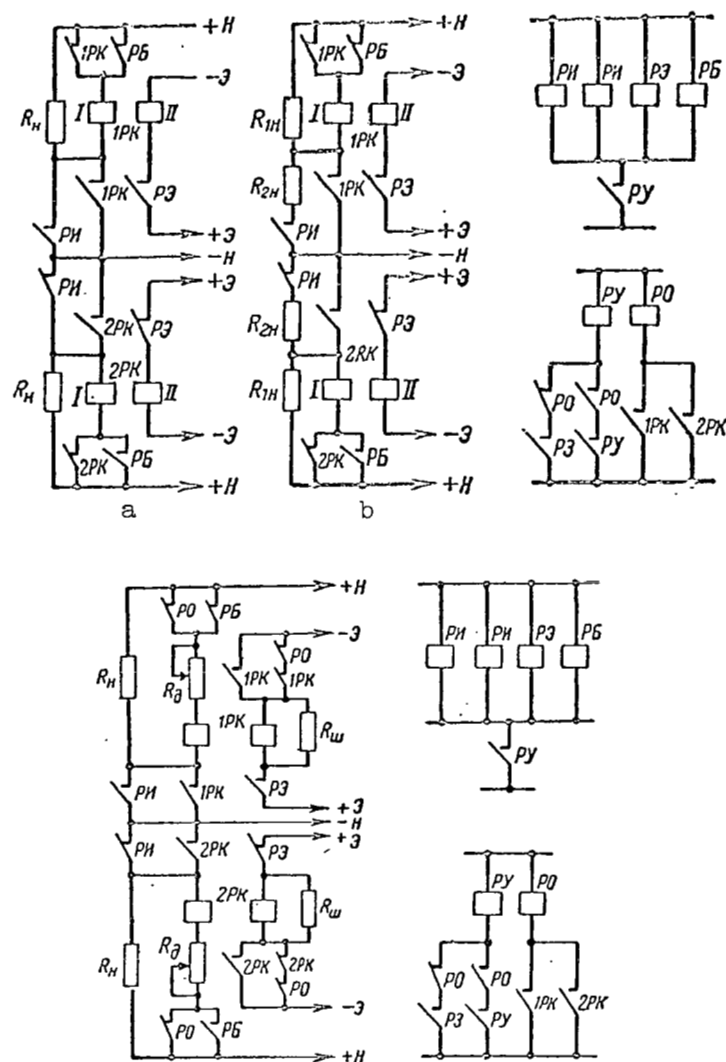


Figure 1. Relay circuits for recording failures during dc switching (comparison with a reference contact).

control relay RK operates, the system stops and the failure is recorded. Relays RB, RE, RZ and RO are common to the entire system. The blocking relay RB operates in synchronization with the test relays RI and prepares the blocking network 1 of the winding during the half period when RI may not open. Contact RZ generates pulses of definite frequency. The control relay RU switches relays RI, RE and RB. Relay RO stops the system when failure occurs such that the position of the test relay is the one in which failure occurred.

The type and position of failure is determined by the number of control relay RK and by the position of relay RI. The operate time of the system is determined primarily by the operate time of relay RK and does not depend on



voltage. The lower voltage level is determined by the sensitivity of relay RK. For voltages which exceed the operate voltage of relay RK, it is necessary to connect the winding I in parallel with part of the load. /489

The system utilizes neutral electromagnetic relays of any type with double windings. The disadvantage of this system is the narrow range of loads and the necessity for tapping the load resistance, as well as the unsuitability of the system for inductive loads. When the system is used to test a large number of contacts, it is desirable to increase the number of RB contacts. The circuit presented in figure 1b proposes the use of common contacts RD and RB in the circuit containing one winding of relay RK. When RI does not close, there is a blocking of the corresponding relay RK in the circuits of the other windings. A resistance of several kilohms and a capacity of a few tenths of a microfarad provide for a clear switching of relay 1 RK.

Figure 2 shows the electronic circuit for recording failures of the "transverse" type during dc operation. This circuit compares the operation of the RI test relay contacts and makes it possible to record failures not associated with the contacts, i.e., failures produced by the sticking of the armature and by breaks in the winding, etc. The input circuits of the system are connected in such a way that under normal operation of the test contacts, no voltage is fed to the grid of the tube. Quiescent current flows in the windings of the RK control relays and is limited by the resistances  $R_C$  in the cathode

circuit. When one of the contacts fails, the inputs of the two tubes which are connected so that they oppose each other, are supplied with a bias which is equal in magnitude but of different sign. One of the tubes conducts while the other is blocked, depending on which contact failed. When the RK control relay operates, the failure is recorded. In addition to this, relay RK stops the test relay in the position in which the failure occurred (see figure 1c).

The type of failure is determined by the number of the RK relay and by the position of the test relays.

The sensitivity of the system depends strongly on the value of the resistance  $R_C$  in the cathode which provides for negative feedback. If we make  $R_C$  variable, we may use the system over a relatively wide range of load

voltages. When we have a constant resistor  $R_C$  in the cathode circuit, /491

the sensitivity of the system may be varied over a small range by controlling the plate. This makes it possible to carry out adjustments so that there is not interference from relay chatter and from the operate time difference between the contacts under test. It should be pointed out that when the polarity of the load voltage is changed, the sensitivity of the system is destroyed and it is not possible to identify the failures. For the polarity shown in figure 2, the sensitivity is higher because the load voltage is added to the plate voltage. When the load polarity is reversed, the sensitivity of the system drops.

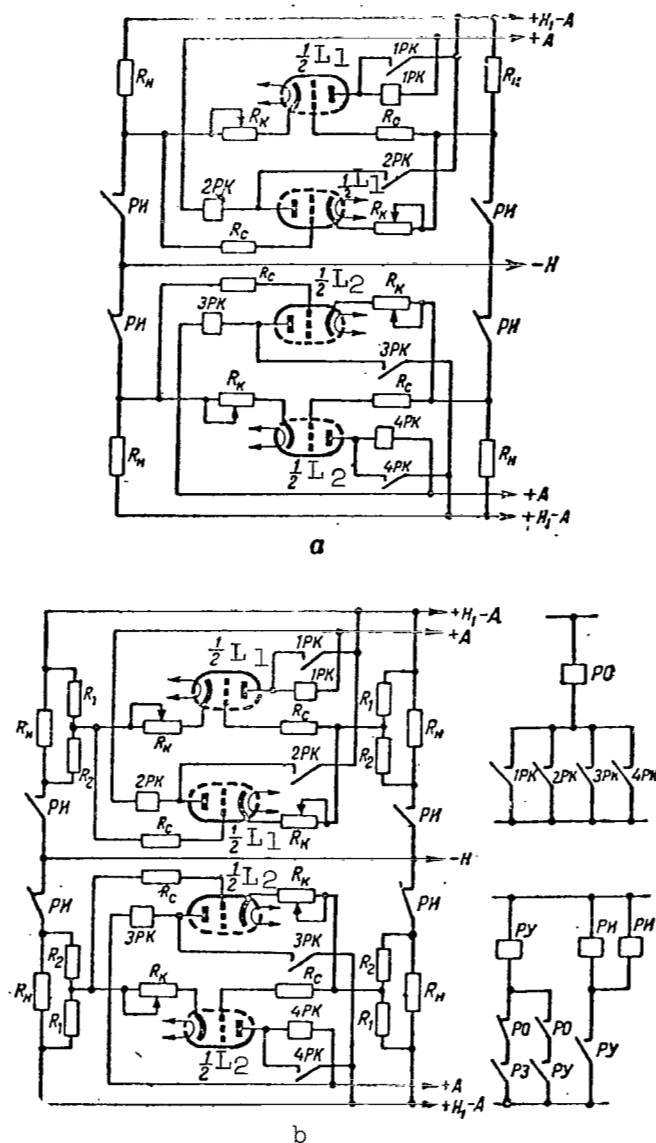


Figure 2. Electronic system for recording failures during the quality control of contacts which switch dc circuits (comparison of test contacts).

The system shown in figure 2 uses a double triode 6N1P and a type RPN relay for the control relay RK. When the sensitivity of the latter is 4-8 mA,  $R_C$  has a value of 3-6 k $\Omega$ . When there is no failure, the current does not exceed 1-2 mA and when failure occurs, the current is greater by a factor of 1.5 than the operate current of the relay. This makes it possible to avoid false indications produced by interference from relay chatter and from the operate time difference between the contacts under test.

When the voltages vary from a few volts to 100 volts, the system shown in figure 2a is recommended. When the voltages are greater than 100 volts, it is desirable to put a voltage divider in parallel with the load. However, when this is done, it is necessary to make sure that the resistance in the cathode circuit does not decrease the sensitivity of the system.

In the grid circuit, the resistance is 1 megohm and for all practical purposes the coupling between the test contacts may be neglected. The system shown in figure 2 may be used over a rather wide range of load values without tapping the load to get the necessary sensitivity.

The disadvantage of the circuit shown in figure 2 is that the cathode circuits also carry the plate currents. This limits the application of these circuits when the loads are of high resistance. Also, for some high voltage operations, it is difficult to test inductive loads because the resistance of the voltage divider varies from 10 to 20 kilohms and its shunting effect cannot be neglected every time.

The circuits shown in figure 3 for dc operation are free from these defects. They are based on the comparison of test contacts with a reference /493 contact and differ from the system shown in figure 1 because the contacts operate out of phase. The tube input circuits are connected in parallel with the load resistance. The polarity of the load voltage is selected so that when the test contact of the relay RI closes, the voltage drop across the load resistance blocks the tube. At the same time, the reference contact breaks the circuit of winding II. In other half periods the test contact of relay RI is open, the input to the tube is shorted by the load resistance, and the tube conducts current whose magnitude depends on the resistance  $R_C$  in the cathode circuit. Windings I and II of the control relay RK are connected so that they oppose each other. Thus, during the normal operation of the test relay RI, relay RK does not operate. When relay RI fails, relay RK operates.

Relays RB, RO, RE and RZ are common. The master contact of relay RZ generates pulses of definite frequency and shape. The blocking relay RB prepares the circuit by blocking winding I. If the contacts do not close, relay RK operates and is blocked, so that the subsequent closing of contacts RI does not lead to a drop-out of RK. The failure relay RO records the position of the test relay during failure.

The diagram shown in figure 3 may use a double triode of the 6N1P type and a double winding RPN type relay. When the sensitivity of winding I is 3-6 mA, the resistance in the cathode circuit is equal to 0.5-1 kilohm. For dc operation when the voltage is greater than 100 volts, it is necessary to use a voltage divider (fig. 3b) with a resistance of approximately 1 megohm. In this case the shunting effect of the voltage divider may be neglected from the standpoint of its effect on the load resistance.

The circuits shown in figure 3 have a series of advantages over the circuits shown in figure 2. Since the voltage drop across the load resistance (fig. 3a) or part of it (fig. 3b) is used to block the vacuum tubes, the circuits have almost the same sensitivity over a wide range of load resistances

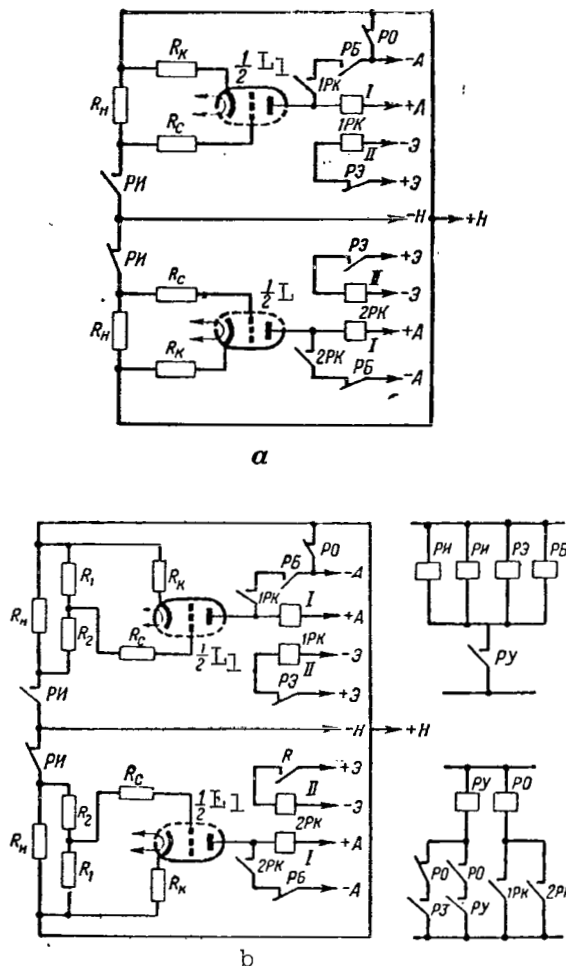


Figure 3. The electronic system for recording failures during the quality control of contacts which switch dc currents (comparison with a reference contact).

without additional adjustment. The sensitivity is determined by the type of vacuum tube which is used, by the parameters of the output relay, and by the magnitude of the resistance in the cathode circuit. To eliminate interference from relay chatter and from the operate time difference between the contacts under test, the characteristics of the circuit can be changed by increasing or decreasing the plate voltage. /494

Thus, this dc scheme has universal application over a wide range of load voltages. When we select  $R_c = 1$  megohm, the coupling between the test contacts

and the reference contacts may be neglected. We should point out that in the circuit shown in figure 3, unlike those shown in figure 2, the load circuits carry grid currents rather than plate currents. This makes this circuit non-critical as far as the load resistance in the contact circuit is concerned.

The system may be used both for active loads and for inductive loads with very little change in the test conditions. However, unlike the circuits in figure 2, this system utilizes a neutral electromagnetic relay with two windings of which one winding (I) has increased sensitivity.

#### ac Operation

Figure 4 shows a system for recording failures during ac operation. The system is analogous to the one shown in figure 1 (windings I and II of control relays RK are connected through rectifying bridges). The windings of relay RK may be fed from a common rectifier. The disadvantages of the circuit shown in figure 4a, like the disadvantage of the circuit shown in figure 1, are its limited sensitivity and low range of loads, particularly when these are inductive. Figure 4b shows another circuit analogous to the one shown in figure 1b. This circuit can be used when it is desirable to test a large number of contacts.

Figure 5 shows an electronic circuit for recording failures during ac operation. In this system, the operation of test contacts is compared with the operation of the reference contact. Under normal operation, a quiescent current flows through the windings of the control relays RI and its value is limited by resistance  $R_c$ . When the test contact fails, the ac load voltage is applied to

the input of the corresponding tube. In this case, the tube is blocked <sup>/497</sup> for half of the load voltage cycle and open for the other half. The capacity smooths out the pulsating plate current of the tube, relay RK operates, is locked by its closing contact and records the failure. It should be pointed out that at a frequency of 50 cps, the RK relay is able to operate during half the period. When the frequency is above 50 cps, for example when it is 400 cps, a clean cut operation of the control relay is impossible without filtering the plate current. The sensitivity is controlled by means of a potentiometer. When the load voltage is greater than 100 volts, a voltage divider must be used.

This system uses a double 6N1P triode and a RPN relay with a sensitivity of the order of 4-8 mA. The resistance in the cathode circuit is 2-4 k $\Omega$ . The resistance is of the order of 1 M $\Omega$ , the capacity is  $C = 0.1$  mf,  $R_1$  and  $R_2$  are several hundred kilohms, the wire rheostat  $R_3$  is several hundred ohms. In

figure 5 we may neglect the coupling between the test and reference contacts and the shunting effect of the voltage divider. These systems may be used over a wide range of resistive and inductive loads.

All the circuit diagrams show the contacts of relay RZ which generates pulses of definite frequency and shape. Synchronous motors or multivibrators may be used to generate pulses. Multivibrators may be used when it is <sup>/499</sup> necessary to achieve a uniform control of pulse repetition rate. Figure 6b shows a typical multivibrator. To improve its frequency stability it utilizes a 6N1P tube with anode-grid couplings. When the frequencies are of the order





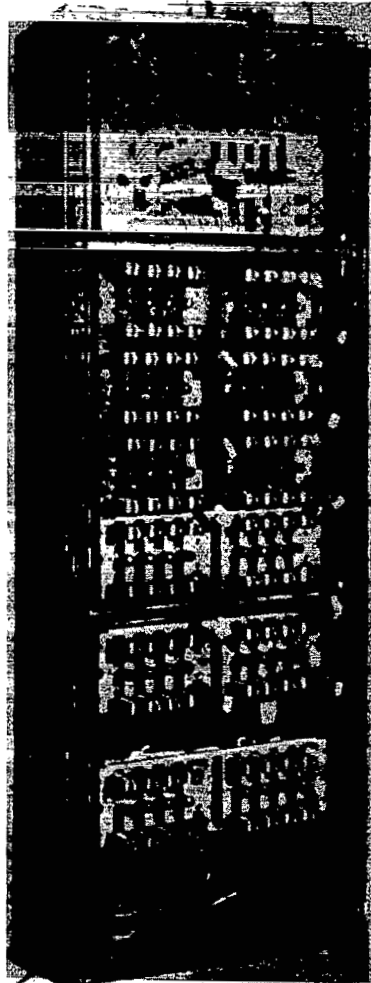


Figure 7. Equipment bay for recording failures.



network with a polarized RP-4 relay. Figure 6a shows the connection of such a network which utilizes a synchronous motor, while figure 6b shows the connection of the differentiating network to one of the arms of the multivibrator.

Relay RP-4, in conjunction with relay R0, memorizes the position of the system during failure.

The control relay RU amplifies the contacts of RP-4 and switches the test relays and other components of the system.

The systems for recording failures utilize sonic signals and light signals. The type of failure is determined from the position of control relay RU which switches the windings of the test relays and from the number of the operated control relay RK. When the control rack has a high capacity, it is not rational to have a separate signal lamp for each RK. In this case RK should be placed in rows and we should have one signal lamp for each longitudinal and transverse row. This will make it possible to determine the number of the RK during failure by using the signal lamps as coordinates.

The general view of the test rack for recording failures is shown in figure 7.

## Conclusions

The circuits which we have described make it possible to record the failure of test contacts to close or to open. The type of failure is determined by the operation of a particular RK relay and by the position of the test relays at the instant of failure. In cases when we are concerned only with failure to close or with failure to open, the circuits which we have presented may be simplified.

The particular system selected for testing relays depends on the specific requirements. If testing is conducted under specific conditions, the circuits with electromagnetic relays, for example, relays of the RPN type may be used. In this case, because these circuits have a limited sensitivity, it is necessary to evaluate the effect of the test circuit on the test conditions. When testing is carried out over a wide range of loads, it is desirable to use electronic circuits which are more universal. /500

The lower range of test voltages is determined by the types of electromagnetic relays and by the types of vacuum tubes. With use of the 6N1P double triodes with a medium amplification factor and with use of the RPN type relay, the electronic circuits may operate with a minimum voltage of 5-10 volts.

Translated for the National Aeronautics and Space Administration  
by John F. Holman and Co. Inc.

*"The aeronautical and space activities of the United States shall be conducted so as to contribute . . . to the expansion of human knowledge of phenomena in the atmosphere and space. The Administration shall provide for the widest practicable and appropriate dissemination of information concerning its activities and the results thereof."*

—NATIONAL AERONAUTICS AND SPACE ACT OF 1958

## NASA SCIENTIFIC AND TECHNICAL PUBLICATIONS

**TECHNICAL REPORTS:** Scientific and technical information considered important, complete, and a lasting contribution to existing knowledge.

**TECHNICAL NOTES:** Information less broad in scope but nevertheless of importance as a contribution to existing knowledge.

**TECHNICAL MEMORANDUMS:** Information receiving limited distribution because of preliminary data, security classification, or other reasons.

**CONTRACTOR REPORTS:** Technical information generated in connection with a NASA contract or grant and released under NASA auspices.

**TECHNICAL TRANSLATIONS:** Information published in a foreign language considered to merit NASA distribution in English.

**SPECIAL PUBLICATIONS:** Information derived from or of value to NASA activities. Publications include conference proceedings, monographs, data compilations, handbooks, sourcebooks, and special bibliographies.

**TECHNOLOGY UTILIZATION PUBLICATIONS:** Information on technology used by NASA that may be of particular interest in commercial and other nonaerospace applications. Publications include Tech Briefs; Technology Utilization Reports and Notes; and Technology Surveys.

*Details on the availability of these publications may be obtained from:*

SCIENTIFIC AND TECHNICAL INFORMATION DIVISION  
NATIONAL AERONAUTICS AND SPACE ADMINISTRATION

Washington, D.C. 20546